

Topics in Organometallic Chemistry 49

Elena Fernández
Andrew Whiting *Editors*

Synthesis and Application of Organoboron Compounds

 Springer

Topics in Organometallic Chemistry

Editorial Board

M. Beller, Rostock, Germany

J.M. Brown, Oxford, United Kingdom

P.H. Dixneuf, Rennes, France

J. Dupont, Porto Alegre, Brazil

A. Fürstner, Mülheim, Germany

Frank Glorius, Münster, Germany

L.J. Gooßen, Kaiserslautern, Germany

T. Ikariya, Tokyo, Japan

S. Nolan, St Andrews, United Kingdom

Jun Okuda, Aachen, Germany

L.A. Oro, Zaragoza, Spain

Q.-L. Zhou, Tianjin, China

Aims and Scope

The series *Topics in Organometallic Chemistry* presents critical overviews of research results in organometallic chemistry. As our understanding of organometallic structure, properties and mechanisms increases, new ways are opened for the design of organometallic compounds and reactions tailored to the needs of such diverse areas as organic synthesis, medical research, biology and materials science. Thus the scope of coverage includes a broad range of topics of pure and applied organometallic chemistry, where new breakthroughs are being achieved that are of significance to a larger scientific audience.

The individual volumes of *Topics in Organometallic Chemistry* are thematic. Review articles are generally invited by the volume editors. All chapters from *Topics in Organometallic Chemistry* are published OnlineFirst with an individual DOI. In references, *Topics in Organometallic Chemistry* is abbreviated as *Top Organomet Chem* and cited as a journal.

More information about this series at
<http://www.springer.com/series/3418>

Elena Fernández • Andrew Whiting
Editors

Synthesis and Application of Organoboron Compounds

With contributions by

V.K. Aggarwal • D.G. Hall • T.N. Hooper • M.J. Ingleson •
N. Ishid • K. Ishihara • F. Jäkle • H.C. Johnson • S. Lee •
D. Leonori • G.A. Molander • M. Murakami • K. Nozaki •
H-Y. Sun • K.M. Traister • A.S. Weller • M. Yamashita •
J. Yun

 Springer

Editors

Elena Fernández
Universitat Rovira i Virgili Directora
TECAT
Tarragona
Spain

Andrew Whiting
Department of Chemistry
Centre for Sustainable Chemical Processes
Durham
United Kingdom

ISSN 1436-6002

ISBN 978-3-319-13053-8

DOI 10.1007/978-3-319-13054-5

Springer Cham Heidelberg New York Dordrecht London

ISSN 1616-8534 (electronic)

ISBN 978-3-319-13054-5 (eBook)

Library of Congress Control Number: 2015933846

© Springer International Publishing Switzerland 2015

This work is subject to copyright. All rights are reserved by the Publisher, whether the whole or part of the material is concerned, specifically the rights of translation, reprinting, reuse of illustrations, recitation, broadcasting, reproduction on microfilms or in any other physical way, and transmission or information storage and retrieval, electronic adaptation, computer software, or by similar or dissimilar methodology now known or hereafter developed. Exempted from this legal reservation are brief excerpts in connection with reviews or scholarly analysis or material supplied specifically for the purpose of being entered and executed on a computer system, for exclusive use by the purchaser of the work. Duplication of this publication or parts thereof is permitted only under the provisions of the Copyright Law of the Publisher's location, in its current version, and permission for use must always be obtained from Springer. Permissions for use may be obtained through RightsLink at the Copyright Clearance Center. Violations are liable to prosecution under the respective Copyright Law.

The use of general descriptive names, registered names, trademarks, service marks, etc. in this publication does not imply, even in the absence of a specific statement, that such names are exempt from the relevant protective laws and regulations and therefore free for general use.

While the advice and information in this book are believed to be true and accurate at the date of publication, neither the authors nor the editors nor the publisher can accept any legal responsibility for any errors or omissions that may be made. The publisher makes no warranty, express or implied, with respect to the material contained herein.

Printed on acid-free paper

Springer is part of Springer Science+Business Media (www.springer.com)

Preface

From the early explorative days of organoboron chemistry to the present day, this area has never ceased to be a vital and exciting area of chemical research. Major themes have emerged, one after another, keeping organoboron chemistry at the forefront of our science, perhaps starting with major and long-term contributions of H. C. Brown. His work gave us the possibility to hydroborate and off-the-shelf hydride reducing agents that we now take for granted, and of course, this contributed to his Nobel Prize in 1979. Organoboron chemistry moved from stoichiometric to a catalytic manifold, and this fact opened up unexpected applications and unlimited possibilities. In addition to these fundamental studies elucidating the basics of organoboron chemistry, there were major strides into asymmetric synthesis and this contributed to our science in innumerable ways, allowing us to routinely achieve non-chiral pool synthesis of chiral molecules. Further remarkable contributions carried out by D. S. Matteson have laid the foundations for considerable amounts of the research reported in this book. Along the way, A. Suzuki and N. Miyaura found new uses for organoboron compounds in cross-coupling reactions, creating major impacts upon the way in which we assemble molecules, especially using automated systems for biological evaluation. In turn, and following fundamental studies by E. Vedejs, new types of organoboron compounds were spun out which pushed forward the boundaries of stability and created an ever-widening range of applications for further synthetic transformations. Interestingly, we still need new ways, not only to make organoboron compounds, but to exploit the huge and untapped potential for these compounds. In this book, we can see how new methods for the introduction of boron into carbon frameworks are creating their own revolutions of what is possible to make, and this science is moving on from simple boron-based Lewis acid catalysis to new types of activation pathways and who knows exactly where this will lead us. One thing is certain of course, for those of us who are addicted to organoboron chemistry, it will continue to stimulate and even better, surprise. We hope this snapshot of where organoboron is today will not only be a vital reference book but we hope it will provide you with an insight into where things might go in the future, and maybe it will spark that idea that opens the way for yet another major advance in our science.

Finally, as editors, we would like to thank all the contributors for their participation in this project, both authors of chapters and reviewers (Holger Braunschweig, Warren E. Piers, Webster Santos, Kalman J. Szabó, Bertrand Carboni, R. Tom Baker, Jörg Pietruszka, Tom Sheppard, and Emmanuel Lacôte). We appreciate their efforts to complete the chapters and revisions on time and for all the constructive and positive comments we have received from them along this period of gestation of the entire book.

Tarragona, Spain
Durham, UK

Elena Fernández
Andrew Whiting

Contents

Boryl Anions	1
Makoto Yamashita and Kyoko Nozaki	
Fundamental and Applied Properties of Borocations	39
Michael J. Ingleson	
Asymmetric Catalytic Borylation of α,β-Unsaturated Acceptors	73
Sumin Lee and Jaesook Yun	
Reactions of Alkynylboron Compounds	93
Naoki Ishida and Masahiro Murakami	
Improving Transformations Through Organotrifluoroborates	117
Kaitlin M. Traister and Gary A. Molander	
The Catalytic Dehydrocoupling of Amine–Boranes and Phosphine–Boranes	153
Heather C. Johnson, Thomas N. Hooper, and Andrew S. Weller	
At the Forefront of the Suzuki–Miyaura Reaction: Advances in Stereoselective Cross-Couplings	221
Ho-Yan Sun and Dennis G. Hall	
Boronic Acid-Catalyzed Reactions of Carboxylic Acids	243
Kazuaki Ishihara	
Reagent-Controlled Lithiation–Borylation	271
Daniele Leonori and Varinder K. Aggarwal	
Recent Advances in the Synthesis and Applications of Organoborane Polymers	297
Frieder Jäkle	
Index	327

Boryl Anions

Makoto Yamashita and Kyoko Nozaki

Contents

1	Introduction: History of Boryl Anions Before 2006	2
2	Chemistry of Boryl Anions	3
2.1	Base-Stabilized Boryl Anions	4
2.2	<i>N</i> -Heterocyclic Boryl Anions	7
2.3	Boryl Anion Derivatives as a Counterpart of Carboanions	12
2.4	Base-Coordinated Diborane(4) as Boryl Anion Equivalents	18
3	Chemistry of Boryl–Transition Metal Complexes Derived from Boryl Anion	22
3.1	Boryl Complexes of Late Transition Metals (Groups 11–12)	23
3.2	Boryl Complexes of Early Transition Metals (Groups 3–5)	25
4	Chemistry of Boryl-Substituted Main Group Element Compounds Derived from Boryl Anions	27
4.1	Boryl-Substituted Group 13 Element Compounds	28
4.2	Boryl-Substituted Group 14 Element Compounds	31
4.3	Boryl-Substituted Group 15 Element Compounds	33
5	Summary and Outlook	33
	References	34

M. Yamashita (✉)

Department of Applied Chemistry, Chuo University, 1-13-27 Kasuga, Bunkyo-ku, Tokyo 112-8551, Japan

e-mail: makoto@oec.chem.chuo-u.ac.jp

K. Nozaki (✉)

Department of Chemistry and Biotechnology, The University of Tokyo, 7-3-1 Hongo, Bunkyo-ku, Tokyo 113-8656, Japan

e-mail: nozaki@chembio.t.u-tokyo.ac.jp

© Springer International Publishing Switzerland 2015

E. Fernández, A. Whiting (eds.), *Synthesis and Application of Organoboron Compounds*, Topics in Organometallic Chemistry 49,

DOI 10.1007/978-3-319-13054-5_1

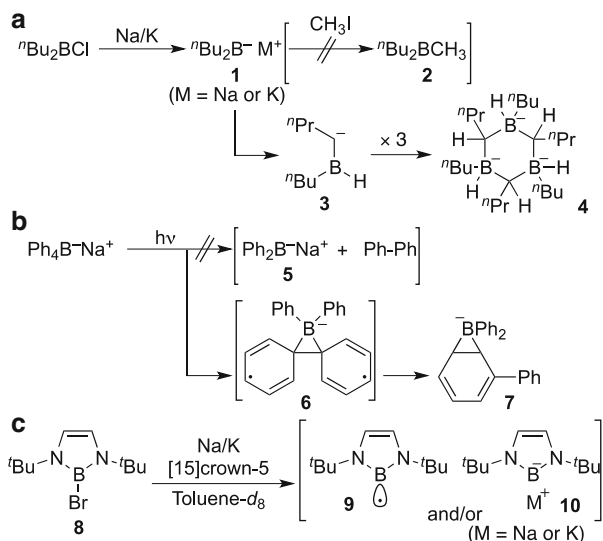
Abstract This chapter focuses on the chemistry of boryl anions. The first section gives a brief history of boryl anion before the first isolated boryl anion equivalent, boryllithium, emerged. Synthesis and properties of all existing boryl anions are summarized in the second section. In the third section, examples of boryl–transition metal complexes synthesized from boryl anion reagents are presented. The following fourth section describes chemistry of boryl-substituted main group element compounds made from boryl anions. At the end of this chapter, the authors provide a summary and their perspective for related fields.

Keywords Boryl anions • Boryl–transition metal complexes • Boryllithium • Boryl-substituted main group elements

1 Introduction: History of Boryl Anions Before 2006

Boron is a group 13 element in the second period, located on the left-hand side of carbon in the periodic table. Since atomic boron has three valence electrons, neutral boron molecules generally have six valence electrons and a vacant p-orbital on the boron center. This nature characterizes the chemistry of boron compounds as electron-deficient species in organic and inorganic chemistry fields. For example, the Lewis acidity of boron-containing compounds has been widely utilized for organic chemistry, such as hydroboration chemistry [1–3], Lewis-acidic boron-mediated chemistry [4], boron-enolate chemistry [5], and Suzuki–Miyaura cross-coupling chemistry [6–8]. To synthesize these types of boron-containing compounds, a boron-containing chemical bond should be constructed. In general, the existence of a vacant p-orbital of the boron atom in boron-containing reagents allows us to add nucleophiles to them to form a boron–nucleophile bond. However, there have been limited examples of “boryl anions,” which have a formal lone pair and nucleophilicity on the boron atom. In this chapter, the authors summarize the chemistry of boryl anions.

A parent boryl anion, $:\text{BH}_2^-$, was calculated to have a singlet ground state [9], in contrast to the case of the isoelectronic parent carbene, $:\text{CH}_2$, which has a triplet ground state [10]. The parent boryl anion could be thermodynamically stabilized by complexation with a lithium cation and by substitution of hydrogen atoms with electronegative nitrogen and oxygen atoms [9]. The latter stabilization could be explained by two factors: (1) σ -accepting character of electronegative nitrogen and oxygen atoms and (2) π -donation from the lone pairs of these heteroatoms. Further stabilization could be expected by the introduction of a boron-containing five-membered ring system [11, 12], as has been common to synthesize the isoelectronic *N*-heterocyclic carbenes (NHCs) [13]. Before the first achievement of the isolation of a boryl anion, as described in Sect. 2, the history of boryl anions should be noted here.

Scheme 1 Proposed boryl anions

The first experimental trial for the generation of boryl anion derivatives in the literature goes back to the early 1950s. Auten and Kraus reported the treatment of ${}^n\text{Bu}_2\text{BCl}$ with Na/K alloy followed by reaction with CH_3I to form ${}^n\text{Bu}_2\text{BCH}_3$ **2** (Scheme 1a) [14]. In this reaction, they assumed the formation of an anionic boron nucleophile ${}^n\text{Bu}_2\text{B}^- \text{M}^+$ (M=Na or K); however, no modern spectroscopic characterization was available for the methylated product and anionic intermediate. Later, Smith revealed that the reaction may proceed to form the boryl-stabilized carbanion **3** by a rapid intramolecular deprotonation of the resulting dibutylboryl anion **1**, followed by trimerization of **3** to give a cyclic six-membered ring tris (borate) **4** [15]. Diphenylboryl anion Ph_2B^- **5** was proposed as an intermediate in the photolysis of $\text{Ph}_4\text{B}^- \text{Na}^+$ according to the formation of biphenyl in 1967 (Scheme 1b) [16]. However, Shuster found that the exposure of $\text{Ph}_4\text{B}^- \text{Na}^+$ to light afforded a biradical species **6** which immediately rearranged to the cyclic three-membered ring borate **7**, followed by protonation to give biphenyl. Weber investigated the reduction of bromoborane **8** with Na/K alloy in toluene- d_8 , where they mentioned the formation of both the boryl radical **9** and boryl anion **10** during the reduction (Scheme 1c). However, no direct evidence for the formation of **10** was obtained.

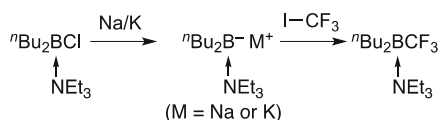
2 Chemistry of Boryl Anions

Prior to the report for the key compound, boryllithium, as an anionic boron nucleophile having a lone pair in an sp^2 orbital, several Lewis base-stabilized boryl anions and catalytically generated borylcopper species were reported having

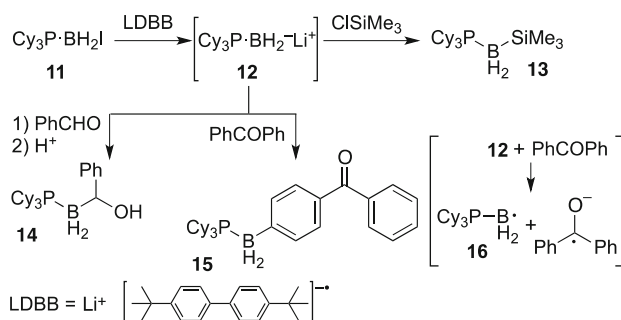
a negative charge or nucleophilicity on the boron center as judged by the structure of their resulting products. Together with earlier examples other than boryllithium, recent progress involving base-stabilized boryl anions is described in the following Sect. 2.1. The history and recent progress of borylcopper species are described as a member of the family of boryl anions in Sect. 2.4.

2.1 Base-Stabilized Boryl Anions

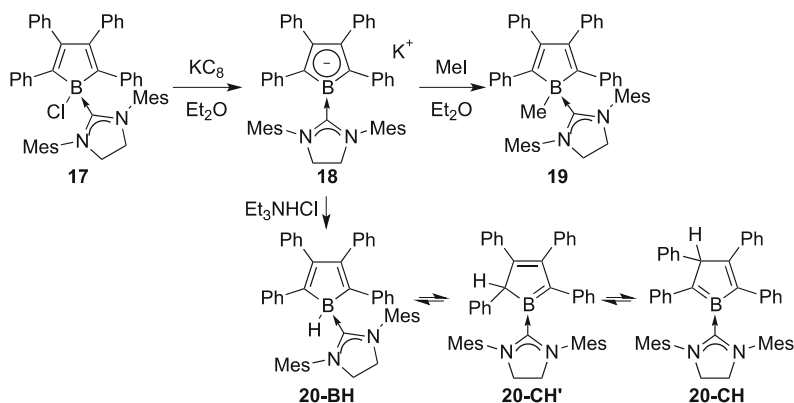
Since the boryl anion has a vacant p-orbital on the boron center, the coordination of a Lewis base leads to thermodynamic stabilization. In 1967, Parsons et al. reported that the reduction of $n\text{Bu}_2\text{BCl}$ with Na/K alloy in NEt_3 afforded the corresponding $\text{Et}_3\text{N}-n\text{Bu}_2\text{B}^-$ anion and subsequent reaction with CF_3I formed $\text{Et}_3\text{N}-n\text{Bu}_2\text{B}-\text{CF}_3$, though with no modern characterization [17] (Scheme 2). It should be noted, however, that the formation of the B-CF₃ bond may not originate from a simple nucleophilic attack on CF₃, because in case of a nucleophilic attack of a carbanion on CF₃I, reaction takes place on the iodine atom rather than the CF₃ carbon in order to avoid the steric and electronic repulsion between the nucleophile and three fluorine atoms of the CF₃ group [18]. Later, in early the 1990s, Schmidbauer and Imamoto independently reported the generation of $\text{Cy}_3\text{P}\cdot\text{BH}_2^-$ **12** by the reduction of $\text{Cy}_3\text{P}\cdot\text{BH}_2\text{I}$ **11** with LDBB (Scheme 3). They also reported a trapping experiment of the resulting anion $\text{Cy}_3\text{P}\cdot\text{BH}_2^-$ with ClSiMe_3 or benzaldehyde to form the corresponding substituted product **13** or adduct **14** by a boron nucleophile. In the case of the reaction of **12** with benzophenone, the *para*-borylated product **15** was



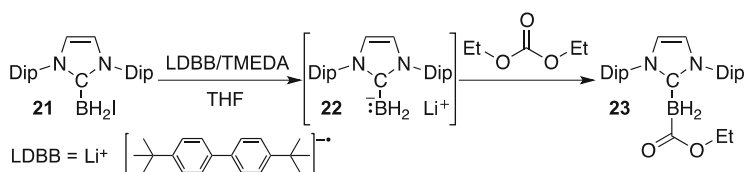
Scheme 2 The early report about NEt_3 -stabilized boryl anion and its trapping with CF_3I



Scheme 3 Generation of PCy_3 -stabilized boryl anion and its trapping experiment



Scheme 4 Synthesis of NHC-stabilized borole anion **18** and its reactivity toward MeI and proton (Mes = 2,4,6-Me₃C₆H₂)

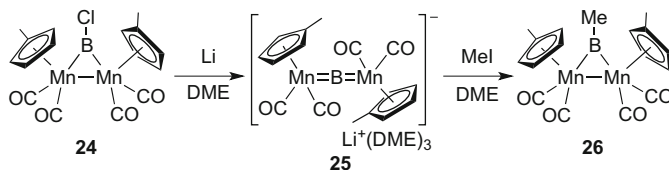


Scheme 5 Synthesis and nucleophilic reactivity of NHC-stabilized dihydroboryl anion **22** (Dip = 2,6-*t*-Pr₂C₆H₃)

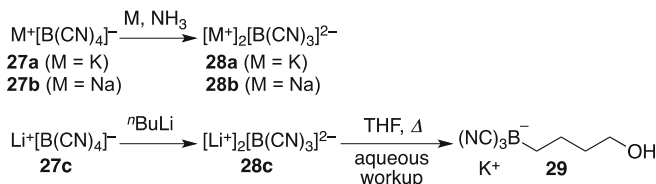
obtained. Imamoto proposed the possibility of a one-electron transfer process through the formation of a base-stabilized boryl radical **16**. Although all the products, **13–15**, were well characterized by modern spectroscopic techniques, no direct observation of the anionic intermediate **12** was reported.

Recently, Braunschweig reported that the reduction of NHC (*N*-heterocyclic carbene)-stabilized chloroborole **17** with KC₈ gave the corresponding NHC-stabilized borole anion **18** (Scheme 4) [19]. The key for stabilization of the borole anion could be attributed to delocalization of the lone-pair electrons on the boron center to the central carbon atom of the NHC. The resulting borole anion **18** has nucleophilicity on the boron center toward CH₃I allowing formation of a substituted product, methylborane **19**. The borole anion **18** also acts as a base upon the addition of Et₃NHCl to form the NHC-stabilized hydroborole **20-BH** [20]. Interestingly, a single crystal of isomeric **20-CH** could be obtained from the solution of **20-BH**. The formation of **20-CH** was explained by two subsequent [1, 5] sigmatropic rearrangement through **20-CH'**. In the reaction of **18** with R₃ECl (E=Sn, Pb; R=Me, Ph), a one-electron transfer reaction was confirmed, instead of direct nucleophilic attack of boron center on R₃ECl (see Sect. 4.2).

Curran and Lacôte recently reported that the NHC-stabilized iodoborane **21** could be reduced by LDBB to the NHC-stabilized dihydroboryl anion **22** (Scheme 5) [21]. The resulting boryl anion **22** could react with a variety of organic electrophiles, such as carbonate esters, carboxylate esters, aldehydes, epoxides,



Scheme 6 Synthesis and nucleophilic reactivity of anionic dimetalloborylene complex **25**



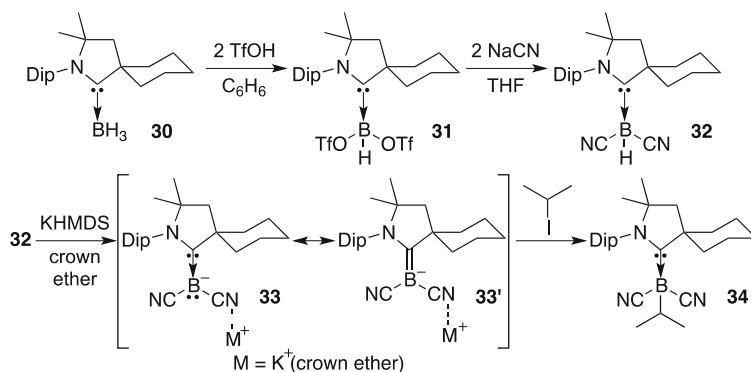
Scheme 7 Generation of base-stabilized boryl dianions and its reaction with THF

nitriles, alkyl and allylic halides, and C_6F_6 to give the corresponding substituted products and adducts. Although **22** was not isolated in a pure form, DFT calculations revealed effective delocalization of the lone pair on the anionic boron atom to the carbon atom of NHC, similar to the case of NHC-stabilized borole anion **18**.

Interaction between an anionic boron center and transition metal center was also shown to be effective to stabilize boryl anions. Braunschweig reported the reduction of bridging chloroborylene dimanganese complex **24** with metallic Li, affording a linear and anionic dimetalloborylene complex **25** as a $[\text{Li}(\text{DME})_3]^+$ salt (Scheme 6) [22]. Crystallographic analysis of **25** showed shortening of the B–Mn bond compared to those in **24**, indicating B=Mn double-bond character. The addition of methyl iodide to **25** gave B-methylated product **26** with a longer B–Mn bond length. The boron center in **25** also underwent boron–metal bond formation with group 10 and 11 metals (see Sect. 3.1).

Replacement of the Lewis base in the base-stabilized boryl anions described above with an anionic ligand produces dianionic sp^3 boryl anions. Bernhardt and Willner reported that the reduction of $\text{M}^+[\text{B}(\text{CN})_4]^-$ (**27a,b**, M=K, Na) with M/ NH_3 formed an alkali metal salt of the boryl dianion, $[\text{M}^+]_2[\text{B}(\text{CN})_3]^{2-}$ (**28a,b**), with a formal double negative charge on the boron center (Scheme 7) [23]. A lithium salt of the same dianion **28c** could be prepared from a similar precursor $\text{Li}^+[\text{B}(\text{CN})_4]^-$ (**27c**). This dianion reacted with THF to open the five-membered ring, indicating the nucleophilic character of the dianionic boron center in **28c**.

Changing of one cyanide in $[\text{B}(\text{CN})_3]^{2-}$ with a neutral ligand also resulted in the formation of a base-stabilized boryl anion. Bertrand reported replacement of two hydride ligands on CAAC [cyclic(amino)(alkyl)carbene]-coordinated BH_3 **30** with triflate ligands, followed by subsequent replacement with two cyanide ligands to afford CAAC-coordinated dicyanoborane **32** [24] (Scheme 8). Because of the strong π -acidity of the CAAC ligand and cyanides, the hydrogen atom on the boron center in **32** could be deprotonated by KHMDS in the presence of dibenzo-18-crown-6 to give



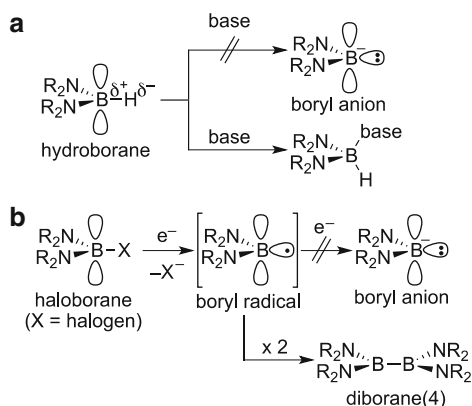
Scheme 8 Generation of base-stabilized boryl dianions and its reaction with THF

the CAAC-stabilized dicyanoboryl anion **33**. It is noteworthy that **33** was the first and the sole example of a boryl anion prepared by deprotonation so far. X-ray crystallographic analysis of the resulting anion **33** showed significant delocalization of anionic charge on the boron center to carbene center of CAAC (described as **33'**) and two cyanides having weak interactions between the nitrogen and potassium atoms [2.7884(15) Å]. Compound **33** reacted with 2-iodopropane to give the CAAC-coordinated isopropylborane **34**, which can be considered as a substituted product.

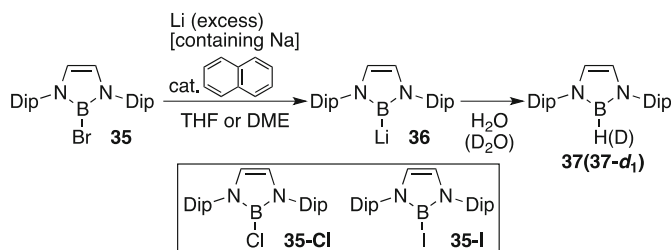
2.2 N-Heterocyclic Boryl Anions

Unlike the base-stabilized boryl anions discussed in Sect. 2.1, it would be expected that an sp²-boryl anion having a vacant p-orbital would have different properties. As described in Sect. 1, the introduction of an electronegative nitrogen atom having a lone pair and small lithium cation can stabilize boryl anions [9]. Considering the chemistry of carbanions, two possible synthetic routes would be expected for boryl anions. However, classically, two methodologies for the preparation of carbanions are not applicable for boryl anions (Scheme 9). Deprotonation of hydroboranes with base is usually difficult because of the negatively polarized hydrogen atom due to the lower electronegativity of the boron atom (Pauling, 2.04) [25] than that of the hydrogen atom (2.20) (Scheme 9a, top).¹ One can also expect the vacant p-orbital on the boron atom to accept a lone pair of the base to form a Lewis-acid–Lewis-base adduct as an undesired reaction (Scheme 9a, bottom). Reductive cleavage of the boron–halogen bond in haloboranes having small substituents with two electrons (Scheme 9b, top) is also not applicable because of the formation of diborane(4)

¹ Recently, Bertrand developed the deprotonation methodology to generate base-stabilized boryl anion **33** by using three strong π -acceptor ligands on the boron center (see the previous section).



Scheme 9 Two conceivable synthetic routes for the boryl anion



Scheme 10 Generation and trapping of boryllithium **36** from haloboranes **35**, **35-Cl**, and **35-I**

species having a B–B single bond via dimerization of the boryl radical intermediate (Scheme 9b, bottom).

In fact, the boryllithium **36** could be generated by a reduction of bromoborane **35** possessing a five-membered ring and bulky Dip groups with an excess of lithium (containing small amounts of sodium) in the presence of a catalytic amount of naphthalene in THF or DME (Scheme 10) [26]. By adjusting the conditions for the reduction, chloroborane **35-Cl** and iodoborane **35-I** could also be used as boron sources [27]. The reaction of a THF solution of **36** with water gave a protonated hydroborane **37**. In a control experiment with D₂O to form deuterioborane **37-d₁**, the hydrogen atom in **37** was confirmed to come from water, instead of the THF solvent. Similar five-membered ring boryllithiums **38–41** (Fig. 1), having a saturated C–C bond, benzoannulated diazaborole ring, and mesityl groups on the nitrogen atoms, could also be synthesized in the same manner as for **36**, where **41** was proven to be less thermally stable compared to **38–40** (see references for details). It is noteworthy that using sodium-incorporated lithium metal was proven to be important for generating the boryllithium efficiently, as reported by Liddle et al. [28], although the original report did not have such information.

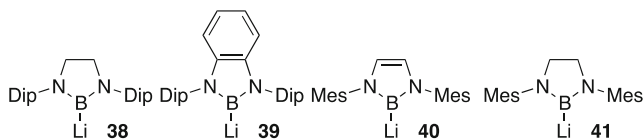


Fig. 1 Structurally varied boryllithiums **38–41**

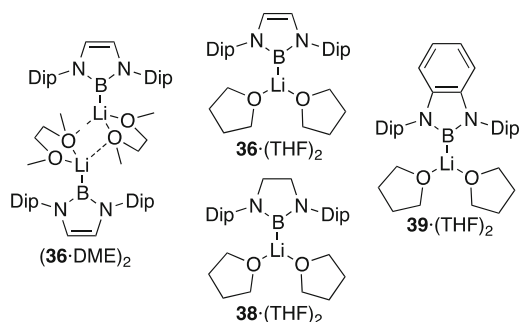


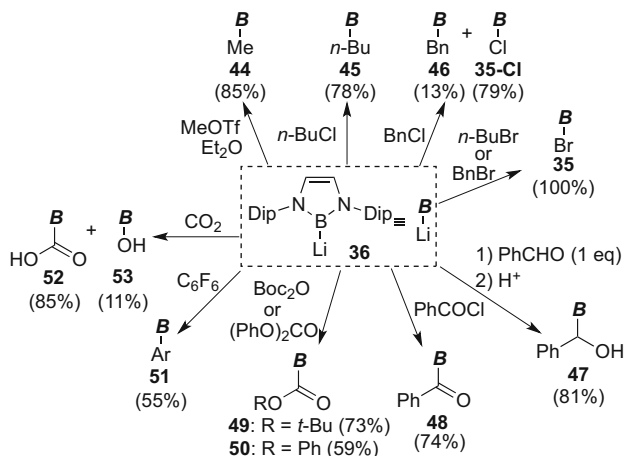
Fig. 2 Structurally characterized boryllithiums as solvate

Boryllithiums were isolated and characterized by using X-ray crystallography (Fig. 2). Currently, two solvents, THF and DME, are known to be incorporated into crystals [26, 27, 29]. In the case of boryllithium **36**, a DME-coordinated dimeric form ($\mathbf{36} \cdot \text{DME}$)₂ with bridging oxygen atoms and a THF-coordinated form $\mathbf{36} \cdot (\text{THF})_2$ with two THF molecules have been characterized. Two other boryllithiums, $\mathbf{38} \cdot (\text{THF})_2$ and $\mathbf{39} \cdot (\text{THF})_2$, were also structurally analyzed. The structural parameters of these boryllithiums were close to those obtained from DFT-calculated free boryl anions, rather than the corresponding hydroboranes, indicating that boryllithiums can be considered as boryl anions (see references for details).

To clarify the structure of boryllithium in solution, NMR spectroscopic studies were also performed. In the ¹H NMR spectrum of isolated crystalline ($\mathbf{36} \cdot \text{DME}$)₂ and $\mathbf{36} \cdot (\text{THF})_2$ in THF-*d*₈, the solvent molecules (which originally coordinated to the central lithium atom in the solid state) were observed in a free form in solution [DME (1 equiv.) or THF (2 equiv.) was detected], indicating that **36** forms the same THF-*d*₈ solvate. In the ¹¹B NMR spectrum of $\mathbf{36} \cdot (\text{THF})_2$, a broad signal was observed at δ_B 45.4 ppm (full width at half maximum, FWHM = 535 Hz). This signal shifted to lower field from that in hydroborane **37** (δ_B 22.9 ppm, FWHM = 379 Hz). This low-field shift was also observed for carbene **42** (δ_C 220.6 in C₆D₆) [30] in comparison with imidazolium salt **43** (δ_C 139.9 in DMSO-*d*₆) [27] (Fig. 3). Accordingly, the boron center in boryllithium can be considered to have a lone pair. In the ⁷Li NMR spectrum of $\mathbf{36} \cdot (\text{THF})_2$, a broad signal (δ_{Li} 0.46 ppm, FWHM = 36 Hz) was observed in contrast to that of LiCl in D₂O (FWHM = 1.2 Hz). The significant broadening may originate from the interaction between the lithium atom with the quadrupolar boron nucleus [31]. Although spin–



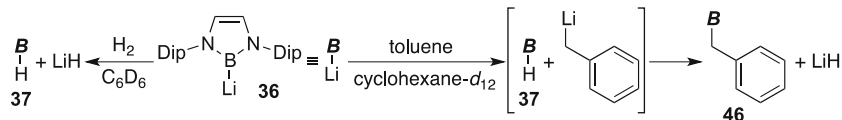
Fig. 3 Reference compounds



Scheme 11 Boryllithium **36** as nucleophile in reaction with various electrophiles

spin coupling among endocyclic atoms is theoretically predicted [32–34], it was difficult to observe this experimentally, probably due to broadening of signals.

Reactivity of boryllithiums toward electrophiles was systematically studied (Scheme 11). The reaction with MeOTf and n -BuCl gave the corresponding alkylborane derivatives **44** and **45**. In contrast, for the reaction with BnCl, the chlorinated product **35-Cl** formed as the major compound with small amount of benzylated product **46**, probably due to the halophilic attack of **36** on BnCl. Reaction with more reactive n -BuBr or BnBr afforded the bromoborane **35** as the sole product. Marder and Lin reported a DFT study to show that boryllithium could undergo halophilic attack on alkyl halides to form the haloborane and alkylolithium [35]. They also indicated that the slow subsequent nucleophilic substitution of the haloborane with alkylolithium would be the reason why the halogenated product was the major product. The reaction with 1 equiv. of PhCHO, followed by protonation, formed the α -borylbenzylalcohol **47** in 81% yield. The reaction with PhCOCl gave a substituted product, benzoylborane **48**, in good yield. The reaction with Boc₂O or (PhO)₂CO afforded borylcarboxylate ester products, **49** and **50**. Boryllithium **36** also reacted with C₆F₆ to afford a pentafluorophenylborane **51** in a moderate yield. Reaction with CO₂, followed by acidic workup, afforded the borylcarboxylic acid **52** and a small amount of hydroxyborane **53**. The formation of the latter compound was explained by a migration of the anionic oxygen atom in borylcarboxylate anion and elimination of CO. The nucleophilic reactivity of boryllithium **36** was also supported by DFT calculations [36].



Scheme 12 Boryllithium **36** as base in reaction with H_2 and toluene

Table 1 Structural parameters (\AA and $^\circ$); NPA charges of B, Li, and N atoms; and calculated ^{11}B NMR chemical shift (ppm) for calculated boryllithium **36** and related compounds

	opt-54	opt-36 · (THF) ₂	opt-36 · (THF) ₃	opt-37
B–Li	–	2.268	2.363	–
B–N	1.495	1.481	1.491 1.487	1.436
N–B–N	97.74	99.22	98.77	105.28
B	0.104	0.072	0.084	0.656
Li	–	0.755	0.768	–
N	–0.770	–0.728	–0.742 –0.739	–0.663
δ_{B}	51.3	41.4	56.9	19.6

Boryllithium **36** also reacted with H_2 and toluene, acting as a strong base (Scheme 12). Exposure of a C_6D_6 solution of **36** to dihydrogen afforded hydroborane **37** and LiH, as confirmed by complexation with $\text{B}(\text{C}_6\text{F}_5)_3$ to form soluble $\text{Li}[\text{HB}(\text{C}_6\text{F}_5)_3]$ [37]. A DFT study on this elementary reaction showed two types of interaction: one between the lone pair on the boron atom and σ^* orbital of the H–H bond and the other being between the σ orbital of the H–H bond and the Li cation. Furthermore, boryllithium **36** reacted with toluene to form benzylborane **46** with LiH, which was confirmed by IR spectroscopy. The formation of **46** could be explained by two consecutive steps, including deprotonation of toluene to form hydroborane **37** and benzyllithium and subsequent nucleophilic attack of benzyllithium to **37** to eliminate LiH. Thus, boryllithium **36** is basic enough to deprotonate H_2 and toluene.

DFT analysis of **36** revealed its bonding properties and solution structure. The structural parameters, NPA charges and calculated ^{11}B NMR chemical shifts (GIAO)² of opt-36 · (THF)₂ and opt-36 · (THF)₃ are summarized in Table 2–1, with two reference compounds, free boryl anion (opt-54) and hydroborane (opt-37). The structural parameters of calculated opt-36 · (THF)₂ are close to the

² Optimized B_2H_6 molecule at B3LYP/6-31 + G* was used as a reference (δ_{B} 16.6 ppm) for the ^{11}B NMR chemical shift (GIAO/B3LYP/6-311++G**). Chemical shift for B_2H_6 in gas phase was reported in the reference [38].

³ A structure with one THF molecule, opt-36 · (THF)₁, could not be optimized to the minimum. A four-membered bridging structure consists of $-(\text{Li}-\text{B})_2^-$, which corresponds to $-(\text{Li}-\text{C})_2^-$ structure observed for alkyl lithium species is less probable because of the bulky substituents on the boron center.

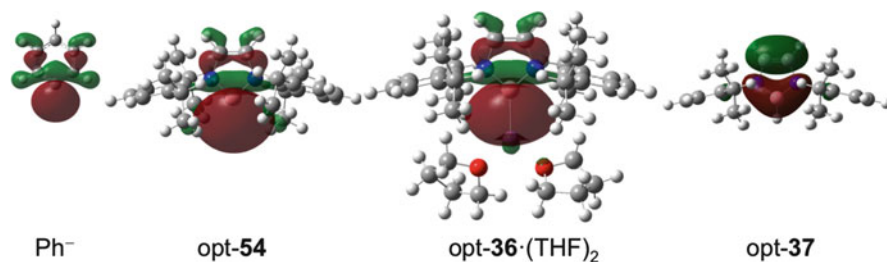
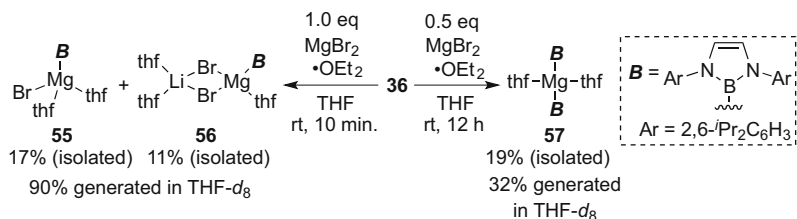


Fig. 4 HOMOs of boryllithium and reference compounds

experimental values obtained from crystallographic studies. The NPA charges showed that all the boryl anions adopted positively charged boron atom due to existence of electronegative nitrogen atoms as Schleyer et al. indicated the stabilization effect of nitrogen atoms [9]. Recent theoretical calculations also supported the stability of diazaborole-based boryl anions [39]. The calculated ^{11}B NMR chemical shift for $\text{opt-36} \cdot (\text{THF})_2$ (δ_{B} 41.4 ppm) was close to the two experimental values at 20°C (δ_{B} 45.4 ppm) and -100°C (δ_{B} 38.5 ppm). In contrast, the chemical shifts for the free anions, opt-54 (δ_{B} 51.3 ppm) and $\text{opt-36} \cdot (\text{THF})_3$ (δ_{B} 56.9 ppm), did not reproduce the experimental values. Thus, boryllithium **36** may exist as $\text{36} \cdot (\text{THF})_2$ in THF solution. The calculated HOMO of the crystallographically confirmed structure of $\text{opt-36} \cdot (\text{THF})_2$ seemed to be similar to those of Ph^- and the calculated free boryl anion opt-54 (Fig. 4), reflecting the lone-pair character of the central carbon and boron atom. Complexation of opt-54 with $\text{Li}(\text{THF})_2$ did not affect the shape of the HOMO, suggesting a polar character to the B–Li bond. On the other hand, the HOMO of hydroborane opt-37 corresponds to the π -orbital of the electron-rich boron-containing heterocycle. One can imagine that replacement of a hydrogen atom in hydroborane with lithium atom induces a localization of electrons at the anionic boron center with raising the orbital having the character of B–Li bonding to become HOMO [40], indicating a high reactivity of boryllithium as a nucleophile at the boron center. AIM analysis [41, 42] for the B–Li [43] bonds showed its polar character with small $\rho(r)$ values ($0.02889 e/a_0^3$) and positive $\nabla^2\rho(r)$ values ($0.08409 e/a_0^5$) much like the polar C–Li bonds of alkyllithiums (this result is consistent with that of the previously reported AIM analyses on non-solvated alkyllithiums having ionic C–Li bonds. See [44, 45]).

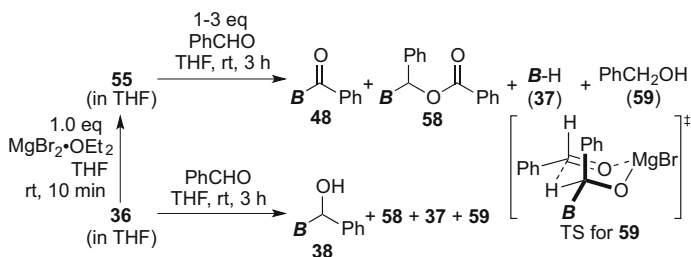
2.3 Boryl Anion Derivatives as a Counterpart of Carboanions

Considering of the rich chemistry of carbanions having C–Li, C–Mg, C–Cu, and C–Zn bonds, exploring the chemistry of the corresponding boryl anions would be expected to open up a wide area of chemistry. This section reviews chemistry of three boryl anions possessing Mg, Cu, and Zn as counter cations.



Scheme 13 Reaction of boryllithium **36** with $\text{MgBr}_2 \cdot \text{OEt}_2$ to generate borylmagnesium species

Table 2 Reactions of boryllithium **36** and borylmagnesium **55** with benzaldehyde



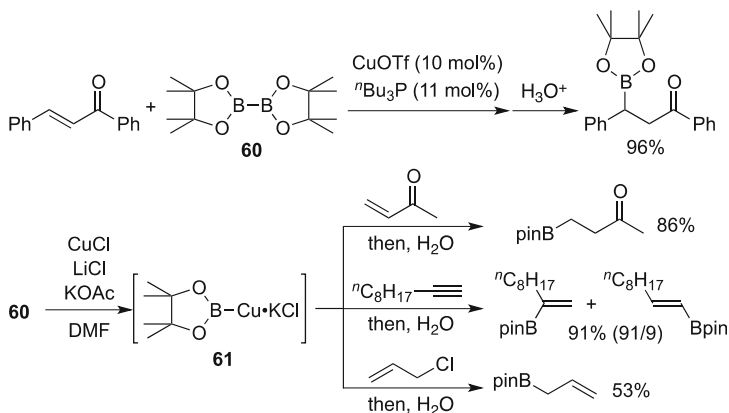
Run	Reactant	PhCHO (equiv.)	48 (%) ^a	58 (%) ^a	37 (%) ^a	59 (%) ^b	38 (%) ^a
1	55	1	18	18	56	27	0
2	55	2	34	24	32	47	0
3	55	3	22	40	16	55	0
4	36	1	0	0	6	0	81
5	36	3	0	51	10	50	0

^a¹H NMR yield

^bGC yield after quenching with HCl aq

Transmetalation of boryllithium with Mg salts can generate the corresponding borylmagnesium species, which can be considered as a boron derivative of a Grignard reagent [46]. In fact, treatment of **36** with 1 equiv. of $\text{MgBr}_2 \cdot \text{OEt}_2$ in THF afforded a solution containing a borylmagnesium species (Scheme 13). Recrystallization of the reaction solution gave two types of single crystals, consisting of colorless borylmagnesium bromide **55** and yellow borylmagnesium bromide-LiBr complex **56**, which could be characterized by X-ray crystallographic studies separately. Changing the stoichiometry of the Mg salt to 0.5 equiv. produced diborylmagnesium **57**, isolated as yellow crystals. All the structural parameters were similar to those of boryllithiums, indicating a strongly, polarized B–Mg bond. Dissolution of the isolated crystals **55** and **56** showed identical ¹H and ¹¹B NMR spectra. In the case of **56**, a ⁷Li NMR chemical shift was identical to that of LiBr in THF-*d*₈, showing that LiBr dissociates to convert **56** to **55** in THF-*d*₈ solution.

The reactivity of borylmagnesium bromide **55** with benzaldehyde was compared with that of boryllithium **36** (Table 2). Reactions of **55** afforded a mixture of

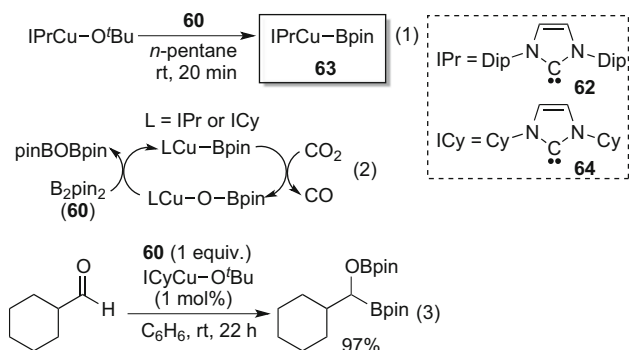


Scheme 14 The first example of copper-catalyzed β -borylation of α,β -unsaturated carbonyl compound using diborane(4) **60**

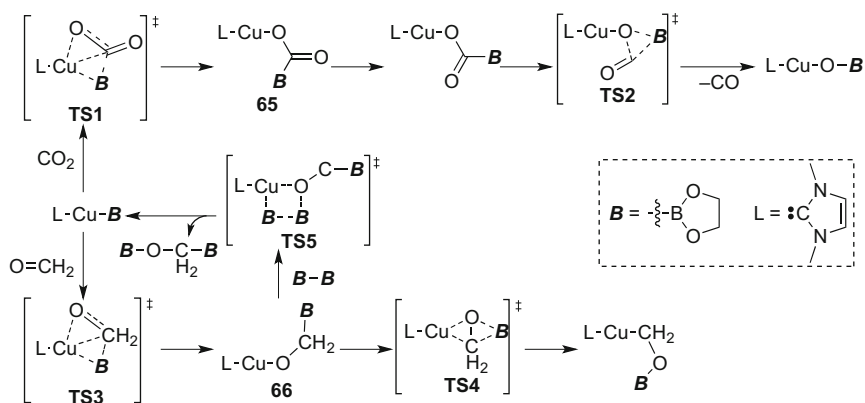
benzoylborane **48**, boron-substituted benzyl ester **58**, and hydroborane **37**. Concomitant formation of benzyl alcohol **59** indicated an intermolecular hydride transfer from a magnesium borylbenzyloxy intermediate to an excess amount of benzaldehyde via a six-membered ring transition state (see TS for **59**) in an Oppenauer oxidation fashion. It is noteworthy that no α -borylbenzylalcohol **38** was formed in the case of borylmagnesium, in sharp contrast to the fact that **38** was obtained in 81% yield by a reaction of boryllithium **36** with 1 equiv. of benzaldehyde (run 4). The addition of a second equivalent of benzaldehyde to **38** also led to an intermolecular hydride transfer to form **58** (run 5). Thus, the counter metal cation affects the reactivity of the α -borylbenzyloxy intermediate.

In the history of boryl anions, borylcopper species having a B–Cu bond is one of the most important species from the viewpoint of synthetic organic chemistry. In 2000, Cu-catalyzed β -borylation of α,β -unsaturated ketones using B_2pin_2 **60** [bis(pinacolato)diborane(4)] has been reported by Ito and Hosomi (Scheme 14, top) [47]. Later, Miyaura and Ishiyama suggested that mixing **60** and CuCl in the presence of LiCl and KOAc gave a borylcopper species **61**, which could undergo the β -borylation of α,β -unsaturated carbonyls, monoborylation of alkynes, and substitution of allyl chloride (Scheme 14, bottom) [48, 49]. After these discoveries, there have been many reports about catalytic borylation reactions involving a borylcopper species as the key intermediate. There have been some review articles on this area, and Lee and Yun [50] of this book also summarize this work [51–53].

Although these copper-catalyzed borylation reactions do not involve an isolation of borylcopper species, Sadighi et al. reported an isolation of $IPrCuBpin$ **63** by a reaction of $IPrCu(O^tBu)$ with diborane(4) **60** (Scheme 15, Eq. 1) [54]. The combination of $Cu(O^tBu)$ complex possessing carbene ligand **64** with **60** could construct active catalyst systems for the reduction of CO_2 to CO (Eq. 2) and 1,2-diboration of aldehydes (Eq. 3) [54, 55]. In the former case, stoichiometric reactions of **63** with CO_2 or benzaldehyde afforded no insertion products which should have metal–oxygen and boron–carbon



Scheme 15 The first example of copper-catalyzed β -borylation of α,β -unsaturated carbonyl compound using diborane(4) **60**

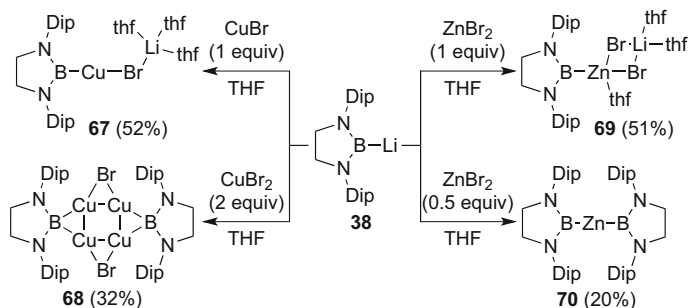


Scheme 16 Calculated reaction pathway for carbonyl insertion to borylcopper species

bonds. Theoretical calculations on the mechanisms of these reactions revealed that the carbonyl-inserted products **65** and **66** easily isomerized or underwent σ -bond metathesis in the presence of diborane(4) reagent to make a boron–oxygen bond and to regenerate the borylcopper species (Scheme 16) [56, 57].

Transmetalation of boryllithium with a copper salt was also effective for forming borylcopper species [58]. A simple mixing of boryllithium **38** with CuBr gave borylcopper products (Scheme 17). In the case of the reaction with 1 equiv. of CuBr, lithium borylbromocuprate **67** could be isolated. The first borylcuprate **67** was crystallographically characterized to show the existence of a B–Cu–Br–Li chain with three THF molecules coordinating to the lithium atom.⁴ Changing the

⁴Two carbyl(halo)cuprates, $[\text{Li}(12\text{-c-4})_2][\text{Cu}(\text{Br})\text{CH}(\text{SiMe}_3)_3]$ [59] and $(\text{Et}_2\text{O})_2\text{Li}[\text{ICuC}_6\text{H}_3\text{-2,6-(2,4,6-}(i\text{-Pr})_3\text{C}_6\text{H}_2)_2]$ [60], were reported to have linear C–Cu–X–Li structure, being similar to that of **67**.



Scheme 17 Calculated reaction pathway for carbonyl insertion to borylcopper species

stoichiometry of the CuBr to 2 equiv. afforded a tetranuclear copper species **68** having two bridging bromides and two bridging boryl ligands. The crystal structure of **68** showed each of the two bromine atoms and two boron atoms bridging two Cu atoms in an alternating fashion.⁵ The longer B–Cu bond lengths in **68** [2.093(4) and 2.073(5) Å] compared to the 2-center-2-electron B–Cu bond lengths [1.983 Å (av.)] in **67** may reflect a bridging situation of the boryl ligand, as were observed for other bridging boryl complexes [62–64].⁶

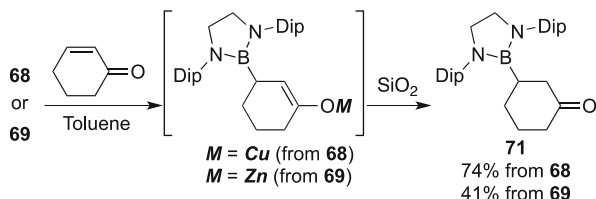
The addition of ZnBr_2 (1 equiv.) to **38** gave lithium dibromoborylzincate **69** as the first example containing a 2-center-2-electron B–Zn bond [B–Zn = 2.075(5) Å]. The related lithium alkyldibromozincate, [(PhNMe) Me_2Si](Me_3Si) $_2\text{C}$ –Zn(μ^2 -Br) $_2\text{Li}$ (thf) $_2$, has also been structurally characterized with C–Zn bond of 2.014(5) Å, being similar to the sum of covalent radii (2.02 Å) of carbon and zinc atoms [65].⁷ A reaction of **38** with 0.5 equiv. of ZnBr_2 afforded a solvent-free diborylzinc species **70** possessing a linear B–Zn–B angle. The linear structure of **70** is in contrast to that of diphenylzinc, which has a dimeric structure containing C–Zn–C–Zn core with bridging phenyl ligands [66]. Recently, Uchiyama reported the generation of related borylzincate species by mixing **60**, Et_2Zn , and $t\text{BuONa}$, although the borylzincate species was not directly observed [67].

The reactivity of isolated borylcopper **68** and borylzincate **69** toward α,β -unsaturated ketones was examined (Scheme 18). The reaction of **68** or **69** with 2-cyclohexen-1-one gave the corresponding conjugate addition product, 3-borylcyclohexan-1-one **71** in 74 and 41% yield after hydrolysis.

⁵In contrast to **68**, a related tetranuclear copper complex possessing two aryl groups and two bromides has been structurally characterized where two bridging bromide shared one copper atom of Cu_4 core [61].

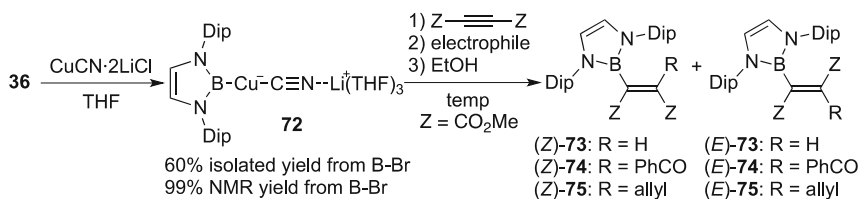
⁶For the previously reported examples for multinuclear transition metal complexes having a bridging boryl ligand, see [62–64].

⁷The Zn–(μ^2 -Br) bonds [2.504 Å (av.)] in **69** were longer than those in **70** [2.4217 Å (av.)], probably due to the coordination of THF molecules toward zinc atom in **69**.



Scheme 18 Conjugate addition of borylcopper and borylzinc species

Table 3 Preparation of lithium borylcyanozincate **72** and its application for carboboration of DEAD



Entry	Electrophile	Temp (°C)	Products (yield ^a)	Syn/anti
1	PhCOCl	-78	(Z)- 73 (48%), (E)- 73 (32%)	60/40
2	PhCOCl	RT	(E)- 74 (71%)	1/99>
3	allylBr	-78	(Z)- 75 (93%)	99>/1
4	allylBr	RT	(Z)- 75 (36%), (E)- 75 (60%)	38/62

^aIsolated yield based on the added DEAD

The regioselectivity of the addition is the same as those for the organo-cuprates, organo-zincates, and transient borylcopper species.

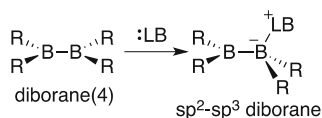
Transmetalation of boryllithium with copper cyanide was also effective to prepare borylcyanozincate **72** (Table 3) [68, 69]. X-ray crystallographic analysis revealed a monomeric linear structure of B–Cu–C≡N–Li linkage in **72** with three THF molecules coordinating to the lithium atom. Reaction of in situ-generated **72** with DEAD (diethyl acetylenedicarboxylate), followed by treatment with benzoyl chloride or allyl bromide at -78 °C or room temperature, gave carboborated, tetrasubstituted alkenylborane products (Table 3). At low temperature, reaction with benzoyl chloride followed by protic quenching afforded a mixture of *syn*- and *anti*-hydroborated products, (Z)-**73** and (E)-**73**, in 48 and 32% yields (entry 1), indicating that the boryl-substituted alkenylcuprate intermediate did not react with benzoyl chloride at -78 °C. Reaction at room temperature afforded the *anti*-product (E)-**74** in 71% yield with a selectivity of *syn/anti*=1/>99 (entry 2). Changing the electrophile to allyl bromide, at -78 °C, gave the *syn*-product (Z)-**75** in 93% yield, accompanied by a trace amount of the *anti*-product (E)-**75** (entry 3). By elevating the temperature to room temperature, a mixture of (Z)-**75** and (E)-

75 was obtained in 36 and 60% yield (entry 4). Thus, the selectivity for carboborated products could be affected by the reaction temperature.

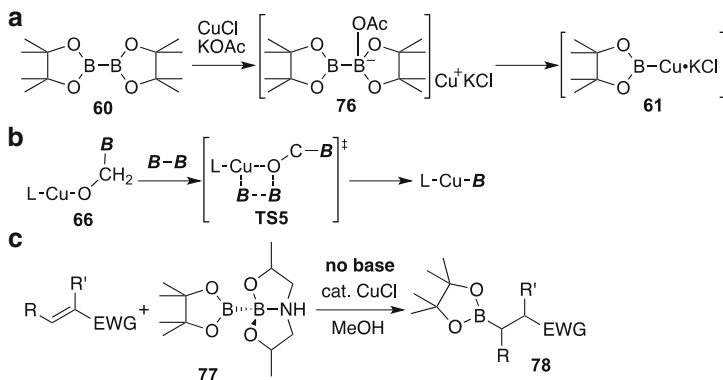
2.4 Base-Coordinated Diborane(4) as Boryl Anion Equivalents

In general, Lewis-acidic sp^2 boron compounds can accept a Lewis base to form an sp^3 Lewis-acid–Lewis-base adduct. In the case of a diborane(4) compound having a B–B single bond, coordination of a Lewis base would be expected to form sp^2 – sp^3 diborane compounds (Scheme 19). Several experimental reports for the formation of sp^2 – sp^3 diborane compounds showed lengthening of the B–B single bond upon coordination of a Lewis base [70–74]. This lengthening may lead to weakening of the B–B bond.

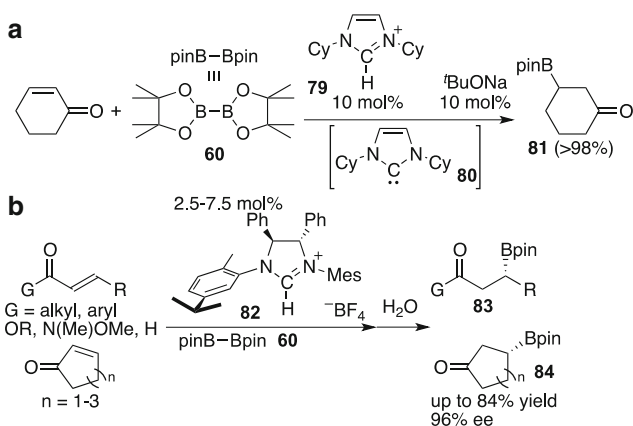
Considering the pathway for generation of borylcopper species **61** from B_2pin_2 **60**, copper salt and additional Lewis base, as described in the previous section (Scheme 14) [49], one can imagine that the transmetalation of a “boryl anion” equivalent to a copper(I) cation from an sp^2 – sp^3 diborane **76** would take place (Scheme 20a). DFT calculations on the copper-catalyzed 1,2-diboration of aldehydes with diborane(4) by Marder and Lin portrayed a picture of a transition state **TS5** for σ -bond metathesis from copper alkoxide **66** and diborane(4), which can be considered as an intermolecular transmetalation of a “boryl anion,” to regenerate a



Scheme 19 Addition of Lewis base to diborane(4) to form sp^2 – sp^3 diborane



Scheme 20 Previous examples indicating the transfer of a “boryl anion” from an sp^2 – sp^3 diborane

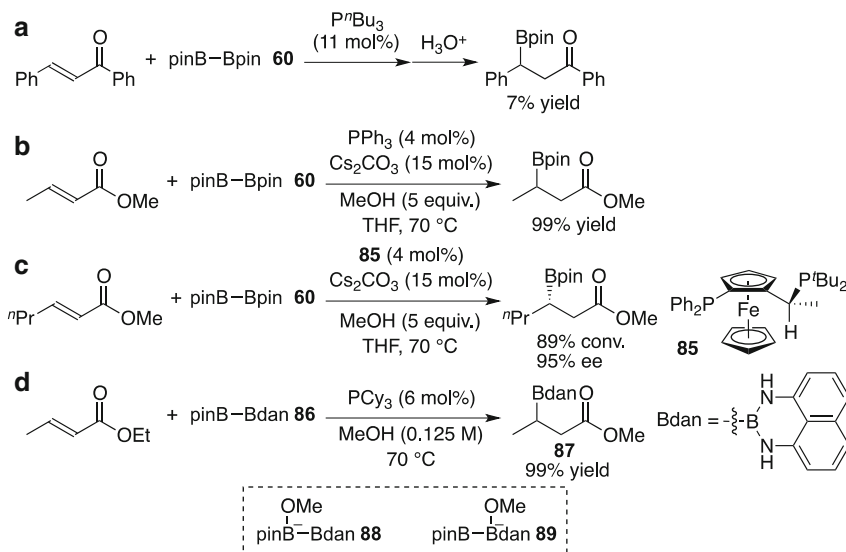


Scheme 21 NHC-catalyzed β -borylation

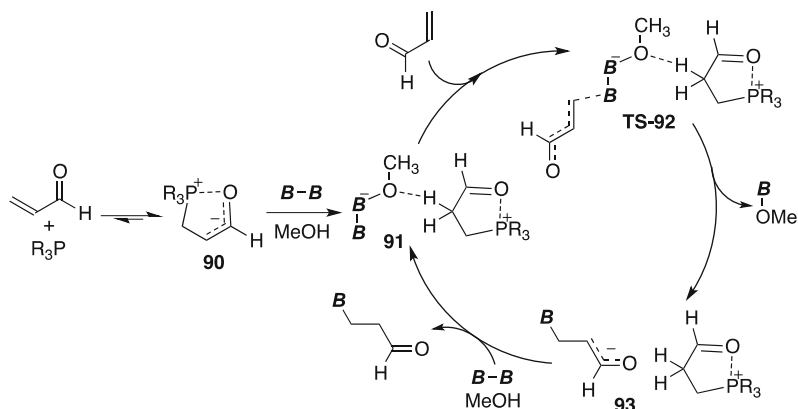
borylcopper species (Scheme 20b) [56, 57, 75]. Recently, Santos reported the copper-catalyzed reaction of electron-deficient alkenes and an isolated sp^2 - sp^3 diborane **77** in the absence of additional base to afford the β -borylated product **78** (Scheme 20c) [76–78]. These three results implicate that the formation of an sp^2 - sp^3 diborane species induces transfer of a “boryl anion.”

The transfer of a “boryl anion” from B_2pin_2 **60** was also achieved by using an *N*-heterocyclic carbene (NHC) as a nucleophilic catalyst by Hoveyda [79–81]. Mixing cyclohexenone and **60** in the presence of a catalytic amount of cyclohexyl-substituted imidazolium salt **79** and ^tBuONa afforded the conjugate adduct **81** in good yield (Scheme 21a). In the reaction solution, NHC **80** may be generated, and **80** was found to be in equilibrium between coordination and dissociation to **60** [82]. The NHC-catalyzed borylation system was successfully expanded to the asymmetric version by using a chiral imidazolium precursor **82** (Scheme 21b).

A phosphine-based simple system for “boryl anion” transfer was also discovered by Fernández (Scheme 22). Some key review papers described this type of “boryl anion” transfer [83, 84]. Inspired by that, the first report for the copper-catalyzed β -borylation reaction of α,β -unsaturated carbonyls by Ito and Hosomi has an entry with low product yield using the sole additive of P^tBu_3 (Scheme 22a). They found that the existence of both methanol and cesium carbonate was best to achieve high yields of the conjugate adducts (Scheme 22b) [85]. Furthermore, they also succeeded in disclosing that Josiphos-type ligand **85** was effective for enantioselective β -boration without a transition metal catalyst (Scheme 22c). This catalytic system was also effective for an unsymmetrical diborane pinB-Bdan **86** to give β -borated product **87** by transfer of the Bdan moiety (Scheme 22d) [86], which was originally developed as a masked boronic acid by Suginome group [87–89]. This characteristic transformation may result from a selective complexation of **86** and methoxide to form sp^2 - sp^3 diborane **88** over **89**. DFT calculations on this catalytic reaction provided an interesting pathway involving phosphine in the catalytic cycle (Scheme 23) [90]. The key role of the phosphine could be attributed to the formation of a phosphonium enolate intermediate **90**. The interaction of **90** with MeOH and



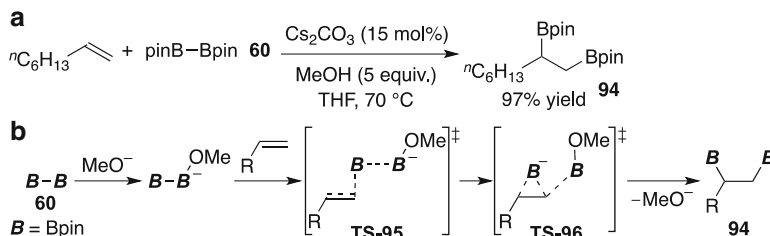
Scheme 22 Phosphine-based catalyst system for β -borylation



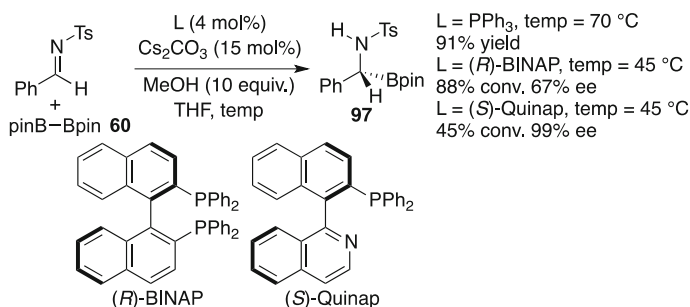
Scheme 23 DFT-based catalytic cycle for β -borylation with the role of the phosphine additive

B_2pin_2 afforded an ion pair **91** consisting of an sp^2 - sp^3 anionic diboron and carbonyl-stabilized phosphonium species. The resulting ion pair **91** could transfer a “boryl anion” to another α,β -unsaturated carbonyl compound through **TS-92** to give another ion pair **93**. Trapping a proton from MeOH by the anionic moiety of **93** liberated the β -borylated product and regenerated the ion pair **91**.

The same research group also found that the removal of the phosphine additive from the previous system led to a “boryl anion” transfer to alkenes and allenes [91]. The treatment of B_2pin_2 with an alkene or allene in the presence of cesium carbonate and methanol in THF gave the corresponding diborylalkane **94**



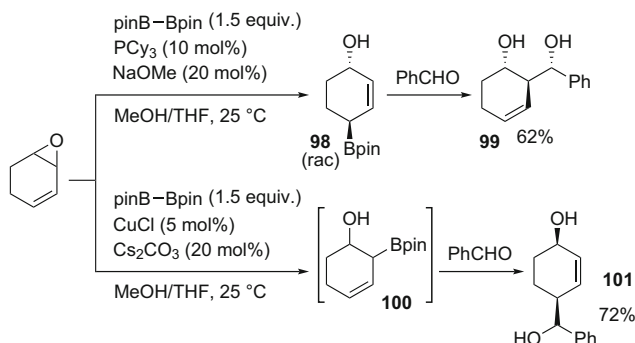
Scheme 24 Diboration of alkenes with simple base catalyst



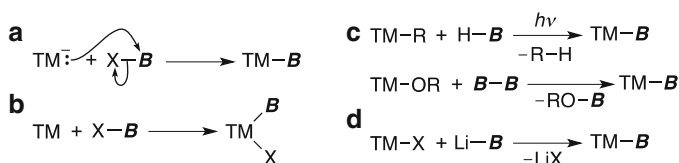
Scheme 25 Enantioselective boration of aldimines

(Scheme 24a). They also analyzed the reaction mechanism by using DFT calculations to show that the Bpin group was transferred from the $\text{sp}^2\text{-sp}^3$ diborane to alkene through **TS-95** and the subsequent cyclic-borate-like **TS-96** to make two B–C bonds in **94** (Scheme 24b).

Fernández also showed the phosphine-based system was applicable to the 1,2-addition of a boryl group to *N*-tosylaldimines to give α -borylamine products (Scheme 25). In the case of using PPh₃, the product was obtained in 91% yield. Changing the phosphine to (*R*)-BINAP led to the formation of the same product with 67% ee at 88% conversion. Using (*S*)-Quinap gave a better enantioselectivity of the same product with 45% conversion [92]. The present catalyst system was also active for borylative ring-opening reactions of alkenyl-substituted epoxides and *N*-tosylaziridines (Scheme 26) [93]. Reaction of 3,4-epoxy-1-cyclohexene with B₂pin₂ **60** under the same phosphorus-based catalyst system gave an S_N2'-type ring-opened allylboronate **98** (racemic mixture). The subsequent treatment of **98** with benzaldehyde formed the allylic alcohol product **99**, showing the *trans*-configuration of the two substituents on the cyclohexene ring. In sharp contrast, copper-based catalytic boration conditions for the same substrate induced boration reaction at the 3-position through a direct ring opening by the “boryl anion” to give the 3,4-disubstituted cyclohexene derivative **100**. After treatment of **100** with benzaldehyde, the isomeric allylic alcohol **101** was obtained to confirm a similar relationship between the two substituents. It should be noted that the exact mechanism



Scheme 26 Borylative ring opening of alkenyl-substituted epoxide and aziridine



Scheme 27 Conventional methods (a–c) to synthesize boryl–transition metal complexes and a new method (d), based on the nucleophilic character of boryllithium

for these transformations is still unclear. Clarifying the role of the phosphine in the mechanism would also be desirable for the future development of the field.

3 Chemistry of Boryl–Transition Metal Complexes Derived from Boryl Anion

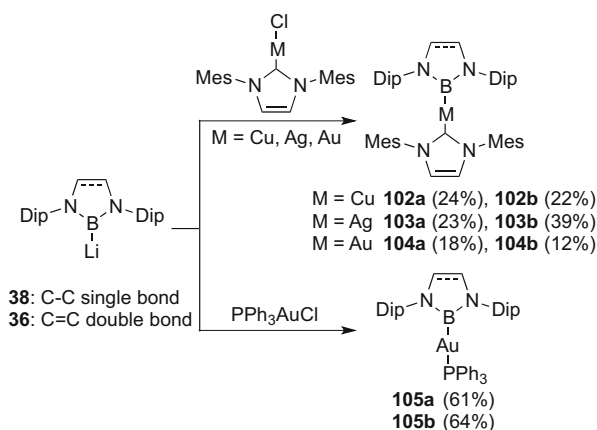
Boryl–transition metal complexes are defined as species possessing 2-center-2-electron boron–transition metal bonds [94–98]. From the viewpoint of synthetic inorganic chemistry, preparative methods for boryl–transition metal complexes are generally limited to the following three methods (Scheme 27): (1) salt elimination reaction through a reaction of nucleophilic anionic metal carbonyls with haloborane;⁸ (2) oxidative addition of boron–hydride, boron–boron, and boron–

⁸ See [99] for the first example of boryl complex synthesized by a salt elimination and see [100] for the first structurally characterized boryl complex made by a salt elimination.

halide bonds to transition metals having low-oxidation states;⁹ and (3) σ -bond metathesis between alkylmetal complexes and hydroborane under the irradiation of light [103] or between oxygen-substituted metal complexes and diborane [49, 54, 104]. Nucleophilic borylation with boryl anions would be a fourth method for the synthesis of boryl–transition metal complexes.

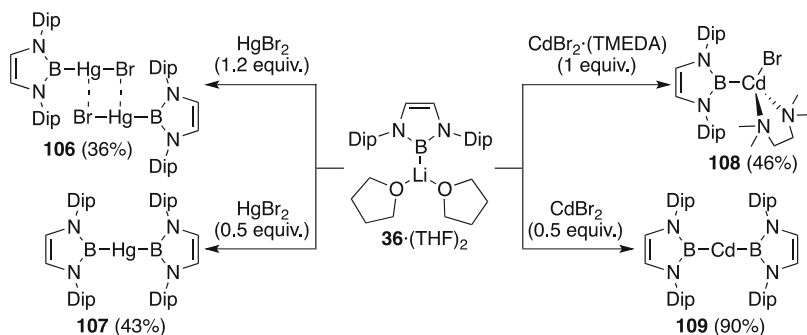
3.1 Boryl Complexes of Late Transition Metals (Groups 11–12)

Some borylcopper species acting as nucleophilic boryl anions were reported as described in Sect. 2.3; therefore, the remaining examples of borylcopper species prepared from boryl anions are shown here. Just after the first report of boryllithium formation, we showed in situ-generated **38** and **36** could be utilized as a source of a boryl ligand on group 11 metal complexes **102–105a, b** (Scheme 28: **a**, C–C single bond in the five-membered ring; **b**, C–C double bond in the five-membered ring) [105]. This result involves the first example of borylsilver and borylgold complexes having 2-center-2-electron B–Ag and B–Au bonds. From the structural and spectroscopic features of the resulting complexes, we can conclude that the boryl ligands have a strong *trans*-influence as a previous theoretical study had indicated [106]. Recently, Aldridge reported reactions of isolated boryllithium–THF solvate with mercury and cadmium bromide to give the corresponding borylmercury and

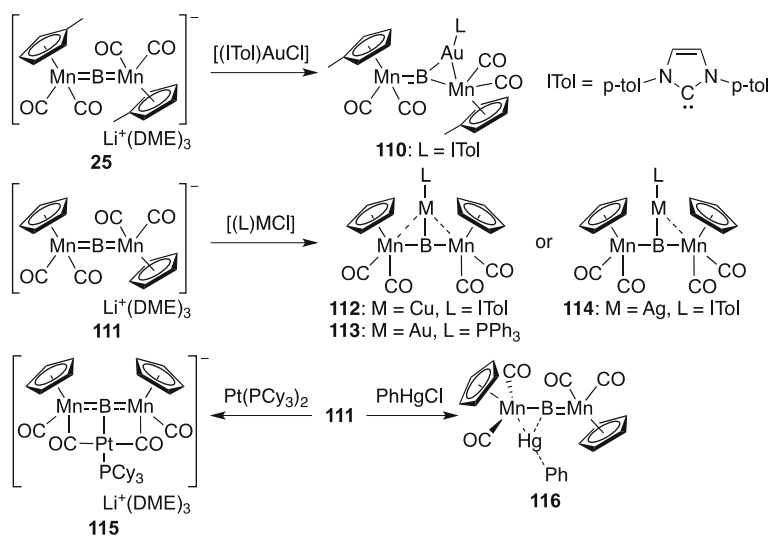


Scheme 28 Synthesis of group 11 boryl–metal complexes having (a) saturated and (b) unsaturated C–C bond from boryllithium **38** or **36**

⁹ See [101] for the first example of boryl complex synthesized by oxidative addition and see [102] for the first structurally characterized boryl complex made by oxidative addition.



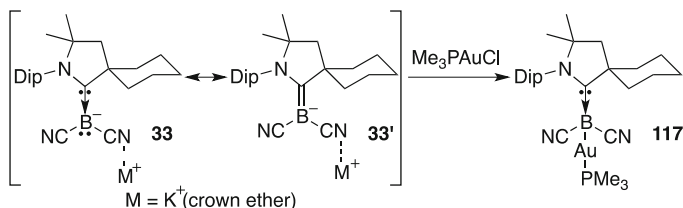
Scheme 29 Synthesis of group 12 boryl–metal complexes using isolated boryllithium **36**·(THF)₂



Scheme 30 Synthesis of group 11 and 12 boryl–metal complexes using anionic dimetalloborylene complexes

borylcadmium species **106–109** (Scheme 29) [107]. The resulting complexes could be considered as the first examples of 2-center-2-electron B–Hg and B–Cd bonds. Borylmercury bromide **106** assembles as a dimeric structure through weak interactions between mercury and bromide, keeping linearity of the B–Hg–Br bond [169.0(1)°], while the structure of borylcadmium bromide **108** was not reported. Linear structures for **107** [B–Hg–B=179.0(1)°] and **109** [B–Cd–B=177.5(1)°] seem to be similar to that of the diborylzinc species [B–Zn–B=178.5(1)°] as we reported [58].

The reported anionic dimetalloborylene complex **25** and its derivative **111** reacts with group 11 and 12 metal halides to give a series of the trimetallic boride complexes (Scheme 30) [108–110]. The formation of these complexes could



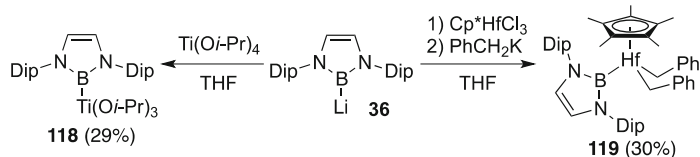
Scheme 31 Synthesis of gold complex **117** from CAAC-stabilized boryl anion **33** generated by deprotonation

be explained by nucleophilic attack of the boron atom in the starting complexes on the metal halide. In the solid-state structure of **110**, the two Mn–B bonds [1.871(3) Å and 1.964(3) Å] were inequivalent. The gold atom in **110** is closer to one of two Mn atoms, resulting in a triangular arrangement, as illustrated. Reaction of **111** with LMX complexes took place to afford the corresponding copper, gold, and silver complexes **112–114**. Among them, silver boride complex **114** showed a similar triangular structure like **110**. On the contrary, copper and gold atoms in **112** and **113** were located in similar positions and with similar distances to the two Mn atoms to form two triangular arrangements. DFT analysis of these complexes showed some characteristic features, such as a positive charge on the boron center. The same reaction of **111** with a Pt(0) precursor also gave the B–Pt complex **115**, but we should consider the central boron atom in **111** as being electrophilic, in this case, because the oxidation state of Pt could be two in **115**. The introduction of mercury could be achieved by a similar simple reaction of **111** with PhHgCl to form mercury-bridging **116**. Although the Mn–Hg–C(ipso) angle was close to linearity (165.3°), the mercury and boron atoms were interacting with each other as confirmed by sharpening the signal in the $^{119}\text{Hg}\{^{11}\text{B}\}$ NMR spectrum upon ^{11}B decoupling.

In a similar manner to simple nucleophilic borylation, Bertrand reported the complexation of their CAAC-stabilized boryl anion **33** with gold to form a base-stabilized borylgold complex **117** (Scheme 31) [24]. Lengthening of the B–CN bond [1.553(2) and 1.552(2) Å for **33** and 1.544 Å for **117**] was observed upon complexation because of the delocalized electrons in **33** used for coordination to the gold in **117**.

3.2 Boryl Complexes of Early Transition Metals (Groups 3–5)

In addition to the reason why the preparative methodology of boryl complex is limited, as described in Scheme 27, additional difficulty could be expected for boryl complexes of early transition metals due to the following reasons: (a) anionic early transition metal complexes have no nucleophilicity at the metal center due to the d^0



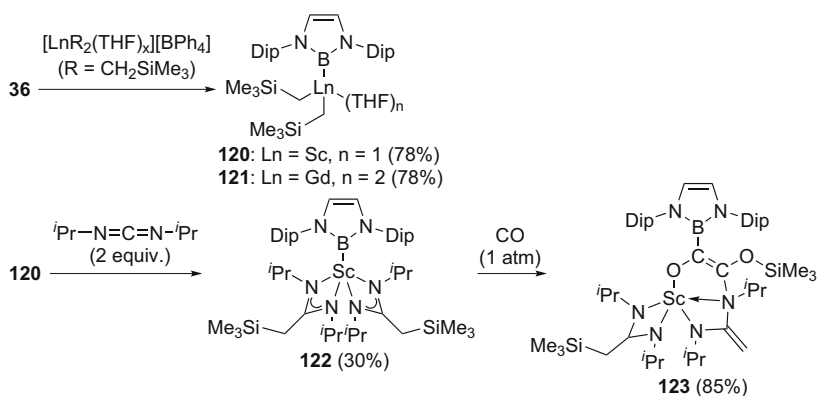
Scheme 32 Synthesis of group 4 boryl complexes **118** and **119** using boryllithium **36**

electron configuration; (b) low-valent early transition metal complexes are not easily available as precursors; and (c) a Lewis-acidic boron reagent may abstract an anionic ligand from early transition metal complexes to form a borate complex rather than σ -bond metathesis. Therefore, nucleophilic substitution by boryl anions may be a sole method to prepare boryl complexes of early transition metals. This section shows examples of boryl complexes of early transition metals formed by using boryl anions.

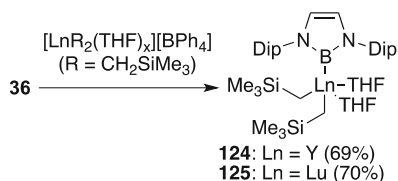
A reaction of boryllithium **36** with $\text{Ti}(\text{O}i\text{-Pr})_4$ gave **118** through an elimination of isopropoxide (Scheme 32) [111]. Additionally, a sequential reaction of **36** with Cp^*HfCl_3 and benzylpotassium afforded **119**. Both complexes **118** and **119** are the first examples of group 4 boryl–metal complexes. Crystallographic analysis revealed a distorted tetrahedral structure of **118** and a typical three-leg piano stool structure of **119**. Both B–M bonds in **118** and **119** are slightly longer than the sum of covalent radii of each of the atoms. Remarkably short Ti–O bonds (av. 1.758 Å) and large Ti–O–C angles (av. 164.9°) in **118** reflect $\pi\text{p}–\text{d}\pi$ interactions between the titanium and oxygen atoms. Two Hf–benzylic carbon bonds (av. 2.219 Å) and five Hf–C(Cp^*) bonds (av. 2.494 Å) in **119** are similar to those observed in conventional Cp^*Hf –alkyl complexes. The hafnium complex **119** was shown to be utilized as a catalyst precursor for polymerization of ethylene and 1-hexene.

Following the above report, Hou reported preparation of scandium and gadolinium boryl complexes **120** and **121** by the same method using boryllithium **36** (Scheme 33) [112]. X-ray crystallographic analysis showed these complexes had tetrahedral and distorted square pyramidal structures. The borylscandium complex **120** reacted with 2 equiv. of N,N' -diisopropylcarbodiimide to give square pyramidal bis(amidato)borylscandium complex **122** through the insertion of carbodiimide into the Sc–C bond. This result indicated that the Me_3SiCH_2 ligand was more reactive than the boryl ligand toward carbodiimide. Subsequently, the complex **122** reacted with atmospheric CO affording double CO insertion product **123** through the formation of a C–C bond between two CO molecules and migration of trimethylsilyl group to the oxygen atom originated from CO. They assumed that stepwise insertions of the two CO molecules into the Sc–B bond followed by an intramolecular migration of a trimethylsilyl group were the key steps to form the new C–C bonds between the two CO molecules.

Subsequently, Aldridge, Jones, and Mountford reported a similar procedure to prepare borylthulium and boryllutetium complexes, based on the boryl anion strategy [113]. The structural features of the resulting boryl complexes **124** and **125**



Scheme 33 Synthesis of scandium and gadolinium boryl complexes **120** and **121** using boryllithium **36**

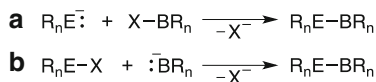


Scheme 34 Synthesis of boryllyttrium and boryllytettium complexes **124** and **125** using boryllithium **36**

were similar to those obtained for **121**, possessing similar square pyramidal structures (Scheme 34). DFT calculations and AIM analysis revealed that the B–metal bonds of **124** and **125** were polarized and the HOMOs of the resulting complexes coincided with the B–metal bonds.

4 Chemistry of Boryl-Substituted Main Group Element Compounds Derived from Boryl Anions

As expected, boryl-substituted main group element compounds can be synthesized by the reaction of anionic main group nucleophiles and boron compounds having leaving groups to achieve nucleophilic substitution at the boron center (Scheme 35a). The emergence of boryl anions has enabled us to expand the synthetic methodology for boryl-substituted main group element compounds in an umpolung manner, where the boron nucleophile can attack the main group element compounds possessing leaving groups on the main group element center (Scheme 35b); borylmagnesium species were synthesized this way (see Sect. 2.3).



Scheme 35 Synthesis of boryl-substituted main group element compound in (a) electrophilic and (b) nucleophilic substitution at the boron center (*E*, main group element; *R*, anionic ligand)

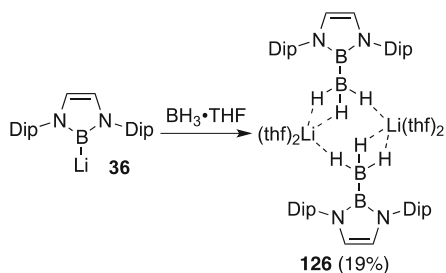
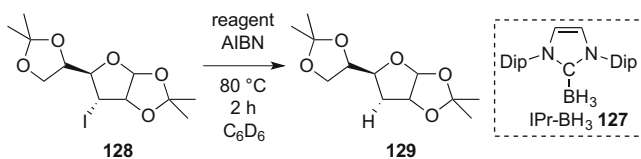
In this section, the application of boryl anions to synthesize boryl-substituted main group element compounds is reviewed.

4.1 Boryl-Substituted Group 13 Element Compounds

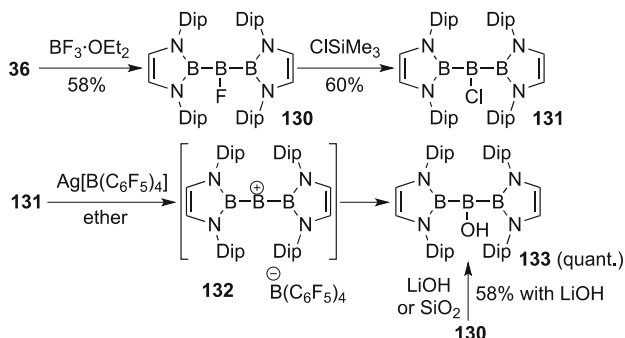
Since the history of nucleophilic group 13 element compounds is short, examples of boryl-substituted group 13 elements are still limited. Therefore, the application of boryl anions plays an important role in the chemistry of boryl-substituted group 13 element compounds.

We demonstrated that the boryl anion could be utilized for the preparation of boryl-substituted boron compounds. Reaction of boryllithium **36** with $\text{BH}_3 \cdot \text{THF}$ gave lithium boryltrihydroborate **126** in 19% isolated yield (Scheme 36) [114]. A broad ^1H NMR signal of **126** at -0.98 ppm could be assigned as BH_3 moiety, because the signal was sharpened by decoupling of ^{11}B nucleus in the $^1\text{H}\{^{11}\text{B}\}$ NMR spectrum. A hindered secondary alkyl iodide **128**, which may resist $\text{S}_{\text{N}}2$ substitution, was subjected to radical reduction with **126**, LiBH_4 , and **127** as a reductant (Table 4). The precursor **128** (and the product **129**) was inseparable, but their combined isolated yields were good. In this sequence of reactions, boryltrihydroborate **126** provided the best result, giving 78% conversion to **129** (entry 1). In contrast, **127** gave only 37% conversion (entry 3) and LiBH_4 gave no conversion, possibly due to its low solubility (entry 2). Thus, **126** is the best hydrogen donor for radical reduction among three reagents, probably due to its high solubility to hydrocarbon solvent and small bond dissociation energy for B–H bond. A theoretical calculation implied the changing counter cation of **126** would afford a more effective reagent toward radical reduction [115].

Boryllithium **36** also reacted with $\text{BF}_3 \cdot \text{OEt}_2$ to give fluorotriborane(5) **130** through double nucleophilic borylation (Scheme 37) [116]. In the ^{11}B NMR spectrum of **130**, two signals at 83 and 25 ppm were observed. Subsequent halogen exchange reaction of **130** could be achieved by a treatment with ClSiMe_3 to give the chlorinated triborane(5) **131**. Treatment of **131** with $\text{Ag}[\text{B}(\text{C}_6\text{F}_5)_4]$ in ether led to the formation of white precipitate and hydroxytriborane(5) **133**, which was independently synthesized from **130** and characterized. It may be assumed that a cationic intermediate **132** was generated by an absorption of chloride with Ag^+ to precipitate AgCl . The diborylboryl cation **131** may be more reactive toward Et_2O than the previously reported example of isolated boryl cations [117, 118], because there is no $\text{p}\pi\text{--p}\pi$ stabilization between the boron center and the substituents in **131**

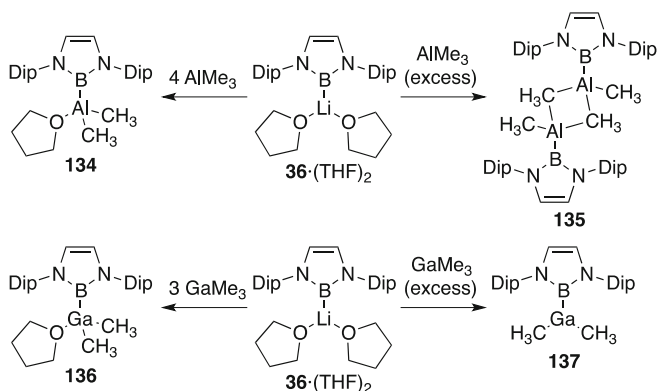
**Scheme 36** Synthesis of boryltrihydroborate **126****Table 4** Reduction of secondary alkyl iodide with **126**, LiBH₄, and IPr-BH₃ **127**

Entry	Reagent	Conv. 128 (%)	Yield (%) ^a
1	126	78	73
2	LiBH ₄	~0	—
3	127	37	65

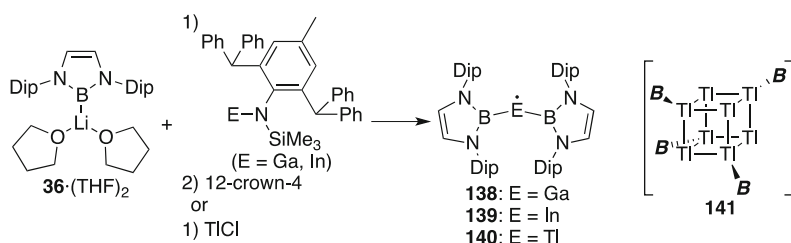
^aIsolated yield of **128** and **129** (inseparable)**Scheme 37** Synthesis and reaction of tritoranes(5)

(recently, a remarkably reactive diarylboryl cation was isolated and its reactivity toward CO₂ was disclosed; see [119]).

Heavier group 13 elements could also have 2-center-2-electron bonds with boron atoms through nucleophilic borylation methods with boryllithium. Anwander reported the synthesis of borylaluminum and borylgallium species (Scheme 38)



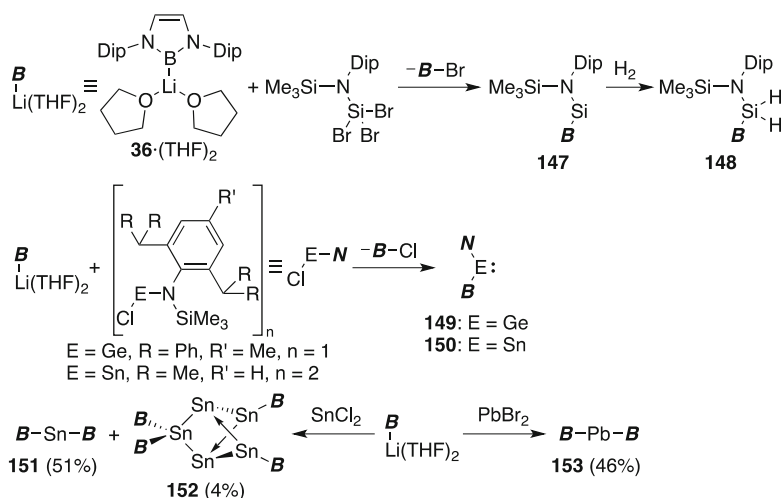
Scheme 38 Nucleophilic introduction of boryl substituent to methylated aluminum and gallium



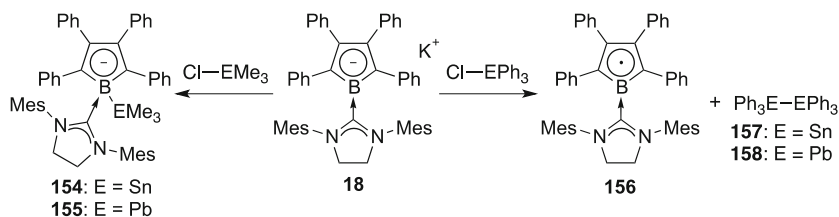
Scheme 39 Generation of divalent group 13 diborylmethyl species **138–140**

[120–122]. Reaction of boryllithium·THF solvate **36**·(THF)₂ with 4 equiv. of AlMe₃ gave boryldimethylaluminum–THF adduct **134**. Addition of an excess amount of AlMe₃ induced an abstraction of all THF molecules to afford a dimeric boryldimethylaluminum **135**. The resulting dimer **135** could be further applied to complexation with lanthanide metals (see references for details). In the case of gallium, boryldimethylgallium–THF adduct **136** was obtained by a reaction with 3 equiv. of GaMe₃, while a reaction with an excess of GaMe₃ afforded monomeric boryldimethylgallium **137**. The structural difference between dimeric **135** and monomeric **137** could be attributed to the difference in Lewis acidity between Al and Ga, as the authors discussed.

Nucleophilic borylation methods were also effective for the preparation of heavier group 13 element compounds. Aldridge reported reactions of M (I) compounds (M = Ga, In, Tl) with boryllithium·THF solvate **36**·(THF)₂ to give the divalent group 13 diborylmethyl species **138–140** (Scheme 39) [123, 124]. Each reaction liberated elemental M(0) species, which was supported by an observation of cluster cubane Tl₈ compound **141** in the reaction of Tl. All the resulting M(II) species were proven to have a bent B–M–B structure, based on X-ray crystallography. Reflecting their open-shell character, these compounds were paramagnetic, since a magnetic moment was observed. The unpaired electron of these



Scheme 41 Synthesis of divalent group 14 element compounds



Scheme 42 Reaction of base-stabilized borole anion **18** with R₃ECl (*E*: Sn, Pb)

pentanuclear cluster **152** was also formed, which could be considered to result from reduction at tin center.

The NHC-stabilized borole anion **18**, having nucleophilicity on the boron center and being introduced in the previous section, reacts with trimethyltin chloride and trimethyllead chloride to give the corresponding formal nucleophilic substitution products **154** and **155** (Scheme 42) [126]. The resulting compounds have 2-center-2-electron boron–tin and boron–lead bonds, as were characterized by NMR spectroscopy and X-ray crystallographic studies. On the other hand, triphenyltin and triphenyllead chloride reagents reacted with **18** to give the reduced distannane **157** and diplumbane **158**. They disclosed that this reaction took place through one-electron transfer reactions to form an oxidized product **156** from **18**. The resulting radical **156** was characterized by X-ray crystallography, ESR spectroscopy, and DFT studies to show the delocalization of the unpaired electron over borole ring.

availability for boron–element bonds, connecting with nearly any type of element. However, currently available boryl anion derivatives still have some limitations. For example, (1) boryllithium needs ethereal solvent and steric bulk to be generated; (2) only nitrogen-substituted boryllithium is available; (3) there is no example of borylsodium and borylpotassium, probably due to their high basicity and reducing ability; (4) there is no direct method to prepare borylmagnesium and borylzinc species, in contrast to the chemistry of Grignard and Reformatsky reagents; (5) insufficient information about the reactivity of boryl anions and their scope of reactivity for various substrates; and (6) no observable sp^2 boryl anion other than the examples shown in this review exists. Any improvement in the properties of boryl anions and solutions for these problems would have further impact on extending this field of chemistry.

Desired advances from the viewpoint of extending the generality of boryl anion chemistry in the future are as follows: (1) preparation of less-hindered boryl anions, especially with oxygen substituents; (2) preparation of boryl anions in hydrocarbon solvents (compared with commercially available butyllithium in *n*-hexane); (3) carbon-substituted boryl anions for more Lewis-acidic boryl anions or for triplet boryl anions; (4) further applications of boryl groups in synthetic organic chemistry through further transformations to other functional groups; and (5) exploring the limits of the basicity of the boryl anion because the boron atom has lower electronegativity compared to the carbon atom. Efforts to realize these new types of boryl anions would extend main group, organometallic, and organic chemistry and related areas substantially.

Acknowledgment The authors acknowledge all the students, postdocs, and colleagues in our papers in the reference section, all friends whom we have discussed this chemistry, and all those who have provided funding resource.

References

1. Brown HC, Rao BCS (1956) *J Am Chem Soc* 78:2582
2. Brown HC (1962) *Hydroboration*. Wiley-Interscience, New York
3. Suzuki A, Dhillon RS (1986) *Top Curr Chem* 130:23
4. Ishihara K (2000) Achiral and chiral B(III) Lewis acids. In: Yamamoto H (ed) *Lewis acids in organic synthesis*, vol 1. Wiley-VCH, Weinheim, pp 89–190
5. Kim BM, Williams SF, Masamune S (1991) The aldol reaction: group III enolates. In: Trost BM (ed) *Comprehensive organic synthesis*, vol 2. Pergamon, Oxford, p 239
6. Miyaura N, Suzuki A (1995) *Chem Rev* 95:2457
7. Miyaura N (2002) Organoboron compounds. In: *Cross-Coupling Reactions: A Practical Guide (Topics in Current Chemistry)*, vol 219. Springer-Verlag, Berlin, p 11
8. Miyaura N (2004) Metal-catalyzed cross-coupling reactions of organoboron compounds with organic halides. In: Meijere AD, Diederich F (eds) *Metal-catalyzed cross-coupling reactions*, vol 1, 2nd edn. Wiley-VCH, Weinheim, p 41
9. Wagner M, van Eikema Hommes NJR, Noeth H, Schleyer PVR (1995) *Inorg Chem* 34:607
10. Schaefer HF III (1986) *Science* 231:1100
11. Sundermann A, Reiher M, Schoeller WW (1998) *Eur J Inorg Chem* 3:305

12. Metzler-Nolte N (1998) *New J Chem* 22:793
13. Arduengo AJ III, Harlow RL, Kline M (1991) *J Am Chem Soc* 113:361
14. Auten RW, Kraus CA (1952) *J Am Chem Soc* 74:3398
15. Smith K, Swaminathan K (1976) *J Chem Soc Dalton* 21:2297
16. Williams JLR, Doty JC, Grisdale PJ, Searle R, Regan TH, Happ GP, Maier DP (1967) *J Am Chem Soc* 89:5153
17. Parsons TD, Self JM, Schaad LH (1967) *J Am Chem Soc* 89:14:3446
18. Umemoto T (1996) *Chem Rev* 96:1757
19. Braunschweig H, Chiu C-W, Radacki K, Kupfer T (2010) *Angew Chem Int Ed* 49:2041
20. Braunschweig H, Chiu C-W, Kupfer T, Radacki K (2011) *Inorg Chem* 50:4247
21. Monot J, Solovyev A, Bonin-Dubarle H, Derat É, Curran DP, Robert M, Fensterbank L, Malacria M, Lacôte E (2010) *Angew Chem Int Ed* 49:9166
22. Braunschweig H, Burzler M, Dewhurst RD, Radacki K (2008) *Angew Chem Int Ed* 47:5650
23. Bernhardt E, Bernhardt-Pitchougina V, Willner H, Ignatiev N (2011) *Angew Chem Int Ed* 50:12085
24. Ruiz DA, Ung G, Melaimi M, Bertrand G (2013) *Angew Chem Int Ed* 52:7590
25. Emsley J (1998) *The elements*, 3rd edn. Oxford University Press, New York
26. Segawa Y, Yamashita M, Nozaki K (2006) *Science* 314:113
27. Segawa Y, Suzuki Y, Yamashita M, Nozaki K (2008) *J Am Chem Soc* 130:16069
28. Robinson S, McMaster J, Lewis W, Blake AJ, Liddle ST (2012) *Chem Commun* 48:5769
29. Yamashita M, Suzuki Y, Segawa Y, Nozaki K (2008) *Chem Lett* 37:802
30. Arduengo AJ III, Krafczyk R, Schmutzler R, Craig HA, Goerlich JR, Marshall WJ, Unverzagt M (1999) *Tetrahedron* 55:14523
31. Rath NP, Fehlner TP (1988) *J Am Chem Soc* 110:5345
32. Del Bene JE, Elguero J (2007) *J Phys Chem A* 111:6443
33. Del Bene JE, Elguero J (2007) *Magn Res Chem* 45:484
34. Del Bene JE, Elguero J, Alkorta I, Yanez M, Mo O (2007) *J Phys Chem A* 111:419
35. Cheung MS, Marder TB, Lin Z (2011) *Organometallics* 30:3018
36. Jaramillo P, Pérez P, Fuentealba P (2009) *J Phys Chem A* 113:6812
37. Dettenrieder N, Aramaki Y, Wolf BM, Maichle-Mössmer C, Zhao X, Yamashita M, Nozaki K, Anwander R (2014) *Angew Chem Int Ed* 53:6259
38. Onak TP, Landesman H, Williams RE, Shapiro I (1959) *J Phys Chem* 63:1533
39. Lai C-H, Chou P-T (2010) *J Mol Model* 16:713
40. Tuononen HM, Roesler R, Dutton JL, Ragoona PJ (2007) *Inorg Chem* 46:10693
41. Bader RFW (1990) *Atoms in molecules - a quantum theory*. Oxford University Press, New York
42. Bader RFW (1991) *Chem Rev* 91:893
43. Lambert C, Schleyer PV (1994) *Angew Chem Int Ed Engl* 33:1129
44. Bader RFW, Macdougall PJ (1985) *J Am Chem Soc* 107:6788
45. Ritchie JP, Bachrach SM (1987) *J Am Chem Soc* 109:5909
46. Yamashita M, Suzuki Y, Segawa Y, Nozaki K (2007) *J Am Chem Soc* 129:9570
47. Ito H, Yamanaka H, Tateiwa J, Hosomi A (2000) *Tetrahedron Lett* 41:6821
48. Takahashi K, Ishiyama T, Miyaura N (2000) *Chem Lett* 29:982
49. Takahashi K, Ishiyama T, Miyaura N (2001) *J Organomet Chem* 625:47
50. Lee S, Yun J (2015) Asymmetric catalytic borylation of α,β -unsaturated acceptors. In: Fernández E, Whiting A (eds) *Synthesis and application of organoboron compounds*. doi:10.1007/978-3-319-13054-5_3
51. Ito H (2008) New synthetic reactions through σ -bond metathesis of group 11 metal catalysts. *J Synth Org Chem Jpn* 66:1168
52. Dang L, Lin Z, Marder TB (2009) *Chem Commun* 27:3987
53. Lillo V, Bonet A, Fernandez E (2009) *Dalton Trans* 16:2899
54. Laitar DS, Mueller P, Sadighi JP (2005) *J Am Chem Soc* 127:17196
55. Laitar DS, Tsui EY, Sadighi JP (2006) *J Am Chem Soc* 128:11036

56. Zhao H, Lin Z, Marder TB (2006) *J Am Chem Soc* 128:15637
57. Zhao H, Dang L, Marder TB, Lin Z (2008) *J Am Chem Soc* 130:5586
58. Kajiwara T, Terabayashi T, Yamashita M, Nozaki K (2008) *Angew Chem Int Ed* 47:6606
59. Hope H, Olmstead MM, Power PP, Sandell J, Xu X (1985) *J Am Chem Soc* 107:4337
60. Hwang CS, Power PP (1999) *Organometallics* 18:697
61. Janssen MD, Corsten MA, Spek AL, Grove DM, van Koten G (1996) *Organometallics* 15:2810
62. Curtis D, Lesley MJG, Norman NC, Orpen AG, Starbuck J (1999) *J Chem Soc Dalton* 10:1687
63. Westcott SA, Marder TB, Baker RT, Harlow RL, Calabrese JC, Lam KC, Lin Z (2004) *Polyhedron* 23:2665
64. Braunschweig H, Radacki K, Rais D, Whittell GR (2005) *Angew Chem Int Ed* 44:1192
65. Azarifar D, Coles MP, El-Hamruni SM, Eaborn C, Hitchcock PB, Smith JD (2004) *J Organomet Chem* 689:1718
66. Markies PR, Schat G, Akkerman OS, Bickelhaupt F, Smeets WJJ, Spek AL (1990) *Organometallics* 9:2243
67. Nagashima Y, Takita R, Yoshida K, Hirano K, Uchiyama M (2013) *J Am Chem Soc* 135:18730
68. Okuno Y, Yamashita M, Nozaki K (2011) *Angew Chem Int Ed* 50:920
69. Okuno Y, Yamashita M, Nozaki K (2011) *Eur J Org Chem* 3951
70. Haubold W, Hrebicek J, Sawitzki G (1984) *Z Naturforsch B Chem Sci* 39:1027
71. Nguyen P, Dai C, Taylor NJ, Power WP, Marder TB, Pickett NL, Norman NC (1995) *Inorg Chem* 34:4290
72. Clegg W, Dai CY, Lawlor FJ, Marder TB, Nguyen P, Norman NC, Pickett NL, Power WP, Scott AJ (1997) *J Chem Soc Dalton* 5:839
73. Grigsby WJ, Power P (1997) *Chem Eur J* 3:368
74. Kaufmann B, Jetzfellner R, Nöth H, Schmidt M, Leissring E, Issleib K (1997) *Chem Ber* 130:1677
75. Dang L, Lin Z, Marder TB (2008) *Organometallics* 27:4443
76. Gao M, Thorpe SB, Santos WL (2009) *Org Lett* 11:3478
77. Gao M, Thorpe SB, Kleeberg C, Slobodnick C, Marder TB, Santos WL (2011) *J Org Chem* 76:3997
78. Thorpe SB, Guo X, Santos WL (2011) *Chem Commun* 47:424
79. Lee K-S, Zhugralin AR, Hoveyda AH (2009) *J Am Chem Soc* 131:7253
80. Wu H, Radomkit S, O'Brien JM, Hoveyda AH (2012) *J Am Chem Soc* 134:8277
81. Lee K-S, Zhugralin AR, Hoveyda AH (2010) *J Am Chem Soc* 132:12766
82. Kleeberg C, Crawford AG, Batsanov AS, Hodgkinson P, Apperley DC, Cheung MS, Lin Z, Marder TB (2011) *J Org Chem* 77:785
83. Cid J, Gulyas H, Carbo JJ, Fernandez E (2012) *Chem Soc Rev* 41:3558
84. Gulyas H, Bonet A, Pubill-Ulldemolins C, Sole C, Cid J, Fernandez E (2012) *Pure Appl Chem* 84:2219
85. Bonet A, Gulyás H, Fernández E (2010) *Angew Chem Int Ed* 49:5130
86. Cid J, Carbó JJ, Fernández E (2014) *Chem Eur J* 20:3616
87. Noguchi H, Hojo K, Suginome M (2007) *J Am Chem Soc* 129:758
88. Iwadata N, Suginome M (2009) *J Organomet Chem* 694:1713
89. Noguchi H, Shioda T, Chou C-M, Suginome M (2008) *Org Lett* 10:377
90. Pubill-Ulldemolins C, Bonet A, Gulyas H, Bo C, Fernandez E (2012) *Org Biomol Chem* 10:9677
91. Bonet A, Pubill-Ulldemolins C, Bo C, Gulyás H, Fernández E (2011) *Angew Chem Int Ed* 50:7158
92. Sole C, Gulyas H, Fernandez E (2012) *Chem Commun* 48:6739
93. Sanz X, Lee GM, Pubill-Ulldemolins C, Bonet A, Gulyas H, Westcott SA, Bo C, Fernandez E (2013) *Org Biomol Chem* 11:7004

94. Irvine GJ, Lesley MJG, Marder TB, Norman NC, Rice CR, Robins EG, Roper WR, Whittell GR, Wright LJ (1998) *Chem Rev* 98:2685
95. Braunschweig H (1998) *Angew Chem Int Ed* 37:1786
96. Braunschweig H, Colling M (2001) *Coord Chem Rev* 223(1):1–51
97. Braunschweig H, Kollann C, Rais D (2006) *Angew Chem Int Ed* 45:5254
98. Aldridge S, Coombs DL (2004) *Coord Chem Rev* 248:535
99. Schmid G, Nöth H (1963) *Angew Chem Int Ed Engl* 2:623
100. Hartwig JF, Huber S (1993) *J Am Chem Soc* 115:4908
101. Schmid G, Nöth H (1965) Diphenylbor-Verbindungen von Kobalt und Platin. *Zeitschrift für Naturforschung Teil B Chemie B* 20b:1008
102. Baker RT, Ovenall DW, Calabrese JC, Westcott SA, Taylor NJ, Williams ID, Marder TB (1990) *J Am Chem Soc* 112:9399
103. Kawano Y, Yasue T, Shimoï M (1999) *J Am Chem Soc* 121:11744
104. Ito H, Kawakami C, Sawamura M (2005) *J Am Chem Soc* 127:16034
105. Segawa Y, Yamashita M, Nozaki K (2007) *Angew Chem Int Ed* 46:6710
106. Zhu J, Lin ZY, Marder TB (2005) *Inorg Chem* 44:9384
107. Protchenko AV, Dange D, Schwarz AD, Tang CY, Phillips N, Mountford P, Jones C, Aldridge S (2014) *Chem Commun* 50:3841
108. Braunschweig H, Brenner P, Dewhurst RD, Kaupp M, Müller R, Östreicher S (2009) *Angew Chem Int Ed* 48:9735
109. Braunschweig H, Damme A, Dewhurst RD, Kramer T, Östreicher S, Radacki K, Vargas A (2013) *J Am Chem Soc* 135:2313
110. Bertermann R, Braunschweig H, Ewing WC, Kramer T, Phukan AK, Vargas A, Werner C (2014) *Chem Commun* 50:5729
111. Terabayashi T, Kajiwara T, Yamashita M, Nozaki K (2009) *J Am Chem Soc* 131:14162
112. Li S, Cheng J, Chen Y, Nishiura M, Hou Z (2011) *Angew Chem Int Ed* 50:6360
113. Saleh LMA, Birjkumar KH, Protchenko AV, Schwarz AD, Aldridge S, Jones C, Kaltsoyannis N, Mountford P (2011) *J Am Chem Soc* 133:3836
114. Nozaki K, Aramaki Y, Yamashita M, Ueng S-H, Malacria M, Lacôte E, Curran DP (2010) *J Am Chem Soc* 132:11449
115. Lai C-H, Chou P-T (2010) *J Comput Chem* 31:2258
116. Hayashi Y, Segawa Y, Yamashita M, Nozaki K (2011) *Chem Commun* 47:5888
117. Koelle P, Nöth H (1985) *Chem Rev* 85:399
118. Piers WE, Bourke SC, Conroy KD (2005) *Angew Chem Int Ed* 44:5016
119. Shoji Y, Tanaka N, Mikami K, Uchiyama M, Fukushima T (2014) *Nat Chem* 6:498
120. Dettenrieder N, Dietrich HM, Schädle C, Maichle-Mössmer C, Törnroos KW, Anwänder R (2012) *Angew Chem Int Ed* 51:4461
121. Dettenrieder N, Hollfelder CO, Jende LN, Maichle-Mössmer C, Anwänder R (2014) *Organometallics* 33:1528
122. Dettenrieder N, Schädle C, Maichle-Mössmer C, Sirsch P, Anwänder R (2014) *J Am Chem Soc* 136:886
123. Protchenko AV, Dange D, Harmer JR, Tang CY, Schwarz AD, Kelly MJ, Phillips N, Tirfoin R, Birjkumar KH, Jones C, Kaltsoyannis N, Mountford P, Aldridge S (2014) *Nat Chem* 6:315
124. Protchenko AV, Dange D, Blake MP, Schwarz AD, Jones C, Mountford P, Aldridge S (2014) *J Am Chem Soc* 136:10902
125. Protchenko AV, Birjkumar KH, Dange D, Schwarz AD, Vidovic D, Jones C, Kaltsoyannis N, Mountford P, Aldridge S (2012) *J Am Chem Soc* 134:6500
126. Bertermann R, Braunschweig H, Dewhurst RD, Hörl C, Kramer T, Krummenacher I (2014) *Angew Chem Int Ed* 53:5453
127. Kaaz M, Bender J, Forster D, Frey W, Nieger M, Gudat D (2014) *Dalton Trans* 43:680

Fundamental and Applied Properties of Borocations

Michael J. Ingleson

Contents

1	Introduction	40
2	Fundamentals	42
2.1	Select Synthetic Considerations	42
2.2	Electrophilicity of Borocations	44
2.3	General Reactivity Pathways of Borocations with Nucleophiles	48
3	Borocations in Dehydroboration	49
3.1	Intramolecular Electrophilic Aromatic Borylation	50
3.2	Intramolecular Electrophilic Aliphatic Borylation	52
3.3	Intermolecular Electrophilic Aromatic Borylation	53
4	Borocations in Elemento-Boration	58
4.1	Hydroboration	58
4.2	Other Elemento-Boration Reactions	59
5	Borocations in Catalysis	61
6	Miscellaneous Applications of Borocations	64
6.1	Materials Applications	64
6.2	Borocations as Precursors to Borylenes and Boryl Radicals	65
6.3	Structural Rearrangement of Borocations	66
7	Conclusions and Future Outlook	67
	References	68

M.J. Ingleson (✉)

School of Chemistry, The University of Manchester, Chemistry Building-4.02 K, Manchester M13 9PL, UK

e-mail: Michael.Ingleson@manchester.ac.uk

© Springer International Publishing Switzerland 2015

E. Fernández, A. Whiting (eds.), *Synthesis and Application of Organoboron*

Compounds, Topics in Organometallic Chemistry 49,

DOI 10.1007/978-3-319-13054-5_2

Abstract The past 5 years has witnessed considerable growth in the field of borocation chemistry with a multitude of new cations containing 2, 3 and 4 coordinate boron centres reported. Perhaps more significant has been the expansion in the synthetic utility of borocations as stoichiometric reagents and catalysts. It is these new applications of borocations that are the primary focus of this article which concentrates on reports from 2009 to the end of June 2014. The correlation between structure and reactivity in these recent studies will be emphasised to aid in the future design of new borocations for specific targeted outcomes.

Keywords Borenium • Borinium • Borocations • Boronium • Borylation • Dehydroboration • Electrophiles • Haloboration • Hydroboration • Lewis acid catalysis

Abbreviations

[NTf ₂] ⁻	Triflimide ⁻ N(SO ₂ CF ₃) ₂
[OTf] ⁻	Triflate ⁻ OSO ₂ CF ₃
BBN	9-Borabicyclo[3.3.1]nonane
Cat	Catecholato ([<i>o</i> -C ₆ H ₄ O ₂] ²⁻)
CatS ₂	Thiocatecholato ([<i>o</i> -C ₆ H ₄ S ₂] ²⁻)
CIA	Chloride ion affinity
DABCO	Diazabicyclo[2.2.2]octane
DIPP	2,6-Disopropylbenzene
DOSY	Diffusion-ordered NMR spectroscopy
FIA	Fluoride ion affinity
FLP	Frustrated Lewis pair
HIA	Hydride ion affinity
KIE	Kinetic isotope effect
Mes	Mesityl (2,4,6-Me ₃ -C ₆ H ₂)
NHC	<i>N</i> -Heterocyclic carbene
PCM	Polarisation continuum model
Pin	Pinacolato ([OC(Me) ₂ C(Me) ₂ O] ²⁻)
S _E Ar	Electrophilic aromatic substitution
X-DMAP	<i>N,N</i> -Dimethylaminopyridine (<i>x</i> = 2 or 4)

1 Introduction

The fundamental chemistry of borocations was first summarised in the seminal review by Koelle and Nöth nearly 30 years ago [1]. This included defining the terminology for borocations of varying coordination number at boron as boronium, borenium and borinium for four, three and two coordinate, respectively (Fig. 1). In 2005, Piers and co-workers provided an updated review and emphasised the

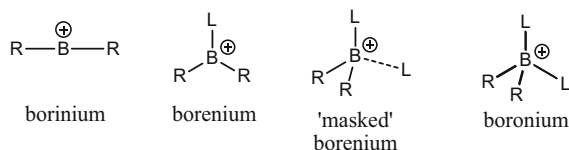


Fig. 1 The terminology for borocations of varying coordination number (where L is formally a neutral two-electron donor and R is formally a monoanionic substituent)

potential of borocations in synthesis and materials applications [2]. In addition to these two articles that cover the fundamental aspects of borocation chemistry in depth, a comprehensive review of the chemistry of borocations from an organic perspective (covering the literature up to the end of 2011) was produced by Vedejs and co-workers [3]. To avoid excessive overlap with these previous reviews, this chapter only briefly discusses the fundamental and early chemistry of borocations. Instead, it focuses on the applications of borocations reported in the last 5 years and emphasises how structural variation of the borocation controls electrophilicity at boron and subsequent reactivity. Current mechanistic hypotheses, limitations and future challenges will also be discussed. Due to space limitations, this article is limited to (i) the condensed phase reactivity of borocations (for gas phase reactivity, see Piers and co-workers [2]), (ii) metal-free borocations (for cationic transition metal borylenes, see references in [4]), and (iii) borocations directly bound to two R groups (Fig. 1), with R_3B with peripheral cationic groups also beyond the scope of this review [5].

As expected for a compound class that carries a unit positive charge and for borinium and borenium cations are formally electron deficient at boron, the reactivity of borocations is dominated by electrophilicity at boron. The majority of this review focuses on the recent applications of borenium cations as these cations combine significant electrophilicity at boron with relatively simple synthetic accessibility. However, it is important to note that a number of boronium cations are also useful electrophiles, particularly examples containing weakly bound Lewis bases in the fourth coordination site. A continuum of electrophilic reactivity with borinium cations at one extreme can be proposed in which boronium cations play an important role either as masked forms of borenium cations (via dissociation of L) or as electrophiles in their own right reacting via a S_N2 -type process. Furthermore, anion-coordinated species can also exhibit borenium-type reactivity provided the anion is sufficiently weakly coordinating and readily displaced by another nucleophile, thus these neutral species are included where appropriate. Finally, we acknowledge that representing the positive charge throughout this review as localised at boron in borenium cations is a simplification and that charge is inherently diffuse. However, we feel that this representation is useful as it emphasises that the locus of electrophilic reactivity is consistently at boron and that boron generally possesses the greatest magnitude of positive charge in these cations (by NBO calculations) [6].

2 Fundamentals

2.1 Select Synthetic Considerations

The major synthetic routes to borenium and “masked” borenium cations remain as outlined originally by Koelle and Nöth, specifically (i) B–Y bond heterolysis (Y=halide or hydride), (ii) anion displacement by a neutral donor and (iii) coordination of an electrophile to a nucleophilic moiety in a neutral borane (Fig. 2). As noted by Vedejs and co-workers [7] for the latter when the electrophile (E) is neutral, this does not actually generate a compound with an overall positive charge. However, a borocation subunit can be identified (e.g. Fig. 2, inset) in these species; furthermore, they are often strong boron-based Lewis acids, thus their inclusion herein has validity [8]. Whilst a more comprehensive discussion of the synthetic routes to borocations is provided in previous reviews, some key observations of particular importance are discussed below.

The dominant synthetic route to borocations utilised in the recent literature is by B–Y bond heterolysis (Y=halide or hydride, route (i)). This can be effected by the addition of a metathesis agent (e.g. $\text{Ag}^+/\text{[Ph}_3\text{C]}^+$ salts), a strong Brønsted acid (e.g. HNTf_2) or a neutral strong Lewis acid, such as AlCl_3 . The latter was in fact the methodology used to generate the first well-characterised borenium cation [9]. For successful borocation formation by route (i), a number of interrelated factors must be considered: (a) the donor L has to bind sufficiently strongly to boron in the neutral precursor to prevent rapid dissociation of L and competitive coordination of L to M on the addition of M[anion] or MX_n . Likewise, strong L→B bonds are necessary to prevent the protonation of L when a strong Brønsted acid reagent is used. (b) The coordination of L to the neutral borane has to weaken the B–Y bond to

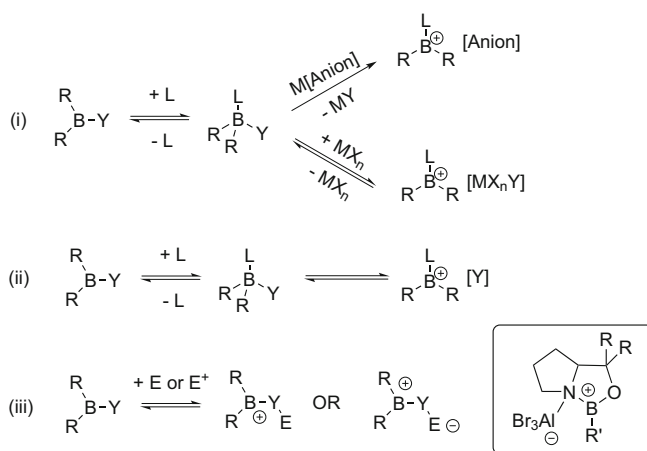


Fig. 2 Common synthetic routes to borenium cations. *Inset*, an example of a neutral compound that can be considered a borenium equivalent [8]

energetically favour B–Y bond heterolysis either on addition of MX_n/M^+ (route (i)) or without any further reagents (route (ii)). (c) L has to provide enough stabilisation, either kinetically through significant L steric bulk and/or electronically (e.g. by π donation), to disfavour strong anion/solvent binding. With borenium cations that have considerable Lewis acidity, B–Y bond heterolysis from the neutral precursor often only proceeds with the strongest MX_n Lewis acids, even when L is bulky and electron donating. Furthermore, B–Y bond heterolysis can be reversible, leading to complex dynamic mixtures in the solution phase that can complicate subsequent reactivity [6, 10].

The anion compatibility of borocations is also an important consideration and is obviously also dependent on the steric and electronic environment around boron. The production of the most electrophilic borocations necessitates the use of extremely robust and weakly coordinating anions, with simple fluorinated anions (e.g. $[\text{BF}_4]^-$, $[\text{SbF}_6]^-$) susceptible to anion decomposition by fluoride abstraction [11–15]. Many recently synthesised borenium cations utilise anions previously proven to be robust and weakly coordinating with the valence isoelectronic silicenium cations [16]. $[\text{B}(\text{C}_6\text{F}_5)_4]^-$ is a popular example, with reports of its decomposition when partnering borocations being extremely rare [7, 17]. It is notable that the $[\text{B}(\text{C}_6\text{H}_3(\text{CF}_3)_2)_4]^-$ anion is much more susceptible to decomposition by fluoride abstraction by highly electrophilic borocations due to the weaker sp^3 C–F bond [12]. Other classic “weakly” coordinating anions, particularly $[\text{OTf}]^-$, often interact strongly with boron in the absence of considerable steric crowding/electronic stabilisation of boron. This can effectively quench the Lewis acidity at boron, precluding subsequent synthetic applications.¹ In contrast, weak anion coordination can actually be beneficial, with stabilising $\text{B} \cdots \text{Cl}-\text{AlCl}_3$ and $\text{B} \cdots \text{NTf}_2$ interactions often observed in the solid state and solution. These weak interactions may well be essential for facilitating the simple synthesis of many borenium equivalents whilst maintaining significant electrophilicity at boron [18]. The determination of a borenium ions position on the continuum between a strongly bound ion pair and a solvent-separated ion pair in solution is complex. The most widely used method is the value of $\delta^{11}\text{B}$; however, this has limitations and is generally only able to unambiguously distinguish between 3 and 4 coordination at boron. This has recently been supplemented by the use of DOSY experiments, with the difference between anion and cation diffusion coefficients, an established method to assess the degree of ion association in solution [19, 20]. This approach was used to confirm the solvent-separated ion pair nature of $[\text{BBN}(\text{IMes})][\text{OTf}]$, whose existence as a borenium cation demonstrates that with sufficient steric bulk around boron even triflate can fulfil the role of a “non”-coordinating anion towards a borenium cation [19].

The coordinating ability of all other possible nucleophiles present in solution also needs to be considered if highly electrophilic borocations are the synthetic

¹ A CCDC search (June 2014) revealed 21 structures with the formula $[\text{R}_2\text{BL}][\text{OTf}]$ where the B–O bond distance is consistent with a significant interaction between the triflate anion and boron.

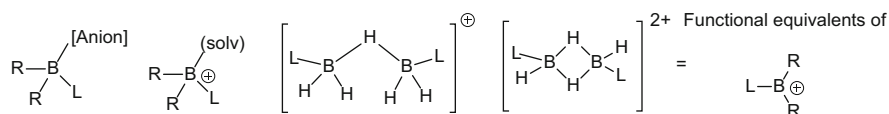


Fig. 3 Functional equivalents, or masked versions, of borenium cations

goal; this includes further equivalents of the neutral boron precursors. For example, Vedejs and co-workers have demonstrated the propensity of $(R_3N)BH_3$ to coordinate to the highly electrophilic borocations $[(R_3N)BH_2]^+$ forming hydride-bridged cations (Fig. 3 centre). More remarkably, borenium cations have been recently reported to dimerise to form dicationic (Fig. 3), further confirming the considerable electrophilicity of weakly stabilised borenium cations [21]. Nevertheless, all the species shown in Fig. 3 can be considered as functional equivalents, or masked versions, of borenium cations for reactivity purposes, and in this review they will all be termed borenium cations. Whether these species react via a true borenium cation intermediate or via S_N2 processes is generally unknown.

Finally, reaction solvent is another important variable. The avoidance of strongly coordinating solvents and the use of a solvent that is stable towards cationic boron electrophiles are obviously essential requirements for harnessing borenium ion reactivity in solution. Whilst ethers unsurprisingly decompose in the presence of many borocations [22, 23], even CH_2Cl_2 will react with certain borocations [24]. One specific example is from attempts to form $[(\text{amine})BBr_2]^+$ borocations in CH_2Cl_2 which instead led to halide exchange and formation of $[(\text{amine})BCl_2]^+$ [25]. Solvent polarity can also significantly effect borocation formation particularly equilibrium positions when using B–Y bond heterolysis effected by neutral Lewis acids as the synthetic route. In these reactions, low-polarity solvents often favour neutral species over the borocation [26]. Therefore, the solvents of last resort for synthesising the most electrophilic borocations are the halogenated arenes which combine sufficient polarity and low nucleophilicity with robustness (e.g. resistance to C–X cleavage). When all the above considerations are met, a multitude of highly electrophilic borenium cations, or functional equivalents, can be readily synthesised thus allowing their electrophilicity to be harnessed in the condensed phase.

2.2 Electrophilicity of Borocations

Borocation reactivity is dominated by Lewis acidity at boron. However, reactivity studies have demonstrated that electrophilicity at boron spans a considerable range. It is therefore important to summarise the key factors controlling Lewis acidity in these cations. Analogous to the neutral boranes [27], the Lewis acidity of borenium cations is dominated by three factors: (i) the degree of positive charge localised at boron (“hard” Lewis acidity using Pearson’s HSAB terminology which is

particularly important when the electrostatic contribution to bonding is significant), (ii) the energy of the lowest unoccupied molecular orbital with significant boron character (“soft” Lewis acidity) and (iii) the substituent steric bulk which effects the energy required to pyramidalise at boron and to increase the coordination number at boron from three to four. Intuitively, the unit positive charge present in a borocation would be expected to lead to higher Lewis acidity towards hard Lewis bases relative to neutral borane Lewis acids. This is consistent with experimental observations that many borocations abstract fluoride from $[\text{BF}_4]^-$ [11–15], whilst $[\text{CatB}(\text{NEt}_3)]^+$, **1**, even abstracts fluoride from $[\text{SbF}_6]^-$ [13]. Cation **1** therefore has a greater fluoride ion affinity (FIA) than SbF_5 (FIA of $\text{SbF}_5 = 489 \text{ KJ mol}^{-1}$), making it considerably more fluorophilic than the neutral borane, $\text{B}(\text{C}_6\text{F}_5)_3$ (FIA = 444 KJ mol^{-1}) [28]. In contrast, the relative Lewis acidity of **1** and $\text{B}(\text{C}_6\text{F}_5)_3$ towards hydride is reversed, with $\text{B}(\text{C}_6\text{F}_5)_3$ able to abstract hydride from $\text{CatB}(\text{H})(\text{NEt}_3)$ to form **1** and $[\text{HB}(\text{C}_6\text{F}_5)_3]^-$. This indicates an enhanced “hard” Lewis acidity in **1** due to increased magnitude of positive charge localised at boron (supported by NBO calculations).

As the Lewis acidity comparison between **1** and $\text{B}(\text{C}_6\text{F}_5)_3$ clearly demonstrates no absolute scale of borocation Lewis acidity can be provided due to the inherent dependence on the probe Lewis base. However, two probe nucleophiles have been widely used to assess electrophilicity, Et_3PO (Gutmann–Beckett method) [29] as a “hard” nucleophile and crotonaldehyde (Childs methods) as a “softer” nucleophile [30]. Piers and co-workers found that the dipyrinato-ligated borenium cation (Fig. 4, **2**) has a Lewis acidity towards crotonaldehyde comparable to BF_3 [31]. The planar chiral borenium cation, **3**, had a Lewis acidity towards Et_3PO that was slightly lower than $\text{B}(\text{C}_6\text{F}_5)_3$ [32]. Our laboratory found that the binding of Et_3PO to **1** produced a greater deshielding of the ^{31}P nucleus than Et_3PO bound to $\text{B}(\text{C}_6\text{F}_5)_3$ indicating greater Lewis acidity for **1** towards Et_3PO , consistent with the relative FIAs [13]. Vedejs and co-workers reported that the non-stabilised borenium cation $[(\text{Me}_3\text{N})\text{BH}_2]^+$ has a comparable Lewis acidity towards Et_3PO to that reported for **1** (based on comparable $\delta_{31\text{P}}$ values) [33]. This result can again be attributed to the large degree of positive charge localised at boron in **1**, which is generated by the bonding of boron to three highly electronegative atoms. Finally, Brunker and co-workers used the Gutmann–Beckett method to probe the Lewis acidity of a number of pentamethylazaferrocene ligated borenium cations including **4** and **5** [14]. Cation **4** was found to be more Lewis acidic towards Et_3PO than **5**, consistent with the reduced electronic stabilisation of boron bonded to two hydride substituents relative to two chloride π donor substituents. Despite the significant $\text{B}=\text{N}$ double bond character in cation **4**, it was still more Lewis acidic than $\text{B}(\text{C}_6\text{F}_5)_3$ towards Et_3PO in competitive binding experiments. The Lewis acidity of compounds **4** and **5** can also be assessed by the magnitude of the dip angle (the ring centroid – N – B angle), with **5** having a dip angle of -9.6° compared to that of -12.3° for $\text{Cp}^*\text{Fe}(\text{C}_5\text{H}_4\text{BBR}_2)$, indicating a greater interaction between Fe and boron for the neutral borane [14]. These results again suggest an enhanced hard Lewis acidity for borocations due to the unit positive charge.

The paradigm of a soft nucleophile is hydride; thus the hydride binding propensity of borocations is an informative indication of “soft” Lewis acidity. Trityl salts are extremely hydridophilic and will abstract hydride from a multitude of L-BY₂H species to generate borenium cations or their functional equivalents. This is exemplified by hydride abstraction from LBH₃ with [Ph₃C][B(C₆F₅)₄] (L=tertiary amines or NHCs) proceeding effectively, producing the transient weakly stabilised borenium cation, [LBH₂]⁺, which rapidly dimerises or interacts with an equivalent of LBH₃ to form [(LBH₂)₂(μ-H)]⁺ [7, 21]. Another informative comparison is to benchmark borenium cation hydridophilicity against that of B(C₆F₅)₃, the ubiquitous Lewis acid used for H₂/R₃SiH activation in frustrated Lewis pair chemistry [34]. A number of [PinB(L)]⁺ and [CatB(L)]⁺ (L=DABCO, PhNMe₂, Et₃N, 2,6-lutidine or P^tBu₃) cations have been synthesised by hydride abstraction from the neutral four-coordinate hydroborane using B(C₆F₅)₃, thus these cations all have lower HIA values than B(C₆F₅)₃. The lower Lewis acidity of these cations towards hydride is partly due to the stabilisation of the p_z orbital on boron by O → B π donation [13, 35–37]. Enhancing π donation by using C → B π donation from a carbodiphosphorane even enabled isolation of a (L)BH₂⁺ borenium cation (Fig. 4, 7) by hydride abstraction from LBH₃ with B(C₆F₅)₃ [38]. π donation to boron and positive charge delocalisation is also important for stabilising highly unusual borocations, as exemplified by the use of a carbodicarbene enabling isolation of the dication, [bis(carbodicarbene)BH]²⁺ [39]. In addition to electronic effects, steric bulk can also greatly modulate HIA, with borocation **8** (Fig. 4) also having a lower hydride ion affinity than B(C₆F₅)₃. In this case, the lower HIA can be attributed in part to significant steric crowding producing a large pyramidalisation energy [40]. Borenium cations with a greater Lewis acidity towards hydride than B(C₆F₅)₃ are accessible provided there is only weak electronic stabilisation of boron and limited substituent steric bulk. For example, the boron centre in [(2,6-lutidine)

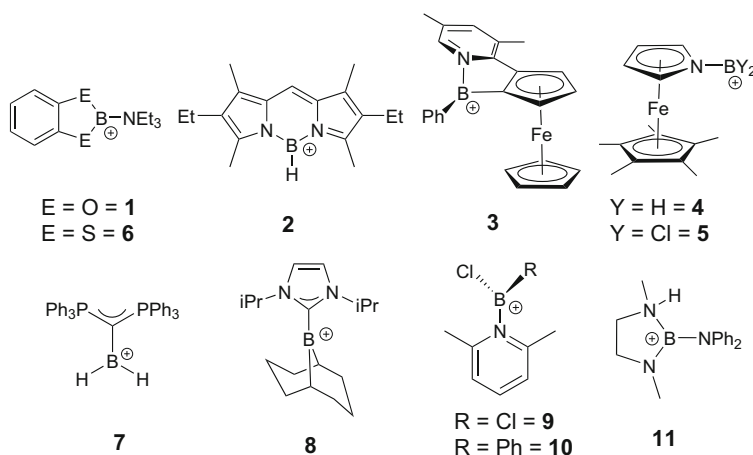
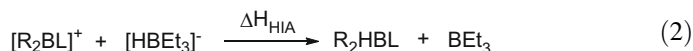
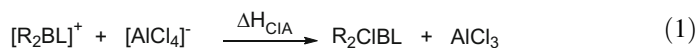


Fig. 4 Borenium cations whose Lewis acidity has been probed experimentally or computationally

$\text{BCl}_2]^+$, **9** (Fig. 4), is electronically stabilised by $\text{Cl} \rightarrow \text{B}$ π donation, with the pyridyl and BCl_2 moieties orthogonal precluding significant $\text{N} \rightarrow \text{B}$ π donation [25]. This cation abstracts hydride from $[\text{HB}(\text{C}_6\text{F}_5)_3]^-$ forming (2,6-lutidine) BHCl_2 and $\text{B}(\text{C}_6\text{F}_5)_3$, confirming that borocations can be extremely strong Lewis acids towards both hard and soft nucleophiles [13].

Alongside these experimental observations, several computational studies have been performed evaluating the Lewis acidity of borenium cations towards various Lewis bases. The binding enthalpy of NH_3 to borocations was probed at the M06-2X/6-311++G(3df,2p)//M06-2X/6-31+G(d,p) level by Vedejs and co-workers [3]. This revealed a considerable range of NH_3 affinities with borenium cations containing good π donor amido substituents, such as **11** (Fig. 4), being at one extreme displaying minimal Lewis acidity towards NH_3 (ΔH for NH_3 binding = -2.3 kcal mol $^{-1}$). At the other extreme, the weakly stabilised and sterically unhindered borocation $[(\text{Me}_3\text{N})\text{BH}_2]^+$ is highly Lewis acidic towards NH_3 (ΔH for NH_3 binding = -48.8 kcal mol $^{-1}$). Related trends were found for the calculated chloride ion affinity (CIA, Eq. 1) of borocations (at the M06-2X/6-311G(d,p) level with a PCM (DCM)), with the steric environment around boron and π donor ability of substituents important factors effecting Lewis acidity (e.g. **10** is considerably less Lewis acidic towards chloride than **9**, Fig. 4) [13].



One point worth reemphasising is the key effect the degree of positive charge localised at boron has on Lewis acidity towards hard bases, including chloride, due to the high electrostatic contribution to bonding. Two related borocations based on catechol and thiocatechol, **1** and **6** (Fig. 4), were found to have calculated relative Lewis acidities towards chloride that was the reverse of the expected order based on π donor ability (calculated CIA of **1** > **6**). The relative CIA was confirmed by reactivity studies. The greater $\text{O} \rightarrow \text{B}$ π donation relative to $\text{S} \rightarrow \text{B}$ π donation would suggest that **6** would be a weaker Lewis acid; however, the significantly greater polarisation of the σ bonding framework in **1** leads to a larger magnitude of positive charge localised at boron in **1** thus contributing to a greater CIA (NBO charges at boron for **1** = $+1.338e$, for **6** = $+0.396e$ at the MPW1K/6-311++G(d,p) level) [6]. The importance of electrostatics in increasing the binding strength of Lewis bases containing highly electronegative donor atoms towards borocations is not limited to borenium cations; Frenking and co-workers reported analogous trends for the borinium cation $[\text{H}_2\text{B}]^+$ with EC_5H_5 (E = N, P, As, Sb, Bi) [41].

The methodology for assessing relative CIA was extended to determining HIA relative to BEt_3 (Eq. 2). Calculated relative HIA values were found to be consistent with the experimental reactivity observed between borocations and $\text{B}(\text{C}_6\text{F}_5)_3$ [13]. Whilst Lewis acidity trends were broadly analogous to those observed for CIA, there are a number of important distinctions: (i) HIA is less effected by steric

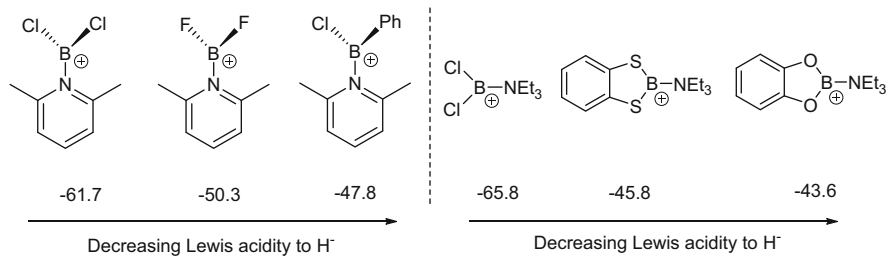


Fig. 5 HIA values of a range of borenium cations. HIA values are relative to BEt_3 (kcal mol^{-1}) calculations at the M06-2X/6311G(d,p) (PCM=DCM) level [13]

bulk around boron relative to CIA due to the smaller size of hydride versus chloride and (ii) the degree of positive charge localised at boron has a lower effect on Lewis acidity as expected for forming a B–H bond in which the electrostatic contribution to overall bond strength will be smaller. Thus **6** is a stronger Lewis acid towards hydride than **1** in contrast to relative CIA. Overall, the effect of altering the halide/chalcogen substituents on the HIA of borenium cations (Fig. 5) mirrors that observed for the Lewis acidity of neutral boranes [27]. A general correlation between the LUMO energy of the borocations in Fig. 5 and HIA was also observed, a trend analogous to that reported for the neutral boranes BF_3 and BCl_3 [42].

2.3 General Reactivity Pathways of Borocations with Nucleophiles

When a sufficiently electrophilic borenium cation, or its functional equivalent, interacts with a nucleophile, the primary product is generally a Lewis adduct. With π nucleophiles (the major area of recent studies), a number of subsequent reaction pathways are followed that are dependent on borocation structure. These can be grouped into three distinct classes: (i) $\text{L} \rightarrow \text{B}$ bond cleavage, which generates a new borenium cation, containing an activated nucleophile and an equivalent of a Lewis base (useful for subsequent deprotonations resulting in overall dehydroboration of the nucleophile); (ii) $\text{R}-\text{B}$ bond cleavage, e.g. leading to intramolecular transfer of an anionic R group to the nucleophile (representing elemento-boration); and (iii) No $\text{L}-\text{B}$ or $\text{R}-\text{B}$ cleavage, in which the activated nucleophile in the Lewis adduct can be attacked by an additional nucleophile (which if the product dissociates from boron represents Lewis acid catalysis) (Fig. 6).

Before discussing recent examples of each type, pathway (i) warrants more attention. The addition of a nucleophile to a borenium cation followed by dissociation of L generates $[\text{R}_2\text{B}(\text{Nuc})]^+$. This is an equivalent outcome to that from reacting a nucleophile directly with a borinium cation, but importantly avoids having to synthesise the borinium cation, which can often be extremely challenging. Borinium cations are in general more electrophilic than borenium cations and

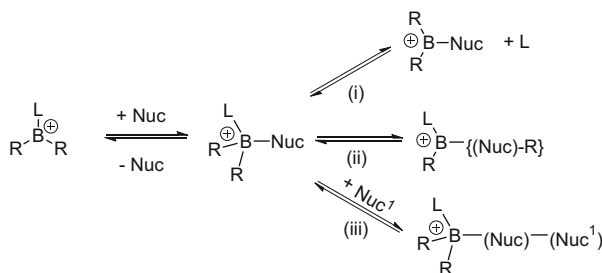


Fig. 6 Possible reaction pathways after initial combination of a boronium cation and a nucleophile (Nuc)

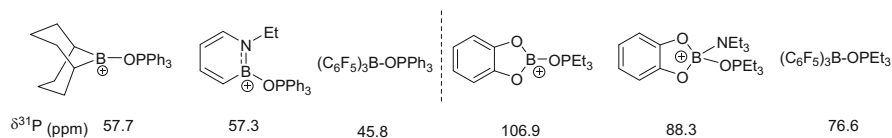


Fig. 7 ^{31}P NMR chemical shifts of phosphine oxide adducts of borocations and $\text{B}(\text{C}_6\text{F}_5)_3$

therefore will activate the coordinated nucleophile to a greater extent [27]. Indeed, the greater downfield shift observed in the ^{31}P NMR spectra of R_3PO coordinated to $[\text{R}_2\text{B}]^+$ species relative to R_3PO coordinated to $\text{B}(\text{C}_6\text{F}_5)_3$ and to boronium cations confirms the considerable Lewis acidity of boronium cations (Fig. 7) [13, 17, 43, 44]. Thus boronium cations can also be considered as masked borinium cations provided they dissociate L at some point during the reaction with a nucleophile.

Specific examples of reactions between borocations and nucleophiles from the recent literature are presented in Sects. 3–5.

3 Borocations in Dehydroboration

The addition of a nucleophile containing a Brønsted acidic moiety to a boronium cation, or a boronium cation equivalent, can ultimately result in the dehydroboration of the nucleophile. The most obvious example of dehydroboration is the reactivity of borocations with ROH generating B–OR moieties (for a recent example, see [45]). More useful products can be accessed from the dehydroboration of C–H bonds in unsaturated hydrocarbons, and this is the primary focus of this section. Direct electrophilic borylation, the conversion of C–H to C–B, is an appealing synthetic conversion installing a highly versatile functional group onto a hydrocarbyl framework. However, this reaction requires significant Lewis acidity at the boron centre towards soft (π) nucleophiles, with neutral boranes, such as BCl_3 , not sufficiently strong Lewis acids [10]. In one mechanistic sequence, L is evolved at some point from boron post binding of the nucleophile (Fig. 8 left) and

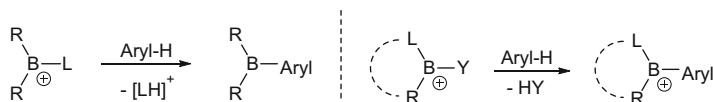


Fig. 8 Two distinct dehydroboration reactions using borenium cations

subsequently acts as a Brønsted base. An alternative dehydroboration pathway that leads to different primary products utilises the anionic substituent on the borocation as a Brønsted basic moiety, generating HY (Y=halide or hydride) as the by-product and producing a new borocation (Fig. 8, right). The latter process dominates particularly when the datively bound L substituent is part of a chelating group, thereby disfavouring dissociation of L from boron.

Historically, multiple intramolecular dehydroborations may proceed via borocations, but the intermediacy of these species was generally not considered [3]. This section therefore predominantly focuses on more recent work where the key role of borocations in C–H borylation has been considered and in some cases unambiguously confirmed.

3.1 Intramolecular Electrophilic Aromatic Borylation

To the best of our knowledge, the first possible observation of a borenium cation in intramolecular electrophilic borylation came from the work of Nagy and co-workers in 2000. In this work, cation **12** (Fig. 9, left) was proposed as an intermediate based on ¹H and ¹³C{¹H} NMR spectroscopy. However, the borenium formulation was not definitive due to the absence of ¹¹B NMR spectroscopic data. On warming to 0°C **12** (or its functional equivalent) was converted into the cyclic borylated structure with loss of HCl [46].

Subsequently, Vedejs and co-workers performed more extensive studies on a related intramolecular borylation proceeding via borocation **13** (Fig. 9, right), or its functional equivalent, to form **15** with H₂ as the only by-product [7]. This dehydroboration reaction could be extended to a number of other amine boranes, including for the formation of six-membered boracycles. Anions Weakly coordinating towards borocations were found to be essential, with [OTf][−] preventing dehydroboration, whereas [NTf₂][−] and [B(C₆F₅)₄][−] proving compatibility with borylation. The authors proposed a C–H insertion mechanism where C–B and H–H bond formations were concerted via a four-membered transition state, a hypothesis supported by high-level calculations. Experimental evidence for a C–H insertion mechanism was provided by using the ^tBu containing borocation **14**, which exclusively borylated at the *ortho* C–H position, with no products derived from loss of ^tBu⁺ observed. The evolution of the *tert*-butyl cation would be expected if the reaction proceeded via an arenium cation and a S_EAr process. The extreme electrophilicity of boron in **13** is presumably essential for generating an interaction between the borocation and the C–H σ bond on the pathway to C–H insertion. It is

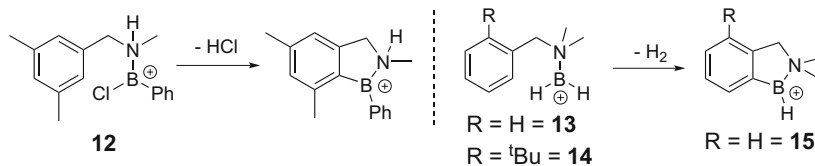


Fig. 9 Intramolecular dehydroboration using borenium cations (or functional equivalents)

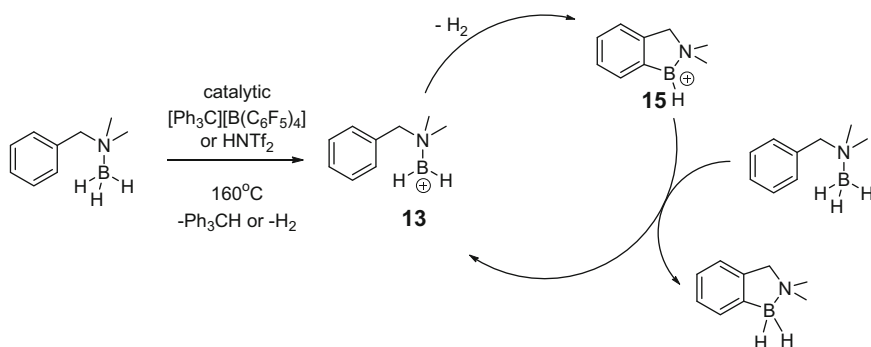


Fig. 10 Catalytic (in cationic activator) intramolecular dehydroboration of arenes

also noteworthy that a related C–H insertion process occurs for the dehydroboration of benzene with BH_3 which produces Ph_3B and H_2 [47, 48]. Catalytic (in activators such as HNTf_2) variants using borenium equivalents were concurrently developed (Fig. 10) [7, 49]. The key step in the catalytic cycle involves hydride transfer from (amine) BH_3 to **15** to regenerate **13** (or its functional equivalent). Catalytic turnover proceeded effectively at raised temperatures down to catalyst loadings of 5 mol% HNTf_2 .

Since Vedejs and co-worker's seminal report in 2009, a number of other intramolecular borylations have been reported where borocations have been proposed as intermediates; this includes pyridyl- [50–52] and phosphinite [53]-directed dehydroborations. In the pyridyl-directed borylation, excess BBr_3 and the hindered base, NEt^iPr_2 , were both essential; the base required either to deprotonate an arenium intermediate if the reaction proceeds by an $\text{S}_{\text{E}}\text{Ar}$ mechanism or sequester HBr to prevent protodeboration. Borenium cation intermediates have also been proposed in pyridyl-directed borodestannylation of a stannylated ferrocene and the related dehydroboration of **16** [54]. Compound **16** underwent dehydroboration at -70°C only in the presence of two equivalents of PhBCl_2 , which the authors suggest supports the intermediacy of **17** (Fig. 11). Borocations (or their equivalent) are also probable intermediates in the synthesis of BN-fused polycyclic aromatics from **18** (and related compounds) by double intramolecular dehydroboration. The addition of AlCl_3 and a hindered base were essential for the dehydroboration of **18**, with AlCl_3 presumably required to generate borenium equivalents by binding to nitrogen or by abstract halide [55, 56].

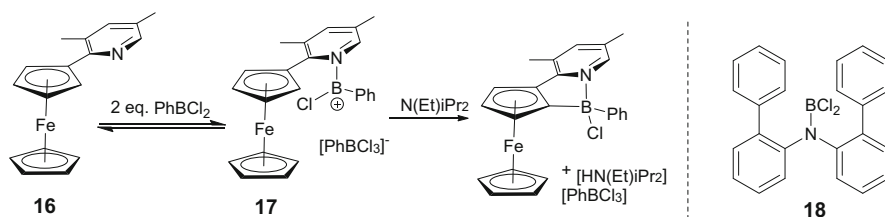


Fig. 11 *Left*, intramolecular borylation proposed to be mediated by borenium cation **17**. *Right*, the precursor **18** used for double electrophilic dehydroboration

3.2 Intramolecular Electrophilic Aliphatic Borylation

The observation of a C–H insertion mechanism in intramolecular electrophilic aromatic borylation using borocations was significant [7], as it had been reported that BH₃ will dehydroborate both arenes and alkanes via a related mechanism [48]. Thus Vedejs and co-workers demonstrated that intramolecular aliphatic C–H borylation using highly electrophilic [(R₃N)BH₂]⁺ borenium cations, or their equivalents, was also possible. Activation of amine borane **19** with [Ph₃C][B(C₆F₅)₄] led to the evolution of H₂ and formation of the *spiro* borenium cation **20** (which was subsequently characterised by X-ray diffraction studies) [49, 57]. A C–H insertion mechanism was proposed proceeding via a four-membered transition state. (Fig. 12). Figure 12 displays the mechanistic pathway assuming monoboron intermediates.

Vedejs and co-workers extended intramolecular aliphatic borylation to other [(NR₃)BH₂]⁺ systems and in internal competition studies determined that the formation of five-membered boracycles is preferred over six membered, whilst the dehydroboration of aromatic and aliphatic C–H bonds was kinetically comparable [49]. Finally, they demonstrated that the replacement of [Ph₃C][B(C₆F₅)₄] with HNTf₂ was possible and that catalytic (in electrophilic activator) aliphatic C–H borylation was also feasible. Braunschweig et al. reported a related intramolecular C–H borylation from the addition of a ^tBu-substituted NHC to BBBr₃ [58]. This rapidly evolved HBr and formed the five-membered boracycle, with the intermediacy of a borenium cation feasible due to ligand steric bulk inducing spontaneous bromide dissociation as previously observed [59]. To date, the dehydroboration of nonactivated aliphatic C–H positions has been limited to the use of highly electrophilic borenium cations (or their functional equivalents). A less remarkable aliphatic intramolecular C–H dehydroboration has been observed starting from **9**, with the addition of a hindered Brønsted base leading to deprotonation of the activated *ortho* methyl group of 2,6-lutidine leading to C–B bond formation and generation of a neutral boracycle [13].

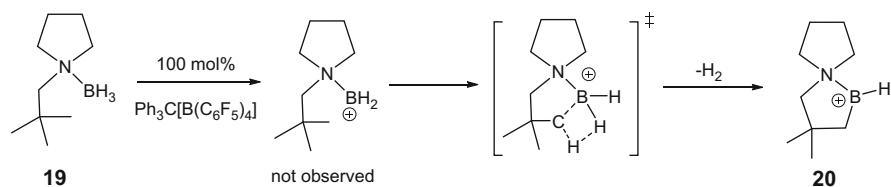


Fig. 12 Intramolecular aliphatic C–H borylation mediated by a borocation

3.3 Intermolecular Electrophilic Aromatic Borylation

The first intermolecular dehydroboration reactions involving borocations or their equivalents came from Muetterties and Lappert [60–63]. Independently, they activated boron trihalides with Lewis acids in arene solvents and observed intermolecular dehydroboration. In both cases, the removal of the Brønsted acidic by-product from S_EAr (either as gaseous HX or as H_2 from the reaction of HX with Al , $X=halide$) was essential [64]. The active boron electrophile(s) was not observed, but two plausible candidates were proposed (Fig. 13, left) [65]. More recently, Ingleson et al. reported that Muetterties-type dehydroborations are viable with hindered amines in place of aluminium as HX scavengers [10]. Furthermore, Wagner and co-workers proposed an analogous intramolecularly activated electrophile **21** in the dehydroboration of arenes [66].

In 2010, Del Grosso and Ingleson activated $CatBCl$ with extremely halophilic silicenium cations partnered with robust weakly coordinating anions and observed intermolecular borylation of arenes, including the deactivated arene *ortho*-dichlorobenzene. The activation of $CatBH$ [17] (or 1-hydrido-1,3,2-benzodiazaboroles) [6] was also reported using trityl salts or the Brønsted superacidic by-product from arene dehydroboration. The latter reaction enabled electrophilic borylation to be catalytic in the initial electrophilic activator with H_2 the only by-product. The active electrophile in each of these reactions was again transient, eluding observation by low-temperature NMR spectroscopy, but related electrophiles to those proposed for the Muetterties/Lappert systems are feasible (Fig. 14, left) [17]. An alternative electrophile where $\{CatB\}^+$ is stabilised by weak interactions with the $[CB_{11}H_6Br_6]^-$ anion is also feasible, and this can be viewed as a masked form of a borinium cation. A related “quasi-borinium” cation, **22**, derived from $[\mu-8,8'-I-3,3'-Co(1,2-C_2B_9H_{10})_2]$ has been proposed by Sivaev and co-workers to be the active electrophile in the dehydroboration of arenes [67, 68]. Other carborane compounds with “naked boron vertices” have been used by Michl et al. to effect the borodesilation of arylsilanes [69].

For the catecholato- and halide-substituted monoboron systems, the active boron electrophile is short-lived preventing its unambiguous characterisation, whilst the extremely Lewis/Brønsted acidic reaction mixtures limited substrate scope [63]. Less electrophilic and more well-defined borocations were subsequently utilised that enabled the expansion of electrophilic arene dehydroboration to heterocycles. These cations included catecholato borenium cations and more

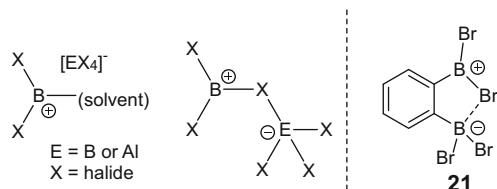


Fig. 13 *Left*, borocation species proposed for Muetterties/Lappert dehydroborations. *Right*, a related boron electrophile proposed by Wagner and co-workers for intermolecular dehydroboration

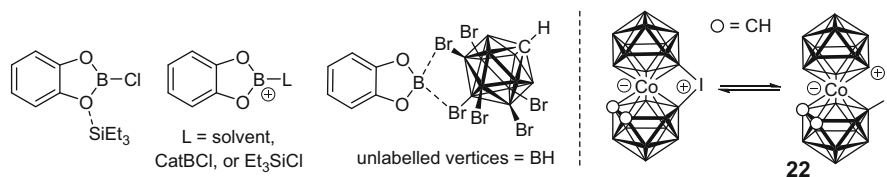


Fig. 14 *Left*, potential boron electrophiles for the intermolecular dehydroboration of arenes using CatBH or CatBCl. *Right*, ring opening of an iodonium cation to generate a "quasi-borinium" cation for arene dehydroboration

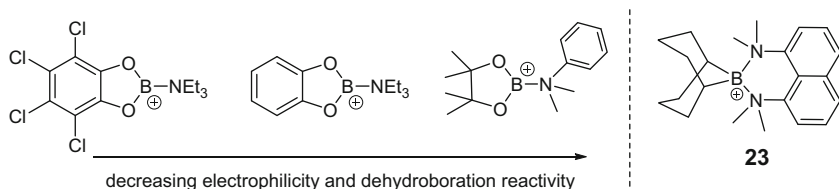


Fig. 15 *Left*, relative reactivity of borenium cations in intermolecular dehydroboration of heteroarenes. *Right*, the boronium cation **23** that dehydroborates activated *N*-heterocycles

electrophilic tetrachlorocatecholato analogues, both generally used as the tetrachloroaluminate salts. As expected based on the lower π donor ability of the aryloxy groups, the tetrachlorocatecholato substituted congener demonstrated an increased arene substrate scope consistent with enhanced electrophilicity at boron (Fig. 15). The solution NMR data and the solid state structure of a tetrachlorocatecholato borenium cation were most consistent with a 3-coordinate boron centre with only weak interactions with the [AlCl₄]⁻ anion [37]. Related amine-ligated pinacolato borenium cations (Fig. 15) did not borylate activated heterocycles, such as *N*-Me-pyrrole, indicating a considerable reduction in electrophilicity at boron towards π nucleophiles on replacing aryloxy for alkoxide substituents. This was confirmed by calculations which revealed that [PinB(NEt₃)]⁺ had an HIA relative to BEt₃ (−23 kcal mol⁻¹) (Unpublished results) considerably lower than the catecholato congener (−43 kcal mol⁻¹).

Concurrently, Vedejs and co-workers synthesised the boronium cation, **23**, from the addition of 1,8-bis(dimethylamino)naphthalene to 9-BBN(NTf₂), with the NTf₂

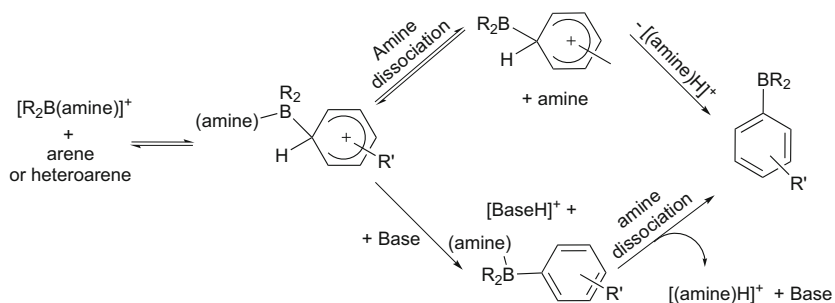


Fig. 17 Mechanisms for the dehydroboration of arenes using $[R_2B(amine)]^+$ varying based on the deprotonation step (R =catecholato or Cl)

$[(pyridine)BCl_2][AlCl_4]$ could be isolated as a solid and crystallographically characterised [71]. *Ortho* disubstituted 2,6-lutidine is particularly effective in reducing the chloride ion affinity of the borenium **9**; therefore, **9** $[AlCl_4]$ is the dominant species on combination of 2,6-lutidine/ BCl_3 and $AlCl_3$. Related equilibria are also present in $[CatB(amine)][AlCl_4]$ as evidenced by low-temperature NMR spectroscopy and reactivity studies [37].

To simplify mechanistic studies, a number of borenium cations were synthesised using robust and weakly coordinating anions, $[CB_{11}H_6Br_6]^-$ and $[B(C_6H_3Cl_2)_4]^-$, that do not participate in any halide transfer equilibria. According to a combined experimental and computational study, the borylation of activated arenes at 20°C proceeds through a S_EAr mechanism with borenium cations as the key electrophiles [10]. For catecholato-borocations, two amine-dependent reaction pathways were identified: (i) with $[CatB(NEt_3)]^+$, an additional base is necessary to accomplish borylation by deprotonation of the borylated arenium cation, which otherwise would rather decompose to the starting materials than liberate the amine from boron to effect deprotonation (Fig. 17, bottom). (ii) When the amine component of the borocation is less nucleophilic (e.g. 2,6-lutidine), no additional base is required due to more facile amine dissociation from the boron centre in the borylated arenium cation intermediate (Fig. 17, top).

Surprisingly, given their high electrophilicity $[Cl_2B(amine)]^+$, borenium cations do not dehydroborate weakly activated arenes (e.g. toluene) to any significant degree even at high temperatures [10]. Instead, the key electrophile for the borylation of less activated arenes is presumably derived from the interaction of $AlCl_3$ with R_2BCl , with the amine fulfilling the roll of proton scavenger. Despite the mechanistic complexity of arene dehydroboration using BCl_3 -derived boreniums or their functional equivalents, it is an attractive one-step methodology for converting C–H to C–B and is complementary in selectivity to iridium-catalysed direct borylation (electronic control versus predominantly steric control) [72].

Recently, Oestreich, Tatsumi and co-workers developed a route to dehydroborate activated heteroarenes directly using pinacol-ligated borenium cations [73]. In contrast to previous studies using amine-ligated pinacol borenium cations that were ineffective for dehydroborations, they used a cationic Ru(II)–SR compound that was bound to $[PinB]^+$ through sulphur. Presumably, the lower

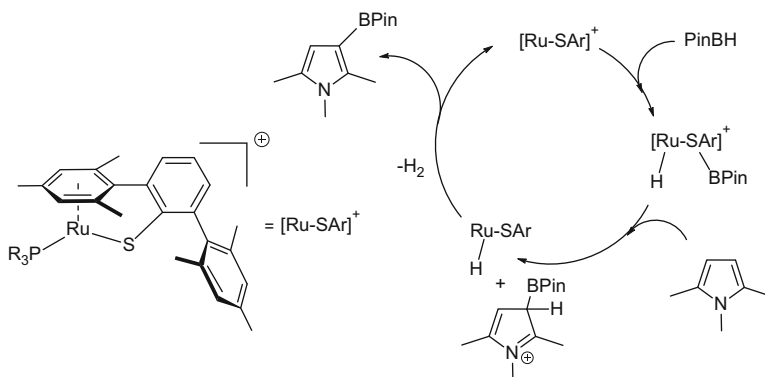


Fig. 18 Catalytic (in cationic ruthenium complex) dehydroboration

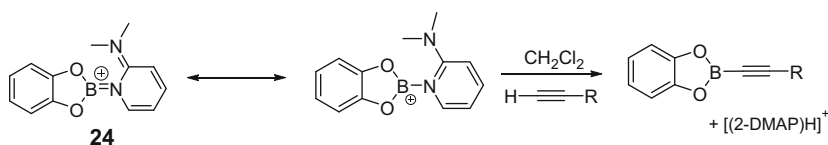


Fig. 19 The dehydroboration of alkynes using borenium cation **24**

nucleophilicity of the cationic Ru–SR moiety relative to the amine Lewis bases previously studied enhances electrophilicity at boron sufficiently to borylate certain activated heteroarenes. It is also noteworthy that borylation is catalytic in the ruthenium complex, with H₂ loss regenerating the key ruthenium complex (Fig. 18), making this an extremely atom-efficient and elegant process. However, the substrate scope reported to date for this process has been limited to highly activated nitrogen heteroarenes, with *N,N*-dimethylaniline and *N*-^{*i*}Pr₃Si-indole not borylated. This indicates that electrophilicity at boron in [PinB(Ru(H)-SR)]⁺ is still significantly lower than the catecholato borenium cations which do borylate these substrates [37].

The expansion of dehydroboration to other unsaturated hydrocarbons is in its infancy. Our laboratory has recently reported [CatB(2-DMAP)][AlCl₄], **24**, which is a borenium cation in the solid state (by X-ray crystallography) and solution (based on δ_{11B}) despite the presence of two nucleophilic nitrogens in 2-DMAP. This can be attributed to O → B π donation and significant B=N double bond character reducing the electrophilicity at boron thereby disfavoring chelation by 2-DMAP. Despite the significant B=N character, **24** is still sufficiently electrophilic to dehydroborate terminal alkynes to produce alkynyl boronic esters (Fig. 19) in moderate to good yields [74]. Whether the pendant NMe₂ basic site plays a role in the deprotonation step is currently unclear, but the related borocation, [CatB(NEt₃)]⁺, only produced alkyne-dehydroborated products in low yields even in the presence of noninteracting bases to effect deprotonation.

4 Borocations in Elemento-Boration

Elemento-boration is the addition of a B–X bond across an unsaturated moiety. Sections 4.1 and 4.2 discuss the borocation analogues of the venerable (with neutral boranes) hydroboration and haloboration reactions.

4.1 Hydroboration

The intermediacy of borenium cations (or their functional equivalents) in hydroboration was first considered by Vedejs and co-workers when studying the reactivity of (L)BH₂X (X=I or OTf, L=amine or phosphine) [75–77]. Importantly, the hydroboration reactivity of the (L)BH₂X species was distinct to that of the free borane, particularly in providing improved regioselectivity. The authors concluded that an S_N2-type process involving concerted attack by the π nucleophile/B–X heterolysis was proceeding. In this case, LBH₂X is therefore a functional equivalent of a borenium rather than a true borenium cation. More recently, this approach was extended by Vedejs, Curran, Lacôte and co-workers to the borenium equivalents (NHC)BH₂NTf₂ and [(Ime)BH₂]₂(μ-H)[NTf₂], **25** (Ime = 1,3-dimethylimidazol-2-ylidene) [78]. In contrast to amine borane adducts, NHCs do not dissociate from boron even under forcing conditions. Therefore, NHC–borane hydroboration is unequivocally due to borenium-type character engendered by the weakly coordinating NTf₂ (or (μ-H) moiety). The product distribution from mono- and di-hydroboration (forming (Ime)B(R)(H)NTf₂ and (Ime)B(R)₂NTf₂, respectively, Fig. 20) of a range of alkenes with these borenium cation equivalents was assessed. Interestingly, hydroboration of a number of internal alkenes resulted in rapid migration and final reaction mixtures in which boron at C2 is the dominant product. In contrast, hydroboration with neutral boranes undergoes slower migration and converges to give primary alkylboranes (boron at C1) [78].

Curran and co-workers subsequently extended this approach to the iodide congener, (Ime)BH₂I. This was more selective for mono-hydroboration and enabled the alkene substrate scope to be expanded [79], particularly towards tri- and tetra-substituted alkenes for which the triflimide analogue gave complex mixtures of products. It is noteworthy that in the presence of excess (Ime)BH₃, the iodide congener (Ime)BH₂I does not react to form **25** confirming the greater coordinating power of iodide versus NTf₂ towards boron. In the same paper, the

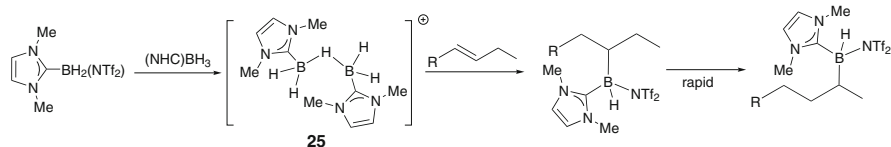


Fig. 20 Hydroboration of alkenes using borenium cation equivalent **25**

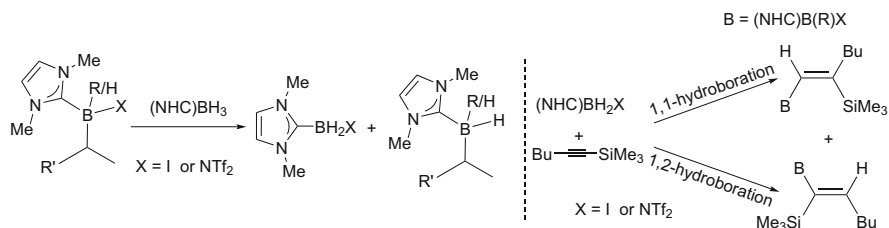


Fig. 21 *Left*, key hydride transfer step in catalytic (in activator) hydroboration. *Right*, 1,1- and 1,2-hydroboration of silyl substituted alkynes

variation of steric bulk on the *N*-substituent of the NHC was investigated, with the most notable effect being bulky aryl groups on nitrogen (mesityl, 2,6-diisopropylbenzene) preventing hydroboration, consistent with an increased barrier for an $\text{S}_{\text{N}}2$ -type process. Hydroboration can be made catalytic in HNtF_2 or I_2 activators (typical loadings are ca. 10 mol%), with a hydride transfer step again key for transferring borenium-type character (Fig. 21 left).

The hydroboration of a range of allyl and alkenyl silanes produced the 1,2 hydroboration products exclusively under stoichiometric and catalytic activation of $(\text{NHC})\text{BH}_3$ with I_2 [80]. The hydroboration of alkynyl silanes was more complex with both syn-1,2- and 1,1-hydroborated products observed (Fig. 21, right). The latter isomer was formed by silicon migration prior to B–H cleavage as it did not form from isomerisation of the 1,2-hydroboration products in the presence of borenium equivalents. 1,1-Hydroboration is related to the “Wrackmeyer reaction” which includes the 1,1-carboboration of alkynyl silanes with BEt_3 [81]. Mesoionic carbene boranes were also effective for the hydroboration of allylbenzene on activation with $[\text{Ph}_3\text{C}][\text{B}(\text{C}_6\text{F}_5)_4]$, presumably proceeding via borenium cations or their functional equivalents [82]. Brunker and co-workers also utilised a borenium cation produced by hydride abstraction, in this case from pentamethylazaferrocene- BH_3 , to hydroborate 1,5-cyclo-octadiene to generate $[\text{pentamethylazaferrocene-}\text{BBN}]^+$ [14]. In contrast to the reactive borenium hydroborating agents discussed above, the B–H containing borenium cation **2** did not hydroborate phenylacetylene, an indication of considerable π delocalisation reducing Lewis acidity towards soft nucleophiles [31]. Finally, the combination of PinBH/THF and $\text{B}(\text{C}_6\text{F}_5)_3$ is essential for hydroboration catalysed by an Rh complex, with a borenium ion intermediate proposed to facilitate the formal oxidative addition of PinBH to Rh [36].

4.2 Other Elemento-Boration Reactions

Haloboration of alkynes using trihaloboranes is well documented but is restricted to terminal alkynes due to limited electrophilicity at boron [83–85]. Calculations on haloboration indicated that increasing electrophilicity at boron results in haloboration becoming more exothermic, and the key transition state barrier also becomes lower in

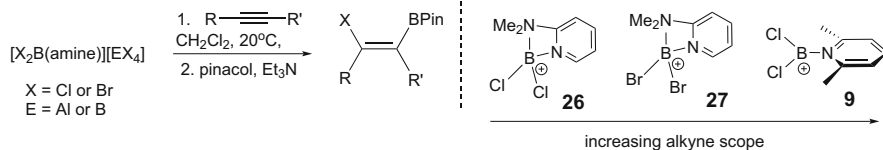


Fig. 22 Haloboration and esterification of alkynes with borenium and boronium cations

energy [86]. Therefore our laboratory investigated the reactivity of alkynes with a series of dihaloborocations, $[X_2B(\text{amine})]^+$ ($X=Cl$ or Br), ligated by 2-DMAP or 2,6-lutidine. $[X_2B(2\text{-DMAP})]^+$ (**26** and **27**, Fig. 22) exist as boronium cations with 2-DMAP a bidentate ligand in contrast to the catechol analogue, **24**. This disparity is presumably due to the lower degree of stabilisation from halide π donation to boron in the ring-opened borenium isomers of **26** and **27** relative to **24** [74]. The chelation of 2-DMAP to boron results in the formation of a significantly strained four-membered boracycle, “consistent with a low calculated barrier to ring opening, was calculated. However, currently, it is not known if $[X_2B(2\text{-DMAP})]^+$ cations react via a borenium cation intermediate or via an S_N2 -type process.

Cation **26** only haloborated terminal alkynes, with 1,2-haloboration the exclusive mode of reaction and the initial $\text{vinyl}BCl_2$ product in situ esterified to the pinacol boronate ester. Increasing the electrophilicity at boron by replacing chloride for bromide increased the scope of 1,2-haloboration, but only to include internal dialkyl alkynes. The use of 2,6-lutidine in place of 2-DMAP increases electrophilicity at boron further, with **9** haloborating a range of internal alkynes. Throughout, haloboration occurred with excellent regio- and stereoselectivity, predominantly controlled by electronic effects. It is noteworthy that attempts to use another boron electrophile highly effective in arene dehydroboration, specifically that derived from $DMT/BCl_3/AlCl_3$, in place of $[(2,6\text{-lutidine})BCl_2][AlCl_4]$ led to complex mixtures with little haloborated product observed. Presumably the different halide transfer equilibrium positions observed when using DMT compared to 2,6-lutidine lead to significant quantities of aluminium Lewis acids which are well documented to react with alkynes to give oligomers/polymers.

Attempts to extend elemento-boration to the carboboration of terminal alkynes using $[Ph(Cl)B(2\text{-DMAP})][AlCl_4]$ led instead to 1,2-haloborated products, with chloride migrating in preference to phenyl. Modification of the substituents on boron to permit only the migration of phenyl was achieved by using the chelating monoanionic ligand, 8-hydroxyquinoline [87]. The borenium cation **28** was accessed in two steps from $PhBCl_2$, whereas the 5-hexylthienyl congener, **29**, was prepared from 5-hexylthiophene using electrophilic dehydroboration to form the thienyl BCl_2 . Both **28** and **29** reacted with the 3-hexyne to give products from 1,2-carboboration (Fig. 23). In contrast, **28** reacted with 1-pentyne to effect alkyne cyclotrimerisation forming 1,3,5-tripropylbenzene. The cyclotrimerisation observed with **28** was attributed to the generation of Lewis acidic “ $AlCl_3$ ” species which rapidly cyclotrimerises terminal alkynes but only slowly cyclotrimerises internal alkynes [88]. The support for the presence of Lewis acidic “ $AlCl_3$ ” species

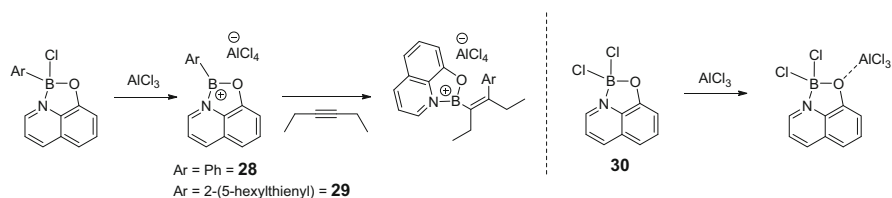


Fig. 23 *Left*, synthesis of borocations **28** and **29** and the 1,2-carbaboration of 3-hexyne. *Right*, coordination of AlCl_3 to oxo functionality instead of the expected mode of reactivity, halide abstraction

was provided by the addition of AlCl_3 to **30** (Fig. 23, right). Instead of boronium cation and $[\text{AlCl}_4]^-$ formation, AlCl_3 interacts with the weakly nucleophilic oxygen. The formation of an $\text{O} \cdots \text{AlCl}_3$ interaction can be disfavoured simply by installing a methyl group *ortho* to oxygen, with the addition of AlCl_3 now forming a boronium cation.

Recently, the remarkable carboboration of CO_2 with a borinium cation has been reported. The dimesityl borinium cation, $[(\text{Mes})_2\text{B}]^+$, **31**, was readily accessed by fluoride abstraction from Mes_2BF with a triethylsilycenium salt. **31** is a linear (at boron) cation stabilised by π donation from the two orthogonally orientated mesityl groups. Cation **31** reacts with CO_2 by 1,2-carbaboration, ultimately forming aroyl cations, $[\text{MesCO}]^+$ and MesBO , with the latter undergoing oligomerisation and further reactions with **31** to give a complex mixture of boron-containing products [89, 90].

5 Borocations in Catalysis

The previous two sections have discussed the chemistry of borocations with a range of nucleophiles that lead to the loss/transfer of one of the substituents originally bound to boron. The final major class of reactions that borocations have been utilised for retains all three substituents on boron throughout with the borocation centre acting as a Lewis acid catalyst or as an intermediate in hydride “shuttling” reactions.

The paradigms of borocations as Lewis acid catalysts come from seminal studies by Corey and co-workers on chiral cations derived from oxazaborolidines. The two major applications are BH_3 -activated oxazaborolidines for chiral hydroborations (the Corey–Bakshi–Shibata reaction, Fig. 24, left) and using AlBr_3 or H^+ activation for catalytic enantioselective cycloadditions (Fig. 24, right). Whilst unambiguous boronium formation is not confirmed by ^{11}B NMR spectroscopy for the majority of these systems, it is clear from reactivity studies that boronium equivalents, if not actual boronium cations, are present in solution (an in-depth discussion on the solution species present in activated oxazaborolidine chemistry is provided by Vedejs and co-workers) [3]. It is noteworthy that oxazaborolidines are both extremely weak

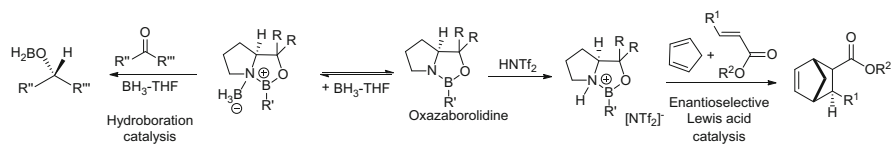


Fig. 24 Oxazaborolidine-derived Lewis acid catalysts for hydroboration and cycloadditions

bases and weak nucleophiles at nitrogen, with Corey and co-workers reporting that there was no significant protonation by methane sulfonic acid and no coordination of AlCl_3 or GaCl_3 observed. Finally, significant reactivity differences are again observed when using $[\text{OTf}]^-$ and $[\text{NTf}_2]^-$ as counterions, with $[\text{OTf}]^-$ giving drastically inferior catalytic activity due to strong coordination of triflate to boron. The considerable body of work in this area is summarised in two reviews by Corey and co-workers, which readers are directed to for further information [8, 91]. Subsequent to these reviews, high-level calculations were reported that support Corey's proposed mechanistic pathways with Lewis or Brønsted acids interacting with nitrogen giving lower energy species and lower barrier processes than the activation of the oxazaborolidines through coordination of acids to oxygen [92, 93].

Concurrently, Yamamoto developed related oxazaborolidines and demonstrated that the most active catalyst was formed by protonating at nitrogen with $\text{C}_6\text{F}_5\text{CH}(\text{SO}_2\text{CF}_3)_2$. This produced a catalyst that outperformed both the HOTf - and HNTf_2 -activated congeners in Diels–Alder reactions. The authors attributed this reactivity trend to the greater steric bulk of the $[\text{C}_6\text{F}_5\text{C}(\text{SO}_2\text{CF}_3)_2]^-$ anion which weakens its coordination to boron relative to $[\text{OTf}]^-$ and $[\text{NTf}_2]^-$ ([94]; [95] and references therein). Finally, catalysis of the allylboration of aldehydes may also proceed via related “borenium-type” intermediates generated from Brønsted/Lewis acid coordination to the oxo functionality present in pinacol allylboronates. This extensive and well-developed area was reviewed in depth in 2011 by Elford and Hall [96]. Furthermore, a detailed discussion of this and other synthetic applications of activated oxazaborolidines has been recently provided by Vedejs and co-workers [3].

The most recent catalytic applications of borenium cations are in the activation of σ bonds, particularly H_2 . The first suggestion that borocations can activate H_2 came from Olah and co-workers who proposed that $[\text{B}_2\text{H}_5]^+$ can reversibly coordinate and cleave H_2 [97]. This area lays unexplored until Vedejs and co-workers heated $13[\text{B}(\text{C}_6\text{F}_5)_4]$ under a D_2 atmosphere and observed H/D exchange concomitant with anion decomposition [7]. Due to the complex/heterogeneous nature of both these examples, H_2 activation by a borocation could not be unambiguously confirmed. Subsequently, Stephan and co-workers unequivocally demonstrated that the borenium cation **8** (Fig. 25, left) activates H_2 in a frustrated Lewis pair (FLP) [40]. Frustrated Lewis pairs use unquenched Lewis acidity/basicity to heterolytically activate H_2 in a concerted manner and have become a highly topical area [34]. Cation **8** forms an FLP with P^tBu_3 due to the combined steric bulk precluding dative bond formation. This FLP when exposed to H_2 (4 atm.)

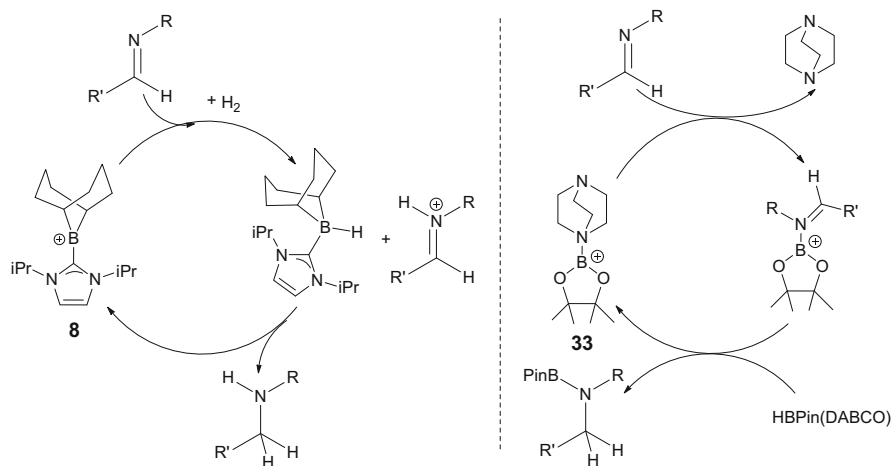


Fig. 25 *Left*, catalytic (in cationic activator) hydrogenation and *right*, hydroboration mediated by borenium cations

heterolytically cleaves H_2 . More significantly, **8** is a catalyst for the hydrogenation of imines and enamines via an FLP mechanism, with a functional group tolerance broader than the ubiquitous neutral borane used for FLP reductions, $\text{B}(\text{C}_6\text{F}_5)_3$. For example, **8** tolerates diarylketones, *ortho*-substituted pyridyls and ethyl benzoates. The lack of reaction between **8** and these oxo functionalities is remarkable given the high Lewis acidity of borocations to hard Lewis bases previously discussed. This is presumably due to the severely sterically congested environment around boron.

Ingleson and co-workers reported two other borocation-based FLPs that were capable of activating H_2 , albeit with competitive reactions observed alongside heterolytic H_2 cleavage [13]. This was followed by the observation that the borenium cation $[(\text{acridine})\text{BCl}_2]^+$, **32**, formed an FLP with hindered pyridines that activated H_2 [98]. Surprisingly, the position of hydride addition to **32** was not at boron, but at the C9 carbon of acridine, consistent with this position being the most Lewis acidic towards hydride by HIA calculations. Concurrent to Stephan's borenium-catalysed hydrogenation work, Crudden and co-workers reported a related reduction (hydroboration followed by hydrolysis of the N–B bond) of imines, nitriles and *N*-heterocycles with HBpin catalysed by $[\text{PinB}(\text{DABCO})]^+$, **33** (Fig. 25, right) [99]. The DABCO Lewis base in the borenium cation is proposed to be displaced by an imine to form $[\text{PinB}(\text{imine})]^+$; however, a boronium, $[\text{PinB}(\text{DABCO})(\text{imine})]^+$, is an alternative intermediate. Regardless, the activated imine is subsequently reduced by HBPin(DABCO), regenerating the borenium cation. Consistent with HIA calculations (the conjugate Lewis acid $[\text{PinB}(\text{amine})]^+$ has a lower HIA than $\text{B}(\text{C}_6\text{F}_5)_3$), HBPin(amine) was found to be a better reductant than $[\text{HB}(\text{C}_6\text{F}_5)_3]^-$. The aldimine substrate scope reduced with $[\text{PinB}(\text{DABCO})]^+$ was greater when compared to hydrogenations using $\text{B}(\text{C}_6\text{F}_5)_3$ containing FLPs, indicating improved functional group tolerance of the borocation relative to $\text{B}(\text{C}_6\text{F}_5)_3$.

Alongside H_2 activation, there is considerable current interest in using boron Lewis acids for the activation of Si–H bonds via B-(μ -H)-Si intermediates [100]. Borocations also form sigma complexes with silanes, with Vedejs and co-workers observing a significant upfield shift in the ^{11}B NMR spectrum for **13** on addition of 1Pr_3SiH [7]. Jäkle and co-workers also reported that the chiral borenium cation **3** interacts with Et_3SiH via B-(μ -H)-Si interactions (as indicated by loss of $^3J_{HH}$ H-Si- CH_2 coupling) and catalyses the hydrosilylation of carbonyls with only modest 20% *ee* [32]. Denmark and co-workers subsequently demonstrated that [9-BBN(2,6-lutidine)] $^+$, **34**, catalysed the hydrosilylation of a range of ketones to silyl ethers [44]. In contrast to the hydrosilylation of ketones with Et_3SiH catalysed by 9-BBN(NTf_2) and $B(C_6F_5)_3$, cation **34** does not catalyse the over reduction of the silyl ether to the alkane under identical conditions. An analogous hydrosilylation mechanism to that elucidated for $B(C_6F_5)_3$ was proposed [101]; this was based in part on the observation that the addition of Et_3SiH to [33][NTf_2] led to the formation of 9-BBN-H and Et_3SiNTf_2 .

6 Miscellaneous Applications of Borocations

6.1 Materials Applications

In 1998, Atwood and co-workers reported the use of a boronium cation that reacted as a masked borenium to initiate the polymerisation of propylene oxide [102]. Since then, one of the major materials applications of borocations is to modify photophysical properties by converting neutral boranes into borenium and boronium cations. Notable examples are the modification of the BODIPY framework independently by the groups of Piers and Gabbai, with the latter demonstrating that a BODIPY boronium cation, **35**, can be used as a switch on fluoride sensor [31]. The use of borocations in this area is discussed in more depth in a number of review articles [3, 5, 103]. More recently, 1,2-azaborine-containing borenium cations, **36** (Fig. 26), have been synthesised that are emissive in the solid state with high quantum yields and narrow emission bands [43]. A subporphyrin

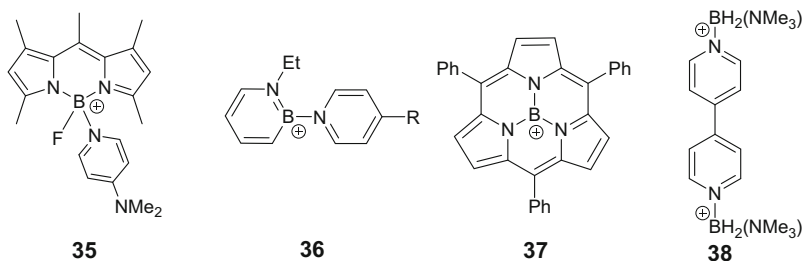


Fig. 26 Select borocations whose photophysical or electrochemical properties have been assessed

borenium cation, **37**, has also been isolated indicating the viability of these species as intermediates in facile boron axial ligand exchange in this class of porphyrinic pigments [104]. The subporphyrin borenium cations were found to have similar absorption and emission spectra to the neutral four coordinates at boron, B-methoxy precursors. Calculations indicate that this is due to a comparable stabilisation of the LUMO+1, LUMO, HOMO and HOMO-1 all by ca. 3.6 eV. Borenium cations have also been demonstrated to be highly emissive, with $[(4\text{-DMAP})_2(9\text{-borafluorene})]^+$ emitting in the blue in halogenated solvents when excited with UV light [105].

A number of boronium-containing polymers were also synthesised [106], with boronium incorporation enabling reversible reduction (by CV) [107], whilst the controlled cleavage of a boron–pyridine bond was used for stoichiometric Brønsted acid–base reactivity [108]. Boronium cations have also been incorporated into ionic liquids to be used as extremely stable electrolytes for lithium batteries [109] and as hypergolic fluids [110]. Finally, Davis Jr. and co-workers have synthesised **38** (Fig. 26), a diboronium dicationic analogue of viologens, and demonstrated its rich redox behaviour indicating its potential as an electroactive material [111]. The nature of related reduced boronium species is discussed further in Sect. 6.2.

6.2 Borocations as Precursors to Borylenes and Boryl Radicals

Borocations have proved to be useful precursors for the synthesis of a range of radicals. For example, 2,2'-bipyridyl (bipy)-ligated boronium cations undergo one-electron reduction to form radicals with the amount of spin density localised on boron that is highly dependent on the other substituents. For example, the radical from one electron reduction of the Lewis acid / base adduct between 2,2'-bipyridine and 9-bora-9,10-dihydroanthracene has significant boron character [112], whilst the calculated Mulliken spin density at boron is only 0.15% for the (2,2'-bipyridyl)BCl₂ radical analogue [113]. A bis-carbene boronium cation, **40**, can be reduced by one and two electrons to give an unusual radical cation (Fig. 27), **41**, and a bis(carbene) borylene, respectively [114]. A related approach was recently utilised by Vidovic

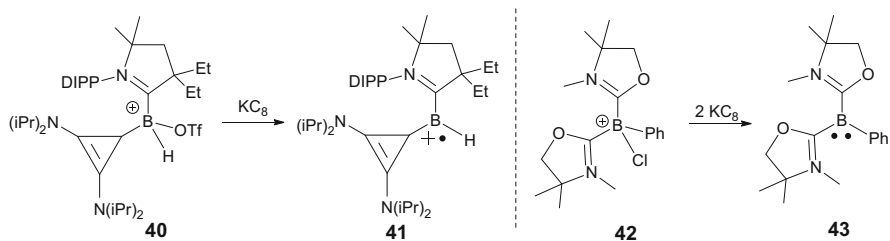


Fig. 27 Reduction of boronium cations to radical cation **41** (*left*) and to the carbene-stabilised borylene **43** (*right*)

and co-workers with the two-electron reduction of boronium cation **42** leading to the bis(oxazol-2-ylidene)borylene, **43**, which can be protonated at boron to form a new boronium cation [115].

Boronium cations also undergo one-electron reductions, and these occur at distinctly more positive potentials than neutral boranes, for example, $[(\text{Mes})_2\text{B}(\text{L})]^+$ ($\text{L} = 4\text{-DMAP}$ and IMe) have $E_{\text{peak}} = -2.03$ V and $E_{1/2} = -1.81$ V, respectively (versus Fc^+/Fc) [114, 115]. The latter can be chemically reduced with magnesium to give a persistent radical that has significant spin density at boron [116, 117].

6.3 Structural Rearrangement of Borocations

Carbocations are well documented to undergo skeletal rearrangements, e.g. 1,2-sigmatropic shifts (Wagner–Meerwein rearrangements), but despite the isoelectronic relationship between carbocations and boronium cations, related conversions in borocations are significantly less common. One example from Braunschweig and co-workers who observed 1,2-halide/mesityl exchange was induced by Lewis base coordination in diborane(4) compounds [118]. This process may involve ionic or zwitterionic borocation intermediates and halide bridge adducts, e.g. **44** (Fig. 28). It is also noteworthy that the replacement of mesityl for NMe_2 leads to the formation of unusual boronium cations based on a diborane(4) backbone, **45** (inset Fig. 28). Himmel and co-workers have also recently synthesised a boronium cation based on a diborane backbone and found that it rapidly undergoes a remarkable B–B coupling reaction to form a tetraborane dication [20].

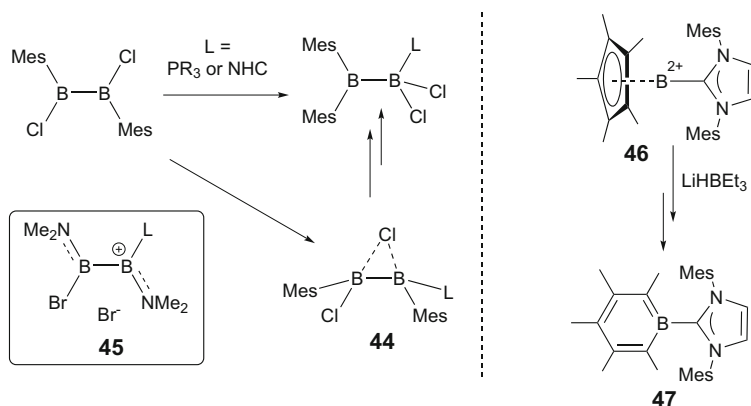


Fig. 28 The inorganic analogue of the Wagner–Meerwein rearrangement (*left*). *Inset bottom left*, a boronium cation based on a diborane(4) backbone. *Right*, the hydride-induced conversion of a dicationic boron compound to an NHC-stabilised borabenzene

A limited number of other structural rearrangements of borocations have also been reported, for example, heating the boronium cation $[\text{B},\text{B}-(N\text{-Me-imidazole})_2(\text{BC}_5\text{H}_5\text{-}2\text{-SiMe}_3)]\text{Cl}$ under vacuum produced the borabenzene complex $\text{B}-(N\text{-methyl-imidazole})\text{BC}_5\text{H}_5$ [119]. The borenium cation $[(\eta^1\text{-C}_5\text{Me}_5)\text{B}(\text{Cl})(\text{IMes})]^+$ undergoes halide abstraction with AlCl_3 to form the dication $[(\eta^5\text{-C}_5\text{Me}_5)\text{B}(\text{IMes})]^{2+}$, **46** (Fig. 28). Subsequent addition of $\text{Li}[\text{HBEt}_3]$ induces the remarkable ring expansion conversion to IMes-stabilised borabenzene, **47** [120].

7 Conclusions and Future Outlook

At the end of 2005 Piers and co-workers predicted that the chemistry of cationic boron compounds was on the verge of a “quantum leap” in activity [2]. This prediction proved prescient with a multitude of synthetic applications using borocations developed over the past 5–6 years. A significant factor in enabling this surge in interest is the considerable versatility of borocations. The myriad of structural permutations for borocations allows for the controlled modulation of electrophilicity and steric environment at boron. This flexibility allows for bespoke borocations to be designed and readily synthesised for targeted applications. For example, the activation of aliphatic C–H bonds requires the extreme electrophilicity of weakly stabilised borocations [49], whilst more functional group-tolerant hydrogenations require combining moderate electrophilicity (to activate H_2) with considerable substituent steric bulk at boron [40]. The structural versatility not only controls key properties but it can also be used to fundamentally alter the reaction pathway followed post combination of a borocation and a nucleophile. This has considerable potential as exemplified by simple structural changes to the borocation enabling selective dehydroboration, haloboration and carboboration of alkynes [74, 87].

Borenium cations are isoelectronic to neutral boranes and carbocations, and Vedejs and co-workers have previously highlighted the similarities and disparities in the fundamental chemistry of carbocations and borenium cations [3]. As synthetic applications of borocations increase, reactivity disparities between neutral boranes and borenium ions are also becoming apparent. Whilst a number of the synthetic applications mentioned throughout this review are conceivable (or have already been reported) with neutral boranes, a considerable proportion require the unique properties of borocations. Most examples require the enhanced electrophilicity of borocations which can surpass that of the neutral boranes BBr_3 and $\text{B}(\text{C}_6\text{F}_5)_3$. This is demonstrated in the intermolecular dehydroboration of arenes, a reaction that utilises two components of the borocation in distinct steps: (i) the strongly Lewis acidic borocation forms the borylated arenium cation and (ii) the evolved Brønsted base acts as a proton scavenger [10]. Related dehydroborations using neutral boranes (particularly $\text{B}(\text{C}_6\text{F}_5)_3$)/noninteracting base combinations are known but are much more limited in arene scope [121]. In addition to the dramatic reactivity differences derived from extremely electrophilic borocations, there are

also more subtle distinctions emerging between the chemistry of neutral boranes and borocations (or their equivalents). One notable example is the alkene hydroboration product distribution observed by Vedejs and Curran and co-workers; with borenium equivalents, this results in predominantly C2-borylated hydroboration products after migration, whereas neutral boranes lead to C1-borylated hydroboration products post migration [78, 79].

The advances discussed herein highlight the burgeoning utility of borocations in synthesis, but this field is still in its infancy. Simply defining the reactivity of borocations towards π nucleophiles other than arenes and alkynes is in itself a vast research area, whilst the ability to activate sigma bonds opens up a multitude of possibilities, both stoichiometric and catalytic in borocation. Furthermore, the recent development of a simple route to the highly electrophilic borinium cation, $[(\text{Mes})_2\text{B}]^+$, and the subsequent unusual reactivity with CO_2 suggests that even the most reactive member of the borocation family, the borinium, is poised for wider exploitation [89]. In comparison to synthetic applications, the incorporation of borenium and boronium ions into functional materials is less developed and opportunities abound in using the unique properties of borocations to produce desirable photophysical properties. Consequently, the next decade should see a continuation of the recent “quantum leap” in activity and see borocations assume a place alongside neutral boranes as widely used reagents and catalysts, rather than simply being niche reagents and curiosities.

References

1. Koelle P, Nöth H (1985) *Chem Rev* 85:399
2. Piers WE, Bourke SC, Conroy KD (2005) *Angew Chem Int Ed* 44:5016
3. De Vries TS, Prokofjevs A, Vedejs E (2012) *Chem Rev* 116:4246
4. Bissinger P, Braunschweig H, Damme A, Dewhurst RD, Kraft K, Kramer T, Radacki K (2013) *Chem Eur J* 19:13402
5. Wade CR, Broomsgrove AEJ, Aldridge S, Gabbai FP (2010) *Chem Rev* 132:3958
6. Solomon SA, Del Grosso A, Clark ER, Bagutski V, McDouall JJW, Ingleson MJ (2012) *Organometallics* 31:1908
7. De Vries TS, Prokofjevs A, Harvey JN, Vedejs E (2009) *J Am Chem Soc* 131:14679
8. Corey EJ (2009) *Angew Chem Int Ed* 48:2100
9. Ryschkewitsch GE, Wiggins JW (1979) *J Am Chem Soc* 92:1790
10. Bagutski V, Del Grosso A, Ayuso Carrillo J, Cade IA, Helm MD, Lawson JR, Singleton PJ, Solomon SA, Marcelli T, Ingleson MJ (2013) *J Am Chem Soc* 135:474
11. Brahmi MM, Malacria M, Curran DP, Fensterbank L, Lacôte E (2013) *Synlett* 24:1260
12. Vedejs E, Nguyen T, Powell DR, Schrimpf MR (1996) *Chem Commun* 2721
13. Clark ER, Del Grosso A, Ingleson MJ (2013) *Chem Eur J* 19:2462
14. Bentivegna B, Mariani CI, Smith JR, Ma S, Rheingold AL, Brunker TJ (2014) *Organometallics* 33:2820
15. Saito M, Matsumoto K, Fujita M, Minoura M (2014) *Heteroatom Chem* 25:354–360
16. Reed CA (1998) *Acc Chem Res* 31:325
17. Del Grosso A, Muryn CA, Pritchard RG, Ingleson MJ (2010) *Organometallics* 29:241

18. Muthaiah S, Do DCH, Ganguly R, Vidovic D (2013) *Organometallics* 32:6718
19. McArthur D, Butts CP, Lindsay DM (2011) *Chem Commun* 47:6650
20. Litters S, Kaifer E, Enders M, Himmel HJ (2013) *Nat Chem* 5:1029
21. Prokofjevs A, Kampf JW, Solovyev A, Curran DP, Vedejs E (2013) *J Am Chem Soc* 135:15686
22. Hayashi Y, Segawa Y, Yamashita M, Nozaki K (2011) *Chem Commun* 47:5888
23. Wang Y, Abraham MY, Gillard RJ, Sexton DR, Wei P, Robinson GH (2013) *Organometallics* 32:6639
24. De Vries TS, Vedejs E (2007) *Organometallics* 26:3079
25. Del Grosso A, Helm MD, Solomon SA, Caras Quintero D, Ingleson MJ (2011) *Chem Commun* 47:12459
26. Reichardt C, Welton TE (2010) *Solvents and solvent effects in organic chemistry*, 4th edn. Wiley, Weinheim
27. Sivaev IB, Bregadze VI (2014) *Coord Chem Rev* 270:75
28. Krossing I, Raabe I (2004) *Angew Chem Int Ed* 43:2066
29. Beckett MA, Brassington DS, Coles SJ, Hursthouse MB (2000) *Inorg Chem Commun* 3:530
30. Childs RF, Mulholland DL, Nixon A (1982) *Can J Chem* 60:801
31. Bonnier C, Piers WE, Parvez M Sorensen, TS (2008) *Chem Commun* 4593
32. Chen J, Lalancette RA, Jäkle F (2013) *Chem Commun* 49:4893
33. Prokofjevs A (2012) DPhil Thesis, University of Michigan
34. Erker G, Stephan DW (eds) (2013) *Frustrated Lewis pairs: uncovering and understanding*. Springer, Berlin
35. Dureen MA, Lough A, Gilbert TM, Stephan DW (2008) *Chem Commun* 4303
36. Lata CJ, Crudden CM (2009) *J Am Chem Soc* 132:131
37. Del Grosso A, Singleton PJ, Muryn CA, Ingleson MJ (2011) *Angew Chem Int Ed* 50:2102
38. Ines B, Patil M, Carreras J, Goddard R, Thiel W, Alcarazo M (2011) *Angew Chem Int Ed* 50:8400
39. Chen WC, Lee CY, Lin BC, Hsu YC, Shen JS, Hsu CP, Yap GPA, Ong TG (2014) *J Am Chem Soc* 136:914
40. Farrell JM, Hatnean JA, Stephan DW (2012) *J Am Chem Soc* 134:15728
41. Erhardt S, Frenking G (2006) *Chem Eur J* 12:4620
42. Bessac F, Frenking G (2003) *Inorg Chem* 42:7990
43. Marwitz AJV, Jenkins JT, Zakharov LV, Liu SY (2010) *Angew Chem Int Ed* 49:7444
44. Denmark SE, Ueki Y (2013) *Organometallics* 32:6631
45. Solovyev A, Geib SJ, Lacôte E, Curran DP (2012) *Organometallics* 31:54
46. Genaev AM, Nagy SM, Salnikov GE, Shubin VG (2000) *Chem Commun* 1587
47. Hurd DT (1948) *J Am Chem Soc* 70:2053
48. Goldfuss B, Knochel P, Bromm LO, Knapp K (2000) *Angew Chem Int Ed* 39:4136
49. Prokofjevs A, Jermaks J, Borovika A, Kampf JW, Vedejs E (2013) *Organometallics* 32:6701
50. Ishida N, Moriya T, Goya T, Murakami M (2010) *J Org Chem* 75:8709
51. Niu L, Yang H, Wang R, Fu H (2012) *Org Lett* 14:2618
52. Zhao Z, Chang Z, He B, Chen B, Deng C, Lu P, Qiu H, Tang BZ (2013) *Chem Eur J* 19:11512
53. Cazorla C, De Vries TS, Vedejs E (2013) *Org Lett* 15:984
54. Chen J, Lalancette RA, Jäkle F (2013) *Organometallics* 32:5483
55. Hatakeyama T, Hashimoto S, Seki S, Nakamura M (2011) *J Am Chem Soc* 133:18614
56. Hatakeyama T, Hashimoto S, Oba T, Nakamura M (2012) *J Am Chem Soc* 134:19600
57. Prokofjevs A, Vedejs E (2011) *J Am Chem Soc* 133:20056
58. Bissinger P, Braunschweig H, Damme A, Dewhurst RD, Kupfer T, Radacki K, Wagner K (2011) *J Am Chem Soc* 133:19044
59. Mansaray HB, Rowe ADL, Phillips N, Niemeyer J, Kelly M, Addy DA, Bates JI, Aldridge S (2011) *Chem Commun* 47:12295
60. Bujwid ZJ, Gerrard W, Lappert MF (1959) *Chem Ind* 1091
61. Muetterties EL (1959) *J Am Chem Soc* 81:2597

62. Muetterties EL (1960) *J Am Chem Soc* 82:4163
63. Muetterties EL, Tebbe FN (1968) *Inorg Chem* 7:2663
64. Ingleson MJ (2012) *Synlett* 23:1411
65. Olah GA (1993) *Angew Chem Int Ed* 32:767
66. Reus C, Weidlich S, Bolte M, Lerner HW, Wagner M (2013) *J Am Chem Soc* 135:12892
67. Bregadze VI, Kosenko ID, Lobanova IA, Starikova ZA, Godovikov IA, Sivaev IB (2010) *Organometallics* 29:5366–5372
68. Kosenko ID, Lobanova IA, Godovikov IA, Starikova ZA, Sivaev IB (2012) *J Organomet Chem* 721:70
69. Zharov I, Havlas Z, Orendt AM, Barich DH, Grant DM, Fete MG, Michl J (2006) *J Am Chem Soc* 128:6089
70. Prokofjevs A, Kampf JW, Vedejs E (2011) *Angew Chem Int Ed* 50:2098
71. Del Grosso A, Clark ER, Montoute N, Ingleson MJ (2012) *Chem Commun* 48:7589
72. Mkhaldid IAI, Barnard JH, Marder TB, Murphy JM, Hartwig JF (2010) *Chem Rev* 110:890
73. Stahl T, Muther K, Ohki Y, Tatsumi K, Oestreich M (2013) *J Am Chem Soc* 135:10978
74. Lawson JR, Clark ER, Cade IA, Solomon SA, Ingleson MJ (2013) *Angew Chem Int Ed* 52:7518
75. Scheideman M, Shapland P, Vedejs E (2003) *J Am Chem Soc* 125:10502
76. Clay JM, Vedejs E (2005) *J Am Chem Soc* 127:5766
77. Scheideman M, Wang G, Vedejs E (2008) *J Am Chem Soc* 130:8669
78. Prokofjevs A, Boussonnière A, Li L, Bonin H, Lacôte E, Curran DP, Vedejs E (2012) *J Am Chem Soc* 134:12281
79. Pan X, Boussonniere A, Curran DP (2013) *J Am Chem Soc* 135:14433
80. Boussonniere A, Pan X, Geib SJ, Curran DP (2013) *Organometallics* 32:7445
81. Wrackmeyer B (1995) *Coord Chem Rev* 145:125
82. Freitas LBO, Eisenberger P, Crudden CM (2013) *Organometallics* 32:6635
83. Lappert MF, Prokai B (1964) *J Organomet Chem* 1:384
84. Wrackmeyer B (1986) *Polyhedron* 5:1709
85. Yao ML, Reddy MS, Zeng W, Hall K, Walfish I, Kabalka GW (2009) *J Org Chem* 74:1385
86. Wang C, Uchiyama M (2012) *Eur J Org Chem* 6548
87. Cade IA, Ingleson MJ (2014) *Chem Eur J* 20:12874
88. Schafer W, Hellmann H (1967) *Angew Chem Int Ed* 6:518
89. Shoji Y, Tanaka N, Mikami K, Uchiyama M, Fukushima T (2014) *Nat Chem* 6:498
90. Reus C, Wagner M (2014) *Nat Chem* 6:466
91. Corey EJ (2002) *Angew Chem Int Ed* 41:1650
92. Sakata K, Fujimoto H (2013) *J Org Chem* 78:3095
93. Paddon-Row MN, Anderson CD, Houk KN (2009) *J Org Chem* 74:861
94. Payette JN, Yamamoto H (2007) *J Am Chem Soc* 129:9536
95. Payette JN, Yamamoto H (2009) *Angew Chem Int Ed Engl* 48:8060
96. Hall DG (2011) *Boronic acids: preparation and applications in organic synthesis, medicine and materials*, 2nd edn. Wiley-VCH, Weinheim
97. Olah GA, Aniszfeld R, Surya-Prakash GK, Williams RE, Lammertsma K, Guner OF (1988) *J Am Chem Soc* 110:7885
98. Clark ER, Ingleson MJ (2013) *Organometallics* 32:6712
99. Eisenberger P, Bailey AM, Crudden CM (2012) *J Am Chem Soc* 134:17384
100. Piers WE, Marwitz AJV, Mercier LG (2011) *Inorg Chem* 50:12252
101. Rendler S, Oestreich M (2008) *Angew Chem Int Ed* 47:5997
102. Wei P, Atwood DA (1998) *Inorg Chem* 37:4934
103. Hudnall TW, Chiu CW, Gabbai FP (2009) *Acc Chem Res* 42:388
104. Tsurumaki E, Hayashi S, Tham FS, Reed CA, Osuka A (2013) *J Am Chem Soc* 133:11956
105. Berger CJ, He G, Merten C, McDonald R, Ferguson MJ, Rivard E (2014) *Inorg Chem* 53:1475
106. Cui C, Jäkle F (2009) *Chem Commun* 2744

107. Cui C, Heilmann-Brohl J, Perucha AS, Thomson MD, Roskos HG, Wagner M, Jäkle F (2010) *Macromolecules* 43:5256
108. Wiggins KM, Hudnall TW, Tennyson AG, Bielawski CW (2011) *J Mater Chem* 21:8355
109. Ruther T, Huynh TD, Huang J, Hollenkamp AF, Salter EA, Wierzbicki A, Mattson K, Lewis AJHD (2010) *Chem Mater* 22:1038
110. Wang K, Zhang Y, Chand D, Parrish DA, Shreeve JM (2012) *Chem Eur J* 18:16931
111. Dorman SC, O'Brien RA, Lewis AT, Salter EA, Wierzbicki A, Hixon PW, Sykora RE, Mirjafari A, Davis JH (2011) *Chem Commun* 47:9072
112. Wood TK, Piers WE, Keay BA, Parvez M (2009) *Chem Commun* 5147
113. Mansell SM, Adams CJ, Bramham G, Haddow MF, Kaim W, Norman NC, McGrady JE, Russell CA, Udeen SJ (2010) *Chem Commun* 5070
114. Ruiz DA, Melaimi M, Bertrand G (2014) *Chem Commun* 50:7837
115. Kong L, Li Y, Ganguly R, Vidovic D, Kinjo R (2014) *Angew Chem Int Ed* 53:9280
116. Matsumoto T, Gabbai FP (2009) *Organometallics* 28:4252
117. Chiu CW, Gabbai FP (2008) *Organometallics* 27:1657
118. Braunschweig H, Damme A, Dewhurst RD, Kramer T, Kupfer T, Radacki K, Siedler E, Trumpp A, Wagner K, Werner C (2013) *J Am Chem Soc* 135:8702
119. Cade IA, Hill AF (2012) *Organometallics* 31:2112
120. Shen CT, Liu YH, Peng SM, Chiu CW (2013) *Angew Chem Int Ed* 52:13293
121. Focante F, Mercandelli P, Sironi A, Resconi L (2006) *Coord Chem Rev* 250:170

Asymmetric Catalytic Borylation of α,β -Unsaturated Acceptors

Sumin Lee and Jaesook Yun

Contents

1	Introduction	74
2	Asymmetric β -Borylation with Transition Metal Catalysts	74
2.1	Cu-Catalyzed β -Borylation	74
2.2	Rh-Catalyzed β -Borylation	84
2.3	Ni- and Pd-Catalyzed β -Borylation	85
3	Asymmetric β -Borylation with Organocatalysts	86
4	Asymmetric β -Borylation in Water	88
5	Conclusions	91
	References	91

Abstract Asymmetric β -borylation (conjugate borylation) of α,β -unsaturated acceptors allows the efficient synthesis of chiral organoboron compounds bearing extra functional groups. In the last 8 years, impressive progress has been made regarding this reaction since the first asymmetric report. While copper catalysis has dominated the field of asymmetric borylation due to its high reactivity and selectivity, various metal-catalyzed and metal-free methods have also been developed. The present chapter covers recent developments in asymmetric borylation of α,β -unsaturated compounds while focusing on the substrate scope and enantioselectivity of each catalytic system. In addition, recent achievements of asymmetric borylation conducted in water are briefly presented.

Keywords Borylation • Catalysis • Enantioselectivity • α,β -Unsaturated compounds

S. Lee • J. Yun (✉)

Department of Chemistry and Institute of Basic Science, Sungkyunkwan University, Suwon 440-746, South Korea

e-mail: jaesook@skku.edu

© Springer International Publishing Switzerland 2015

E. Fernández, A. Whiting (eds.), *Synthesis and Application of Organoboron Compounds*, Topics in Organometallic Chemistry 49, DOI 10.1007/978-3-319-13054-5_3

73

1 Introduction

The asymmetric β -borylation (conjugate borylation) of α,β -unsaturated acceptors involves conjugate addition of a nucleophilic boryl moiety to the β -carbon. This reaction allows efficient synthesis of chiral organoboron compounds with extra functionality. The reaction has received increased attention in recent years and has become a useful tool for preparing chiral organoboron derivatives, which are versatile intermediates in organic synthesis. Various catalytic processes for borylation have been developed with a large variety of acceptors and catalysts based on transition metals and organocatalysts.

Marder, Norman and co-workers provided the initial report of racemic β -borylation carried out with Pt in 1997 [1]. Other groups subsequently introduced racemic β -borylation using Cu (2000) [2, 3] and Rh (2002) [4] catalytic systems. However, an asymmetric variant of the reaction did not appear until Yun's report in 2006 [5], which expanded the substrate scope under copper catalysis in the presence of methanol and included the first example of asymmetric β -borylation of an α,β -unsaturated nitrile. A more detailed study of the asymmetric β -borylation of α,β -unsaturated esters and nitriles was reported in 2008 by the same group [6]. Various asymmetric β -borylation reactions have followed since then, with the use of other transition metal catalysts including Rh, Ni, and Pd. Copper is by far the most frequently employed and extensively studied metal in borylation because it is an inexpensive and less toxic metal source. Asymmetric β -borylation reactions in water and 1,6-borylation of extended Michael acceptors have recently been reported with copper catalysts as well.

On the other hand, transition-metal-free, organocatalytic asymmetric β -borylation methodologies have been developed by Fernández [7] and Hoveyda [8]. These methods use chiral phosphines and *N*-heterocyclic carbenes (NHCs), respectively, as chiral additives.

This chapter covers recent developments in the asymmetric borylation of α,β -unsaturated compounds while focusing on the substrate scope and enantioselectivity of each catalytic system. In addition, recent achievements of asymmetric borylation in water are briefly presented.

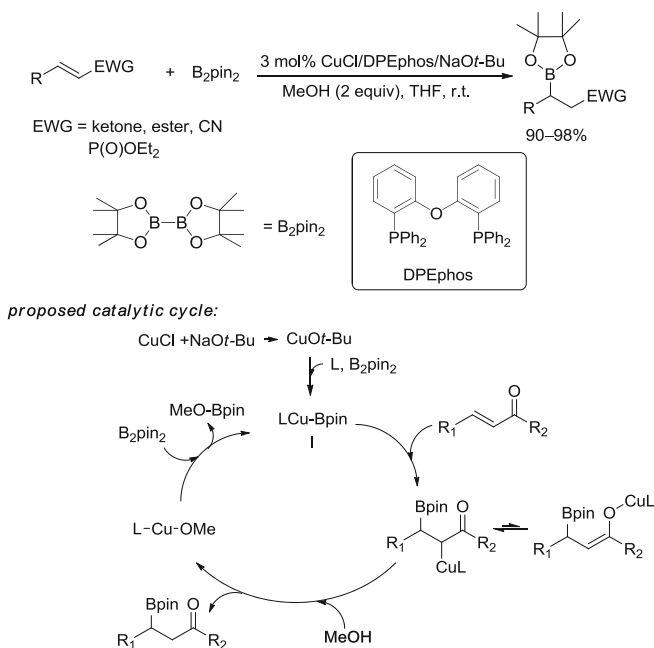
2 Asymmetric β -Borylation with Transition Metal Catalysts

2.1 *Cu-Catalyzed β -Borylation*

In 2000, the Hosomi and Miyaura groups independently reported copper-catalyzed borylation of α,β -unsaturated carbonyl compounds with bis(pinacolato)diboron (B_2pin_2) [2, 3]. In their seminal work, Hosomi and co-workers reported that a catalytic combination of $Cu(OTf)$ (OTf = trifluoromethanesulfonyl) and tri-*n*-

butylphosphine was effective for borylation of α,β -unsaturated ketones [2]. The use of tri-*n*-butylphosphine greatly improved the reaction to give β -borylated products in good yields, whereas reactions with no ligand or with a bidentate phosphine, dppp (dppp = 1,3-bis(diphenylphosphino)propane), did not afford the desired products. At the same time, Miyaura and co-workers reported a similar copper-promoted addition of bis(pinacolato)diboron to α,β -unsaturated ketones, esters, and nitriles using a stoichiometric amount of CuCl/LiCl and KOAc [3]. A catalytic version of this reaction soon followed from the same group, but this catalytic reaction was possible only for α,β -unsaturated ketones, similar to Hosomi's report [9]. Miyaura et al. also proposed a copper-boryl species as an active nucleophilic boron source in the β -borylation reaction. The contributions of Hosomi and Miyaura set the stage for the development of copper-catalyzed borylation reactions, but the insufficient activity of their catalytic systems limited their applicability. Moreover, the inactivity of the bidentate phosphine–Cu(OTf) catalyst implied that the development of enantioselective β -borylation would be challenging.

Yun and co-workers made a major advance in this area in 2006 [5]. In their report, the addition of alcohol dramatically accelerated copper-catalyzed β -borylation, expanding the substrate scope to a variety of α,β -unsaturated acceptors. α,β -Unsaturated esters, nitriles, and hindered enones were reacted to produce the corresponding β -boryl compounds in high yields (>90%) at room temperature in the presence of a copper–bidentate phosphine catalyst (Scheme 1). The first enantioselective β -borylation example with cinnamitrile is included in this



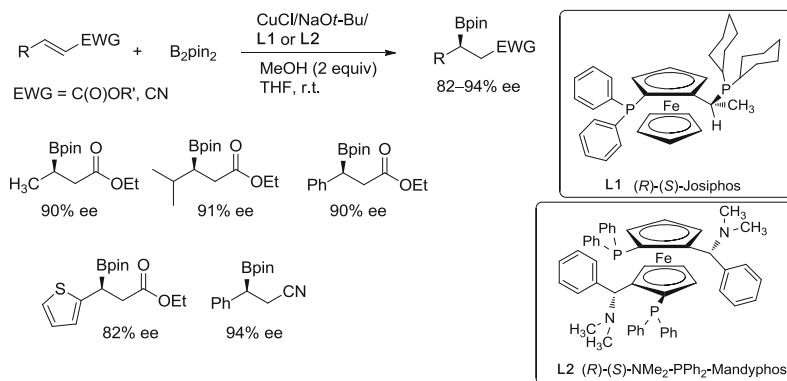
Scheme 1 Methanol-promoted, Cu-catalyzed β -borylation of α,β -unsaturated acceptors

contribution. A phosphine-bound copper-boryl species (**I**) is proposed as the active catalytic species in β -borylation. Its addition to an α,β -unsaturated carbonyl substrate produces an alkyl copper-enolate intermediate that is cleaved by methanol to generate a copper alkoxide and the protonated product. The copper alkoxide regenerates the active copper-boryl catalyst by reaction with the diboron reagent (Scheme 1). Theoretical calculations by Marder et al. supported Yun's proposed mechanism [10]. Marder et al. elucidated that a 3,4-addition of Cu–B to the substrate occurs with subsequent isomerization to the *O*-copper enolate. This provides a pathway for facile σ -bond metathesis with the diboron reagent, as is true for enones. Such isomerization does not occur for α,β -unsaturated esters, and thus, protonolysis of the C-bound copper enolate by an alcohol is necessary because of a low activation energy barrier.

2.1.1 β -Monosubstituted Acyclic Substrates

Although the conditions developed by Yun and co-workers resulted in greatly enhanced reaction rates, the alcohol additive can cause nonselective background reactions via copper species noncoordinated by the chiral ligand. The use of optimal ligands with high binding affinities for copper and high selectivities is necessary to achieve high enantioselectivities.

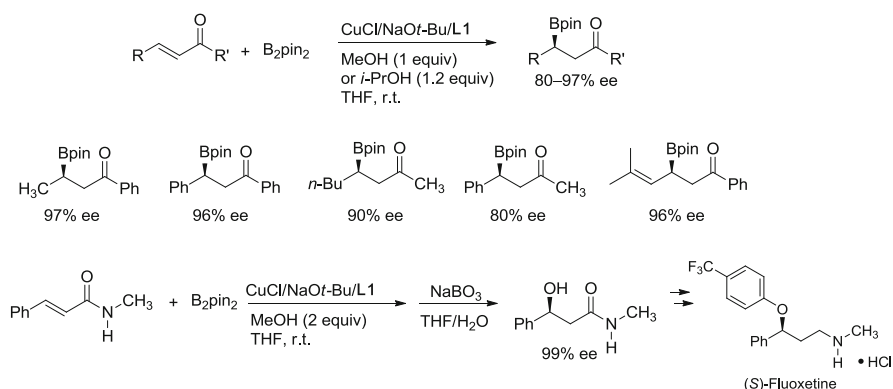
In 2008, Yun and co-workers reported a general enantioselective protocol for β -borylation using a CuCl/NaOt-Bu/bisphosphine catalytic combination for a variety of acyclic α,β -unsaturated esters and nitriles in the presence of 2 equiv. of methanol [6]. Of the studied substrates, ligand screening demonstrated that Josiphos-type ligand **L1** and Mandyphos **L2** were optimal, since Cu(I) modified with these ligands gave products in 82–94% *ee* (Scheme 2). The catalysts were not very sensitive to the β -substituent (i.e., alkyl or aryl) or to the ester moiety of substrates, resulting in similar *ee* values.



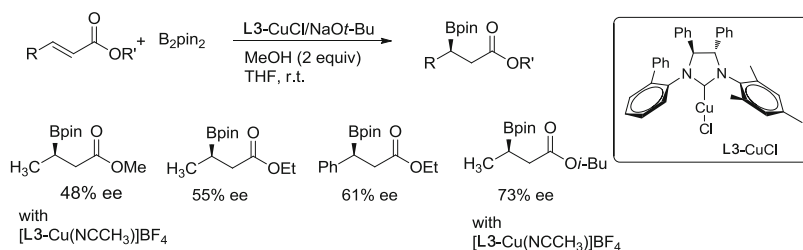
Scheme 2 Phosphine (**L1**)–Cu-catalyzed enantioselective β -borylation of α,β -unsaturated esters and nitriles

Subsequent reports demonstrated that Cu(I) modified with Josiphos (**L1**) was also an optimal catalytic system for the enantioselective β -borylation of acyclic β -monosubstituted enones [11] and amides [12] (Scheme 3). β -Borylation of acyclic enones was carried out with 1 equiv. of methanol or with bulkier isopropanol to reduce nonselective background reactions that deteriorate *ee* values. Using Cu(I)–**L1**, enantioselectivities up to 97% *ee* were observed for a range of acyclic enones. The catalysts accommodated structural variation of β - and α' -substituents of acyclic enones. Enantioselective borylation of α,β -unsaturated amides was investigated using a similar method, and the utility of borylated amide products was demonstrated by formal synthesis of (*S*)-fluxetine.

N-Heterocyclic carbene (NHC) ligands are strong σ -donors and have replaced phosphine ligands in many transition-metal-catalyzed transformations [13–15]. Due to their strong affinity for metals, chiral NHCs are good candidate ligands for asymmetric β -borylation. In 2009, Fernández and co-workers reported that chiral NHC–copper catalysts can perform the β -borylation of α,β -unsaturated esters and cinnamaldehyde [16]. The reactions generally proceeded to good conversion with either **L3**–CuCl or **L3**–[Cu(NCCH₃)]BF₄ as precatalyst, in the presence of methanol, but only modest enantioselectivities were observed (Scheme 4). Among



Scheme 3 Phosphine (**L1**)–Cu-catalyzed enantioselective β -borylation of α,β -unsaturated ketones and amides

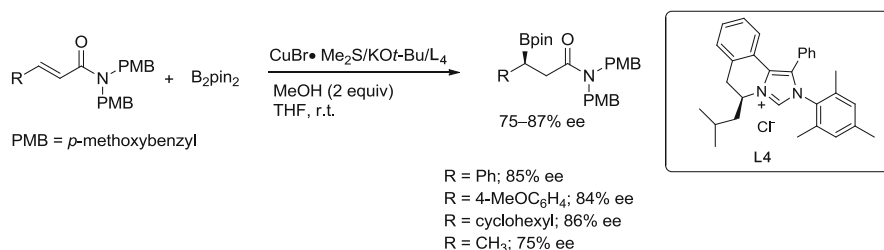


Scheme 4 NHC (**L3**)–Cu-catalyzed enantioselective β -borylation of α,β -unsaturated esters

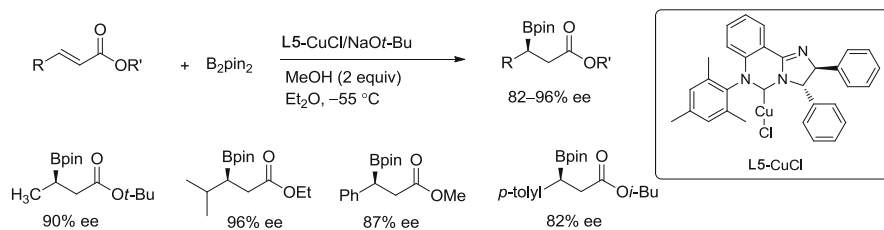
the crotonate series, the highest *ee* (73%) was obtained with bulky isobutyl crotonate ($R = \text{CH}_3$). A range of α -methyl α,β -unsaturated esters proceeded to high conversion as well, but moderate *syn/anti*-ratios and *ee* values were reported. The same group assessed the efficiency of axially chiral *P,N*-type ligands in borylation and found that quinap–CuCl catalyst [(*S*)-quinap = (*S*)-1-(2-diphenylphosphino-1-naphthyl)-isoquinoline] gave the best results from isobutyl crotonate, forming the product in 79% *ee* [17].

Several chiral NHCs with different scaffolds have been synthesized and tested in Cu(I)-catalyzed asymmetric β -borylation since the report by Fernández et al. NHC–Cu catalysts are generally reactive enough to cover less electrophilic unsaturated esters and amides. In 2010, Hong and co-workers reported the β -borylation of α,β -unsaturated amides using isoquinoline-based chiral diaminocarbene (**L4**) as a ligand [18]. The new isoquinoline-based NHC–Cu catalyst displayed good enantioselectivities for borylation of *N,N*-di(*p*-methoxybenzyl)amides, but the catalyst resulted in decreased enantioselectivities (53–78% *ee*) for nitrile, ester, Weinreb amide, and dialkyl amide derivatives of cinnamic acid (Scheme 5).

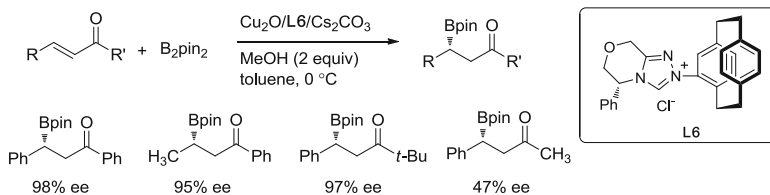
MaQuade and co-workers also reported that a chiral 6-membered NHC–copper complex (**L5**–CuCl) is effective for the β -borylation of α,β -unsaturated esters (Scheme 6) [19]. The catalyst was highly active for esters, and its selectivity was optimized at -55°C . The catalyst was sensitive to the ester moiety and β -substituent, giving methyl cinnamate in the highest *ee* (87% *ee*) among a series of cinnamates ($R = \text{Ph}$, $R' = \text{methyl, ethyl, isobutyl}$). The opposite trend was observed for the crotonate series, in which bulky *tert*-butyl crotonate gave the



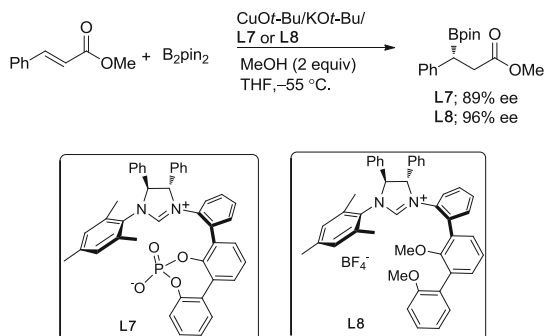
Scheme 5 NHC (**L4**)–Cu-catalyzed enantioselective β -borylation of α,β -unsaturated amides



Scheme 6 NHC (**L5**)–Cu-catalyzed enantioselective β -borylation of α,β -unsaturated esters



Scheme 7 NHC (**L6**)–Cu-catalyzed enantioselective β -borylation of α,β -unsaturated ketones



Scheme 8 NHC–Cu-catalyzed enantioselective β -borylation of methyl cinnamate

best result (90% *ee*). Other substrate types, such as amides and ketones, were not investigated with the same catalyst.

A new triazolium-based chiral NHC ligand was developed by Song et al. and employed for the enantioselective β -borylation of enones [20]. The carbene–copper complex generated in situ by the reaction of triazolium salt (**L6**) and Cu_2O produced β -boryl ketones in high yields and enantioselectivities up to 99% *ee* at 0°C (Scheme 7). The catalyst worked well for a range of aryl ketones ($\text{R}' = \text{Ar}$), including chalcone ($\text{R}, \text{R}' = \text{Ph}$), with excellent enantioselectivities up to 98% *ee*. However, the reaction of methyl ketone ($\text{R}' = \text{CH}_3$) resulted in a product with low enantioselectivity.

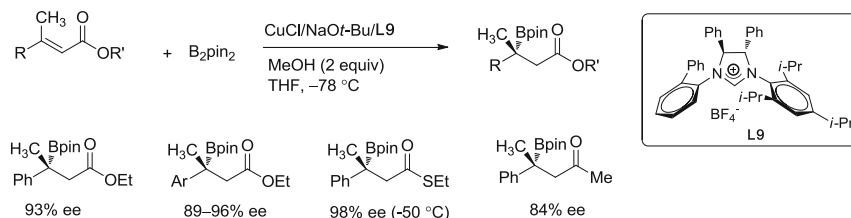
Sawamura and co-workers synthesized chiral NHC ligands (**L7** and **L8**) with an *m*-terphenyl-based moiety and demonstrated its efficiency on the enantioselective β -borylation of methyl cinnamate [21]. In situ generated catalysts with CuOt-Bu and **L7** or **L8** resulted in high enantioselectivities, affording products in 89 and 96% *ee* at -55°C , respectively (Scheme 8). However, catalyst efficiency was not investigated further on a broader range of substrates.

2.1.2 β,β -Disubstituted Acyclic Substrates: Formation of Organoboronates with a Quaternary Carbon

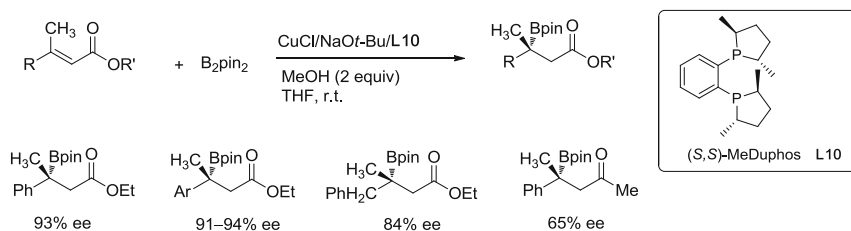
As in other copper-catalyzed conjugate addition reactions [22], the reactivity of substrates in copper-catalyzed β -borylations is dependent on the nature of the electron-withdrawing group (ketone > ester > amide) and steric hindrance around the reaction site (no substitution > β -mono- > β,β -disubstitution). Due to low reactivity and selectivity, the formation of chiral quaternary carbon stereogenic centers from acyclic β,β -disubstituted α,β -unsaturated substrates remained challenging.

In 2010, Hoveyda and co-workers reported an enantioselective β -borylation of β,β -disubstituted esters, ketones, and thioesters using a chiral monodentate NHC (**L9**)–Cu complex [23]. The reactions were efficient and delivered products with high enantioselectivities up to 98% *ee* at low temperatures (-50 or -78°C) (Scheme 9). Unsaturated thioesters displayed better enantioselectivity (89–98% *ee*) than unsaturated esters, but enones were less enantioselective in the NHC–Cu-catalyzed protocol.

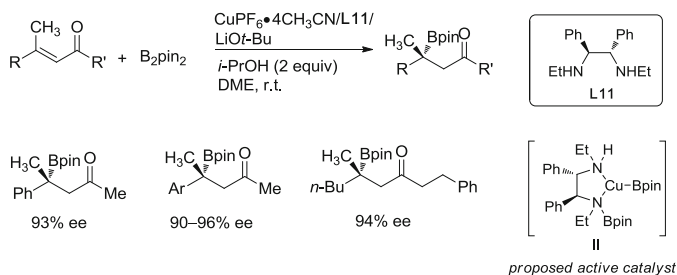
Simultaneously, Yun and co-workers reported in 2010 an enantioselective β -borylation of β,β -disubstituted esters catalyzed by a bisphosphine (**L10**)–Cu complex, overcoming the reactivity limitation of their previous **L1**–Cu catalyst [24]. Enantioselective borylation by (**L10**)–Cu catalyst proceeded at room temperature with high enantioselectivity (Scheme 10). The reaction of enones or *t*-butyl ester (88% *ee*) was less selective compared to that of the ethyl ester (93% *ee*), indicating that the (**L10**)–Cu catalyst is sensitive to the size and nature of electron-withdrawing groups.



Scheme 9 NHC (**L9**)–Cu-catalyzed enantioselective β -borylation of β,β -disubstituted unsaturated carbonyl compounds



Scheme 10 Phosphine (**L10**)–Cu-catalyzed enantioselective β -borylation of β,β -disubstituted unsaturated carbonyl compounds



Scheme 11 Diamine (**L11**)–Cu-catalyzed enantioselective β -borylation of β,β -disubstituted enones

Shibasaki and co-workers also reported a copper-secondary diamine (**L11**)-catalyzed enantioselective β -borylation of β,β -disubstituted enones (Scheme 11) [25]. Chiral tertiary organoboronates were produced in high yield with high enantioselectivity using 2 equiv. of isopropanol as an additive in DME. The authors suggested a copper–boronate complex (**II**) containing an *N*-borylated ligand based on ESI-MS experimental results. However, the activity of this catalyst was not reported for other substrate types, such as the less reactive unsaturated ester compounds in this work.

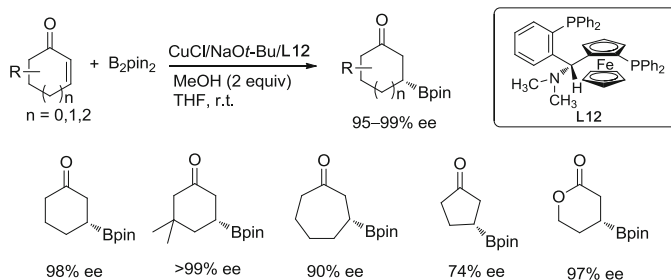
2.1.3 Cyclic Compounds

Enantioselective β -borylation of cyclic substrates was first reported by Yun and co-workers using a Cu–Taniaphos (**L12**) catalyst [26]. While the catalyst provided β -borylated 6- and 7-membered cyclic carbonyls as products with enantioselective ties up to 99% *ee*, it was less selective for 5-membered cyclopentenone and β -methyl cyclohexenone (Scheme 12).

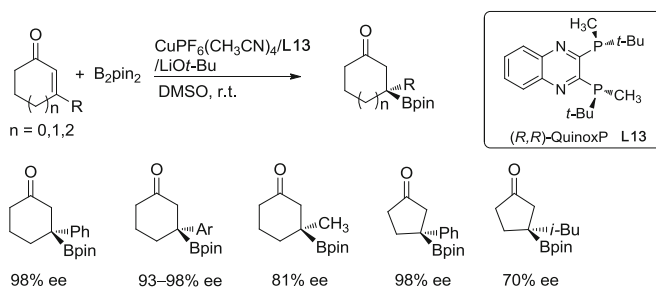
Shibasaki and co-workers reported that Cu–QuinoxP (**L13**) complex catalyzed the enantioselective borylation of β -substituted cyclic enones in DMSO [27]. β -Aryl-substituted cyclohexenone and cyclopentenone resulted with high enantioselectivities (93–98% *ee*), but β -methyl- or isobutyl-substituted cyclic compounds gave lower enantioselectivities (70–85% *ee*) (Scheme 13). The reaction protocol did not use an alcohol additive, so the resulting boron enolates could be used for further aldol addition reactions. Only enone substrates were reported, while the reactivity of less reactive substrates was not reported using the same catalytic conditions.

2.1.4 α,β -Unsaturated C = N Compounds and *N*-Containing Compounds

α,β -Unsaturated imines or iminium ions, isolated or formed in situ from carbonyl compounds and amines, are good substrates for β -borylation. Fernández and



Scheme 12 Phosphine (**L12**)-Cu-catalyzed enantioselective β -borylation of cyclic enones

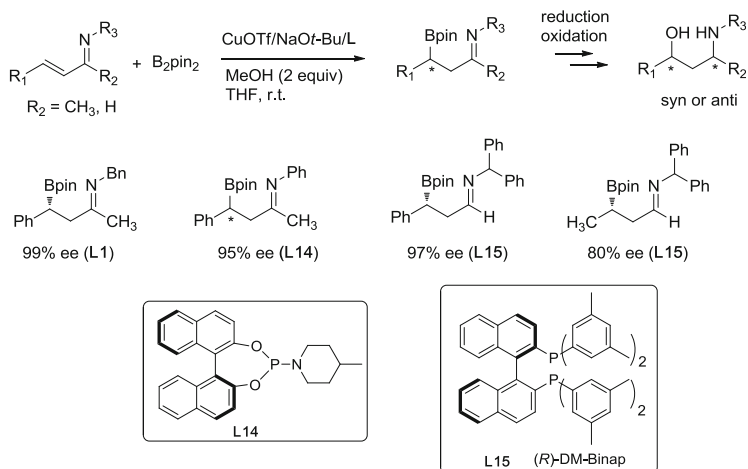
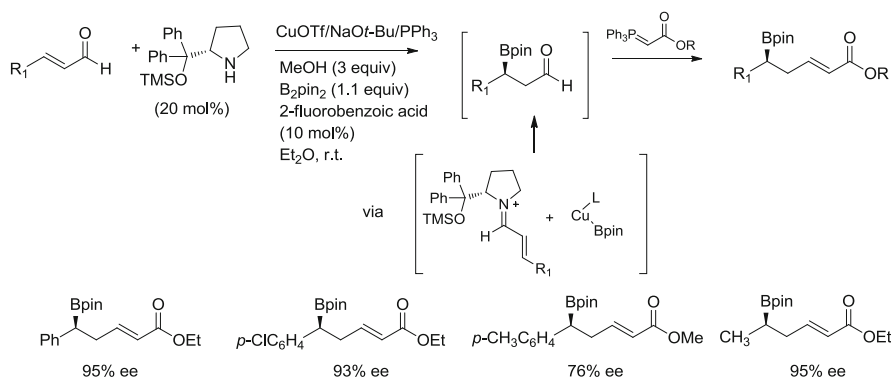
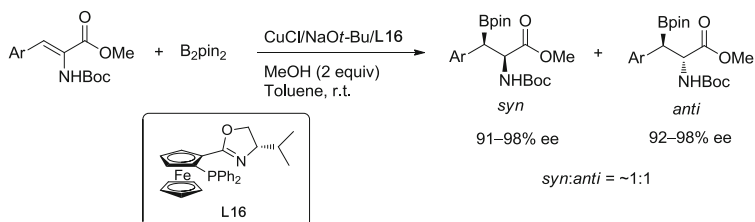


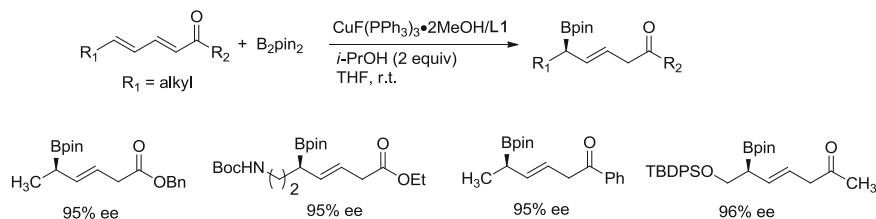
Scheme 13 Phosphine (**L13**)-Cu-catalyzed enantioselective β -borylation of β -substituted cyclic enones

co-workers published a series of reports on this subject with various copper-catalytic systems [28–30]. Selected examples with good conversion and high *ee* values were obtained (Scheme 14). In general, the *N*-substituent of the imines greatly affected the resulting enantioselectivity of each catalytic system. Cu complexes modified with chiral bisphosphine ligands (**L1** and **L15**) and phosphoramidites displayed good enantioselectivities. The resulting β -borylated imines were further converted to the corresponding γ -amino alcohols through sequential diastereoselective reduction and oxidation.

Córdoba and co-workers reported an enantioselective synthesis of homoallylboronates through the enantioselective β -borylation of enals and sequential Wittig reaction [31]. The presence of chiral iminium intermediates was confirmed by ^1H NMR and HRMS analyses, which induced enantio-control of the copper catalyst. Amine-catalyzed chiral iminium ion formation from enals and copper-catalyzed activation of diboron reagents were combined in this investigation to achieve enantioselective borylations (Scheme 15).

Recently, Lin and co-workers reported an enantioselective β -borylation of substituted α -amidoacrylate esters catalyzed by copper-**L16** complex [32]. The *syn*- and *anti*-products were obtained with excellent enantioselectivities but the diastereomeric ratio was not completely controlled (~1:1) (Scheme 16). This method provides a pathway for the facile synthesis of chiral β -hydroxy- α -amino acids.

**Scheme 14** Cu-catalyzed enantioselective β -borylation of α,β -unsaturated imines**Scheme 15** One-pot catalytic enantioselective synthesis of homoallylboronates**Scheme 16** Cu-catalyzed enantioselective β -borylation of α -amidoacrylates



Scheme 17 Cu-catalyzed enantioselective δ -borylation of dienones and dienooates

2.1.5 Extended Michael Acceptors

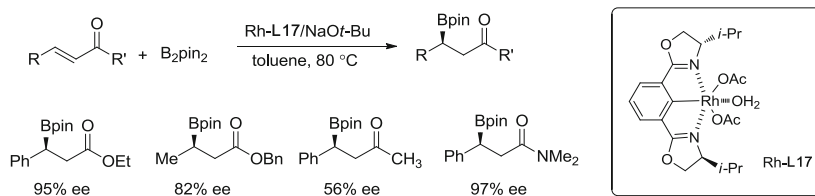
Copper-catalyzed borylation of dienones and dienooates has not been extensively studied due to the possible complex formation of isomeric products. Scattered examples in the literature indicate that 1,4-addition occurs preferentially over 1,6-addition. Yun and co-workers obtained the corresponding β -borylated product from a δ -disubstituted dienone in high *ee* with CuCl–**L1** catalyst [11]. Córdova and co-workers obtained a racemic β -borylation product from phenyl-2,4-dienoate by using Cu(OTf)₂–PPh₃ catalytic complex [31]. Kobayashi and co-workers recently reported catalytic systems highly effective for β -borylation of acyclic dienones and dienooates in water [33] (these will be discussed in more detail in a later section).

Recently, Lam and co-workers reported that chiral secondary allyboronates can be obtained by selective 1,6-addition (boron addition to the δ -carbon) of $\alpha,\beta,\gamma,\delta$ -unsaturated esters and ketones [34]. The regioselectivity was greatly affected by the choice of copper–ligand complexes. The best results were obtained with CuF(PPh₃)₃·2MeOH/**L1** complex in THF in the presence of *i*-PrOH as a protic additive. The benzyl sorbate reaction resulted in the δ -addition product with 96% *ee* in a >19:1 regioisomeric ratio (Scheme 17). While δ -alkyl-substituted substrates were suitable for the reaction, substrates containing a phenyl group at the δ -carbon (R₁ = Ph, Ar) provided a mixture of unidentified impurities under catalytic conditions.

Copper-catalyzed borylation of allenooates and allenamides has been investigated as well. Santos and co-workers reported an efficient borylation of 2,3-allenooates [35] and Ma and co-workers reported that of 2,3-allenamides [36]. Both methods produced (*Z*)- β -borylated β,γ -unsaturated compounds by installing a boron moiety on the β -position, which had an achiral C–B (sp² C–B) bond.

2.2 Rh-Catalyzed β -Borylation

The first rhodium-catalyzed β -borylation of α,β -unsaturated acceptors was reported by Kabalka and co-workers in 2002 [4]. The addition of bis(pinacolato)diboron and bis(neopentyl glycolato)diboron to α,β -unsaturated ketones, esters, aldehydes, and



Scheme 18 Rh/Phebox (**L17**)-catalyzed enantioselective β -borylation of unsaturated carbonyl compounds

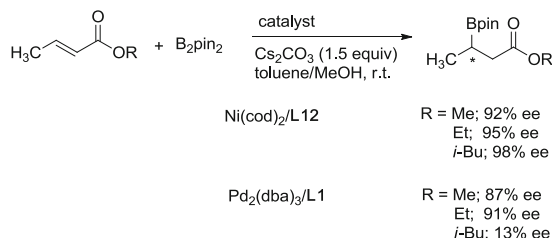
nitriles was performed using a nonchiral 10 mol% $\text{RhCl}(\text{PPh}_3)_3$ catalyst at 80°C . The desired products were obtained in 62–78% yields.

Nishiyama and co-workers devised asymmetric rhodium-catalyzed β -borylation in 2009 [37]. Chiral rhodium–bisoxazolinylphenyl acetate complexes catalyzed the reaction of α,β -unsaturated carbonyl compounds with enantioselectivity up to 97% *ee* (Scheme 18). While substrate variants were limited, especially for unsaturated amides, the catalyst was highly enantioselective for esters and amides. However, it was not highly enantioselective for unsaturated ketones.

2.3 Ni- and Pd-Catalyzed β -Borylation

In 2007, Oshima and co-workers developed an achiral nickel catalyst system for the β -borylation of α,β -unsaturated esters and amides [38]. A catalytic combination of $\text{Ni}(\text{cod})_2$ and PCy_3 was used in the presence of Cs_2CO_3 in toluene/MeOH solvent. In this system, the addition of MeOH was proven to increase the isolated yield of products. The nickel system was effective for the borylation of di-, tri-, and tetrasubstituted substrates. The reactions of cinnamate and other β -aryl-substituted substrates were limited, producing unstable borylated products under catalytic conditions in low isolation yields.

In 2009, Fernández and co-workers were the first to report that chiral catalyst systems based on Ni and Pd were effective for enantioselective β -borylation of (*E*)-crotonates (Scheme 19) [39]. A $\text{Ni}(\text{cod})_2$ and Taniaphos (**L12**) complex was effective for the β -borylation of crotonates, resulting in products with high enantioselectivity up to 98% *ee*. Pd_2dba_3 –Josiphos (**L1**) catalyst catalyzed the ethyl crotonate reaction, affording the product in 91% *ee*. In both systems, enantioselectivity was affected by the ester moiety. In particular, the palladium catalyst displayed variable enantioselectivity depending on the substrate. However, only crotonate was investigated with both catalysts, so the effect of substrate variants on enantioselectivity is difficult to predict.



Scheme 19 Ni- and Pd-catalyzed enantioselective β -borylation of crotonates

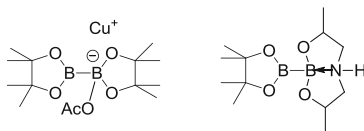
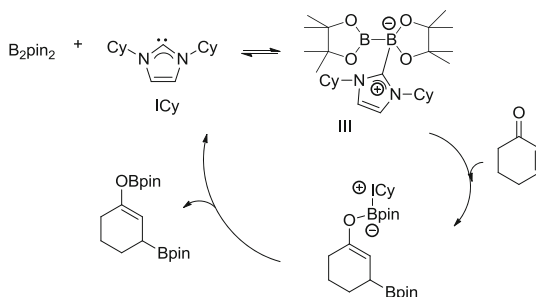
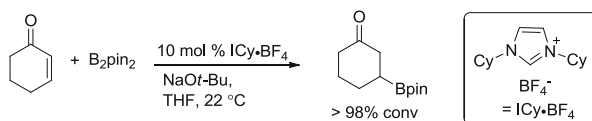
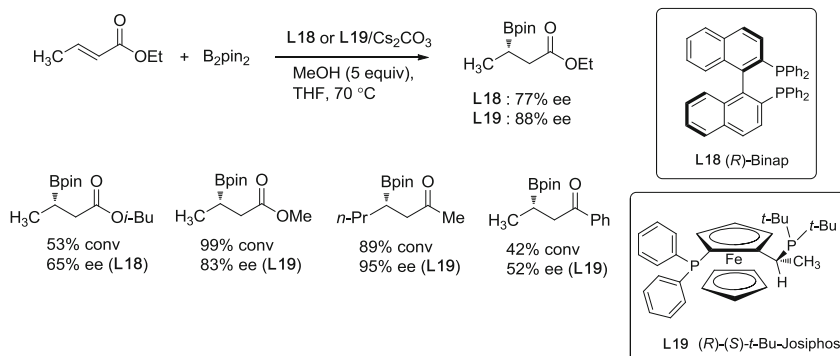
3 Asymmetric β -Borylation with Organocatalysts

It was previously postulated that $\text{sp}^2\text{-sp}^3$ diboron compounds acted as boron intermediates in copper-catalyzed borylation reactions. Miyaura and co-workers postulated a diboron–acetate complex before transmetalation to copper [9], while Santos and co-workers used $\text{sp}^2\text{-sp}^3$ mixed diboron for the copper-catalyzed reaction [35, 40] (Fig. 1). However, the reactivity of $\text{sp}^2\text{-sp}^3$ diboron compounds without a transition-metal catalyst has not been studied in detail until recently.

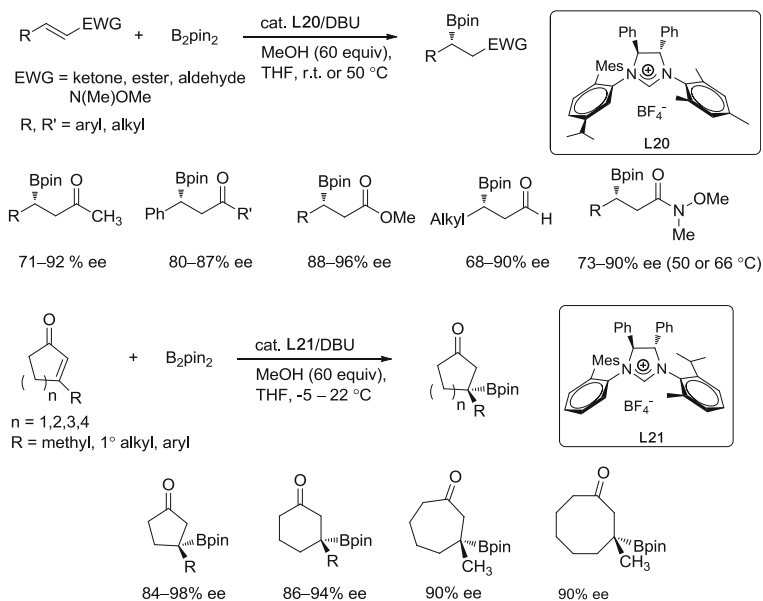
Hoveyda and co-workers made a breakthrough in nonmetal catalyzed β -borylation in 2009 [41]. They investigated Lewis acid–base complexes of bis(pinacolato)diboron and *N*-heterocyclic carbenes as a nucleophilic boron reagent and first reported the metal-free β -borylation of cyclic and acyclic α,β -unsaturated ketones and esters in a racemic version (Scheme 20). They proposed a model for diboron activation by the coordination of a nucleophilic NHC. NHC-bound diboron (**III**) adds to the substrate and a carbene intermediate is regenerated. Marder and co-workers carried out the spectroscopic and structural characterization of the Lewis adduct [42]. The crystal structure of the Lewis adduct was elucidated, and NMR revealed weak binding and rapid exchange of the NHC between the two boron centers in solution.

In 2010, Fernández and co-workers reported the first asymmetric metal-free β -borylation using a chiral bisphosphine as an additive at 70°C (Scheme 21) [7]. Among the screened ligands, binap (**L18**) and *t*-Bu-Josiphos ligand (**L19**) displayed higher activities for ethyl crotonate (>99% conversion) with 77 and 88% *ee* values, respectively. However, both catalysts resulted in partial conversion (~50% conversion) of bulkier isobutyl crotonate with lower enantioselectivity. The organocatalysts were also active for enone substrates, but the conversion and *ee* values varied with substituents. For most cases, **L19** resulted in better enantioselectivities than **L18**.

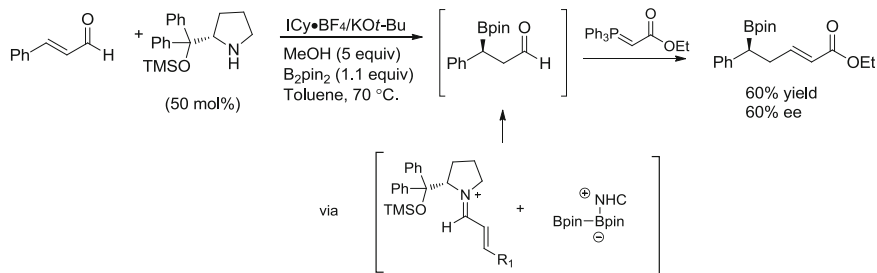
Hoveyda and co-workers carried out an extensive study of metal-free asymmetric β -borylation of α,β -unsaturated carbonyl compounds with chiral imidazolium salts (**L20** and **L21**) (Scheme 22) [8]. Chiral NHC, in situ generated by the 1,8-diazabicyclo[5,4,0]undec-7-ene (DBU), catalyzed the asymmetric addition of a Bpin moiety to various α,β -unsaturated carbonyls in the presence of MeOH. Acyclic α,β -unsaturated ketones, esters, and aldehydes were suitable substrates, affording the desired β -boryl-carbonyl compounds up to 96% *ee* with **L20**. However, the reactions did not proceed to a full conversion in certain cases. In particular, the less reactive Weinreb amides required elevated reaction temperatures

**Fig. 1** Diboron-ate complexes as active diboron species**Scheme 20** NHC-catalyzed boron conjugate addition to cyclic enones**Scheme 21** Asymmetric metal-free β-borylation of α,β -unsaturated carbonyl compounds in the presence of chiral phosphines as additives

(50–66 °C), higher catalyst loadings, and longer reaction times for substantial conversion (67–98% conversion). For the transformation of β-substituted cyclic enones, a slightly modified NHC organocatalyst (**L21**) from **L20** was effective in affording products in good conversions and high enantioselectivities [43].



Scheme 22 Chiral NHC-catalyzed β -borylation of α,β -unsaturated carbonyl compounds

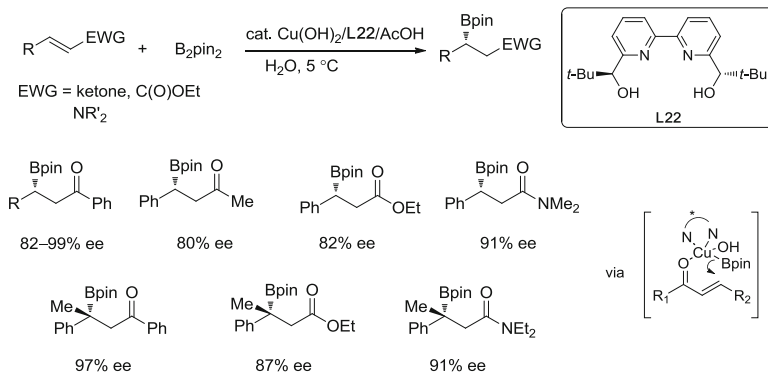


Scheme 23 Metal-free three-component synthesis of homoallylboronates

Córdova and co-workers reported a metal-free version of their homoallylboronate synthesis in a one-pot process [44] (Scheme 23). However, the isolated yield and *ee* values varied depending on the amount of chiral amine, indicating a nonselective background reaction involved in this protocol.

4 Asymmetric β -Borylation in Water

The use of water as a reaction medium, instead of organic solvents, provides environmentally friendly protocols in organic synthesis [45]. Because protic additives such as alcohols are commonly employed for catalytic β -borylation as a

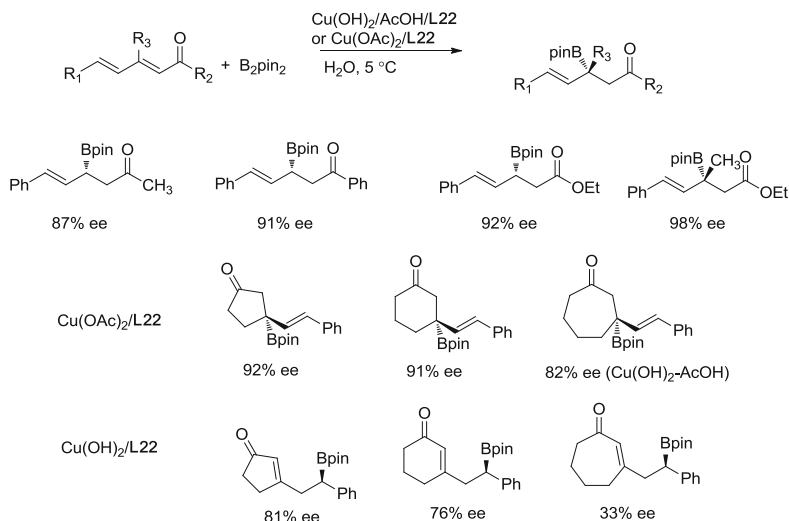


Scheme 24 Cu-catalyzed enantioselective β -borylation of α,β -unsaturated carbonyl compounds in water

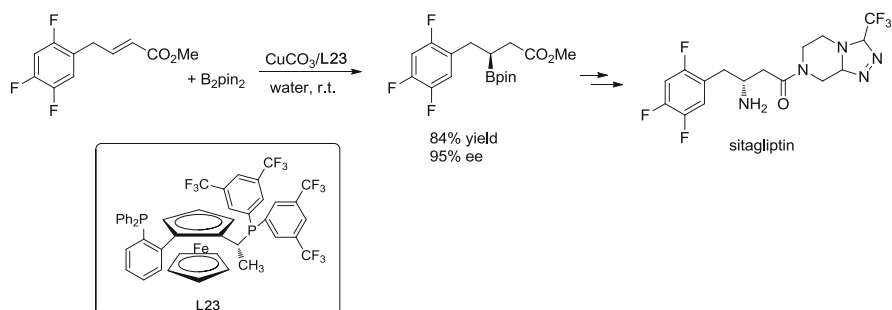
reaction promotor, efforts have been made to develop the same transformation in aqueous media. Yun and co-workers reported ligandless copper-catalyzed β -borylation in aqueous solution using a catalytic amount of copper(I) precursors or copper(II) oxide in combination with $NaOt\text{-}Bu$ base [46]. This protocol resulted in β -borylation of α,β -unsaturated ketones, esters, and unsubstituted amides. Santos and co-workers also reported β -borylation of α,β -unsaturated esters and ketones in water catalyzed by $CuSO_4 \cdot 5H_2O$ and picoline [47]. Although not in aqueous media, Molander and co-workers demonstrated that tetrahydroxydiborane (bisboronic acid) could be used in ethanol solvent [48].

In 2012, Kobayashi and co-workers reported the first enantioselective boron conjugate additions to various α,β -unsaturated carbonyl compounds and nitriles in water using a chiral 2,2'-bipyridine **L22**- $Cu(OH)_2$ catalyst [33, 49]. α,β -Unsaturated ketones, including cyclic enones, afforded the desired products with high yields and enantioselectivities (Scheme 24). While chalcone ($R = Ph$, EWG = $COPh$) resulted in the highest *ee* (99% *ee*), the same catalyst afforded 82% *ee* for cyclohexenone. The catalyst was also reactive for unsaturated esters, nitriles, and amides, but was less enantioselective for esters and cinnamonnitrile (81% *ee*). Of note was the fact that β,β -disubstituted enones reacted with the same catalyst to give products with high enantioselectivities [33]. Further investigation of β,β -disubstituted esters or amides with the same catalyst proved that the catalytic systems were effective for such less reactive substrates and generally applicable for various types of α,β -unsaturated carbonyl compounds [49].

The same authors reported enantioselective borylation of dienones and dienesters in water (Scheme 25) [50]. A strong preference for 1,4-addition over 1,6-addition was observed for acyclic $\alpha,\beta,\gamma,\delta$ -unsaturated dienones and diesters with either $Cu(OH)_2$ or $Cu(OAc)_2$ catalysts, even for substrates with an extra β -substituent. An interesting switch of regioselectivity was observed for 5-, 6-, and 7-membered cyclic dienones. While the use of a $Cu(OH)_2/AcOH$ combination or $Cu(OAc)_2$ resulted in exclusive formation of 1,4-adduct with high



Scheme 25 Enantioselective borylation of $\alpha,\beta,\gamma,\delta$ -unsaturated carbonyl compounds



Scheme 26 Enantioselective β -borylation of an ester in water

enantioselectivity, the use of Cu(OH)_2 as catalytic precursor gave a 1,6-addition product with moderate enantioselectivity (Scheme 25). The authors claimed that the former catalyst constituted homogeneous system, while the latter catalyst results in a heterogeneous catalysis in water as evidenced by a filtration test. Although the role of Cu(II) and water has not been clearly elucidated, water was considered effective in the activation of a copper-boryl species and the protonation of a reaction intermediate.

Casar and co-workers recently reported an example of asymmetric β -borylation of α,β -unsaturated esters using water as the reaction medium [51]. A β -boryl-carbonyl precursor to the antidiabetic drug sitagliptin [52] was synthesized in 84% yield and 95% *ee* using CuCO_3 as a catalyst in combination with chiral bisphosphine **L23** at room temperature. Oxidation afforded the corresponding β -alcohol product (Scheme 26).

5 Conclusions

In the last 8 years, impressive progress has been made in the catalytic asymmetric β -borylation (conjugate borylation) of α,β -unsaturated acceptors. Various metal-catalyzed and metal-free methods have been developed. Some of these methods meet standards of high efficiency in terms of yield, enantioselectivity, and substrate scope.

Copper catalysis has dominated the field of asymmetric borylation since the first report of its efficacy because it exhibits high reactivity and selectivity for various substrates, including challenging β,β -disubstituted esters and amides. Copper catalysis also allows high versatility in asymmetric β -borylation reactions in water. Other promising transition-metal-catalyzed and metal-free methods have also been developed. Asymmetric β -borylation can provide a platform to test the efficiency of newly developed chiral organocatalysts, ligands, and ligand–metal catalysts. Future challenges in this field will be addressed with the development of more efficient asymmetric catalytic systems for the borylation and with related organic transformations of involving complex molecules or cooperative catalysis [53, 54].

Acknowledgments We are grateful for the financial support of the Basic Science Research Program through the National Research Foundation of Korea (NRF) funded by the Ministry of Education (2013R1A1A2058160).

References

1. Lawson YG, Lesley MJG, Marder TB, Norman NC, Rice CG (1997) *Chem Commun* 2051
2. Ito H, Yamanaka H, Tateiwa J, Hosomi A (2000) *Tetrahedron Lett* 41:6821
3. Takahashi K, Ishiyama T, Miyaura N (2000) *Chem Lett* 982
4. Kabalka GW, Das BC, Das S (2002) *Tetrahedron Lett* 43:2323
5. Mun S, Lee JE, Yun J (2006) *Org Lett* 8:4887
6. Lee JE, Yun J (2008) *Angew Chem Int Ed* 47:145
7. Bonet A, Gulyás H, Fernández E (2010) *Angew Chem Int Ed* 49:5130
8. Wu H, Radomkit S, O'Brien JM, Hoveyda AH (2012) *J Am Chem Soc* 134:8277
9. Takahashi K, Ishiyama T, Miyaura N (2001) *J Orgmetal Chem* 625:47
10. Dang L, Lin Z, Marder TB (2008) *Organometallics* 27:4443
11. Sim HS, Feng X, Yun J (2009) *Chem Eur J* 15:1939
12. Chea H, Sim HS, Yun J (2009) *Adv Synth Catal* 351:855
13. Herrmann WA (2002) *Angew Chem Int Ed* 41:1290
14. Díez-González S, Marion N, Nolan SP (2009) *Chem Rev* 109:3612
15. Snead DR, Seo H, Hong S (2008) *Curr Org Chem* 12:1370
16. Lillo V, Prieto A, Bonet A, Díaz-Requejo MM, Ramírez J, Pérez PJ, Fernández E (2009) *Organometallics* 28:659
17. Fleming WJ, Müller-Bunz H, Lillo V, Fernández E, Guiry PJ (2009) *Org Biomol Chem* 7:2520
18. Hirsch-Weil D, Abboud KA, Hong S (2010) *Chem Commun* 46:7525
19. Park JK, Lackey HH, Rexford MD, Kovnir K, Shatruk M, McQuade DT (2010) *Org Lett* 12:5008

20. Zhao L, Ma Y, He F, Duan W, Chen J, Song C (2013) *J Org Chem* 78:1677
21. Iwai T, Akiyama Y, Sawamura M (2013) *Tetrahedron Asymmetry* 24:729
22. Krause N (ed) (2002) *Modern organocopper chemistry*. Wiley-VCH, Weinheim
23. O'Brien JM, Lee K, Hoveyda AH (2010) *J Am Chem Soc* 132:10630
24. Feng X, Yun J (2010) *Chem Eur J* 16:13609
25. Chen IH, Kanai M, Shibasaki M (2010) *Org Lett* 12:4098
26. Feng X, Yun J (2009) *Chem Commun* 6577
27. Chen IH, Yin L, Itano W, Kanai M, Shibasaki M (2009) *J Am Chem Soc* 131:11664
28. Solé C, Whiting A, Gulyás H, Fernández E (2011) *Adv Synth Catal* 353:376
29. Solé C, Bonet A, de Vries AHM, de Vries JG, Lefort L, Gulyás H, Fernández E (2012) *Organometallics* 31:7855
30. Calow ADJ, Batsanov AS, Pujol A, Solé C, Fernández E, Whiting A (2013) *Org Lett* 15:4810
31. Ibrahim I, Breistein P, Córdova A (2011) *Angew Chem Int Ed* 50:12036
32. He ZT, Zhao YS, Tian ZP, Wang CC, Dong HQ, Lin GQ (2014) *Org Lett* 16:1426
33. Kobayashi S, Xu P, Endo T, Ueno M, Kitanosono T (2012) *Angew Chem Int Ed* 51:12763
34. Luo Y, Roy ID, Madec AGE, Lam HW (2014) *Angew Chem Int Ed* 53:4186
35. Thorpe SB, Guo X, Santos WL (2011) *Chem Commun* 424
36. Yuan W, Zhang X, Yu Y, Ma S (2013) *Chem Eur J* 19:7193
37. Shiomi T, Adachi T, Toribatake K, Zhou L, Nishiyama H (2009) *Chem Commun* 5987
38. Hirano K, Yorimitsu H, Oshima K (2007) *Org Lett* 9:5031
39. Lillo V, Geier MJ, Westcott SA, Fernández E (2009) *Org Biomol Chem* 7:4674
40. Gao M, Thorpe SB, Santos WL (2009) *Org Lett* 11:3478
41. Lee K, Zhugralin AR, Hoveyda AH (2009) *J Am Chem Soc* 131:7253
42. Kleeberg C, Crawford AG, Batsanov AS, Hodgkinson P, Apperley DC, Cheung MS, Lin Z, Marder TB (2011) *J Org Chem* 77:785
43. Radomkit S, Hoveyda AH (2014) *Angew Chem Int Ed* 53:3387
44. Ibrahim I, Breistein P, Córdova A (2012) *Chem Eur J* 18:5175
45. Lindstroem UM (ed) (2007) *Organic reactions in water*. Wiley-Blackwell, Oxford
46. Chea H, Sim HS, Yun J (2010) *Bull Korean Chem Soc* 31:551
47. Thorpe SB, Calderone JA, Santos WL (2012) *Org Lett* 14:1918
48. Molander GA, McKee SA (2011) *Org Lett* 13:4684
49. Kitanosono T, Xu P, Kobayashi S (2014) *Chem Asian J* 9:179
50. Kitanosono T, Xu P, Kobayashi S (2013) *Chem Commun* 49:8184
51. Stavber G, Casar Z (2013) *Appl Organomet Chem* 27:159
52. Hansen KB, Balsells J, Dreher S, Hsiao Y, Kubryk M, Palucki M, Rivera N, Steinhuebel D, Armstrong JD III, Askin D, Grabowski EJJ (2005) *Org Process Res Dev* 9:634
53. Burns AR, González JS, Lam HW (2012) *Angew Chem Int Ed* 51:10827
54. Semba K, Nakao Y (2014) *J Am Chem Soc* 136:7567

Reactions of Alkynylboron Compounds

Naoki Ishida and Masahiro Murakami

Contents

1	Introduction	94
2	Alkynylboronates (Esters of Alkynylboronic Acids)	94
2.1	Preparations	94
2.2	Insertion Reactions	95
2.3	Cycloaddition Reactions	95
2.4	Miscellaneous	102
3	Alkynylborates (Ate-Complexes)	105
3.1	Preparations	105
3.2	Uncatalyzed Reactions	106
3.3	Transition Metal-Catalyzed Reactions	108
3.4	Reactions Through Intermediacy of Alkynyl(Triorganyl)Borates	110
4	Conclusions	113
	References	113

Abstract This chapter overviews reactions of alkynylboron compounds, in which the carbon–carbon triple bond is transformed into a different form, with the boryl group remaining in the product. Most of the reactions produce multiply substituted alkenyl- and aryl-boron compounds.

Keywords Alkyne • Boron • Catalysis • Directing group • Organic synthesis • Regioselectivity • Transition metal

N. Ishida • M. Murakami (✉)

Department of Synthetic Chemistry and Biological Chemistry, Kyoto University, Katsura,
Kyoto 615-8510, Japan

e-mail: naisida@sbchem.kyoto-u.ac.jp; murakami@sbchem.kyoto-u.ac.jp

© Springer International Publishing Switzerland 2015

E. Fernández, A. Whiting (eds.), *Synthesis and Application of Organoboron Compounds*, Topics in Organometallic Chemistry 49,

DOI 10.1007/978-3-319-13054-5_4

1 Introduction

Organoboron compounds are stable enough for storage, in general. Nonetheless, they acquire a variety of reactivities when subjected to appropriate conditions. This feature is favored by synthetic chemists and thus widely utilized in organic synthesis. One of the most typical examples is the Suzuki–Miyaura cross-coupling reaction, in which the carbon–boron bond is exchanged with a carbon–halogen bond to form a carbon–carbon bond by means of a transition metal catalyst [1].

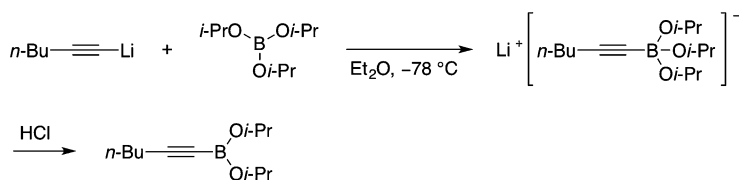
Alkynylboron compounds also react at the carbon–carbon triple bond. The boryl group influences their reactivities both sterically and electronically, leading to regioselective reactions. The carbon–boron bond is retained in the product and can be utilized for further transformations. This chapter overviews the latter type of reactions of alkynylboron compounds in which the carbon–carbon triple bonds are transformed. The former reactions, in which an *sp*-hybridized carbon–boron bond is substituted, are outside the coverage of this review. Excellent reviews on alkynylboron compounds in organic synthesis are available from references [2–6].

2 Alkynylboronates (Esters of Alkynylboronic Acids)

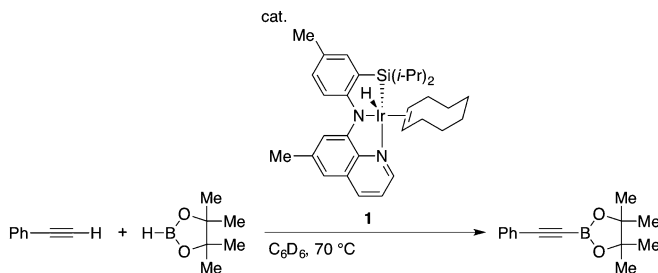
2.1 Preparations

The reaction of alkynyllithiums with triisopropyl borate ($\text{B}(\text{O}i\text{-Pr})_3$) is often utilized for the preparation of alkynylboronates (Scheme 1) [7]. Alkynyl(triisopropoxy)borates are initially generated and, upon treatment with anhydrous HCl, decompose to produce alkynylboronates. Other esters are synthesized by using other borates or transesterification of the resulting alkynylboronates with diols.

A totally different pathway is available by using a C–H borylation reaction of terminal alkynes with hydroboranes (Scheme 2) [8]. The iridium complex **1**, having an SiNN pincer ligand, prompts a dehydrogenative coupling in priority to hydroboration across the carbon–carbon triple bond, producing alkynylboronates.



Scheme 1 Preparation of alkynylboronate from alkynyllithium with triisopropyl borate



Scheme 2 C–H borylation reaction of terminal alkyne

2.2 Insertion Reactions

A unique reactivity of alkynylboronates is demonstrated by a hydrozirconation reaction; 1-boryl-1-alkenylzirconiums are selectively obtained upon treatment with Schwartz's reagent ($\text{Cp}_2\text{Zr(H)Cl}$) (Scheme 3) [9]. The resulting 1,1-heterobimetallic alkenes are applied to the synthesis of a wide variety of alkenylboronates that are inaccessible by conventional hydroboration reactions.

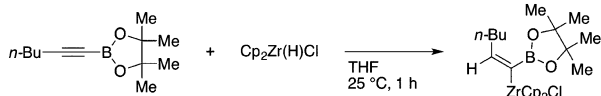
A hydroboration reaction of a catechol ester of ethynylboronic acid provides 1,1-diborylethene as the major product (Scheme 4) [10]. Pinacol esters [11], amides [12], and borinates [13] also exhibit similar regioselectivities in hydroboration reactions. In sharp contrast, hydroboration of the *N*-methyliminodiacetic acid (MIDA) ester **2** affords 1,2-diborylalkene **3** regioselectively (Scheme 5) [14]. Radical-mediated hydrostannylation of **2** also shows an analogous regioselectivity.

Silylboranes can be added across carbon–carbon unsaturated bonds with the aid of a transition metal catalyst [15]. The palladium-catalyzed silylboration reaction of alkynylboronates gives 1,1-diboryl-2-silylalkenes regioselectively (Scheme 6) [16]. The resulting multimetallic alkenes serve as versatile intermediates for the stereoselective synthesis of tetrasubstituted alkenes.

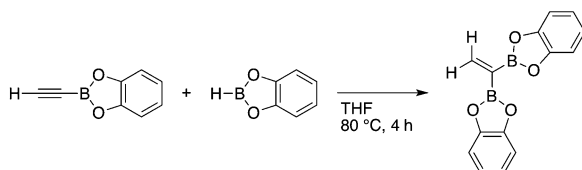
2.3 Cycloaddition Reactions

Alkynylboronates participate in a wide variety of cycloaddition reactions at the carbon–carbon triple bond. Early examples include a [4+2]-cycloaddition reaction of an ethynylboronate with cyclopentadiene furnishing a norbornadieneboronate (Scheme 7) [17] and an analogous [4+2]-cycloaddition reaction with 1,3-butadiene furnishing a cyclohexa-1,4-dienylboronate [18].

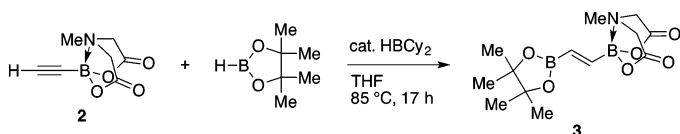
Trimethylsilylethynyl-9-BBN reacts with 2-siloxy-1,3-butadiene at 100°C to give cyclohexadienylborane **4** in a regioselective manner (Scheme 8) [19]. Ab initio calculations suggest that the bonding between the nucleophilic C1 atom of the butadiene and the electrophilic boron in TS is responsible for the regioselectivity.



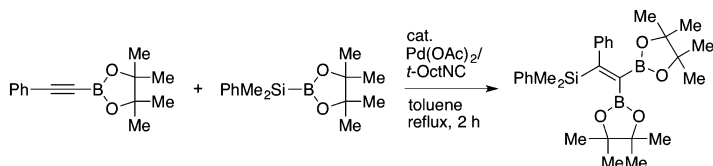
Scheme 3 Hydrozirconation of alkynylboronate



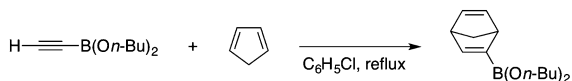
Scheme 4 Hydroboration of ethynylboronic acid catechol ester



Scheme 5 Hydroboration of ethynylboronic acid MIDA ester



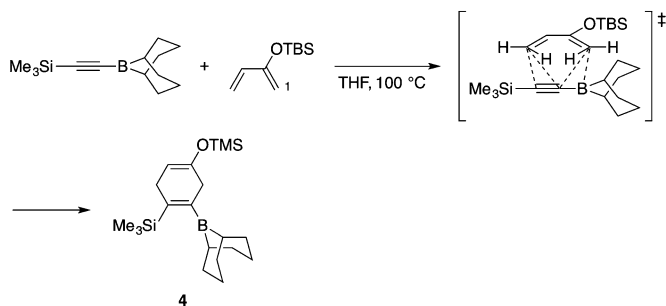
Scheme 6 Silylboration of alkynylboronate



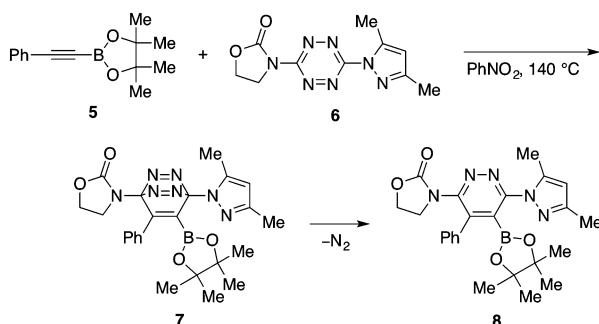
Scheme 7 [4+2]-Cycloaddition reaction of ethynylboronate with cyclopentadiene

An analogous [4+2]-cycloaddition between alkynyl(dihalo)boranes with 1,3-butadienes proceeds at room temperature, indicating that a highly Lewis acidic dihaloborane moiety facilitates the cycloaddition reaction [20–22].

Alkynylboronates (alkynyl(dialkoxy)boranes) also seem to act as electron-deficient alkynes. In fact, however, they undergo a [4+2]-cycloaddition reaction with electron-deficient dienes, rather than with electron-rich dienes. For example, alkynylboronate **5** reacts with 1,2,4,5-tetrazine **6** upon heating at 140 °C to give 1,2,3,4-tetraaza[2.2.2]bicyclooctatriene **7**, which is then denitrogenated to afford pyridazine **8** (Scheme 9) [23, 24]. This seemingly counterintuitive reactivity of



Scheme 8 [4+2]-Cycloaddition reaction of trimethylsilylethynyl-9-BBN with 2-siloxy-1,3-butadiene

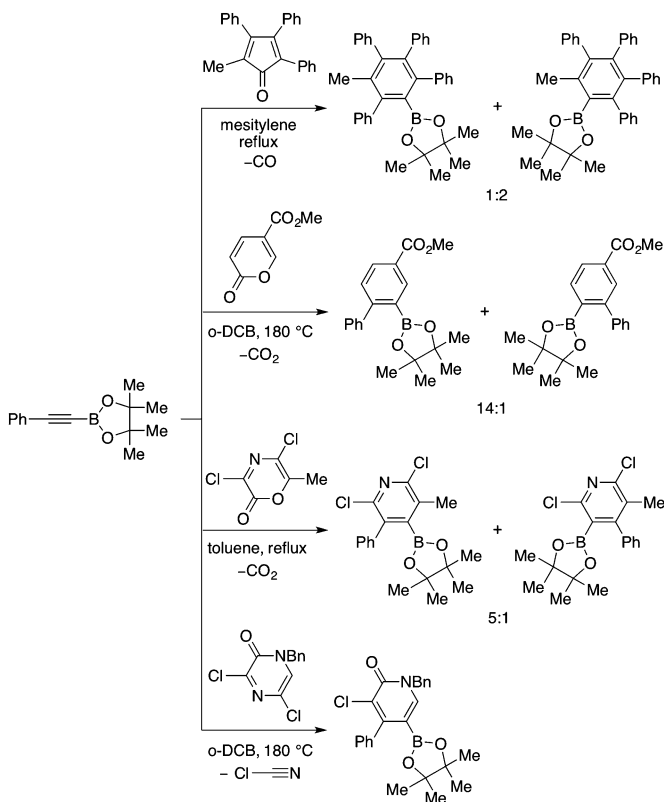


Scheme 9 Denitrogenative cycloaddition reaction of alkynylboronate with 1,2,4,5-tetrazine

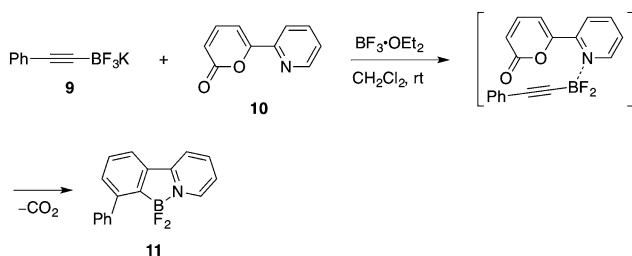
alkynylboronates can be ascribed to the energy levels of their frontier orbitals. The π -electron donation from oxygen to a vacant p-orbital on boron mitigates the electron deficiency of the boron atom. Hence, the LUMO level is not low enough to react with electron-rich dienes. Instead, the HOMO level of the alkynylboronates is increased due to the inductive effect of the electropositive boron atom [25].

Analogous inverse electron demand Diels–Alder reactions proceed with cyclopentadienones [26], pyrones [27–29], 3,5-dihalo-2*H*-1,4-oxazin-2-ones [30], and 2[1*H*]-pyrazinones [30] (Scheme 10).

The [4+2]-cycloaddition reactions are facilitated by coordination with electrophilic species, particularly with Lewis acids. When a mixture of alkynyltrifluoroborate **9** and pyrone **10** is treated with $\text{BF}_3 \cdot \text{OEt}_2$, an alkynyldifluoroborane is generated (Scheme 11) [31, 32]. The Lewis basic nitrogen atom coordinates to the trivalent boron, locating the alkyne in close proximity to the diene unit. A regioselective cycloaddition occurs even at room temperature to produce 2-arylp yridine **11**. The cycloaddition reaction with 1,2,4,5-tetrazines is also facilitated by an analogous coordination-mediated reaction [33].



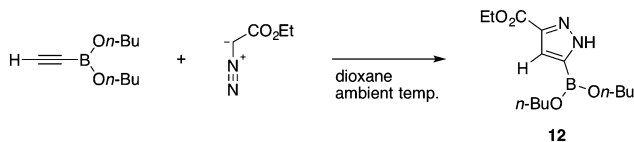
Scheme 10 Cycloaddition reactions of alkynylboronate with electron-deficient dienes



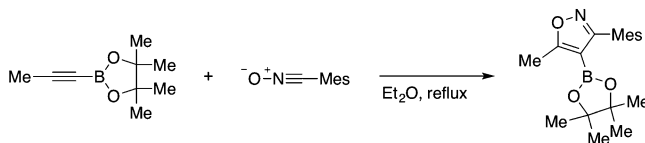
Scheme 11 Coordination-assisted cycloaddition reaction

Alkynylboronates also act as the dipolarophile in 1,3-dipolar cycloaddition reactions. A reaction with diazo ester producing pyrazole **12** is an early example (Scheme 12) [34] of such a reaction.

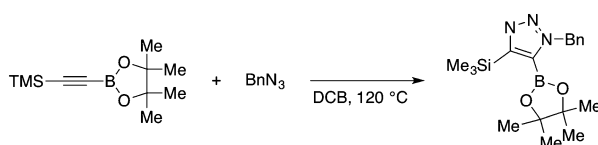
The 1,3-dipolar cycloaddition reaction with nitrile oxides furnishes isoxazoleboronates as a single regioisomer (Scheme 13) [35]. The reaction with azides produces triazoles (Scheme 14) [36]. Sydnone, which are readily synthesized in



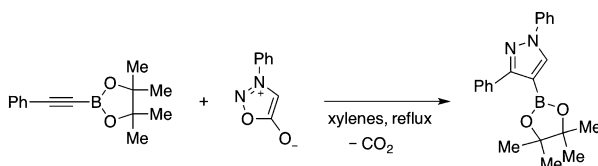
Scheme 12 1,3-Dipolar cycloaddition reaction of ethynylboronate with α -diazo ester



Scheme 13 1,3-Dipolar cycloaddition reaction of alkynylboronate with nitrile oxide



Scheme 14 1,3-Dipolar cycloaddition reaction of alkynylboronate with azide



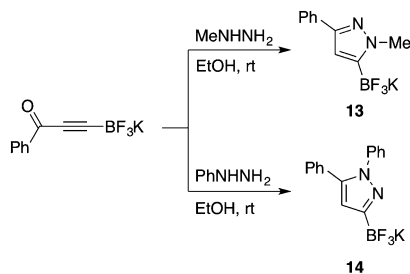
Scheme 15 Decarboxylative cycloaddition reaction of alkynylboronate with sydnone

two steps from amino acids, also react with alkynylboronates (Scheme 15) [37, 38] and spontaneous decarboxylation follows to give pyrazoles.

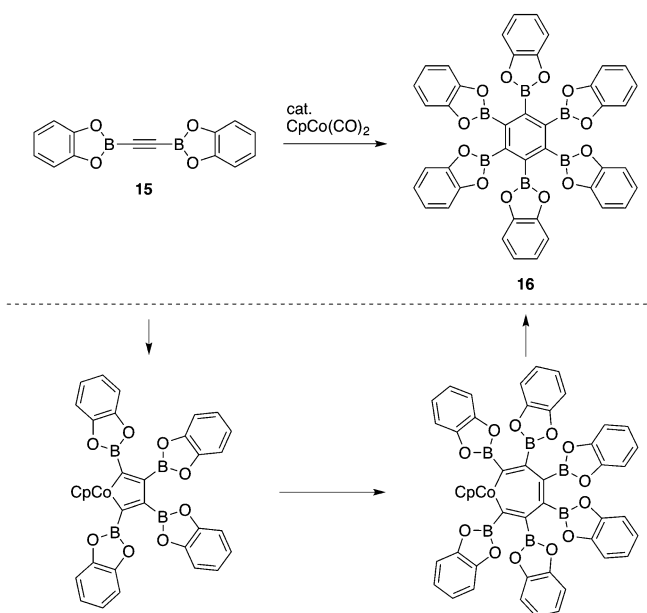
Borylated pyrazoles are synthesized by the reaction of 3-oxoalkynyltrifluoroborates with hydrazines (Scheme 16) [39]. The regioselectivity significantly depends upon the substituents on the hydrazine; methylhydrazine gives **13**, while phenylhydrazine provides **14**.

Transition metal catalysis offers another avenue for cycloaddition reactions. Diborylacetylene **15** is cyclotrimerized upon treatment with a cobalt catalyst to afford hexaborylbenzene **16** (Scheme 17) [40]. Oxidative cyclization, insertion of alkynes, and reductive elimination are assumed as part of the reaction pathway [41]. $\text{Co}_2(\text{CO})_8$ and $\text{Ni}(\text{cod})_2$ also serve as a catalyst for this type of cyclotrimerization reaction.

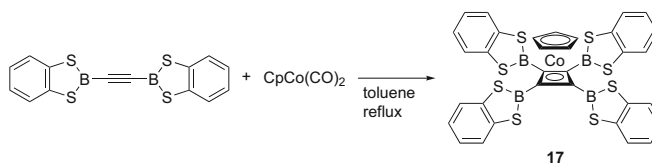
Monoborylacetylenes also undergo analogous cyclotrimerizations to give a mixture of 1,2,4- and 1,3,5-triborylbenzenes [10]. In contrast, when oxygen atoms are replaced with sulfur, cyclodimerization occurs to furnish cobalt-cyclobutadiene complex **17** (Scheme 18) [42].



Scheme 16 Synthesis of borylated pyrazoles from 3-oxoalkynyltrifluoroborate with hydrazines

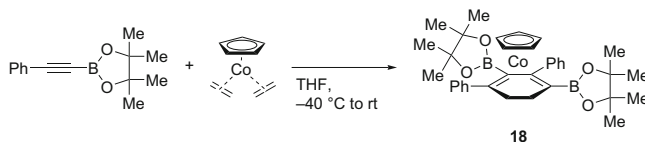


Scheme 17 Cobalt-catalyzed cyclotrimerization reaction of diborylacetylene

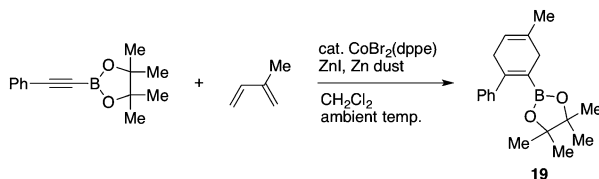


Scheme 18 Cyclodimerization reaction of diborylacetylene on cobalt

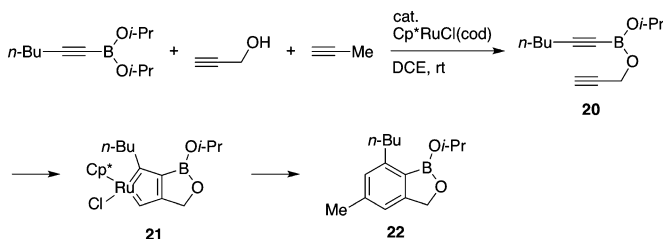
CpCo(CO)_2 also mediates the [2+2+2]cycloaddition of alkynylboronates with 1,6-diynes to produce arylboronates [43]. Alkenes and alkynylboronates are also coupled using cobalt(I)-based catalysts to produce cobalt–cyclohexadiene complex **18** (Scheme 19) [44, 45].



Scheme 19 [2+2+2]-Cycloaddition reaction of alkynylboronate with ethylene on cobalt



Scheme 20 Cobalt-catalyzed [4+2]-cycloaddition reaction of alkynylboronate with 1,3-diene

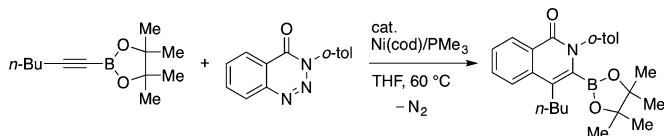


Scheme 21 Ruthenium-catalyzed [2+2+2]-cycloaddition reaction of alkynylboronate, propargyl alcohol, and terminal alkyne

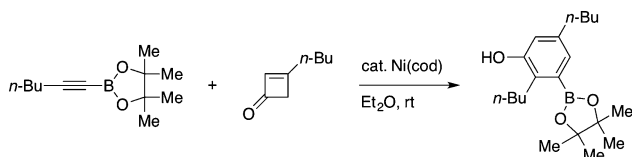
A cobalt catalyst generated by reduction of $\text{CoBr}_2(\text{dppe})$ with zinc promotes the [4+2]-cycloaddition reaction of alkynylboronates with 1,3-dienes (Scheme 20) [46, 47]. 1,4-Cyclohexadienylboronic esters like **19** are obtained in a regioselective fashion.

It is a formidable challenge to catalytically cyclotrimerize three different alkynes in a chemo- and regioselective fashion. Yamamoto and coworkers have reported a ruthenium-catalyzed [2+2+2]-cycloaddition reaction of alkynylboronates, propargyl alcohol, and terminal alkynes (Scheme 21) [48, 49]. At the outset of the reaction, condensation of an alkynylboronate with propargyl alcohol furnishes a boronate-tethered 1,6-diyne **20**, which undergoes oxidative cyclization using a ruthenium catalyst. The resulting ruthenacycle **21** reacts with a terminal alkyne to produce arylboronate **22**. The boronate can also be directly employed for Suzuki–Miyaura coupling reactions, in a one-pot process. The same ruthenium catalyst prompts [2+2+2]-cycloaddition of alkynylboronates with 1,6-diyne [50].

A denitrogenative cycloaddition reaction of 1,2,3-benzotriazin-4(3*H*)-ones with alkynes is induced by nickel catalysis (Scheme 22) [51]. When alkynylboronates are employed as the alkyne, 3-borylated isoquinolones are obtained in a regioselective manner.



Scheme 22 Nickel-catalyzed denitrogenative cycloaddition reaction of alkynylboronate with 1,2,3-benzotriazin-4(3H)-one



Scheme 23 Nickel-catalyzed cycloaddition reaction of alkynylboronate with cyclobutenone

A cycloaddition reaction of cyclobutenones with alkynes (formal insertion of alkynes into a carbon–carbon bond of cyclobutenones) is induced by nickel catalysis [52]. When alkynylboronates are employed as the alkynes, phenols having a boronate moiety are produced (Scheme 23) [53]. The regioselectivity is highly dependent upon the substituents on the alkyne moiety.

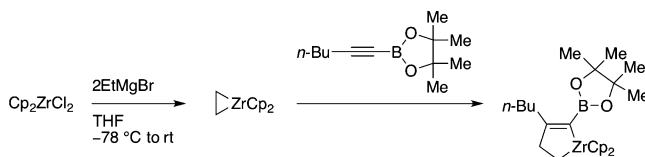
2.4 Miscellaneous

When Cp_2ZrCl_2 is treated with organolithium or organomagnesium reagents, a low-valent zirconocene complex is generated [54], which reacts with unsaturated molecules to produce zirconacycles. The reaction with alkynylboronates affords zirconacycles having the boryl group on the sp^2 carbon next to the zirconium center regioselectively (Scheme 24) [55], as with the case of hydrozirconation reactions [9]. This zirconacycle has been exploited for the stereoselective synthesis of multiply substituted alkenes through selective functionalization of the carbon–zirconium and carbon–boron bonds [56, 57].

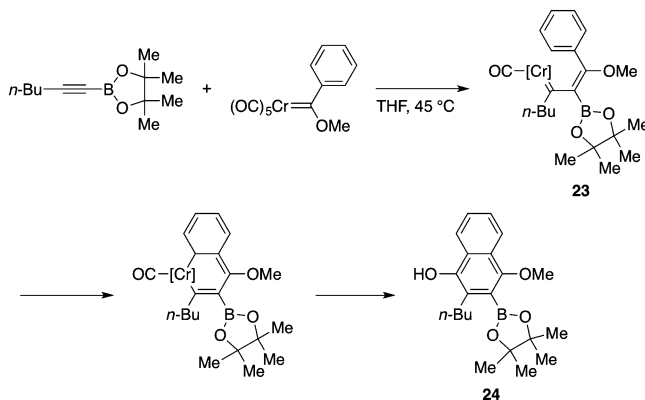
A low-valent zirconocene generated by treatment of Cp_2ZrCl_2 with *n*-butyllithium reacts with two molecules of alkynylboronates to produce a borylated zirconacycle as a mixture of the regioisomers [58]. Di(alkynylboryl)methanes also participate in the cyclization reaction with the low-valent zirconocene [59], as does diborylacetylene which provides an analogous zirconacycle [60].

Fischer carbene complexes react with alkynylboronates in a regioselective manner to give borylated hydroquinones of type **24** (Dötz reaction) (Scheme 25) [61–63].

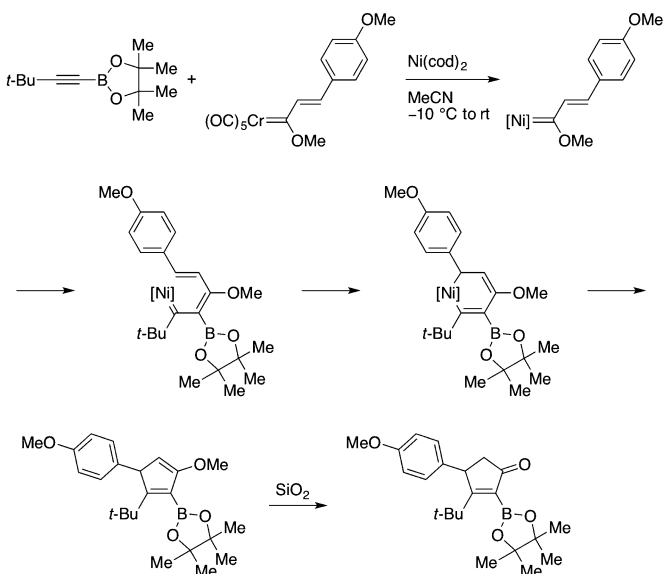
In sharp contrast to the thermal Dötz reaction, the nickel-mediated reaction of alkynylboronates with vinylcarbene complexes proceeds without incorporation of CO to afford cyclopentenones (Scheme 26) [64].



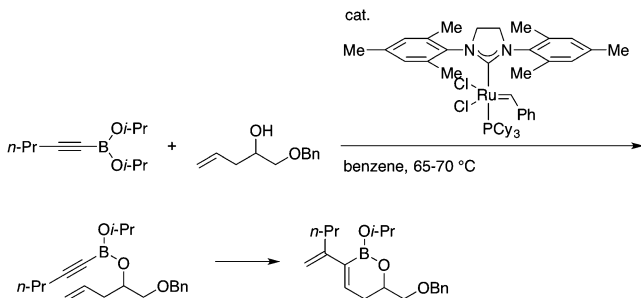
Scheme 24 Regioselective formation of zirconacycle from low-valent zirconocene and alkynylboronate



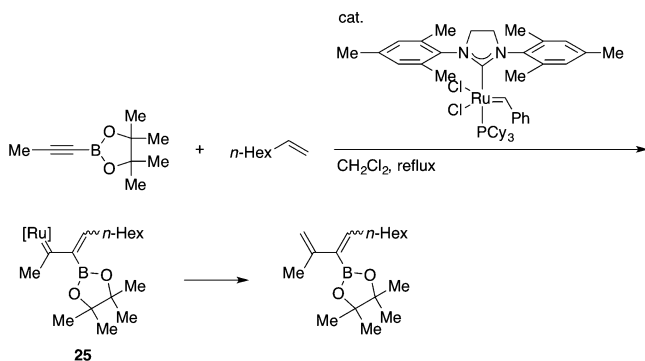
Scheme 25 Dötz reaction of alkynylboronate with Fischer carbene complex



Scheme 26 Nickel-mediated reaction of alkynylboronates with vinylcarbene chromium complex



Scheme 27 Enyne metathesis reaction between alkynylboronate with homoallyl alcohol



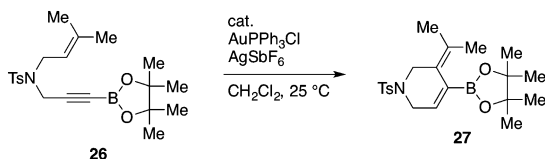
Scheme 28 Enyne metathesis reaction between alkynylboronate and 1-alkene

The enyne metathesis reaction [65, 66] between alkynylboronates and homoallyl alcohols proceeds in a regioselective manner through in situ formation of boron tethered 1,6-enynes (Scheme 27) [67]. The resulting boroxacycles having a dienylboronate unit serve as versatile intermediates for diversity-oriented synthesis.

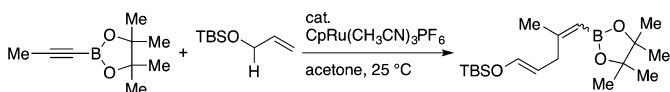
The enyne metathesis reaction of alkynylboronates with 1-alkenes affords alkenylboronates regioselectively (Scheme 28) [68] (for an intramolecular enyne metathesis reaction, see [69]), resulting in the suggested formation of vinylcarbene intermediate **25**, which is similar to the intermediate **23** generated in the Dötz reaction [60]. This regioselective enyne metathesis reaction has been applied to the total synthesis of (–)-amphidinolide **K** [70].

Cationic gold complexes electrophilically activate alkynes to initiate various cyclization reactions [71]. The borylated 1,6-enyne **26** is cycloisomerized by a gold catalyst to give six-membered dienylborane **27** (Scheme 29) [72].

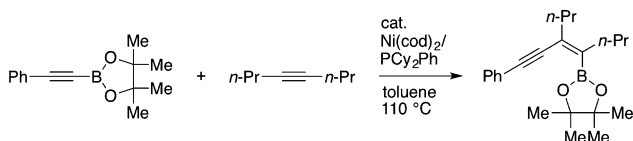
The Alder-ene reaction between alkynes and alkenes (formal addition of allylic C–H bond to alkynes) is promoted by a ruthenium(II) catalyst to furnish a 1,4-dienes [73]. The reaction of alkynylboronates with 1-alkenes generates 1,4-dienylboronates in a regioselective fashion (Scheme 30) [74] with the major



Scheme 29 Gold-catalyzed cycloisomerization reaction of borylated 1,6-enyne



Scheme 30 Ruthenium-catalyzed Alder-ene reaction of alkynylboronate with 1-alkene



Scheme 31 Nickel-catalyzed alkyne-ene reaction of alkynylboronate with 1-alkene

stereoisomer being the *trans*-adducts. This stereoselectivity is in contrast to that of alkynylsilanes, which affords *cis*-adducts as the major products [75].

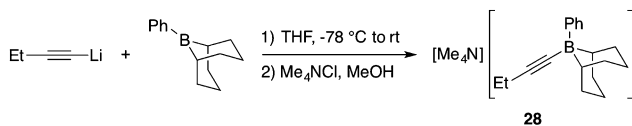
The carbon–boron bond of alkynylboronates is cleaved and adds across alkynes upon treatment with a nickel catalyst (Scheme 31) [76]. Borylated enynes are obtained in a stereoselective manner.

3 Alkynylborates (Ate-Complexes)

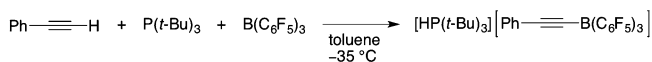
3.1 Preparations

Alkynyl(triorganyl)borates are prepared by the reaction of trialkylborohydrides with terminal alkynes [77] or addition of alkynyllithiums to (triorganyl)boranes [78]. For example, ammonium borate **28** is prepared by the reaction of but-1-nyllithium with Ph-9-BBN in THF at -78°C followed by cation exchange with tetramethylammonium chloride in methanol (Scheme 32) [79]. The borate **28** is reasonably stable in air and to moisture and, therefore, storable for several months in a freezer.

Alkynyl(triaryl)borates are also synthesized by the reaction of terminal alkynes with frustrated Lewis pairs consisting of tris(pentafluorophenyl)borane and bulky phosphines or amines, such as tri(*t*-butyl)phosphine (Scheme 33) [80].



Scheme 32 Preparation of alkynylborate by addition of alkynyllithium to Ph-9-BBN



Scheme 33 Preparation of alkynylborate from terminal alkyne, P(*t*-Bu)₃, and B(C₆F₅)₃

3.2 *Uncatalyzed Reactions*

Alkynyl(triorganyl)borates react with various electrophiles at the β -alkynyl carbon. The addition reaction is accompanied by migration of substituents on boron to the α -carbon, giving rise to (substituted alkenyl)boranes, which is typically followed by protonation. For example, when alkynyl(triethyl)borate **29** is treated with hydrochloric acid, alkenyl(dialkyl)borane **30** is produced as a mixture of (*E*)- and (*Z*)-isomers (Scheme 34) [77, 81–83].

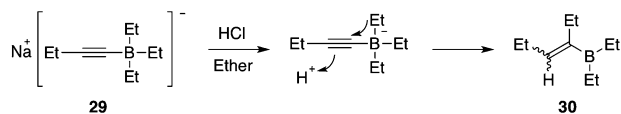
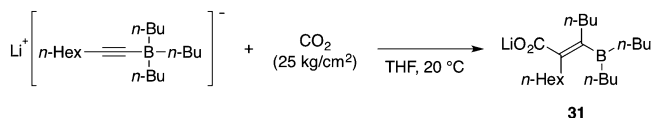
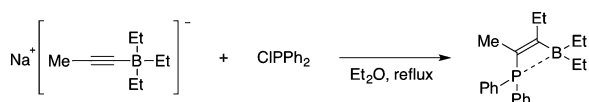
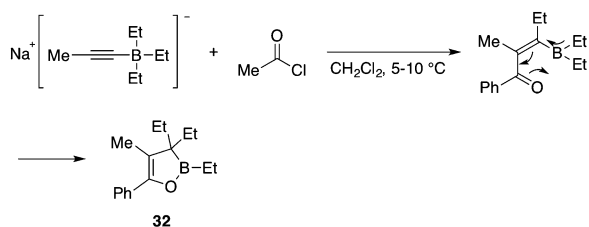
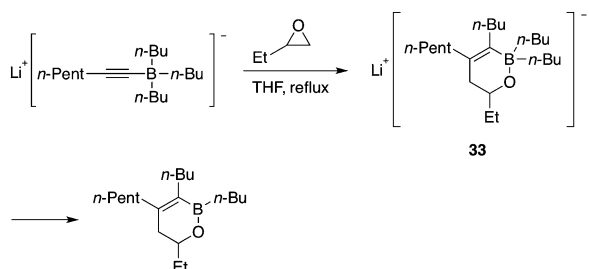
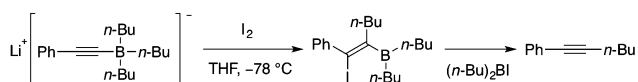
The stereoselectivity depends on the electrophile used to quench the reaction. Alkyl halides afford a mixture of the (*E*)- and (*Z*)-isomers [84–87]. Carbon dioxide furnishes carboxylate **31** in a stereoselective manner (Scheme 35) [88]. Chlorophosphanes [89], sulfonyl chlorides [90], and metal halides [77, 91, 92] provide alkenylboranes in which the boron and heteroatoms are located *cis* across the resulting carbon–carbon double bond (Scheme 36).

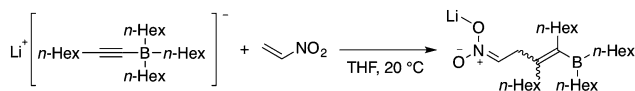
The reaction with acyl halides induces double alkyl migration from boron to the α -carbon, forming boroxacycle **32** (Scheme 37) [93]. Diiodomethane and dibromomethane also react to induce analogous double alkyl migration, resulting in the formation of allylhaloboranes [94].

Oxiranes react with alkynylborates (Scheme 38) [95] resulting in the formation of the cyclic borate **33**. Subsequent thermolysis eliminates one butyl group on boron to produce the corresponding cyclic borinate ester.

A reaction with iodine produces internal alkynes (Scheme 39) [96]. It is assumed that 2-iodoalkenylboranes are initially produced and subsequent deiodoborylation affords alkynes. Treatment with sulfinyl chlorides brings about an analogous reaction [97, 98].

Alkynyl(trialkyl)borates undergo conjugate addition to nitroalkenes at ambient temperature (Scheme 40) [99]. *N*-Acetylpyridinium salts react with alkynyl (trialkyl)borates at the C4 position [100]. Although vinyl ketones are not reactive enough to undergo direct addition, Lewis acids such as TiCl₄ can be used to induce the conjugate addition reaction to afford alkenylboranes [101].

**Scheme 34** Protonation of alkynylborate**Scheme 35** Carboxylation of alkynylborate**Scheme 36** Reaction of alkynylborate with chlorophosphane**Scheme 37** Reaction of alkynylborate with acid chloride**Scheme 38** Reaction of alkynylborate with oxirane**Scheme 39** Reaction of alkynylborate with iodine



Scheme 40 Conjugate addition reaction of alkynylborate to nitroalkene

3.3 Transition Metal-Catalyzed Reactions

The advent of transition metal catalysis has expanded the scope of the electrophiles that can be used and has also made it possible to control the stereoselectivity. A reaction of alkynylborates with aryl halides is promoted by palladium catalysts to produce (trisubstituted alkenyl)boranes (Scheme 41) [79, 102]. In the case of the 9-BBN derivative **34**, the aryl group on boron selectively migrates and the 9-BBN framework is retained in the product. The stereoselectivity is significantly dependent upon the ligand employed. When $P(o\text{-tol})_3$ is used, two aryl groups are incorporated in a *cis* manner. In sharp contrast, the use of xantphos results in the formation of the *trans*-adducts.

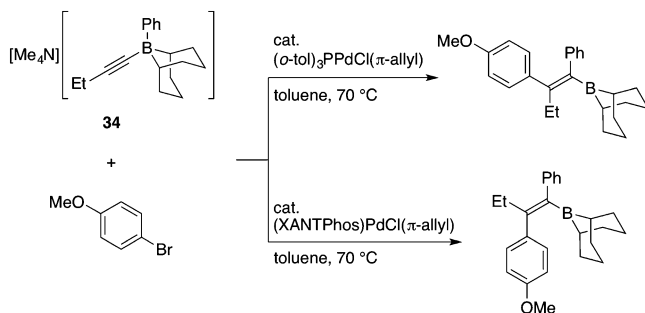
Oligo(arylenevinylene)s having tetrasubstituted vinylene units are stereoselectively synthesized by repetition of the reaction of alkynylborates with 4-iodobromobenzene and Suzuki–Miyaura cross-coupling (Scheme 42) [103]. Initially, 4-bromoanisole is treated with alkynylborate **35** in the presence of (xantphos) $Pd(\pi\text{-allyl})Cl$ to synthesize (trisubstituted alkenyl)-9-BBN **36** stereoselectively. Although the product **36** contains an alkenylborane moiety, it does not couple with 4-bromoanisole in the absence of a base. After completion of the initial reaction, 4-bromoiodobenzene and NaOH are added to the reaction mixture in one pot. The Suzuki–Miyaura coupling reaction takes place chemoselectively at the iodide moiety to give the 2nd generation aryl bromide **37** stereoselectively (*E/Z* < 1/99). Repetition of this sequential procedure grows the arylenevinylene chain without erosion of the stereoselectivity, giving the oligomers as a single stereoisomer.

When alkynyltriarylborates are reacted with bromopyridines, pyridine–borane complexes are obtained (Scheme 43) [104]. This class of compounds generally exhibits fluorescence and has high electron affinity [105, 106].

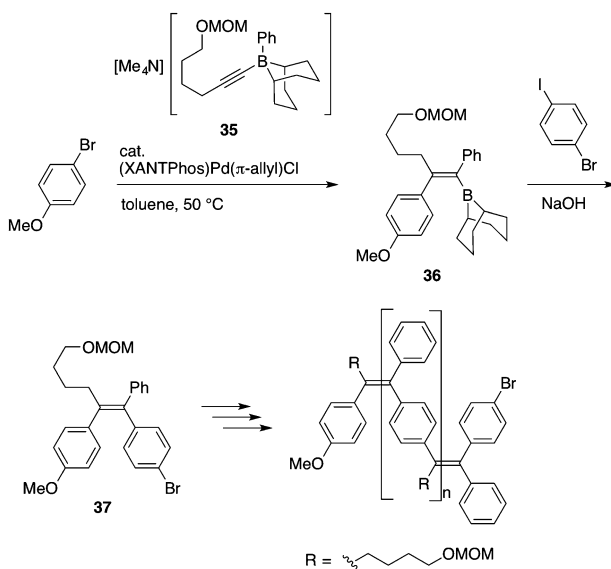
Pyridine-*N*-oxide–borane complexes are also synthesized by an analogous reaction with 2-bromopyridine-*N*-oxides (Scheme 44) [107]. This class of compounds is non-fluorescent but has higher electron affinity than pyridine–borane complexes.

The palladium-catalyzed reaction of *o*-iodophenyl ketones with alkynylborates gives indenenes with site-specific installation of the 2,3-substituents (Scheme 45) [108]. Alkenylborane **38** is initially formed in a regioselective fashion, and the carbon–boron bond subsequently attacks to the carbonyl group to cyclize in a 5-*exo* mode to construct the indene skeleton.

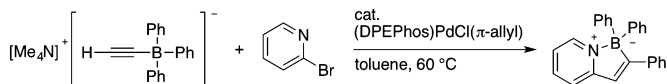
Ammonioalkynylborate **39** is rearranged upon treatment with a palladium catalyst (Scheme 46) [109]. The proton on nitrogen migrates onto the β -alkynyl carbon and the phenyl group on boron migrates onto the α -alkynyl carbon. The resulting



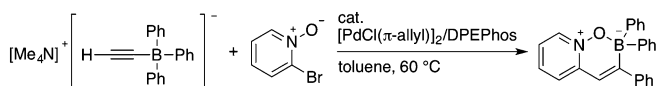
Scheme 41 Palladium-catalyzed reaction of alkynylborate with aryl halide



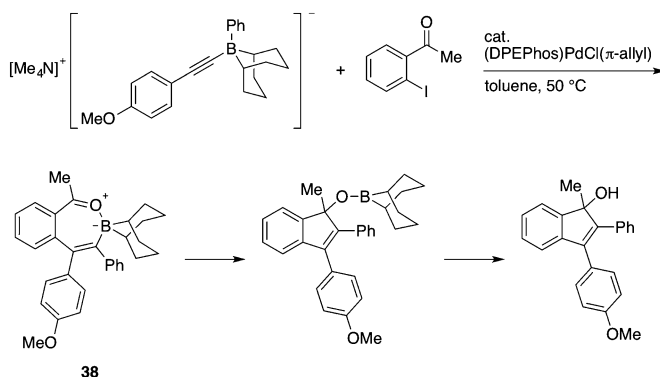
Scheme 42 Iterative procedure for the synthesis of oligo(phenylene)vinylenes having tetrasubstituted vinylene units



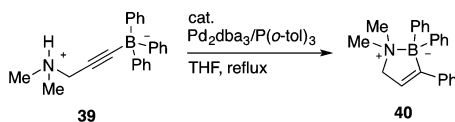
Scheme 43 Synthesis of pyridine-borane complex from alkynylborate and 2-bromopyridine



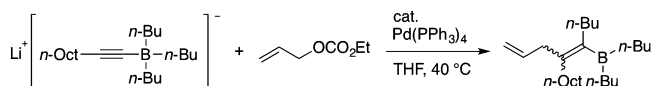
Scheme 44 Synthesis of pyridine-*N*-oxide-borane complex from alkynylborate and 2-bromopyridine-*N*-oxide



Scheme 45 Construction of indene skeleton by a reaction of alkynylborate with *o*-iodoacetophenone



Scheme 46 Palladium-catalyzed rearrangement reaction of ammonioalkynylborate



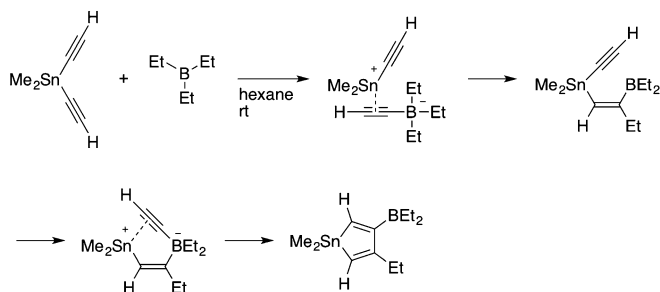
Scheme 47 Palladium-catalyzed allylation reaction of alkynylborate

amine moiety coordinates to the trivalent boron center to form amine–borane complex **40**.

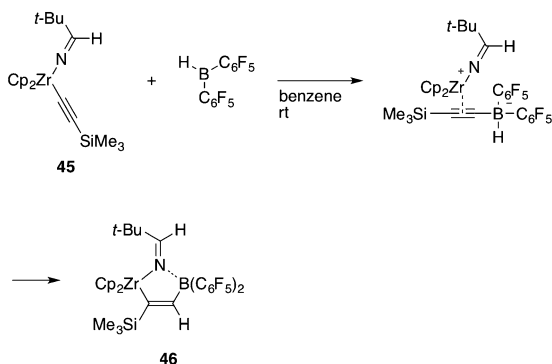
Alkynyl(trialkyl)borates react with allyl carbonates in the presence of $\text{Pd}(\text{PPh}_3)_4$ to furnish (trisubstituted alkenyl)boranes (Scheme 47) [110]. Alkynyl(triaryl)borates, which are less nucleophilic than alkynyl(trialkyl)borates, react with allyl bromide by action of a palladium–xantphos catalyst [111].

3.4 Reactions Through Intermediacy of Alkynyl(Triorganyl) Borates

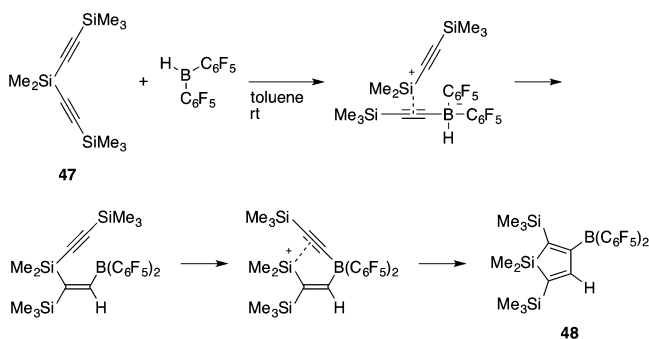
It has been proposed that a palladium-catalyzed three-component reaction of terminal alkynes, allyl alcohols, and trialkylboranes proceeds through the intermediacy of alkynyl(triorganyl)borates (Scheme 48) [112]. Initially, the allyl alcohol undergoes oxidative addition onto palladium(0) with the assistance of the trialkylborane. Then, the acidic hydrogen at the alkyne terminus is deprotonated.



Scheme 50 Formation of stannacyclopentadiene by a reaction of di(ethynyl)stannane with triethylborane

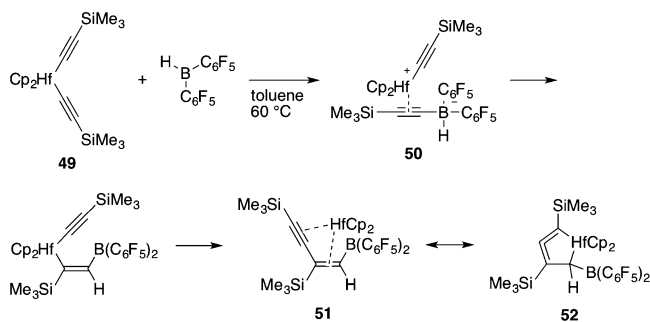


Scheme 51 1,1-Hydroboration of alkynylzircononium with $\text{HB}(\text{C}_6\text{F}_5)_2$



Scheme 52 Formation of silacyclopentadiene by a reaction of di(alkynyl)silane with $\text{HB}(\text{C}_6\text{F}_5)_2$

A hydroboration reaction of di(alkynyl)silane **47** with $\text{HB}(\text{C}_6\text{F}_5)_2$ affords silacyclopentadiene **48** via a 1,1-hydroboration reaction followed by an intramolecular 1,1-alkenylboration reaction (Scheme 52) [133].



Scheme 53 Hydroboration of di(alkynyl)hafnocene with $\text{HB}(\text{C}_6\text{F}_5)_2$

Hydroboration of di(alkynyl)hafnocene **49** with $\text{HB}(\text{C}_6\text{F}_5)_2$ affords metallacyclic allene **52** (Scheme 53) [134]. This reaction is also initiated by alkynyl migration from hafnium to boron. The resulting alkynylborate **50** adds to the cationic hafnium center to induce 1,2-hydride migration. Subsequent reductive elimination of hafnocene yields **51**, which is a resonance structure of metallacyclic allene **52**. Dialkynylzirconocene also exhibits similar reactivities [135].

4 Conclusions

Alkynylboron compounds are easily prepared from alkynes and boron reagents. Many reactions have been developed which pave the way for convenient ways to synthesize alkenyl- and aryl-boron compounds. The products include densely substituted derivatives that are difficult to prepare by other, well-established methods such as the hydroboration of alkynes and the addition of organometallic reagents to electrophilic boron compounds. The subsequent transformations of the C–B bonds of the products would further lead to the synthesis of a variety of complex organic molecules.

References

1. Miyaura N, Suzuki A (1995) *Chem Rev* 95:2457
2. Negishi E (1976) *J Organomet Chem* 108:281
3. Cragg GML, Koch KR (1977) *Chem Soc Rev* 6:393
4. Suzuki A (1982) *Acc Chem Res* 15:78
5. Hilt G, Bolze P (2005) *Synthesis* 2091
6. Jiao J, Nishihara Y (2012) *J Organomet Chem* 721–722:3
7. Brown HC, Bhat NG, Srebnik M (1988) *Tetrahedron Lett* 29:2631
8. Lee C-I, Zhou J, Ozerov OV (2013) *J Am Chem Soc* 135:3560
9. Deloux L, Skrzypczak-Jankun E, Cheesman BV, Srebnik M, Savat M (1994) *J Am Chem Soc* 116:10302

10. Gu Y, Pritzkow H, Siebert W (2001) *Eur J Inorg Chem* 373
11. Li H, Carroll PJ, Walsh PJ (2008) *J Am Chem Soc* 130:3521
12. Weber L, Eickhoff D, Halama J, Werner S, Kahlert J, Stammler H-G, Neumann B (2013) *Eur J Inorg Chem* 2608
13. Soderquist JA, Rane AM, Matos K, Ramos J (1995) *Tetrahedron Lett* 36:6847
14. Struble JR, Lee SJ, Burke MD (2010) *Tetrahedron* 66:4710
15. Ohmura T, Suginome M (2009) *Bull Chem Soc Jpn* 82:29
16. Jiao J, Nakajima K, Nishihara Y (2013) *Org Lett* 15:3294
17. Matteson DS, Waldbillig JO (1963) *J Org Chem* 28:366
18. Woods WG, Strong PL (1967) *J Organomet Chem* 7:371
19. Singleton DA, Leunt S-W (1992) *J Org Chem* 57:4796
20. Leung S-W, Singleton DA (1997) *J Org Chem* 62:1955
21. Silva MA, Pellegrinet SC, Goodman JM (2002) *J Org Chem* 67:8203
22. Silva MA, Pellegrinet SC, Goodman JM (2003) *J Org Chem* 68:4059
23. Seitz G, Haenel F (1994) *Arch Pharm* 327:673
24. Helm MD, Moore JE, Plant A, Harrity JPA (2005) *Angew Chem Int Ed* 44:3889
25. Gomez-Bengoa E, Helm MD, Plant A, Harrity JPA (2007) *J Am Chem Soc* 129:2691
26. Moore JE, York M, Harrity JPA (2005) *Synlett* 860
27. Delaney PM, Moore JE, Harrity JPA (2006) *Chem Commun* 3323
28. Delaney PM, Browne DL, Adams H, Plant A, Harrity JPA (2008) *Tetrahedron* 64:866
29. Kirkham JD, Leach AG, Row EC, Harrity JPA (2012) *Synthesis* 44:1964
30. Delaney PM, Huang J, Macdonald SJF, Harrity JPA (2007) *Org Lett* 10:781
31. Kirkham JD, Butlin RJ, Harrity JPA (2012) *Angew Chem Int Ed* 51:6402
32. Crepin DFP, Harrity JPA, Jiang J, Meijer AJHM, Nassoy A-CMA, Raubo P (2014) *J Am Chem Soc* 136:8642
33. Vivat JF, Adams H, Harrity JPA (2010) *Org Lett* 12:160
34. Matteson DS (1962) *J Org Chem* 27:4293
35. Davies MW, Wybrow RAJ, Johnson CN, Harrity JPA (2001) *Chem Commun* 1558
36. Huang J, Macdonald SJF, Harrity JPA (2009) *Chem Commun* 436
37. Browne DL, Helm MD, Plant A, Harrity JPA (2007) *Angew Chem Int Ed* 46:8656
38. Browne DL, Vivat JF, Plant A, Gomez-Bengoa E, Harrity JPA (2009) *J Am Chem Soc* 131:7762
39. Kirkham JD, Edeson SJ, Stokes S, Harrity JPA (2012) *Org Lett* 14:5354
40. Maderna A, Pritzkow H, Siebert W (1996) *Angew Chem Int Ed* 35:1501
41. Ester C, Maderna A, Pritzkow H, Siebert W (2000) *Eur J Inorg Chem* 1177
42. Goswami A, Pritzkow H, Rominger F, Siebert W (2004) *Eur J Inorg Chem* 4223
43. Gandon V, Leca D, Aechtner T, Vollhardt KPC, Malacria M, Aubert C (2004) *Org Lett* 6:3405
44. Gandon V, Leboeuf D, Amslinger S, Vollhardt KPC, Malacria M, Aubert C (2005) *Angew Chem Int Ed* 44:7114
45. Geny A, Leboeuf D, Rouquie G, Vollhardt KPC, Malacria M, Gandon V, Aubert C (2007) *Chem Eur J* 13:5408
46. Hilt G, Smolko KI (2003) *Angew Chem Int Ed* 42:2795
47. Auvinet A-L, Harrity JPA, Hilt G (2010) *J Org Chem* 75:3893
48. Yamamoto Y, Ishii J, Nishiyama H, Itoh K (2004) *J Am Chem Soc* 126:3712
49. Yamamoto Y, Ishii J, Nishiyama H, Itoh K (2005) *Tetrahedron* 61:11501
50. Yamamoto Y, Hattori K, Ishii J, Nishiyama H (2006) *Tetrahedron* 62:4294
51. Miura T, Yamauchi M, Murakami M (2008) *Org Lett* 10:3085
52. Huffman MA, Liebeskind LS (1991) *J Am Chem Soc* 113:2771
53. Auvinet A-L, Harrity JPA (2011) *Angew Chem Int Ed* 50:2769
54. Negishi E, Takahashi T (1998) *Synthesis* 1
55. Quintar AAA, Srebnik M (2004) *Org Lett* 6:4243

56. Nishihara Y, Miyasaka M, Okamoto M, Takahashi H, Inoue E, Tanemura K, Takagi K (2007) *J Am Chem Soc* 129:12634
57. Nishihara Y, Okada Y, Jiao J, Suetsugu M, Lan M-T, Kinoshita M, Iwasaki M, Takagi K (2011) *Angew Chem Int Ed* 50:8660
58. Desurmont G, Klein R, Uhlenbrock S, Laloe E, Deloux L, Giolando DM, Kim YW, Pereira S, Srebnik M (1996) *Organometallics* 15:3323
59. Metzler N, Nöth H, Thomann M (1993) *Organometallics* 12:2423
60. Altenburger K, Arndt P, Spannenberg A, Baumann W, Rosenthal U (2013) *Eur J Inorg Chem* 3200
61. Davies MW, Harrity JPA, Johnson CN (1999) *Chem Commun* 2107
62. Davies MW, Johnson CN, Harrity JPA (2001) *J Org Chem* 3525
63. Dötz KH, Tomuschat P (1999) *Chem Soc Rev* 28:187
64. Barluenga J, Barrio P, Riesgo L, Lopez LA, Tomas M (2007) *J Am Chem Soc* 129:14422
65. Poulsen CS, Madsen R (2003) *Synthesis* 1
66. Giessert AJ, Diver ST (2004) *Chem Rev* 104:1317
67. Micalizio GC, Schreiber SL (2002) *Angew Chem Int Ed* 41:3272
68. Kim M, Lee D (2005) *Org Lett* 7:1865
69. Renaud J, Graf C-D, Oberer L (2000) *Angew Chem Int Ed* 39:3101
70. Ko HM, Lee CW, Kwon HK, Chung HS, Choi SY, Chung YK, Lee E (2009) *Angew Chem Int Ed* 48:2364
71. Belmont P, Parker E (2009) *Eur J Org Chem* 6075
72. Lee JCH, Hall DG (2011) *Tetrahedron Lett* 52:321
73. Trost BM, Toste FD, Pinkerton AB (2001) *Chem Rev* 101:2067
74. Hansen EC, Lee D (2005) *J Am Chem Soc* 127:3252
75. Trost BM, Machacek M, Schnaderbeck MJ (2000) *Org Lett* 2:1761
76. Suginome M, Shirakura M, Yamamoto A (2006) *J Am Chem Soc* 128:14438
77. Binger P, Köster R (1965) *Tetrahedron Lett* 6:1901
78. Binger P, Benedikt G, Rotermund GW, Köster R (1968) *Liebigs Ann Chem* 717:21
79. Ishida N, Shimamoto Y, Murakami M (2009) *Org Lett* 11:5434
80. Dureen MA, Stephan DW (2009) *J Am Chem Soc* 131:8396
81. Miyaura N, Yoshinari T, Itoh M, Suzuki A (1974) *Tetrahedron Lett* 15:2961
82. Brown HC, Levy AB, Midland MM (1975) *J Am Chem Soc* 97:501
83. Pelter A, Harrison CR, Subrahmanyam C, Kirkpatrick D (1976) *J Chem Soc Perkin Trans* 1:2435
84. Pelter A, Harrison CR, Kirkpatrick (1973) *J Chem Soc Chem Commun* 544
85. Pelter A, Subrahmanyam C, Laub RJ, Gould KJ, Harrison CR (1975) *Tetrahedron Lett* 1633
86. Pelter A, Bentley TW, Harrison CR, Subrahmanyam C, Laub RJ (1976) *J Chem Soc Perkin Trans* 1:2419
87. Pelter A, Gould KJ, Harrison CR (1976) *J Chem Soc Perkin Trans* 1:2428
88. Deng M, Tang Y, Xu W (1984) *Tetrahedron* 25:1797
89. Binger P, Köster R (1974) *J Organomet Chem* 73:205
90. Gerard J, Hevesi L (2001) *Tetrahedron* 57:9109
91. Binger P, Köster R (1973) *Synthesis* 309
92. Hooz J, Mortimer R (1976) *Tetrahedron Lett* 17:805
93. Binger P (1967) *Angew Chem Int Ed* 6:84
94. Pelter A, Harrison CR (1974) *J Chem Soc Chem Commun* 829
95. Naruse M, Utimoto K, Nozaki H (1974) *Tetrahedron* 30:3037
96. Suzuki A, Miyaura N, Abiko S, Itoh M, Brown HC, Sinclair JA, Midland MM (1973) *J Am Chem Soc* 95:3080
97. Naruse M, Utimoto K, Nozaki H (1973) *Tetrahedron Lett* 14:1847
98. Naruse M, Utimoto K, Nozaki H (1973) *Tetrahedron* 30:2159
99. Pelter A, Hughes L (1977) *J Chem Soc Chem Commun* 913
100. Pelter A, Gould KJ (1974) *J Chem Soc Chem Commun* 347

101. Hara S, Kishimura K, Suzuki A (1980) *Chem Lett* 9:221
102. Ishida N, Miura T, Murakami M (2007) *Chem Commun* 4381
103. Ishida N, Shimamoto Y, Murakami M (2010) *Org Lett* 12:3179
104. Ishida N, Narumi M, Murakami M (2012) *Helv Chim Acta* 95:474
105. Wakamiya A, Taniguchi T, Yamaguchi S (2006) *Angew Chem Int Ed* 45:3170
106. Yoshino J, Kano N, Kawashima T (2007) *Chem Commun* 559
107. Ishida N, Ikemoto W, Narumi M, Murakami M (2011) *Org Lett* 13:3008
108. Shimamoto Y, Sunaba H, Ishida N, Murakami M (2013) *Eur J Org Chem* 1421
109. Ishida N, Narumi M, Murakami M (2008) *Org Lett* 10:1279
110. Chen Y, Li N, Deng M (1990) *Tetrahedron Lett* 31:2405
111. Ishida N, Shinmoto T, Sawano S, Miura T, Murakami M (2010) *Bull Chem Soc Jpn* 83:1380
112. Fukushima M, Takushima D, Satomura H, Onodera G, Kimura M (2012) *Chem Eur J* 18:8019
113. Wrackmeyer B (1995) *Coord Chem Rev* 145:125
114. Kehr G, Erker G (2012) *Chem Commun* 48:1839
115. Wrackmeyer B, Nöth H (1976) *J Organomet Chem* 108:C21
116. Menz G, Wrackmeyer B (1977) *Z Naturforsch* 32b:1400
117. Chen C, Voss T, Fröhlich R, Kehr G, Erker G (2011) *Org Lett* 13:62
118. Köster R, Seidel G, Wrackmeyer B (1989) *Chem Ber* 122:1825
119. Ekkert O, Kehr G, Fröhlich R, Erker G (2011) *J Am Chem Soc* 133:4610
120. Wrackmeyer B, Horchler K, Boese R (1989) *Angew Chem Int Ed* 28:1500
121. Sebald A, Wrackmeyer B (1983) *J Chem Soc Chem Commun* 309
122. Chen C, Kehr G, Fröhlich R, Erker G (2010) *J Am Chem Soc* 132:13594
123. Fan C, Piers WE, Parves M, McDonald R (2010) *Organometallics* 29:5132
124. Ekkert O, Kehr G, Fröhlich R, Erker G (2011) *Chem Commun* 47:10482
125. Wrackmeyer B, Kehr G, Boese R (1991) *Angew Chem Int Ed* 30:1370
126. Killian L, Wrackmeyer B (1977) *J Organomet Chem* 132:213
127. Ge F, Kehr G, Daniliuc CG, Erker G (2014) *J Am Chem Soc* 136:68
128. Wrackmeyer B (1986) *J Chem Soc Chem Commun* 397
129. Wrackmeyer B (1986) *J Organomet Chem* 310:151
130. Wrackmeyer B, Pedall A, Weidinger J (2002) *J Organomet Chem* 649:225
131. Sebald A, Wrackmeyer B (1983) *J Chem Soc Chem Commun* 1293
132. Podiyanachari SK, Fröhlich R, Daniliuc CG, Petersen JL, Mück-Lichtenfeld C, Kehr G, Erker G (2012) *Angew Chem Int Ed* 51:8830
133. Ugolotti J, Kehr G, Fröhlich R, Erker G (2010) *Chem Commun* 46:3016
134. Ugolotti J, Dierker G, Kehr G, Fröhlich R, Grimme S, Erker G (2008) *Angew Chem Int Ed* 47:2622
135. Ugolotti J, Kehr G, Fröhlich R, Grimme S, Erker G (2009) *J Am Chem Soc* 131:1996

Improving Transformations Through Organotrifluoroborates

Kaitlin M. Traister and Gary A. Molander

Contents

1	Introduction	118
2	Improvements Toward Organotrifluoroborate Synthesis	118
3	Recent Advances in C–C Bond Formation with Organotrifluoroborates	122
3.1	Cross-Coupling of Novel Organotrifluoroborates	122
3.2	Improved Incorporation of Important Scaffolds	127
3.3	C–H Functionalization with Organotrifluoroborates	131
3.4	Enantioselective C–C Bond Formation	133
3.5	Radical Reactions with Organotrifluoroborates	136
4	C–Y Bond Formation from Organotrifluoroborates	141
4.1	C–O Bond Formation	141
4.2	C–N Bond Formation	142
4.3	C–X Bond Formation	145
5	Using Organotrifluoroborates to Construct Novel Scaffolds	147
6	Conclusions and Outlook	149
	References	149

Abstract Organotrifluoroborates have emerged as choice reagents for a number of diverse transformations, providing reactivity patterns that complement those of other available organoboron reagents. Over the last several years, numerous potassium organotrifluoroborates have become commercially available owing to their long shelf-lives. As a result of this and their unique reactivity patterns, a significant amount of progress has been made in the synthesis and utilization of organotrifluoroborate salts in organic transformations.

K.M. Traister • G.A. Molander (✉)
Roy and Diana Vagelos Laboratories, Department of Chemistry, University of Pennsylvania,
Philadelphia, PA 19104-6323, USA
e-mail: gmolandr@sas.upenn.edu

Keywords Cross-coupling • Heteroatom conversion • Organotrifluoroborates

1 Introduction

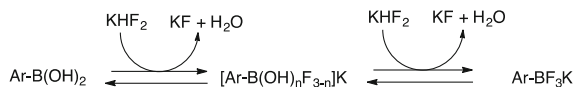
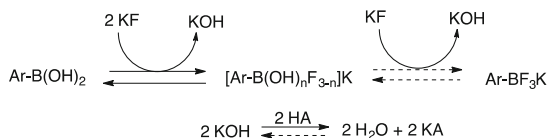
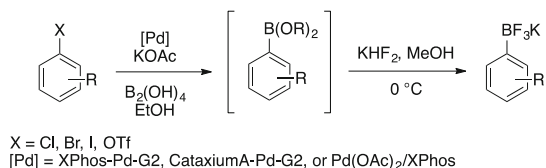
Organotrifluoroborates have emerged as a powerful group of reagents for both carbon–carbon and carbon–heteroatom bond-forming processes. Several desirable features afford them inherent advantages over other boronic acid derivatives. For example, new methods in organotrifluoroborate synthesis have allowed more convenient and selective syntheses of existing substructures, as well as access to novel building blocks that are unknown among other boronic acid surrogates. The trifluoroborates are often more atom economical than boronate ester analogues, and the potassium salts are reliably stable, monomeric, crystalline solids with indefinite shelf-lives, in contrast to many boronic acids and boronate esters.

Within cross-coupling forums, organotrifluoroborates serve as “protected” forms of boronic acids that can be slowly hydrolyzed to their reactive boronate form under basic reaction conditions. In this manner, they represent stable reservoirs for their more reactive counterparts; as a result, they can generally be used stoichiometrically or in slight excess relative to their coupling partners [1]. Organotrifluoroborates, therefore, often afford practical improvements over other boron-based reagents in many transition metal-catalyzed cross-coupling protocols.

Although there has been substantial progress over the last decade in the application of organotrifluoroborates in these transformations, numerous other areas of synthetic methods development have also benefitted as a result of the increased attention paid to these reagents (for other reviews on potassium organotrifluoroborates, see [2–6]). This chapter provides a summary of the major advances made possible through the use of organotrifluoroborates in areas that include cross-coupling and a variety of other carbon–carbon bond-forming processes, but also surveys their application in other important synthetic regimes.

2 Improvements Toward Organotrifluoroborate Synthesis

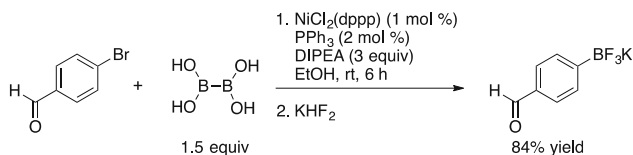
The last decade has seen a significant progress in the area of organotrifluoroborate preparation. The seminal breakthrough that opened the floodgates for research in organotrifluoroborate research came with Vedejs’ development of a convenient way to generate these materials using inexpensive KHF_2 (Scheme 1) [7]. This method has proven to be rapid, efficient, and amazingly general. However, although this protocol reliably effects the desired transformation, the KF and excess

**Scheme 1** Preparation of aryltrifluoroborates from arylboronic acids using KHF_2 **Scheme 2** Preparation of aryltrifluoroborates from arylboronic acids using KF /tartrate [8]**Scheme 3** Borylation of aryl halides with bisboronic acid

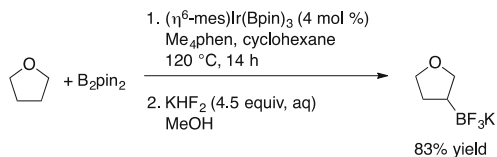
KHF_2 by-products must be removed from the product by Soxhlet extraction or repeated hot filtrations. The use of KHF_2 also results in etching of commonly used borosilicate glassware.

To avoid these drawbacks, a recent procedure was developed for the conversion of boronic acid and boronate ester species to organotrifluoroborates under non-etching conditions that used KF in the presence of tartaric acid [8]. The use of a stoichiometric amount of tartaric acid allows the precipitation of bitartrate through the reaction of tartaric acid with KOH , which drives the equilibrium toward the organotrifluoroborate salt. This method eliminates the need for Soxhlet extraction techniques because the by-products precipitate out of organic solution (Scheme 2).

Bis(pinacolato)diboron has nearly always been the reagent of choice in various borylation reactions owing to its stability and crystalline form. However, procedures have more recently been developed that makes use of bisboronic acid (BBA) as a stable, crystalline reagent that is not only a more atom-economical borylating agent but also avoids the task of having to remove pinacol from the desired products. Under conditions that were determined using high-throughput experimentation, arylboronic acids and a variety of boronate ester derivatives were accessed directly from aryl chlorides under Pd catalysis (Scheme 3) [9]. Because isolation of the boronate ester is not necessary, this method allows in situ coupling of organoboron compounds that are potentially unstable toward isolation [10]. A large variety of functional groups are tolerated on the starting aryl chloride, including ester, nitrile, nitro, ketone, alcohol, amino, and trifluoromethyl groups. Notably, *ortho*-substitution on the aromatic ring can be accommodated. Aryl aldehydes, nitro compounds, and ketones underwent reduction to various extents under the Pd-catalyzed conditions.



Scheme 4 Nickel-catalyzed borylation of 4-bromoacetophenone

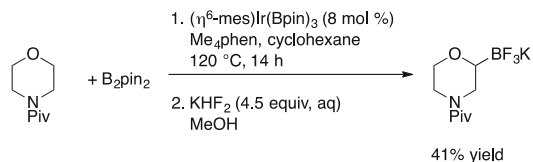
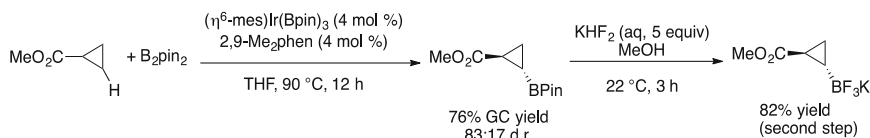
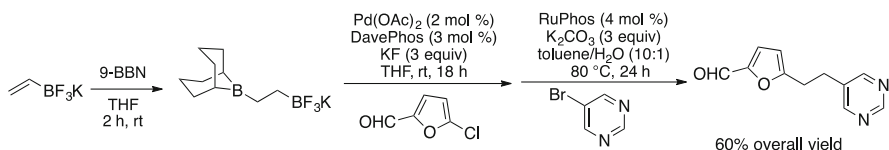


Scheme 5 Ir-catalyzed borylation of cyclic ethers

As an extension of this palladium-catalyzed borylation protocol, a Ni-catalyzed borylation procedure with BBA was developed for aryl and heteroaryl halides as well as pseudohalides. This method offers advantages over the Pd-catalyzed method in terms of cost and substrate scope, in addition to being able to carry out the reactions under much milder conditions (Scheme 4) [11]. As with the Pd-catalyzed method, this protocol was found to be extremely tolerant of a wide variety of functional groups on the aryl substrate, including nitrile, ketone, ester, aldehyde, trifluoromethyl, nitro, alcohol, and amino moieties. Because of the lower temperatures and shorter reaction times employed in this method, no reduction of carbonyl-containing structures was observed. Importantly, the Ni-catalyzed method also allowed extension to a wide range of heteroaryltrifluoroborates, including thiophene, benzothiophene, furan, benzofuran, indole, pyridyl, quinoline, pyrazole, and azaindole substrates that were not possible using Pd catalysis. In addition to aryl bromides, under the developed conditions, aryl chlorides, iodides, triflates, tosylates, mesylates, and sulfamates were also borylated in good yields.

Access to boronic acids and derivatives, which are the ultimate precursors to organotrifluoroborates, has historically been achieved from the corresponding organic halides through metal halogen exchange and/or transmetalation methods. More recently developed methods, which avoid the use of organic halides, include Rh- and Ru-catalyzed C–H borylations of unactivated alkanes and arenes [12–14]. As one example, Hartwig et al. have demonstrated the application of Ir-catalysis toward aryl C–H borylation [15]. The activation of secondary C–H bonds in cyclic ethers has also been achieved using an iridium catalyst, $(\eta^6\text{-mes})\text{Ir}(\text{BPin})_3$, (*mes*=mesitylene), in the presence of 3,4,7,8-tetramethyl-1,10-phenanthroline (*Me*₄phen) (Scheme 5) [16].

As shown, the borylation is typically selective for the C–H bond β to the oxygen atom, and a variety of cyclic ethers can be employed as substrates. However, because of the steric bulk of the pivalate group in *N*-pivaloyl morpholine substrates, the borylation in this substrate proceeds α to the oxygen atom (Scheme 6).

**Scheme 6** Ir-catalyzed borylation of *N*-pivaloyl morpholine**Scheme 7** Ir-catalyzed borylation of cyclopropanes**Scheme 8** Synthesis of orthogonally reactive dibora species from vinyltrifluoroborate

The Ir-catalyzed C–H borylation protocol was further extended to cyclopropyl systems, and it was demonstrated that in the presence of either (η^6 -mes)Ir(BPin)₃ or [Ir(COD)OMe]₂, the borylation was selective for the methylene C–H bonds even on substituted structures (Scheme 7) [17]. Although most of the products were isolated as cyclopropylboronate esters, it was demonstrated that these compounds could be readily converted to the corresponding potassium trifluoroborate salts as well.

Because trifluoroborates represent a protected organoboron moiety, several advancements have focused on taking advantage of the orthogonal reactivity of trifluoroborates and more reactive (tricoordinate) boron species [18]. Functionalized organotrifluoroborates have been prepared through the selective coupling of bifunctional borane/trifluoroborate species. For example, a 1,2-dianion equivalent has been prepared through the borylation of vinyltrifluoroborate with 9-BBN [19, 20]. Using the developed conditions, the trialkylborane can be selectively coupled with an aryl or heteroaryl halide under anhydrous conditions, leaving the organotrifluoroborate untouched (Scheme 8). Using a second set of (aqueous) conditions, the organotrifluoroborate is unmasked and subsequently cross-coupled with a different aryl or heteroaryl halide. The dibora species allows preparation of an array of ethyl-linked substructures. A variety of aryl and heteroaryl bromides and chlorides were successfully employed in this reaction, and the method boasts tolerance of ketone, ester, aldehyde, and nitrile groups.

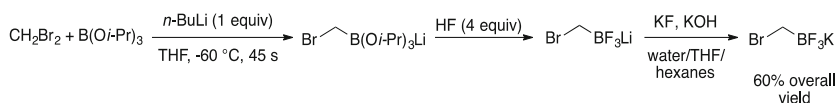
3 Recent Advances in C–C Bond Formation with Organotrifluoroborates

3.1 Cross-Coupling of Novel Organotrifluoroborates

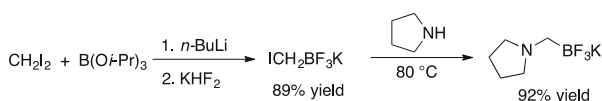
Although organotrifluoroborates have proven efficient and often advantageous when compared to even the most generic boronic acid and boronate ester analogues [21], one advantage of these reagents that has been exploited recently is the availability of novel and highly useful organotrifluoroborates whose complements do not exist among other boronic acid derivatives. One such set of example are the halomethyltrifluoroborates, the syntheses of which spawned whole new families of highly valuable building blocks for organic synthesis (Scheme 9) [22]. Both bromomethyl- and iodomethyl-trifluoroborates were originally prepared on multi-gram scale from the corresponding dihalomethane and a trialkylborate. Subsequently, a spectacular advance was made by the application of flow chemistry, providing improved large-scale preparation of potassium bromomethyltrifluoroborate [23]. A continuous-flow process was thus developed that allowed production of 100 kg of this important building block in less than 4 weeks. This development makes feasible the use of bromomethyltrifluoroborate in synthetic strategies employing multi-kilogram quantities of the reagent.

Once prepared, the halomethyltrifluoroborates were reacted with a wide variety of carbon-, oxygen-, sulfur-, and nitrogen-based nucleophiles, providing access to diverse organotrifluoroborates. The employed nucleophiles include organolithiums, primary and secondary amines, organomagnesium, alkoxides, carbanions, cyanide, and thiolates. It was demonstrated that nucleophilic displacement could also be carried out on 5-bromopentyltrifluoroborate, providing support for the presumed S_N2 nature of the reaction as opposed to an α -transfer mechanism, normally observed with tri-coordinate organoboron derivatives (Scheme 10).

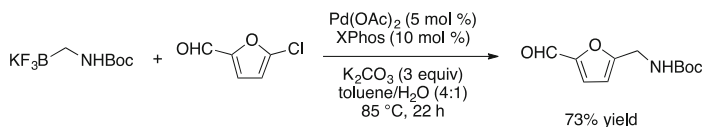
A method for the cross-coupling of potassium Boc-protected aminomethyltrifluoroborates with a variety of aryl and heteroaryl chlorides was developed [24], providing an alternative to reductive aminations for the introduction of aminomethyl groups into aromatic systems. An advantage of the cross-coupling



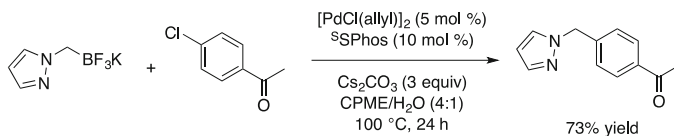
Scheme 9 Preparation of bromomethyltrifluoroborate through continuous-flow chemistry



Scheme 10 Preparation and nucleophilic substitution of potassium iodomethyltrifluoroborate



Scheme 11 Cross-coupling of *N*-Boc-aminomethyltrifluoroborate

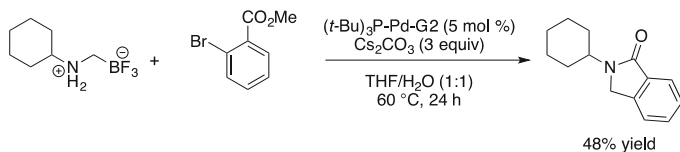


Scheme 12 Cross-coupling of potassium trifluoro(*N*-methylpyrazolo)borate

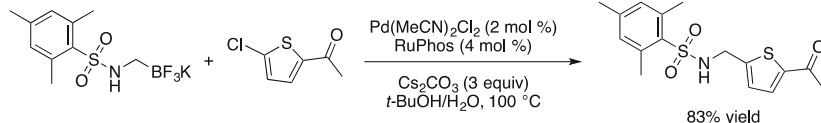
approach is that aryl and heteroaryl chlorides could be utilized as starting materials for the transformation, in place of less readily available and less stable aryl and heteroaryl aldehydes. For both aryl and heteroaryl chlorides, good to excellent yields were obtained with both XPhos and SPhos as ligands, which were shown to provide complementary reactivity. The substrate scope of this reaction was shown to include nitrile, nitro, ester, aldehyde, and ketone functional groups as well as di-*ortho*-substitution. The heteroaryl chlorides that were successfully cross-coupled included substituted thiophene, pyridine, quinoline, isoquinoline, furan, and indole systems (Scheme 11). Only 1.05 equiv. of the aminomethyltrifluoroborate were required to drive this reaction to completion.

This method was later extended to the coupling of trifluoro(*N*-methylheteroaryl) borates [25], secondary ammoniomethyltrifluoroborates [26], and sulfonamido-methyltrifluoroborates [27] by using slightly modified reaction conditions. These methods allow access to a variety of highly valued aminomethylated arene cores. Potassium trifluoro(*N*-methylheteroaryl)borates were prepared from the reaction of pyrrole, pyrazole, or indole with potassium chloromethyltrifluoroborate in the presence of KHMDS. Once prepared, these trifluoro(*N*-methylheteroaryl)borates were cross-coupled with a variety of aryl and heteroaryl chlorides. Slightly different conditions were required, however, for the coupling of each trifluoroborate. Although the pyrazole system was optimized with the use of $[\text{PdCl}(\text{allyl})]_2$ and sodium 2'-dicyclohexylphosphino-2,6-dimethoxy-1,1'-biphenyl-3-sulfonate hydrate ($^{\text{S}}\text{SPhos}$) (Scheme 12), the pyrrole and indole systems gave higher conversions with $\text{Pd}(\text{OAc})_2$ in the presence of RuPhos. All three trifluoro(*N*-methylheteroaryl)borates were successfully cross-coupled with a variety of aryl and heteroaryl chlorides. The substrate scope was shown to include nitrile, nitro, ketone, ester, aldehyde, and amino functional groups. The heteroaryl chlorides illustrated as electrophilic coupling partners included pyridine, thiophene, quinoline, pyrazine, furan, and indole systems.

A variety of secondary potassium ammoniomethyltrifluoroborates were prepared through the reaction of primary amines with bromomethyltrifluoroborate



Scheme 13 Cross-coupling of secondary potassium ammoniomethyltrifluoroborate



Scheme 14 Cross-coupling of potassium sulfonamidomethyltrifluoroborate

[26]. Although conversion to the desired products was achieved with chloromethyltrifluoroborate, the reaction did not go to completion, even using elevated temperatures. The use of bromomethyltrifluoroborate, however, allowed the preparation of numerous potassium ammoniomethyltrifluoroborates, several of which contain multiple heteroatoms. The use of a palladium biphenyl tri-*tert*-butylphosphine precatalyst, $(t\text{-Bu})_3\text{P-Pd-G2}$, allowed the cross-coupling of these compounds with aryl and heteroaryl bromides to proceed in good to excellent yields (Scheme 13). Aryl bromides bearing *ortho*-substitution as well as nitrile, amino, nitro, and ester functional groups were cross-coupled in good yields. The scope of the heteroaryl bromides employed as electrophilic coupling partners includes quinoline, isoquinoline, indole, pyridine, and thiophene moieties. Cross-coupling with methyl 2-bromobenzoate allows subsequent intramolecular cyclization to take place, yielding a substituted isoindolinone.

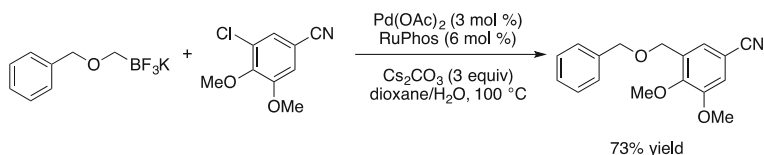
Potassium sulfonamidomethyltrifluoroborates were prepared from the pinacol ester of chloromethylboronic acid [27]. A variety of aryl and heteroaryl sulfonyl chlorides were used to create a library of diverse sulfonamidomethyltrifluoroborates, bearing chloride, bromide, nitro, and amide substituents. Cross-couplings with aryl and heteroaryl chlorides were carried out under catalysis with $\text{Pd}(\text{MeCN})_2\text{Cl}_2$ in the presence of RuPhos , requiring only 1.2 equiv. of the corresponding trifluoroborate (Scheme 14). Aryl chlorides bearing ketone, ester, aldehyde, and nitrile moieties as well as pyridine, thiophene, and furan substrates were successfully coupled under this set of conditions. The reaction was shown to extend beyond aryl chlorides to limited examples of aryl bromide, iodide, triflate, tosylate, and mesylate substrates.

Another important and unique class of organotrifluoroborates that has emerged is that of alkoxymethyltrifluoroborates, which were cross-coupled with aryl chlorides to provide access to complex ethers [28]. The strategic bond connection brought about by this process avoids multistep approaches to the same materials that normally transpire through reduction of carboxylic acid derivatives. To initiate this program, a variety of alkoxymethyltrifluoroborates were prepared from the

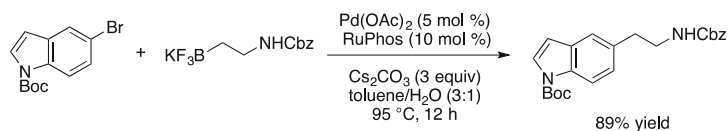
reaction of bromomethyltrifluoroborate with benzyl, aryl, as well as primary, secondary, and tertiary aliphatic alcohols. The cross-coupling of these alkoxymethyltrifluoroborates was demonstrated to proceed in the presence of several monodentate and bidentate phosphine ligands, but ultimately RuPhos appeared to be the optimal ligand (Scheme 15). The cross-coupling of alkoxymethyltrifluoroborates with aryl chlorides was demonstrated, but extension to heteroaryl chloride substrates was challenging and thus proved to be a limitation of the developed method. Although a general method for the coupling of potassium (2-(trimethylsilyl)ethoxy)methyltrifluoroborate with heteroaryl chlorides and bromides.

In addition to the progress that has been made in accessing organotrifluoroborates that provide methyl linkers to heteroatoms, methods have been developed over the last several years to provide access to organotrifluoroborates that serve as ethyl linkers to heteroatoms as well. Several potassium β -aminoethyltrifluoroborates have been prepared through the hydroboration of *N*-vinyl substrates with di(isopropylprenyl)borane (*i*-PP₂BH) followed by treatment with KHF₂ [29], giving rise to aminoethylating reagents [30]. These reagents were initially cross-coupled with a variety of aryl and heteroaryl bromides in good yields in the presence of PdCl₂(dppf) · CH₂Cl₂ (Scheme 16) [31]. The substrate scope of this reaction included aryl and heteroaryl bromides bearing nitrile, ketone, ester, aldehyde, nitro, and amide functional groups. Subsequent to the initial report, slight modification of the reaction conditions allowed extension of the substrate scope to include aryl triflates and iodides [32]. The heteroaryl bromide scope was also expanded to include isoquinoline and pyrazine systems in addition to the furan, pyridine, indole, and thiophene systems that had previously been demonstrated.

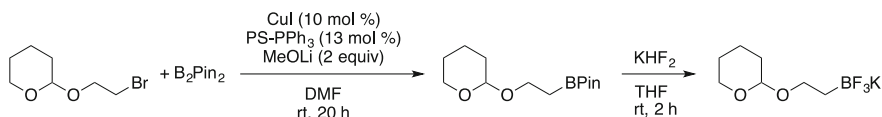
Alkoxyethylboron building blocks remained challenging to access because of the instability of alkoxyethylmetallics that, in principle, could serve as precursors to the corresponding organoborons via transmetalation. Unfortunately, nucleophilic



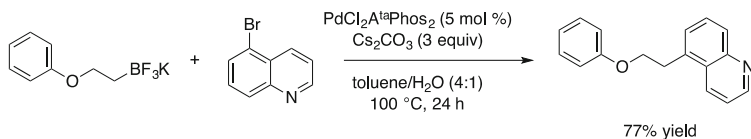
Scheme 15 Cross-coupling of potassium alkoxymethyltrifluoroborate



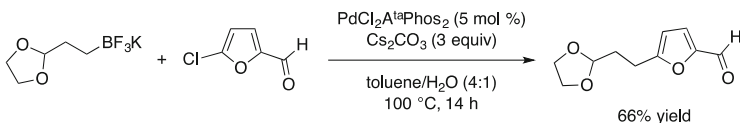
Scheme 16 Cross-coupling of potassium β -aminoethyltrifluoroborate



Scheme 17 Preparation of potassium alkoxyethyltrifluoroborates



Scheme 18 Cross-coupling of potassium alkoxyethyltrifluoroborates



Scheme 19 Cross-coupling of potassium dioxolanylethyltrifluoroborates

alkoxyethylmetallics decompose rapidly through facile β -elimination processes [33–36]. Alkoxyethyltrifluoroborates were thus eventually prepared through the Cu-catalyzed borylation of β -bromoethers with bis(pinacolato)diboron (Scheme 17). Through this process, a variety of alkoxyethyltrifluoroborates were prepared, a number of which were derived from bromoethyl ethers of protected alcohols, including those with benzyl, acetate, and THP and TBDPS groups [37].

These structures were subsequently cross-coupled with a variety of aryl and heteroaryl chlorides bearing nitrile, aldehyde, ketone, ester, nitro, amide, and sulfonamide functional groups. The heteroaryl substrate scope illustrated with this reaction include pyridine, quinoline, isoquinoline, indole, pyrazine, and thiophene systems (Scheme 18).

Interestingly, under the developed cross-coupling conditions, potassium dioxolanylethyltrifluoroborate was also demonstrated to undergo cross-coupling with aryl and heteroaryl chlorides and bromides, providing access to a variety of dioxolanylethylaryl substrates (Scheme 19) [38]. The scope of this reaction was demonstrated to include aryl and heteroaryl amide, amine, nitrile, nitro, ketone, and aldehyde functional groups and complemented previous routes to arylpropanal derivatives that relied upon air- and moisture-sensitive organomagnesium and organozinc reagents.

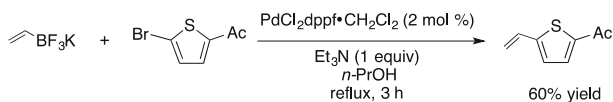
3.2 Improved Incorporation of Important Scaffolds

In the realm of Suzuki–Miyaura cross-couplings, the incorporation of aryl, heteroaryl, alkenyl, alkynyl, and alkyl groups derived from a variety of different organoborons has proven extremely successful. In these regimes, as noted previously, the use of organotrifluoroborates provides what might be described as noncritical practical advantages, e.g., the ability to use stable, crystalline, monomeric reagents as well as the capability of using atom-economical reagents that can be used stoichiometrically. Several key molecular scaffolds, however, represent significant challenges that could be addressed most efficaciously and often only through the use of organotrifluoroborates.

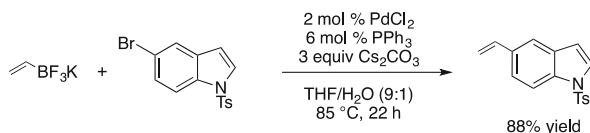
For example, although vinylborons had been previously employed in cross-couplings, severe limitations existed with available reagents. Vinylboronic acid is unstable, being prone to facile polymerization [39], and the corresponding vinylboronic esters undergo Heck–Mizoroki couplings in competition with Suzuki–Miyaura couplings under Pd catalysis [40, 41]. The development of conditions for the preparation and cross-coupling of vinyltrifluoroborate, therefore, represented a good alternative for the introduction of a vinyl moiety into a desired substrate.

Potassium vinyltrifluoroborate was readily prepared as an indefinitely stable crystalline solid from a vinyl Grignard reagent and has been shown to cross-couple successfully with a variety of electrophilic partners [42, 43]. In the presence of $\text{PdCl}_2(\text{dppf}) \cdot \text{CH}_2\text{Cl}_2$ and Et_3N , potassium vinyltrifluoroborate was coupled with 2-acetyl-5-bromothiophene (Scheme 20). The scope of this vinylation reaction includes aryl bromides, iodides, and triflates bearing acetate, nitrile, aldehyde, and nitro groups as well as a substituted pyridyl chloride. Unactivated aryl chlorides proved problematic under these conditions.

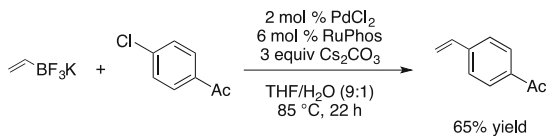
Later work in the area of vinyltrifluoroborate cross-coupling revealed a set of conditions that allowed greater functional group tolerance using PdCl_2 in the presence of PPh_3 and Cs_2CO_3 (Scheme 21). This method allowed the presence of nitrile, ketone, aldehyde, ester, alcohol, amine, and nitro functional groups as well as illustrating examples with a variety of *N*-, *S*-, and *O*-containing heteroaryls [44].



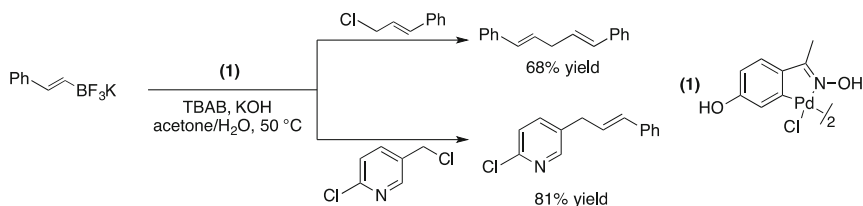
Scheme 20 Cross-coupling of potassium vinyltrifluoroborate



Scheme 21 Cross-coupling of potassium vinyltrifluoroborate



Scheme 22 Cross-coupling of potassium vinyltrifluoroborate

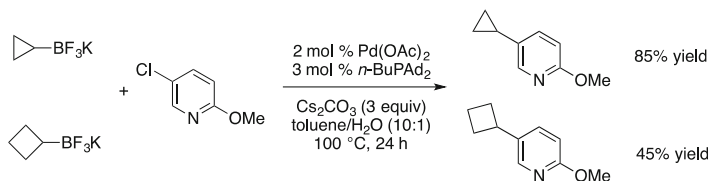


Scheme 23 Cross-coupling of potassium styryltrifluoroborate with allyl and benzyl chlorides

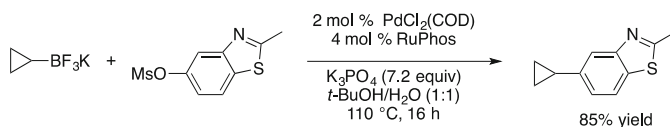
Although the cross-coupling of vinyltrifluoroborate with unactivated aryl chlorides remained challenging, a single example was illustrated in which 4-chloroacetophenone was successfully coupled with potassium vinyltrifluoroborate. A moderate yield was obtained with the use of RuPhos in place of PPh_3 , but homocoupling and Heck–Mizoroki products were observed (Scheme 22). Attempts to extend these conditions to deactivated aryl chlorides were unsuccessful.

The cross-coupling of alkenyltrifluoroborates has been achieved using water as a reaction solvent, albeit under Pd-catalyzed conditions that afforded a mixture of isomers [45]. More recently, a modified method has been developed for the diastereoselective cross-coupling of vinyl and alkenyltrifluoroborates with aryl, heteroaryl, allyl, and benzyl halides under aqueous conditions in the presence of palladacycle (1) (Scheme 23). The palladacycle, used as a precatalyst, can be recycled up to five times under the developed conditions and does not require a phosphine ligand [46]. Aryl and heteroaryl bromides bearing ester, ketone, nitrile, and aldehyde functional groups were successfully cross-coupled with vinyl and (*E*)-styryltrifluoroborate. With modifications to the reaction base and solvent, a variety of substituted allyl and benzyl chlorides were employed in the developed reaction to afford 1,4-dienes and allylbenzene derivatives.

Cyclopropyl and cyclobutyl moieties are substructures that have gained increasing attention as desired subunits of biologically active molecules within the pharmaceutical and agrochemical industries [47, 48]. The incorporation of cyclopropyl units through a Suzuki–Miyaura cross-coupling reaction has, until recently, required a large excess of the cyclopropylboronic acid, which is prone to protodeboronation [49]. Furthermore, examples of cyclopropylboronic acid cross-couplings with aryl and heteroaryl chlorides are limited. Cyclobutyl units pose a distinct challenge in Pd-catalyzed cross-couplings because of the tendency of secondary alkyl groups to undergo competitive β -hydride elimination [50]. In 2008, both of these challenging couplings were addressed by Molander et al., who demonstrated Pd-catalyzed conditions that allow both potassium cyclopropyl



Scheme 24 Cross-coupling of potassium cyclopropyl and cyclobutyltrifluoroborate

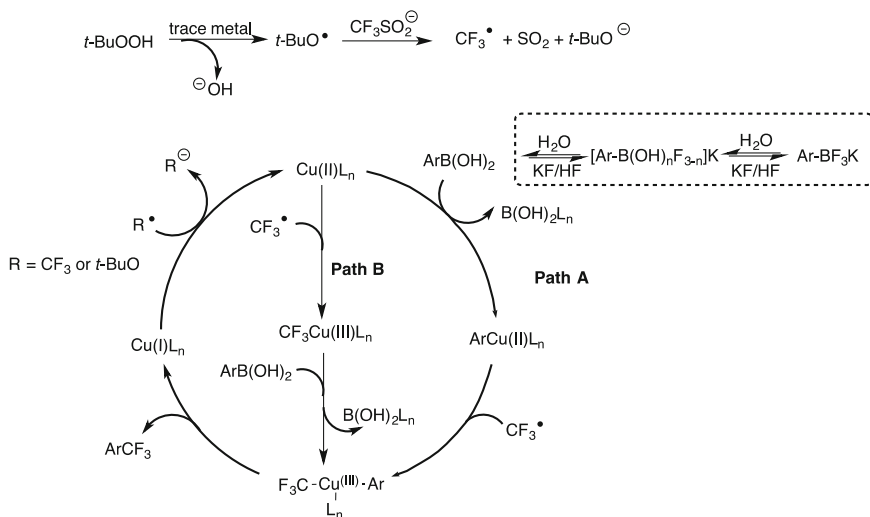


Scheme 25 Cross-coupling of cyclopropyltrifluoroborate with aryl and heteroaryl mesylates

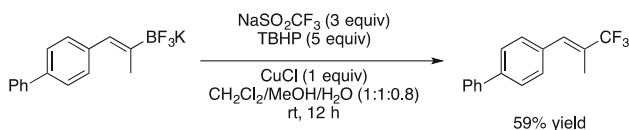
and cyclobutyltrifluoroborate to be cross-coupled with aryl and heteroaryl chlorides (Scheme 24) [51]. Using XPhos as a ligand in the presence of $\text{Pd}(\text{OAc})_2$, cyclopropyltrifluoroborate was cross-coupled with a variety of aryl chlorides bearing ketone, ester, and nitrile groups. Modification of the ligand, base, and solvent allowed the cross-coupling of cyclopropyltrifluoroborate to be extended to heteroaryl chlorides. Under the same conditions, cyclobutyltrifluoroborate was coupled with both aryl and heteroaryl chlorides. Ester, ketone, and aldehyde functional groups were tolerated under these conditions, as was *ortho*-substitution on the electrophilic partner.

The cross-coupling protocol for cyclopropyltrifluoroborate was later modified to allow the C–O activation of aryl and heteroaryl mesylates, expanding the scope of the electrophilic coupling partner [52]. Aryl mesylates bearing ketone, ester, and nitrile functional groups were successfully cross-coupled with cyclopropyltrifluoroborate in the presence of $\text{Pd}(\text{OAc})_2$ and RuPhos under aqueous conditions. Modification of the Pd source to $\text{PdCl}_2(\text{COD})$ allowed extension of the developed method to a variety of heteroaryl mesylates, including quinoline, dibenzofuran, benzothiophene, benzothiazole, and dibenzothiophene systems (Scheme 25).

Another unique and critical subunit that has gained attention in the area of medicinal chemistry is the trifluoromethyl group, which has the ability to alter the lipophilicity and metabolism of a drug molecule upon its incorporation [53]. Over the last decade, Cu-catalyzed electrophilic [54–56], nucleophilic [57, 58], and radical trifluoromethylations [59] of various boronic acids have been demonstrated. Electrophilic trifluoromethylation protocols have been extended to both aryltrifluoroborates and arylboronic esters [60, 61]. Recently, progress toward the cost-effectiveness and substrate scope expansion for the conversion of organotrifluoroborates to the corresponding trifluoromethylated substructures has been made. A Cu(II)-mediated trifluoromethylation protocol for aryl and alkenylboronic acids has been demonstrated using the Langlois reagent (NaSO_2CF_3) as a cost-effective source of trifluoromethyl radicals (Scheme 26) [62]. In the proposed mechanism, trifluoromethyl radicals are generated by the reaction *t*-BuOOH with NaSO_2CF_3 . The trifluoromethyl radicals are intercepted by the cuprate species



Scheme 26 Formation of trifluoromethyl radicals from NaSO_2CF_3 [62]

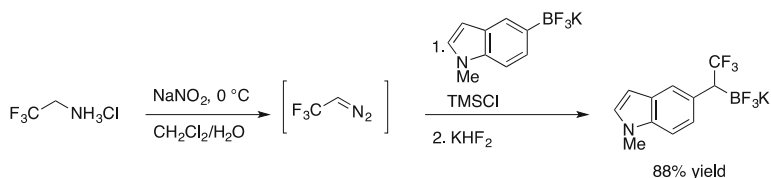


Scheme 27 Trifluoromethylation of organotrifluoroborates

either before (Path B) or after (Path A) transmetalation of the arylboronic acid to yield a trifluoromethyl-Cu(III)-Ar complex. The product is formed through reductive elimination from the Cu(III) complex to give a Cu(I) species that is oxidized to Cu(II) by radical components in the reaction mixture.

Using this method for the generation of trifluoromethyl radicals, in the presence of CuCl, alkenyl- and alkynyltrifluoroborates were transformed to trifluoromethylated compounds (Scheme 27) [63] based on previously reported conditions for the trifluoromethylation of aryl and heteroaryl boronic acids [59]. Under the same conditions, electron-rich aryl and heteroaryl trifluoroborates underwent trifluoromethylation in moderate to good yields. Electron-poor aryl and heteroaryl substrates represented a challenge under the developed method, but the use of $(\text{CH}_3\text{CN})\text{CuPF}_6$ under slightly modified reaction conditions allowed the successful trifluoromethylation of these structures. Ketone and ester functional groups were tolerated, as was *ortho*-substitution.

In addition to organotrifluoroborates serving as precursors toward trifluoromethylated compounds, a protocol has been developed for the synthesis of α -trifluoromethylated alkylboron compounds [64]. These materials are remarkable for their demonstrated bench stability, as most β -fluorometalloid species undergo ready elimination to form alkenes and metal fluorides. Under the developed



Scheme 28 Preparation of α -trifluoromethylated alkyltrifluoroborates

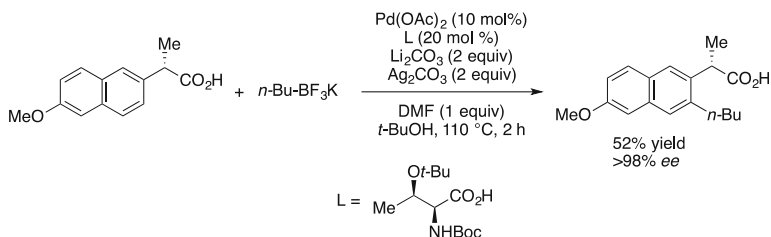
protocol, 2,2,2-trifluorodiazoethane is produced from the corresponding ammonium salt and undergoes an α -transfer reaction with a trivalent organoboron species produced in situ by using either TMSCl or *p*-tolyl-SiCl₃ as a fluorophile. Quenching the reaction with KHF₂ allows isolation of α -trifluoromethylated trifluoroborate moieties (Scheme 28). A variety of primary and secondary alkyl, alkenyl, alkynyl, aryl, and heteroaryl trifluoroborates were successfully employed in this method, enabling the preparation of a variety of unprecedented, shelf-stable, trifluoromethylated building blocks.

3.3 C–H Functionalization with Organotrifluoroborates

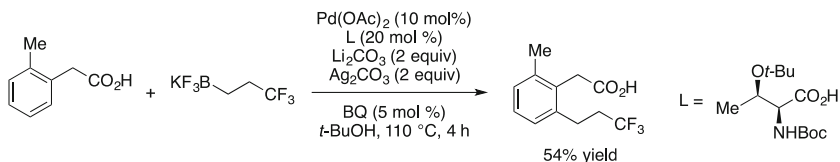
Organotrifluoroborate cross-coupling has been demonstrated in recent years in conjunction with C–H functionalization of aryl substrates. In the presence of Pd, C–H activation on an arene *ortho* to an activating group (e.g., carboxylic acid or amide) allows subsequent alkylation using alkyltrifluoroborate substrates [65, 66]. The addition of *n*-BuBF₃K to a variety of phenylacetic acid derivatives was demonstrated, and it was noted that the presence of an aryl chloride did not inhibit the reaction. Also noteworthy was the retention of stereochemistry at the α -carbon center of an enantiopure NSAID, naproxen (Scheme 29).

Yields varied based on substitution around the arene, and modifications to the ligand were necessary in some cases to obtain enhanced yields. A variety of potassium alkyltrifluoroborates were employed in the reaction, including cyclopropyl, benzyl, and methyltrifluoroborate. Alkyltrifluoroborates bearing amine, ester, and ketone functional groups were also tolerated. The method was also extended to allow addition of alkyltrifluoroborates to a variety of arylbenzoic acids (Scheme 30).

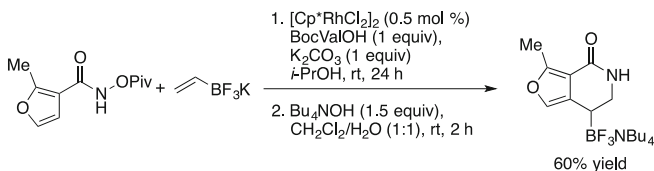
Rh-catalyzed annulations were carried out through an initial C–H activation of aryl and heteroaryl hydroxamates followed by insertion of potassium vinyltrifluoroborate. Conditions were varied slightly to allow isolation of either the potassium or tetrabutylammonium salt of the product. Aryl hydroxamates bearing nitro, bromo, and trifluoromethyl groups as well as pyridyl, furyl, and thienyl hydroxamates were among the substrates successfully employed under the developed conditions (Scheme 31). The resulting 4-trifluoroboratotetrahydroisoquinolones were then subjected to oxidation or protodeboronation to provide access to bicyclic cores, in



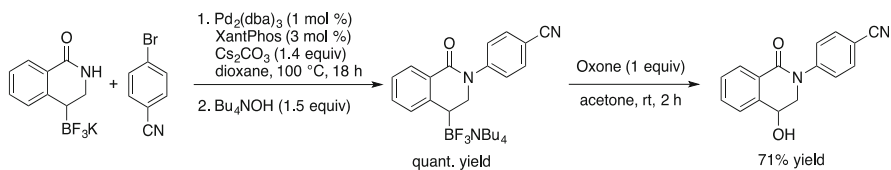
Scheme 29 C–H activation and alkylation of naproxen with *n*-butyltrifluoroborate



Scheme 30 C–H activation and subsequent alkylation with organotrifluoroborates



Scheme 31 C–H insertion of vinyltrifluoroborate



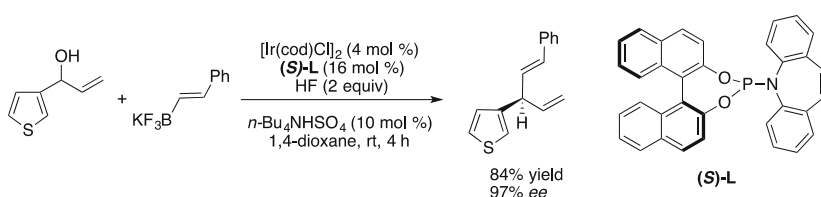
Scheme 32 Selective Buchwald–Hartwig arylation and subsequent oxidation

which vinyltrifluoroborate ultimately acted as ethylene and enol equivalents [67]. Additionally, these substrates were shown to undergo Buchwald–Hartwig coupling with aryl bromides under Pd-catalysis, yielding *N*-arylated products selectively, with none of the Suzuki–Miyaura product observed (Scheme 32).

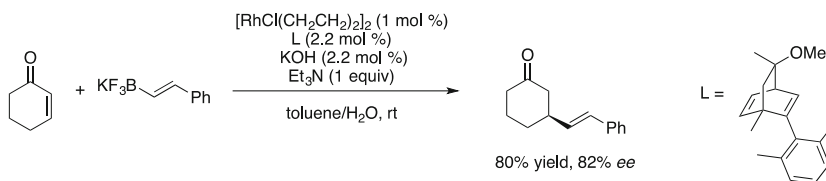
3.4 Enantioselective C–C Bond Formation

Iridium-catalyzed alkenylations have been carried out with potassium alkenyltrifluoroborates that show high site selectivity and enantioselectivity [68]. This method is the first example of an Ir-catalyzed asymmetric substitution using alkenyltrifluoroborates, and it allows selective access to a wide array of 1,4-dienes (Scheme 33). The conditions make use of a phosphoramidite ligand and tetrabutylammonium sulfate ($n\text{-Bu}_4\text{NHSO}_4$), which acts as a phase-transfer catalyst as well as an acidic activator of the allylic alcohols. Potassium styryltrifluoroborate was coupled with a variety of allylic alcohols bearing substituted arenes and heteroarenes. The substrate scope was shown to include aryl bromide and iodide, ester, aldehyde, and nitro functional groups, as well as naphthalene, thiophene, and indole moieties. The scope of the trifluoroborate partner was expanded to include a variety of alkenyltrifluoroborates, including conjugated diene structures. Mixtures of branched and linear regioisomers were isolated, but in most cases, the branched to linear ratio was greater than 50:1 and the obtained *ees* of the products were greater than 97%.

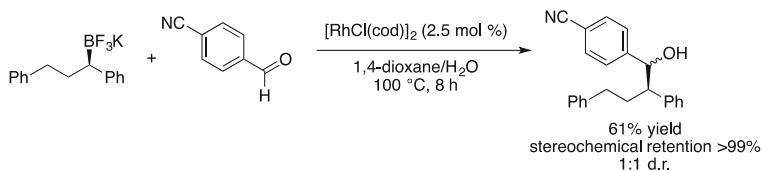
Asymmetric 1,4-additions of aryl and alkenyl trifluoroborates to α,β -unsaturated substrates in the presence of Rh and a chiral diene ligand have been reported. This method allows the formation of substituted lactones and cyclic ketones with a high degree of enantioselectivity [69]. A variety of chiral phosphorus ligands were explored to promote this transformation, but diene ligand **L** was found to promote the reaction with the highest yield and degree of enantioselectivity (Scheme 34). The method was extended to cyclic enones of 5-, 6-, and 7-membered rings as well as a cyclic lactone. Several aryl and alkenyl trifluoroborates successfully underwent 1,4-additions to the enone substrates, including aryl chloride, aryl bromide, and naphthalene moieties.



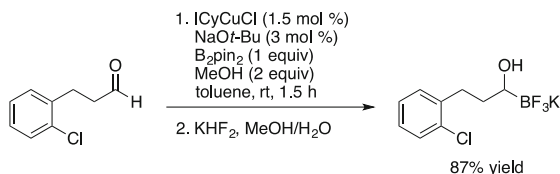
Scheme 33 Ir-catalyzed enantioselective vinylation with a styryltrifluoroborate



Scheme 34 Asymmetric 1,4-additions of aryl and alkenyltrifluoroborates



Scheme 35 Addition of chiral alkyltrifluoroborates to aldehydes

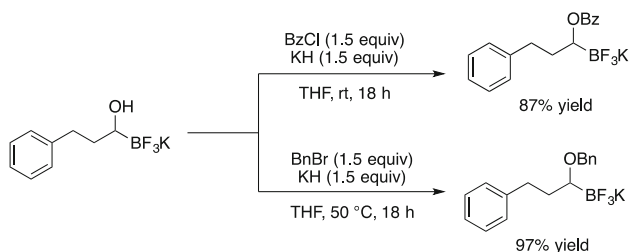


Scheme 36 Preparation of 1-(hydroxy)alkyltrifluoroborates

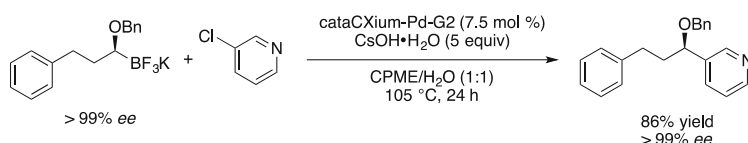
Aggarwal et al. have demonstrated the synthesis and reactivity of chiral secondary and tertiary alkyltrifluoroborates, which are prepared enantioselectively from lithiated carbamates (preparation of corresponding boronate esters [70, 71]). The chiral alkyltrifluoroborates are shown to undergo 1,2-addition to aldehydes to form alcohols with retention of stereochemistry at the benzylic center (Scheme 35) [72]. Interestingly, potassium 1,1-diaryltrifluoroboratomethanes were able to undergo addition to aldehyde substrates under the same conditions developed for the secondary alkyltrifluoroborates without erosion of stereochemistry. The aldehydes demonstrated as successful coupling partners in this reaction bear nitro, nitrile, and ester functional groups. The isolated alcohol products are 1:1 mixtures of diastereomers at the newly formed carbinol center, but the alcohols were readily oxidized to the corresponding enantioenriched ketones using TEMPO.

The preparation and cross-coupling of secondary organotrifluoroborates in a stereospecific fashion has recently been demonstrated. A variety of 1-(hydroxy)alkyltrifluoroborates have been prepared from the corresponding aldehydes through a Cu-catalyzed diboration protocol employing ICyCuCl (ICy = 1,3-dicyclohexylimidazol-2-ylidene) (Scheme 36) [73]. The developed method, which was based on a previously reported aldehyde diboration protocol [74], allows isolation of air-stable trifluoroborate salts upon quenching with KHF₂. It was demonstrated that substrates bearing alkenes as well as protected alcohols and amines could be successfully prepared.

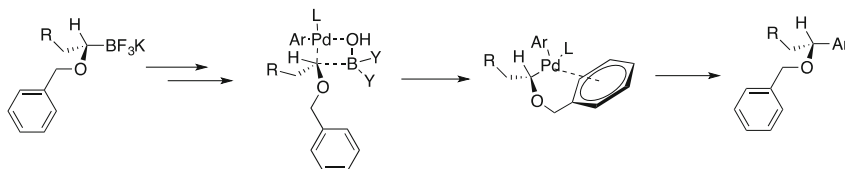
Several 1-(acyloxy)alkyltrifluoroborates were prepared from the corresponding hydroxy substrates through treatment with acyl chlorides or anhydrides. Similarly, a variety of 1-(alkoxy)alkyltrifluoroborates were prepared through reaction of alkyl bromides with the corresponding 1-(hydroxy)alkyltrifluoroborate. The alkyl bromides employed included substituted benzyl, 2-pyridyl, 2-thienyl, and allyl substrates (Scheme 37).



Scheme 37 Preparation of 1-(acyloxy)alkyltrifluoroborates and 1-(alkoxy)alkyltrifluoroborates



Scheme 38 Cross-coupling of 1-(benzyloxy)alkyltrifluoroborates

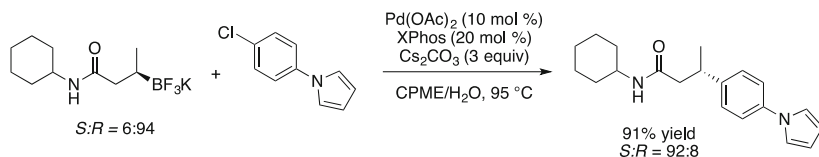


Scheme 39 Retention of stereochemistry in the cross-coupling of 1-(benzyloxy)alkyltrifluoroborates [73]

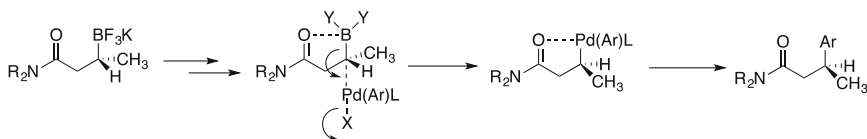
The cross-coupling of enantiomerically enriched 1-(benzyloxy)alkyltrifluoroborates with aryl and heteroaryl chlorides was illustrated (Scheme 38). With the use of a benzyl moiety as a coordinating group, stereospecific cross-couplings with aryl and heteroaryl chlorides bearing a variety of functional groups including ketones, esters, and amines have been achieved. Successfully coupled heteroaryl chlorides include pyridine, quinoline, isoquinoline, and thiophene derivatives.

These reactions occur with retention of stereochemistry. This has been rationalized by transformation through a four-membered transition structure during the transmetalation process (Scheme 39). In the diorganopalladium intermediate, it was postulated that β -hydride elimination was inhibited by coordination of the arene to the metal center.

The stereochemistry of this process contrasts with that previously observed in the stereospecific cross-coupling of secondary alkyl β -trifluoroboratoamides with aryl halides, which occurs with overall inversion of configuration [75]. Under the developed conditions, a variety of aryl chlorides and bromides were successfully cross-coupled, with tolerance of nitrile, aldehyde, ester, and nitro moieties



Scheme 40 Cross-coupling of β -trifluoroboratoamides



Scheme 41 Inversion of stereochemistry in the cross-coupling of β -trifluoroboratoamides [75]

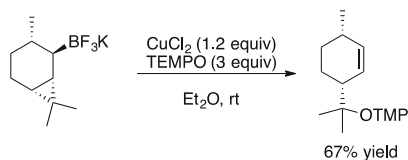
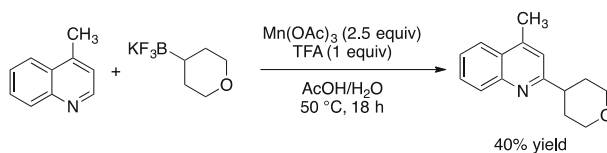
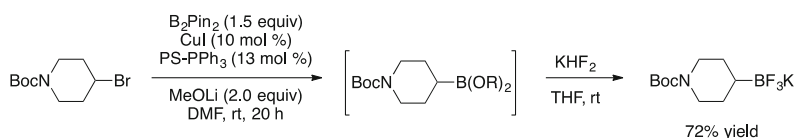
(Scheme 40). The nucleophilic partner of the reaction was varied to include amides with primary and secondary alkyl, benzyl, and aryl units on the amide nitrogen.

In these substrates, the amide carbonyl of the β -trifluoroboratoamides provides stabilization through coordination to the boron and also to the Pd after transmetalation. Inversion of configuration is observed in the cross-coupling of enantioenriched amides because the strong intramolecular coordination of the amide to the boronic acid intermediate facilitates S_E2 -type reactivity during the transmetalation process (Scheme 41).

3.5 Radical Reactions with Organotrifluoroborates

Organotrifluoroborates may serve as radical precursors under oxidative conditions. For example, the Cu(II)-promoted oxidation of alkyltrifluoroborates to carbon radicals has been demonstrated (Scheme 42) [76]. Primary and secondary alkyltrifluoroborates served as radical precursors in the presence of either CuCl_2 , $\text{Cu}(\text{EH})_2$, or DMP ($\text{EH} = 2$ -ethyl hexanoate). Evidence for the generation of a radical intermediate is provided by the opening of a cyclopropylcarbinyl radical intermediate in a bicyclic system, producing a cyclohexene product. Functionalized alkyltrifluoroborates bearing a benzyl ether, ketone, and alkenylsilane were successfully oxidized without reaction of these embedded functional groups. The radicals generated from secondary alkyltrifluoroborates were also trapped by methyl vinyl ketone to demonstrate application of the method to C–C bond formation.

Protocols for Minisci reactions have been developed, taking advantage of the facile oxidation of alkyl and alkoxyethyltrifluoroborates to the corresponding radicals. Oxidation of the organotrifluoroborates to the requisite radicals was optimized to employ $\text{Mn}(\text{OAc})_3$ and trifluoroacetic acid to allow the alkylation of heteroaryls in selective positions (Scheme 43) [77]. Potassium

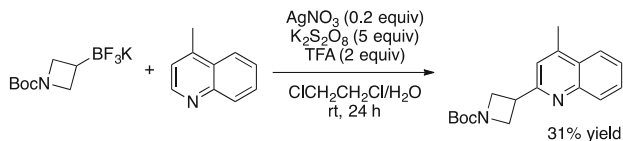
**Scheme 42** Cu-promoted radical generation from alkyltrifluoroborates**Scheme 43** Minisci reaction with organotrifluoroborates**Scheme 44** Synthesis of nonaromatic heterocyclic trifluoroborates

cyclobutyltrifluoroborate was coupled with a wide array of heteroaryl substrates including quinoline, isoquinoline, pyridine, quinoxaline, imidazole, benzimidazole, thiazole, and benzothiazole substrates. The reaction was extended to a variety of primary and secondary alkyltrifluoroborates, including cyclic substrates and a tetrahydropyranyltrifluoroborate. Stoichiometric amounts of both the heteroaryl and the alkyltrifluoroborate could be utilized to achieve moderate to good yields of the Minisci products. Several alkoxyethyltrifluoroborates were also illustrated to alkylate lepidine selectively in the 2-position.

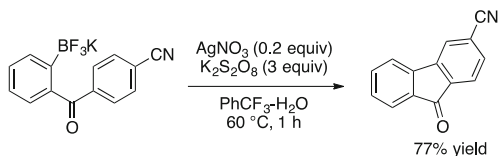
Several nonaromatic heterocyclic trifluoroborates were prepared from their corresponding halides using a copper-catalyzed borylation procedure (Scheme 44) [78]. Using this mild borylation protocol, piperidinyl, pyrrolidinyl, azetidynyl, tetrahydropyranyl, tetrahydrofuranyl, and oxetanyl trifluoroborate structures were isolated as free-flowing white solids.

These trifluoroborate building blocks were then incorporated into heteroaryls using slightly modified silver-mediated Minisci conditions previously developed by Baran et al. for the reaction of arylboronic acids [79, 80]. The heteroaryl substrates illustrated in the developed reaction include quinoline, quinoxaline, and pyridazine cores (Scheme 45).

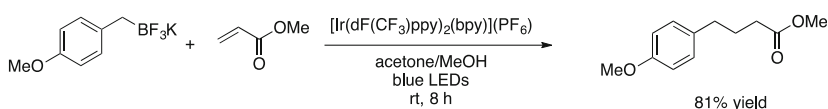
In addition to Minisci reactions, organotrifluoroborates have been used as radical precursors in Pschorr reactions for the formation of polycyclic scaffolds [81]. These reactions, termed “borono-Pschorr” transformations, have been illustrated on substrates bearing ester, nitrile, and trifluoromethyl functional groups. Under the developed conditions, a Minisci-type reaction was also demonstrated by extending



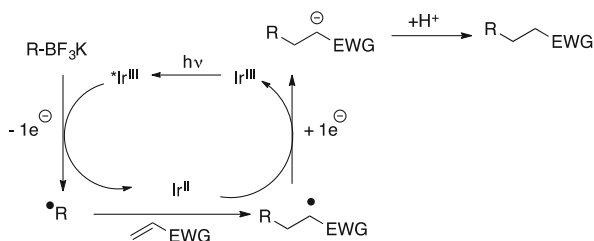
Scheme 45 Minisci reactions of nonaromatic heterocyclic trifluoroborates



Scheme 46 Pschorr reaction with aryltrifluoroborates



Scheme 47 Photocatalytic addition of aryltrifluoroborates to electron-poor olefins

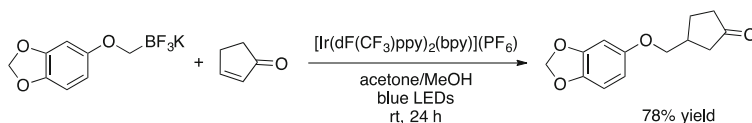


Scheme 48 Proposed mechanism for photocatalytic reaction of organotrifluoroborate [82]

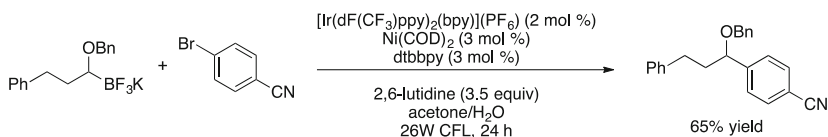
the substrate scope to include a pyridine derivative. A tandem radical cyclization/trap cascade protocol was also demonstrated by using 1,4-benzoquinone as a radical trap. The development of this protocol allowed access to polycyclic cores under mild, functional-group-tolerant conditions (Scheme 46).

A unique method of generating radicals from organotrifluoroborates derives from photoredox catalysis. Single-electron oxidation of benzyltrifluoroborates and subsequent addition to electron-poor olefins is carried out in the presence of visible light and an iridium catalyst (Scheme 47) [82, 83].

A proposed mechanism for this transformation involves the excitation of an Ir(III) catalyst by visible light, which then generates an alkyl radical from an organotrifluoroborate through a single-electron transfer (Scheme 48). The carbon-centered radical then adds to the electron-poor olefin to generate a radical intermediate. The



Scheme 49 Photocatalytic addition of alkoxyethyltrifluoroborates to electron-poor olefins



Scheme 50 Photoredox/nickel dual catalytic cross-coupling of organotrifluoroborates

Ir(II) catalyst reduces the carbon-centered radical, which is subsequently deprotonated to yield the cross-coupled product.

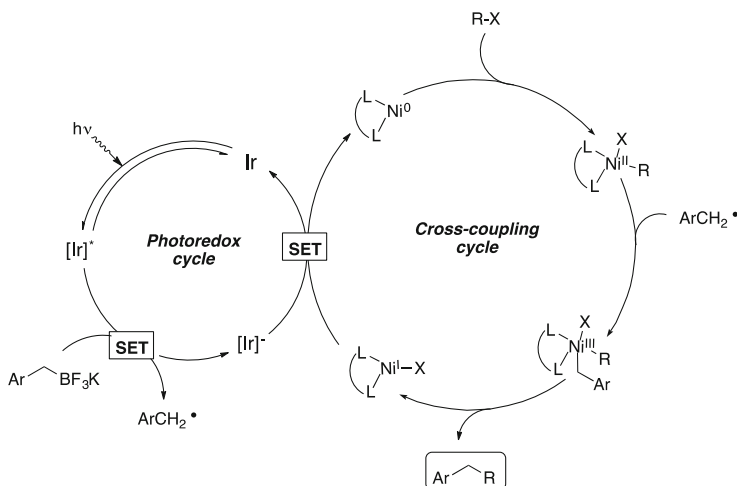
The scope of this protocol has been extended to include alkoxyethyltrifluoroborates (Scheme 49) [84]. The olefins participating in this C–C bond-forming process bear ketone, ester, amide, and nitrile moieties and also include cyclic enones, demonstrating the mild nature of the photoredox method which, therefore, boasts a high degree of functional group tolerance.

A further extension of photocatalytic methods involving organotrifluoroborates has been achieved through the application of a dual catalytic system that allows the cross-coupling of benzyl- and alkoxyalkyltrifluoroborates with a variety of aryl bromides (Scheme 50) [85]. This method, which employs an iridium photocatalyst in conjunction with a nickel catalyst, allows extremely mild coupling of challenging sp^3 -hybridized carbon centers.

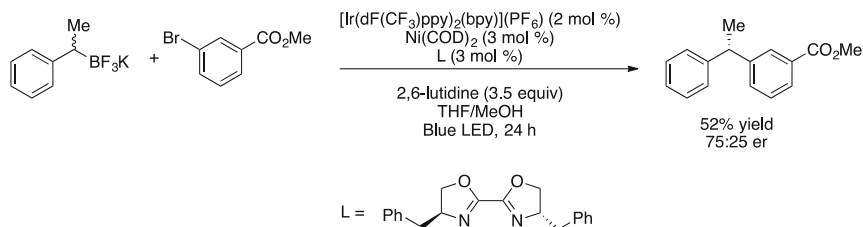
The reaction is proposed to proceed through a cross-coupling/photoredox dual catalytic pathway (Scheme 51). An aryl halide undergoes oxidative addition to a Ni(0) catalyst to produce an organo-Ni(II) species. At the same time, a benzylic radical is generated from the single-electron oxidation of a benzylic trifluoroborate salt by an excited-state iridium complex. Single-electron transmetalation of the benzylic radical to the organo-Ni(II) species generates a diorgano-Ni(III) complex. Reductive elimination from the Ni center yields the diarylmethyl product. The resulting Ni(I) species undergoes single-electron reduction by the reduced iridium complex to regenerate both the Ni(0) species and the iridium catalyst.

Use of a chiral ligand under slightly modified reaction conditions allowed the transmetalation process to be stereoconvergent. In one preliminary example, an enantioenriched 1,1-diarylethane product was obtained from a racemic secondary benzylic trifluoroborate (Scheme 52).

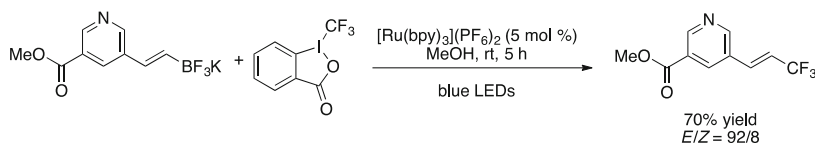
In addition to serving as radical precursors, organotrifluoroborates may serve in other roles in transformations involving radical intermediates. Visible light-induced radical formation from Togni's reagent has been developed in a method that provides access to trifluoromethylated alkenes (Scheme 53) [86]. The alkenes shown to undergo trifluoromethylation are substituted with various arenes as well as



Scheme 51 Proposed mechanism for photoredox/nickel cross-coupling of benzyltrifluoroborates [85]



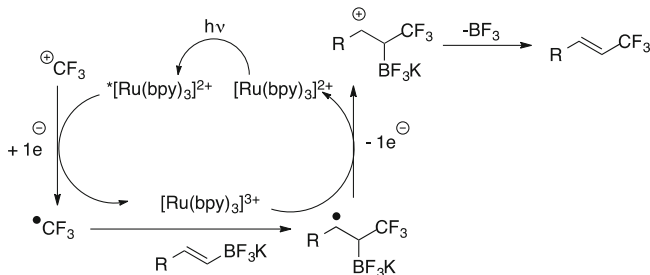
Scheme 52 Stereoconvergent cross-coupling of a racemic secondary benzylic trifluoroborate



Scheme 53 Trifluoromethylation of alkenyltrifluoroborates

heteroarenes, including pyridine, quinoline, thiophene, and benzothiazole structures. Functional groups that were tolerated under the developed reaction conditions include nitrile, amine, and ester moieties as well as aryl and heteroaryl chlorides and bromides.

Although these structures have previously been synthesized through Cu(I) or Fe(II) catalysis [54–56, 87], this method boasts an improved substrate scope and a high degree of stereoselectivity. The use of the electrophilic Togni reagent allows generation of a trifluoromethyl radical through a single-electron reduction. In a proposed



Scheme 54 Proposed mechanism for radical trifluoromethylation of alkenyltrifluoroborates [86]

mechanism (Scheme 54), the generated radical combines with the olefin of the alkenyltrifluoroborate to produce a stabilized radical intermediate regioselectively. After single-electron oxidation of the radical intermediate to a cation, *trans*-selective elimination of the trifluoroborate produces an (*E*)-alkenyl product.

4 C–Y Bond Formation from Organotrifluoroborates

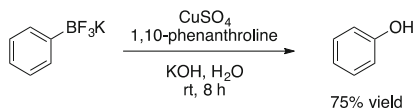
4.1 C–O Bond Formation

Several methods have been developed that allow the conversion of organotrifluoroborates to the corresponding alcohols. In 2010, Wang et al. reported a Cu-catalyzed synthesis of phenols from arylboronic acids. The developed method was demonstrated to be effective for a variety of arylboronic acid derivatives, including potassium phenyltrifluoroborate (Scheme 55) [88]. Although only one isolated trifluoroborate was demonstrated under the reaction conditions, a variety of functional groups were tolerated on arylboronic acid substrates, including amine, aldehyde, nitrile, nitro, and carboxylic acid moieties.

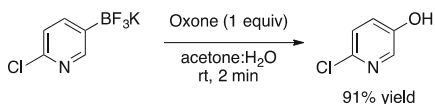
A mild and effective method for the oxidation of organotrifluoroborates to the corresponding alcohols was revealed that takes place in only 2–5 min in the presence of Oxone[®] (Scheme 56). This method expanded the scope of aryltrifluoroborates that undergo oxidation to include a variety of electron-rich and electron-poor arenes. In addition, to aryltrifluoroborates, the method was extended to numerous heteroaryls, including dibenzofuran, dibenzothiophene, pyridine, benzothiophene, benzofuran, thiophene, and furan substrates.

Primary and secondary alkyl, as well as alkenyltrifluoroborates were also illustrated to participate in this oxidation reaction. Interestingly, oxidation of an enantioenriched organotrifluoroborate proceeded with retention of configuration (Scheme 57).

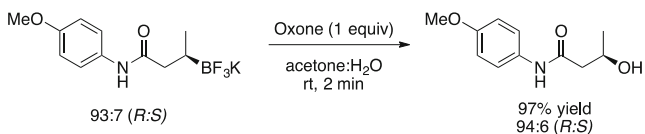
Alkenyltrifluoroborates underwent oxidation to yield the corresponding aldehyde product. This method allows the presence of a variety of functional groups on



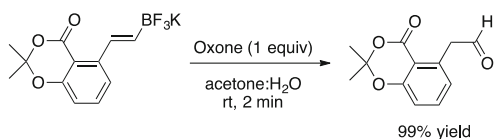
Scheme 55 Cu-catalyzed oxidation of potassium phenyltrifluoroborate to phenol



Scheme 56 Oxidation of heteroaryltrifluoroborate with Oxone[®]



Scheme 57 Oxidation of enantioenriched potassium trifluoroborate with Oxone[®]



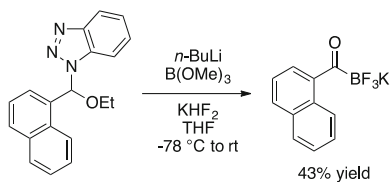
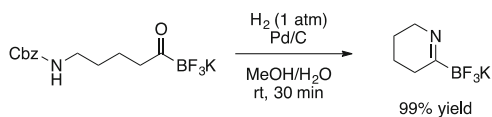
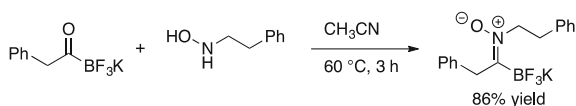
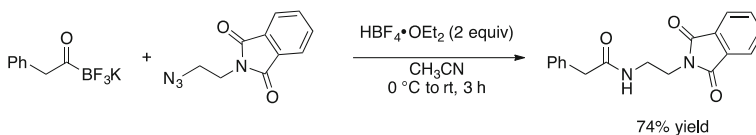
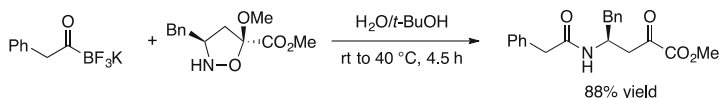
Scheme 58 Mild oxidation of organotrifluoroborates with Oxone[®]

the organotrifluoroborate, including alkene, nitrile, nitro, aldehyde, ester, ketone, and aryl halides (Scheme 58) [89].

4.2 C–N Bond Formation

A variety of acyl trifluoroborates have been prepared from a class of benzotriazole-based *N,O* acetals. Substituted benzoyltrifluoroborates were prepared, and it was illustrated that an aryl chloride and alkynylsilane were undisturbed under the reaction conditions. Substrates with *ortho*-substitution could be readily converted under the reaction conditions developed. Several phenylacetyltrifluoroborates as well as non-benzylic acyltrifluoroborates were prepared under similar conditions, and both an alkyl chloride and a terminal olefin were tolerated (Scheme 59) [90].

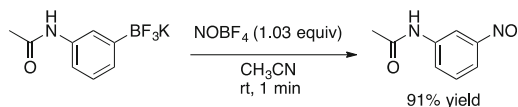
These important substructures have been demonstrated to react like typical carbonyl-containing molecules by their formation of imines and nitrones. Hydrogenation of a Cbz-protected amine on an acyltrifluoroborate led to cyclization of the free amine onto the carbonyl, resulting in the formation of an imine (Scheme 60).

**Scheme 59** Synthesis of acyltrifluoroborates**Scheme 60** Imine formation of acyltrifluoroborate**Scheme 61** Nitron formation of acyltrifluoroborate**Scheme 62** Preparation of amides from acyltrifluoroborates and alkyl azides**Scheme 63** Preparation of amides from acyltrifluoroborates and isoxazolidines

Phenylacetyltrifluoroborate was also demonstrated to react like a typical carbonyl upon condensation with a hydroxylamine to form a nitron as a single isomer (Scheme 61).

Acyltrifluoroborates have been employed in the preparation of amides through the reaction with organic azides (Scheme 62) [91]. Under mild conditions, a variety of primary and secondary alkyl and aryl azides, including those bearing ester, nitrile, and alkene functional groups, have been reacted stoichiometrically with (2-phenylacetyl)trifluoroborate to yield structurally diverse amides.

This method has been extended to demonstrate the coupling of acyltrifluoroborates with hydroxylamines under aqueous conditions (Scheme 63) [92]. In this later work, the scope of the trifluoroborate was expanded to show reaction of both



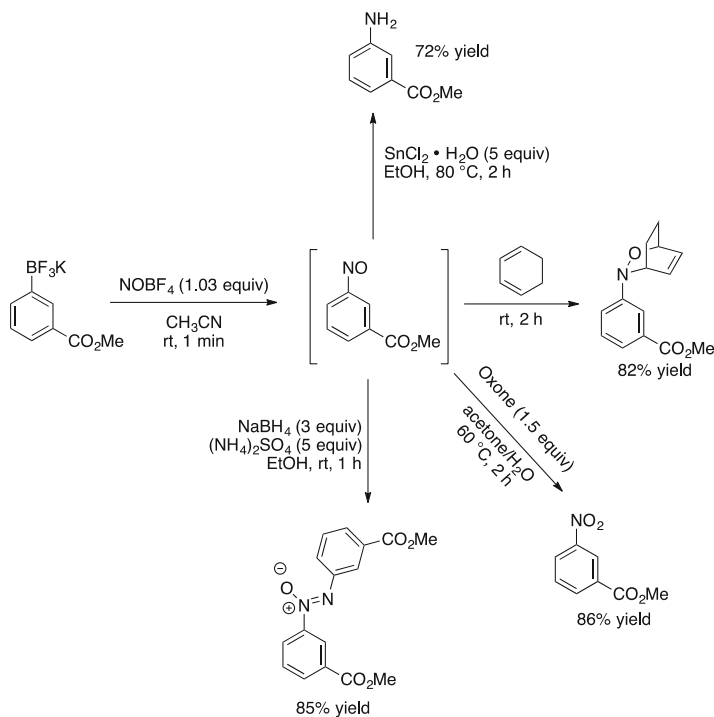
Scheme 64 Nitrosation of aryltrifluoroborates

aryl- and alkyl-substituted acyltrifluoroborates. Among the functional groups tolerated by this method are terminal olefin, alkynylsilane, aldehyde, amine, free alcohol, and carbamate. The use of hydroxylamines as the nitrogen component for the amide formation allowed an expansion of the reaction scope even further. Isoxazolidines and *O*-benzoyl hydroxylamines served as coupling partners in the reaction, and the conditions allowed the presence of alkene, ester, and amine moieties.

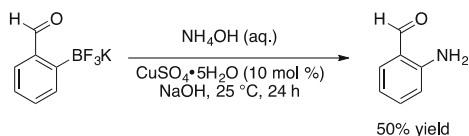
Nitrosation of aryl and heteroaryltrifluoroborates with nitrosonium tetrafluoroborate serves as another method for C–N bond formation from organotrifluoroborates and, more importantly, as a facile entry to nitrosoarenes. Access to nitrosoarenes had previously been limited by existing methods of oxidation of anilines and use of electrophilic nitrosonium reagents (Scheme 64). Oxidation methods suffered from a lack of toleration of various functional groups and heteroaryl compatibility as well as the generation of azo and azoxy by-products [93–95]. The use of electrophilic nitrosonium reagents is limited by the necessity of using aryl substrates bearing electron-donating groups, thus significantly limiting the scope of the method [96–98]. A recently developed nitrosation of aryltrifluoroborates represents a significant improvement over existing protocols to access nitrosoarenes, as it is tolerant of a wide array of functional groups on the arene, including aldehyde, ketone, amide, ester, carboxylic acid, and nitrile moieties [99]. The presence of aryl halides does not interfere with the nitrosation reaction, which takes place on most substrates in less than one minute in a flask that can be open to the air at room temperature. The heteroaryl substrates illustrated to react efficiently under the developed conditions include dibenzofuran, dibenzothiophene, benzothiophene, indole, pyridine, isoquinoline, and pyrimidine.

Several one-pot transformations were demonstrated on potassium methyl 3-trifluoroboratobenzoate, including oxidation to a nitroarene and reduction to an aniline derivative, illustrating the applicability of the developed method toward synthesis of important synthetic building blocks (Scheme 65).

Oliveira et al. have demonstrated a Cu-catalyzed amination of aryltrifluoroborates using aqueous ammonia under mild reaction conditions [100]. This method allows direct access to arylamines and can be carried out in the presence of a variety of functional groups, including aryl bromide, nitrile, nitro, ketone, and aldehyde moieties (Scheme 66).



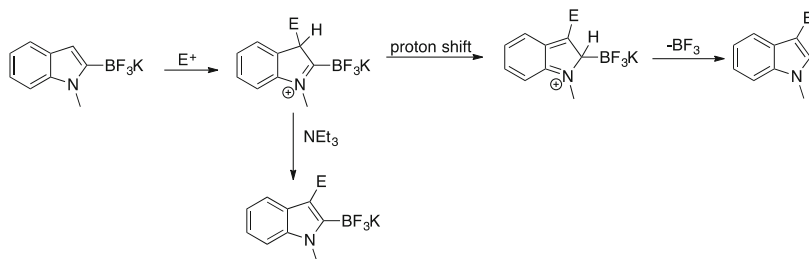
Scheme 65 One-pot transformations of nitrosoarenes [99]



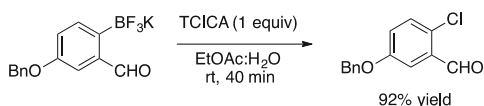
Scheme 66 Amination of aryltrifluoroborates with ammonia

4.3 C–X Bond Formation

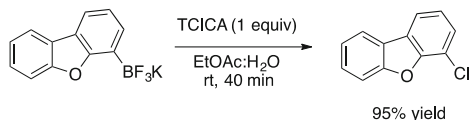
The kinetics and mechanism of electrophilic aromatic substitution reactions for select heteroaryltrifluoroborates have recently been studied [101]. Under transition-metal-free conditions, electrophiles are sometimes observed to participate at sites remote to the trifluoroborate group, typically at the *ortho*-position. Although the trifluoroborate substituent has a strong *ipso*-activating effect on the attached carbon (on the order of 10^3 – 10^4), the adjacent C–H bond is often activated by a factor of 10^5 – 10^6 . It was observed that the electrophilic aromatic substitution of *N*-methylindol-2-yltrifluoroborate takes place with initial attack at the C3 position (Scheme 67). In the absence of base, a proton shift occurs followed by deboronation. In the presence of base, however, the proton at the site of the



Scheme 67 Possible pathways for electrophilic aromatic substitution of *N*-methylindol-2-yltrifluoroborate [101]



Scheme 68 Metal-free chlorination of aryltrifluoroborates



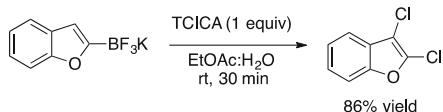
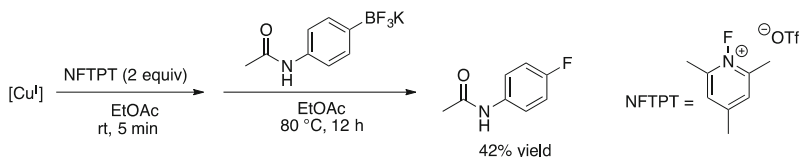
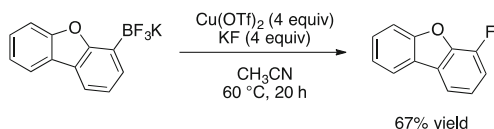
Scheme 69 Metal-free chlorination of heteroaryltrifluoroborates

electrophilic attack is scavenged, and the trifluoroborate remains intact. This observation suggests that many reactions on symmetrical aromatic systems previously presumed to proceed through *ipso*-substitution may actually undergo remote electrophilic attack followed by protodeboronation.

The metal-free *ipso*-chlorination of organotrifluoroborates has been developed. This method allows rapid access to site-specific chlorination using the commodity reagent trichloroisocyanuric acid (TCICA) under aqueous conditions (Scheme 68) [102]. Both electron-rich and electron-poor aryltrifluoroborates react efficiently under the developed conditions, and most reactions proceed to completion in one hour or less.

The addition of 1 equiv. of NaBr to the standard conditions was illustrated in an isolated example to provide access to an aryl bromide as an extension of the developed method. Heteroaryl substrates, including those possessing dibenzofuran, quinoline, pyrimidine, pyridine, and benzofuran cores, also participated in the chlorination reaction, albeit requiring slightly longer reaction times (Scheme 69).

It was noted that under the developed conditions, 1:1 mixtures of mono- and dichlorinated species were obtained with benzofuran and pyridine substrates. Use of 1 equiv. of the chlorinating agent (standard conditions use 0.33 equiv.) led to complete conversion to the dichlorinated product (Scheme 70). Limited examples of alkenyl, alkynyl, and alkyltrifluoroborate substrates were also illustrated to undergo chlorination in good yields.

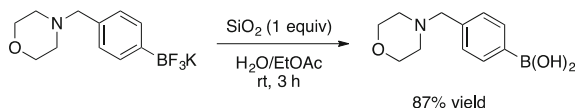
**Scheme 70** Metal-free dichlorination of heteroaryltrifluoroborates**Scheme 71** Fluorination of aryltrifluoroborates with NFTPT**Scheme 72** Fluorination of aryl and heteroaryltrifluoroborates with KF

Recently, methods have been developed to address the fluorination of aryltrifluoroborates [53, 103, 104]. Sanford et al. reported a copper-mediated method for fluorination of aryltrifluoroborates with *N*-fluoro-2,4,6-trimethylpyridinium triflate (NFTPT) (Scheme 71) [105]. This method, which can also be applied to arylstannanes, employs an electrophilic fluorinating agent under mild, functional-group-tolerant conditions. Both electron-rich and electron-poor substrates react in moderate to good yield. Functional groups tolerated by the developed conditions include aldehyde, ketone, amide, and ester moieties.

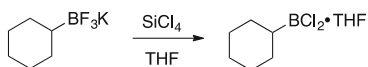
Subsequently, the Sanford group reported an improved fluorination protocol that uses KF as a fluoride source and proceeds under mild reaction conditions that allow a variety of functional groups to be present on the aryl or heteroaryltrifluoroborate (Scheme 72) [106]. In addition to functional groups tolerated by the method employing NFTPT, this protocol allows the presence of aryl nitro and nitrile groups. Additionally, the fluorination reaction is demonstrated on dibenzofuran, pyridine, and quinoline substructures.

5 Using Organotrifluoroborates to Construct Novel Scaffolds

Organotrifluoroborates have successfully been employed in various contexts as tetracoordinate, protected boronic acids, owing to their resilience toward numerous reagents [3]. In this manner, the trifluoroborate moiety allows functionalization of



Scheme 73 Hydrolysis of organotrifluoroborates to corresponding boronic acids



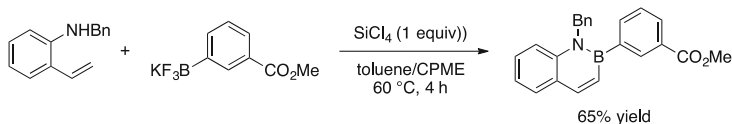
Scheme 74 Synthesis of reactive organodihaloboranes from organotrifluoroborates

the organic substructures without disturbance of the C–B bond. Once desired molecular complexity has been achieved, the organotrifluoroborates can be unmasked by suitable fluorophiles to reveal a reactive, tricoordinate boron species.

One approach to deprotection of organotrifluoroborates is hydrolysis to their corresponding boronic acids. A protocol was developed that allows the mild, yet extremely efficient, hydrolysis of aryl, heteroaryl, alkyl, and alkenyltrifluoroborates with aqueous silica gel [107]. Using this procedure, a variety of aminomethyl-substituted arylboronic acids were prepared in good yields after only a few hours at room temperature (Scheme 73). This method demonstrates an effective protocol for late-stage unveiling of a reactive boron moiety within a functionalized molecule. Complimentary methods for the hydrolysis of organotrifluoroborates to boronic acids were later developed, making use of either alumina or iron trichloride under aqueous conditions to promote the transformations [108, 109].

Other methods for unmasking a reactive boron species from an organotrifluoroborate include the addition of either trimethylsilyl chloride (TMSCl) or silicon tetrachloride (SiCl_4) as fluorophiles to generate organodihaloboranes (Scheme 74) [7, 110]. There currently exist few commercially available organodihaloboranes, and there are in fact limited convenient ways to synthesize these materials cleanly and efficiently. The use of fluorophilic silicon reagents thus permits the in situ formation of organodihaloboranes from diverse, shelf-stable organotrifluoroborates, allowing these sensitive reagents to be generated and utilized at will for use in further transformations.

This deprotection approach was recently utilized in a protocol developed for the construction of azaborine cores from organotrifluoroborates and aminostyrenes. Azaborines represent a class of molecular scaffolds that has garnered attention in the medicinal chemistry and materials science fields [111–113]. In the approach developed, a variety of aminostyrenes were shown to participate, with substitution being tolerated both on the arene and on the nitrogen. Several aryl, heteroaryl, alkynyl, alkenyl, and alkyltrifluoroborates served as the source of the intermediate organodihaloborane for the borazine preparation, including dibenzofuranyl, dibenzothienyl, trifluoroethyl, and cyclopropyltrifluoroborate. The developed method boasts a large functional group tolerance, allowing the presence of aryl nitro, nitrile, and ester substituents as well as alkyl bromide and iodide moieties. These structures have been shown to undergo halogenation reactions and subsequent cross-couplings, allowing formation of a large library of functionalized isosteres of naphthalene cores (Scheme 75) [114].



Scheme 75 Synthesis of 2,1-borazaronaphthalenes with organotrifluoroborates

6 Conclusions and Outlook

Organotrifluoroborates have found use in several useful niches in synthetic organic chemistry. Their desirable physical properties make them an attractive alternative in many transformations to tricoordinate organoboron compounds, whose sensitivity to moisture, air, and in fact many reagents make them less than ideal in complex molecule synthesis. More and more, however, it is becoming clear that the organotrifluoroborates exhibit unique and powerful reactivity patterns of their own that set them apart from all other organoborons. It is this regime, just in its infancy, that promises to launch this important class of reagents to new heights.

References

1. Lennox AJJ, Lloyd-Jones GC (2014) *Chem Soc Rev* 43:412
2. Darses S, Genet JP (2008) *Chem Rev* 108:288
3. Molander GA, Ellis N (2007) *Acc Chem Res* 40:275
4. Doucet H (2008) *Eur J Org Chem* 2013
5. Stefani HA, Cella R, Vieira AS (2007) *Tetrahedron* 63:3623
6. Molander GA, Sandrock DL (2009) *Curr Opin Drug Discov Devel* 12:811
7. Vedejs E, Chapman RW, Fields SC, Lin S, Schrimpf MR (1995) *J Org Chem* 60:3020
8. Lennox AJJ, Lloyd-Jones GC (2012) *Angew Chem Int Ed* 51:9385
9. Molander GA, Trice SLJ, Dreher SD (2010) *J Am Chem Soc* 132:17701
10. Molander GA, Trice SLJ, Kennedy SM, Dreher SD, Tudge MT (2012) *J Am Chem Soc* 134:11667
11. Molander GA, Cavalcanti LN, Garcia-Garcia C (2013) *J Org Chem* 78:6427
12. Chen H, Schlecht S, Sample TC, Hartwig JF (2000) *Science* 287:1995
13. Lawrence JD, Takahashi M, Bae C, Hartwig JF (2004) *J Am Chem Soc* 126:15334
14. Murphy JM, Lawrence JD, Kawamura K, Incarvito C, Hartwig JF (2006) *J Am Chem Soc* 128:13684
15. Murphy JM, Tzschucke CC, Hartwig JF (2007) *Org Lett* 9:757
16. Liskey CW, Hartwig JF (2012) *J Am Chem Soc* 134:12422
17. Liskey CW, Hartwig JF (2013) *J Am Chem Soc* 135:3375
18. Tobisu M, Chatani N (2009) *Angew Chem Int Ed* 48:3565
19. Molander GA, Sandrock DL (2008) *J Am Chem Soc* 130:15792
20. Molander GA, Sandrock DL (2009) *Org Lett* 11:2369
21. Molander GA, Jean-Gérard L (2013) *Org Reactions* 79:1
22. Molander GA, Ham J (2006) *Org Lett* 8:2031
23. Broom T, Hughes M, Szczepankiewicz BG, Ace K, Hagger B, Lacking G, Chima R, Marchbank G, Alford G, Evans P, Cunningham C, Roberts JC, Perni RB, Berry M, Rutter A, Watson SA (2013) *Org Process Res Dev*. doi:10.1021/op400090a

24. Molander GA, Shin I (2011) *Org Lett* 13:3956
25. Molander GA, Ryu D, Hosseini-Sarvari M, Devulapally R, Seapy DG (2013) *J Org Chem* 78:6648
26. Fleury-Brégeot N, Raushel J, Sandrock DL, Dreher SD, Molander GA (2012) *Chem Eur J* 18:9564
27. Molander GA, Fleury-Brégeot N, Hiebel M-A (2011) *Org Lett* 13:1694
28. Molander GA, Canturk B (2008) *Org Lett* 10:2135
29. Kalinin AV, Scherer S, Snieckus V (2003) *Angew Chem Int Ed* 42:3399
30. Kamatani A, Overman LE (1999) *J Org Chem* 64:8743
31. Molander GA, Vargas F (2007) *Org Lett* 9:203
32. Molander GA, Jean-Gérard L (2007) *J Org Chem* 72:8422
33. Tallman RC (1934) *J Am Chem Soc* 56:126
34. Hawthorne MF, Dupont JA (1958) *J Am Chem Soc* 80:5830
35. Matteson DS, Liedtke JD (1963) *J Org Chem* 28:1924
36. Matteson DS, Peacock K (1964) *J Organomet Chem* 2:190
37. Fleury-Brégeot N, Pisset M, Beaumard F, Colombel V, Oehlich D, Rombouts F, Molander GA (2012) *J Org Chem* 77:10399
38. Fleury-Brégeot N, Oehlich D, Rombouts F, Molander GA (2013) *Org Lett* 15:1536
39. Matteson DS (1960) *J Am Chem Soc* 82:4228
40. Hunt AR, Stewart SK, Whiting A (1993) *Tetrahedron Lett* 34:3599
41. Lightfoot AP, Twiddle SJR, Whiting A (2005) *Synlett* 529–531
42. Molander GA, Rodríguez Rivero M (2002) *Org Lett* 4:107
43. Molander GA, Bernardi CR (2002) *J Org Chem* 67:8424
44. Molander GA, Brown AR (2006) *J Org Chem* 71:9681
45. Arvela RK, Leadbeater NE, Mack TL, Kormos CM (2006) *Tetrahedron Lett* 47:217
46. Alacid E, Najera C (2009) *J Org Chem* 74:2321
47. Patai S, Rappoport Z (eds) (1987) *The chemistry of the cyclopropyl group*. Wiley, New York
48. Patai S, Rappoport Z (2006) *The chemistry of cyclobutanes*. Wiley, New York
49. Knapp DM, Gillis EP, Burke MD (2009) *J Am Chem Soc* 131:6961
50. Jana R, Pathak TP, Sigman MS (2011) *Chem Rev* 111:1417
51. Molander GA, Gormisky PE (2008) *J Org Chem* 73:7481
52. Molander GA, Beaumard F, Niethamer TK (2011) *J Org Chem* 76:8126
53. Pursler S, Moore PR, Swallow S, Gouverneur V (2008) *Chem Soc Rev* 37:320
54. Xu J, Luo DF, Liu ZJ, Gong TJ, Fu Y, Liu L (2011) *Chem Commun* 47:4300
55. Zhang CP, Cai J, Zhou CB, Wang XP, Zheng X, Gu YC, Xiao JC (2011) *Chem Commun* 47:9516
56. Liu T, Shen Q (2011) *Org Lett* 13:2342
57. Chu L, Qing FL (2010) *Org Lett* 12:5060
58. Senecal TD, Parsons AT, Buchwald SL (2011) *J Org Chem* 76:1174
59. Ye Y, Kunzi SA, Sanford MS (2012) *Org Lett* 14:4979
60. Liu T, Shao X, Wu Y, Shen Q (2012) *Angew Chem Int Ed* 51:540
61. Huang Y, Fang X, Lin X, Li H, He W, Huang KW, Yuan Y, Weng Z (2012) *Tetrahedron* 68:9949
62. Li Y, Wu L, Neumann H, Beller M (2013) *Chem Commun* 49:2628
63. Pisset M, Oehlich D, Rombouts F, Molander GA (2013) *J Org Chem* 78:12837
64. Argintaru OA, Ryu D, Aron I, Molander GA (2013) *Angew Chem Int Ed* 52:13656
65. Wasa M, Chan KSL, Yu JQ (2011) *Chem Lett* 40:1004
66. Thuy-Boun PS, Villa G, Dang D, Richardson P, Su S, Yu JQ (2013) *J Am Chem Soc* 135:17508
67. Pisset M, Oehlich D, Rombouts F, Molander GA (2013) *Org Lett* 15:1528
68. Hamilton JY, Sarlah D, Carreira EM (2013) *J Am Chem Soc* 135:994
69. Gendrineau T, Genet JP, Darses S (2009) *Org Lett* 11:3486
70. Szymiest JL, Dutheil G, Mahmood A, Aggarwal VK (2007) *Angew Chem Int Ed* 46:7491

71. Stymiest JL, Bagutski V, French RM, Aggarwal VK (2008) *Nature* 456:778
72. Ros A, Aggarwal VK (2009) *Angew Chem Int Ed* 48:6289
73. Molander GA, Wisniewski SR (2012) *J Am Chem Soc* 134:16856
74. Zhao H, Dang L, Marder TB, Lin Z (2008) *J Am Chem Soc* 128:11036
75. Sandrock DL, Jean-Gerard L, Chen C, Dreher SD, Molander GA (2010) *J Am Chem Soc* 132:17108
76. Sorin G, Martinez Mallorquin R, Contie Y, Baralle A, Malacria M, Goddard JP, Fensterbank L (2010) *Angew Chem Int Ed* 49:8721
77. Molander GA, Colombel V, Braz VA (2011) *Org Lett* 13:1852
78. Presset M, Fleury-Brégeot N, Oehlrich D, Rombouts F, Molander GA (2013) *J Org Chem* 78:4615
79. Fujiwara Y, Domingo V, Seiple IB, Gianatassio R, Del Bel M, Baran PS (2011) *J Am Chem Soc* 133:3292
80. Seiple IB, Su S, Rodriguez RA, Gianatassio R, Fujiwara Y, Sobel AL, Baran PS (2010) *J Am Chem Soc* 132:13194
81. Lockner JW, Dixon DD, Risgaard R, Baran PS (2011) *Org Lett* 13:5628
82. Koike T, Akita M (2013) *Synlett* 24:2492
83. Yasu Y, Koike T, Akita M (2012) *Adv Synth Catal* 354:3414
84. Miyazawa K, Yasu Y, Koike T, Akita M (2013) *Chem Commun* 49:7249
85. Tellis JC, Primer DN, Molander GA (2014) *Science* 345:433
86. Yasu Y, Koike T, Akita M (2013) *Chem Commun* 49:2037
87. Parsons AT, Senecal TD, Buchwald SL (2012) *Angew Chem Int Ed* 51:2947
88. Xu J, Wang X, Shao C, Su D, Cheng G, Hu Y (2010) *Org Lett* 12:1964
89. Molander GA, Cavalcanti LN (2011) *J Org Chem* 76:623
90. Dumas AM, Bode JW (2012) *Org Lett* 14:2138
91. Molander GA, Raushel J, Ellis NM (2010) *J Org Chem* 75:4304
92. Dumas AM, Molander GA, Bode JW (2012) *Angew Chem Int Ed* 51:5683
93. Gowenlock BG, Richter-Addo GB (2004) *Chem Rev* 104:3315
94. Zhao D, Johansson M, Backvall JE (2007) *Eur J Org Chem* 4431
95. Bordoloi A, Halligudi SB (2007) *Adv Synth Catal* 2085
96. Bosch E, Kochi JK (1994) *J Org Chem* 59:5573
97. Atherton JH, Moodie RB, Noble R (1999) *J Chem Soc Perkin Trans 2* 699
98. D'Amicoc JJ, Tung CC, Walker LA (1959) *J Am Chem Soc* 81:5957
99. Molander GA, Cavalcanti LN (2012) *J Org Chem* 77:4402
100. Liesen AP, Silva AT, Sousa JC, Menezes PH, Oliveira RA (2012) *Tetrahedron Lett* 53:4240
101. Berionni G, Morozova V, Heining M, Mayer P, Knochel P, Mayr H (2013) *J Am Chem Soc* 135:6317
102. Molander GA, Cavalcanti LN (2011) *J Org Chem* 76:7195
103. Hagmann WK (2008) *J Med Chem* 51:4359
104. Jeschke P (2010) *Pest Manag Sci* 66:10
105. Ye Y, Sanford MS (2013) *J Am Chem Soc* 135:4648
106. Ye Y, Schimler SD, Hanley PS, Sanford MS (2013) *J Am Chem Soc* 135:16292
107. Molander GA, Cavalcanti LN, Canturk B, Pan P-S, Kennedy LE (2009) *J Org Chem* 74:7364
108. Kabalka GW, Coltuclu V (2009) *Tetrahedron Lett* 50:6271
109. Blevins DW, Yao M-L, Yong L, Kabalka GW (2011) *Tetrahedron Lett* 52:6534
110. Kim BJ, Matteson DS (2004) *Angew Chem Int Ed* 43:3056
111. Liu Z, Marder TB (2008) *Angew Chem Int Ed* 47:242
112. Campbell PG, Marwitz AJV, Liu SY (2012) *Angew Chem Int Ed* 51:6074
113. Bosdet MJD, Piers WE (2009) *Can J Chem* 87:8
114. Wisniewski SR, Guenther CL, Argintaru OA, Molander GA (2014) *J Org Chem* 79:365

The Catalytic Dehydrocoupling of Amine–Boranes and Phosphine–Boranes

Heather C. Johnson, Thomas N. Hooper, and Andrew S. Weller

Contents

1	Introduction	154
2	Transition-Metal-Catalysed Dehydrocoupling of Amine–Boranes	155
2.1	General Considerations	155
2.2	Aminoboranes: Observation and Trapping	155
2.3	Linear Diborazanes	157
2.4	Early Examples of Metal-Catalysed Dehydrocoupling	157
2.5	Heterogeneous Catalysts for the Dehydrocoupling of Amine–Boranes	158
2.6	Transition-Metal-Catalysed Dehydrocoupling of $H_3B \cdot NH_3$ Promoted by Ionic Liquids	162
2.7	Homogeneous Dehydrocoupling of Amine–Boranes	163
2.8	Mechanistic Studies on Homogeneous Dehydrocoupling Systems	166
2.9	Generic Mechanisms for Dehydrocoupling of $H_3B \cdot NMe_2H$ Using Transition Metals	189
2.10	Main-Group Element-Catalysed Dehydrocoupling of Amine–Boranes	192
3	Dehydrocoupling of Phosphine–Boranes	201
3.1	Transition-Metal-Catalysed Dehydrocoupling of Phosphine–Boranes	201
3.2	Determination of the Active Catalytic Species: Hetero- or Homogeneous	203
3.3	Sigma Complexes and B-Agostic Interactions of Phosphine–Boranes	205
3.4	Stabilised Phosphinoboranes	206
3.5	Group 8 Metal-Catalysed Dehydrocoupling of Phosphine–Boranes	207
3.6	Mechanistic Investigations into the Rhodium-Catalysed Dehydrocoupling of Secondary Phosphine–Boranes	207
3.7	Mechanistic Investigation into the Rhodium-Catalysed Dehydrocoupling of Primary Phosphine–Boranes	211
3.8	Lewis Acid-Catalysed Dehydrocoupling of Phosphine–Boranes	214
4	Future Prospects	215
	References	216

H.C. Johnson • T.N. Hooper • A.S. Weller (✉)
Department of Chemistry, University of Oxford, Oxford OX1 3TA, UK
e-mail: andrew.weller@chem.ox.ac.uk

Abstract Mechanistic studies into the catalysed dehydrocoupling of amine–boranes and phosphine–boranes have seen a rapid development over the last 5 years. The primary driver for this intense research effort has been the development of catalysts that might offer significant benefits with regard to the kinetics of hydrogen release, for potential use when linked with a fuel cell. Secondary to this, although becoming increasingly important, is the use of dehydrocoupling approaches to afford well-defined polymeric materials with B–N or B–P backbones that offer potential as high-performance polymers, as pre-ceramic materials and as precursors to white graphene. There have been many systems studied using catalysts incorporating metals from across the periodic table. This review attempts to bring together the insight revealed from these studies, which shows a rich and complex mechanistic landscape for the dehydrocoupling of phosphine–boranes and amine–boranes.

Keywords Amine–Borane • Catalysis • Dehydrocoupling • Mechanism • Phosphine–Borane

1 Introduction

The transition-metal-catalysed dehydrocoupling of amine–boranes and, to a lesser extent, phosphine–boranes has received much attention in recent years [1, 2]. For amine–boranes, the parent compound, $\text{H}_3\text{B} \cdot \text{NH}_3$, is an air-stable solid containing a high weight percentage of hydrogen (19.6%) and thus has been explored extensively as a potential candidate for chemical hydrogen storage vectors [3]. Although $\text{H}_3\text{B} \cdot \text{NH}_3$ can release dihydrogen on heating to temperatures above 120°C , leading to mixtures of products including polyborazylene and polyaminoboranes, metal catalysts have led to more efficient and controlled dehydrogenation [4]. Amine–boranes have also been studied with respect to the formation of BN-based materials. In particular polyaminoboranes, which are isoelectronic with societally and technologically ubiquitous polyolefins, have potential applications as piezoelectric materials or as precursors to BN-based ceramics [5] or white graphene [6]. Likewise, the analogous dehydrocoupling of phosphine–boranes produces oligomeric and polymeric materials that show promise as electron beam resists and precursors to semiconducting boron phosphide [7].

In this review we outline recent developments to elucidate, and thus harness, the mechanism of catalytic dehydrocoupling of amine–boranes and phosphine–boranes. Although there is yet to be developed a common, detailed, overarching mechanism that encompasses all catalysed systems, we hope that this contribution serves to mark the current state of the art in the field and provide a background to aid future developments in the area. It is the control of these processes, to either afford well-defined final products or the maximum rate and yield of hydrogen evolution, that makes catalytic routes attractive for dehydrocoupling. This is not

the first time that dehydrocoupling of amine–boranes and phosphine–boranes has been reviewed, and there have been recent overviews dealing with their general chemistry and properties [1, 2], role in hydrogen storage applications [4, 8, 9], as well as dehydrocoupling processes [5, 7, 10, 11]. We do not attempt to review the extensive literature on the catalysed hydrolysis of amine–boranes to produce H_2 as the principal product of interest [3].

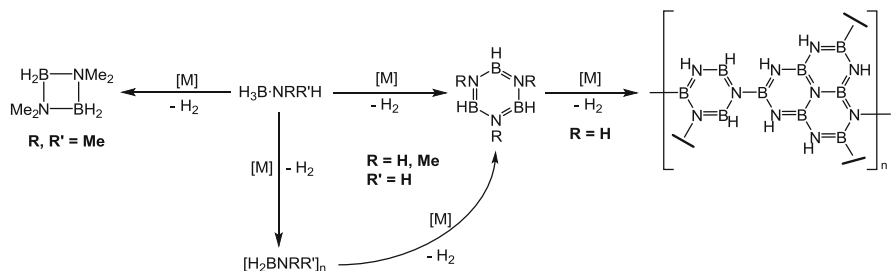
2 Transition-Metal-Catalysed Dehydrocoupling of Amine–Boranes

2.1 General Considerations

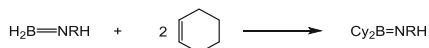
A generalised scheme for the products observed from amine–borane dehydrocoupling is shown in Scheme 1. The parent $H_3B \cdot NH_3$ can also lose over 2 equiv. of hydrogen to form polyborazylene, as well as often insoluble oligomeric and polymeric materials that arise from loss of less than 2 equiv. of H_2 [8]. Primary amine–boranes, $H_3B \cdot NRH_2$, can undergo loss of 1 equiv. of hydrogen during dehydrocoupling to afford polyaminoboranes $[H_2BNRH]_n$ ($R=H, Me, ^iBu$), while borazines, $[HBNR]_3$ ($R=H, Me, ^iBu$), can result from the loss of 2 equiv. of dihydrogen and should be considered to be the thermodynamic product of the dehydrocoupling of primary amine–boranes. Secondary amine–boranes $H_3B \cdot NR_2H$ can lose 1 equiv. of dihydrogen and dehydrocouple through soluble and well-defined intermediates; for $H_3B \cdot NMe_2H$, the most commonly observed are the aminoborane $H_2B=NMe_2$ and the linear diborazane $H_3B \cdot NMe_2BH_2 \cdot NMe_2H$ (see Sect. 2.2 and 2.3). Consequently, $H_3B \cdot NMe_2H$ is often used as a model for the dehydrocoupling of $H_3B \cdot NH_3$ and $H_3B \cdot NMe_2H$ [12, 13], the products of which are often insoluble or poorly defined polymeric or oligomeric materials [14]. The cyclic dimer $[H_2BNR_2]_2$ ($R=e.g. Me, Et$) is generally formed as the major dehydrocoupling product of $H_3B \cdot NR_2H$. With bulky *N*-substituents, e.g. iPr or *Cy*, dimerisation is prevented and instead the aminoborane $H_2B=NR_2$ results [15, 16].

2.2 Aminoboranes: Observation and Trapping

The dehydrocoupling of amine–boranes is often proposed to proceed via formation of aminoboranes $H_2B=NRR'$ that arise from initial dehydrogenation, and aminoboranes such as $H_2B=N^iBuH$ and $H_2B=NMe_2$ have been directly observed as intermediates in catalytic dehydrocoupling of their respective amine–boranes [17, 18]. The kinetics for the “off-metal” dimerisation of $H_2B=NMe_2$ to form $[H_2BNMe_2]_2$ have been explored and found to be a second-order process with a large negative entropy of activation [19]. Interestingly, a significant solvent effect on the relative rate of dimerisation has also been noted, with acetonitrile



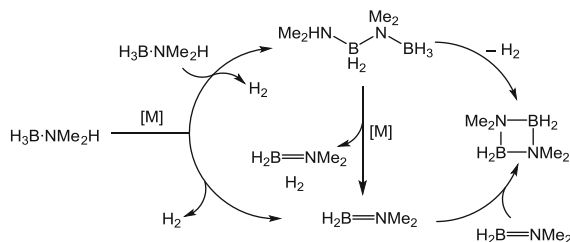
Scheme 1 Simplified dehydrocoupling pathway for $\text{H}_3\text{B} \cdot \text{NMe}_2\text{H}$, $\text{H}_3\text{B} \cdot \text{NMe}_2$ and $\text{H}_3\text{B} \cdot \text{NH}_3$. The generation of intermediate aminoboranes is not shown but is implicit for many processes



Scheme 2 Trapping of aminoboranes by cyclohexene. $\text{R} = \text{Me}, \text{H}$

accelerating the process [13, 20]. The less bulky congeners $\text{H}_2\text{B}=\text{NH}_2$ [21] and $\text{H}_2\text{B}=\text{NMeH}$ [22, 23], however, have not been directly observed as intermediates in dehydrocoupling, although they have been isolated coordinated to a transition metal fragment, being formed from dehydrogenation of the corresponding amine–borane [24]. In 2008, Baker, Dixon and co-workers proposed that $\text{H}_2\text{B}=\text{NH}_2$ liberated from the metal results in the eventual production of borazine, whereas $\text{H}_2\text{B}=\text{NH}_2$ (or derivatives thereof) remaining bound to the metal results in oligomeric or polymeric products [25]. To detect free aminoborane, cyclohexene was added to reaction mixtures, as cyclohexene can be hydroborated by $\text{H}_2\text{B}=\text{NRH}$ ($\text{R} = \text{H}, \text{Me}$), forming $\text{Cy}_2\text{B}=\text{NRH}$ (Scheme 2) thereby acting as a useful marker for free aminoboranes.

Accordingly, when cyclohexene was added to a reaction mixture of $\text{H}_3\text{B} \cdot \text{NH}_3$ and $[\text{Rh}(1,5\text{-cod})(\mu\text{-Cl})_2]_2$, $\text{Cy}_2\text{B}=\text{NH}_2$ was the major product observed, instead of the expected borazine (see Sect. 2.4 [26]). However, upon addition of cyclohexene to a solution of $\text{H}_3\text{B} \cdot \text{NH}_3$ and catalyst $\text{Ir}(\text{tBuPOCOP}^t\text{Bu})(\text{H})_2$ [27], the same oligomeric products were observed as in the absence of cyclohexene, i.e. no hydroboration product was observed (Sect. 2.8.3). Although cyclohexene trapping is still regarded as a useful method for detecting free aminoboranes, more recent studies have suggested that the absence of hydroboration does not necessarily reflect an absence of free aminoborane. It has been suggested that, if borazine formation (from aminoborane trimerisation/dehydrogenation) or hydroboration of cyclohexene are not kinetically competitive with metal-based BN oligomerisation/polymerisation processes, $\text{Cy}_2\text{B}=\text{NH}_2$ will not be observed even if $\text{H}_2\text{B}=\text{NH}_2$ is present [21, 28, 29].



Scheme 3 Schneider's early model for dehydrocoupling $\text{H}_3\text{B} \cdot \text{NMe}_2\text{H}$ to form $[\text{H}_2\text{BNMe}_2]_2$

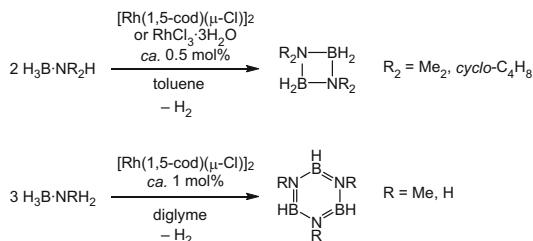
2.3 Linear Diborazanes

Another intermediate often observed in the dehydrocoupling of $\text{H}_3\text{B} \cdot \text{NMe}_2\text{H}$ is the linear diborazane $\text{H}_3\text{B} \cdot \text{NMe}_2\text{BH}_2 \cdot \text{NMe}_2\text{H}$ [15]. Schneider has calculated that the pathway for B–N bond cleavage of $\text{H}_3\text{B} \cdot \text{NMe}_2\text{BH}_2 \cdot \text{NMe}_2\text{H}$ to generate $\text{H}_3\text{B} \cdot \text{NMe}_2\text{H}$ and $\text{H}_2\text{B}=\text{NMMe}_2$ is close to thermoneutral ($\Delta G = -2.3 \text{ kcal mol}^{-1}$) [30]. Therefore, if this process is reversible, the position of the equilibrium (and hence whether $\text{H}_3\text{B} \cdot \text{NMe}_2\text{BH}_2 \cdot \text{NMe}_2\text{H}$ is observed in catalysis) is likely to be dependent upon these species relative concentrations and rates of formation with a particular catalyst. A general pathway for the dehydrocoupling of $\text{H}_3\text{B} \cdot \text{NMe}_2\text{H}$ with Schneider's ruthenium catalysts (see Sect. 2.8.4) was developed (Scheme 3), suggesting that the formation of $\text{H}_3\text{B} \cdot \text{NMe}_2\text{BH}_2 \cdot \text{NMe}_2\text{H}$ is a metal-based process. The role of this diborazane in the dehydrocoupling of $\text{H}_3\text{B} \cdot \text{NMe}_2\text{H}$ has been further discussed by others [15, 19, 28, 31, 32].

Weller and Manners have since reported that the diborazane $\text{H}_3\text{B} \cdot \text{NMeHBH}_2 \cdot \text{NMeH}_2$, the product of one dehydrooligomerisation of $\text{H}_3\text{B} \cdot \text{NMeH}_2$, can be formed by catalytic methods [33], and its role as a possible intermediate in dehydropolymerisation has been further explored (see Sect. 2.8.3) [28]. Shore and co-workers have also reported the synthesis by stoichiometric methods of the $\text{H}_3\text{B} \cdot \text{NH}_3$ analogue, $\text{H}_3\text{B} \cdot \text{NH}_2\text{BH}_2 \cdot \text{NH}_3$ [34], while Sneddon and co-workers have reported the synthesis of triborazanes, such as $\text{H}_3\text{B} \cdot (\text{NH}_2\text{BH}_2)_2 \cdot \text{NH}_3$ [35], which are implicated in dehydropolymerisation processes [36].

2.4 Early Examples of Metal-Catalysed Dehydrocoupling

The first example of transition-metal-catalysed dehydrocoupling was reported in 1989 by Roberts and co-workers. The amine–borane $\text{H}_3\text{B} \cdot \text{N}^t\text{BuMeH}$ was dehydrogenated at 120°C by 10% Pd on charcoal to form the aminoborane $\text{H}_2\text{B}=\text{N}^t\text{BuMe}$, which dimerised to form $[\text{H}_2\text{BN}^t\text{BuMe}]_2$ [37]. In 2001, Manners and co-workers reported that Rh^{I} or Rh^{III} precursors catalytically dehydrocoupled secondary amine–boranes $\text{H}_3\text{B} \cdot \text{NR}_2\text{H}$ ($\text{R}_2=\text{Me}_2$, *cyclo*- C_4H_8) to yield the corresponding cyclic dimer $[\text{H}_2\text{BNR}_2]_2$ (Scheme 4). The Rh^{I} precursor was also



Scheme 4 Dehydrocoupling of amine–boranes by $[\text{Rh}(1,5\text{-cod})(\mu\text{-Cl})_2]$ and $\text{RhCl}_3 \cdot 3\text{H}_2\text{O}$

an effective catalyst for the dehydrocoupling of $\text{H}_3\text{B} \cdot \text{NH}_3$ and $\text{H}_3\text{B} \cdot \text{NMe}_2$ to form their respective borazines, although in both cases insoluble material, indicative of oligomeric chains, was also observed in the reaction mixtures [26].

2.5 Heterogeneous Catalysts for the Dehydrocoupling of Amine–Boranes

Various systems act as heterogeneous catalysts for amine–borane dehydrocoupling by the formation in situ of catalytically active nanoparticles, although the nature of the actual catalytic component has been the subject of debate. Nonetheless, heterogeneous catalysis is attractive due to the facile separation of the products and catalyst. The dehydrocoupling of $\text{H}_3\text{B} \cdot \text{NMe}_2\text{H}$ by $[\text{Rh}(1,5\text{-cod})(\mu\text{-Cl})_2]$ showed a reaction profile with an induction period, during which a black precipitate was observed to form. Tests, originally developed by Finke [38], were performed to probe for heterogeneous catalysis. For example, both filtration and catalyst poisoning with mercury halted catalysis (Fig. 1), suggesting a heterogeneous system in which the dehydrocoupling is catalysed by rhodium nanoparticles [39].

Later EXAFS studies by Autrey and co-workers suggested that, instead, soluble Rh_6 clusters are responsible for the dehydrocoupling activity in this system [40]. Interestingly, the catalytic dehydrocoupling of $\text{H}_3\text{B} \cdot \text{PPh}_2\text{H}$ with $[\text{Rh}(1,5\text{-cod})(\mu\text{-Cl})_2]$ to form $\text{H}_3\text{B} \cdot \text{PPh}_2\text{BH}_2 \cdot \text{PPh}_2\text{H}$ was reported by Manners as homogeneous (see Sect. 3.2) [39].

Some heterogeneous systems are among the fastest reported dehydrocoupling catalysts. A system using $[\text{Fe}(\text{NCMe})_2(\text{PNNP})][\text{BF}_4]_2/\text{KO}^t\text{Bu}$ [$\text{PNNP} = (\text{Ph}_2\text{PC}_6\text{H}_4\text{CH}=\text{NCH}_2)_2$], reported by Morris and co-workers, was highly active in the dehydrogenation of $\text{H}_3\text{B} \cdot \text{NH}_3$. At 2.5 mol% catalyst loading, an equivalent of H_2 is released within a minute, representing a turnover frequency (TOF) of approximately $2,400 \text{ h}^{-1}$, to yield a mixture of products: borazine, polyborazylene and B–N oligomers or partially cross-linked polyborazylene, as well as unreacted $\text{H}_3\text{B} \cdot \text{NH}_3$ [41]. The active species are proposed to be iron(0) nanoparticles stabilised by PNNP ligands. Catalysis slowed after the initial fast dehydrogenation, and free PNNP ligand was observed by $^{31}\text{P}\{^1\text{H}\}$ NMR spectroscopy, implying that

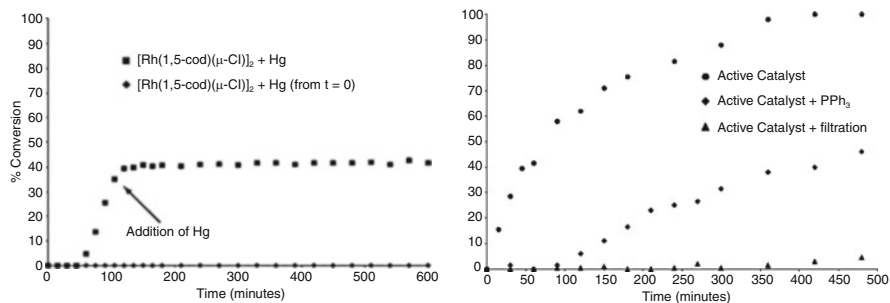


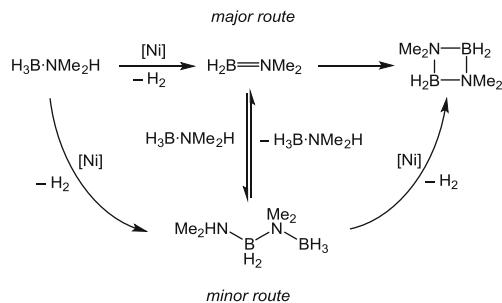
Fig. 1 *Left:* addition of mercury to the reaction mixture. *Right:* the effect of filtration and poisoning with PPh_3 . Both figures reprinted (adapted) with permission from Jaska and Manners [39]. Copyright 2004 American Chemical Society

catalyst deactivation was occurring and active sites on the iron nanoparticle were being blocked. Consistent with this, attempts to recycle the catalyst resulted in slower dehydrocoupling.

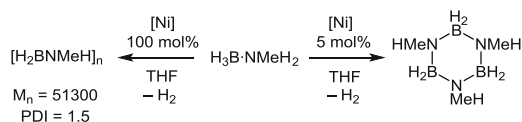
Systems based upon ruthenium nanoparticles have been explored by Ozkar et al. for the dehydrocoupling of $\text{H}_3\text{B} \cdot \text{NMe}_2\text{H}$ to yield $[\text{H}_2\text{BNMe}_2]_2$ and show good activities. Oleylamine-stabilised ruthenium(0) nanoparticles (generated in situ from RuCl_3) effect dehydrocoupling of this amine–borane with a TOF of 137 h^{-1} [42], while ruthenium(0) nanoparticles stabilised by 3–aminopropyltriethoxysilane gave a TOF of 55 h^{-1} [43]. Ozkar also obtained turnover frequencies of $\sim 60 \text{ h}^{-1}$ for the dehydrocoupling of $\text{H}_3\text{B} \cdot \text{NMe}_2\text{H}$ when using rhodium(0) nanoclusters ($\sim \text{Rh}_{190}\text{--}\text{Rh}_{460}$), produced from $[(\text{C}_5\text{H}_{11}\text{CO}_2)_2\text{Rh}]_2$ [44]. Zahmakiran and co-workers dehydrogenated $\text{H}_3\text{B} \cdot \text{NH}_3$ to form $[\text{H}_2\text{BNH}_2]_n$ and polyborazylene (average TOF $\sim 24 \text{ h}^{-1}$) with a ruthenium nanocatalyst that is formed from the in situ hydrogenation of $[\text{Ru}(\text{cod})(\text{cot})]$. Poisoning experiments suggested sub-nanometer Ru_n clusters as the dominant catalytically active species rather than $\text{Ru}(0)$ nanoparticles [45]. Iron-doped $\text{H}_3\text{B} \cdot \text{NH}_3$ (5 mol% Fe) has been shown to produce crystalline $[\text{H}_2\text{BNH}_2]_n$ on heating the solid to 60°C , the mechanism being proposed to operate via an FeB alloy [46].

A skeletal nickel catalyst, produced from base-leaching a Ni/Al alloy, for the heterogeneous dehydrocoupling of amine–boranes was reported by Manners and co-workers [22]. Although the dehydrocoupling is relatively slow (TOF $\sim 3 \text{ h}^{-1}$ for $\text{H}_3\text{B} \cdot \text{NMe}_2\text{H}$, 5 mol% Ni), mechanistic insight into heterogeneous dehydrocoupling was obtained. The major route for dehydrocoupling $\text{H}_3\text{B} \cdot \text{NMe}_2\text{H}$ was proposed to be dehydrogenation to afford the aminoborane $\text{H}_2\text{B}=\text{NMe}_2$, which dimerises off-metal to form the final product $[\text{H}_2\text{BNMe}_2]_2$. A minor pathway was also suggested, involving the on-metal formation of the linear dimer $\text{H}_3\text{B} \cdot \text{NMe}_2\text{BH}_2 \cdot \text{NMe}_2\text{H}$, followed by on-metal dehydrocyclisation to form $[\text{H}_2\text{BNMe}_2]_2$ (Scheme 5).

Dehydrocoupling of the primary amine–borane $\text{H}_3\text{B} \cdot \text{NMe}_2\text{H}$ was also investigated with this system. At a catalyst loading of 5 mol%, slow conversion (TOF $\sim 0.2 \text{ h}^{-1}$) to form the cyclic triborazane $[\text{H}_2\text{BNMeH}]_3$ resulted. Interestingly at



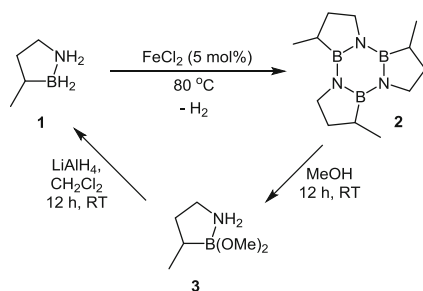
Scheme 5 Suggested dehydrocoupling pathway for the dehydrocoupling of $\text{H}_3\text{B}\cdot\text{NMe}_2\text{H}$ by skeletal Ni (5 mol%, toluene)



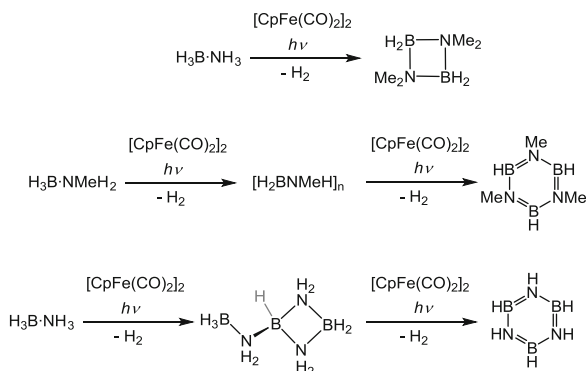
Scheme 6 Dehydrocoupling of $\text{H}_3\text{B}\cdot\text{NMeH}_2$ with skeletal Ni

100 mol% Ni, polyaminoborane $[\text{H}_2\text{BNMeH}]_n$ was formed ($M_n = 51,300 \text{ g mol}^{-1}$, PDI = 1.5), Scheme 6. This effect of catalyst loading on the identity of the final product was attributed to initial dehydrogenation of $\text{H}_3\text{B}\cdot\text{NMeH}_2$ to form the monomer $\text{H}_2\text{B}=\text{NMeH}$, which is formed in higher concentrations with higher catalyst loadings and, under such a kinetic regime, polymerisation is favoured over cyclisation. Similarly, in the dehydrocoupling of $\text{H}_3\text{B}\cdot\text{NH}_3$, 5 mol% of Ni produced *B*-(cyclodiborazanyl)-aminoborohydride, whereas stoichiometric quantities of Ni formed polyaminoborane $[\text{H}_2\text{BNH}_2]_n$.

An important result for the potential development of amine–boranes as hydrogen storage materials originated from Liu and co-workers using a heterogeneous system. The cyclic amine–borane BN-methylcyclopentane (**1**, Scheme 7), an air- and moisture-stable liquid at room temperature, was shown to release 2 equiv. of H_2 (4.7 wt%) at 80°C to cleanly generate the trimer **2**, also a liquid, using 5 mol% FeCl_2 (TOF 120 h^{-1}) in a neat solution of **1** [47]. The reaction profile showed an induction period, and a black powder was produced during the reaction, with mercury experiments suggesting a heterogeneous catalyst as the active species. The catalyst was recyclable, with three successive experiments all showing similar activities. Significantly **2** could be treated with MeOH (to form **3**), followed by LiAlH_4 to regenerate **1** (Scheme 7) in 92% yield. Although a more efficient regeneration method is desirable, these results illustrate the potential of this system as a hydrogen storage candidate, with the additional benefit of using cheap and abundant iron as the catalyst. The properties of the materials produced by this process have been described (e.g. viscosity, thermal stability, purity) [48]. A related system was recently reported in which $\text{MeH}_2\text{B}\cdot\text{NMeH}_2$ is dehydrogenated by CoCl_2 (5 mol%, 80°C , diglyme) to form the borazine product $[\text{MeBNMe}]_3$ in



Scheme 7 Dehydrogenation of **1** to yield **2** and regeneration of **1** from **2**



Scheme 8 Catalytic dehydrocoupling of $\text{H}_3\text{B} \cdot \text{NMe}_2\text{H}$, $\text{H}_3\text{B} \cdot \text{NMeH}_2$ and $\text{H}_3\text{B} \cdot \text{NH}_3$ with 5 mol % $[\text{CpFe}(\text{CO})_2]_2$

71% yield. Subsequent treatment of $[\text{MeBNMe}]_3$ with HCOOH and then LiAlH_4 regenerated $\text{MeH}_2\text{B} \cdot \text{NMeH}_2$ in a 46% yield [49].

Manners and co-workers recently illustrated that subtle changes in the ligand set can have significant effects on whether the catalysis is homogeneous or heterogeneous. $[\text{CpFe}(\text{CO})_2]_2$ (5 mol%) dehydrocouples the amine–boranes $\text{H}_3\text{B} \cdot \text{NMe}_2\text{H}$, $\text{H}_3\text{B} \cdot \text{NMeH}_2$ and $\text{H}_3\text{B} \cdot \text{NH}_3$ under photoirradiation (Scheme 8). With $\text{H}_3\text{B} \cdot \text{NMeH}_2$, high molecular weight $[\text{H}_2\text{BNMeH}]_n$ was produced ($M_n = 64,300 \text{ g mol}^{-1}$, $\text{PDI} = 1.8$) after 3 h (90% conversion), although after 16 h of irradiation, the borazine $[\text{HBNMe}]_3$ was the major product [50].

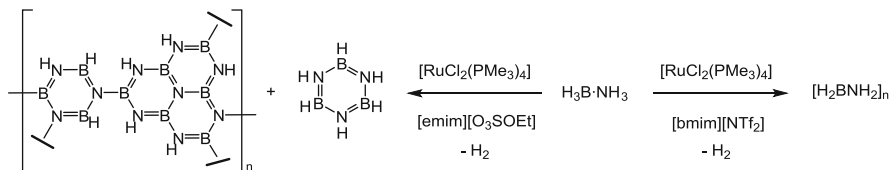
Further mechanistic investigations were undertaken with a range of iron carbonyl cyclopentadienyl complexes and $\text{H}_3\text{B} \cdot \text{NMe}_2\text{H}$ [51]. When using $[\text{CpFe}(\text{CO})_2]_2$ under photoirradiation and $\text{Cp}_2\text{Fe}_2(\text{CO})_3(\text{NCMe})$ (no photoirradiation), $\text{H}_2\text{B}=\text{NMe}_2$ was observed as the sole intermediate during the dehydrocoupling. With $\text{CpFe}(\text{CO})_2\text{I}$, however, under photoirradiation, the linear diborazane $\text{H}_3\text{B} \cdot \text{NMe}_2\text{BH}_2 \cdot \text{NMe}_2\text{H}$ was observed as an intermediate, with $\text{H}_2\text{B}=\text{NMe}_2$ observed in no significant quantities. Investigations into the nature of the reaction mixtures showed that $[\text{CpFe}(\text{CO})_2]_2$ and $\text{Cp}_2\text{Fe}_2(\text{CO})_3(\text{NCMe})$ were producing iron nanoparticles as the active catalyst, thought to form via the loss of CO and NCMe,

respectively. The heterogeneous mechanism is thought to involve initial dehydrogenation of $\text{H}_3\text{B} \cdot \text{NMe}_2\text{H}$ on the nanoparticle surface to form $\text{H}_2\text{B}=\text{NMe}_2$, which then dimerises off-metal. By contrast, $\text{CpFe}(\text{CO})_2\text{I}$ appeared to be acting as a homogeneous catalyst, and this mechanism is discussed in more detail in Sect. 2.8.3.

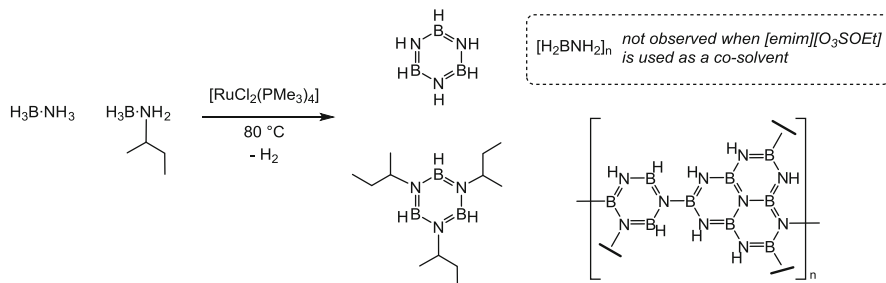
2.6 Transition-Metal-Catalysed Dehydrocoupling of $\text{H}_3\text{B} \cdot \text{NH}_3$ Promoted by Ionic Liquids

In 2006 Sneddon and co-workers noted that dissolving $\text{H}_3\text{B} \cdot \text{NH}_3$ in ionic liquids increased the rate and extent of *thermal* dehydrocoupling relative to that of solid $\text{H}_3\text{B} \cdot \text{NH}_3$ [52, 53]. In 2011, Baker and Sneddon sought to utilise this enhancement by combining transition metal catalysts with ionic liquid solvents. A range of transition metal catalysts were screened for the dehydrocoupling of $\text{H}_3\text{B} \cdot \text{NH}_3$ in the ionic liquid $[\text{bmim}][\text{Cl}]$ (bmim=1-butyl-3-methylimidazole) [54], all at 5 mol% loading, including $[\text{Rh}(1,5\text{-cod})(\mu\text{-Cl})_2]$, $\text{Ru}(1,5\text{-cod})\text{Cl}_2$, RhCl_3 , $\text{Ni}(1,5\text{-cod})_2$ and NiCl_2 . All showed enhanced dehydrocoupling activity at 65°C compared with the analogous reaction in $[\text{bmim}][\text{Cl}]$ in the absence of catalyst. However, increasing the temperature to 85°C with the catalyst $[\text{Rh}(1,5\text{-cod})(\mu\text{-Cl})_2]$ led to lower total H_2 release than that in the absence of catalyst. Similar effects were observed with $[\text{RuCl}_2(\text{PMe}_3)_4]$ (0.78 mol%) in $[\text{emim}][\text{O}_3\text{SOEt}]$ (emim = 1-ethyl-3-methylimidazole), implying that transition metal catalysts can enhance the rate of H_2 release in ionic liquids, but the advantage is most apparent below 85°C . Moreover, different products were observed with changing the ionic liquid: catalysis with $[\text{RuCl}_2(\text{PMe}_3)_4]$ in $[\text{emim}][\text{O}_3\text{SOEt}]$ resulted in borazine and polyborazylene, whereas the same reaction in $[\text{bmim}][\text{NTf}_2]$ resulted in $[\text{H}_2\text{BNH}_2]_n$ (Scheme 9).

This selectivity could have useful implications in the future design of chemical hydrogen storage systems, which was exploited by Baker in the dehydrocoupling of mixtures of $\text{H}_3\text{B} \cdot \text{NH}_3$ and *sec*-butylamine-borane, $\text{H}_3\text{B} \cdot \text{N}^s\text{BuH}_2$ [55]. $\text{H}_3\text{B} \cdot \text{N}^s\text{BuH}_2$ can solubilise $\text{H}_3\text{B} \cdot \text{NH}_3$, resulting in liquid fuel mixtures that have an upper limit for H_2 release of 12.8 wt%. With the $[\text{RuCl}_2(\text{PMe}_3)_4]$ catalyst (~ 1 mol%), the system released over 5.0 wt% of hydrogen in 1 h at 80°C , affording $[\text{HBN}^s\text{Bu}]_3$, $[\text{HBNH}]_3$ and polyborazylene. However, insoluble $[\text{H}_2\text{BNH}_2]_n$ was also observed in the reaction mixture, which is undesirable for a liquid fuel cell, and prevailed on testing diglyme and sulfolane as co-solvents (Scheme 10). The addition of $[\text{emim}][\text{O}_3\text{SOEt}]$ as the co-solvent, however, released 3.6 wt% H_2 at 80°C over 18 h (a lower overall storage capacity due to the ionic liquid) with no insoluble $[\text{H}_2\text{BNH}_2]_n$ observed, making $\text{H}_3\text{B} \cdot \text{N}^s\text{BuH}_2/\text{H}_3\text{B} \cdot \text{NH}_3$ mixtures more appealing as potential liquid fuel cells.



Scheme 9 Different product distributions for the Ru-catalysed dehydrocoupling of $\text{H}_3\text{B} \cdot \text{NH}_3$ with different ionic liquids



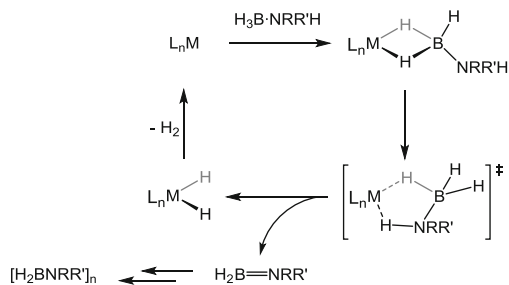
Scheme 10 Products resulting from the dehydrogenation of $\text{H}_3\text{B} \cdot \text{N}^t\text{BuH}_2/\text{H}_3\text{B} \cdot \text{NH}_3$ with $[\text{RuCl}_2(\text{PMe}_3)_4]$ (~1 mol%) with and without $[\text{emim}][\text{O}_3\text{SOEt}]$ as co-solvent

2.7 Homogeneous Dehydrocoupling of Amine–Boranes

Although heterogeneous catalysts can produce high turnover numbers, homogeneous catalysts are more readily studied due to the well-defined coordination sites that can allow for control of catalytic processes by modification of the metal and ligand environment. Homogeneous catalysts can operate via inner-sphere or outer-sphere mechanisms. Outer-sphere mechanisms allow dehydrogenation of amine–boranes without the direct coordination to the metal centre by using metal–ligand cooperativity [21, 30, 56–59]. By contrast, inner-sphere mechanisms involve initial coordination of the amine–borane to the metal forming a sigma complex, followed by dehydrogenation of the amine–borane (Scheme 11). Various mechanistic scenarios have been implicated for the mechanism of dehydrogenation and will be discussed in detail in Sect. 2.8.

2.7.1 Sigma Complexes of Amine–Boranes

Inner-sphere mechanisms for the dehydrocoupling of amine–boranes often invoke coordination of an amine–borane to the metal via 3-centre, 2-electron M-H-B interactions [60], forming a sigma complex, $[\text{L}_n\text{M-H}_3\text{B} \cdot \text{NR}_3]$. These weak interactions arise primarily from donation from the σ B–H orbital to the metal; the B–H σ^* orbital is high in energy, meaning that back-donation from the metal is negligible [11, 61]. Often, sigma complexes are isolated using tertiary amine–boranes,



Scheme 11 Simplified pathway for inner-sphere dehydrogenation

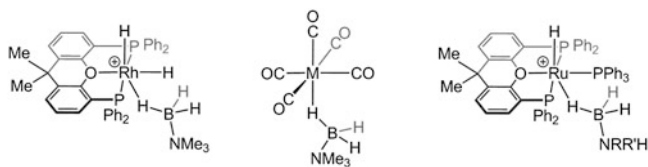


Fig. 2 Examples of η^1 -sigma amine–borane complexes. $M = Cr, Mo$ or W . $NRR'H = N^tBuH_2, NMe_2H$ or NH_3 . $[BAR^F_4]^-$ anions not shown

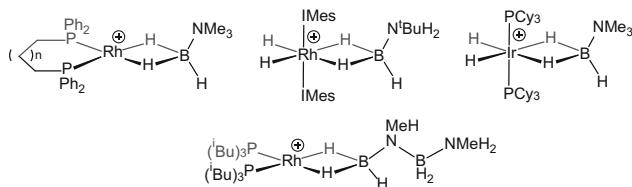


Fig. 3 Examples of η^2 -sigma amine–borane complexes. $[BAR^F_4]^-$ anions not shown. $IMes = N,N'$ -bis(2,4,6-trimethylphenyl)imidazol-2-ylidene, $n = 1-3$

e.g. $H_3B \cdot NMe_3$, as the lack of N–H bonds generally prevents further reactivity. The first example of a simple amine–borane coordinated to a metal was reported by Shimoi and co-workers in 1999, in which $[M(CO)_5(\eta^1-H_3B \cdot NMe_3)]$ ($M = Cr, Mo, W$) is formed through photolysis of $[M(CO)_6]$ in the presence of $H_3B \cdot NMe_3$ [61]. This “end-on” η^1 binding of the amine–borane occurs through one B–H bond, and various other η^1 sigma complexes of amine–boranes have since been reported (a selection shown in Fig. 2) [61–63].

Amine–boranes can also bind to the metal centre through two B–H sigma bonds, resulting in η^2 complexes [19, 64, 65]. Oligomeric species such as $H_3B \cdot NMe_2BH_2 \cdot NMe_2H$ have also been observed to bind in this manner (Fig. 3) [31, 66, 67].

Examples have also been isolated in which multiple amine–borane moieties are bound to a metal centre, similar to intermediates often invoked for dimerisation and polymerisation mechanisms (vide infra) [12, 62, 68–70]. In

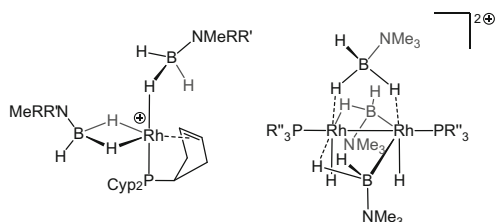
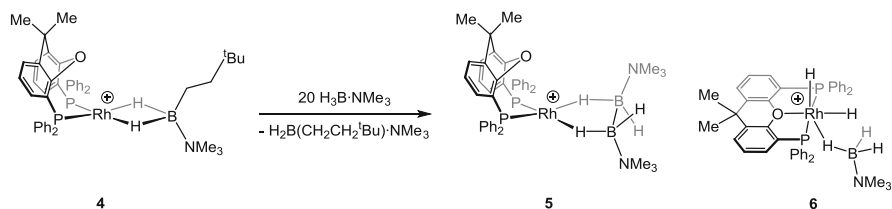


Fig. 4 Examples of multiple amine–borane bonding to transition metal fragments. $R''=^i\text{Pr}$, Cy. Cyp=cyclopentyl. $R=\text{Me}$, H . $R'=\text{Me}$, H . $[\text{BAR}^{\text{F}}_4]^-$ not shown



Scheme 12 B–B homocoupling using the $[\text{Rh}(\text{Xantphos})]^+$ fragment. $[\text{BAR}^{\text{F}}_4]^-$ not shown

2010, Weller and co-workers reported a bimetallic hydridoboryl species formed from two $\{\text{Rh}(\text{PR}_3)\}^+$ ($R=^i\text{Pr}$, Cy) fragments bridged by three $\text{H}_3\text{B}\cdot\text{NMe}_3$ ligands, two of which have undergone B–H activation (Fig. 4) [71]. The same group also reported cationic rhodium species with two amine–boranes bound to one rhodium centre, $[\text{Rh}\{\text{P}(\text{C}_5\text{H}_9)_2(\eta^2\text{-C}_5\text{H}_7)\}(\eta^2\text{-H}_3\text{B}\cdot\text{NMeRR}')](\eta^1\text{-H}_3\text{B}\cdot\text{NMeRR}')][\text{BAR}^{\text{F}}_4]$ ($R, R'=\text{Me}$, H) [72].

In 2013, Weller and MacGregor reported the first well-characterised example of the B–B homocoupling of an amine–borane to yield the diborane (4) $\text{Me}_3\text{N}\cdot\text{BH}_2\text{BH}_2\cdot\text{NMe}_3$ ligand sigma bound to rhodium [62]. B–B homocoupling of boranes has been otherwise limited to B–B bond formation in polyhedral boranes [73, 74], guanidine bases [75] and catechol- and pinacolboranes [76–78]. Pd^{II} catalysts have been demonstrated to rapidly (TOF $\sim 2,000\text{ h}^{-1}$) dehydrocouple $\text{H}_3\text{B}\cdot\text{NH}_3$ to yield poorly defined materials proposed to contain B–B bonds [79]. Addition of excess $\text{H}_3\text{B}\cdot\text{NMe}_3$ to the sigma complex $[\text{Rh}(\kappa^2\text{-P,P-Xantphos})(\eta^2\text{-H}_2\text{B}(\text{CH}_2\text{CH}_2^t\text{Bu})\cdot\text{NMe}_3)][\text{BAR}^{\text{F}}_4]$ (4) yielded $[\text{Rh}(\kappa^2\text{-P,P-Xantphos})(\eta^2\text{-H}_4\text{B}_2\cdot 2\text{NMe}_3)][\text{BAR}^{\text{F}}_4]$ (5) alongside the Rh^{III} complex $[\text{Rh}(\kappa^3\text{-P,O,P-Xantphos})(\text{H})_2(\eta^1\text{-H}_3\text{B}\cdot\text{NMe}_3)][\text{BAR}^{\text{F}}_4]$ (6) in an approximate 50:50 ratio (Scheme 12).

The homocoupling mechanism was probed by DFT calculations. Starting from the putative complex $[\text{Rh}(\kappa^2\text{-P,P-Xantphos})(\eta^2\text{-H}_3\text{B}\cdot\text{NMe}_3)][\text{BAR}^{\text{F}}_4]$, a low-energy initial B–H activation of the coordinated $\text{H}_3\text{B}\cdot\text{NMe}_3$ is followed by the coordination of a second $\text{H}_3\text{B}\cdot\text{NMe}_3$ molecule, with a higher-energy combined second B–H activation/B–B coupling step. Addition of excess cyclohexene to the reaction mixture resulted in nearly quantitative yields of 5 by reducing 6 to $[\text{Rh}(\kappa^2\text{-P,P-Xantphos})(\eta^2\text{-H}_3\text{B}\cdot\text{NMe}_3)][\text{BAR}^{\text{F}}_4]$, enabling further homocoupling at a Rh^{I} centre.

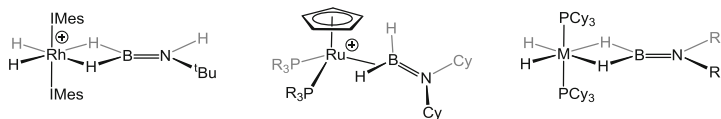


Fig. 5 Aminoborane complexes. $(\text{PR}_3)_2 = (\text{Ph}_3\text{P})_2$ or $(\text{Cy}_2\text{PCH}_2\text{CH}_2\text{PCy}_2)$. $\text{M} = \text{Ru}$, $\text{R}' = ^i\text{Pr}$, Me , H ; $\text{M} = \text{Rh}^+$ or Ir^+ , $\text{R}' = ^i\text{Pr}$, Me . $[\text{BAR}^F_4]^-$ not shown

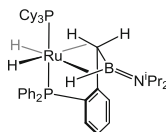


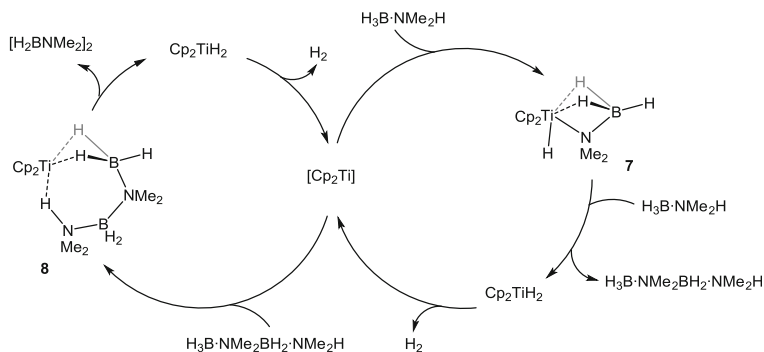
Fig. 6 Sabo-Etienne and Alcaraz's bis(agostic) phosphinobenzyl-(amino)borane ruthenium complex

Sigma complexes of aminoboranes have also been isolated, where donation from the B–H bonds into a vacant metal orbital is reinforced by π back-donation from the metal into the π^* B–N orbital of the aminoborane [80]. Various examples have been characterised with rhodium [13, 66, 80, 81], iridium [17, 19, 80, 82] and ruthenium [24, 80, 83, 84], and a selection is presented in Fig. 5. Sabo-Etienne and Alcaraz have recently reported an unusual aminoborane complex exhibiting adjacent agostic B–H and C–H interactions (Fig. 6) [85]. The isolation of aminoborane complexes is of interest mechanistically, as aminoboranes bound to the metal centre have been implicated in dehydrocoupling mechanisms, although often not observed directly (*vide infra*) [12, 70, 86]. These aminoborane complexes are also closely related to transition metal complexes of three-coordinate boranes, e.g. H_2BR or HBR_2 [87].

2.8 Mechanistic Studies on Homogeneous Dehydrocoupling Systems

2.8.1 Early Transition Metals

In 2006, Manners demonstrated the first well-defined homogeneous catalytic dehydrocoupling of $\text{H}_3\text{B} \cdot \text{NMe}_2\text{H}$ to form $[\text{H}_2\text{BNMe}_2]_2$ by using the $[\text{Cp}_2\text{Ti}]$ fragment, generated *in situ* from $\text{Cp}_2\text{TiCl}_2/{}^t\text{BuLi}$ [88]. After this initial report, calculations by Ohno and Luo suggested a stepwise mechanism for dehydrocoupling in which N–H bond activation is followed by B–H activation to form $\text{H}_2\text{B} = \text{NMe}_2$, which dimerises off-metal [89]. A more detailed kinetic–mechanistic study by Manners, Lloyd-Jones and co-workers on the $[\text{Cp}_2\text{Ti}]$ system contradicted this mechanism; significantly, the linear diborazane $\text{H}_3\text{B} \cdot \text{NMe}_2\text{BH}_2 \cdot \text{NMe}_2\text{H}$ was identified as an intermediate in the dehydrocoupling reaction (2 mol% $[\text{Cp}_2\text{Ti}]$, $\text{TOF} = 12.5 \text{ h}^{-1}$) [69]. The proposed mechanism



Scheme 13 Mechanism proposed by Manners and Lloyd-Jones for the dehydrocoupling of $\text{H}_3\text{B} \cdot \text{NMe}_2\text{H}$

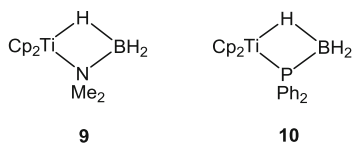


Fig. 7 Ti^{III} complexes **9** and **10**

(Scheme 13) involves two cycles. Initial coordination of $\text{H}_3\text{B} \cdot \text{NMe}_2\text{H}$ to $[\text{Cp}_2\text{Ti}]$ to form $[\text{Cp}_2\text{Ti}(\eta^2\text{-H}_3\text{B} \cdot \text{NMe}_2\text{H})]$ is suggested to be followed by N–H activation of the protic hydrogen with the Ti^{III} centre to yield the amidoborane $[\text{Cp}_2\text{Ti}(\text{H})(\text{NMe}_2 \cdot \text{BH}_3)]$, **7**. A second equivalent of $\text{H}_3\text{B} \cdot \text{NMe}_2\text{H}$ reacts with **7**, resulting in B–N bond formation to give Cp_2TiH_2 with loss of $\text{H}_3\text{B} \cdot \text{NMe}_2\text{BH}_2 \cdot \text{NMe}_2\text{H}$. The second cycle invokes reaction of $\text{H}_3\text{B} \cdot \text{NMe}_2\text{BH}_2 \cdot \text{NMe}_2\text{H}$ with $[\text{Cp}_2\text{Ti}]$ to form **8**, which undergoes on-metal dehydrocyclisation to form $[\text{H}_2\text{BNMe}_2]_2$ and Cp_2TiH_2 . The proposed scheme is consistent with experimental and kinetic observations, in particular that reaction of independently prepared $\text{H}_3\text{B} \cdot \text{NMe}_2\text{BH}_2 \cdot \text{NMe}_2\text{H}$ with $[\text{Cp}_2\text{Ti}]$ resulted in the complete consumption of $\text{H}_3\text{B} \cdot \text{NMe}_2\text{BH}_2 \cdot \text{NMe}_2\text{H}$ to form $[\text{H}_2\text{BNMe}_2]_2$, with only negligible amounts of $\text{H}_2\text{B}=\text{NMe}_2$ observed. This implies that $\text{H}_3\text{B} \cdot \text{NMe}_2\text{BH}_2 \cdot \text{NMe}_2\text{H}$ is the sole intermediate in the formation of $[\text{H}_2\text{BNMe}_2]_2$ in this case, contrary to Luo and Ohno's mechanism. Interestingly, the same system was unreactive towards $\text{H}_3\text{B} \cdot \text{NMe}_2\text{H}$ (20°C) and $\text{H}_3\text{B} \cdot \text{PPh}_2\text{H}$ (up to 40°C). Zirconium analogues of amidoboranes such as **7** have been synthesised and structurally characterised by Roesler and co-workers [90].

More recent work has found that paramagnetic Ti^{III} species may play a significant role in the $[\text{Cp}_2\text{Ti}]$ system. Following the report of the isolation of the Ti^{III} complex $[\text{Cp}_2\text{Ti}(\text{NH}_2 \cdot \text{BH}_3)]$ by McGrady [91], the analogous complexes $[\text{Cp}_2\text{Ti}(\text{NMe}_2 \cdot \text{BH}_3)]$ (**9**) and $[\text{Cp}_2\text{Ti}(\text{PPh}_2 \cdot \text{BH}_3)]$ (**10**) (Fig. 7) were synthesised and employed as catalysts under the same conditions as with the titanocene fragment (2 mol%, toluene) [92]. **9** and **10** were shown to be effective catalysts, promoting 83 and 97% consumption of $\text{H}_3\text{B} \cdot \text{NMe}_2\text{H}$ after 2 h, respectively. Similar to $[\text{Cp}_2\text{Ti}]$, both reaction profiles showed $\text{H}_3\text{B} \cdot \text{NMe}_2\text{BH}_2 \cdot \text{NMe}_2\text{H}$ as an

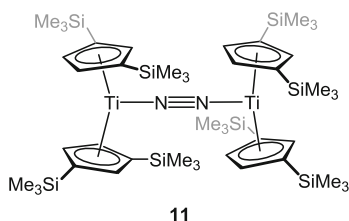
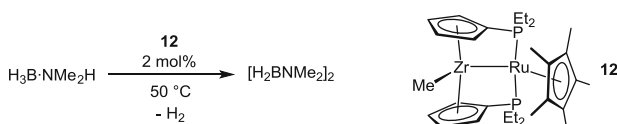


Fig. 8 Chirik's dehydrocoupling catalyst **11**

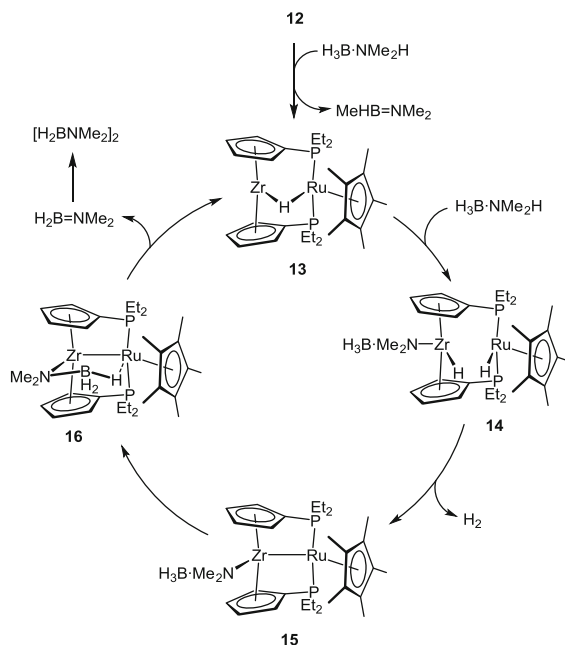


Scheme 14 Dehydrocoupling of $\text{H}_3\text{B} \cdot \text{NMe}_2\text{H}$ using **12**

intermediate, followed by the formation of $[\text{H}_2\text{BNMe}_2]_2$, with **9** showing comparable activity to $[\text{Cp}_2\text{Ti}]$ (TOF of 10.7 h^{-1} for **9**, cf. 12.5 h^{-1} for $[\text{Cp}_2\text{Ti}]$). Analysis by UV/Vis and EPR spectroscopies of reaction solutions using $[\text{Cp}_2\text{Ti}]$ and **9** as precatalysts resulted in spectra comparable with those of isolated **9**. These results imply that the Ti^{III} complex **9** may be of importance in the catalytic dehydrocoupling by titanocene, in contrast to the Ti^{II} and Ti^{IV} cycle depicted in Scheme 13. The zirconocene analogue of **10**, $[\text{Cp}_2\text{Zr}(\text{PPh}_2 \cdot \text{BH}_3)]$, was a far less active catalyst, achieving negligible consumption of $\text{H}_3\text{B} \cdot \text{NMe}_2\text{H}$ after 2 h. Related work on metallocene complexes by Rosenthal and co-workers using the alkyne complex $[\text{Cp}_2\text{M}(\eta^2\text{-Me}_3\text{SiCCSiMe}_3)(\text{L})]$ ($\text{M}=\text{Ti}, \text{Zr}$; $\text{L}=\text{pyridine}$ for Zr , no L for Ti) as a source of $[\text{Cp}_2\text{M}]$ showed turnover frequencies of 3 h^{-1} and 1 h^{-1} for $\text{M}=\text{Ti}$ and $\text{M}=\text{Zr}$, respectively, for the dehydrocoupling of $\text{H}_3\text{B} \cdot \text{NMe}_2\text{H}$ [93]. The closely related precatalyst $[(\eta^5\text{-C}_5\text{H}_4\text{Pr})_2\text{Ti}(\eta^2\text{-Me}_3\text{SiCCSiMe}_3)]$ was explored shortly afterwards and showed improved dehydrocoupling activity (TOF = 32 h^{-1} at 40°C , 6 h^{-1} at 24°C) [94]. The Cp^* analogue, however, showed no dehydrocoupling activity, highlighting the importance of sterics in designing systems for dehydrocoupling with early transition metal systems [93].

The fastest group IV systems reported include Chirik's Ti^{II} complex **11** (Fig. 8), which dehydrocoupled $\text{H}_3\text{B} \cdot \text{NMe}_2\text{H}$ with a TOF of 420 h^{-1} [95]. Based on kinetic and isotopic labelling experiments, a mechanism was proposed that involved reversible B–H oxidative addition followed by β -H elimination. A rapid Zr^{IV} catalyst based on a frustrated Lewis pair (TOF $\sim 600 \text{ h}^{-1}$) published by Wass is discussed further in Sect. 2.8.4.

Nishibayashi and co-workers reported the heterobimetallic group IV/VIII complex $[\text{ZrMe}(\mu\text{-}\eta^5\text{-}\eta^1\text{-C}_5\text{H}_4\text{PEt}_2)_2\text{RuCp}^*]$, **12**, and showed that it was a slow catalyst for the dehydrocoupling of $\text{H}_3\text{B} \cdot \text{NMe}_2\text{H}$ to form $[\text{H}_2\text{BNMe}_2]_2$ (2 mol% **12**, TOF $\sim 8 \text{ h}^{-1}$, 50°C) (Scheme 14) [96]. The system was less active for the dehydrocoupling of $\text{H}_3\text{B} \cdot \text{NMe}_2\text{H}$ and $\text{H}_3\text{B} \cdot \text{NH}_3$, reaching 92 and 56% completion, respectively, after 24 h (10 mol% **12** at 50°C) to form B–N oligomeric



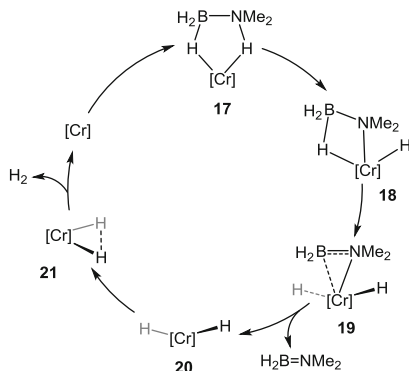
Scheme 15 Proposed mechanism for the dehydrocoupling of $\text{H}_3\text{B} \cdot \text{NMe}_2\text{H}$ with **12**

materials. Accordingly, mechanistic studies were conducted with $\text{H}_3\text{B} \cdot \text{NMe}_2\text{H}$, and the proposed catalytic cycle is presented in Scheme 15.

The initial conversion of **12** to **13** is proposed to occur via ligand exchange of the hydride on $\text{H}_3\text{B} \cdot \text{NMe}_2\text{H}$ with the methyl group at Zr, forming $\text{MeH}_2\text{B} \cdot \text{NMe}_2\text{H}$ and **13**, which is suggested to be the true catalyst. The thus formed $\text{MeH}_2\text{B} \cdot \text{NMe}_2\text{H}$ undergoes dehydrogenation to afford $\text{MeHB}=\text{NMe}_2$ (observed) in an analogous manner to the subsequent catalytic dehydrogenation of $\text{H}_3\text{B} \cdot \text{NMe}_2\text{H}$. From **13**, the dehydrogenation of $\text{H}_3\text{B} \cdot \text{NMe}_2\text{H}$ proceeds via initial N–H activation of $\text{H}_3\text{B} \cdot \text{NMe}_2\text{H}$ on the Zr centre, forming the amidoborane dihydride **14**. Bimetallic reductive elimination of H_2 forms **15**, and B–H activation by the Ru centre can then occur (**16**), releasing $\text{H}_2\text{B}=\text{NMe}_2$, which yields $[\text{H}_2\text{BNMe}_2]_2$ upon dimerisation, and reforming **13**. This cycle highlights that the cooperative effect of two metals in close proximity could be of potential use in designing future catalysts, although the activity of **12** is only moderate compared with some other homogeneous systems [12, 21, 59, 65]. Rousseau has also explored multimetallic dehydrocoupling of $\text{H}_3\text{B} \cdot \text{NMe}_2\text{H}$ with Rh_4 clusters [97].

2.8.2 Mid-Transition Metals

Shimoi and co-workers have shown that photoactivated $[\text{M}(\text{CO})_6]$ ($\text{M}=\text{Cr}, \text{Mo}, \text{W}$) act as dehydrocoupling catalysts yielding $[\text{H}_2\text{BNMe}_2]_2$ from $\text{H}_3\text{B} \cdot \text{NMe}_2\text{H}$ ($\text{TOF } 19 \text{ h}^{-1}$ when $\text{M}=\text{Cr}$) and a mixture of $[\text{HBNMe}]_3$ and $[\text{H}_2\text{BNMeH}]_n$ from



Scheme 16 Shimoi's proposed mechanism for the dehydrocoupling of $\text{H}_3\text{B} \cdot \text{NMe}_2\text{H}$. $[\text{Cr}] = [\text{Cr}(\text{CO})_4]$

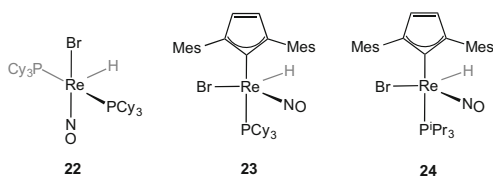
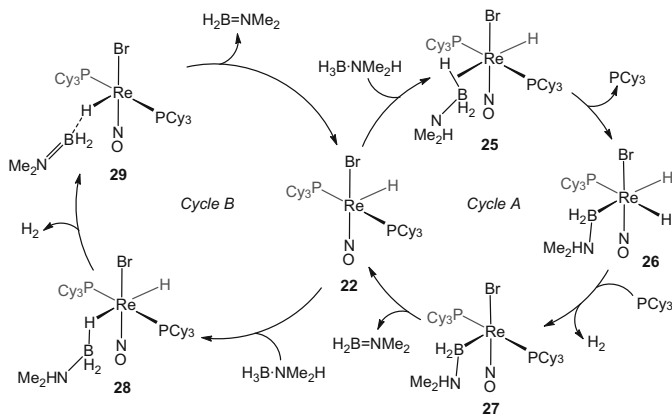


Fig. 9 Rhenium catalysts for the dehydrocoupling of $\text{H}_3\text{B} \cdot \text{NMe}_2\text{H}$

$\text{H}_3\text{B} \cdot \text{NMe}_2\text{H}$ [98]. The mechanism of dehydrocoupling $\text{H}_3\text{B} \cdot \text{NMe}_2\text{H}$ with $[\text{Cr}(\text{CO})_6]$ was investigated by DFT calculations and suggested that the active species is the 14-electron $[\text{Cr}(\text{CO})_4]$ fragment, which can coordinate $\text{H}_3\text{B} \cdot \text{NMe}_2\text{H}$ to form the sigma complex **17** (Scheme 16). From this, N–H activation to form an amidoborane (**18**) precedes B–H activation to release $\text{H}_2\text{B}=\text{NMe}_2$ from **19**. $[\text{Cr}(\text{CO})_4]$ is regenerated from $[\text{Cr}(\text{CO})_4(\text{H})_2]$ (**20**) (Scheme 16). Interestingly, although the sigma complex $[\text{Cr}(\text{CO})_5(\eta^1\text{-H}_3\text{B} \cdot \text{NMe}_2\text{H})]$ was observed in the reaction mixture, it was calculated to sit outside the cycle, acting simply as a source of $[\text{Cr}(\text{CO})_4]$.

In 2009, Berke and co-workers explored a range of nitrosyl rhenium catalysts for the dehydrocoupling of $\text{H}_3\text{B} \cdot \text{NMe}_2\text{H}$ to form $[\text{H}_2\text{BNMe}_2]_2$ [86]. The most active catalysts were **22**, **23** and **24** (Fig. 9), showing turnover frequencies of 77, 100 and 92 h^{-1} , respectively. All three catalysts were also active for the transfer hydrogenation of *n*-octene using $\text{H}_3\text{B} \cdot \text{NMe}_2\text{H}$ as the hydrogen source. Two possible mechanisms for the dehydrocoupling reaction using **22** were suggested (Scheme 17). Cycle A involves coordination of $\text{H}_3\text{B} \cdot \text{NMe}_2\text{H}$ to **22**, forming the sigma complex **25**. Loss of a PCy_3 ligand reveals a vacant coordination site, allowing B–H activation to form the base-stabilised boryl species **26**. Reductive elimination of H_2 forms **27**, from which a β -H elimination yields free $\text{H}_2\text{B}=\text{NMe}_2$ and reforms **22**. An alternative pathway (B) involves the formation of the sigma compound **28**, followed by N–H protonation of Re–H to form **29**. B–H cleavage



Scheme 17 Suggested mechanisms for the dehydrocoupling of $\text{H}_3\text{B}\cdot\text{NMe}_2\text{H}$ using **22**

then forms $\text{H}_2\text{B}=\text{NMe}_2$ and **22**. During catalysis, a dihydrogen complex $[\text{Re}(\text{PCy}_3)_2(\text{H})(\text{H}_2)(\text{NO})]$ was the observed resting state in the presence of hydrogen, being in equilibrium with the active species **22**.

2.8.3 Late Transition Metals

Many studies regarding the mechanisms of catalytic dehydrocoupling have used late transition metal systems. Early reports by Manners on Rh systems indicated that these were operating as heterogeneous catalysts (see Sect. 2.5) [15, 26]. In 2006 Heinekey and Goldberg used Brookhart's $\text{Ir}(\text{tBuPOCOP}^t\text{Bu})\text{H}_2$ ($\text{tBuPOCOP}^t\text{Bu} = \kappa^3\text{-P}_{\text{C,C,P}}\text{-1,3-(OP}^t\text{Bu)}_2\text{C}_6\text{H}_3$) catalyst (**30**) to efficiently dehydrocouple $\text{H}_3\text{B}\cdot\text{NH}_3$ to form the purported cyclic pentamer $[\text{H}_2\text{BNH}_2]_5$ [27], although this product was later reassigned by Manners and co-workers as $[\text{H}_2\text{BNH}_2]_n$ ($n \sim 20$) [23]. At 1 mol% an impressive ToF of $1,500 \text{ h}^{-1}$ was recorded. At long reaction times, a dormant new species is formed, assigned as the sigma-borane complex $\text{Ir}(\text{tBuPOCOP}^t\text{Bu})\text{H}_2(\text{BH}_3)$ **31** (Fig. 10) [99], which can be regenerated to form a catalytically active species on addition of H_2 . Related sigma complexes of **30** bound to pinacolborane and 9-BBN have also been reported. Various kinetic data of the hydrogen release using catalyst **30** have been determined, and follow a first-order dependence on amine–borane, for both $\text{H}_3\text{B}\cdot\text{NH}_3$ and $\text{H}_3\text{B}\cdot\text{NMe}_2\text{H}$ [100]. Interestingly, for this system, dehydrocoupling of $\text{H}_3\text{B}\cdot\text{NMe}_2\text{H}$ is sluggish at best. Calculations suggest a concerted process for B–H/N–H activation at the Ir centre [101].

In 2007 Baker reported that $\text{Ni}(\text{NHC})_2$ systems were active catalysts for the dehydrogenation of ammonia–borane [102]. A variety of NHC ligands were used, with Enders' carbene (1,3,4-triphenyl-4,5-dihydro-1H-1,2,4-triazol-5-ylidene) affording the most active catalyst (Scheme 18). First-order rate constants were determined, and KIE experiments indicated that both B–H and N–H bonds were being broken in the rate-determining step(s). This report generated considerable

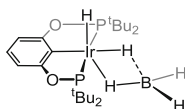
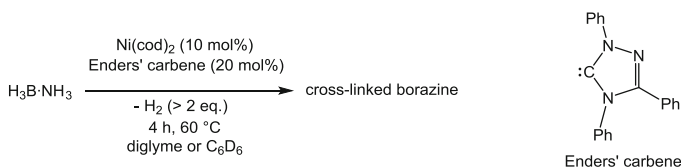
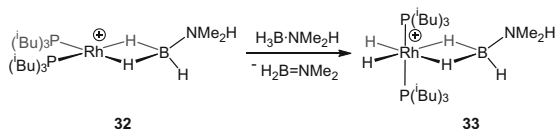


Fig. 10 The structure of Ir(^tBuPOCOP^tBu)(H)₂(BH₃) (**31**)



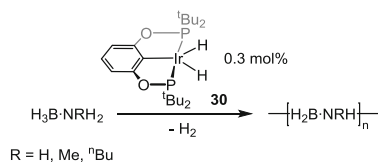
Scheme 18 Dehydrocoupling of H₃B·NH₃ with Ni(cod)₂ and Enders' carbene



Scheme 19 Initial dehydrogenation of **32**. [BAR^F₄][−] anions not shown

interest with regard to mapping the processes occurring using computational methods [103–107]. In particular the non-innocent role of the NHC ligands, by mediating hydrogen transfer from the amine–borane to the Ni centre, and the role of free carbene in dehydrogenation were revealed.

In 2009, Weller and Hall conducted a detailed experimental and computational study [66] on the dehydrocoupling of H₃B·NMe₂H by the latent low-coordinate complex [Rh(P^tBu₃)₂][BAR^F₄] [108] (5 mol%, TOF = 34 h^{−1}) to afford [H₂BNMe₂]₂. Coordination of H₃B·NMe₂H to [Rh(P^tBu₃)₂][BAR^F₄] forms the sigma complex [Rh(P^tBu₃)₂(η²-H₃B·NMe₂H)][BAR^F₄] (**32**, Scheme 19). This is short-lived in the presence of excess H₃B·NMe₂H, rapidly forming [Rh(P^tBu₃)₂(H)₂(η²-H₃B·NMe₂H)][BAR^F₄] (**33**). A complex pathway was calculated for the lowest energy dehydrogenation of **32**. Either initial B–H activation and N–H transfer or initial N–H activation and B–H transfer occurs to yield the aminoborane complex [Rh(P^tBu₃)₂(H₂)(η²-H₂B=NMe₂)][BAR^F₄], which is observed at the end of catalysis. N–H activation was calculated to be rate limiting in either pathway. Then, H₂ loss followed by dissociation of H₂B=NMe₂, or vice versa, forms [H₂BNMe₂]₂ and regenerates the Rh^I fragment. A constant oxidation state Rh^{III} cycle was also proposed. Experimentally H₃B·NMe₂BH₂·NMe₂H was observed as an intermediate during catalytic dehydrocoupling and its role probed further. The linear diborazane complex [Rh(P^tBu₃)₂(η²-H₃B·NMe₂BH₂·NMe₂H)][BAR^F₄] was stable in 1,2-C₆H₄F₂ solution but, upon addition of excess H₃B·NMe₂BH₂·NMe₂H, formed [H₂BNMe₂]₂ with H₂B=NMe₂ also observed, suggesting that B–N cleavage is occurring rather than a simple intramolecular dehydrocyclisation.



Scheme 20 Catalytic dehydrocoupling of amine–boranes using **30**

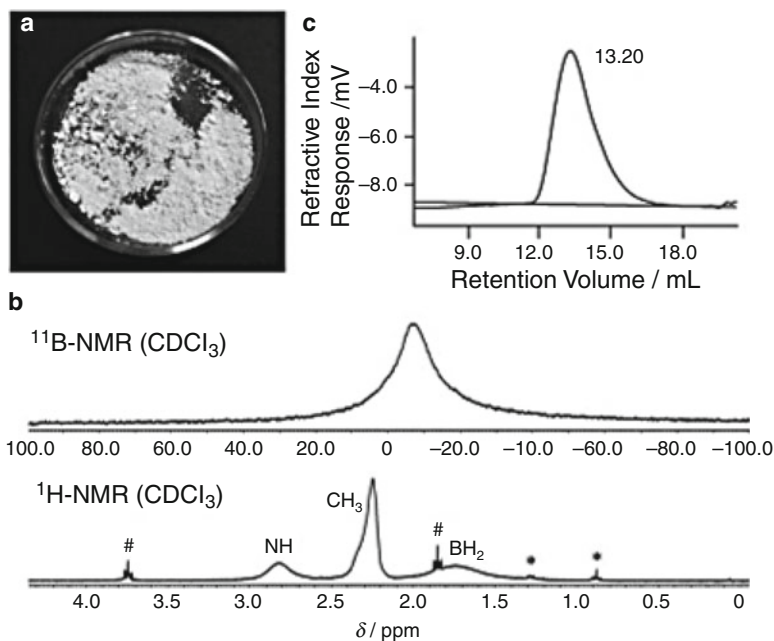
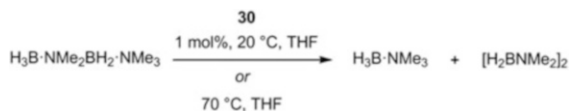


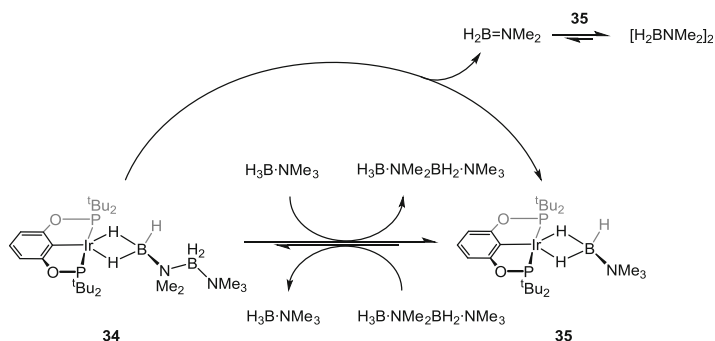
Fig. 11 (a) [H₂BNMeH]_n. (b) ¹¹B and ¹H NMR spectra. # = THF, * = butane. (c) GPC trace (THF with 0.1% w/w ⁿBu₄NBr). Staubitz et al. [14]. Copyright 2008 Wiley-VCH

The first example of well-defined homogeneous catalytic dehydrocoupling of amine–boranes was reported by Manners and co-workers in 2008 [14]. The dehydrocoupling of H₃B·NRH₂ (R=H, Me, ⁿBu) mediated by **30** formed [H₂BNRH]_n (Scheme 20). With R=Me, high molecular weight [H₂BNMeH]_n was isolated (M_n = 55,200 g mol⁻¹, PDI = 2.9, Fig. 11c). The ¹¹B NMR spectrum of the polymer shows a broad resonance consistent with multiple ¹¹B environments within the polymer chain (Fig. 11b).

In a detailed follow-up paper, on the basis of molecular weight versus conversion experiments alongside other markers, a modified chain growth mechanism was proposed for this system, in which a slow initial dehydrogenation of H₃B·NMeH₂ is followed by fast insertion of the resulting H₂B=NMeH [23]. A variety of other catalysts based on rhodium and ruthenium were also active in dehydrocoupling. A recent computational study explored the mechanism of



Scheme 21 Hydrogen redistribution reaction of $\text{H}_3\text{B} \cdot \text{NMe}_2\text{BH}_2 \cdot \text{NMe}_3$

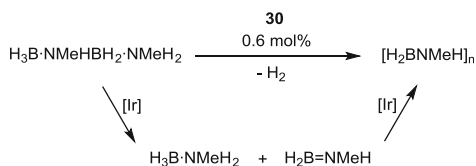


Scheme 22 Model suggested for the metal-catalysed hydrogen redistribution reaction

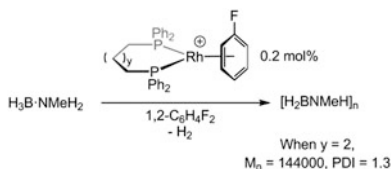
the polymerisation of $\text{H}_2\text{B}=\text{NH}_2$ by **30** (although concomitant dehydrogenation of the amine–borane was not probed) and also implicated a chain growth mechanism, as suggested experimentally by Manners. The proposed mechanism for propagation involves end chain growth; the lone pair on the NH_2 end of the chain interacts with the Lewis acidic BH_2 group of the entering $\text{H}_2\text{B}=\text{NH}_2$ molecule [29]. This suggested mechanism contrasts with a coordination insertion mechanism, in which a transient aminoborane inserts into a growing polymer chain at the metal centre, similar to Ziegler–Natta olefin polymerisation.

The role of **30** in the redistribution of linear diborazanes has also been probed [28]. The diborazane $\text{H}_3\text{B} \cdot \text{NMe}_2\text{BH}_2 \cdot \text{NMe}_3$ was prepared as a “model” diborazane as it does not have a functional N–H group. This can undergo both thermal (70°C , THF) and metal-catalysed (20°C , 1 mol% [Ir], THF) redistribution reactions to form $\text{H}_3\text{B} \cdot \text{NMe}_3$ and $[\text{H}_2\text{BNMe}_2]_2$ (Scheme 21). Kinetic analyses and simulations were used to probe the metal-catalysed pathway. The model suggested that **30** reacts with $\text{H}_3\text{B} \cdot \text{NMe}_2\text{BH}_2 \cdot \text{NMe}_3$ to form a proposed sigma complex **34**, from which a direct redistribution reaction gives $\text{H}_2\text{B}=\text{NMe}_2$ and a sigma complex **35** (Scheme 22). Dimerisation of $\text{H}_2\text{B}=\text{NMe}_2$ affords $[\text{H}_2\text{BNMe}_2]_2$, and the kinetic simulations showed that, as well as the expected off-metal dimerisation, the dimerisation was also being catalysed by **35**, or a closely related fragment. Related to this, the pincer complex $[\text{Pd}(\text{}^t\text{BuPCP}^t\text{Bu})(\text{OH}_2)][\text{PF}_6]$ ($\text{}^t\text{BuPCP}^t\text{Bu} = 2,6\text{-C}_6\text{H}_3(\text{CH}_2\text{P}^t\text{Bu}_2)_2$) has been shown to release 1 equiv. of H_2 upon reaction with $\text{H}_3\text{B} \cdot \text{NH}_3$, and DFT modelling also suggested an on-metal cyclodimerisation to form $[\text{H}_2\text{BNH}_2]_2$ [109].

The redistribution chemistry of the more complex (i.e. containing N–H groups) linear diborazane $\text{H}_3\text{B} \cdot \text{NMeHBH}_2 \cdot \text{NMeH}_2$, first noted by Weller and Manners as the product of a single oligomerisation of $\text{H}_3\text{B} \cdot \text{NMeH}_2$ [33], was also explored by



Scheme 23 Proposed mechanism for the metal-catalysed redistribution of $\text{H}_3\text{B} \cdot \text{NMeHBH}_2 \cdot \text{NMeH}_2$

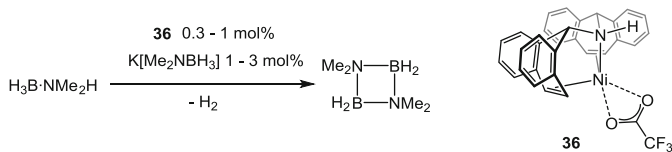


Scheme 24 Dehydropolymerisation by $[\text{Rh}(\text{Ph}_2\text{P}(\text{CH}_2)_x\text{PPh}_2)(\eta^6\text{-C}_6\text{H}_5\text{F})][\text{BAR}^{\text{F}}_4]$ ($x = 3\text{--}5$). $[\text{BAR}^{\text{F}}_4]^-$ not shown

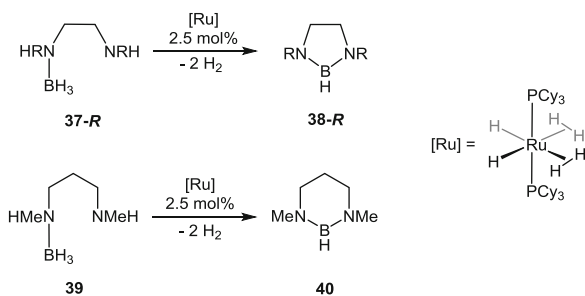
Manners and co-workers [110]. Treatment of $\text{H}_3\text{B} \cdot \text{NMeHBH}_2 \cdot \text{NMeH}_2$ with 0.6 mol% **30** yielded high molecular weight $[\text{H}_2\text{BNMeH}]_n$ ($M_n = 67,400$, $\text{PDI} = 1.4$), with the parent amine–borane $\text{H}_3\text{B} \cdot \text{NMeH}_2$ observed as an intermediate (Scheme 23). Hydroboration trapping experiments with cyclohexene (Sect. 2.2) did not lead to $\text{C}_y\text{B}=\text{NMeH}$. Nonetheless, the observation of $\text{H}_3\text{B} \cdot \text{NMeH}_2$ suggests that $\text{H}_2\text{B}=\text{NMeH}$ is formed, either remaining on-metal or polymerising rapidly relative to the rate of hydroboration. By contrast, metal-free thermolysis of $\text{H}_3\text{B} \cdot \text{NMeHBH}_2 \cdot \text{NMeH}_2$ at 70°C in THF led to the formation of $\text{H}_3\text{B} \cdot \text{NMeH}_2$ and the cyclic trimer $[\text{H}_2\text{BNMeH}]_3$, presumed to arise from trimerisation of $\text{H}_2\text{B}=\text{NMeH}$. Addition of cyclohexene resulted in the formation of the trapping product $\text{C}_y\text{B}=\text{NMeH}$, implying free $\text{H}_2\text{B}=\text{NMeH}$ is present in the solution and that hydroboration is kinetically competitive with trimerisation.

In 2011, Weller and Manners reported that the dehydrocoupling of $\text{H}_3\text{B} \cdot \text{NMeH}_2$ with the cationic rhodium chelating phosphine system $[\text{Rh}(\text{Ph}_2\text{P}(\text{CH}_2)_x\text{PPh}_2)(\eta^6\text{-C}_6\text{H}_5\text{F})][\text{BAR}^{\text{F}}_4]$ ($x = 3\text{--}5$) produced high molecular weight and narrow polydispersity polyaminoborane $[\text{H}_2\text{BNMeH}]_n$ (when $x = 4$, $M_n = 144,000 \text{ g mol}^{-1}$, $\text{PDI} = 1.3$) (Scheme 24) [65].

These catalysts were also efficient in dehydrocoupling $\text{H}_3\text{B} \cdot \text{NMe}_2\text{H}$ to form $[\text{H}_2\text{BNMe}_2]_2$ (fastest TOF $\sim 1,250 \text{ h}^{-1}$ when $x = 3$) following an induction period of approximately 5 min. The bite angle correlated with binding strength in the related sigma complexes $[\text{Rh}(\text{Ph}_2\text{P}(\text{CH}_2)_x\text{PPh}_2)(\eta^2\text{-H}_3\text{B} \cdot \text{NMe}_3)][\text{BAR}^{\text{F}}_4]$ ($x = 3\text{--}5$); the smallest bite angle ($x = 3$) has the weakest sigma binding of $\text{H}_3\text{B} \cdot \text{NMe}_3$ and the fastest dehydrocoupling activity of $\text{H}_3\text{B} \cdot \text{NMe}_2\text{H}$. Tests indicated a homogeneous catalyst, and, although the reason for the induction period is yet to be deduced, it was speculated on the basis of ESI–MS experiments that this temporal profile was due to the formation of an initial inactive dimeric species, possibly in a slow equilibrium with an active monomeric species. Independent computational work



Scheme 25 Dehydrocoupling of $\text{H}_3\text{B}\cdot\text{NMe}_2\text{H}$ with **36**



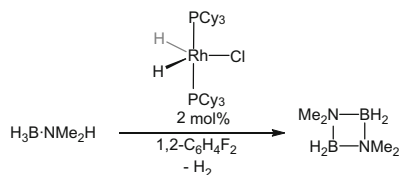
Scheme 26 Dehydrocyclisation of amine–boranes using $[\text{Ru}(\text{PCy}_3)_2(\text{H})_2(\text{H}_2)_2]$. R=Me, *i*Pr

on this system has suggested that dimerisation forms an inactive hydridoboryl species, and the active catalyst is monomeric [111].

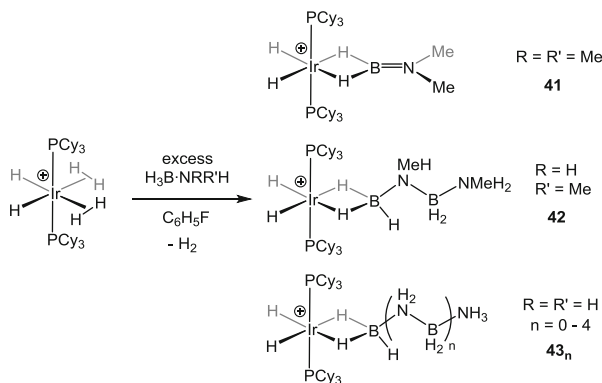
One of the fastest dehydrocoupling catalysts that has been reported is the Ni^{I} species $[\text{Ni}(\text{trop}_2\text{NH})(\text{OOC}\text{CF}_3)]$ (trop_2NH =bistropyliideneamine) (**36**, Scheme 25) [112]. At 0.3 mol% of **36**, one molar equivalent of hydrogen is released from a solution of $\text{H}_3\text{B}\cdot\text{NMe}_2\text{H}$ in less than 1 min (TOF $\sim 20,000 \text{ h}^{-1}$) to form $[\text{H}_2\text{BNMe}_2]_2$. Interestingly the amidoborane $\text{K}[\text{NMe}_2\text{BH}_3]$ is used as cocatalyst (1–3 mol%), and, although its role was not commented upon, it is tempting to speculate that the active species is a Ni–amidoborane. During dehydrocoupling, the aminoborane $\text{H}_2\text{B}=\text{NMe}_2$ is observed as an intermediate, although further mechanistic details were not reported.

Alcaraz and Sabo-Etienne reported the novel dehydrogenative cyclisation of the diamine–monoboranes **37-Me**, **37-*i*Pr** and **39** leading to cyclic diamineboranes **38-Me**, **38-*i*Pr** and **40**, respectively, using the $[\text{Ru}(\text{PCy}_3)_2(\text{H})_2(\text{H}_2)_2]$ catalyst at 2.5 mol% loading (Scheme 26) [113]. The reaction was slower in the presence of bulkier *N*-substituents (3 h for complete formation of **38-Me** versus 8 h for complete formation of **38-*i*Pr**), but lengthening the alkyl chain length of the starting amine–borane (**37-Me** versus **39**) did not significantly affect the rate. $[\text{Ru}(\text{PCy}_3)_2(\text{H})_2(\text{H}_2)_2]$ remained the resting state throughout catalysis and could be reused twice.

In 2013, Weller explored the mechanism of the dehydrocoupling of $\text{H}_3\text{B}\cdot\text{NMe}_2\text{H}$ with the neutral rhodium catalyst $\text{Rh}(\text{PCy}_3)_2(\text{H})_2\text{Cl}$ after its catalytic activity had been implicated in an earlier study with $[\text{Rh}(\text{PCy}_3)_2][\text{BAR}^{\text{F}}_4]$ (vide infra) [13, 32]. Investigations showed that $\text{Rh}(\text{PCy}_3)_2(\text{H})_2\text{Cl}$ is a moderate catalyst for dehydrogenation of $\text{H}_3\text{B}\cdot\text{NMe}_2\text{H}$ (2 mol% $[\text{Rh}]$, TOF = 28 h^{-1}) to form $\text{H}_2\text{B}=\text{NMe}_2$, which dimerises to form $[\text{H}_2\text{BNMe}_2]_2$ (Scheme 27) [32].



Scheme 27 Dehydrocoupling of $\text{H}_3\text{B} \cdot \text{NMe}_2\text{H}$ with $\text{Rh}(\text{PCy}_3)_2(\text{H})_2\text{Cl}$

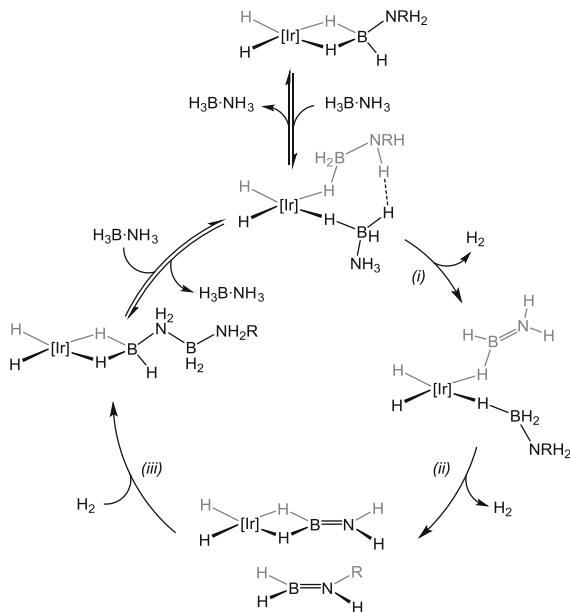


Scheme 28 Metal-bound products in the reaction of excess amine–borane with $\{\text{Ir}(\text{PCy}_3)_2(\text{H})_2\}^+$. $[\text{BAR}^{\text{F}}_4]^-$ not shown

Mechanistic investigations indicated that N–H activation (either preceding or following B–H activation) is turnover-limiting in this system, indicated by a large primary kinetic isotope effect observed using $\text{H}_3\text{B} \cdot \text{NMe}_2\text{D}$.

The $\{\text{Ir}(\text{PCy}_3)_2(\text{H})_2\}^+$ fragment has proved a useful, albeit slow (10–20 mol%, TOF $\sim 0.1 \text{ h}^{-1}$), catalyst for the dehydrogenation and dehydrocoupling of $\text{H}_3\text{B} \cdot \text{NMe}_2\text{H}$ [19], $\text{H}_3\text{B} \cdot \text{NMeH}_2$ [33] and $\text{H}_3\text{B} \cdot \text{NH}_3$ [70], in which metal-bound products and intermediates can be observed, allowing direct comparisons between the different amine–boranes. Reaction of the bis-dihydrogen complex $[\text{Ir}(\text{PCy}_3)_2(\text{H})_2(\text{H}_2)_2][\text{BAR}^{\text{F}}_4]$, a source of $\{\text{Ir}(\text{PCy}_3)_2(\text{H})_2\}^+$, with $\text{H}_3\text{B} \cdot \text{NMe}_2\text{H}$ forms ultimately $[\text{H}_2\text{BNMe}_2]_2$, and the major metal-containing product is the bound aminoborane complex $[\text{Ir}(\text{PCy}_3)_2(\text{H})_2(\eta^2\text{-H}_2\text{B}=\text{NMe}_2)][\text{BAR}^{\text{F}}_4]$ (**41**). The mechanism of dehydrogenation of $[\text{Ir}(\text{PCy}_3)_2(\text{H})_2(\eta^2\text{-H}_3\text{B} \cdot \text{NMe}_2\text{H})][\text{BAR}^{\text{F}}_4]$ to form **41** has been suggested by calculation to be sequential B–H activation, H_2 loss from the metal and rate-limiting N–H activation [19]. By contrast, $\text{H}_3\text{B} \cdot \text{NMeH}_2$ catalytically undergoes an on-metal oligomerisation event to yield the diborazane $\text{H}_3\text{B} \cdot \text{NMeHBH}_2 \cdot \text{NMeH}_2$, with the sigma complex $[\text{Ir}(\text{PCy}_3)_2(\text{H})_2(\eta^2\text{-H}_3\text{B} \cdot \text{NMeHBH}_2 \cdot \text{NMeH}_2)][\text{BAR}^{\text{F}}_4]$ (**42**) observed during the dehydrocoupling. Furthermore, $\text{H}_3\text{B} \cdot \text{NH}_3$ undergoes additional oligomerisation events, yielding insoluble $[\text{H}_2\text{BNH}_2]_n$. During the dehydrocoupling, various species with bound oligomeric units, $[\text{Ir}(\text{PCy}_3)_2(\text{H})_2(\eta^2\text{-H}_3\text{B} \cdot (\text{NH}_2\text{BH}_2)_n \cdot \text{NH}_3)][\text{BAR}^{\text{F}}_4]$ (**43_n**) ($n = 0\text{--}4$), were observed using ESI–MS techniques (Scheme 28).

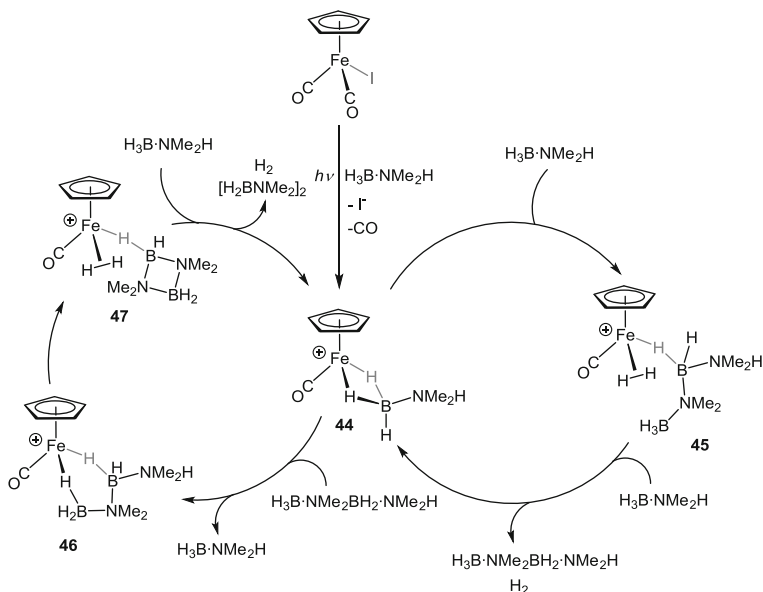
Scheme 29 Calculated pathway by MacGregor and Weller for the dehydrogenation and coupling of $\text{H}_3\text{B} \cdot \text{NH}_3$. $\text{R}=\text{H}$ (first oligomerisation), $\text{R}=\text{BH}_2\text{NH}_2$ (second oligomerisation). $[\text{Ir}]=\{\text{Ir}(\text{PR}'_3)_2\}^+$ ($\text{R}'=\text{Cy}$, experiment; Me , computation)



Calculations conducted on the model system $\{\text{Ir}(\text{PMe}_3)_2(\text{H})_2\}^+$ for the dehydrogenation and oligomerisation of $\text{H}_3\text{B} \cdot \text{NH}_3$ propose a pathway (Scheme 29) involving (i) initial dehydrogenation of the amine-borane, (ii) dehydrogenation of a second amine-borane and (iii) B–N coupling. Step (i) was calculated to have the highest barrier, and the B–N coupling step (iii) had the lowest barrier. Calculations showed that subsequent oligomerisations were also viable for this system, as observed experimentally. With $\text{H}_3\text{B} \cdot \text{NMe}_2\text{H}$, the B–N coupling barrier for subsequent oligomerisations was significantly raised, consistent with the experimental observations of a single oligomerisation event. With the more sterically encumbered $\text{H}_3\text{B} \cdot \text{NMe}_2\text{H}$, the calculated B–N coupling barrier was prohibitively high, consistent with no experimental observation of linear diborazane. Although likely to be system specific, this selectivity illustrates the potential importance of sterics in the dehydrocoupling of amine-boranes. Moreover, the calculations point to outersphere $\text{N}-\text{H} \cdots \text{H}-\text{B}$ interactions as being important to lowering barriers to dehydrogenation processes, as has been reviewed by others more generally for amine-boranes [114].

As introduced in Sect. 2.5, Manners and co-workers recently found that $[\text{CpFe}(\text{CO})_2\text{I}]$, under conditions of photoirradiation, acts as a homogeneous catalyst in the dehydrocoupling of $\text{H}_3\text{B} \cdot \text{NMe}_2\text{H}$ to form $[\text{H}_2\text{BNMe}_2]_2$ [51]. A two-stage mechanism was proposed for this system to account for the formation of $\text{H}_3\text{B} \cdot \text{NMe}_2\text{BH}_2 \cdot \text{NMe}_2\text{H}$ and the on-metal dehydrocyclisation to yield $[\text{H}_2\text{BNMe}_2]_2$ (Scheme 30), similar to that invoked for Cp_2Ti systems [69].

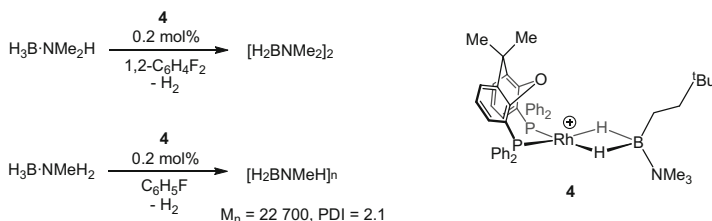
Experimental evidence and DFT calculations support initial coordination of $\text{H}_3\text{B} \cdot \text{NMe}_2\text{H}$ to the photogenerated $[\text{FeCp}(\text{CO})]^\dagger$ fragment, forming the sigma



Scheme 30 Proposed two-stage mechanism for the homogeneous dehydrocoupling of $\text{H}_3\text{B} \cdot \text{NMe}_2\text{H}$ using $\text{CpFe}(\text{CO})_2\text{I}$

complex **44**. Addition of a second equivalent of $\text{H}_3\text{B} \cdot \text{NMe}_2\text{H}$ results in a B–N bond formation process to yield the bound $\text{H}_3\text{B} \cdot \text{NMe}_2\text{BH}_2 \cdot \text{NMe}_2\text{H}$ complex **45**. Complex $\text{H}_3\text{B} \cdot \text{NMe}_2\text{BH}_2 \cdot \text{NMe}_2\text{H}$ and dihydrogen are displaced by $\text{H}_3\text{B} \cdot \text{NMe}_2\text{H}$ to reform **44**. The second cycle proposes that the just formed $\text{H}_3\text{B} \cdot \text{NMe}_2\text{BH}_2 \cdot \text{NMe}_2\text{H}$ displaces $\text{H}_3\text{B} \cdot \text{NMe}_2\text{H}$ in **44** to form the chelate sigma complex **46**, not unrelated to Rh complexes crystallographically characterised with this motif [31]. Subsequent on-metal dehydrocyclisation occurs to form $[\text{H}_2\text{BNMe}_2]_2$ sigma bound to the metal (**47**). $[\text{H}_2\text{BNMe}_2]_2$ and dihydrogen are displaced by $\text{H}_3\text{B} \cdot \text{NMe}_2\text{H}$, reforming **44**. It was speculated that the electronegative iodide ligand enables heterolytic Fe–I cleavage under photoirradiation, maintaining an Fe^{II} species. However, the dimeric complexes $[\text{CpFe}(\text{CO})_2]_2$ and $\text{Cp}_2\text{Fe}_2(\text{CO})_3(\text{NCMe})$ formally are in the lower Fe^{I} oxidation state and already have Fe–Fe interactions; these factors aid nanoparticle formation and hence heterogeneous catalysis is observed (Sect. 2.5).

A recent report by Weller, Manners and Lloyd-Jones has explored in detail the catalytic dehydrocoupling of $\text{H}_3\text{B} \cdot \text{NMe}_2\text{H}$ and $\text{H}_3\text{B} \cdot \text{NMe}_2\text{H}_2$ with **4** (Scheme 31) [12]. Open to argon, thus allowing for release of H_2 , complex **4** (0.2 mol%) dehydrocouples $\text{H}_3\text{B} \cdot \text{NMe}_2\text{H}$ rapidly, forming $[\text{H}_2\text{BNMe}_2]_2$ (TOF $\sim 1,000 \text{ h}^{-1}$), following an induction period of approximately 5 min. $\text{H}_2\text{B}=\text{NMe}_2$ was observed as an intermediate with only negligible amounts of $\text{H}_3\text{B} \cdot \text{NMe}_2\text{BH}_2 \cdot \text{NMe}_2\text{H}$ detected, a similar reaction profile to the closely related $[\text{Rh}(\text{Ph}_2\text{P}(\text{CH}_2)_x\text{PPh}_2)(\eta^6\text{-C}_6\text{H}_5\text{F})][\text{BAR}^{\text{F}}_4]$ system (TOF $\sim 1,250 \text{ h}^{-1}$ for $x = 3$). Under these conditions, the decay of $[\text{H}_3\text{B} \cdot \text{NMe}_2\text{H}]$ appeared *pseudo-zero* order at high $[\text{H}_3\text{B} \cdot \text{NMe}_2\text{H}]$



Scheme 31 Dehydrocoupling of $\text{H}_3\text{B}\cdot\text{NMe}_2\text{H}$ and $\text{H}_3\text{B}\cdot\text{NMeH}_2$ using **4**. $[\text{BAr}^{\text{F}}_4]^-$ not shown

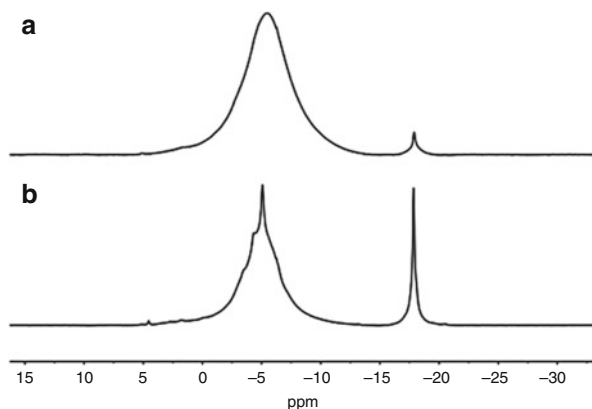
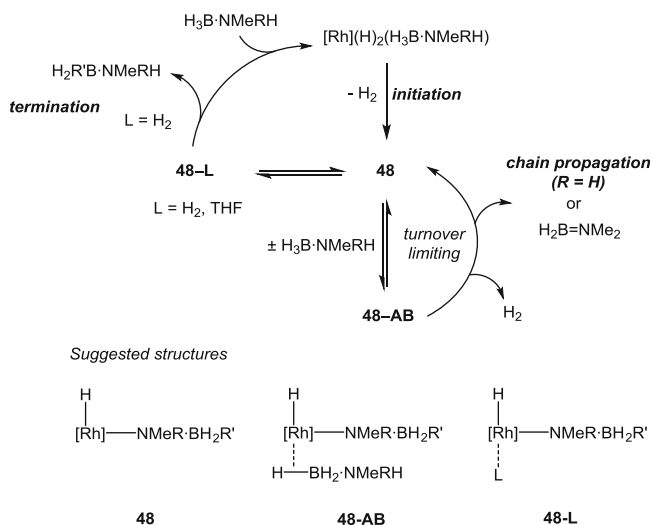


Fig. 12 (a) $^{11}\text{B}\{^1\text{H}\}$ NMR spectrum of $[\text{H}_2\text{BNMeH}]_n$ ($\delta \sim -5$) isolated after dehydropolymerisation of $\text{H}_3\text{B}\cdot\text{NMeH}_2$ (**4**, 0.2 mol%) under open conditions (signal at δ -17 is unreacted $\text{H}_3\text{B}\cdot\text{NMeH}_2$). (b) $^{11}\text{B}\{^1\text{H}\}$ NMR spectrum of material isolated after reaction under sealed conditions (**4**, 0.2 mol%). Johnson et al. [115]. Copyright 2014 American Chemical Society

(approximately 0.1 M), becoming *pseudo*-first order at lower $[\text{H}_3\text{B}\cdot\text{NMe}_2\text{H}]$. This suggested that saturation kinetics were operating, corroborated by kinetic modelling. By contrast, under closed conditions, in which a pressure of H_2 can build, the reaction profile appeared *pseudo*-first order over the entire concentration range (post induction period). With $\text{H}_3\text{B}\cdot\text{NMeH}_2$, in an open system, 0.2 mol% **4** catalysed the formation of $[\text{H}_2\text{BNMeH}]_n$ ($M_n = 22,700 \text{ g mol}^{-1}$, $\text{PDI} = 2.1$) in $\text{C}_6\text{H}_5\text{F}$ solution within 2 h, also with an induction period observed. Similar to $\text{H}_3\text{B}\cdot\text{NMe}_2\text{H}$, saturation kinetics were apparent. Molecular weight versus conversion experiments indicated a chain growth mechanism; in particular, high molecular weights were achieved at less than 20% conversion. In THF solvent, the catalysis was slower (85% completion, 19 h) but produced higher molecular weight $[\text{H}_2\text{BNMeH}]_n$ ($M_n = 52,200 \text{ g mol}^{-1}$, $\text{PDI} = 1.4$). Conversely, in a sealed system, the molecular weight was significantly lower ($M_n = 2,800 \text{ g mol}^{-1}$, $\text{PDI} = 1.8$) and took approximately 24 h to reach $\sim 95\%$ completion. $^{11}\text{B}\{^1\text{H}\}$ NMR spectroscopy of the product isolated from the closed system provided evidence for the presence of shorter-chain oligomers (Fig. 12).



Scheme 32 Suggested cycle for the dehydropolymerisation of $\text{H}_3\text{B} \cdot \text{NMe}_2\text{H}$ ($\text{R}'=\text{H}$ or growing polymer chain; $\text{R}=\text{H}$) and dehydrogenation of $\text{H}_3\text{B} \cdot \text{NMe}_2\text{H}$ ($\text{R}'=\text{H}$, $\text{R}=\text{Me}$). $[\text{Rh}]=\{\text{Rh}(\text{Xantphos})\}^+$

Exploring the rationale behind the induction period, heterogeneous catalysis was ruled out. Additionally, the authors noted that the induction period was approximately twice as long using $\text{H}_3\text{B} \cdot \text{NMe}_2\text{D}$ compared with $\text{H}_3\text{B} \cdot \text{NMe}_2\text{H}$, whereas no change was observed using $\text{D}_3\text{B} \cdot \text{NMe}_2\text{H}$. This implied that N–H activation was rate limiting in the formation of the active species, which is proposed to be an amido-boryl complex **48**. These, and other observations, led to a proposed catalytic cycle applicable for both the dehydropolymerisation of $\text{H}_3\text{B} \cdot \text{NMe}_2\text{H}$ and dehydrogenation of $\text{H}_3\text{B} \cdot \text{NMe}_2\text{H}$ (Scheme 32).

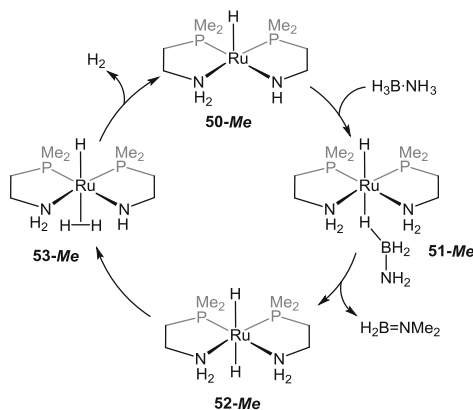
Stoichiometric reactions of **4** with 2 equiv. of $\text{H}_3\text{B} \cdot \text{NMe}_2\text{H}$ or $\text{H}_3\text{B} \cdot \text{NMe}_2\text{H}_2$ led to the immediate formation of the Rh^{III} dihydride $[\text{Rh}(\kappa^3\text{-P}_2\text{O}_2\text{P-Xantphos})(\text{H})_2(\eta^1\text{-H}_3\text{B} \cdot \text{NMeRH})][\text{BAR}^{\text{F}}_4]$ ($\text{R}=\text{Me}$, H), and it was speculated that these species were the starting points in the catalytic cycle. The induction period (i.e. initiation) occurs, involving N–H activation, to yield **48**. Complex **48**, as written, would have a vacant site, allowing the reversible binding of another equivalent of amine–borane, forming **48-AB**, as implicated by saturation kinetics. From **48-AB**, dehydrogenation (with $\text{H}_3\text{B} \cdot \text{NMe}_2\text{H}$) or chain propagation (with $\text{H}_3\text{B} \cdot \text{NMe}_2\text{H}$) occurs, for the latter leading to a growing polymer from the metal centre. At high [amine–borane], the turnover-limiting step occurs after the formation of **48-AB**, resulting in a *pseudo-zero-order* decay of [amine–borane], but at lower [amine–borane], the formation of **48-AB** is dependent upon [amine–borane], giving *pseudo-first-order* kinetics. Chain termination can arise from H_2 binding to **48** and undergoing heterolytic H_2 cleavage [116], consistent with the observations of shorter polymer chains, and first-order decay of $[\text{H}_3\text{B} \cdot \text{NMe}_2\text{H}]$, under an atmosphere of H_2 . THF can also bind competitively with H_2 and $\text{H}_3\text{B} \cdot \text{NMe}_2\text{H}$, slowing catalysis but

attenuating chain termination, resulting in higher molecular weight $[\text{H}_2\text{BNMeH}]_n$. This tuning of molecular weight has provided valuable insight into methods of controlling polyaminoborane formation.

2.8.4 Dehydrocoupling of Amine–Boranes Involving Ligand Cooperativity

In 2008, Fagnou and co-workers reported the rapid dehydrogenation of $\text{H}_3\text{B} \cdot \text{NH}_3$ to form $[\text{H}_2\text{BNH}_2]_n$ with 0.03 mol% loadings of the catalyst $[\text{Ru}(\text{P}^i\text{Pr}_2\text{CH}_2\text{CH}_2\text{NH}_2)_2\text{Cl}_2]$ (**49**), activated by 0.9 mol% KO^tBu (TOF $\sim 20,000 \text{ h}^{-1}$) [59]. Furthermore, 0.5 mol% of **49** could promote the release of 2 equiv. of H_2 from $\text{H}_3\text{B} \cdot \text{NMeH}_2$ within 10 min. An outer-sphere mechanism was proposed using DFT calculations on the model complex $[\text{Ru}(\text{PMe}_2\text{CH}_2\text{CH}_2\text{NH}_2)(\text{PMe}_2\text{CH}_2\text{CH}_2\text{NH})\text{H}]$ (**50-Me**), the product of the activation of $[\text{Ru}(\text{PMe}_2\text{CH}_2\text{CH}_2\text{NH}_2)_2\text{Cl}_2]$ (**49-Me**) with KO^tBu (Scheme 33). The mechanism proposed invokes protonation of the ligand by the amine (**51-Me**), loss of $\text{H}_2\text{B}=\text{NH}_2$ to form **52-Me** and rate-limiting formation of the dihydrogen complex **53-Me**.

In 2009, Schneider and co-workers reported that the related bifunctional catalyst $[\text{Ru}(\text{PNP})(\text{H})(\text{PMe}_3)]$ {Fig. 13, $\text{PNP}=\text{N}(\text{CH}_2\text{CH}_2\text{P}^i\text{Pr}_2)_2$ } (**54**) was extremely active in the dehydrocoupling of $\text{H}_3\text{B} \cdot \text{NH}_3$ to release approximately 1 equiv. of dihydrogen (TOF $\sim 12,000 \text{ h}^{-1}$ at 0.1 mol% **54**) to form $[\text{H}_2\text{BNH}_2]_n$, with small amounts of borazine also observed [57]. $\text{H}_3\text{B} \cdot \text{NMe}_2\text{H}$ was also rapidly dehydrocoupled by **54** (2 mol%), forming $[\text{H}_2\text{BNMe}_2]_2$, until approximately 70% conversion (initial TOF $\sim 3,600 \text{ h}^{-1}$); after this point, a much slower regime operates (TOF $\sim 1.5 \text{ h}^{-1}$), suggesting a change in mechanism [30]. During the fast regime, the species *trans*- $[\text{Ru}(\text{PNP}^{\text{H}})(\text{H})_2(\text{PMe}_3)]$ { $\text{PNP}^{\text{H}}=\text{HN}(\text{CH}_2\text{CH}_2\text{P}^i\text{Pr}_2)_2$ } (**55**) was observed as the resting state and, indeed, starting catalysis with **55** showed very similar kinetics as with **54**. However, a new species evolved throughout the dehydrocoupling, $[\text{Ru}(\text{PNP}^{\text{B}})(\text{H})_2(\text{PMe}_3)]$ { $\text{PNP}^{\text{B}}=\text{NMe}_2\text{BH}_2\text{N}(\text{CH}_2\text{CH}_2\text{P}^i\text{Pr}_2)_2$ }



Scheme 33 Proposed mechanism for the dehydrogenation of $\text{H}_3\text{B} \cdot \text{NH}_3$ by **50-Me**

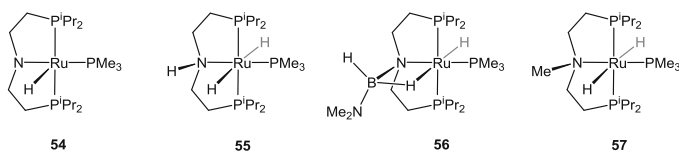
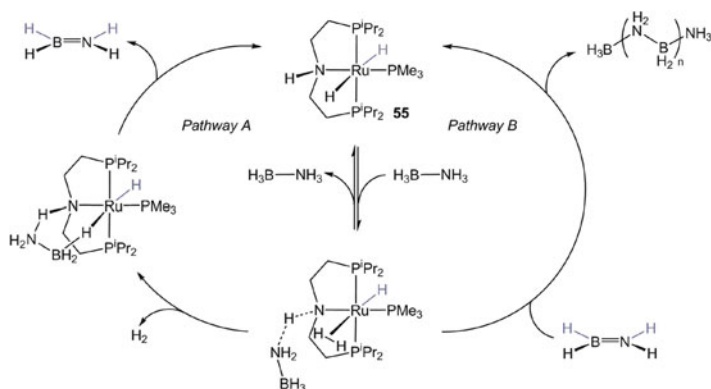


Fig. 13 Schneider's bifunctional ruthenium complexes



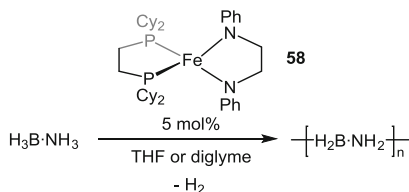
Scheme 34 Dehydrogenation and dehydrocoupling pathways proposed by Schneider and co-workers

(**56**), containing a four-membered bora-metallacycle. The use of isolated **56** as the dehydrocoupling catalyst gave essentially the same catalytic activity as for the slow regime.

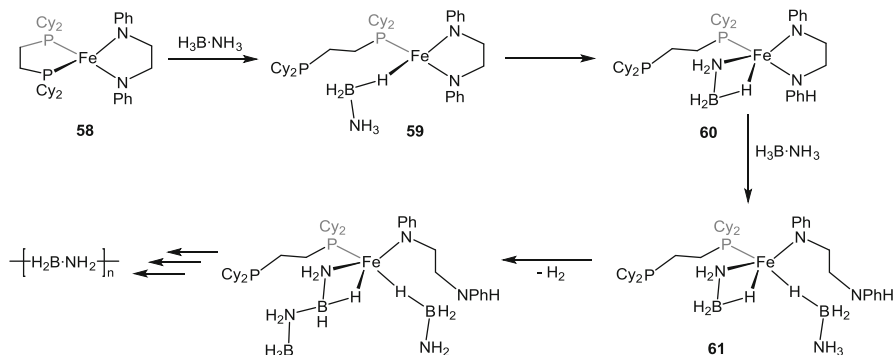
A more detailed study published in 2013 focused on the catalytic dehydrocoupling of $\text{H}_3\text{B} \cdot \text{NH}_3$ with **54**, **55** and $[\text{Ru}(\text{M}^c\text{PNP})(\text{H})(\text{PMe}_3)] \{\text{M}^c\text{PNP} = \text{MeN}(\text{CH}_2\text{CH}_2\text{P}^i\text{Pr}_2)_2\}$ (**57**) [21]. The methylation of the pincer nitrogen atom in **57** prevents the bifunctional reactivity that is thought to be key in rationalising the high activities of these complexes. Accordingly, catalysis using **57** exhibited a rate of H_2 evolution two orders of magnitude lower than with **54** or **55**, confirming the importance of amine cooperativity in these systems.

In contrast to the previous results, in which **54** and **55** appeared to operate within the same catalytic cycle [30], on closer examination, differences were found between the two, suggesting different mechanisms for each [21]. Both catalysts demonstrated first-order kinetics for H_2 evolution on dehydrocoupling $\text{H}_3\text{B} \cdot \text{NH}_3$. On using the *N*-deuterated analogue $\text{H}_3\text{B} \cdot \text{ND}_3$, first-order kinetics were retained with **55**. However, the H_2 evolution became zero order with **54**, implying a change in the turnover-limiting step upon deuteration for this system. Additionally, some cross-linking of $[\text{H}_2\text{BNH}_2]_n$ was observed with **55**, which was not detected in $[\text{H}_2\text{BNH}_2]_n$ produced with **54**.

For catalysis with **55**, a combination of DFT (using a PMe_2 -truncated model) and experimental methods led to a proposed mechanism for the formation of $[\text{H}_2\text{BNH}_2]_n$ from $\text{H}_3\text{B} \cdot \text{NH}_3$, depicted in Scheme 34.



Scheme 35 Dehydrocoupling of $\text{H}_3\text{B}\cdot\text{NH}_3$ by **58**

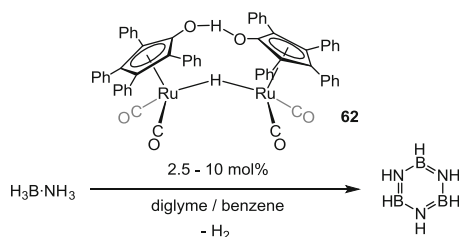


Scheme 36 A proposed mechanism for the dehydropolymerisation of $\text{H}_3\text{B}\cdot\text{NH}_3$ by **58**

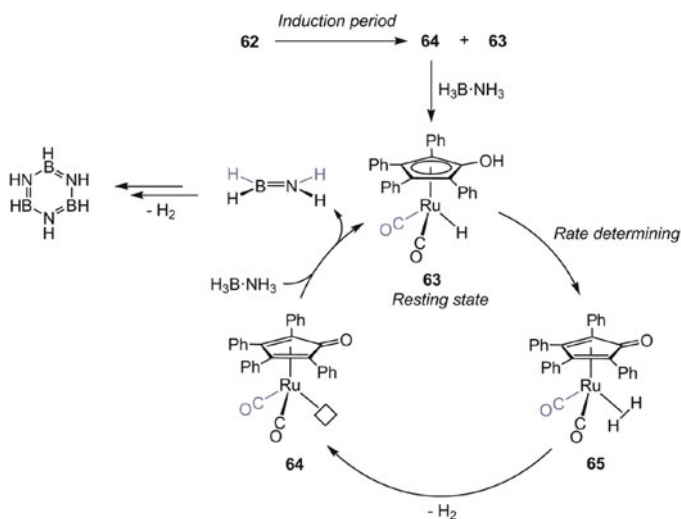
The mechanism involves dehydrogenation of $\text{H}_3\text{B}\cdot\text{NH}_3$, via initial N–H activation, to form $\text{H}_2\text{B}=\text{NH}_2$ (Pathway A), which undergoes oligomerisation by catalytic insertion of $\text{H}_2\text{B}=\text{NH}_2$ into the N–H bond of the substrate (Pathway B). Experiments with $\text{H}_3\text{B}\cdot\text{NMe}_3$ and $\text{Et}_3\text{B}\cdot\text{NH}_3$ in the presence of 1 mol% **55** showed that “head-to-tail” coupling to yield $\text{Et}_3\text{B}\cdot\text{NH}_2\text{BH}_2\cdot\text{NMe}_3$ did not occur, indicating that proton and hydride transfer from the same substrate molecule to the catalyst is required in this system, as suggested in the proposed mechanism.

Further mechanistic insight into dehydropolymerisation of amine–boranes was also obtained by Gordon and Baker et al. in the dehydrocoupling of $\text{H}_3\text{B}\cdot\text{NH}_3$ to selectively form $[\text{H}_2\text{BNH}_2]_n$ using $[\text{Fe}(\text{PCy}_2\text{CH}_2\text{CH}_2\text{PCy}_2)(\text{NPhCH}_2\text{CH}_2\text{NPh})]$ (**58**) at 5 mol% loading (TOF $\sim 80 \text{ h}^{-1}$) (Scheme 35) [68]. The catalyst could not be recycled; during catalysis, a black precipitate (presumed to be iron metal) was observed, indicating catalyst decomposition during dehydrocoupling. In situ NMR spectroscopy suggested de-coordination of one of the chelating phosphine arms during catalysis, possibly responsible for the observed induction period (ca. 2 min). Two mechanisms were proposed to account for experimental observations, one of which is shown in Scheme 36.

Initial dissociation of a phosphine arm enables coordination of $\text{H}_3\text{B}\cdot\text{NH}_3$ to form **59**. Protonation of one arm of the amido ligand by the amine–borane (affording a bound amidoborane, **60**) follows, and the resulting amino arm of the ligand can dissociate, allowing ligation of a second equivalent of $\text{H}_3\text{B}\cdot\text{NH}_3$ (**61**). From this, successive dehydrogenation and insertion steps yield $[\text{H}_2\text{BNH}_2]_n$. Throughout the proposed mechanism, no free $\text{H}_2\text{B}=\text{NH}_2$ is implicated, and



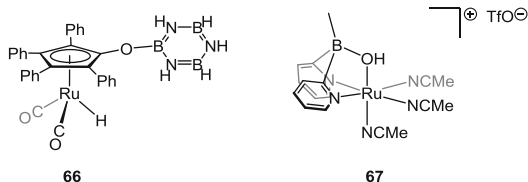
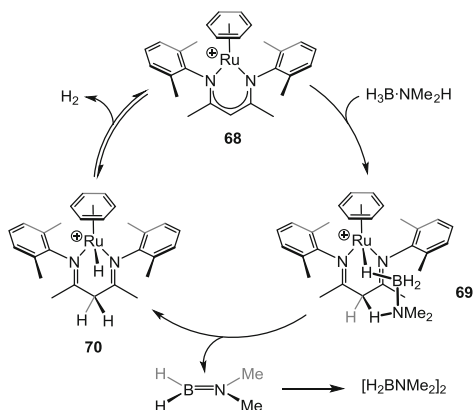
Scheme 37 Dehydrocoupling of $\text{H}_3\text{B}\cdot\text{NH}_3$ by **62**



Scheme 38 Suggested catalytic cycle for the catalyst initiation and fast dehydrocoupling of $\text{H}_3\text{B}\cdot\text{NH}_3$

experimentally $\text{H}_2\text{B}=\text{NH}_2$ was neither detected directly nor with cyclohexene trapping. This is consistent with previous work by some of the authors [25] and others [17], suggesting that $\text{H}_2\text{B}=\text{NH}_2$ must remain bound to the metal to oligomerise (Sect. 2.2), although other work has suggested that cyclohexene trapping does not necessarily rule out the presence of free $\text{H}_2\text{B}=\text{NH}_2$ if the hydroboration is not kinetically competitive with oligomerisation [21, 28].

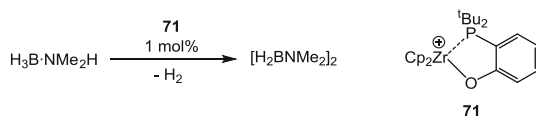
Williams also reported ligand cooperativity in the dehydrocoupling of $\text{H}_3\text{B}\cdot\text{NH}_3$ to yield borazane using Shvo's ruthenium catalyst, **62** (Scheme 37). The catalyst showed reasonable activity at 5 mol% **62** and 2 mol% EtOH (TOF $\sim 18 \text{ h}^{-1}$ for release of 2 equiv. H_2 at 70°C) [58]. H_2 release measurements (total 2 equiv.) produced a kinetic profile with three regimes evident: (i) initiation period, (ii) fast catalysis showing a zero-order decay of $[\text{H}_3\text{B}\cdot\text{NH}_3]$ and (iii) slow catalysis showing a first-order decay of $[\text{H}_3\text{B}\cdot\text{NH}_3]$. The induction period was attributed to the dissociation of **62** into **63** and **64** (Scheme 38). Fast dehydrogenation follows, in which H–H bond formation is the rate-determining step, similar to Fagnou's

Fig. 14 Complexes **66** and **67****Scheme 39** Proposed mechanism for the initial dehydrogenation of $\text{H}_3\text{B} \cdot \text{NMe}_2\text{H}$ using **68**. $[\text{OTf}]^-$ anions not shown

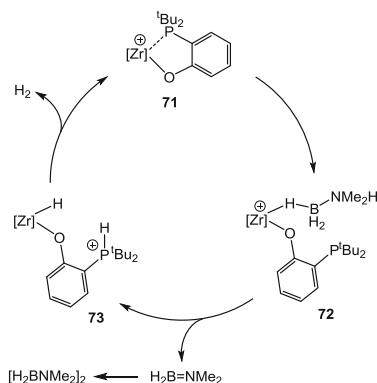
mechanism [59], and **63** is the resting state observed during catalysis [58]. At high borazine concentrations, the third regime dominates. This is attributed to the hydroboration of **64** by borazine, to form **66** (Fig. 14). $\text{H}_3\text{B} \cdot \text{NH}_3$ is required to convert **66** back into **63**, which is the rate-limiting step in this slow regime, and, thus, the reaction becomes first order in $[\text{H}_3\text{B} \cdot \text{NH}_3]$ [117].

To avoid deactivation by borazine, the same group developed a Ruthenium catalyst with an oxygen atom already borylated, **67** (Fig. 12). Complex **67** catalysed the dehydropolymerisation of $\text{H}_3\text{B} \cdot \text{NH}_3$ to form a mixture of borazine and polyborazylene (2 mol%, 70°C, TOF $\sim 25 \text{ h}^{-1}$ for the release of 2 equiv. of H_2 in a tetraglyme slurry). Significantly for potential practical applications, the catalysis could be conducted under air and the catalyst could be reused; four successive runs in a single reactor produced similar rates and quantities of H_2 loss in each run (2.1–2.3 equiv.). To date, mechanistic details have not been unravelled, although a mechanism involving dual-site cooperativity is likely [118].

Phillips and co-workers recently reported the fast dehydrocoupling of $\text{H}_3\text{B} \cdot \text{NH}_3$ and $\text{H}_3\text{B} \cdot \text{NMe}_2\text{H}$ (TOF $\sim 400 \text{ h}^{-1}$ for $\text{H}_3\text{B} \cdot \text{NMe}_2\text{H}$ at 42°C in THF) using 0.5 mol% of the bifunctional Ru^{II} β -diketiminate complex, **68** (Scheme 39) [119]. Mechanistic studies focused on $\text{H}_3\text{B} \cdot \text{NMe}_2\text{H}$ as, under these reaction conditions, $\text{H}_3\text{B} \cdot \text{NH}_3$ can thermally release H_2 in the absence of a catalyst. The proposed mechanism for initial dehydrogenation is that of hydride coordination from BH_3 by the Ru^{II} centre, forming **69**. The acidic NMe_2H proton can then protonate the β -carbon position of the β -diketiminate ligand, resulting in **70**. Complex **68** had been previously shown to reversibly heterolytically cleave H_2 to yield **70** [120].



Scheme 40 Dehydrocoupling of $\text{H}_3\text{B}\cdot\text{NMe}_2\text{H}$ with **71**. $[\text{B}(\text{C}_6\text{F}_5)_4]^-$ anion not shown

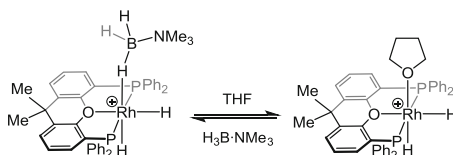


Scheme 41 Suggested mechanism for dehydrocoupling of $\text{H}_3\text{B}\cdot\text{NMe}_2\text{H}$ by **71**. $[\text{Zr}] = \text{Cp}_2\text{Zr}$. $[\text{B}(\text{C}_6\text{F}_5)_4]^-$ anions not shown

An induction period was observed in the dehydrocoupling, thought to be the slow initial formation of **70**, which is the active catalyst for subsequent dehydrogenations. An experiment performed using a THF solution that had been saturated with H_2 resulted in faster dehydrogenation and a reduced induction period compared with the N_2 -flushed THF used as the normal reaction solvent, demonstrating the rate is dependent on the rate of formation of **70**.

Wass and co-workers reported a fast dehydrocoupling catalyst based upon a “frustrated” Lewis pair, but where the Lewis acid (typically a fluorinated aryl borane) was replaced with an electrophilic Zr^{IV} centre. The species $[\text{Cp}_2\text{ZrOC}_6\text{H}_4\text{P}^+\text{Bu}_2][\text{B}(\text{C}_6\text{F}_5)_4]^-$ (**71**) dehydrocoupled $\text{H}_3\text{B}\cdot\text{NMe}_2\text{H}$ rapidly (1 mol% **71**, TOF $\sim 600 \text{ h}^{-1}$), being the fastest reported group IV catalyst to our knowledge (Scheme 40) [121]. Wass’ proposed mechanism (Scheme 41) is different from those of other group IV metallocene catalysts (Sect. 2.8.1). Following sigma coordination of $\text{H}_3\text{B}\cdot\text{NMe}_2\text{H}$ to the Zr^{IV} centre to form **72**, ligand-assisted dehydrogenation yields $\text{H}_2\text{B}=\text{NMe}_2$ and **73**. The loss of hydrogen from **73** is facile, regenerating **71**. The reaction using $[\text{Cp}_2\text{ZrO}^t\text{Bu}][\text{B}(\text{C}_6\text{F}_5)_4]^-$ did not dehydrogenate $\text{H}_3\text{B}\cdot\text{NMe}_2\text{H}$, illustrating the importance of the phosphine in this cooperative system.

Ligand cooperativity in $\text{Ni}(\text{NHC})$ systems has been discussed in Sect. 2.8.3.



Scheme 44 Equilibrium between $[\text{Rh}(\kappa^3\text{-P,O,P-Xantphos})(\text{H})_2(\eta^1\text{-H}_3\text{B}\cdot\text{NMe}_3)]^+[\text{BARF}_4]^-$ and $[\text{Rh}(\kappa^3\text{-P,O,P-Xantphos})(\text{H})_2(\text{THF})]^+[\text{BARF}_4]^-$. $[\text{BARF}_4]^-$ anions not shown

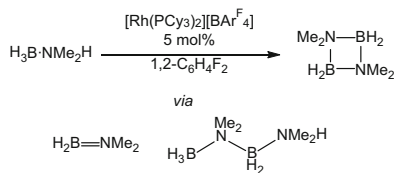
(Me_2O and NH_3 used as model analogues in the calculations) lowers the barrier to B–H activation. In THF solution, $[(\text{NMe}_2\text{H})_2\text{BH}_2]^+$ and $[(\text{NMe}_2\text{H})\text{BH}_2(\text{THF})]^+$ are in equilibrium. The THF adduct reacts with **76** to reform **74** and $\text{H}_2\text{B}=\text{NMe}_2$ with H_2 loss. Stoichiometric experiments showed that $[(\text{NMe}_2\text{H})_2\text{BH}_2]^+$ reacted slowly with **76**, leading to unidentified products, whereas $[(\text{NMe}_2\text{H})\text{BH}_2(\text{THF})]^+$ reacted rapidly, producing $\text{H}_2\text{B}=\text{NMe}_2$ and supporting the proposed cycle.

Many dehydrocoupling reactions involving cationic complexes have been studied in essentially non-coordinating solvents such as $\text{C}_6\text{H}_5\text{F}$ or 1,2- $\text{C}_6\text{H}_4\text{F}_2$, enabling the observation of weakly sigma-bound intermediates [13, 66, 70]. Weller and co-workers have shown that sigma-bound amine–boranes can be displaced by excess THF (Scheme 44) [12].

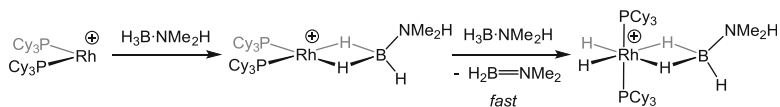
As mentioned in Sect. 2.8.3, however, the formation of $[\text{H}_2\text{BNMeH}]_n$ using the cationic rhodium species **4** produced higher molecular weight material in THF than $\text{C}_6\text{H}_5\text{F}$, although the polymerisation took longer to reach completion. It was suggested that THF can bind to the Rh centre competitively with both amine–borane (slowing catalysis) and H_2 (hindering chain transfer). Solvent effects have also been noted by Manners and Weller in the off-metal dimerisation of $\text{H}_2\text{B}=\text{NMe}_2$, with the rate of dimerisation being accelerated in MeCN [19, 20].

2.9 Generic Mechanisms for Dehydrocoupling of $\text{H}_3\text{B}\cdot\text{NMe}_2\text{H}$ Using Transition Metals

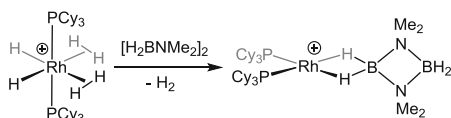
In 2012, Weller and Lloyd-Jones conducted a thorough mechanistic study on the dehydrocoupling of $\text{H}_3\text{B}\cdot\text{NMe}_2\text{H}$ to form $[\text{H}_2\text{BNMe}_2]_2$ using the $\{\text{Rh}(\text{PCy}_3)_2\}^+$ fragment (Scheme 45) [13]. During catalysis (5 mol% [Rh], TOF 10 h^{-1}), both the aminoborane $\text{H}_2\text{B}=\text{NMe}_2$ and the linear diborazane $\text{H}_3\text{B}\cdot\text{NMe}_2\text{BH}_2\cdot\text{NMe}_2\text{H}$ were observed by ^{11}B NMR spectroscopy. Several important observations were noted for this system. Addition of 2 equiv. of $\text{H}_3\text{B}\cdot\text{NMe}_2\text{H}$ to $\{\text{Rh}(\text{PCy}_3)_2\}^+$ led first to the Rh^{I} sigma complex $[\text{Rh}(\text{PCy}_3)_2(\eta^2\text{-H}_3\text{B}\cdot\text{NMe}_2\text{H})]^+[\text{BARF}_4]^-$, which then rapidly formed the Rh^{III} species $[\text{Rh}(\text{PCy}_3)_2(\text{H})_2(\eta^2\text{-H}_3\text{B}\cdot\text{NMe}_2\text{H})]^+[\text{BARF}_4]^-$ with concomitant loss of $\text{H}_2\text{B}=\text{NMe}_2$ (Scheme 46). This species does not lose H_2 easily, implying the active catalyst is a Rh^{III} complex, operating at a constant oxidation state, after the initial dehydrogenation.



Scheme 45 Catalytic dehydrocoupling of $\text{H}_3\text{B}\cdot\text{NMe}_2\text{H}$ by $[\text{Rh}(\text{PCy}_3)_2\text{L}_n][\text{BAR}^{\text{F}}_4]$



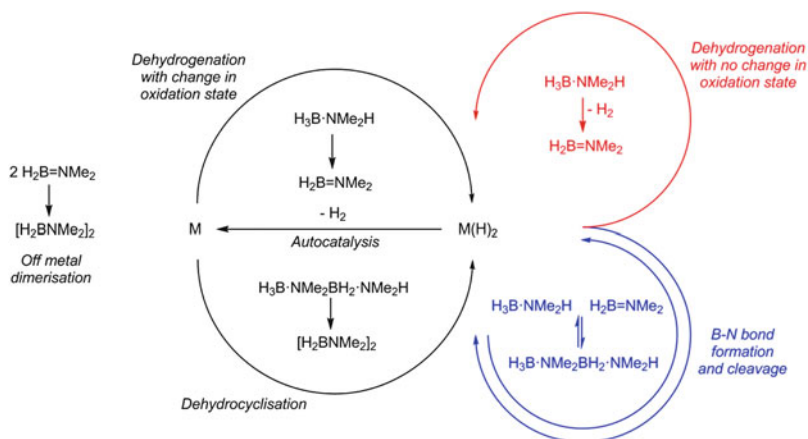
Scheme 46 Stoichiometric reactivity of $\{\text{Rh}(\text{PCy}_3)_2\text{L}_n\}^+$ with $\text{H}_3\text{B}\cdot\text{NMe}_2\text{H}$. $[\text{BAR}^{\text{F}}_4]^-$ not shown



Scheme 47 Reduction from Rh^{III} to Rh^{I} by addition of $[\text{H}_2\text{BNMe}_2]_2$. $[\text{BAR}^{\text{F}}_4]^-$ not shown

However, addition of the product $[\text{H}_2\text{BNMe}_2]_2$ to the Rh^{III} species $[\text{Rh}(\text{PCy}_3)_2(\text{H})_2(\eta^2\text{-H}_2)][\text{BAR}^{\text{F}}_4]$ resulted in the immediate formation of the Rh^{I} complex $[\text{Rh}(\text{PCy}_3)_2(\eta^2\text{-}(\text{H}_2\text{BNMe}_2)_2)][\text{BAR}^{\text{F}}_4]$, indicating that $[\text{H}_2\text{BNMe}_2]_2$ can drive the reductive elimination of H_2 to reform a Rh^{I} species (Scheme 47). Consistent with this, under catalytic conditions, $[\text{H}_2\text{BNMe}_2]_2$ was found to have an autocatalytic role in the dehydrocoupling catalysis by acting as a modifier to produce kinetically significant amounts of a Rh^{I} catalytically active species alongside the Rh^{III} species. Thus, the dehydrocoupling was shown to exist in both a constant oxidation state $\text{Rh}^{\text{III}}/\text{Rh}^{\text{III}}$ cycle (slower) and a $\text{Rh}^{\text{I}}/\text{Rh}^{\text{III}}$ cycle (faster).

Kinetic simulations indicated the presence of an additional catalyst present in constant (low) concentrations that promoted the first-order dehydrogenation of $\text{H}_3\text{B}\cdot\text{NMe}_2\text{H}$ to give $\text{H}_2\text{B}=\text{NMe}_2$. Due to a constant concentration of chloride ions in solution (arising from the catalyst preparation method), it was determined that the active catalyst was the neutral species $\text{Rh}(\text{PCy}_3)_2(\text{H})_2\text{Cl}$, whose catalytic activity was separately examined (see Sect. 2.8.3) [32].

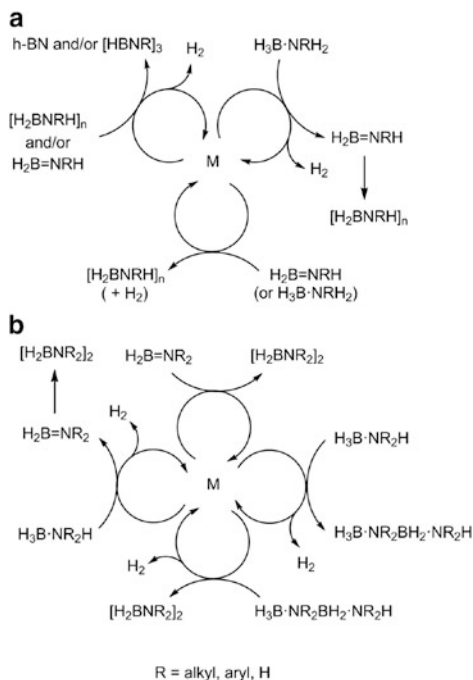


Scheme 48 General mechanistic cycle for the dehydrocoupling of $\text{H}_3\text{B}\cdot\text{NMe}_2\text{H}$. M=metal catalyst

The observations led to a generalised mechanistic scenario (Scheme 48) simplified into several parts: (1) dehydrogenation of $\text{H}_3\text{B}\cdot\text{NMe}_2\text{H}$ with a change in the oxidation state of the catalyst, (2) dehydrogenation of $\text{H}_3\text{B}\cdot\text{NMe}_2\text{H}$ with no change in the oxidation state of the catalyst, (3) the formation and cleavage of $\text{H}_3\text{B}\cdot\text{NMe}_2\text{BH}_2\cdot\text{NMe}_2\text{H}$, (4) dehydrocyclisation of $\text{H}_3\text{B}\cdot\text{NMe}_2\text{BH}_2\cdot\text{NMe}_2\text{H}$ and (5) the off-metal dimerisation of $\text{H}_2\text{B}=\text{NMe}_2$ to give $[\text{H}_2\text{BNMe}_2]_2$. This cycle, or parts thereof, is generally applicable to various homogeneous transition-metal-catalysed systems reported. For example, dehydrogenation with a change in oxidation state has been implicated for systems based upon Ti [69, 92], Re [86], Cr [98] and Rh [65]. Systems remaining in a constant oxidation state, however, include cationic Rh [66] and Ir [19, 70], as well as bifunctional Ru catalysts [21, 59]. The formation of $\text{H}_3\text{B}\cdot\text{NMe}_2\text{BH}_2\cdot\text{NMe}_2\text{H}$ from $\text{H}_3\text{B}\cdot\text{NMe}_2\text{H}$ and $\text{H}_2\text{B}=\text{NMe}_2$ has been observed with Ti [69], Rh [66], Ir [19] and Ru [30] systems, which also catalyse the dehydrocyclisation of $\text{H}_3\text{B}\cdot\text{NMe}_2\text{BH}_2\cdot\text{NMe}_2\text{H}$ to form $[\text{H}_2\text{BNMe}_2]_2$.

Manners and co-workers have suggested closely related, but alternative, schemes for the processes occurring in the dehydrogenation and dehydrocoupling of ammonia–borane and primary and secondary amine–boranes, as shown in Scheme 49 [5, 123].

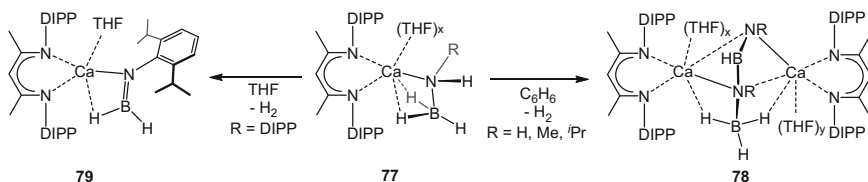
Scheme 49 (a)
Generalised series of catalytic cycles summarising common transformations for primary amine–boranes and ammonia–borane. **(b)** A generalised series of catalytic cycles summarising common transformations for secondary amine–boranes. *M* metal catalyst



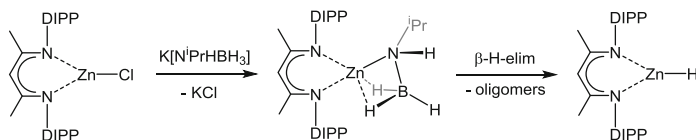
2.10 Main-Group Element-Catalysed Dehydrocoupling of Amine–Boranes

2.10.1 Main-Group Amidoboranes: Stoichiometric Studies

The use of amine–boranes as a means of chemical hydrogen storage prompted great interest in the dehydrogenation of these species. However, in the case of the parent ammonia–borane, which has the highest weight percentage of hydrogen, some of the dehydrocoupling products are insoluble and poorly characterised. A promising avenue of study was that of group 1 and 2 amidoboranes [124, 125]. Characterised as having the general formula $[M(\text{NH}_2 \cdot \text{BH}_3)_n]$ (M =group 1 or 2 metal; $n = 1$ for group 1, $n = 2$ for group 2), these simple amidoboranes were found to have a lower release temperature for 2 equiv. of dihydrogen than parent ammonia–borane (90°C for lithium and sodium amidoborane and 120–170°C for calcium bis(amidoborane) compared to 110–200°C for ammonia–borane). The dehydrogenation of the amidoboranes also proceeds more cleanly with little formation of borazine and other by-products observed for ammonia–borane. The structure of the calcium analogue $[\text{Ca}(\text{NH}_2 \cdot \text{BH}_3)_2(\text{THF})_2]$ was determined by X-ray crystallography, and the molecules were found to form long chains with intermolecular sigma interactions between the B–H bonds and the calcium centres of adjacent molecules. The



Scheme 50 Dehydrogenation of [(DIPP-nacnac)Ca(NRH·BH₃)(THF)₂] (**77**). DIPP=2,6-di(isopropyl)phenyl

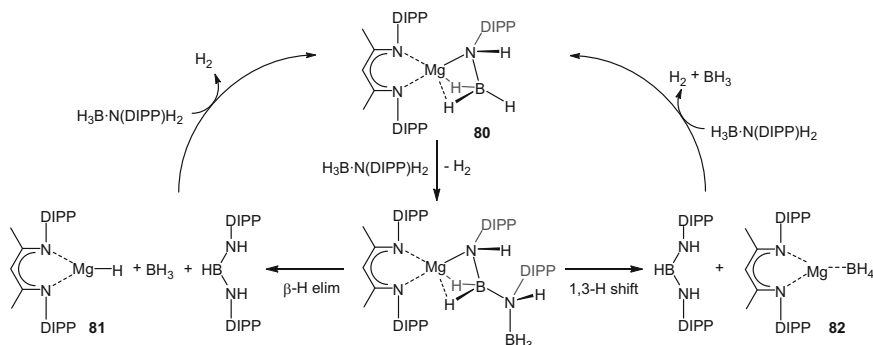


Scheme 51 Formation of [(DIPP-nacnac)ZnH]. DIPP=2,6-di(isopropyl)phenyl

THF solvent could be removed under vacuum at room temperature to form [Ca(NH₂·BH₃)₂] [125].

The first example of a monomeric calcium amidoborane was reported by Harder et al. who used the bulky β -diketiminate ligand {2,6-^{*t*}Pr₂C₆H₃NC(Me)C(H)C(Me)N(2,6-^{*t*}Pr₂C₆H₃)=DIPP-nacnac} to stabilise the calcium centre. Reaction of the dimeric calcium hydride starting material [(DIPP-nacnac)CaH(THF)]₂, with ammonia–borane in a mixture of toluene and THF, led to the elimination of dihydrogen and formation of the amidoborane complex [(DIPP-nacnac)Ca(NH₂·BH₃)(THF)₂] (**77**), Scheme 50. In THF solution, this complex was stable, even at elevated temperatures, but in benzene solution, hydrogen loss was observed and dimerisation occurred. The product was the dinuclear species [{(DIPP-nacnac)Ca(THF)}₂(HNBH₂·BH₃)²⁻] (**78**) with a dianionic (HNBH₂·BH₃)²⁻ fragment bridging the calcium centres [126]. If a bulky substituent was attached to the nitrogen centre of the amine–borane (e.g. DIPP), a similar monomeric amidoborane complex was formed initially. This complex lost dihydrogen, but did not dimerise to form a dinuclear species and remained mononuclear with a borylamide ligand at the calcium centre (**79**), being a deprotonated analogue of an aminoborane (Scheme 50) [127].

This ligand system was also used in an attempt to form a zinc amidoborane complex. The reaction of [(DIPP-nacnac)ZnCl] with the amidoborane salt K[H₃B·N^{*i*}PrH] did not give the amidoborane complex as expected, but a hydride species was formed, [(DIPP-nacnac)ZnH], along with oligomeric aminoborane species. The authors postulated that an amidoborane complex did form but underwent rapid β -hydride elimination of a B–H bond to form the zinc hydride and free, reactive aminoborane which quickly formed oligomers (Scheme 51) [128]. Although this reaction was not catalytic, it did suggest that main-group metals could be used to dehydrogenate amine–boranes.



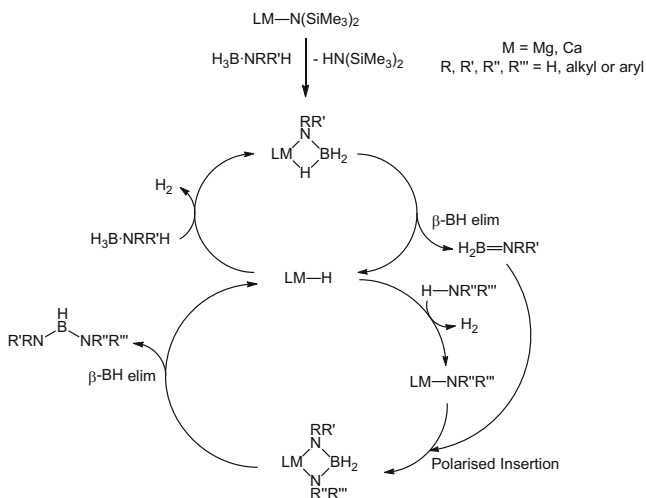
Scheme 52 Suggested mechanism for the dehydrocoupling of $\text{H}_3\text{B} \cdot \text{N}(\text{DIPP})\text{H}_2$ to form bis(amine)borane and BH_3 . DIPP=2,6-di(isopropyl)phenyl

2.10.2 Group 2 Metal-Catalysed Dehydrocoupling of Amine–Boranes

The first catalytic use of a main-group metal for the dehydrogenation of an amine–borane also came from the group of Harder who used the same bulky β -diketiminate ligand DIPP-nacnac on a magnesium centre to dehydrocouple $\text{H}_3\text{B} \cdot \text{N}(\text{DIPP})\text{H}_2$ to form a diaminoborane $\text{HB}\{\text{N}(\text{DIPP})\text{H}\}_2$ and BH_3 (detected as B_2H_6). The authors were able to improve the atom efficiency of the system by using a 2:1 ratio of $\text{N}(\text{DIPP})\text{H}_2$ and $\text{H}_3\text{B} \cdot \text{SMe}_2$ as the substrates and commercially available Mg^nBu_2 (2.5 mol%) as the precatalyst. Heating this mixture to 60°C for 14 h led to complete conversion to the diaminoborane product [129].

The first stage of the reaction involves the formation of the amidoborane complex **80**, Scheme 52. The authors then propose that B–N coupling occurs at the metal centre, followed by either a β -hydride elimination to form a magnesium hydride species **81** or a 1,3-hydride shift from one boron centre to the other to form a magnesium borohydride species **82**. Evidence for this latter mechanism was obtained by isolation of the $[(\text{DIPP-nacnac})\text{Mg}(\text{BH}_4)]_2$ species as a product of the reaction, although the first mechanism could not be ruled out as a reactive Mg–H bond could react with the BH_3 released to form a borohydride species. In a follow-up report, the authors suggested that the β -hydride elimination mechanism was the most likely to occur with the formation of the metal hydride and aminoborane. The reactivity of these intermediates then depends on the metal and the nitrogen substituents of the aminoborane [130].

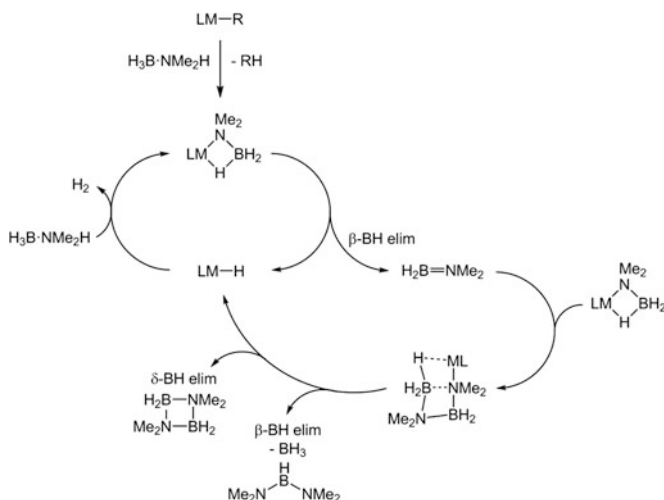
A more general route to a variety of diaminoboranes, including unsymmetrical ones, was reported by Hill and co-workers. Using the group 2 metal catalysts $[\text{M}\{\text{N}(\text{SiMe}_3)_2\}_2]$ ($\text{M} = \text{Mg}, \text{Ca}$), a mixture of primary and secondary amines and amine–boranes in a 1:1 ratio could be dehydrocoupled to form the $[\text{RR}'\text{NBHNR}''\text{R}''']$ ($\text{R}, \text{R}', \text{R}'', \text{R}''' = \text{H}, \text{alkyl or aryl}$) species with little or no formation of the symmetrical products. The mechanism of formation of these species is proposed to proceed via the formation of an amidoborane complex which undergoes β -hydride elimination to give an aminoborane and a metal hydride. The free amine then reacts with the



Scheme 53 Suggested mechanism for the formation of unsymmetrical bis(amine)borane from $\text{H}_3\text{B}\cdot\text{NRR}'\text{H}$ and $\text{HNR}''\text{R}'''$

metal hydride releasing H_2 and the aminoborane inserts into the $\text{M-NRR}'$ bond. A further β -hydride elimination regenerates the metal hydride and releases the diaminoborane product (Scheme 53) [131].

The first example of a main-group catalyst which formed a product with an equal B:N ratio was also from the group of Hill [132]. Stoichiometric reactions between either Mg^nBu_2 or $[\text{Mg}\{\text{CH}(\text{SiMe}_3)_2\}_2(\text{THF})_2]$ and 4 equiv. of $\text{H}_3\text{B}\cdot\text{NMe}_2\text{H}$ produced H_2 and $[\text{Mg}(\text{NMe}_2\text{BH}_2\text{NMe}_2\text{BH}_3)_2(\text{THF})]$ in which the amine–borane units have formed anionic linear diborazane coordinated to the Mg centre through an amide bond and an η^2 -agostic interaction from the terminal BH_3 . Heating this species to 60°C led to the formation of the cyclic $[\text{H}_2\text{BNMe}_2]_2$ dimer; however, the corresponding metal species was not able to be identified. In order to attempt to create a soluble, stable metal species, the same bulky β -diketiminate ligand used by Harder et al. [129] was employed to synthesise $[(\text{DIPP-nacnac})\text{Mg}^n\text{Bu}]$. Reaction of this complex with 2 equiv. of $\text{H}_3\text{B}\cdot\text{NMe}_2\text{H}$ again produced hydrogen, and the product with bound linear diborazane was isolated $[(\text{DIPP-nacnac})\text{Mg}(\text{NMe}_2\text{BH}_2\text{NMe}_2\text{BH}_3)]$. Heating this species to 60°C resulted in a slower reaction, but the cyclic $[\text{H}_2\text{BNMe}_2]_2$ dimer was again observed and the metal–ligand species formed could be identified as $[(\text{DIPP-nacnac})\text{MgH}(\text{THF})_2]$. The formation of the metal hydride means reaction with a further 2 equiv. of amine–borane could again form the bound linear diborazane species, and the reaction could turn over in a catalytic sense. This hypothesis was tested by heating 5 mol% of $[\text{Mg}\{\text{CH}(\text{SiMe}_3)_2\}_2(\text{THF})_2]$ with $\text{H}_3\text{B}\cdot\text{NMe}_2\text{H}$. Although the reaction was slow, taking 72 h for 80% conversion, $[\text{H}_2\text{BNMe}_2]_2$ was produced along with a small amount of the diaminoborane $\text{HB}(\text{NMe}_2)_2$. The proposed reaction mechanism is detailed in Scheme 54.



Scheme 54 Proposed mechanism of group 2-catalysed dehydrocoupling of $\text{H}_3\text{B} \cdot \text{NMe}_2\text{H}$

Hill and co-workers also employed a calcium β -diketiminate ligand system to dehydrocouple the primary amine–borane $\text{H}_3\text{B} \cdot \text{N}^t\text{BuH}_2$. 5 mol% of $[(\text{DIPP-nacnac})\text{Ca}\{\text{N}(\text{SiMe}_3)_2\}(\text{THF})]$ was heated to 60°C in the presence of the substrate to form a mixture of boron-containing compounds. After 24 h, 68% of the $\text{H}_3\text{B} \cdot \text{N}^t\text{BuH}_2$ remained unreacted, and the products were found to be $[\text{H}_2\text{BN}^t\text{BuH}]_2$ (5%), $\text{H}_2\text{B}=\text{N}^t\text{BuH}$ (1%), $\text{HB}(\text{N}^t\text{BuH})_2$ (13%), $\text{H}_3\text{B} \cdot \text{N}^t\text{BuHBH}_2$ (7%) and $[\text{Ca}(\text{BH}_4)_2]$ (6%). Heating of this reaction mixture for a further 5 days led to the formation of the borazine product $[\text{HBN}^t\text{Bu}]_3$ (20%) and an increased amount of $[\text{H}_2\text{BN}^t\text{BuH}]_2$ (45%) although 14% of the starting substrate remained unreacted [133].

Sicilia and co-workers performed a computational DFT analysis on the group II metal- β -diketiminate-catalysed dehydrocoupling of secondary amine–boranes [134]. Using magnesium as the metal, they found that the calculated mechanism was broadly the same as that proposed by Hill et al. [132] (Scheme 54) in which the amidoborane undergoes β -hydride elimination to form the metal hydride and free aminoborane. The aminoborane inserts into the M–N bond of a metal-bound amidoborane to form the bound diborazane. The rate-determining step of the reaction was found computationally to be the δ -hydride elimination to form $[\text{H}_2\text{BNMe}_2]_2$. In contrast, when a DFT analysis was carried out on the analogous calcium system, the β -hydride elimination from the amidoborane species was not found to occur. In order for dehydrogenation to take place, a further equivalent of amine–borane must also coordinate to the metal centre, and the interaction of the N–H of the bound amine–borane with the B–H of the amidoborane releases H_2 and aminoborane, regenerating the amidoborane. This difference in mechanism was ascribed to the larger ionic radius of the calcium ion and the calculated relative instability of the calcium hydride species compared to the amidoborane complex.

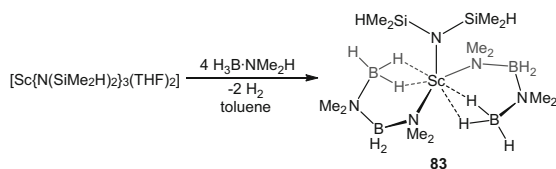
2.10.3 Group 3 Metal-Catalysed Dehydrocoupling of Amine–Boranes

Hypothesising that an increase in charge density at the metal centre would increase the dehydrocoupling activity, Hill and co-workers used group 3 metals as catalysts for the dehydrocoupling of amine–boranes. Reaction of 3 mol% of $[Y\{N(SiMe_3)_2\}_3]$ with $H_3B \cdot NMe_2H$ at $60^\circ C$ led to the complete consumption of the substrate and formation of $[H_2BNMe_2]_2$ dimer (90%) and $HB(NMe_2)_2$ (10%) in 12 h. The first stage of the reaction was observed to be the protonation of the amide ligands with the formation of amidoborane ligands as seen with the group 2 metals. Use of the more reactive scandium starting material $[Sc\{N(SiHMe_2)_2\}_3(THF)_2]$ (3 mol%) provided a much faster reaction with complete consumption of the amine–borane and near quantitative conversion to $[H_2BNMe_2]_2$ in 1 h at $60^\circ C$. In an attempt to elucidate the active species, when 4 equiv. of $H_3B \cdot NMe_2H$ was reacted with $[Sc\{N(SiHMe_2)_2\}_3(THF)_2]$, the dehydrocoupling product $[Sc\{N(SiHMe_2)_2\}(NMe_2BH_2NMe_2BH_3)_2]$ (**83**) was isolated (Scheme 55). The linear diborazane species coordinates in a similar fashion to the group 2 metal complexes with a metal–amido bond from the deprotonated nitrogen centre and a η^2 -B-agostic interaction from the terminal BH_3 [135].

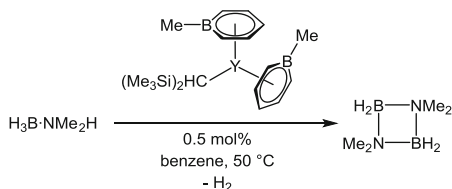
The increased activity of the rare-earth metals in oxidation state (III) was further exploited by Chen et al. who used an yttrium complex with two unusual 1-methyl boratabenzene ligands to catalyse the dehydrocoupling of a secondary amine–borane [136]. $[(MeBC_5H_5)_2Y\{CH(SiMe_3)_2\}]$ (0.5 mol%) was used to dehydrocouple $H_3B \cdot NMe_2H$ at $50^\circ C$ with the reaction reaching completion in ca. 12 min (Scheme 56). The products of the reaction observed after this were $[H_2BNMe_2]_2$ (98%) and a small portion of as yet undimerised aminoborane $H_2B=NMe_2$ (2%). A turnover frequency of $1,015 h^{-1}$ is by far the largest observed for the main-group catalysts and comparable with some of the best transition metal catalysts. The reaction using the lutetium analogue of this system reached completion in 29 min with a similar product distribution.

The extremely high activity of this system was ascribed to either the electron-withdrawing nature of the ligand or a possible interaction between the electron-

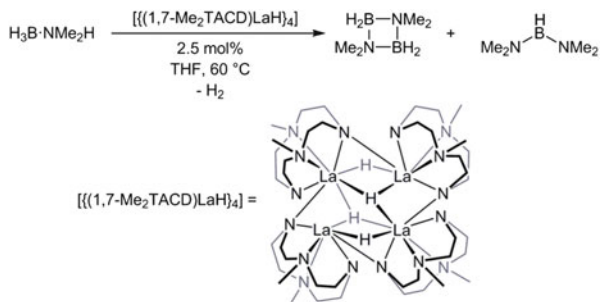
Scheme 55 Formation of $[Sc\{N(SiHMe_2)_2\}(NMe_2BH_2NMe_2BH_3)_2]$ (**83**)



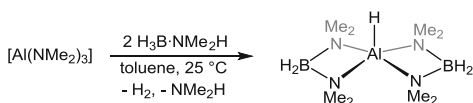
Scheme 56 Catalytic dehydrocoupling of $H_3B \cdot NMe_2H$ using $[(MeBC_5H_5)_2Y\{CH(SiMe_3)_2\}]$



Scheme 57 Catalytic dehydrocoupling of $\text{H}_3\text{B} \cdot \text{NMe}_2\text{H}$ using $[\{(1,7\text{-Me}_2\text{TACD})\text{LaH}\}_4]$



Scheme 58 Formation of $[\text{AlH}\{\text{H}_2\text{B}(\text{NMe}_2)_2\}_2]$

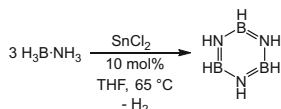


deficient boron centre of the 1-methyl boratabenzene ligand and the hydridic B–H bonds of the substrate. An analogous complex with an electron-donating substituent (NEt_2) on the boratabenzene $[(\text{Et}_2\text{NBC}_5\text{H}_5)_2\text{Y}\{\text{CH}(\text{SiMe}_3)_2\}]$ proved to be much less active in catalysis indicating either the electron-withdrawing nature of the ligand or the Lewis acidic centre was important for high activity. While the authors were unable to elucidate the mechanism of the reaction, they did observe free diborazane $\text{H}_3\text{B} \cdot \text{NMe}_2\text{BH}_2 \cdot \text{NMe}_2\text{H}$ as an intermediate in the reaction mixture, suggesting the mechanism is different than those reported by Harder and Hill in which free linear diborazane was never observed [130, 137].

Rare-earth metal catalysts were used by Okuda et al. for which the hydride tetramers $[\{(1,7\text{-Me}_2\text{TACD})\text{MH}\}_4]$ ($\text{M} = \text{La, Y}$; $1,7\text{-Me}_2\text{TACD} = 1,7\text{-dimethyl-1,4,7,10-tetraazacyclododecane}$) were used to catalyse the dehydrocoupling of $\text{H}_3\text{B} \cdot \text{NMe}_2\text{H}$ (2.5 mol%, 60°C , THF), with the lanthanum complex giving full conversion to $[\text{H}_2\text{BNMe}_2]_2$ (79%) and diamino-borane (21%) in 2 h, Scheme 57. The yttrium analogue took significantly longer with 95% conversion reached after 48 h to form a similar product ratio. Stoichiometric reactivity of $[\{(1,7\text{-Me}_2\text{TACD})\text{LaH}\}_4]$ demonstrated the non-innocent behaviour of the ligand in reactivity with the secondary amine–borane. The basic amido-groups of the $1,7\text{-Me}_2\text{TACD}$ ligand were shown to deprotonate the acidic amine protons of the amine–borane to form coordinated amidoborane species. The lone pair of these amido-groups was also able to provide stabilisation for the boron centre of a coordinated aminoborane by acting as a Lewis base [138].

2.10.4 P-Block-Catalysed Dehydrocoupling of Amine–Boranes

Wright et al. reported that the reaction of $[\text{Al}(\text{NMe}_2)_3]$ with $\text{H}_3\text{B} \cdot \text{NMe}_2\text{H}$ led to the formation of $[\text{AlH}\{\text{H}_2\text{B}(\text{NMe}_2)_2\}_2]$ (Scheme 58) by formation of an amidoborane complex and migration of the NMe_2 amido ligands to the boron centre. This complex (at 5 mol%) was able to catalyse the dehydrocoupling of $\text{H}_3\text{B} \cdot \text{NMe}_2\text{H}$



Scheme 59 SnCl₂-catalysed dehydrocoupling of H₃B·NH₃ to give borazine (87%)

at 50°C to give [H₂BNMe₂]₂ and HB(NMe₂)₂ in a 6:1 molar ratio after 48 h [139]. In a follow-up report, [Al(N^{*t*}Pr₂)₃] was used to catalytically form the aminoborane H₂B=N^{*t*}Pr₂ from the corresponding secondary amine–borane (10 mol%, 60°C, 2 h). As with the system reported by Okuda et al., the amido ligands of the starting material were found to be non-innocent, and if [Al(NMe₂)₃] was used instead, by-products containing the NMe₂ moiety were observed. Extending this investigation to a primary amine–borane, the precatalyst [Al(NMe₂)₃] was able to slowly dehydrocouple H₃B·N^{*t*}BuH₂ to form first the cyclic trimer borazane [H₂BN^{*t*}BuH]₃ which was then further dehydrogenated to the borazine product [HBN^{*t*}Bu]₃. Because the borazine can be observed early in the reaction, this suggests the rate of formation of borazine from borazane is comparable to the rate of initial dehydrocoupling to form the borazane from the monomers. However, overall this reaction was slow with only 30% conversion of the amine–borane after 4 days at 20°C [140]. Wright et al. have also found that Li [AlH₄] can be used as a catalyst to dehydrocouple H₃B·NMe₂H to give [H₂BNMe₂]₂ along with HB(NMe₂)₂ as a minor product [141]. Stoichiometric reactions of amine–boranes with aluminium species have revealed possible reaction intermediates although the mechanism of the dehydrocoupling has not been unambiguously determined [139–142].

The group IV metal tin, in both II and IV oxidation states, was utilised by Waterman et al. to catalyse the dehydrocoupling of H₃B·NMe₂H, H₃B·N^{*t*}BuH₂ and H₃B·NH₃. The majority of the catalytic reactions occurred slowly with most taking at least 24 h and producing a range of BN-containing products. The best performing was the SnCl₂-catalysed (10 mol%) dehydrocoupling of H₃B·NH₃ to borazine (87%) in 1 h at 65°C (Scheme 59). Attempts to identify the active species in catalysis were not successful as no tin-containing intermediates could be characterised or isolated. NMR spectroscopic investigations could not determine whether the active species was a Sn^{II} or Sn^{IV} complex, although several different active species could be present. It was determined that the likely method of catalyst deactivation was by reduction to Sn⁰ [143].

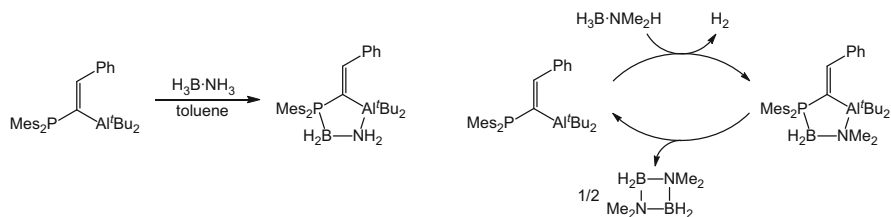
Sneddon has reported that Verkade's base (VB) acts as an initiator for base-promoted anionic dehydropolymerisation of H₃B·NH₃ to form anionic aminoborane chain growth products, such as the structurally characterised [VBH]⁺[H₃BNH₂BH₂NH₂BH₃]⁻ [9]. The mechanism proposed for this dehydrocoupling invokes initial deprotonation of H₃B·NH₃ by VB to form [VBH]⁺[BH₃NH₂]⁻, which then reacts with further H₃B·NH₃ to form the borane-capped [VBH]⁺[BH₃NH₂BH₃]⁻ and NH₃. Subsequent, sequential, dehydrocoupling affords the longer-chain oligomers. Such steps are suggested to

be facilitated by N–H \cdots H–B dihydrogen bonding as informed by a solid-state structural analysis. This result builds upon earlier studies in which proton sponge was used as the base initiator [36], as well as work by Girolami and co-workers that reported mild thermal conversion of Na[NH₂BH₃] leads to NaNH₂ and Na[NH₂(BH₃)₂] [144]. By contrast, Baker and Dixon have reported that the strong Lewis acid, B(C₆F₅)₃, or Brønsted acid, HOSO₂CF₃, promotes dehydrocoupling of amine–borane by a *hydride* abstraction pathway to form a boronium cation [102]. This is not dissimilar to the mechanism suggested for the Pt–catalysed dehydrocoupling of H₃B·NMe₂H (Scheme 43).

2.10.5 Frustrated Lewis Pair Dehydrogenation of Amine–Boranes

Since the discovery that frustrated Lewis pairs can activate dihydrogen, interest has focussed on the activation of other small molecules [145, 146]. The abstraction of dihydrogen from amine–boranes, particularly if it could be performed catalytically, would provide an alternative method to the traditional metal-based catalysis. The first to develop the dehydrogenation of H₃B·NMe₂H using frustrated Lewis pairs were Miller and Bercaw, who used a stoichiometric combination of P^tBu₃ and B(C₆F₅)₃ to ultimately form [H₂BNMe₂]₂ along with trace amounts of other BN-containing products. However, this reaction could not be carried out catalytically, and heating the reaction mixture in an attempt to release hydrogen gas from [HP^tBu₃][HB(C₆F₅)₃] and regenerate the frustrated Lewis pair was unsuccessful. Ammonia–borane could also be dehydrocoupled by a stoichiometric amount of these reagents to give polyaminoborane [H₂BNH₂]_n and [HP^tBu₃][HB(C₆F₅)₃]. Addition of further P^tBu₃ and B(C₆F₅)₃ did not appear to result in further dehydrogenation to form borazine or other products. The authors suggested the mechanism of dehydrogenation was likely to proceed via hydride abstraction by B(C₆F₅)₃, followed by rapid deprotonation by P^tBu₃ to form the aminoborane. This then undergoes rapid oligomerisation to form the products [147]. The group of Manners used a variety of less expensive frustrated Lewis pairs to dehydrocouple H₃B·NMe₂H, with a combination of [Me₃SiO₃SCF₃] and 2,2,6,6-tetramethylpiperidine performing best in forming [H₂BNMe₂]₂, with only traces of side products observed. The reaction could only be performed by a stoichiometric amount of Lewis pair, and therefore the reaction was not catalytic. Attempts to dehydrogenate the primary amine–borane H₃B·NMeH₂ did not result in readily characterised products [148].

An early example of use of a frustrated Lewis pair to *catalytically* dehydrocouple an amine–borane was reported by Uhl et al. who used a compound containing both a Lewis basic bulky phosphine and a Lewis acidic aluminium centre (Scheme 60). Stoichiometric reaction between this compound and ammonia–borane led to the dehydrogenation and formation of the aminoborane adduct. However, this final complex was thermally stable and the aminoborane could not be liberated to regenerate the original Lewis pair. Computational analysis of this reaction gave a mechanism contrasting that suggested by Miller and Manners where the first step of the reaction is now deprotonation of the N–H by the phosphine



Scheme 60 Reaction of the FLP with $\text{H}_3\text{B}\cdot\text{NH}_3$ (top) and catalytic dehydrocoupling of $\text{H}_3\text{B}\cdot\text{NMe}_2\text{H}$ (bottom)

centre and formation of an Al–N bond. Rearrangement, followed by loss of H_2 from the complex, gives the aminoborane and the 5-membered cyclic product quickly forms. The forced proximity of the Lewis acid and base in this compound may be the cause of this alternative mechanism. When the secondary amine–borane $\text{H}_3\text{B}\cdot\text{NMe}_2\text{H}$ was used, dihydrogen was again produced and the five-membered cyclic species was formed, but this was found to only be stable below -30°C . Above this temperature, the aminoborane $\text{H}_2\text{B}=\text{NMe}_2$ is released, which quickly dimerises to form $[\text{H}_2\text{BNMe}_2]_2$, and the frustrated Lewis pair catalyst is regenerated. A melt reaction of $\text{H}_3\text{B}\cdot\text{NMe}_2\text{H}$ (45°C then 90°C) with 9.3 mol% of catalyst produced $[\text{H}_2\text{BNMe}_2]_2$ in 71% isolated yield after 45 min. A lower catalyst loading (0.4 mol%) gave 77% $[\text{H}_2\text{BNMe}_2]_2$ in 44 h under similar conditions [149].

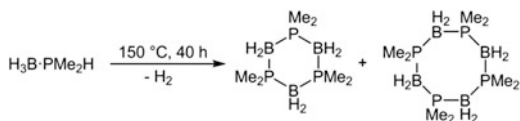
3 Dehydrocoupling of Phosphine–Boranes

3.1 Transition-Metal-Catalysed Dehydrocoupling of Phosphine–Boranes

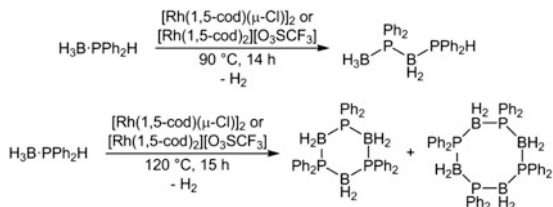
Phosphine–boranes were first found to undergo thermal dehydrocoupling in the 1950s when monomers were heated to 150°C and released hydrogen to form a mixture of cyclic trimer and tetramers [150]. Some polymerisation was reported at higher temperature but the products were ill-defined (Scheme 61) [151].

The breakthrough in *catalytic* dehydrocoupling came at the turn of the century when the group of Manners reported dehydrocoupling of both secondary and primary phosphine–boranes to give a variety of products. The precatalysts used were initially simple rhodium(I) species $[\text{Rh}(1,5\text{-cod})(\mu\text{-Cl})_2]$ or the salt $[\text{Rh}(1,5\text{-cod})_2][\text{O}_3\text{SCF}_3]$. The secondary phosphine–borane $\text{H}_3\text{B}\cdot\text{PPh}_2\text{H}$ was found to selectively form the linear diboraphosphine species $[\text{H}_3\text{B}\cdot\text{PPh}_2\text{BH}_2\cdot\text{PPh}_2\text{H}]$ at 90°C in the presence of 0.3 mol% of the rhodium(I) precatalyst in the absence of solvent (melt conditions) after 14 h. Heating a similar reaction mixture to 120°C for 15 h gave cyclic trimer and tetramers as the sole products (Scheme 62) [152, 153]. Analysis of this reaction mixture after 4 h showed complete consumption of the $\text{H}_3\text{B}\cdot\text{PPh}_2\text{H}$

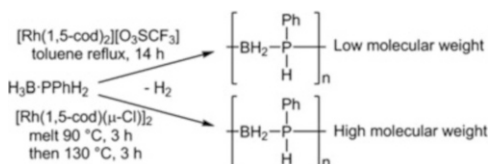
Scheme 61 Thermal dehydrocoupling of dimethyl phosphine–borane



Scheme 62 Rhodium (I)-catalysed dehydrocoupling of secondary phosphine–borane



Scheme 63 Catalytic formation of polyphosphinoboranes



starting material and a mixture of diboraphosphine, $\text{H}_3\text{B} \cdot \text{PPh}_2\text{BH}_2 \cdot \text{PPh}_2\text{H}$, and the cyclic species. It was suggested that $\text{H}_3\text{B} \cdot \text{PPh}_2\text{BH}_2 \cdot \text{PPh}_2\text{H}$ is an intermediate in the formation of the cyclic oligomers.

When the primary phosphine–borane $\text{H}_3\text{B} \cdot \text{PPhH}_2$ was used, 0.3 mol% of $[\text{Rh}(1,5\text{-cod})_2][\text{O}_3\text{SCF}_3]$ in refluxing toluene gave an air- and moisture-stable, off-white solid product found to be low molecular weight polyphenylphosphinoborane ($M_w = 5,600$). If melt conditions were used with $[\text{Rh}(1,5\text{-cod})(\mu\text{-Cl})_2]$ as the catalyst, a similar product could be made with a higher molecular weight ($M_w = 31,000$) (Scheme 63 and Fig. 15) [152].

In a follow-up report, Manners et al. screened a range of precatalysts for the dehydrocoupling of $\text{H}_3\text{B} \cdot \text{PPh}_2\text{H}$. In addition to the species tested above, the best performing precatalysts under melt conditions were found to be either Rh^{I} or Rh^{III} compounds, with species containing other metals (Ir, Pd, Pt) giving lower conversions and slower turnover. The scope of the polymerisation of primary phosphine–boranes was also expanded to the alkyl-substituted $\text{H}_3\text{B} \cdot \text{P}^i\text{BuH}_2$, which was dehydrocoupled in 13 h at 120°C [153].

The alkyl-substituted secondary phosphine–borane $\text{H}_3\text{B} \cdot \text{P}^i\text{Bu}_2\text{H}$ could be dehydrocoupled by similar rhodium-based precatalysts under melt conditions at elevated temperatures. Full conversion of the phosphine–borane was not achieved for any of the catalysts although the major product formed was the diboraphosphine, $\text{H}_3\text{B} \cdot \text{P}^i\text{Bu}_2\text{BH}_2 \cdot \text{P}^i\text{Bu}_2\text{H}$. Other products were also observed including in some cases the chloride-terminated diboraphosphine ($\text{ClH}_2\text{B} \cdot \text{P}^i\text{Bu}_2\text{BH}_2 \cdot \text{P}^i\text{Bu}_2\text{H}$) with the chloride provided by the precatalyst. One of the best catalysts was found to be $[\text{Rh}(1,5\text{-cod})(\mu\text{-Cl})_2]$ which had also been used

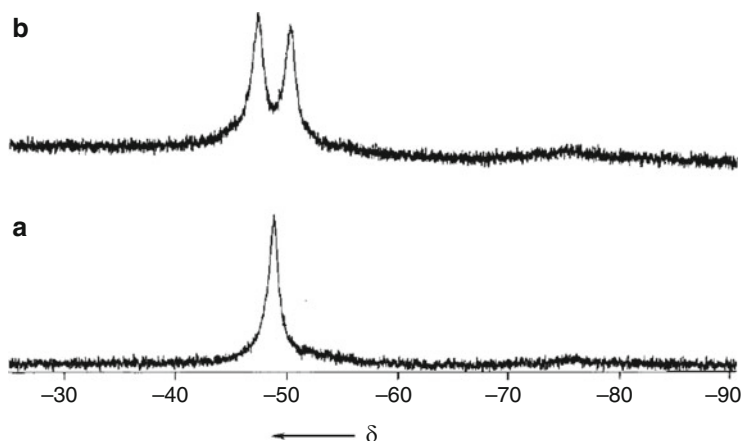


Fig. 15 ^{31}P NMR spectrum of $[\text{H}_2\text{BPPPhH}]_n$ in CDCl_3 (121 MHz): (a) ^1H -decoupled and (b) ^1H -coupled, $J_{\text{PH}} = 360$ Hz. Reprinted (adapted) with permission from Dorn et al. [153]. Copyright 2000, American Chemical Society

for the previous systems [154]. Another report from Manners and co-workers focussed on the formation of polymers from the dehydrocoupling of primary phosphine–boranes; aryl-substituted phosphine–boranes $\text{H}_3\text{B} \cdot \text{P}(p\text{-}^t\text{Bu-C}_6\text{H}_4)_2$ and $\text{H}_3\text{B} \cdot \text{P}(p\text{-(C}_{12}\text{H}_{25}\text{)-C}_6\text{H}_4)_2$ were polymerised by $[\text{Rh}(1,5\text{-cod})(\mu\text{-Cl})_2]$ under melt conditions [155].

3.2 Determination of the Active Catalytic Species: Hetero- or Homogeneous

In all of these reports from the group of Manners, the active catalytic species and mechanism of polymerisation were not investigated in detail. While in general rhodium-based precatalysts under melt conditions performed best, precatalysts with different oxidation states and ligands could all give catalytic turnover for dehydrocoupling. Since the formation of rhodium nanoparticles had been found to be an important step in the catalytic dehydrocoupling of amine–boranes, Manners et al. investigated whether the phosphine–borane catalysis operated in a hetero- or homogeneous mode. Addition of 10 mol% of $[\text{Rh}(1,5\text{-cod})(\mu\text{-Cl})_2]$ to a toluene solution of $\text{H}_3\text{B} \cdot \text{PPh}_2\text{H}$ at 90°C resulted in a colour change from orange to red, but no evidence of black material was observed, which is often characteristic of nanoparticle formation [156]. In addition to this, no induction period was observed, and filtration and mercury poisoning experiments also suggested the catalyst was a heterogeneous species. Similar results were found for the ion-separated precatalyst $[\text{Rh}(1,5\text{-cod})_2][\text{O}_3\text{SCF}_3]$ (Fig. 16).

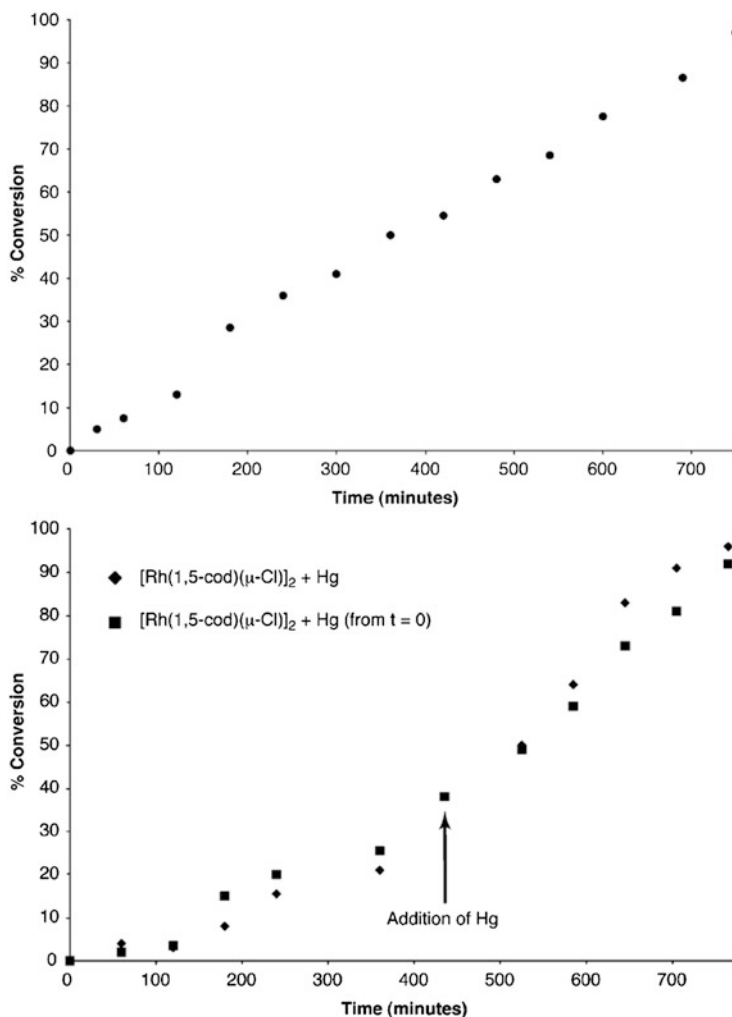


Fig. 16 Top: graph of % conversion vs. time for the catalytic dehydrocoupling of $\text{H}_3\text{B} \cdot \text{PPh}_2\text{H}$ using $[\text{Rh}(1,5\text{-cod})(\mu\text{-Cl})_2]$ (ca. 10 mol% Rh, toluene, 90°C). Bottom: graph of % conversion vs. time for the catalytic dehydrocoupling of $\text{H}_3\text{B} \cdot \text{PPh}_2\text{H}$ using $[\text{Rh}(1,5\text{-cod})(\mu\text{-Cl})_2]$ (ca. 10 mol% Rh, toluene, 90°C). At ca. 35% conversion, excess Hg was added to the reaction mixture (curve filled diamond). The dehydrocoupling reaction was initiated in the presence of excess Hg (curve filled square). Reprinted (adapted) with permission from Jaska and Manners [39]. Copyright 2004, American Chemical Society

Dehydrocoupling was attempted using the heterogeneous $\text{Rh}/\text{Al}_2\text{O}_3$ (5 wt% Rh) precatalyst and, interestingly, catalysis was found to occur. However, filtration of the solution showed the soluble portion to be orange, suggesting some rhodium had leached into the solution to form a homogeneous catalytically active species. Addition of further $\text{H}_3\text{B} \cdot \text{PPh}_2\text{H}$ to both soluble and insoluble portions showed

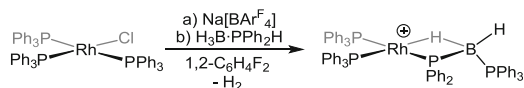
them to be active and inactive, respectively, confirming the homogeneous nature of the catalyst. While the authors were unable to identify the true catalytic species, they were able to speculate that the phosphine–boranes were not reducing enough to form Rh^0 from the Rh^I precatalyst. In addition to this, the relative weakness of the P–B bond (compared to the N–B bond in amine–boranes) allowed dissociation and formation of free phosphine which could act as ligands for solubilising heterogeneous species. However, an excess of free phosphine could act as a catalyst poison, and they suggest higher temperatures required for phosphine–borane dehydrocoupling might be needed to create a vacant site at the metal centre, which is often required in polymerisation catalysis [39].

3.3 *Sigma Complexes and B-Agostic Interactions of Phosphine–Boranes*

An important step in the dehydrocoupling of amine–boranes is thought to be the formation of σ -complexes where the metal centre interacts with the H–B bond of the borane moiety (Sect. 2.7.1). Similarly, in phosphine–borane dehydrocoupling, the creation of a vacant site at the metal centre to which the phosphine–borane can bind, or displacement of a ligand by a phosphine–borane, is likely to be an important step [39]. The initial interaction between the metal centre and the substrate is likely through formation of a σ -complex with the hydridic B–H bonds. A number of phosphine–borane σ -complexes and B-agostic interactions (where the phosphine–borane is further tethered to the metal centre) have been reported in the literature. An early example of a σ -complex was reported in 1984 in which zinc is complexed with diphosphine–diborane(4), $[\text{ZnCl}_2\{\text{B}_2\text{H}_4 \cdot (\text{PMe}_3)_2\}]$ [157], and a phosphidoborane complex with a β -B-agostic interaction $[\text{CpMo}(\text{CO})_2\{\text{P}\{\text{N}(\text{SiMe}_3)_2\}\text{Ph} \cdot \text{BH}_3\}]$ was published 2 years later [158]. The first σ -complex with a monomeric phosphine–borane was synthesised by the photolysis of $[\text{M}(\text{CO})_6]$ (M=Cr, Mo, W) in the presence of $\text{H}_3\text{B} \cdot \text{PR}_3$ (R=Me, Ph) to form the η^1 -complexes $[\text{M}(\text{CO})_5(\text{H}_3\text{B} \cdot \text{PR}_3)]$ [61]. There are a number of reports of similar compounds [159–161] including examples of η^2 -B-agostic interactions in rhodium complexes [162–164].

An interesting observation came from Whittlesey et al. who reported that reaction of $[\text{RuH}(\text{Xantphos})(\text{PPh}_3)(\text{OH}_2)][\text{BAR}^{\text{F}}_4]$ with amine–boranes produced σ -complexes by displacement of the water ligand, but reaction with the phosphine–borane $\text{H}_3\text{B} \cdot \text{PPh}_2\text{H}$ gave only the P–B cleavage product $[\text{RuH}(\text{Xantphos})(\text{PPh}_2\text{H})_2][\text{BAR}^{\text{F}}_4]$. This shows the relative weakness of the P–B bond compared to the N–B bond in amine–boranes and suggests P–B cleavage is likely to play a role in metal-catalysed dehydrocoupling of phosphine–boranes [63].

In 2013, Weller et al. described an attempt to form a σ -complex from the reaction between $[\text{RhCl}(\text{PPh}_3)_3]$ and $\text{Na}[\text{BAR}^{\text{F}}_4]$ in the presence of a secondary phosphine–borane $\text{H}_3\text{B} \cdot \text{PPh}_2\text{H}$. However, this reaction led to dehydrocoupling and



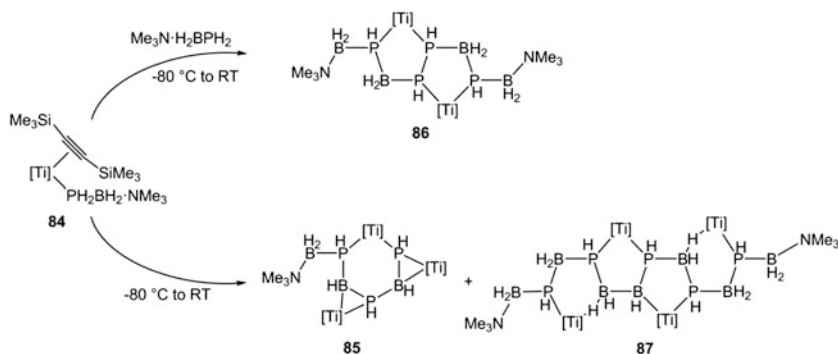
Scheme 64 Formation of $[\text{Rh}(\text{PPh}_3)_2(\text{PPh}_2\text{BH}_2 \cdot \text{PPh}_3)][\text{BAr}^{\text{F}}_4]$ from the dehydrogenation of $\text{H}_3\text{B} \cdot \text{PPh}_2\text{H}$. $[\text{BAr}^{\text{F}}_4]^-$ anion not shown

the formation of the complex $[\text{Rh}(\text{PPh}_3)_2(\text{PPh}_2\text{BH}_2 \cdot \text{PPh}_3)][\text{BAr}^{\text{F}}_4]$ (Scheme 64). One triphenylphosphine ligand has migrated to the boron centre, and a B–H bond has formed a β -B-agostic interaction with the rhodium centre. While the mechanism of this transformation was not determined, it was postulated that the reaction could occur either via P–H activation, B–H activation or the formation of a transient phosphinoborane intermediate $\text{H}_2\text{B} = \text{PPh}_2$ at the metal centre [165]. In contrast, aminoboranes have been shown to be crucial, if often short-lived, intermediates in the metal-catalysed dehydrocoupling of amine–boranes (vide supra); however, free phosphinoboranes have yet to be observed during phosphine–borane dehydrocoupling.

There are examples of group X phosphidoborane complexes that have been synthesised by the reaction of a metal fragment with $\text{H}_3\text{B} \cdot \text{PR}_2\text{H}$ and oxidative addition of the P–H bond [166, 167]. These examples, however, are not active in dehydrocoupling either stoichiometric or catalytic, although, as will be shown in Sect. 3.6, such motifs can be strongly implicated in the dehydrocoupling process with different metal–ligand fragments.

3.4 Stabilised Phosphinoboranes

Although not directly observed during dehydrocoupling, there are phosphinoboranes which have been synthesised that rely on stabilisation by the presence of bulky substituents or by coordination of a Lewis acid or Lewis base. Those with large substituents do not oligomerise due to the steric crowding of the phosphorus and boron centres [168]. However, those with Lewis acid or base stabilisation can undergo further reaction [169, 170]. The Lewis base-stabilised unsubstituted phosphinoborane $\text{Me}_3\text{N} \cdot \text{H}_2\text{BPH}_2$ was synthesised by Scheer et al. and was found to oligomerise in the presence of $[\text{Cp}_2\text{Ti}(\eta_2\text{Me}_3\text{SiCCSiMe}_3)]$, with different products observed depending on the temperature and stoichiometry. The first step of the reaction is the coordination of the stabilised phosphinoborane through the lone pair at the phosphorus centre to form $[\text{Cp}_2\text{Ti}(\eta_2\text{Me}_3\text{SiCCSiMe}_3)(\text{PH}_2\text{BH}_2 \cdot \text{NMe}_3)]$ (**84**) (Scheme 65). This complex is only stable below -80°C in solution, and above this temperature alkyne dissociates and oligomerisation occurs in both head-to-tail and head-to-head fashion, along with some Lewis base dissociation. The complexes formed are oligomeric chains of 3 (**85**), 4 (**86**) and 6 (**87**) phosphinoborane monomers stabilised by the coordination of the $[\text{Cp}_2\text{Ti}]$ fragment [171].



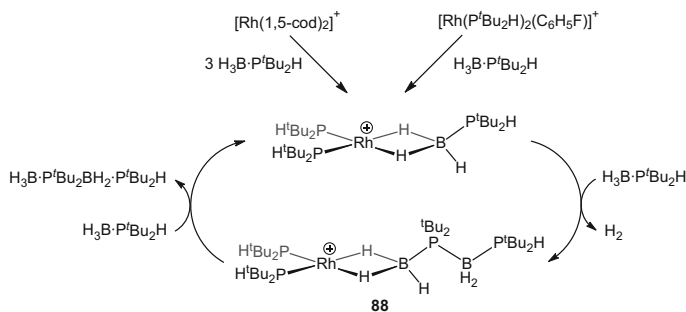
Scheme 65 [Cp₂Ti]-catalysed oligomerisation of Me₃N·H₂BPH₂. [Ti]=Cp₂Ti

3.5 Group 8 Metal-Catalysed Dehydrocoupling of Phosphine–Boranes

Complexes based on group 8 metals were first used in 2008 as precatalysts for dehydrocoupling, when Manners et al. reported the use of [CpM(CO)₂(PPh₂·BH₃)] (M=Fe, Ru) to form diboraphosphine, H₃B·PPh₂BH₂·PPh₂H, from the secondary phosphine–borane H₃B·PPh₂H under both melt conditions and in solution. The phosphidoborane precatalyst complexes were synthesised by a reaction of [CpMI(CO)₂] (M=Fe, Ru) with (H₃B·PPh₂)Li. In toluene solution at 110°C, the Fe complex performed poorly only converting 50% of H₃B·PPh₂H at 25 mol% catalyst loading. However, under melt conditions (120°C), the iron and ruthenium complexes were able to convert 65 and 60% of the starting material to linear diboraphosphine, respectively (1.5 mol%, 15 h). Under the same melt conditions, Fe₂(CO)₉ was also found to catalyse the dehydrocoupling of H₃B·PPh₂H to form the same product (80% conversion in 15 h). The authors postulated that the loss of a carbonyl ligand at high temperatures allowed dehydrocoupling to occur in the vacant coordination site created [172]. This is closely related to the mechanism proposed for amine–borane dehydrocoupling using the same metal–ligand system (Scheme 30).

3.6 Mechanistic Investigations into the Rhodium-Catalysed Dehydrocoupling of Secondary Phosphine–Boranes

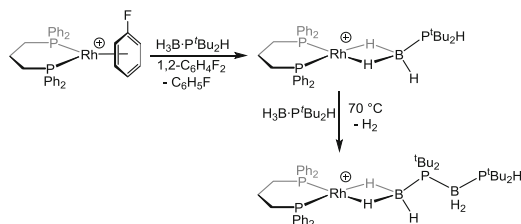
The first detailed investigation into the mechanism of the rhodium-catalysed dehydrocoupling of phosphine–boranes was reported by Huertos and Weller in 2012. The precatalyst used was [Rh(1,5-cod)₂][BAR^F₄] similar to the [Rh(1,5-cod)₂][O₃SCF₃] complex used previously by Manners and co-workers [7]. Heating 5 mol % of the precatalyst with H₃B·P^tBu₂H under melt conditions (140°C) for 20 h led



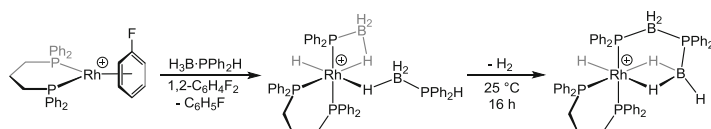
Scheme 66 Proposed mechanism for rhodium-catalysed formation of linear diboraphosphine from $\text{H}_3\text{B} \cdot \text{P}'\text{Bu}_2\text{H}$. $[\text{BAR}^{\text{F}}_4]^-$ omitted for clarity

to the formation of $\text{H}_3\text{B} \cdot \text{P}'\text{Bu}_2\text{BH}_2 \cdot \text{P}'\text{Bu}_2\text{H}$ (65%) along with a bis(phosphine) boronium salt $[\text{H}_2\text{B}(\text{P}'\text{Bu}_2\text{H})_2][\text{BH}_4]$ (10%) as a side product from P–B cleavage. Interrogation of the melt reaction by addition of 1,2-difluorobenzene solvent and analysis by ^{31}P NMR spectroscopy and ESI mass spectrometry revealed the organometallic species present to be $[\text{Rh}(\text{P}'\text{Bu}_2\text{H})_2(\eta^2\text{-H}_3\text{B} \cdot \text{P}'\text{Bu}_2\text{BH}_2 \cdot \text{P}'\text{Bu}_2\text{H})]^+$ (**88**) and $[\text{Rh}(\text{P}'\text{Bu}_2\text{H})_2(\eta^6\text{-C}_6\text{H}_4\text{F}_2)]^+$. The secondary phosphine ligands at the rhodium centre originate from the phosphine–borane having undergone P–B cleavage, and the rest of the coordination sphere of the Rh^{I} centre is filled by a solvent molecule or the σ -bound phosphine–borane or diboraphosphine. These observations suggested that the $[\text{Rh}(\text{P}'\text{Bu}_2\text{H})_2]^+$ fragment was the active species in the catalysis. $[\text{Rh}(\text{P}'\text{Bu}_2\text{H})_2(\eta^6\text{-C}_6\text{H}_5\text{F})][\text{BAR}^{\text{F}}_4]$ was independently synthesised and was found to catalyse the dehydrocoupling of $\text{H}_3\text{B} \cdot \text{P}'\text{Bu}_2\text{H}$ under melt conditions to form the same intermediates and final products as $[\text{Rh}(1,5\text{-cod})_2][\text{BAR}^{\text{F}}_4]$. This provided further evidence that the $[\text{Rh}(\text{P}'\text{Bu}_2\text{H})_2]^+$ fragment is the active catalyst, and a simple mechanism was postulated (Scheme 66) [173].

In an attempt to find a more stable catalytic fragment, $[\text{Rh}(\text{P}'\text{Bu}_3)_2(\eta^6\text{-C}_6\text{H}_5\text{F})][\text{BAR}^{\text{F}}_4]$, which had been shown to be an effective dehydrocoupling catalyst for amine–boranes, was used as a precatalyst for the dimerisation of $\text{H}_3\text{B} \cdot \text{P}'\text{Bu}_2\text{H}$. However, analysis of the reaction mixture found a mixture of organometallic species with the tri-*i*-butylphosphine ligand replaced on the rhodium centre by $\text{P}'\text{Bu}_2\text{H}$ ligands, presumably from P–B cleavage of the substrate. In a further development of this system, Huertos and Weller were able to form a more stable catalytic fragment by replacement of the monodentate phosphine ligands with a chelating phosphine ligand 1,3-bis(diphenylphosphino)propane ($\text{Ph}_2\text{PCH}_2\text{CH}_2\text{CH}_2\text{PPh}_2$, dppp) [174]. Under the harsh melt conditions required for catalysis to occur, the chelating ligand was not displaced by any free phosphine formed from P–B cleavage of the substrate, allowing further investigation into the $[\text{Rh}(\text{dppp})]^+$ fragment as the active catalytic species. A stoichiometric reaction between the precatalyst $[\text{Rh}(\text{dppp})(\eta^6\text{-C}_6\text{H}_5\text{F})][\text{BAR}^{\text{F}}_4]$ and $\text{H}_3\text{B} \cdot \text{P}'\text{Bu}_2\text{H}$ led to the formation of the σ -complex $[\text{Rh}(\text{dppp})(\eta^2\text{-H}_3\text{B} \cdot \text{P}'\text{Bu}_2\text{H})][\text{BAR}^{\text{F}}_4]$ by displacement of the labile fluorobenzene ligand (Scheme 67). In the presence of another



Scheme 67 Formation of $[\text{Rh}(\text{dppp})(\eta^2\text{-H}_3\text{B}\cdot\text{P}'\text{Bu}_2\text{H})]^+$ and dehydrocoupling. $[\text{BAr}^{\text{F}}_4]^-$ omitted for clarity



Scheme 68 Formation of $[\text{RhH}(\text{dppp})(\text{PPh}_2\cdot\text{BH}_3)(\eta^1\text{-H}_3\text{B}\cdot\text{PPh}_2\text{H})]^+$ and dehydrocoupling. $[\text{BAr}^{\text{F}}_4]^-$ omitted for clarity

equivalent of $\text{H}_3\text{B}\cdot\text{P}'\text{Bu}_2\text{H}$, the complex was found to undergo dehydrocoupling at 70°C in 1,2-difluorobenzene to form the σ -bound linear diboraphosphine product $[\text{Rh}(\text{dppp})(\text{H}_3\text{B}\cdot\text{P}'\text{Bu}_2\text{BH}_2\cdot\text{P}'\text{Bu}_2\text{H})]^+$ although the reaction produced several side products.

Extending the study to $\text{H}_3\text{B}\cdot\text{PPh}_2\text{H}$ resulted in quite different complexes being isolated from these stoichiometric studies. Reaction of $[\text{Rh}(\text{dppp})(\eta^6\text{-C}_6\text{H}_5\text{F})][\text{BAr}^{\text{F}}_4]$ with 2 equiv. of $\text{H}_3\text{B}\cdot\text{PPh}_2\text{H}$ in 1,2-difluorobenzene gave a Rh^{III} complex in which one phosphine–borane unit had undergone P–H activation to form a rhodium hydride and a β -B-agostic phosphidoborane, and the second molecule was σ -bound through one hydrogen atom of the borane moiety. The two phosphine–borane units on this complex were found to cleanly dehydrocouple in a first-order process at room temperature to form a linear diboraphosphine product which is also P–H activated, and the remainder of the Rh^{III} coordination sphere is filled by two β -B-agostic interactions from the terminal BH_3 moiety (Scheme 68, Fig. 17). These data, when combined with H/D labelling experiments, allowed the rate-determining step for dehydrocoupling to be suggested to lie in the second B–H activation and ligand reorganisation step(s). In catalysis, the turnover-limiting step, however, is the substitution of the chelating linear diboraphosphine by another molecule of $\text{H}_3\text{B}\cdot\text{PPh}_2\text{H}$ (Scheme 69).

The substituents at the phosphorus position of the phosphine–borane unit were found to have an effect on the reactivity both stoichiometrically and in catalysis. The phosphine–borane with the bulky, electron-donating *t*-butyl substituent was found to dehydrocouple slowly (16 h at 140°C , 60% conversion), and complexes with this ligand were observed in the Rh^{I} oxidation state. Contrastingly, when the phosphine–borane with the electron-withdrawing phenyl substituent was used, dehydrocoupling proceeded faster (4 h at 90°C) while Rh^{III} complexes were

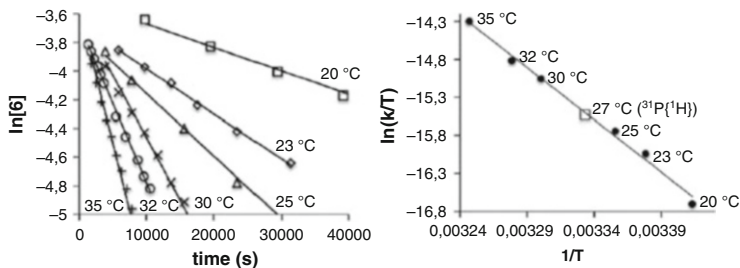
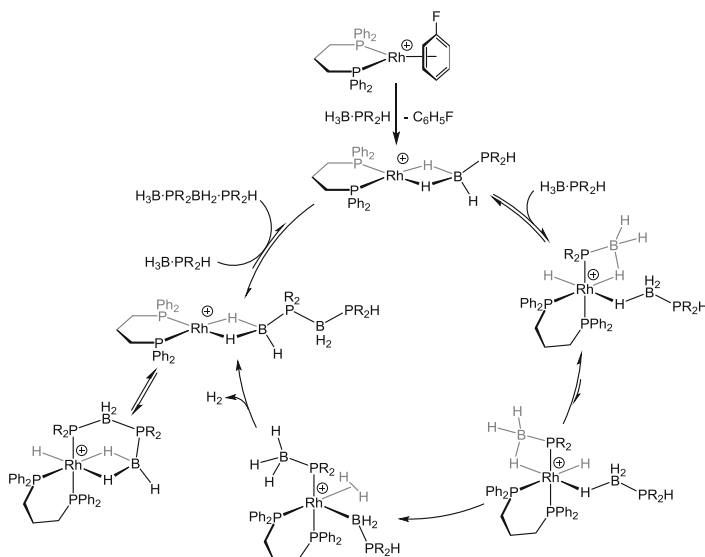


Fig. 17 First-order plots and Eyring analysis of dehydrocoupling of $[\text{RhH}(\text{dppp})(\text{PPh}_2 \cdot \text{BH}_3)(\eta^1\text{-H}_3\text{B} \cdot \text{PPh}_2\text{H})][\text{BAr}^{\text{F}}_4]$ to $[\text{RhH}(\text{dppp})(\text{PPh}_2 \cdot \text{BH}_2\text{PPh}_2 \cdot \text{BH}_3)][\text{BAr}^{\text{F}}_4]$. Reprinted (adapted) with permission from Huertos and Weller [174]. Copyright 2014, Royal Society of Chemistry



Scheme 69 Detailed mechanism for the dehydrocoupling of secondary phosphine-borane by the $[\text{Rh}(\text{dppp})]^+$ fragment. $[\text{BAr}^{\text{F}}_4]^-$ omitted for clarity

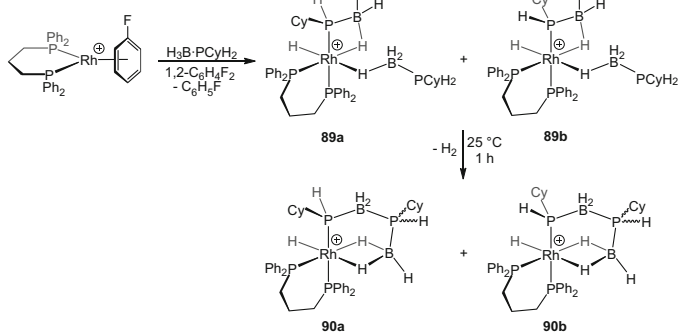
favoured. The difference in oxidation state of the rhodium centre in these cases is likely due to the acidity of the P–H bond. When electron-withdrawing substituents are present on phosphorus, the P–H bond more readily undergoes P–H oxidative addition, making Rh^{III} species favoured [174].

In a follow-up report, secondary phosphine-boranes bearing fluorinated substituents $\text{H}_3\text{B} \cdot \text{P}(p\text{-F}_3\text{C-C}_6\text{H}_4)_2\text{H}$ and $\text{H}_3\text{B} \cdot \text{P}(m\text{-(F}_3\text{C)}_2\text{C}_6\text{H}_3)_2\text{H}$ were found to dehydrocouple at a faster rate than $\text{H}_3\text{B} \cdot \text{PPh}_2\text{H}$ using the same $[\text{Rh}(\text{dppp})]^+$ system [175]. However, stoichiometric reactions showed that the weakening of the P–B bond by the presence of the electron-withdrawing groups caused P–B bond cleavage and hence catalyst deactivation by the formation of $[\text{Rh}(\text{dppp})(\text{PR}_2\text{H})_2]^+$. The

faster dehydrocoupling of fluorinated phosphine–boranes is in agreement with Manners et al. who found that these substrates could be catalytically dehydrocoupled at lower temperature than the non-fluorinated aryl analogues (vide infra). Conversely, the presence of an electron-donating group $\text{H}_3\text{B}\cdot\text{P}(p\text{-MeO-C}_6\text{H}_4)_2\text{H}$ at the phosphorus centre was found to reduce the rate of dehydrocoupling. However, the increased strength of the P–B bond meant cleavage and hence catalyst deactivation was largely avoided. Fluorinated phosphine–boranes can be also catalytically dehydrocoupled using different catalyst systems. The secondary phosphine–borane $\text{H}_3\text{B}\cdot\text{P}(p\text{-F}_3\text{C-C}_6\text{H}_4)_2\text{H}$ was converted to the corresponding linear diboraphosphine product by heating with $[\text{Rh}(1,5\text{-cod})(\mu\text{-Cl})_2]$ (2 mol% based on Rh) to 60°C for 15 h under melt conditions [176]. The cyclic trimer and tetramer species observed for the high-temperature dehydrocoupling of $\text{H}_3\text{B}\cdot\text{PPh}_2\text{H}$ were also formed at lower temperature (100°C , 15 h). The fluorinated primary phosphine–borane $\text{H}_3\text{B}\cdot\text{P}(p\text{-F}_3\text{C-C}_6\text{H}_4)\text{H}_2$ was found to form high molecular weight polymer under similar conditions, $[\text{Rh}(1,5\text{-cod})(\mu\text{-Cl})_2]$ precatalyst (2.5 mol% based on Rh), 60°C , 9 h in melt conditions. The lowering of the reaction temperature was ascribed to the increased acidity of the P–H bond due to the electron-withdrawing substituents and therefore its ability to react more readily with the hydridic B–H bonds to dehydrocouple.

3.7 Mechanistic Investigation into the Rhodium-Catalysed Dehydrocoupling of Primary Phosphine–Boranes

The mechanism of dehydrocoupling of primary phosphine–boranes using $[\text{Rh}(\text{dppp})(\eta^6\text{-C}_6\text{H}_5\text{F})][\text{BAR}^{\text{F}}_4]$ has also been reported. $\text{H}_3\text{B}\cdot\text{PCyH}_2$ was used as the substrate, and under stoichiometric conditions, it reacted in a similar way to $\text{H}_3\text{B}\cdot\text{PPh}_2\text{H}$ with the formation of a Rh^{III} complex with a hydride, a phosphidoborane and a σ -bound $\eta^1\text{-H}_3\text{B}\cdot\text{PCyH}_2$ (Scheme 70). This complex was found to exist as an approximately 1:1 mixture of two diastereoisomers (**89a** and **89b**) due to the P–H activation at the prochiral phosphorus centre. As with the secondary aryl phosphine–boranes, this complex underwent dehydrocoupling, although faster than the secondary analogues, being complete in 1 h at room temperature. The dehydrocoupled complex formed was again equivalent to the $\text{H}_3\text{B}\cdot\text{PPh}_2\text{H}$ reaction with the linear diboraphosphine having undergone P–H activation and chelating via 2 β -B-agostic bonds from the terminal borane moiety. The complex is formed as a mixture of two, unresolved, diastereoisomer (**90a** and **90b**) because of P–H activation at the prochiral phosphorus centre although the diastereoisomers are present as a 6:1 mixture with one thermodynamically favoured. This complex can also be synthesised by the reaction of the preformed linear diboraphosphine with $[\text{Rh}(\text{dppp})(\eta^6\text{-C}_6\text{H}_5\text{F})][\text{BAR}^{\text{F}}_4]$, which initially forms a kinetic 1:1 diastereomeric mixture and over 18 h reaches the 6:1 ratio observed from dehydrocoupling. This provides evidence for the mechanism proposed in



Scheme 70 Reaction of $[\text{Rh}(\text{dppp})(\eta^6\text{-C}_6\text{H}_5\text{F})][\text{BAR}^{\text{F}}_4]$ with primary phosphine–borane $\text{H}_3\text{B} \cdot \text{PCyH}_2$. $[\text{BAR}^{\text{F}}_4]^-$ omitted for clarity

Scheme 69 in which the Rh^{I} σ -bound linear diboraphosphine complex is in equilibrium with the P-H -activated Rh^{III} octahedral complex as such a process would allow interconversion of the Rh^{III} diastereomers. Such a diastereomeric bias may afford some control of polymer tacticity in dehydropolymerisation reactions [175]. Interestingly, the use of a chiral chelating phosphine ligand on rhodium resulted in a further bias towards one diastereoisomer, but the absolute configuration was not determined.

The $[\text{Rh}(\text{dppp})]^+$ fragment performed competently as a catalyst for the polymerisation of the more reactive primary phosphine–borane $\text{H}_3\text{B} \cdot \text{PPhH}_2$ under melt conditions. Heating 5 mol% of precatalyst $[\text{Rh}(\text{dppp})(\eta^6\text{-C}_6\text{H}_5\text{F})][\text{BAR}^{\text{F}}_4]$ with neat $\text{H}_3\text{B} \cdot \text{PPhH}_2$ to 90°C for 4 h led to a peak in the ^{31}P NMR spectrum matching previous literature reports for polyphenylphosphinoborane along with minor signals thought to be short-chain oligomers and cyclic species [153].

An expansion of the scope of dehydrocoupling of primary phosphine–boranes was reported in 2014 when ferrocenylphosphine–boranes were dehydrocoupled to form polymeric material. Using the catalytic system developed by Manners et al., $\text{H}_3\text{B} \cdot \text{P}\{(\text{CH}_2)_x\text{Fc}\}_2$ (Fc = ferrocenyl, $x = 0$ or 1) was dehydrocoupled using 0.6 mol% $[\text{Rh}(1,5\text{-cod})(\mu\text{-Cl})]_2$ (based on Rh) with the products characterised by NMR spectroscopy (Fig. 18). Low molecular weight polymer was formed when the reaction was carried out in toluene solution (110°C), but in melt conditions, higher molecular weights could be obtained (Scheme 71) [177].

The same group reported the dehydrocoupling of secondary phosphine–boranes bearing ferrocenyl substituents. The $\text{H}_3\text{B} \cdot \text{P}^i\text{Bu}(\text{Fc})\text{H}$ substrate could be dehydrocoupled to form the linear diboraphosphine under melt conditions (160°C) using $[\text{Rh}(1,5\text{-cod})(\mu\text{-Cl})]_2$ as the catalyst. The product was found to be a mixture of $\text{H}_3\text{B} \cdot \text{P}^i\text{Bu}(\text{Fc})\text{H}_2\text{B} \cdot \text{P}^i\text{Bu}(\text{Fc})\text{H}$ and $\text{ClH}_2\text{B} \cdot \text{P}^i\text{Bu}(\text{Fc})\text{H}_2\text{B} \cdot \text{P}^i\text{Bu}(\text{Fc})\text{H}$ (Scheme 72), which is a similar observation to that made by Manners et al. in the dimerisation of $\text{H}_3\text{B} \cdot \text{P}^i\text{Bu}_2\text{H}$ where the terminal chloride was thought to originate from the precatalyst [154]. Interestingly, the authors were able to couple two different phosphine–boranes to form a mixed diboraphosphine, the first time this

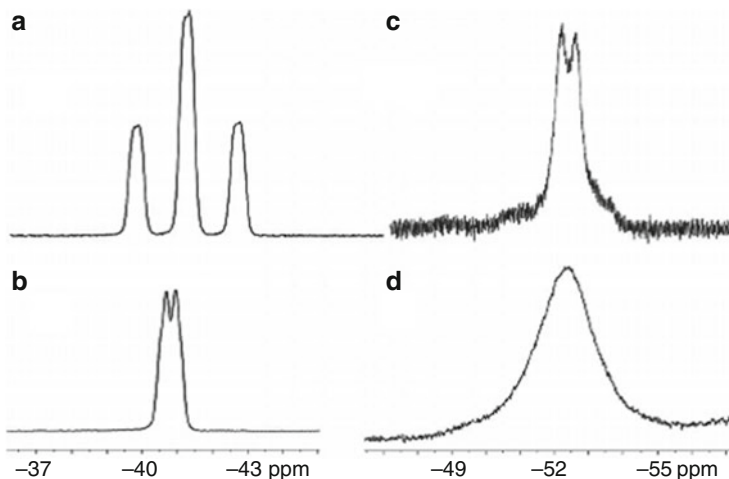
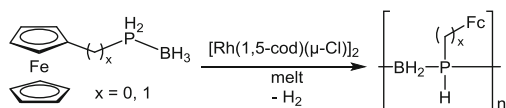
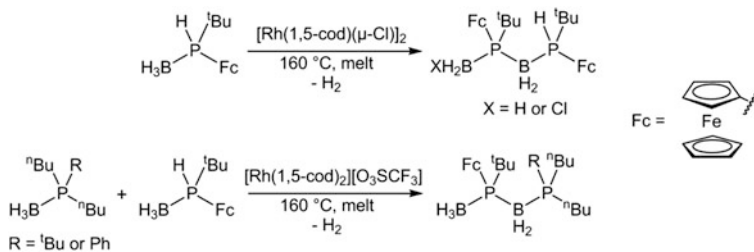


Fig. 18 ^{31}P NMR spectra of monomer $\text{H}_3\text{B} \cdot \text{P}(\text{CH}_2\text{Fc})\text{H}_2$ (a, b) and polymer $[\text{H}_2\text{BP}(\text{CH}_2\text{Fc})\text{H}]_n$ (c, d) in CDCl_3 (161.9 MHz): (a) ^1H -coupled, $^1J_{\text{PH}} = 358$ Hz; (b) ^1H -decoupled; (c) ^1H -coupled, $^1J_{\text{PH}} = 352$ Hz; (d) ^1H -decoupled. Reprinted (adapted) with permission from Pandey et al. [177]. Copyright 2014, John Wiley and Sons



Scheme 71 Rh^{I} -catalysed dehydrocoupling of primary ferrocenyl phosphine–boranes

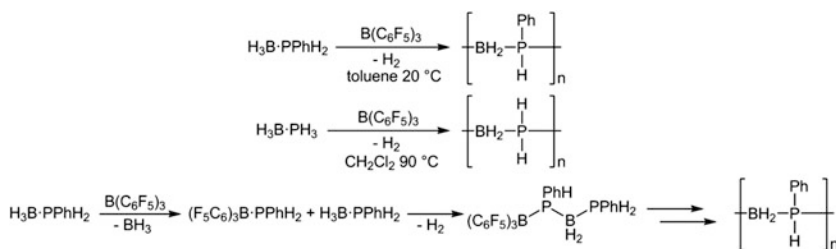


Scheme 72 Catalytic dehydrocoupling of secondary phosphine–boranes bearing ferrocenyl substituents

had been achieved. If a mixture of $\text{H}_3\text{B} \cdot \text{P}^i\text{Bu}(\text{Fc})\text{H}$ and a slight excess of either $\text{H}_3\text{B} \cdot \text{P}^i\text{Bu}(\text{}^n\text{Bu})_2$ or $\text{H}_3\text{B} \cdot \text{PPh}(\text{}^n\text{Bu})_2$ was heated under melt conditions (160°C) with a $[\text{Rh}(1,5\text{-cod})_2][\text{O}_3\text{SCF}_3]$ pre-catalyst (4 mol%), the linear diboraphosphines could be synthesised in moderate isolated yield with the tertiary phosphine in the terminal position due to its lack of P–H functionality (Scheme 72) [178].

3.8 Lewis Acid-Catalysed Dehydrocoupling of Phosphine–Boranes

In 2003 came the first report of a non-transition-metal-catalysed dehydrocoupling of primary phosphine–boranes. The strong Lewis acid $B(C_6F_5)_3$ was used as the catalyst, and heating a solution of $H_3B \cdot PPhH_2$ to $90^\circ C$ in toluene (0.5 mol% catalyst) for 3 h resulted in short oligomers and cyclic species characterised by ^{31}P NMR spectroscopy and size-exclusion chromatography. Alternatively, a longer reaction time at a lower temperature (3 days at $20^\circ C$) resulted in high molecular weight polymeric material. This catalyst was also found to dehydropolymerise $H_3B \cdot PH_3$ (formed from bubbling PH_3 and B_2H_6 through dichloromethane) to form oligomers at $70^\circ C$ and polymer at $90^\circ C$ (Scheme 73). The mechanism of polymerisation was thought to involve an initial exchange reaction of the strong Lewis acid with the BH_3 of one phosphine–borane to form $(C_6F_5)_3B \cdot PPhH_2$. The coordination of the electron-withdrawing group thus increased the acidity of the P–H bond, allowing reaction with the hydridic B–H bond on another phosphine–borane. This argument is similar to that made by Manners et al. for the reason that phosphine–boranes with fluorinated substituents dehydrocouple at lower temperatures than simple aryl phosphine–boranes [179].



Scheme 73 Formation of polyphosphinoboranes using Lewis acid $B(C_6F_5)_3$ as a precatalyst along with a suggested mechanism

4 Future Prospects

It is clear from this review that the mechanistic studies into the dehydrocoupling of amine–boranes and phosphine–boranes have seen a rapid development over the last 5 years, with many systems studied, using catalysts based on metals from across the whole periodic table. The primary driver for this intense research has been the development of catalysts that might offer significant benefits with regard to the kinetics of hydrogen release, for potential use when this gaseous product is linked with a fuel cell. Although it is unlikely that any of these sometimes elegant and well-defined molecular systems would be capable of delivering a truly practicable system for long-term commercial use (i.e. with the constraints of total system weight, cost, extended recyclability, stability, operating conditions), although notable examples do exist of systems that show promise [118], this overarching goal has provided a focus for the elucidation of the mechanism of dehydrocoupling. More likely is that any commercial catalyst will be based around heterogeneous systems that utilise relatively cheap metal–ligand precursors, such as first-row transition metals [47]. Attention is now turning to the use of molecular, single-site catalysts for the closely related dehydropolymerisation of amine–boranes. In this process, the end product of value is the aminoborane, rather than the hydrogen released. It is probable that many of the major developments will likely arise from this area in the near future, as polyaminoboranes (and their closely related polyphosphinoboranes) have an essentially untapped potential with regard to their use as high-performance polymeric materials, as pre-ceramics or as precursors to extended B–N materials, such as white graphene.

Although complex and nuanced, with different catalysts and amine–borane starting materials offering a variety of final products, intermediates and observed catalyst resting states, a number of mechanistic scenarios are now becoming apparent for dehydrocoupling. The intermediate role of aminoboranes is now becoming clear, but whether such species remain associated with the metal centre once formed or are released into solution is still to be completely resolved. This is important as free aminoborane oligomerises to form cyclic products (i.e. borazines), whereas if B–N bond formation at the metal centre is fast, then polymerisation can occur. In some systems aminoborane formation and B–N bond-forming reactions may be closely correlated. Likewise, the propagating species in dehydropolymerisation and dehydrooligomerisation still remain to be fully resolved. Given the regular occurrence of amidoboranes (and phosphidoboranes) with supporting β -B-agostic interactions in many of these mechanistic studies, such species are perhaps likely candidates as key intermediates. If the current pace of discovery continues over the next 5 years, it is likely that the resulting mechanistic insight will lead to the production of catalysts that can dehydrocouple amine–boranes and phosphine–boranes “to order”, to provide high-value bespoke materials such as polyaminoboranes or pre-ceramics in an atom-efficient process, recognising that hydrogen is the only by-product. Indeed, linking such bond-forming processes with hydrogen transfer reactions might prove profitable if it generates two products of value with true 100% atom economy [86]. As recently enunciated [5], the formation

of main-group element–element bonds using catalytic techniques lags behind those developed for carbon–carbon bond-forming reactions that are so important for the synthesis of state-of-the-art organic molecules and macromolecules. The development of robust, and scalable, catalysts for amine–borane and phosphine–borane dehydrocoupling is thus one promising area to develop with regard to opening up the field to all those interested in main-group element–element bond-forming reactions: whether ultimately more interested in the release of gaseous hydrogen from such processes or the products and functional materials that arise directly from such events. Either way, it will certainly be interesting to see how the field develops.

The key intermediate in the dehydrocoupling of $\text{H}_3\text{B} \cdot \text{NH}_3$, B-(cyclotriorazanyl)amine–borane has been synthesized using a Cp_2ZrCl catalyst, allowing for its structural characterization [180].

The kinetics of $\text{H}_3\text{B} \cdot \text{NH}_3$ dehydrogenation using a Os dihydride catalyst have been studied, and show a zero order dependence on amine borane. Calculations suggest a mechanism in which H_2 loss from the catalyst is turnover limiting [181].

Acknowledgment The authors would like to thank EPSRC for the support (EP/J02127X/1).

References

1. Staubitz A, Robertson APM, Sloan ME, Manners I (2010) *Chem Rev* 110:4023
2. Huang Z, Autrey T (2012) *Energy Environ Sci* 5:9257
3. Hügler T, Hartl M, Lentz D (2011) *Chem Eur J* 17:10184
4. Staubitz A, Robertson APM, Manners I (2010) *Chem Rev* 110:4079
5. Leitao EM, Jurca T, Manners I (2013) *Nat Chem* 5:817
6. Liu Z, Song L, Zhao S, Huang J, Ma L, Zhang J, Lou J, Ajayan PM (2011) *Nano Lett* 11:2032
7. Clark TJ, Lee K, Manners I (2006) *Chem Eur J* 12:8634
8. Stephens FH, Pons V, Tom Baker R (2007) *Dalton Trans* 25:2613
9. Ewing WC, Marchione A, Himmelberger DW, Carroll PJ, Sneddon LG (2011) *J Am Chem Soc* 133:17093
10. Waterman R (2013) *Chem Soc Rev* 42:5629
11. Alcaraz G, Sabo-Etienne S (2010) *Angew Chem Int Ed* 49:7170
12. Johnson HC, Leitao EM, Whittell GR, Manners I, Lloyd-Jones GC, Weller AS (2014) *J Am Chem Soc* 136:9078
13. Sewell LJ, Lloyd-Jones GC, Weller AS (2012) *J Am Chem Soc* 134:3598
14. Staubitz A, Soto AP, Manners I (2008) *Angew Chem Int Ed* 47:6212
15. Jaska CA, Temple K, Lough AJ, Manners I (2003) *J Am Chem Soc* 125:9424
16. Pasumansky L, Haddenham D, Clary JW, Fisher GB, Goralski CT, Singaram B (2008) *J Org Chem* 73:1898
17. Johnson HC, Weller AS (2012) *J Organomet Chem* 721:17
18. Garcia-Vivo D, Huergo E, Ruiz MA, Travieso-Puente R (2013) *Eur J Inorg Chem* 4998
19. Stevens CJ, Dallanegra R, Chaplin AB, Weller AS, Macgregor SA, Ward B, McKay D, Alcaraz G, Sabo-Etienne S (2011) *Chem Eur J* 17:3011
20. Leitao EM, Stubbs NE, Robertson APM, Helten H, Cox RJ, Lloyd-Jones GC, Manners I (2012) *J Am Chem Soc* 134:16805
21. Marziale AN, Friedrich A, Klopsch I, Drees M, Celinski VR, Günne J, Schneider S (2013) *J Am Chem Soc* 135:13342
22. Robertson APM, Suter R, Chabanne L, Whittell GR, Manners I (2011) *Inorg Chem* 50:12680

23. Staubitz A, Sloan ME, Robertson APM, Friedrich A, Schneider S, Gates PJ, Günne J, Manners I (2010) *J Am Chem Soc* 132:13332
24. Alcaraz G, Vendier L, Clot E, Sabo-Etienne S (2010) *Angew Chem Int Ed* 49:918
25. Pons V, Baker RT, Szymczak NK, Heldebrant DJ, Linehan JC, Matus MH, Grant DJ, Dixon DA (2008) *Chem Commun* 6597
26. Jaska CA, Temple K, Lough AJ, Manners I (2001) *Chem Commun* 962
27. Denney MC, Pons V, Hebden TJ, Heinekey DM, Goldberg KI (2006) *J Am Chem Soc* 128:12048
28. Robertson APM, Leitao EM, Jurca T, Haddow MF, Helten H, Lloyd-Jones GC, Manners I (2013) *J Am Chem Soc* 135:12670
29. Bhunya S, Malakar T, Paul A (2014) *Chem Commun* 50:5919
30. Friedrich A, Drees M, Schneider S (2009) *Chem Eur J* 15:10339
31. Dallanegra R, Chaplin AB, Tsim J, Weller AS (2010) *Chem Commun* 46:3092
32. Sewell LJ, Huertos MA, Dickinson ME, Weller AS, Lloyd-Jones GC (2013) *Inorg Chem* 52:4509
33. Johnson HC, Robertson APM, Chaplin AB, Sewell LJ, Thompson AL, Haddow MF, Manners I, Weller AS (2011) *J Am Chem Soc* 133:11076
34. Chen X, Zhao J-C, Shore SG (2010) *J Am Chem Soc* 132:10658
35. Ewing WC, Carroll PJ, Sneddon LG (2013) *Inorg Chem* 52:10690
36. Himmelberger DW, Yoon CW, Bluhm ME, Carroll PJ, Sneddon LG (2009) *J Am Chem Soc* 131:14101
37. Green IG, Johnson KM, Roberts BP (1989) *J Chem Soc Perkin Trans* 2:1963
38. Widegren JA, Finke RG (2003) *J Mol Catal A Chem* 198:317
39. Jaska CA, Manners I (2004) *J Am Chem Soc* 126:9776
40. Chen YS, Fulton JL, Linehan JC, Autrey T (2005) *J Am Chem Soc* 127:3254
41. Sonnenberg JF, Morris RH (2013) *ACS Catal* 3:1092
42. Duman S, Ozkar S (2013) *Int J Hydrog Energy* 38:10000
43. Zahmakiran M, Philippot K, Ozkar S, Chaudret B (2012) *Dalton Trans* 41:590
44. Zahmakiran M, Ozkar S (2009) *Inorg Chem* 48:8955
45. Zahmakiran M, Ayvali T, Philippot K (2012) *Langmuir* 28:4908
46. He T, Wang JH, Wu GT, Kim H, Proffen T, Wu AA, Li W, Liu T, Xiong ZT, Wu CZ, Chu HL, Guo JP, Autrey T, Zhang T, Chen P (2010) *Chem Eur J* 16:12814
47. Luo W, Campbell PG, Zakharov LN, Liu SY (2011) *J Am Chem Soc* 133:19326
48. Luo W, Neiner D, Karkamkar A, Parab K, Garner III EB, Dixon DA, Matson D, Autrey T, Liu S-Y (2013) *Dalton Trans* 42:611
49. Campbell PG, Ishibashi JSA, Zakharov LN, Liu S-Y (2014) *Aust J Chem* 67:521
50. Vance JR, Robertson APM, Lee K, Manners I (2011) *Chem Eur J* 17:4099
51. Vance JR, Schafer A, Robertson APM, Lee K, Turner J, Whittell GR, Manners I (2014) *J Am Chem Soc* 136:3048
52. Bluhm ME, Bradley MG, Butterick R, Kusari U, Sneddon LG (2006) *J Am Chem Soc* 128:7748
53. Himmelberger DW, Alden LR, Bluhm ME, Sneddon LG (2009) *Inorg Chem* 48:9883
54. Wright WRH, Berkeley ER, Alden LR, Baker RT, Sneddon LG (2011) *Chem Commun* 47:3177
55. Mal SS, Stephens FH, Baker RT (2011) *Chem Commun* 47:2922
56. Boulho C, Djukic J-P (2010) *Dalton Trans* 39:8893
57. Kass M, Friedrich A, Drees M, Schneider S (2009) *Angew Chem Int Ed* 48:905
58. Conley BL, Williams TJ (2010) *Chem Commun* 46:4815
59. Blaquiere N, Diallo-Garcia S, Gorelsky SI, Black DA, Fagnou K (2008) *J Am Chem Soc* 130:14034
60. Kubas GJ (2001) *Metal dihydrogen and σ -bond complexes*. Kluwer, New York
61. Shimoi M, Nagai S, Ichikawa M, Kawano Y, Katoh K, Uruichi M, Ogino H (1999) *J Am Chem Soc* 121:11704
62. Johnson HC, McMullin CL, Pike SD, Macgregor SA, Weller AS (2013) *Angew Chem Int Ed* 52:9776

63. Ledger AEW, Ellul CE, Mahon MF, Williams MJ, Whittlesey MK (2011) *Chem Eur J* 17:8704
64. Tang CY, Thompson AL, Aldridge S (2010) *J Am Chem Soc* 132:10578
65. Dallanegra R, Robertson APM, Chaplin AB, Manners I, Weller AS (2011) *Chem Commun* 47:3763
66. Douglas TM, Chaplin AB, Weller AS, Yang XZ, Hall MB (2009) *J Am Chem Soc* 131:15440
67. Chaplin AB, Weller AS (2011) *Acta Cryst Sect C Cryst Struct Commun* 67:M355
68. Baker RT, Gordon JC, Hamilton CW, Henson NJ, Lin PH, Maguire S, Murugesu M, Scott BL, Smythe NC (2012) *J Am Chem Soc* 134:5598
69. Sloan ME, Staubitz A, Clark TJ, Russell CA, Lloyd-Jones GC, Manners I (2010) *J Am Chem Soc* 132:3831
70. Kumar A, Johnson HC, Hooper TN, Weller AS, Algarra AG, Macgregor SA (2014) *Chem Sci* 5:2546
71. Chaplin AB, Weller AS (2010) *Angew Chem Int Ed* 49:581
72. Dallanegra R, Chaplin AB, Weller AS (2009) *Angew Chem Int Ed* 48:6875
73. Corcoran EW, Sneddon LG (1984) *J Am Chem Soc* 106:7793
74. Corcoran EW, Sneddon LG (1985) *J Am Chem Soc* 107:7446
75. Ciobanu O, Kaifer E, Enders M, Himmel HJ (2009) *Angew Chem Int Ed* 48:5538
76. Braunschweig H, Guethlein F (2011) *Angew Chem Int Ed* 50:12613
77. Braunschweig H, Claes C, Guethlein F (2012) *J Organomet Chem* 706:144
78. Braunschweig H, Brenner P, Dewhurst RD, Guethlein F, Jimenez-Halla JOC, Radacki K, Wolf J, Zollner L (2012) *Chem Eur J* 18:8605
79. Kim S-K, Han W-S, Kim T-J, Kim T-Y, Nam SW, Mitoraj M, Piekoś Ł, Michalak A, Hwang S-J, Kang SO (2010) *J Am Chem Soc* 132:9954
80. Alcaraz G, Chaplin AB, Stevens CJ, Clot E, Vendier L, Weller AS, Sabo-Etienne S (2010) *Organometallics* 29:5591
81. Tang CY, Thompson AL, Aldridge S (2010) *Angew Chem Int Ed* 49:921
82. Tang CY, Phillips N, Bates JI, Thompson AL, Gutmann MJ, Aldridge S (2012) *Chem Commun* 48:8096
83. Vidovic D, Addy DA, Kramer T, McGrady J, Aldridge S (2011) *J Am Chem Soc* 133:8494
84. MacInnis MC, McDonald R, Ferguson MJ, Tobisch S, Turculet L (2011) *J Am Chem Soc* 133:13622
85. Cassen A, Gloaguen Y, Vendier L, Duhayon C, Poblador-Bahamonde A, Raynaud C, Clot E, Alcaraz G, Sabo-Etienne S (2014) *Angew Chem Int Ed* 53:7569
86. Jiang YF, Blacque O, Fox T, Frech CM, Berke H (2009) *Organometallics* 28:5493
87. Alcaraz G, Grellier M, Sabo-Etienne S (2009) *Acc Chem Res* 42:1640
88. Clark TJ, Russell CA, Manners I (2006) *J Am Chem Soc* 128:9582
89. Luo Y, Ohno K (2007) *Organometallics* 26:3597
90. Forster TD, Tuononen HM, Parvez M, Roesler R (2009) *J Am Chem Soc* 131:6689
91. Wolstenholme DJ, Traboulsee KT, Decken A, McGrady GS (2010) *Organometallics* 29:5769
92. Helten H, Dutta B, Vance JR, Sloan ME, Haddow MF, Sproules S, Collison D, Whittell GR, Lloyd-Jones GC, Manners I (2013) *Angew Chem Int Ed* 52:437
93. Beweries T, Hansen S, Kessler M, Klahn M, Rosenthal U (2011) *Dalton Trans* 40:7689
94. Beweries T, Thomas J, Klahn M, Schulz A, Heller D, Rosenthal U (2011) *ChemCatChem* 3:1865
95. Pun D, Lobkovsky E, Chirik PJ (2007) *Chem Commun* 2397
96. Miyazaki T, Tanabe Y, Yuki M, Miyake Y, Nishibayashi Y (2011) *Organometallics* 30:2394
97. Rousseau R, Schenter GK, Fulton JL, Linehan JC, Engelhard MH, Autrey T (2009) *J Am Chem Soc* 131:10516
98. Kawano Y, Uruichi M, Shimoi M, Taki S, Kawaguchi T, Kakizawa T, Ogino H (2009) *J Am Chem Soc* 131:14946
99. Hebden TJ, Denney MC, Pons V, Piccoli PMB, Koetzle TF, Schultz AJ, Kaminsky W, Goldberg KI, Heinekey DM (2008) *J Am Chem Soc* 130:10812
100. Dietrich BL, Goldberg KI, Heinekey DM, Autrey T, Linehan JC (2008) *Inorg Chem* 47:8583
101. Paul A, Musgrave CB (2007) *Angew Chem Int Ed* 46:8153

102. Keaton RJ, Blacquiere JM, Baker RT (2007) *J Am Chem Soc* 129:1844
103. Yang X, Hall MB (2008) *J Am Chem Soc* 130:1798
104. Yang X, Hall MB (2009) *J Organomet Chem* 694:2831
105. Zimmerman PM, Paul A, Musgrave CB (2009) *Inorg Chem* 48:5418
106. Zimmerman PM, Paul A, Zhang Z, Musgrave CB (2009) *Angew Chem Int Ed* 48:2201
107. Ai D, Guo Y, Liu W, Wang Y (2014) *J Phys Org Chem* 27:597
108. Douglas TM, Chaplin AB, Weller AS (2008) *J Am Chem Soc* 130:14432
109. Rossin A, Bottari G, Lozano-Vila AM, Paneque M, Peruzzini M, Rossi A, Zanobini F (2013) *Dalton Trans* 42:3533
110. Robertson APM, Leitao EM, Manners I (2011) *J Am Chem Soc* 133:19322
111. Butera V, Russo N, Sicilia E (2014) *ACS Catal* 4:1104
112. Vogt M, de Bruin B, Berke H, Trincado M, Grützmacher H (2011) *Chem Sci* 2:723
113. Wallis CJ, Dyer H, Vendier L, Alcaraz G, Sabo-Etienne S (2012) *Angew Chem Int Ed* 51:3646
114. Chen X, Zhao J-C, Shore SG (2013) *Acc Chem Res* 46:2666
115. Johnson HC, Leitao EM, Whittell GR, Manners I, Lloyd-Jones GC, Weller AS (2014) *J Am Chem Soc* 134:1520
116. Kubas GJ (2004) *Adv Inorg Chem* 56:127
117. Lu ZY, Conley BL, Williams TJ (2012) *Organometallics* 31:6705
118. Conley BL, Guess D, Williams TJ (2011) *J Am Chem Soc* 133:14212
119. Schreiber DF, O'Connor C, Grave C, Ortin Y, Muller-Bunz H, Phillips AD (2012) *ACS Catal* 2:2505
120. Phillips AD, Laurenczy G, Scopelliti R, Dyson PJ (2007) *Organometallics* 26:1120
121. Chapman AM, Haddow MF, Wass DF (2011) *J Am Chem Soc* 133:8826
122. Rosello-Merino M, López-Serrano J, Conejero S (2013) *J Am Chem Soc* 135:10910
123. Stubbs NE, Robertson APM, Leitao EM, Manners I (2013) *J Organomet Chem* 730:84
124. Xiong ZT, Yong CK, Wu GT, Chen P, Shaw W, Karkamkar A, Autrey T, Jones MO, Johnson SR, Edwards PP, David WIF (2008) *Nat Mater* 7:138
125. Diyabalana HVK, Shrestha RP, Semelsberger TA, Scott BL, Bowden ME, Davis BL, Burrell AK (2007) *Angew Chem Int Ed* 46:8995
126. Spielmann J, Jansen G, Bandmann H, Harder S (2008) *Angew Chem Int Ed* 47:6290
127. Spielmann J, Harder S (2009) *J Am Chem Soc* 131:5064
128. Spielmann J, Piesik D, Wittkamp B, Jansen G, Harder S (2009) *Chem Commun* 3455
129. Spielmann J, Bolte M, Harder S (2009) *Chem Commun* 6934
130. Spielmann J, Piesik DFJ, Harder S (2010) *Chem Eur J* 16:8307
131. Bellham P, Hill MS, Kociok-Kohn G, Liptrot DJ (2013) *Chem Commun* 49:1960
132. Liptrot DJ, Hill MS, Mahon MF, MacDougall DJ (2010) *Chem Eur J* 16:8508
133. Bellham P, Hill MS, Kociok-Köhn G (2014) *Organometallics*. doi:[10.1021/om500467b](https://doi.org/10.1021/om500467b)
134. Butera V, Russo N, Sicilia E (2014) *Chem Eur J* 20:5967
135. Hill MS, Kociok-Kohn G, Robinson TP (2010) *Chem Commun* 46:7587
136. Lu E, Yuan Y, Chen Y, Xia W (2013) *ACS Catal* 3:521
137. Hill MS, Hodgson M, Liptrot DJ, Mahon MF (2011) *Dalton Trans* 40:7783
138. Cui P, Spaniol TP, Maron L, Okuda J (2013) *Chem Eur J* 19:13437
139. Cowley HJ, Holt MS, Melen RL, Rawson JM, Wright DS (2011) *Chem Commun* 47:2682
140. Hansmann MM, Melen RL, Wright DS (2011) *Chem Sci* 2:1554
141. Less RJ, Simmonds HR, Dane SBJ, Wright DS (2013) *Dalton Trans* 42:6337
142. Harder S, Spielmann J (2011) *Chem Commun* 47:11945
143. Erickson KA, Wright DS, Waterman R (2014) *J Organomet Chem* 751:541
144. Daly SR, Bellott BJ, Kim DY, Girolami GS (2010) *J Am Chem Soc* 132:7254
145. Welch GC, Juan RRS, Masuda JD, Stephan DW (2006) *Science* 314:1124
146. Stephan DW, Erker G (2010) *Angew Chem Int Ed* 49:46
147. Miller AJM, Bercaw JE (2010) *Chem Commun* 46:1709
148. Whittell GR, Balmoud EI, Robertson APM, Patra SK, Haddow MF, Manners I (2010) *Eur J Inorg Chem* 3967

149. Appelt C, Slootweg JC, Lammertsma K, Uhl W (2013) *Angew Chem Int Ed* 52:4256
150. Burg AB, Wagner RI (1953) *J Am Chem Soc* 75:3872
151. Burg AB (1959) *J Inorg Nuc Chem* 11:258
152. Dorn H, Singh RA, Massey JA, Lough AJ, Manners I (1999) *Angew Chem Int Ed* 38:3321
153. Dorn H, Singh RA, Massey JA, Nelson JM, Jaska CA, Lough AJ, Manners I (2000) *J Am Chem Soc* 122:6669
154. Dorn H, Vejsovic E, Lough AJ, Manners I (2001) *Inorg Chem* 40:4327
155. Dorn H, Rodezno JM, Brunnhöfer B, Rivard E, Massey JA, Manners I (2003) *Macromolecules* 36:291
156. Jaska CA, Manners I (2004) *J Am Chem Soc* 126:1334
157. Snow SA, Shimoi M, Ostler CD, Thompson BK, Kodama G, Parry RW (1984) *Inorg Chem* 23:511
158. McNamara WF, Duesler EN, Paine RT, Ortiz JV, Koelle P, Noeth H (1986) *Organometallics* 5:380
159. Frank N, Hanau K, Flosdorf K, Langer R (2013) *Dalton Trans* 42:11252
160. Merle N, Koicok-Köhn G, Mahon MF, Frost CG, Ruggiero GD, Weller AS, Willis MC (2004) *Dalton Trans* 3883
161. Kawano Y, Yamaguchi K, Miyake S-y, Kakizawa T, Shimoi M (2007) *Chem Eur J* 13:6920
162. Macías R, Rath NP, Barton L (1999) *Angew Chem Int Ed* 38:162
163. Volkov O, Macías R, Rath NP, Barton L (2002) *Inorg Chem* 41:5837
164. Ingleson M, Patmore NJ, Ruggiero GD, Frost CG, Mahon MF, Willis MC, Weller AS (2001) *Organometallics* 20:4434
165. Shuttleworth TA, Huertos MA, Pernik I, Young RD, Weller AS (2013) *Dalton Trans* 42:12917
166. Jaska CA, Dorn H, Lough AJ, Manners I (2003) *Chem Eur J* 9:271
167. Jaska CA, Lough AJ, Manners I (2005) *Dalton Trans* 326
168. Paine RT, Noeth H (1995) *Chem Rev* 95:343
169. Vogel U, Hoemensch P, Schwan K-C, Timoshkin AY, Scheer M (2003) *Chem Eur J* 9:515
170. Schwan K-C, Timoshkin AY, Zabel M, Scheer M (2006) *Chem Eur J* 12:4900
171. Thoms C, Marquardt C, Timoshkin AY, Bodensteiner M, Scheer M (2013) *Angew Chem Int Ed* 52:5150
172. Lee K, Clark TJ, Lough AJ, Manners I (2008) *Dalton Trans* 2732
173. Huertos MA, Weller AS (2012) *Chem Commun* 48:7185
174. Huertos MA, Weller AS (2013) *Chem Sci* 4:1881
175. Hooper TN, Huertos MA, Jurca T, Pike SD, Weller AS, Manners I (2014) *Inorg Chem* 53:3716
176. Clark TJ, Rodezno JM, Clendenning SB, Aouba S, Brodersen PM, Lough AJ, Ruda HE, Manners I (2005) *Chem Eur J* 11:4526
177. Pandey S, Lonneck P, Hey-Hawkins E (2014) *Eur J Inorg Chem* 2456
178. Pandey S, Lonneck P, Hey-Hawkins E (2014) *Inorg Chem* 53:8242
179. Denis JM, Forintos H, Szelke H, Toupet L, Pham TN, Madec PJ, Gaumont AC (2003) *Chem Commun* 54
180. Kalviri HA, Gartner F, Ye G, Korobkov I, Baker RT (2014) *Chem Sci* 6:618
181. Esteruelas MA, Lopez AM, Mora M, Onate E (2014) *ACS Catal* 5:187

At the Forefront of the Suzuki–Miyaura Reaction: Advances in Stereoselective Cross-Couplings

Ho-Yan Sun and Dennis G. Hall

Contents

1	Introduction	222
2	Applications to the Synthesis of Enantioenriched Atropisomers	224
3	Mechanistic Considerations in the Suzuki–Miyaura Cross-Coupling of sp^3 Centres	227
3.1	Challenges Associated with the Coupling of Saturated Carbon Centres	227
3.2	Stereochemistry of Various Steps in the Suzuki–Miyaura Cross-Coupling Mechanism	228
4	Stereoselective $C(sp^3)$ – $C(sp^2)$ Suzuki–Miyaura Cross-Coupling Reactions	229
4.1	Stereoselective Couplings of Alkyl Boronates with Aryl or Alkenyl Halides	229
4.2	Stereoselective Couplings of Alkyl Halides and Pseudohalides with Aryl or Alkenyl Boronates	234
5	Stereoselective $C(sp^3)$ – $C(sp^3)$ Suzuki–Miyaura Cross-Coupling Reactions	237
5.1	Stereoselective Couplings of Alkyl Boranes with Alkyl Halides	238
6	Summary and Outlook	239
	References	240

Abstract The synthesis of optically enriched compounds is a continuing challenge in organic synthesis. While the Suzuki–Miyaura cross-coupling has been used extensively in the construction of sp^2 – sp^2 bonds, only recently has it come to prominence as a useful means to construct stereogenic centres. This chapter describes the latest achievements in the development of stereoselective Suzuki–

H.-Y. Sun • D.G. Hall (✉)

Department of Chemistry, University of Alberta, 11227 Saskatchewan Drive, Edmonton, AB T6G 2G2, Canada

e-mail: dennis.hall@ualberta.ca

© Springer International Publishing Switzerland 2015

E. Fernández, A. Whiting (eds.), *Synthesis and Application of Organoboron Compounds*, Topics in Organometallic Chemistry 49,
DOI 10.1007/978-3-319-13054-5_7

221

Miyaura cross-coupling reactions, including advances made both in atroposelective couplings as well as stereoselective C(sp³) couplings. Focus is also given to the mechanistic details of these cross-coupling processes.

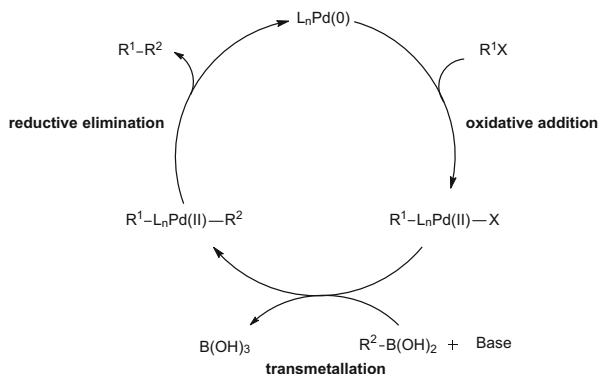
Keywords Catalysis • C–C bond formation • Cross-coupling • Nickel • Organoboron reagents • Palladium • Stereoselectivity

1 Introduction

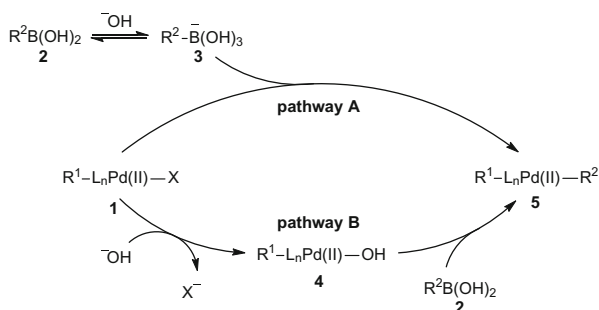
As carbon–carbon bonds make up the framework of most organic molecules, the construction of these bonds lies at the heart of organic synthesis. For over a century, chemists have been in pursuit of various means to construct carbon–carbon bonds, which has led to landmark discoveries like the aldol condensation, Wittig olefination and Friedel–Crafts alkylations, to name only a few. In current times, the formation of carbon–carbon bonds through transition metal-catalysed cross-coupling reactions has found ubiquity in organic synthesis, having been employed in a broad selection of research areas including medicinal chemistry, materials and nanotechnology and agrochemistry. The value of this class of reactions is evidenced by the awarding of the 2010 Nobel Prize in Chemistry to Richard Heck, Ei-ichi Negishi and Akira Suzuki for their contributions to developing Pd-catalysed cross-coupling reactions. Among these processes, the Suzuki–Miyaura reaction, which involves the coupling of an organoboron reagent with an organohalide partner, has become a fundamental synthetic tool in both academic and industrial settings [1, 2]. Its success may be attributed to several factors: the general ease of accessibility of organoboron reagents, the robustness of these reagents, allowing for mild reaction conditions and good functional group tolerance, and the generation of non-toxic by-products such as boric acid. Over the years, the use of the Suzuki–Miyaura reaction for the construction of sp²–sp² bonds in “flat” compounds has been thoroughly studied, and this process is now considered to be well understood. In contrast, there are far fewer examples of applying the Suzuki–Miyaura cross-coupling towards the generation of axial chirality or stereogenic carbon centres due to various mechanistic challenges associated with these processes.

In order to assess the challenges of stereoselective Suzuki–Miyaura cross-couplings, an understanding of the reaction mechanism is required. The generally accepted mechanism of the Suzuki–Miyaura cross-coupling involves three key steps: oxidative addition, transmetallation and reductive elimination (Scheme 1). While the oxidative addition and reductive elimination processes are considered to be well understood, transmetallation, in contrast, has been significantly less studied. To date, there have been two main proposed pathways for the transmetallation step of the Suzuki–Miyaura reaction (Scheme 2), both of which have been corroborated by various computational studies [3–12]. The first involves the coordination of a preformed borate **3** to the product of oxidative addition, R¹PdX **1**, to eventually

Scheme 1 General mechanism for a Suzuki–Miyaura cross-coupling reaction



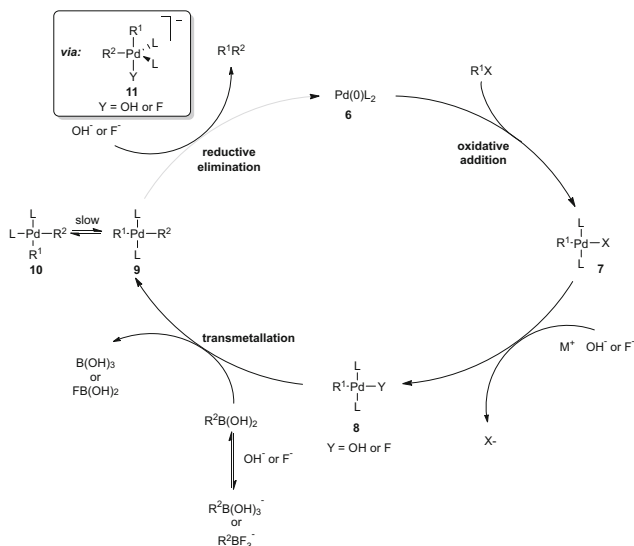
Scheme 2 Proposed pathways for transmetalation



give the transmetalated Pd intermediate **5**. The second pathway proposes that transmetalation occurs between the palladium hydroxo complex **4** and the neutral boronic acid **2**.

Recently, independent efforts have been made by the Amatore [13, 14] and Hartwig [15] groups towards a more thorough understanding of the transmetalation process leading to the formation of key complex **5**. The Hartwig group provided a quantitative assessment of the rates of pathways A and B by isolating key catalytic intermediates and using these intermediates in various stoichiometric and catalytic studies. The chosen reaction conditions used common ligands such as PPh_3 and PCy_3 and mild base like K_2CO_3 in aqueous THF, which is representative of some of the most common reaction conditions for Suzuki–Miyaura reactions. These studies showed that the rate of reaction of hydroxo complex **4** with neutral boronic acid is several orders of magnitude faster than the reaction of halide complex **1** with borate **3**, suggesting pathway B as the dominant pathway for transmetalation. These conclusions, however, do not rule out pathway A for systems employing other metal/ligand systems or systems which employ stronger bases and would thus have higher concentrations of borate.

In line with Hartwig's findings, the Amatore group used electrochemical techniques to obtain kinetic data that also indicated that reaction of **4** with boronic acid was much more rapid than the reaction of the halide complex **1** with the borate

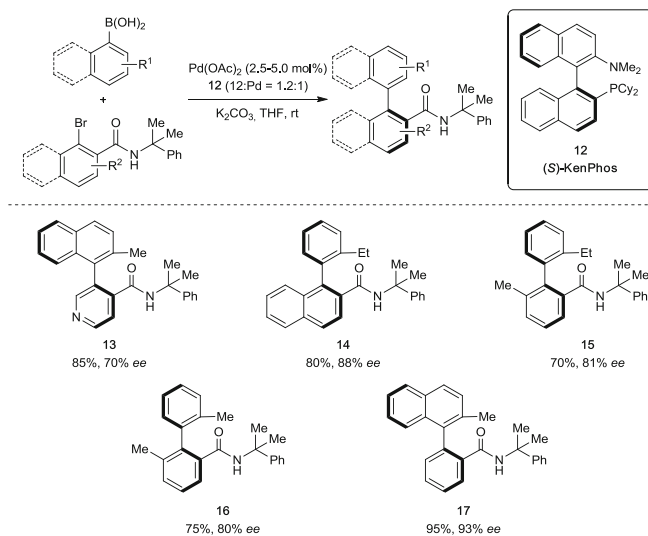


Scheme 3 Detailed catalytic cycle as proposed by the Amatore group

species [13]. In addition to forming the palladium hydroxo species, the Amatore group also identified a secondary role for hydroxide ion in the acceleration of the reductive elimination step through promoting the formation of pentacoordinate complex **11** (Scheme 3). In the absence of base, the product of transmetalation was found to be the *trans*-complex **9**, which needs to isomerize to the corresponding *cis*-complex **10** prior to reductive elimination. Previous work from this group [16] has shown that **9** is energetically more stable than **10**, thus this isomerization is often slow and can potentially reduce the overall reaction rate. This problem is avoided when base is used, as hydroxide will coordinate to palladium to give pentacoordinated palladium complex **11** which can then undergo facile reductive elimination to give the cross-coupled product and regenerated Pd(0) catalyst. In a more recent report, the Amatore group reported that fluoride may behave similarly to hydroxide in the catalytic cycle [14].

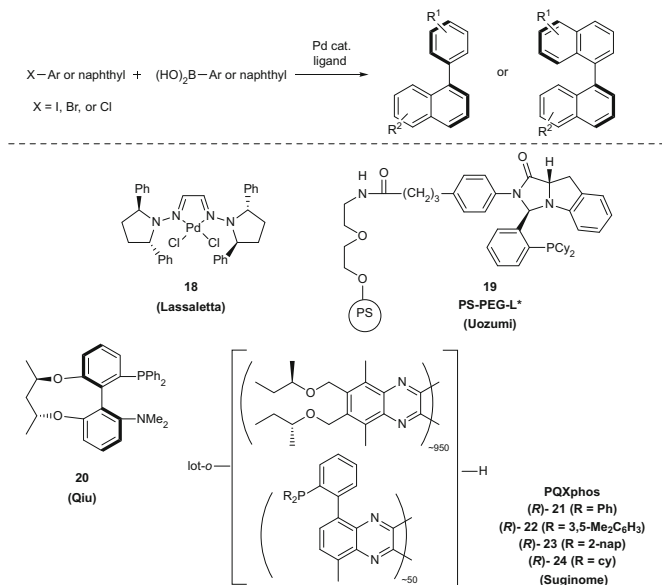
2 Applications to the Synthesis of Enantioenriched Atropisomers

While the use of the Suzuki–Miyaura cross-coupling reaction to form planar C(sp²)–C(sp²) bonds has been well established, it is only in recent years that significant progress has been made in its application towards generating biaryl compounds containing axial chirality [17–19]. Axially chiral biaryl compounds constitute an important class of organic molecules. They are structural components of a number of natural products such as the antibiotic drug vancomycin, and, as



Scheme 4 Buchwald's enantioselective synthesis of axially chiral biaryls

exemplified with the famed ligands Binap and Binol, they are tremendously useful in asymmetric catalysis [20–22]. Transition metal-catalysed asymmetric cross-couplings represent a potentially effective class of reactions for the synthesis of atropisomeric biaryl compounds. Biaryl compounds, however, can display atropisomerism only if there is a significant rotational barrier between the two aryl units. In other words, there must be a high degree of steric hindrance at the *ortho*-positions of the arenes. This requirement makes the cross-coupling between two different, hindered aryl units challenging. While a number of diastereoselective approaches have been reported using coupling partners with pre-embedded chirality, the challenge of enantioselective cross-coupling using chiral catalysts is even greater. Despite these hurdles, many groups have reported advances towards efficient atroposelective Suzuki–Miyaura cross-coupling reactions with different chiral ligands [23–30]. Buchwald and co-workers were the first to report the use of an effective chiral ligand, KenPhos **12**, to cross-couple aryl halides and arylboronic acids to form atropisomeric biaryls with up to 92% enantiomeric excess [31]. In 2010, the same group conducted a comprehensive study on the scope of cross-coupling reactions with KenPhos **12** (Scheme 4) [32]. Variations on the functionalities at the *ortho*-position of the naphthyl halides were explored, and the reaction conditions were found to tolerate functional groups such as phosphonates, phosphine oxides and amides. High yields with enantioselectivities ranging from 88 to 93% *ee* were observed, and the origin of the stereoselectivity was examined using DFT calculations. According to these studies, the high atroposelectivity arises from a combination of weak H-bonding effects and steric interactions in the transition structure for the selectivity-determining reductive elimination step. All attempts to install carboxyester groups at the *ortho*-position of aryl halides, however, only resulted in low enantiomeric excesses. In 2008,



Scheme 5 Synthesis of atropisomers through Suzuki–Miyaura cross-coupling reactions

the Lassaletta group was able to achieve highly atroposelective Suzuki–Miyaura cross-coupling reactions by using chiral bis-hydrazones **18** as chiral ligands (Scheme 5) [33]. While various chiral biaryls could be synthesized with excellent yields and enantioselectivities, the functional groups studied in this communication were restricted to methyl and methoxy substituents.

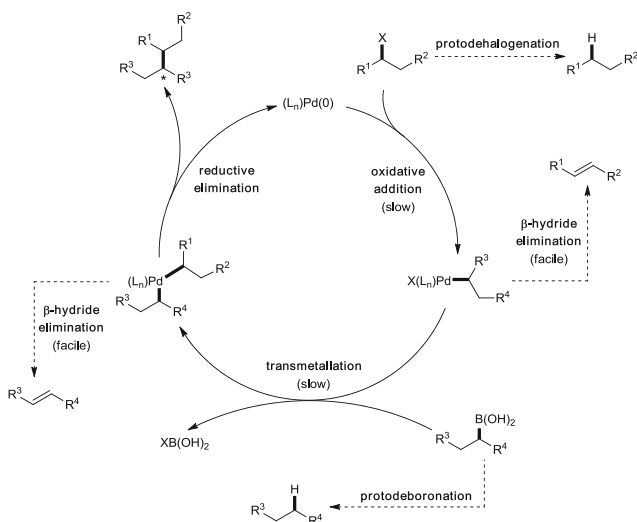
In 2009, an environmentally attractive system for highly enantioselective Suzuki–Miyaura cross-coupling reactions was developed by Uozumi and co-workers [34]. The authors immobilized imidazoleindole dicyclohexylphosphine to an amphiphilic polystyrene–poly(ethylene glycol) copolymer (PS–PEG) resin **19** and employed this catalyst in Suzuki–Miyaura cross-coupling reactions in water. Under the optimized conditions, a variety of biaryls were obtained in excellent enantiomeric excesses. It is important to note here that since the catalyst is immobilized onto PS-PEG, it is recyclable and therefore greatly enhances the economic aspects associated with the reaction. Recently, Suginome and co-workers employed helical chiral polymer PQXPhos **21–24** for the asymmetric syntheses of biaryls through Suzuki–Miyaura cross-coupling reactions [35]. By using these chiral ligands as catalysts, numerous biaryls bearing *ortho*-phosphonate groups could be synthesized with excellent enantiomeric excesses. Interestingly, simply by heating the (*P*)-(*R*)-PQXPhos **23** in 1,1,2-trichloroethane and THF, the left-handed polymer (*M*)-(*R*)-PQXPhos could be obtained. This catalyst also demonstrated catalytic abilities in promoting atroposelective Suzuki–Miyaura cross-couplings, affording the biaryl products as the opposite enantiomers in similar levels of enantioselectivity. The optical properties of this chirality-switchable polymeric ligand were subsequently studied in detail [36].

3 Mechanistic Considerations in the Suzuki–Miyaura Cross-Coupling of sp^3 Centres

3.1 Challenges Associated with the Coupling of Saturated Carbon Centres

In contrast to the well-established $C(sp^2)–C(sp^2)$ coupling, the coupling of sp^3 centres using the Suzuki–Miyaura cross-coupling has remained somewhat elusive. The challenge of these couplings lies in mechanistic pitfalls at various stages in the catalytic cycle (Scheme 6). The oxidative addition of the metal catalyst into the $C–X$ bond of an alkyl halide has been observed to be slower than the aryl/alkenyl counterpart [37–43]. Aryl and alkenyl groups also have the added advantage of π -stabilizing interactions with the empty d-orbitals of the transition metal. The absence of this interaction in alkyl couplings results in a less stable $C–M$ bond, which will be prone to undergo various side reactions such as protodehalogenation or β -hydride elimination [37–43].

Similarly, when performing a cross-coupling reaction of a sp^3 alkyl borane or boronate, the transmetalation step can be slow due to steric hindrance, especially in the case of secondary alkyl boranes and boronates [2]. In this case, protodeboronation becomes a competing side reaction, resulting in the frequent need for the use of excess organoboron reagent. In addition to protodeboronation, the transmetalated organometallic intermediate is also at risk of undergoing undesired β -hydride elimination, if the reductive elimination step is too slow. Most of the initial reports on the coupling of secondary alkyl boronates have been limited to cyclopropyl boronic acids [44]. The unique carbon hybridization of these



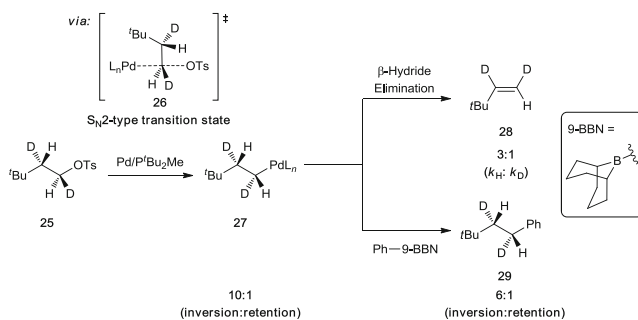
Scheme 6 Mechanistic challenges in sp^3 Suzuki–Miyaura cross-coupling reactions

substrates imparts significant *s*-character to the exocyclic C–B bond thus making the cross-coupling of these compounds more similar to the coupling of sp^2 boronates.

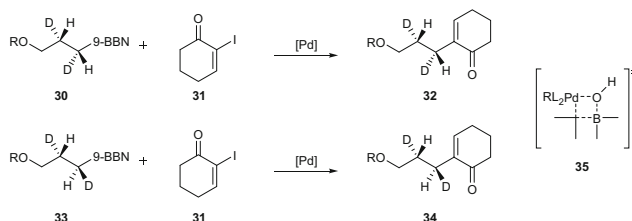
Despite these challenges, advances have been made in the area of sp^3 couplings. The first catalytic cross-coupling of an alkyl borane with aryl or alkenyl halides was reported by Suzuki and Miyaura in 1986 [45], and since then, numerous other alkyl Suzuki–Miyaura reactions have been developed and studied [38, 44, 46–58]. It is only recently, however, that significant advances have been made in the area of stereoselective sp^3 cross-couplings.

3.2 Stereochemistry of Various Steps in the Suzuki–Miyaura Cross-Coupling Mechanism

When designing a stereoselective cross-coupling reaction, the stereochemical consequence of each individual step of the catalytic cycle must be considered since every stage could have a potential impact on the overall outcome of the reaction. Studies have shown that the oxidative addition of palladium into an alkyl halide C–X bond occurs via an S_N2 -type mechanism (Scheme 7) [59–61]. The stereochemical outcome of the oxidative addition step was studied by Fu and co-workers in 2002 through a deuterium labelling study (Scheme 7). Diastereomerically pure tosylate **25** was treated with Pd/ P^t Bu₂Me in the absence of the organoborane coupling partner and base, and the olefins resulting from oxidative addition followed by β -hydride elimination were then examined. Based on NMR analysis of the products, it was found that oxidative addition occurred primarily with overall inversion of configuration [26]. Since β -hydride elimination is known to proceed with the hydride and palladium in a *syn*-conformation, the stereochemistry of the oxidative addition step may be inferred by the stereochemistry of the olefin products, which is analyzable by NMR. The authors then went on to explore the stereochemical course of the coupling of **27** with an organoborane. It was found that the coupled product occurs primarily with inversion of configuration. Since oxidative addition was found to occur with inversion of stereochemistry and reductive



Scheme 7 Stereochemical studies showing evidence of an invertive oxidative addition step



Scheme 8 Stereochemical studies showing evidence of a retentive transmetallation step

elimination is well-known to occur in a stereoretentive manner [62], these results are indicative of a stereoretentive transmetallation step.

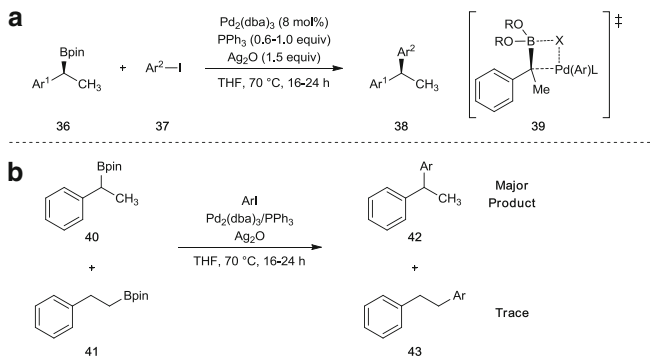
The stereochemistry of the transmetallation step in the Suzuki–Miyaura coupling of aryl and alkenyl halides with sp^3 organoboranes was independently studied by Woerpel [63] and Soderquist [64], and more recently by Jarvo [65]. Deuterium-labelled substrates **30** and **33** were subjected to the coupling conditions and revealed a stereoretentive transmetallation step, leading to products **32** and **34**, respectively (Scheme 8). This observation was attributed to a 4-membered transition state **35**, which was first proposed by Soderquist in 1998 [64].

4 Stereoselective $C(sp^3)$ – $C(sp^2)$ Suzuki–Miyaura Cross-Coupling Reactions

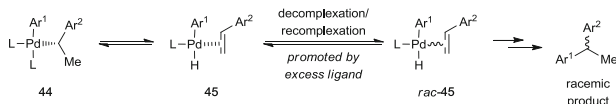
4.1 Stereoselective Couplings of Alkyl Boronates with Aryl or Alkenyl Halides

Due in part to their versatility as synthetic intermediates towards the synthesis of enantioenriched alcohols and amines via C–B bond oxidation, significant efforts, in recent years, have been placed into the synthesis of optically enriched organoboron compounds. With improved access to these substrates [66], optically enriched organoboronates have emerged as useful substrates in stereoselective Suzuki–Miyaura cross-coupling reactions.

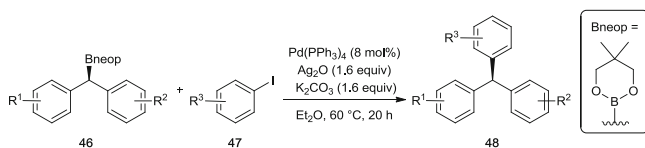
In 2009, Crudden and co-workers reported the seminal example of a cross-coupling between chiral secondary benzyl boronates with aryl iodides which proceeded with good stereochemical integrity (Scheme 9a) [67]. Benzylic boronates **36** were synthesized with high levels of regio- and enantio-control using a Rh-catalysed asymmetric hydroboration previously developed by Hayashi and Ito [68, 69]. While modification of the phosphine ligand did little to improve the yield of the process in the initial stages of the study, using silver oxide as the base dramatically improved the yield of the reaction. The authors proposed that the silver oxide played a role in accelerating a potentially slow transmetallation step. It was found that this process proceeded with good stereoretention, presumably via 4-membered transition state **39**, as previously proposed by Soderquist [64] and



Scheme 9 Stereoretentive Suzuki–Miyaura coupling of benzylic boronates



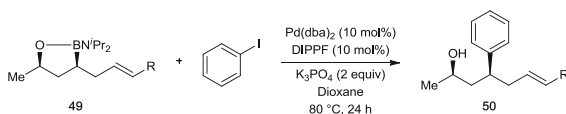
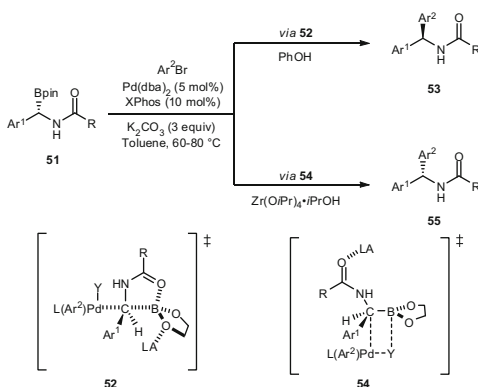
Scheme 10 Potential pathway for product racemization by the presence of excess ligand



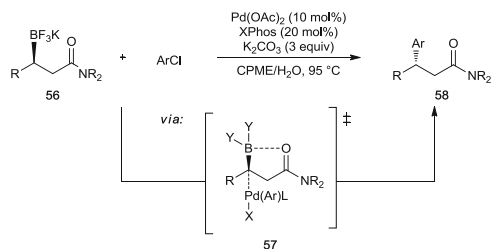
Scheme 11 Synthesis of enantiomerically enriched triarylmethanes

Woerpel [63] (see Sect. 3.2). Furthermore, upon subjection of a branched boronate **40** and a linear boronate **41** to the reaction conditions in a competitive situation, it was observed that there was a complete selectivity for the branched boronate, an indication that there is an important role imparted upon the benzylic nature of the boronate functionality (Scheme 9b). Recently, it was found that these reaction conditions can also be applied towards the stereospecific cross-coupling of optically enriched allylic and propargylic boronates [70].

In a later report [71], it was found that the amount of triphenylphosphine had a direct impact on both the yield and stereochemical outcome of the reaction. At high loadings of phosphine ligand (8–12 equiv. with respect to Pd), a higher yield was obtained but at the cost of lower enantioselectivity. This phenomenon was eventually attributed to a racemization pathway involving hydride elimination of the post-transmetallation intermediate **44**, followed by racemization via decomplexation of the resulting olefin, which is promoted by excess phosphine (Scheme 10). With their newly optimized conditions in hand, the Crudden group was able to apply their method to the construction of enantiomerically enriched triarylmethanes **48** (Scheme 11), motifs which are known to have various biological activities as well as important materials properties [72].

Scheme 12 Stereospecific Suzuki–Miyaura cross-coupling with aryl iodides**Scheme 13** Control of stereoselectivity in the coupling of α -(acylamino)benzylboronic esters

In 2011, Suginome and co-workers reported a Pd-catalysed stereoselective cyclizative alkenylboration of olefins to give products of type **49**. In this report, the authors showed that **49** could undergo stereospecific Suzuki–Miyaura cross-coupling with aryl iodides, giving the cross-coupled product **50** with complete retention of configuration at the stereogenic carbon atom (Scheme 12) [73]. As an extension of this finding, the Suginome group also developed a highly stereoselective Suzuki–Miyaura reaction involving the coupling of enantioenriched α -(acylamino)benzylboronic esters with aryl bromides and chlorides [74]. In contrast to the Crudden system, it was found that this process occurred with inversion of stereochemistry. In a later report [75], the Suginome group described a remarkable ability to direct the stereochemical course of their system simply by modifying their choice of acidic additives (Scheme 13). While using phenol as an additive promoted enantiospecific invertive C–C bond formation leading to product **53**, the use of Zr(O*i*-Pr)₄ · *i*-PrOH conversely resulted in an enantiospecific, retentive C–C bond formation to give **55**. Based on these observations, the authors proposed that the intramolecular coordination of the amide oxygen atom to the boron centre of the boronate results in the approach of the oxidatively inserted palladium(II) species only from the opposite side of the boronate, thus leading to transition state **52**, which results in an invertive transmetalation step. It is believed that phenol enhances this intramolecular interaction by protonating the pinacolate ligand thus leading to enhanced enantioselectivity in the invertive coupling reaction. In the case of Zr(O*i*-Pr)₄ · *i*-PrOH, it was proposed that competitive coordination of the Lewis acid to the carbonyl oxygen of the amide prevents the intramolecular coordination between the carbonyl and the boronate. As a result, the process is thought to proceed through transition state **54** which, as in Crudden's cross-coupling, leads to overall retention of configuration.



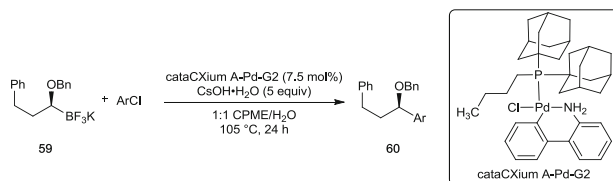
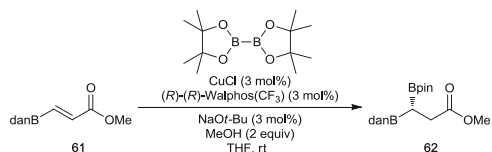
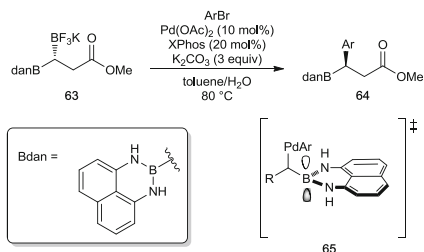
Scheme 14 Invertive cross-coupling of β -trifluoroboratoamides

In 2010, Molander and co-workers reported a successful stereospecific cross-coupling of enantioenriched non-benzylic secondary alkyl trifluoroborates (Scheme 14) [76]. As in Suginome's system, Molander's chosen substrates, acyclic secondary β -trifluoroboratoamides **56**, benefit from intramolecular coordination from the amide carbonyl to the boron group, thus similarly resulting in a transmetalation occurring with inversion of stereochemistry to give products **58**.

Notably, these β -trifluoroboratoamides are substrates that have the potential to undergo β -hydride elimination, yet with their optimized conditions, the authors observed less than 2% of products resulting from this competitive side pathway. The lack of competing β -hydride elimination was attributed to the complexation of the amide carbonyl to the boron atom of the intermediate diorganopalladium complex as seen in **57**. This coordination may restrict the reaction intermediate from adopting the necessary *syn*-coplanar arrangement of the palladium and β -hydrogens in order for elimination to occur.

Following this initial report, Molander and co-workers have also reported the successful stereospecific cross-coupling of secondary organotrifluoroborates containing an α -benzyloxy group **59** (Scheme 15). The benzyloxy group is thought to prevent competing β -hydride elimination by acting as a hemilabile ligand [77]. Prior research has demonstrated that these types of ligands can serve several roles in the prevention of β -hydride elimination. One important advantage is their ability to reduce the necessary agostic interactions between the metal and the neighbouring β -hydrogens [78] in two ways: (1) by acting as an inductively electron withdrawing group, thus reducing the electron density of the β -hydrogens, and (2) by coordinating to the metal centre, which reduces the electron deficiency of the metal. Coordination to the metal centre also has the added benefit of potentially inhibiting *syn*- β -hydride elimination by restricting the conformation of the organometallic intermediate. Due to the lack of a coordinating group to boron, however, this coupling proceeds with the usual retention of configuration (Scheme 15).

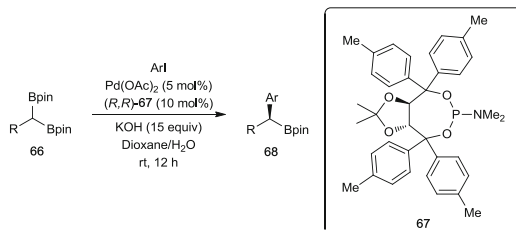
In 2011, the Hall group developed a chemoselective and stereospecific cross-coupling of optically enriched 3,3-diboronyl carboxyesters **63** (Scheme 17) [79]. It was previously shown by Shibata and co-workers that achiral 1,1-diboronyl compounds [80] are capable of undergoing chemoselective cross-coupling resulting only in mono-coupled products [81]. It has been suggested that one boronyl unit serves as an activator for the cross-coupling of the second boronyl unit via

**Scheme 15** Retentive cross-coupling of α -benzyloxytrifluoroborates**Scheme 16** Copper-catalysed synthesis of optically enriched 3,3-diboronyl carboxyesters**Scheme 17** Chemo- and stereoselective cross-coupling of 3,3-diboronyl carboxyesters

stabilization of the transient α -B-Pd(II) intermediate. In this regard, Hall and co-workers proposed that optically pure 3,3-diboronyl carboxyesters could be cross-coupled in a chemoselective and stereospecific fashion. Their efforts led to the first report of the synthesis of optically enriched diboryl compounds **62**, prepared by a Cu-catalysed conjugate addition process using the chiral ligand (*R*)-(*R*)-Walphos(CF₃) (Scheme 16) [79].

These enantioenriched 3,3-diboryl carboxyesters were then cross-coupled chemoselectively with various aryl and alkenylbromides with high stereoselectivity by first transforming the boron pinacolate **62** to the corresponding trifluoroborate **63** (Scheme 17). The cross-coupling process benefits from two modes of stabilization: (1) coordination of the carbonyl oxygen to the boron atom and (2) stabilization of the α -B-Pd(II) intermediate by the second boronyl unit **65**, both of which are thought to assist in the transmetallation process. Predictably, as in the Suginome and Molander studies, the cross-coupling occurs with overall inversion of stereochemistry due to the coordination of the carbonyl oxygen to the boron atom.

In 2014, the Morken group reported the successful cross-coupling of prochiral 1,1-diboryl compounds of type **66** to give optically enriched organoboronates by

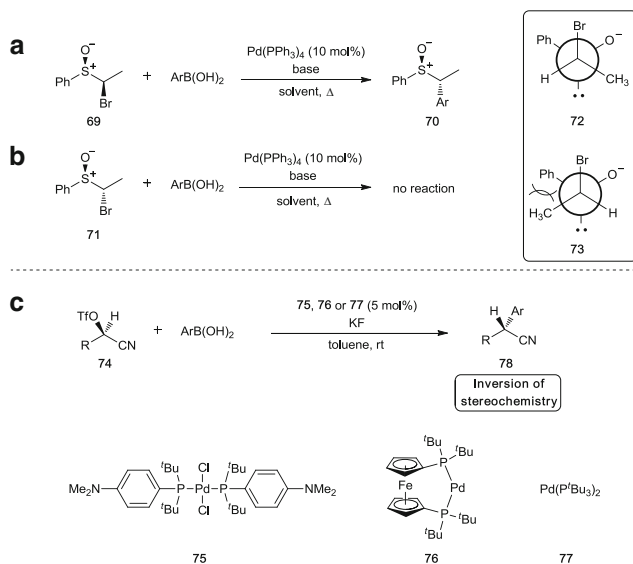


Scheme 18 Catalytic enantioselective cross-coupling of 1,1-diboryl compounds

using a chiral catalyst (Scheme 18) [82]. In this catalytic, enantioselective desymmetrization process, the optimal ligand was found to be TADDOL-derived phosphoramidite **67**. The cross-coupled products were obtained in moderate to good yields and *ees*. Using isotopic boron labelling experiments, the authors determined that transmetalation is stereospecific and likely the stereodetermining step in the reaction mechanism.

4.2 Stereoselective Couplings of Alkyl Halides and Pseudohalides with Aryl or Alkenyl Boronates

Stereoselective Suzuki–Miyaura cross-coupling reactions of stereodefined secondary alkyl halides are a new and valuable synthetic strategy with great potential in the formation of saturated C–C bonds. In order to explore the feasibility of stereoselective Suzuki–Miyaura cross-coupling reactions, Asensio and co-workers first examined diastereoselective variants using configurationally defined α -bromosulfoxides **69** as substrates (Scheme 19a) [83–85]. Using this method, either enantioenriched or racemic *syn*- α -bromosulfoxides **69** could be cross-coupled with arylboronic acids to furnish α -arylsulfoxide **70** with inversion of stereochemistry at the stereogenic α -carbon centre. Cross-coupling reactions of this class of compounds afforded products with only moderate yields due to side reactions such as protodehalogenation and β -hydride elimination. The inversion of stereochemistry observed at the α -carbon can be explained based on the expected mechanistic course of the cross-coupling process. While oxidative addition of sp^3 alkyl bromides proceeds with inversion of stereochemistry (see Sect. 3.2), transmetalation and reductive elimination both feature retention of stereochemistry, leading to the observed products with an overall inversion of stereochemistry. Interestingly, in contrast to *syn*- α -bromosulfoxide **69**, *anti*- α -bromosulfoxide **71** failed to cross-couple with aryl boronic acids, implying the important influence of a stereogenic centre at the sulphur atom (Scheme 19b). The authors rationalized this result by assuming that *syn*- α -bromosulfoxides **69** would preferentially adopt a preferred conformation **72**. In this stereoelectronically favoured conformation, the lone electron pair lies *anti* to the bromide, thus allowing the Pd-catalyst to approach

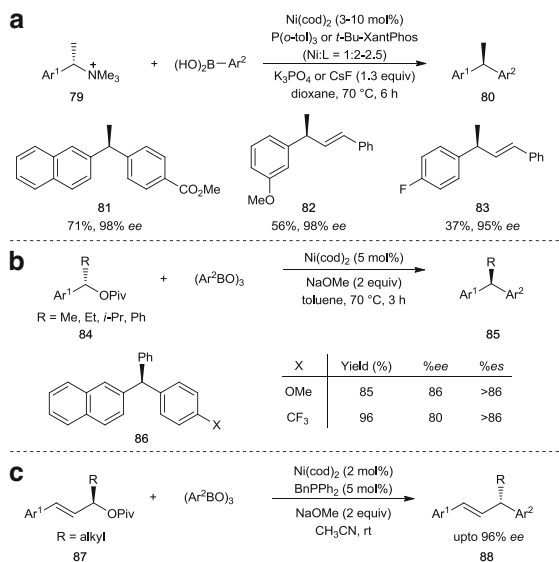


Scheme 19 Stereoselective Suzuki–Miyaura cross-couplings of stereodefined alkyl halides

the substrate from a S_N2 -like trajectory during the oxidative addition step. With this model, the *anti*- α -bromosulfoxide **71** would have difficulty adopting this specific orientation due to the gauche interaction between the methyl and the phenyl groups in conformation **73**.

In 2010, Falck and co-workers conducted stereospecific Suzuki–Miyaura cross-coupling reactions with enantioenriched α -cyanohydrin triflates **74** (Scheme 19c) [86]. This substrate class was chosen because nitriles are a versatile functional group, which can also act as electron-withdrawing groups to facilitate the key oxidative addition step. By employing enantiomerically enriched α -cyanohydrin triflates **74** under the optimized conditions, the authors found that various α -aryl nitriles **78** could be produced with inversion of stereochemistry. The stereochemical outcome can be explained as outlined in Sect. 3.2.

Because of the limited availability and potential instability of chiral secondary alkyl halides and triflates, there has been interest in the identification of alternative electrophiles for use in stereoselective cross-coupling reactions of organoboron derivatives. Based on the precedent of using aryl ammonium salts as cross-coupling partners in nickel-catalysed Suzuki–Miyaura cross-couplings [87], Watson and co-workers developed a mild and effective variant involving benzylic trimethyl ammonium salts **79** [88]. Careful optimization of reaction conditions led to a stereospecific preparation of diarylethane compounds **80** from optically enriched secondary benzylic amines as stable precursors (Scheme 20a). The nature of the ligand was found to exert a significant influence on the chirality transfer, with tri-*o*-tolylphosphine and *t*-butyl-xantphos providing the highest level of enantioselectivity. While various benzylic ammonium substrates can be employed, naphthyl



Scheme 20 Nickel-catalysed stereospecific coupling of benzylic and allylic electrophiles

ammonium salts provide higher yields of products. The reaction was found to be general with respect to the boronic acid and tolerates various common functional groups such as aryl ethers, esters, nitrile, amides, sulfones and fluoride. Alkenylboronic acids are suitable substrates that provide coupling products with high enantiomeric excesses, however, in lower yields compared to arylboronic acids. Likewise, one example of heteroaromatic boronic acid, quinolineboronic acid, only afforded a low product yield.

Based on limited mechanistic studies, a catalytic cycle was proposed whereby the electron-rich Ni(0) catalyst undergoes oxidative addition into the ammonium benzylic C–N bond with inversion of stereochemistry to provide a configurationally stable η^1 or η^3 benzylic Ni(II) complex. This step is followed by a stereochemically retentive transmetalation with the boronic acid, then reductive elimination, a mechanistic step well precedented to occur with retention of stereochemistry. The resulting diarylethane products **80** are formed by overall inversion of configuration and are isolated in up to 99% enantiomeric excess. Recently, Watson and co-workers reported an improved procedure with a phosphine-free catalyst that provides an expanded reaction scope including heteroaromatic boronic acids [89].

The same group reported the use of chiral secondary benzylic pivalates **84** in stereoselective Suzuki–Miyaura cross-couplings with arylboroxines (Scheme 20b) [90]. By making use of sodium methoxide as the optimal base and phosphine-free conditions, the nickel-catalysed couplings afforded the corresponding diarylalkane and triarylmethane products **85** with modest to high retention of optical purity. Like the ammonium salts described above, overall inversion of stereochemistry is also observed with these trimethylacetic esters. Interestingly, arylboroxines were found

to afford higher yields of products with superior enantioselectivity compared to the use of the corresponding arylboronic acids. As demonstrated with control experiments, the presence of water is detrimental to the reaction, thus explaining the advantage provided by the use of boronic anhydrides as a dry form of boronic acids. Although the reaction is limited to 2-naphthyl-substituted secondary alkylpivalates (a single example of a benzylic pivalate led to a lower yield of 33%), it displays a wide scope of suitable arylboroxines in the formation of diarylalkane products. Triarylmethane compounds can be obtained in high yield from coupling of the corresponding diaryl methanol esters, however, with significant erosion of optical purity. Using similar conditions, allylic pivalates **87** can also be used as substrates to produce the cross-coupled products **88** with high regioselectivity and stereochemical fidelity (Scheme 20c) [91].

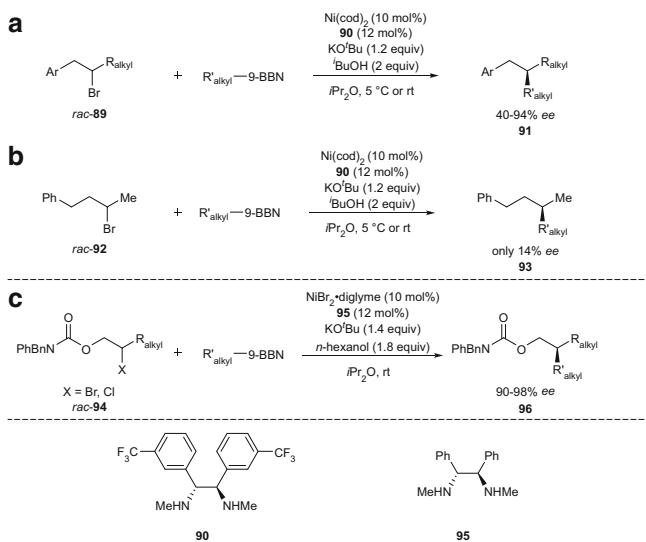
5 Stereoselective C(sp³)–C(sp³) Suzuki–Miyaura Cross-Coupling Reactions

Since the seminal report by Suzuki and Miyaura in 1992 on the successful cross-coupling of primary alkyl iodides with alkyl boranes [92], very little progress was made in the following years in the area of alkyl–alkyl couplings [93] due to the numerous challenges associated with these processes (see Sect. 3.1). In recent years, Fu and co-workers have been the key players in the development of C(sp³)–C(sp³) couplings. By using a nickel catalyst in conjunction with a chiral amine ligand, Suzuki–Miyaura cross-couplings of racemic alkyl halides with alkyl boranes may be achieved with high enantioselectivities. The key feature leading to the success of this reaction lies in the use of nickel as the catalyst in place of palladium. First-row transition metals such as nickel are more prone to undergo oxidative additions by one-electron mechanisms, whereas lower elements like palladium tend to proceed through two-electron processes. The factors leading to reaction via a radical or two-electron process is dependent not only on the metal but also the substrate. Unlike Watson's cross-couplings of alkyl ammonium salts and pivalates (Sect. 4.2), Fu made use of alkyl bromides and chlorides as their choice electrophiles. In this case, the electrochemical potential between the nickel catalyst and the electrophile is high enough for a radical process to occur. As a result, the racemic alkyl halides are converted to prochiral alkyl radicals from which enantiomerically enriched products may be obtained through chiral information transferred from the chiral catalyst. Through this strategy, the Fu group has developed a range of successful alkyl–alkyl Suzuki–Miyaura cross-couplings.

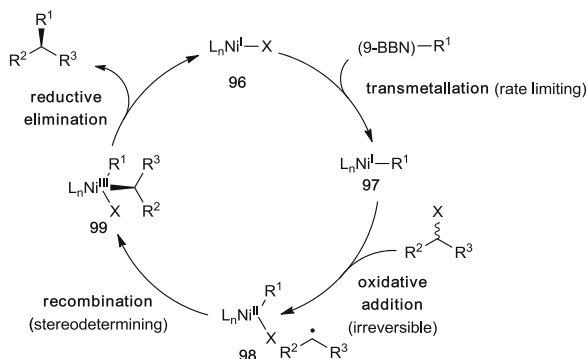
5.1 Stereoselective Couplings of Alkyl Boranes with Alkyl Halides

The first enantioselective cross-coupling of unactivated racemic secondary alkyl bromides with organoborane reagents was first reported by Fu and co-workers in 2008 [94]. Until this breakthrough, stereoselective cross-couplings of this type were limited to substrates bearing activated electrophiles, such as allylic and benzylic halides or α -halocarbonyl compounds. In the presence of $\text{Ni}(\text{cod})_2$ and chiral diamine **90**, the cross-coupled products **91** were obtained with good enantioselectivity (Scheme 21a). The selectivity of the reaction was found to be dependent on the presence and proper placement of the aromatic group on the electrophile (Scheme 21b). It was proposed that this phenomenon was due to coordination of the aromatic group to the Ni catalyst during the enantiodetermining step. This coordination allows for successful stereoinduction from the metal-bound chiral ligand.

During these studies, it was noted that lower enantioselectivities were achieved with ether containing substrates. Fu and co-workers speculated that these observations could be due to coordination of the ether oxygen to the Ni catalyst and that this finding could be exploited to develop a method for the cross-coupling of oxygenated unactivated electrophiles **94** (Scheme 21c) [95]. Over the years, the same group has developed a number of methods for the coupling of unactivated electrophiles employing a variety of coordinating groups, including nitrogen [96], amides [97] and carbamates [98]. The scope of these processes has also been expanded to include secondary alkyl chlorides as well as aryl boranes, aryl boronates and



Scheme 21 Stereoconvergent Suzuki–Miyaura cross-coupling reactions of racemic secondary alkyl halides with alkyl boranes



Scheme 22 Proposed catalytic cycle of Ni-catalysed stereoconvergent Suzuki–Miyaura cross-coupling reactions (L = Chiral ligand)

secondary alkyl boranes. In all cases, the coordinating ability of the heteroatom on the electrophile is essential to the stereochemical outcome of the reaction.

The stereoselectivity of these reactions stems from a stereoconvergent mechanism in which the oxidative addition step proceeds through a radical process. As a result, the initial stereogenic centre of the racemic electrophilic coupling partner is lost at the oxidative addition step, and the stereochemical outcome of the reaction is determined solely by the chiral catalyst during the recombination step. Kinetic studies showed that the rate law is first order in the catalyst and the organoborane, but zeroth order in the electrophile, which is consistent with a turnover-limiting transmetalation step [96]. Monitoring the reaction of optically pure alkyl halide showed no erosion of *ee* of the electrophile over time, suggesting an irreversible oxidative addition step [97]. Based on these findings, the following catalytic cycle may be proposed (Scheme 22): first, rate-limiting transmetalation of the organoborane with the Ni(I) catalyst **96** occurs to give **97**, which may then undergo an irreversible oxidative addition into the alkyl halide to give catalytic intermediate **98** and an alkyl radical. The alkyl radical and **98** may then undergo recombination to give Ni(III) species **99**. This recombination process occurs with stereoselectivity by virtue of the asymmetric environment provided by the chiral ligand L . Subsequent reductive elimination with retention of stereochemistry gives the cross-coupled product and regenerates the Ni(I) catalyst.

6 Summary and Outlook

Since its original discovery in 1979, the Suzuki–Miyaura cross-coupling reaction has continued to receive significant interest from both academic and industrial chemists due to its tremendous success in $C(sp^2)-C(sp^2)$ bond formation. With the recent advances made in stereoselective cross-coupling reactions for the formation of enantiomerically enriched atropisomers and stereogenic centres, the value of this synthetic method has increased even further.

Nevertheless, there is still much to be explored in this area of cross-coupling. Recent breakthroughs notwithstanding, the Suzuki–Miyaura reaction is still by no means a fully matured method. Cross-coupling of aliphatic substrates, in spite of recent developments, is still in its infancy in terms of its applications to organic synthesis. Most catalytic systems in cross-coupling reactions of alkyl substrates still require a high catalyst loading, and the current state of the art is still not applicable towards the coupling of tertiary alkyl substrates for the formation of quaternary stereogenic centres [99–101]. Better mechanistic understanding coupled with improved reaction conditions will be essential for future achievements in these areas. These examples demonstrate that there is still an immense potential in this field, and it is certain that Suzuki–Miyaura cross-coupling reactions will continue to attract attention from chemists both in the form of fundamental advances and practical applications.

References

1. de Meijere A, Diederich F (eds) (2004) *Metal-catalyzed cross-coupling reactions*, 2nd edn. Wiley-VCH, Weinheim
2. Jana R, Pathak TP, Sigman MS (2011) *Chem Rev* 111:1417
3. Sumimoto M, Iwane N, Takahama T, Sakaki S (2004) *J Am Chem Soc* 126:10457
4. Goossen LJ, Koley D, Hermann HL, Thiel W (2006) *Organometallics* 25:54
5. Goossen LJ, Koley D, Hermann HL, Thiel W (2005) *J Am Chem Soc* 127:11102
6. Braga AAC, Morgon NH, Ujaque G, Maseras F (2005) *J Am Chem Soc* 127:9298
7. Braga AAC, Morgon NH, Ujaque G, Lledos A, Maseras F (2006) *J Organomet Chem* 691:4459
8. Braga AAC, Ujaque G, Maseras F (2006) *Organometallics* 25:3647
9. Huang YL, Weng CM, Hong FE (2008) *Chem Eur J* 14:4426
10. Sicre C, Braga AAC, Maseras F, Cid MM (2008) *Tetrahedron* 64:7437
11. Li Z, Zhang SL, Fu Y, Guo QX, Liu L (2009) *J Am Chem Soc* 131:8815
12. Jover J, Fey N, Purdie M, Lloyd-Jones GC, Harvey JN (2010) *J Mol Catal A* 324:39
13. Amatore C, Jutand A, Le Duc G (2011) *Chem Eur J* 17:2492
14. Amatore C, Jutand A, Le Duc G (2012) *Angew Chem Int Ed* 51:1379
15. Carrow BP, Hartwig JF (2011) *J Am Chem Soc* 133:2116
16. Adamo C, Amatore C, Ciofini I, Jutand A, Lakmini H (2006) *J Am Chem Soc* 128:6829
17. Wu W, Wang S, Zhou Y, He Y, Zhuang Y, Li L, Wan P, Wang L, Zhou Z, Qiu L (2012) *Adv Synth Catal* 354:2395
18. Zhou Y, Wang S, Wu W, Li Q, He Y, Zhuang Y, Li L, Pang J, Zhou Z, Qiu L (2013) *Org Lett* 15:5508
19. Benhamou L, Besnard C, Kündig EP (2014) *Organometallics* 33:260
20. Kamikawa K, Uemura M (2000) *Synlett* 938
21. Bringmann G, Mortimer AJP, Keller PA, Gresser MJ, Garner J, Breuning M (2005) *Angew Chem Int Ed* 44:5384
22. Baudoin O (2005) *Eur J Org Chem* 4223
23. Cammidge AN, Crépy KVL (2000) *Chem Commun* 1723
24. Cammidge AN, Crépy KVL (2004) *Tetrahedron* 60:4377
25. Herrbach A, Marinetti A, Baudoin O, Guénard D, Guéritte F (2003) *J Org Chem* 68:4897
26. Jensen JF, Johannsen M (2003) *Org Lett* 5:3025
27. Mikami K, Miyamoto T, Hatano M (2004) *Chem Commun* 2082

28. Genov M, Almorín A, Espinet P (2006) *Chem Eur J* 12:9346
29. Genov M, Almorín A, Espinet P (2007) *Tetrahedron Asymmetry* 18:625
30. Sawai K, Tatum R, Nakahodo T, Fujihara H (2008) *Angew Chem Int Ed* 47:6917
31. Yin J, Buchwald SL (2000) *J Am Chem Soc* 122:12051
32. Shen X, Jones GO, Watson DA, Bhayana B, Buchwald SL (2010) *J Am Chem Soc* 132:11278
33. Bermejo A, Ros A, Fernández R, Lassaletta JM (2008) *J Am Chem Soc* 130:15798
34. Uozumi Y, Matsuura Y, Arakawa T, Yamada YMA (2009) *Angew Chem Int Ed* 48:2708
35. Yamamoto T, Akai Y, Nagata Y, Suginome M (2011) *Angew Chem Int Ed* 50:8844
36. Suginome M, Yamamoto T, Nagata Y, Yamada T, Akai Y (2012) *Pure Appl Chem* 84:1759
37. Cárdenas DJ (1999) *Angew Chem Int Ed* 38:3018
38. Chemler SR, Trauner D, Danishefsky SJ (2001) *Angew Chem Int Ed* 40:4544
39. Netherton MR, Fu GC (2004) *Adv Synth Catal* 346:1525
40. Frisch AC, Beller M (2005) *Angew Chem Int Ed* 44:674
41. Glorius F (2008) *Angew Chem Int Ed* 47:8347
42. Rudolph A, Lautens M (2009) *Angew Chem Int Ed* 48:2656
43. Taylor BLH, Jarvo ER (2011) *Synlett* 2761
44. Doucet H (2008) *Eur J Org Chem* 2013
45. Miyaura N, Ishiyama T, Ishikawa M, Suzuki A (1986) *Tetrahedron Lett* 27:6369
46. Miyaura N, Suzuki A (1995) *Chem Rev* 95:2457
47. Suzuki A (1999) *J Organomet Chem* 576:147
48. Fu GC, Littke AF (2002) *Angew Chem Int Ed* 41:4176
49. Miyaura N (2002) *J Organomet Chem* 653:54
50. Bellina F, Carpita A, Rossi R (2004) *Synthesis* 2419
51. Franzén R, Xu Y (2005) *Can J Chem* 83:266
52. Suzuki A (2005) *Chem Commun* 4759
53. Alonso F, Beletskaya IP, Yus M (2008) *Tetrahedron* 64:3047
54. Molander GA, Canturk B (2009) *Angew Chem Int Ed* 48:9240
55. Suzuki A (2011) *Angew Chem Int Ed* 50:6723
56. Hall DG (ed) (2011) *Boronic acids: preparation and applications in organic synthesis, medicine and materials*, vol 1, 2nd edn. Wiley-VCH, Weinheim
57. Bonin H, Fouquet E, Felpin F-X (2011) *Adv Synth Catal* 353:3063
58. Lennox AJ, Lloyd-Jones GC (2010) *Isr J Chem* 50:664
59. Fitton P, Johnson MP, McKoen JE (1968) *J Chem Soc Chem Commun* 1968
60. Lau KSY, Wong PK, Stille JK (1976) *J Am Chem Soc* 98:5832
61. Wong PK, Lau KSY, Stille JK (1974) *J Am Chem Soc* 96:5956
62. Hartley FR, Patai S (eds) (1985) *The chemistry of the metal-carbon bond*, vol 2. Wiley, New York
63. Ridgway BH, Woerpel KA (1998) *J Org Chem* 63:458
64. Matos K, Soderquist JA (1998) *J Org Chem* 63:461
65. Taylor BLH, Jarvo ER (2011) *J Org Chem* 76:7573
66. Hall DG, Lee JCH, Ding J (2012) *Pure Appl Chem* 84:2263
67. Imao D, Glasspoole BW, Laberge VS, Crudden CM (2009) *J Am Chem Soc* 131:5024
68. Hayashi T, Matsumoto Y, Ito Y (1989) *J Am Chem Soc* 111:3426
69. Uozumi Y, Hayashi T (1991) *J Am Chem Soc* 113:9887
70. Chausset-Boissarie L, Ghazati K, LaBine E, Chen JL-Y, Aggarwal VK, Crudden CM (2013) *Chem Eur J* 19:17698
71. Glasspoole BW, Oderinde MS, Moore BD, Antoft-Finch A, Crudden CM (2013) *Synthesis* 45:1759
72. Matthew SC, Glasspoole BW, Eisenberger P, Crudden CM (2014) *J Am Chem Soc* 136:5828
73. Daini M, Suginome M (2011) *J Am Chem Soc* 133:4758
74. Ohmura T, Awano T, Suginome M (2010) *J Am Chem Soc* 132:13191
75. Awano T, Ohmura T, Suginome M (2011) *J Am Chem Soc* 133:20738

76. Sandrock DL, Jean-Gérard L, Chen C-Y, Dreher SD, Molander GA (2010) *J Am Chem Soc* 132:17108
77. Molander GA, Wisniewski SR (2012) *J Am Chem Soc* 134:16856
78. Pudasaini B, Janesko BG (2011) *Organometallics* 30:4564
79. Lee JCH, McDonald R, Hall DG (2011) *Nat Chem* 3:894
80. Endo K, Hirokami M, Shibata T (2009) *Synlett* 1331
81. Endo K, Ohkubo T, Hirokami M, Shibata T (2010) *J Am Chem Soc* 132:11033
82. Sun C, Potter B, Morken JP (2014) *J Am Chem Soc* 136:6534
83. Rodríguez N, Cuenca A, de Arellano CR, Medio-Simón M, Asensio G (2003) *Org Lett* 5:1705
84. Rodríguez N, Cuenca A, de Arellano CR, Medio-Simón M, Peine D, Asensio G (2004) *J Org Chem* 69:8070
85. Rodríguez N, de Arellano CR, Asensio G, Medio-Simón M (2007) *Chem Eur J* 13:4223
86. He A, Falck JR (2010) *J Am Chem Soc* 132:2524
87. Blakey SB, MacMillan DWC (2003) *J Am Chem Soc* 125:6046
88. Maity P, Shacklady-McAtee DM, Yap GPA, Sirianni ER, Watson MP (2013) *J Am Chem Soc* 135:280
89. Shacklady-McAtee DM, Roberts KM, Basch CH, Song Y-G, Watson MP (2014) *Tetrahedron* 70:4257
90. Zhou Q, Srinivas HD, Dasgupta S, Watson MP (2013) *J Am Chem Soc* 135:3307
91. Srinivas HD, Zhou Q, Watson MP (2014) *Org Lett* 16:3596
92. Ishiyama T, Abe S, Miyaura N, Suzuki A (1992) *Chem Lett* 691
93. Rubina M, Rubin M, Gevorgyan V (2003) *J Am Chem Soc* 125:7198
94. Saito B, Fu GCJ (2008) *J Am Chem Soc* 130:6694
95. Owston NA, Fu GC (2010) *J Am Chem Soc* 132:11908
96. Lu Z, Wilsily A, Fu GC (2011) *J Am Chem Soc* 133:8154
97. Zultanski SL, Fu GC (2011) *J Am Chem Soc* 133:15362
98. Wilsily A, Tramutola F, Owston NA, Fu GC (2012) *J Am Chem Soc* 134:5794
99. Mei T-S, Patel HH, Sigman MS (2014) *Nature* 508:340
100. Bonet A, Odachowski M, Leonori D, Essafi S, Aggarwal VK (2014) *Nat Chem* 6:584
101. Minko Y, Pasco M, Lercher L, Botoshansky M, Marek I (2012) *Nature* 490:522

Boronic Acid-Catalyzed Reactions of Carboxylic Acids

Kazuaki Ishihara

Contents

1	Introduction	244
2	B(III)-Catalyzed Reactions of α,β -Unsaturated Carboxylic Acids	244
3	B(III)-Catalyzed Dehydrative Condensation to Carboxamides	247
4	B(III)-Catalyzed Dehydrative Condensation to Carboxylic Acid Esters	260
5	B(III)-Catalyzed Dehydrative Condensation to Carboxylic Anhydrides	265
6	Other B(III)-Catalyzed Reactions	266
7	Conclusions	268
	References	268

Abstract Although boric acid ($B(OH)_3$) and boronic acids ($RB(OH)_2$) behave as oligomeric mixtures, these boron compounds, as well as borane, electrophilically activate carboxylic acids as a mixed anhydride under equilibrium. In particular, electron-deficient arylboronic acids are useful as Lewis or Brønsted acid catalysts. The pK_a of boronic acids is in the range of 5–9, which is significantly higher than that of the strong protic acids. However, *diortho*-substituted arylboronic acids with electron-withdrawing groups are unstable and are easily decomposed by base-promoted protodeboronation. In this chapter, the main emphasis is upon the recent progress on boronic acid-catalyzed reactions of carboxylic acids, as well as a few other reactions which can be catalyzed by boronic acids.

Keywords (Acyloxy)boron • Amidation • Boronic acid • Brønsted acid • Catalyst • Dehydrative condensation • Esterification • Lewis acid

K. Ishihara (✉)

Nagoya University, Furo-cho, Chikusa, Nagoya 464-8603, Japan

e-mail: ishihara@cc.nagoya-u.ac.jp

© Springer International Publishing Switzerland 2015

E. Fernández, A. Whiting (eds.), *Synthesis and Application of Organoboron*

Compounds, Topics in Organometallic Chemistry 49,

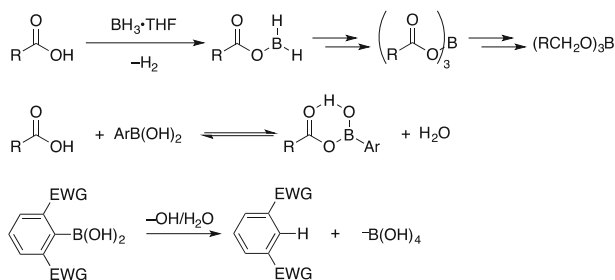
DOI 10.1007/978-3-319-13054-5_8

1 Introduction

The remarkable reactivity of borane toward carboxylic acids over esters is one of the conspicuous characteristics of this element which is hardly seen in any of the other hydride reagents, such as aluminum hydride. The rapid reaction between carboxylic acids and borane is related to the electrophilicity of borane. A mono(acyloxy)borane is recognized to be an initial intermediate (Scheme 1) [1, 2]. The carbonyl group in this molecule, which is essentially a mixed anhydride, is activated by the electronegative nature of the trivalent boron atom. The acyloxy moiety of an (acyloxy)borane is electrophilically increased in the order mono(acyloxy)borane, di(acyloxy)borane, and tri(acyloxy)borane [3]. Although boric acid ($B(OH)_3$) and boronic acids ($RB(OH)_2$) behave as oligomeric mixtures, these boron compounds, as well as borane, electrophilically activate carboxylic acids as a mixed anhydride under equilibrium. In particular, electron-deficient arylboronic acids are useful as Lewis or Brønsted acid catalysts. The pK_a of boronic acids is in the range of 5–9, which is significantly higher than that of the strong protic acids usually required in cationic cyclizations [4]. However, *diortho*-substituted arylboronic acids with electron-withdrawing groups are unstable and are easily decomposed by base-promoted protodeboronation [5]. In this chapter, recent progress on boronic acid-catalyzed reactions of carboxylic acids is overviewed [6, 7], together with a few other examples of other boronic acid-catalyzed reactions.

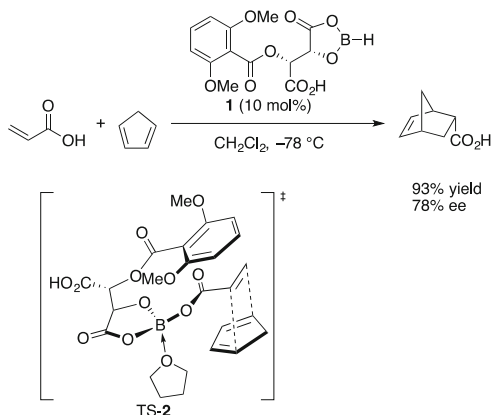
2 B(III)-Catalyzed Reactions of α,β -Unsaturated Carboxylic Acids

In 1988, Yamamoto et al. reported Diels–Alder reactions between α,β -unsaturated carboxylic acids and dienes promoted in the presence of 10 mol% of borane·THF [8]. Furthermore, they found that chiral (acyloxy)borane **1**, which was prepared in situ from monoacylated tartaric acid and borane·THF, was effective as a chiral catalyst for the enantioselective Diels–Alder reaction. Transition state assembly **2** is

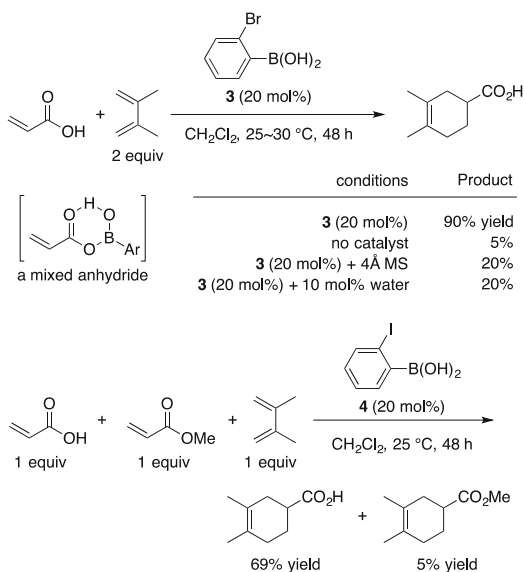


Scheme 1 Generation of (acyloxy)boron species

Scheme 2 The enantioselective Diels–Alder reaction catalyzed by chiral (acyloxy)borane **1**

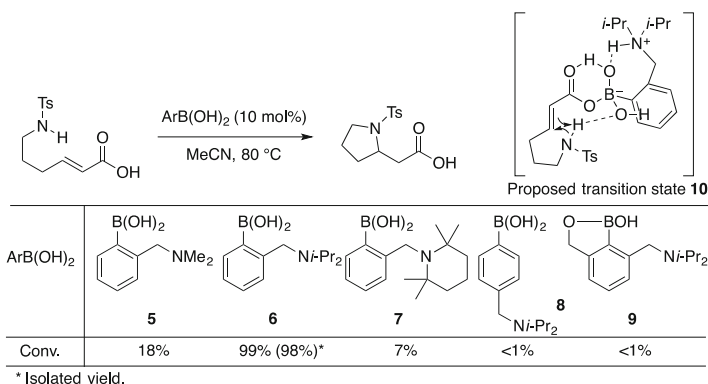


Scheme 3 The Diels–Alder Reaction of α,β -unsaturated carboxylic acids catalyzed by 2-halophenylboronic acids **3** and **4**

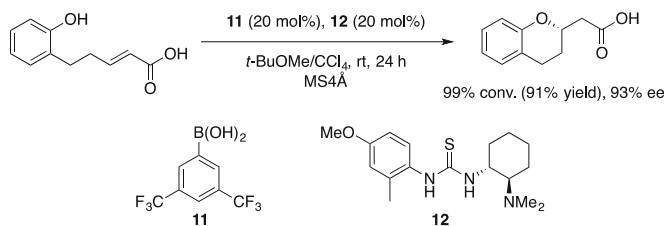


stabilized through π – π attractive interactions between the alkenyl moiety of dienophile and the 2,6-dimethoxyphenyl moiety of the ligand (Scheme 2) [9].

In 2008, Hall et al. reported that 2-halophenylboronic acids **3** and **4** were also effective as catalysts for the Diels–Alder reactions of α,β -unsaturated carboxylic acids with dienes even at room temperature (Scheme 3) [10–12]. The addition of water suppresses the Diels–Alder reaction under equilibrium. However, interestingly, in the absence of water, i.e., in the presence of molecular sieves (4 Å), catalyst turnover is prevented, and this leads to low yields. Boronic acid **4** chemoselectively activates acrylic acid in the presence of the corresponding methyl ester through a mixed anhydride.



Scheme 4 The intramolecular hetero-Michael reaction of α,β -unsaturated carboxylic acids catalyzed by aminoboronic acid



Scheme 5 The enantioselective intramolecular hetero-Michael reaction of α,β -unsaturated carboxylic acid **11** and aminothiourea **12**

In 2014, Takemoto et al. reported that 2-(*N,N*-diisopropylaminomethyl) phenylboronic acid **6** catalyzed the intramolecular hetero-Michael reaction of α,β -unsaturated carboxylic acids (Scheme 4). The *ortho*-diisopropylaminomethyl moiety of phenylboronic acid plays an important role for promoting the reaction. On the basis of the comparison with the catalytic activities of other arylboronic acids **5** and **7–9**, the *s-trans* transition state **10** has been proposed [13].

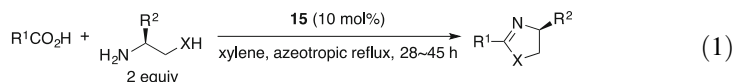
More importantly, the combination of 20 mol% of both 3,5-bis(trifluoromethyl) phenylboronic acid **11** and chiral aminothiourea **12** gives the desired products with high enantioselectivity (Scheme 5) [13]. The reaction proceeds via an (acyloxy) borane species with subsequent activation by **12**. This reaction does not proceed at all in the presence of either **11** or **12**, and hence, the combined use of **11** and **12** is required. Although the exact function and role of **12** remain unclear at this stage, the decreased H bond-donating ability of the thiourea moiety may have prevented the formation of an inert complex between **12** and the substrate through anion binding and consequently enhances the formation of an (acyloxy)borane species. The overall utility of this dual catalytic system has been demonstrated by a one-pot enantioselective synthesis of (+)-erythrocoamide **B**, which proceeds via sequential Michael and amidation reactions.

3 B(III)-Catalyzed Dehydrative Condensation to Carboxamides

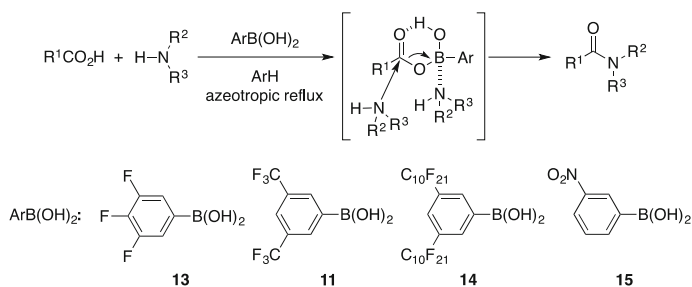
The most desirable method for preparing carboxamides is a catalytic direct condensation between carboxylic acids and amines, which is generally understood to be impossible, due to the formation of unreactive carboxylate ammonium salts. Although the direct formation of amide bonds by heating without catalysts has been known since 1858 ([14] and references therein; [15]), this process has found little synthetic utility, with a few exceptions. More recently, Whiting et al., followed by Williams et al., reported that some direct amide condensations smoothly occur under thermal conditions without catalysts [16, 17]. In particular, benzylamine is highly reactive. In 2002, Loupy et al. reported that carboxamides could be efficiently obtained by mixing neat carboxylic acids and primary amines under microwave irradiation [18]. However, this method is not effective for aromatic substrates such as benzoic acids and anilines. (Acyloxy)boron intermediates generated from carboxylic acids and boron reagents such as BR_3 ($\text{R}=\text{C}_8\text{H}_{17}$, OMe) [19], $\text{CIB}(\text{OMe})_2$ [19], $\text{HB}(\text{OR})_2$ ($\text{R}=\textit{i}\text{-Pr}$, $\textit{t}\text{-Am}$) [19], $\text{BH}_3 \cdot \text{R}_3\text{N}$ ($\text{R}=\text{Me}$, Bu) [20], $\text{BF}_3 \cdot \text{Et}_2\text{O}$ [21], and catecholborane [22] were shown to react with amines to furnish amides in moderate to good yields, but only under uniformly stoichiometric reaction conditions. In these boron-mediated amidations, boron reagents transform into inactive boron species after the reaction of (acyloxy)boron derivatives and amines.

In contrast, arylboronic acids with electron-withdrawing substituents at the aryl group can be used to circumvent these difficulties, since they are water-, acid-, and base-tolerant Lewis and Brønsted acids that can generate (acyloxy)boron species. They are also thermally stable and can be readily handled in air. In 1996, Yamamoto and Ishihara et al. found that the dehydrative condensation of equimolar mixtures of carboxylic acids with amines or ureas proceeds under azeotropic reflux conditions with the removal of water in less polar solvents such as toluene or xylene in the presence of phenylboronic acids bearing electron-withdrawing groups at the *meta*- or *para*-positions such as 3,4,5-trifluorophenylboronic acid **13** [23–25], 3,5-bis(trifluoromethyl)phenylboronic acid **11** [23–26], and 3,5-bis(perfluorodecyl)phenylboronic acid **14** [27] which is reusable in a fluorous biphasic system (FBS) (Scheme 6). In 2002, Wipf et al. reported that 3-nitrophenylboronic acid **15** was also effective as a dehydration catalyst [28]. However, **13** is slightly more active than **15**.

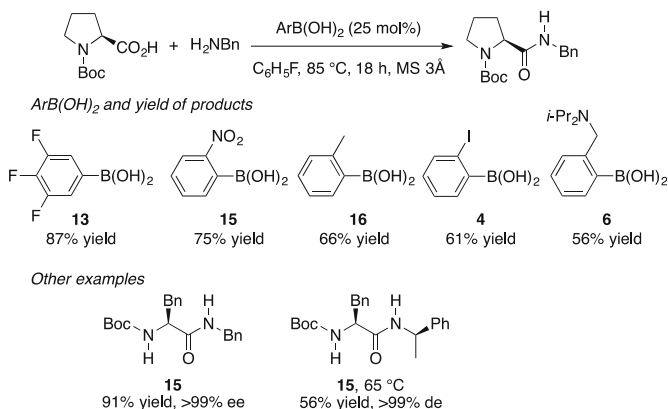
Furthermore, Wipf et al. developed a cyclodehydration of carboxylic acids with amino alcohols and aminothiols catalyzed by **15** to synthesize oxazolines and thiazolines in moderate to excellent yields (Eq. 1) [28].



In 2013, Whiting et al. successfully applied the direct amide condensation of amino acid derivatives catalyzed by arylboronic acids [29]. The direct condensation



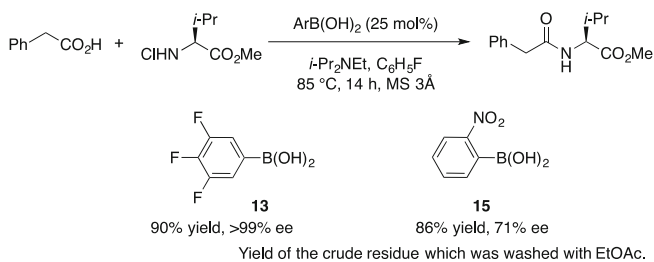
Scheme 6 Boronic acid-catalyzed dehydrative amide condensation reaction



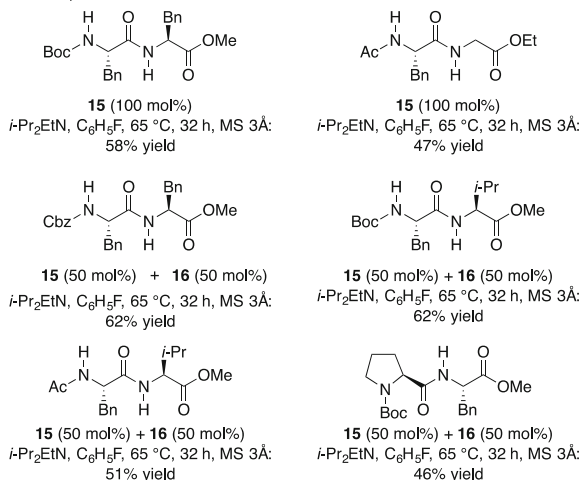
Scheme 7 Boronic acid-catalyzed dehydrative amide condensation reaction of *N*-protected amino acid derivatives

of amino acid derivatives is generally slow relative to simple amine–carboxylic acid combinations. They found that **13** and **15** are more effective catalysts than other arylboronic acids, and fluorobenzene (bp. 85°C) was the best solvent for the amide condensation of *N*-protected amino acid derivatives (Scheme 7). The reaction proceeds under azeotropic reflux conditions at 85°C or in the presence of molecular sieves 3 Å at 65°C to avoid racemization.

The amide condensation of simple carboxylic acids with *C*-protected amino acid derivatives such as methyl ester HCl salts also proceeds, catalyzed by **13** or **15** in the presence of *i*-Pr₂EtN (Scheme 8). Hünig's base (*i*-Pr₂EtN) is used for in situ neutralization of methyl ester HCl salts. Compound **13** is more effective for the less reactive phenylalanine analogues in order to avoid racemization. Furthermore, this method has been applied in dipeptide synthesis; however, even when 100 mol% of arylboronic acids were used at 65°C, dipeptides are obtained in only moderate yield. Dipeptide formation is, therefore, considerably more challenging, and it appears as though a binary arylboronic acid catalyst system is preferable, i.e., a 1:1 mixture of both 2-tolylboronic acids **16** and **15**. This cooperative catalytic system is particularly effective with the least reactive amino acid combinations



Other examples

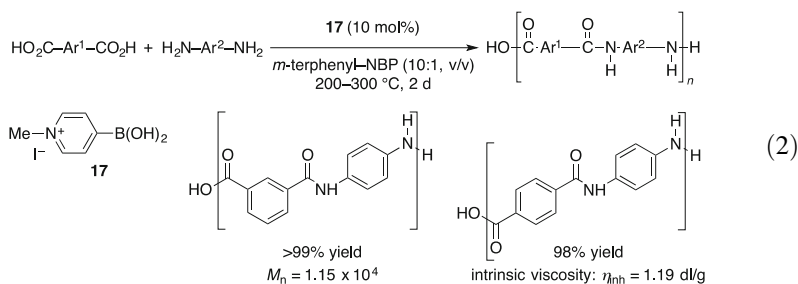
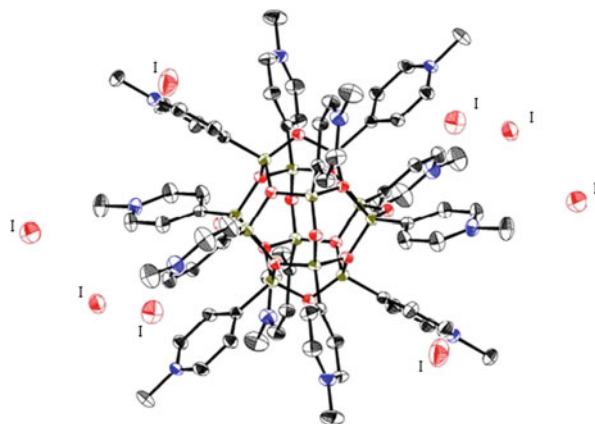


Scheme 8 Boronic acid-catalyzed dehydrative amide condensation reaction of amino acid derivatives

although the overall catalyst loading remains high and the mode of action is not understood.

However, the scope of suitable substrates has been limited, because the catalytic activities of these neutral boronic acids are greatly reduced in polar solvents and for sterically demanding substrates. In 2000, Ishihara and Yamamoto et al. found that 4-borono-*N*-methylpyridinium iodide **17** was effective as a polar solvent-tolerant catalyst for amide condensation [30–32]. Cationic boronic acid **17** is much more active than neutral boronic acids in polar solvents, such as anisole, acetonitrile, and *N*-methylpyrrolidone (NMP), because the boron atom in **17** shows greater Lewis acidity in polar solvents. Thus, **17** is useful as a catalyst for the direct polycondensation of arenedicarboxylic acids with diaminoarenes in a mixed solvent of triphenyl and *N*-butylpyrrolidone (Eq. 2) [24, 30, 31].

Fig. 1 X-ray crystal structure of dodecamer $[17]_{12}$, $[\text{CH}_3\text{N}^+\text{C}_5\text{H}_4\text{BO}_{14/12}]_{12}\text{I}_8 \cdot 10\text{H}_2\text{O}$ (water is omitted for clarity)



When **17** is heated in DMF at 120°C , **17** is completely changed to a yellow precipitate, which is a dodecamer of **17**, $[17]_{12}$, within 1 h, and then gradually undergoes hydrolytic protodeboronation (Fig. 1) [32]. Interestingly, $[17]_{12}$ can be dissolved and is stable, even in water, because the 12 hydrophilic pyridinium ion moieties are oriented on the outside of $[17]_{12}$.

The catalytic activities of **17** and $[17]_{12}$ (5 mol% for B atom) were compared in the amide condensation of 4-phenylbutyric acid with benzylamine under azeotropic reflux conditions in toluene with the removal of water (entries 1 and 2, Table 1). Although background reaction yields, without catalysts, have not been examined [16, 17], the catalytic activity of $[17]_{12}$ was shown to be much lower than that of **17**. However, the catalytic activities of **17** and $[17]_{12}$ were dramatically improved in biphasic solvents of toluene and [emim][OTf] (entries 3 and 4). These results can be understood in terms of the good stability of **8** and the good solubility of **17** and $[17]_{12}$ in the presence of [emim][OTf]. In contrast, **17** is partially soluble in toluene, while $[17]_{12}$ is insoluble. It is likely that **17** is regenerated from $[17]_{12}$ by hydrolysis in the presence of [emim][OTf]. Furthermore, [emim][OTf] plays an important role in suppressing the condensation of **17** to $[17]_{12}$. Thus, the amide condensation proceeds to completion in the presence of 5 mol% of **17** in toluene–[emim][OTf] (5:1 (v/v)) within 5 h (entry 5). After amide condensation, the desired amide is obtained in quantitative yield by repeated extraction with Et_2O from an [emim]

Table 1 Catalytic activities of **17** and [17]₁₂ for amide condensation

$$\text{Ph-CH}_2\text{-CH}_2\text{-CO}_2\text{H} + \text{H}_2\text{NBn} \xrightarrow[\text{toluene (5 mL), [emim][OTf], azeotropic reflux}]{\text{catalyst}} \text{Ph-CH}_2\text{-CH}_2\text{-CONHBn}$$

Entry	Catalyst (mol%)	Time (h)	Yield (%)
1 ^a	17 (5)	1	41
2 ^a	[17] ₁₂ (10) ^b	1	15
3	17 (5)	1	74
4	[17] ₁₂ (5) ^c	1	75
5	17 (5)	5	>99

^aOnly toluene is used as solvent^b[17]₁₂ (10 mol% for B atom) is used^c[17]₁₂ (5 mol% for B atom) is used

[OTf] layer. Compound **17** remains in the [emim][OTf] layer. Thus, a solution of **17** in [emim][OTf] can be repeatedly reused for the same amide condensation reaction without any loss of catalytic activity.

The generality and scope of the amide condensation catalyzed by **17** in the presence of [emim][OTf] are shown in Table 2 (entries 1–8). Not only aliphatic, but also aromatic, substrates are condensed in the presence of 5 mol% of **17**. The amide condensation of less reactive substrates proceeds well under azeotropic reflux conditions in *o*-xylene in place of toluene. Functionalized substrates such as conjugated carboxylic acids, α -hydroxycarboxylic acids, α -alkoxycarboxylic acids, and cyanobenzoic acids are also applicable. Furthermore, a solution of **17** in [emim][OTf] can be repeatedly reused without any loss of activity.

N-Polystyrene-bound 4-boronopyridinium chloride **18a** and *N*-polystyrene-bound 3-boronopyridinium chloride **19** were developed by Yamamoto and Ishihara et al. [30–32] and Wang et al. [33], respectively, to allow recovery and reuse of the *N*-alkyl-4-boronopyridinium halides without any ionic liquids (Table 3). Compound **19** gradually decomposes to *N*-polystyrene-bound pyridinium chloride and boric acid by hydrolytic protodeboronation. In contrast, **18a** can be reused repeatedly. The high catalytic activity of **18a**, which is observed even in the absence of [emim][OTf], can be understood by assuming that the polymer support may prevent dodecamerization of the 4-boronopyridinium chloride moiety in **18a**. After the amide condensation reaction, **18a** can be repeatedly washed with an aqueous solution of 1 M HCl and ethyl acetate, to allow it to be reused in the next reaction. When the treatment of **18a** with an aqueous solution of 1 M HCl is not carried out, the catalytic activity is reduced, since the chloride anions of **18a** are partially exchanged to carboxylate anions through the amide condensation. Therefore, the treatment of **18a** with acid is necessary for reactivating **18a**.

In 2014, Gu and Lee et al. reported mesocellular siliceous foam-supported boronic acids as efficient catalysts for direct amide condensation of carboxylic

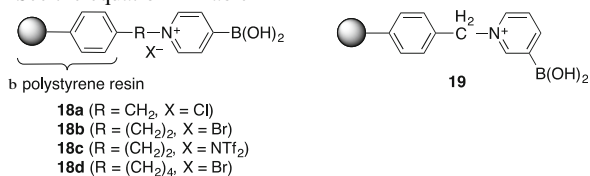
Table 2 Direct amide condensation reaction catalyzed by **17**

Entry	R ¹ CO ₂ H + R ² R ³ NH (2 mmol)		17 (5 mol%) toluene (5 mL), [emim][OTf] (1 mL) azeotropic reflux		Time (h)	Yield (%)	Product	Yield (%)
	Time (h)	Product	Entry	Time (h)				
1	6		92	5 ^b	18	80		80
2	18		95	6 ^b	10	91		91
3 ^a	5 (first)		98 (first)	7 ^b	3	90		90
	5 (second)		93 (second)					
	5 (third)		95 (third)					
4 ^b	18		91	8 ^{a,b}	5 (first)	99 (first)		
					5 (second)	98 (second)		
					5 (third)	99 (third)		

^aSolution of **17** in [emim][OTf] is reused threefold^b*o*-Xylene is used as solvent in place of toluene

Table 3 Recovery and reuse of **19** and **18a**^a

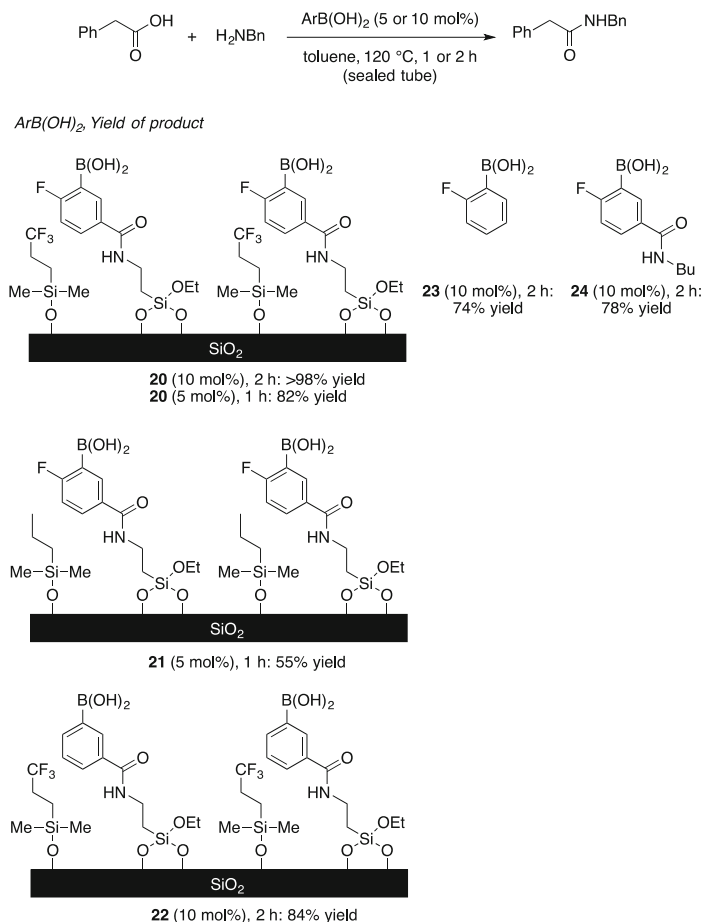
Run	Conversion (%)					
	Catalyst 19 ^b			Catalyst 18a ^b		
	1 h	3 h	5 h	1 h	3 h	5 h
1	64	93	98	68	94	98
2	53	90	98	67	94	98
3	50	85	94	69	93	98
4	40	76	88	69	93	98
5	28	60	74	70	92	96

^aSee the equation in Table 1

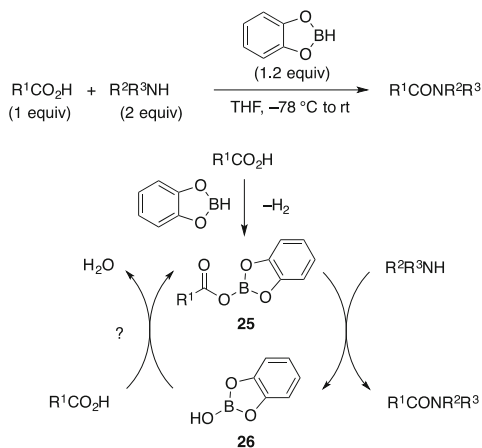
acids and amines (Scheme 9) [34]. Associated with their large pores, the microenvironments surrounding the immobilized active species greatly influence the catalytic activity. The fluoroalkyl moieties on the silica surface significantly enhance the catalytic performance along with making it easy for recovery and reuse. Interestingly, the introduction of the fluoroalkyl moiety in the capping propyl group significantly improves the catalytic efficiency. The isolated yield produced by **20** reached up to 82%, remarkably from 55%, by the fluoro-free derivative **21**, presumably due to the beneficial role of the fluoroalkyl group as a Lewis base or a better water-repelling agent (or both). Similar halogen group effects are also observed in the aromatic substituents of boronic acid (e.g., **20** versus **22**).

In 1970, Levitt et al. reported that several boron reagents such as X_nB(OR)_{3-n} (X=H, Cl, etc.), B(NR²R³)₃, and BR₃ were effective for synthesizing carboxamides [19]. In 1978, Ganem et al. reported that carboxylic acids condensed with amines via a 2-acyloxy-1,3,2-benzodioxaborolane **25** in the presence of stoichiometric amounts of catecholborane under mild conditions (THF, -78°C to rt) ([22]. For resin-bound catecholborane which can be used as a solid-phase amidation reagent, see [35]). As shown in Scheme 10, 2 equiv. of amine were required, because the reaction proceeds via nucleophilic attack of amine on [25·amine]. Catecholborane is converted into benzo[*d*][1,3,2]dioxaborol-2-ol **26**, which is inert through the condensation reaction.

In 2012, Sheppard et al. reported that the use of 2 equiv. of B(OCH₂CF₃)₃, prepared from readily available B₂O₃ and 2,2,2-trifluoroethanol, is effective for the direct amidation of a variety of carboxylic acids with a broad range of amines in acetonitrile at 80 or 100°C in a sealed tube [36]. In most cases, the amide products can be purified by a simple filtration procedure using commercially available resins, with no need for aqueous workup or chromatography. The amidation of *N*-protected amino acids with both primary and secondary amines proceeds effectively, with very low levels of racemization.



Scheme 9 Mesocellular siliceous foam-supported boronic acid-catalyzed dehydrative amide condensation reaction



Scheme 10 Ganem's amide condensation of carboxylic acids with amines using catecholborane as a condensing agent and a possible catalytic pathway

Table 4 Catalytic activities of 1,3,2-dioxaborolan-2-ol derivatives for amide condensation of 4-phenylbutyric acid with benzylamine

Entry	Catalyst	Conversion (%)
1	26	61
2	 27	93
3 ^a	$\text{B}(\text{OH})_3$	31
4 ^a	 11	96

^aBoric acid and **11** are used instead of 1,3,2-dioxaborolan-2-ol derivatives

In contrast, 4,5,6,7-tetrachlorobenzo[*d*][1,3,2]dioxaborol-2-ol **27**, which is prepared in situ from tetrachlorocatechol and boric acid, is sufficiently active as a catalyst for the dehydrative condensation of equimolar mixtures of carboxylic acids with amines (Table 4, entries 1–4) [37]. Although background reaction yields without catalysts have not been examined [16, 17], the catalytic activities can be compared. The catalytic activity of **27** is almost the same as that of **11**. According to the *Chemicals* price catalog (*Chemicals*, 33rd ed.; Wako Pure Chemical Industries, Ltd.: Japan, 2004), **11** is 40-fold more expensive than tetrachlorocatechol. Since boric acid [38, 39] is also available at a rather low price, **27**, which can be prepared from this in situ, is very economical and practical.

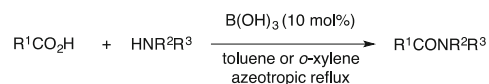
Catalyst **27** is greatly superior to **11** for the amide condensation of not only sterically bulky aliphatic and aromatic carboxylic acids but also functionalized carboxylic acids such as Boc-L-Ala-OH (Table 5, entries 1–9). In contrast, **27** and **11** show a similar trend in catalytic activity with regard to the steric bulk of the amines. The less-hindered **27** has an advantage over **11** at the regeneration step from the hydroxyboron by-product compounds after amidation, back to the (acyloxy)boron species.

In 2005, Tang reported that the cheap, readily available, nontoxic, and eco-friendly boric acid, $\text{B}(\text{OH})_3$, was also usable as a catalyst for the dehydrative amidation process [38]. This amidation procedure has been applied in the synthesis of several active pharmaceutical ingredients (APIs) by Bandichhor et al. (Eq. 3) [39].

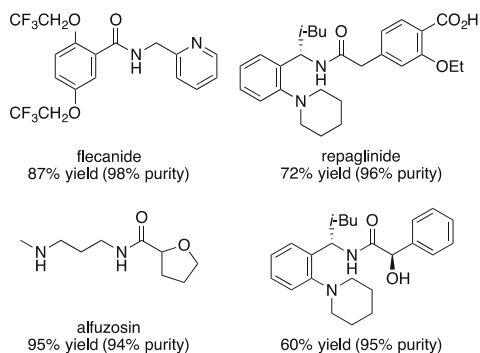
Table 5 Amide condensation of various carboxylic acids with amines catalyzed by **11** or **27**

Entry	Product	Solvent	Time (h)	Yield (%)	
				11	27
1		Toluene	1	32	62
		Toluene	5	–	94
2		Toluene	19	11	55
		<i>o</i> -Xylene	24	–	99
3	<i>t</i> -BuCONHBn	Toluene	20	5	55
		<i>o</i> -Xylene	15	–	94
4		Toluene	2	25	77
		Toluene	5	–	95
5		Toluene	24	15	22
		<i>o</i> -Xylene	20	20	99
6	Ph ₂ CHCONHBn	Toluene	2	30	32
		Toluene	11	–	93
7		<i>o</i> -Xylene	5	47	53
		<i>o</i> -Xylene	19	–	93
8		Toluene	5	35	42
		Toluene	20	–	91 ^a
9		<i>o</i> -Xylene	1	32	62
		<i>o</i> -Xylene	9	–	92

^aOptical purity of amide reduced from >99 to 86% ee through amide condensation



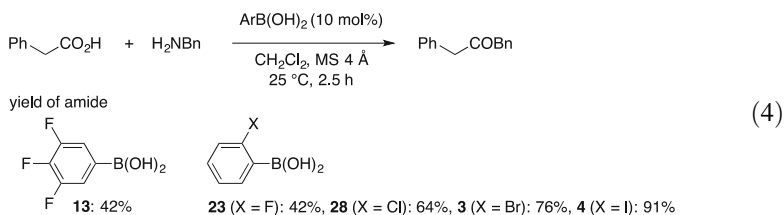
Examples



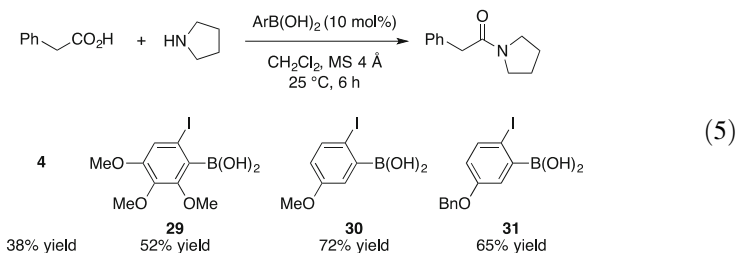
(3)

In 2008, Hall et al. reported that 2-halophenylboronic acids were superior to **13** as amide condensation catalysts in the presence of 4 Å MSs at 25°C (Eq. 4) [10–12]. In particular, 2-iodophenylboronic acid **4** gave amides in higher yields.

However, the substrates were limited to sterically less-hindered compounds such as phenylacetic acids, primary amines, and pyrrolidine.



Furthermore, Hall et al. also investigated some electron-rich arylboronic acids in the model direct amidation reaction between phenylacetic acid and pyrrolidine for a set time of 6 h before the reaction reaches completion (Eq. 5) [12]. All new electron-rich arylboronic acids **29–31** reproducibly showed superior reactivity compared to **4**. For example, electronically enriched catalyst **30** led to 72% of the amide product, while catalyst **4** provided only 38% yield under identical conditions. When compared with the outcome of catalyst **29**, this data tends to confirm the detrimental effect of a methoxy substituent positioned *para* to the boron atom.



The representative results for the amide condensation catalyzed by **30** or **4** at room temperature are shown in Table 6. In all cases, **30** is more active than **4**. The use of 10 mol% of **30** is required for nonconjugated carboxylic acids at room temperature (entries 1, 2, 6–10). In contrast, 20 mol% of **30** is required for less reactive conjugated carboxylic acids at 50°C (entries 3–5). Ibuprofen amide was obtained without racemization at room temperature in the presence of 20 mol% of **30**.

Marcelli's DFT calculations imply the formation of an acylborate intermediate **32** en route to an *ortho*-aminal transition state (TS-**34**) shown in Scheme 11 [40]. Strangely, according to the theoretical transition state, a water molecule is involved in the *ortho*-aminal breakdown. Thus, Hall et al. proposed that a non-hydrated monoacylborate **35** would form during the initiation phase. Its formation may be inhibited in the presence of the amine. However, once formed in the absence of amine, **35** can react with added amine via transition structure TS-**36**. In TS-**36**, a molecule of carboxylic acid (in lieu of H₂O in TS) can assist the *ortho*-aminal breakdown to eliminate water and regenerate **35**. According to more recent theoretical calculations by Fu et al. which take specific account of solvent effects,

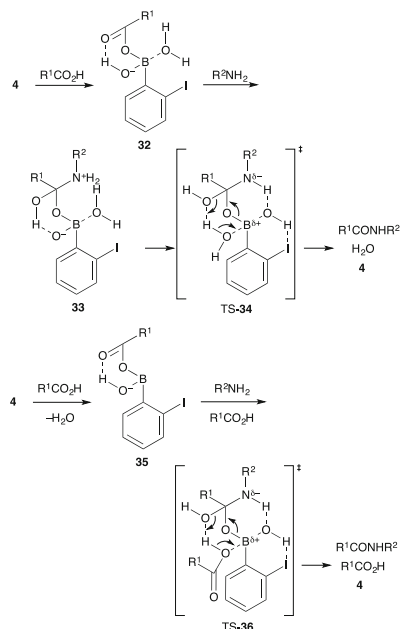
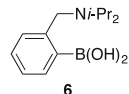
Table 6 Amide condensation of various carboxylic acids with amines catalyzed by **30** or **4**

Entry	Product	Temperature (°C)	Time (h)	Yield (%)	
				4	30
	$\text{R}^1\text{CO}_2\text{H} + \text{R}^2\text{R}^3\text{NH} \xrightarrow[\text{4\AA MS, CH}_2\text{Cl}_2 [70 \text{ mM}]]{\text{4 or 30 (10 mol\%)}} \text{R}^1\text{CONR}^2\text{R}^3$ (1.1 equiv) (1 equiv)				
1	BnCONHi-Bu	rt	2	68	90
2	Ph ₂ CHCONHi-Bu	rt	6	44	58
3 ^{a,b}		50	48	22	30
4		50	48	38	53
5		50	48	51	73
6	BnCO-N	rt	6	66	91
7	BnCO-N	rt	48	55	70
8	BnCO-N	rt	48	0	0
9		rt	6	50	65
10		rt	2	62	85
11 ^a		rt	48	55 ^c	80 ^c

^aWith 20 mol% catalyst^bWith toluene as solvent^cLess than 5% racemization

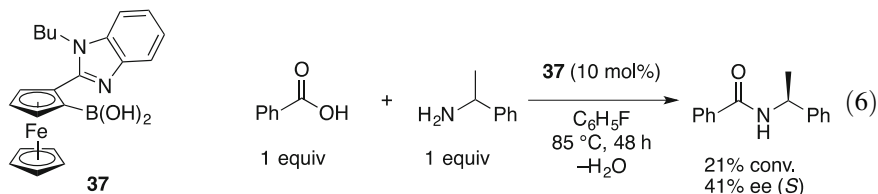
there is no need for a water molecule in the transition state. Not only are arylboronic acids predicted to react through monoacyloxyboronates, but the high catalytic activity of 2-iodophenylboronic acid **4** is attributed to the steric effect of the iodine as well as the orbital interaction between the iodine and the boron atom [41].

According to kinetic studies on the direct formation of amides from amines and carboxylic acids both with and without boron(III) catalysts by Whiting et al. [42], the efficiency of amide formation under thermal and catalyzed conditions is highly substrate dependent. For alkyl carboxylic acids such as 4-phenylbutyric acid, the addition of boron-based catalysts improves the reaction rate and the yield of amide, despite the competing thermal reaction. However, there is an even greater improvement with aryl carboxylic acids such as benzoic acid, where the thermal reaction is truly nonexistent. Interestingly, the use of an aminoboronic acid catalyst **6** clearly

Scheme 11 Proposed mechanisms for direct amide formation**Fig. 2** Aminoboronic acid catalyst **6**

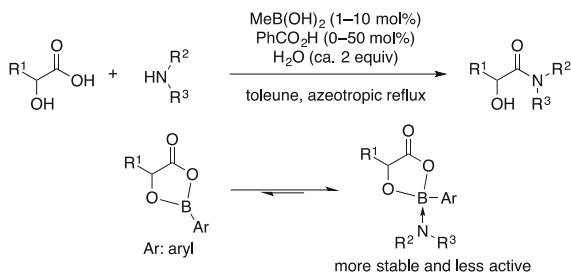
improves amide formation, particularly for aryl carboxylic acids and at lower reaction temperatures. This catalyst has also been shown to act through a bifunctional mechanism; the exact nature of which has not yet been fully elucidated. However, **6** is superior to other monofunctional boronic acid catalysts for more difficult amidations (Fig. 2).

In 2008, Whiting et al. reported that (*pS*)-2-(2-boronofero-cenyl)-*N*-*n*-butylbenzimidazole (**37**) could induce the kinetic resolution of racemic α -substituted benzylamines through direct amide condensation with achiral carboxylic acids (Eq. 6) [43].



In 2013, Ishihara et al. reported that primary alkylboronic acids such as methylboronic acid and butylboronic acid are highly active catalysts for the

Scheme 12 Selective amidation of α -hydroxycarboxylic acids catalyzed by methylboronic acid



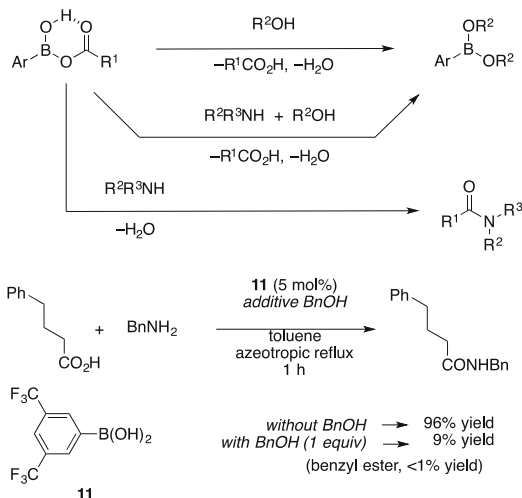
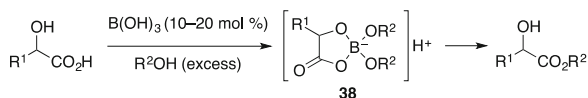
dehydrative amide condensation of α -hydroxycarboxylic acids (Scheme 12) [44]. The catalytic activities of these primary alkylboronic acids are much higher than those of the previously reported more Lewis acidic arylboronic acids, because in situ-generated cyclic boronates easily coordinate with amines, and the catalytic activity is suppressed. This method is easily applied to a large-scale synthesis, and 14 g of an amide was obtained in a single reaction.

4 B(III)-Catalyzed Dehydrative Condensation to Carboxylic Acid Esters

Generally, boron(III) compounds such as 3,5-bis(trifluoromethyl)phenylboronic acid **11** are thought to promote the amide condensation of carboxylic acids with amines via the corresponding (acyloxy)borane intermediates, but are less effective for the esterification of carboxylic acids with alcohols, because an alkoxyborane species is preferentially produced, rather than the desired (acyloxy)borane species (Scheme 13) [45].

In 2004, Houston et al. reported that boric acid [B(OH)₃, 10–20 mol%] was effective as a catalyst for the chemoselective esterification of α -hydroxycarboxylic acids with excess alcohol as a solvent, even at ambient temperature (Scheme 14) [46]. This unexpected reactivity of α -hydroxycarboxylic acids with alcohols can be understood by considering that a thermally stable 2,2-dialkoxy-4-oxo-1,3,2-dioxaborolan-2-uide (**38**) is preferentially produced as an anionic active intermediate, even in the presence of excess alcohol.

In 2005, Yamamoto and Ishihara et al. reported that 4-borono-*N*-methylpyridinium iodide **8** was a more effective catalyst than boric acid for the esterification of α -hydroxycarboxylic acids in excess alcohol solvents (Houston's conditions), probably because **8** is a tolerant cationic Lewis acid catalyst in polar alcohols [45, 47]. On the other hand, boric acid is a more effective esterification catalyst for equimolar mixtures of α -hydroxycarboxylic acids and alcohols. Representative results are shown in Table 7. Not only α -hydroxycarboxylic acids (entries 1–6) but also β -hydroxycarboxylic acids (entries 7 and 8) are condensed. In the esterification of 4-hydroxyisophthalic acid, the *ortho*-hydroxycarbonyl group selectively reacts (entry 7). The esterification condensation of less reactive secondary

Scheme 13 Amide versus ester condensation**Scheme 14** Houston's boric acid-catalyzed esterification

alcohols and aromatic carboxylic acids proceeds well with the use of 10 mol% of **17** (entries 3 and 7). β -Hydroxycarboxylic acids bearing a benzyloxycarbonylamino group at the α -position also reacted (entry 8). Although ethylene glycol is known to react with boronic acid, leading to the corresponding cyclic boronic ester, esterification with mandelic acid is unexpectedly preferred (entry 4).

N-Polystyrene-bound 4-boropyridinium salts (**18a-d**) are effective as heterogeneous catalysts. Compounds **18a-d** can be recovered by filtration and reused tenfold without any loss of activity for the esterification of mandelic acid in excess isobutanol under reflux conditions [45, 47].

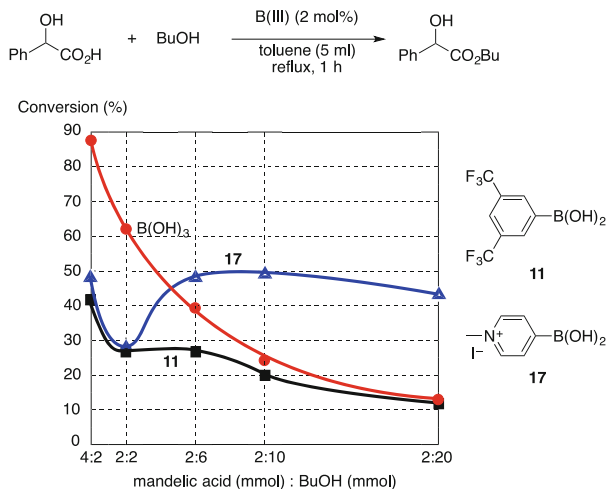
Figure 3 shows the correlation between the catalytic activity of boron(III) compounds and the molar ratio of mandelic acid and butanol for esterifications catalyzed by 2 mol% of boric acid, **11** and **17**. The conversion into butyl mandelate after heating under reflux conditions in toluene for 1 h is plotted in terms of the molar ratio of mandelic acid to butanol. Boric acid is the most active catalyst for a molar ratio of mandelic acid/butanol of $>1/2$. On the other hand, **17** is the most active catalyst for a molar ratio of mandelic acid/butanol of $<1/3$. In contrast, **11** is less active than boric acid and **17**, regardless of the molar ratio of mandelic acid/butanol. These three catalysts share two common phenomena: (1) excess mandelic acid accelerates the esterification and (2) excess butanol suppresses the esterification, probably because excess butanol dilutes the concentration of mandelic acid and the Lewis basicity of excess butanol weakens the Lewis acidity of the catalysts. However, **17** is still active in the presence of excess butanol because of its ability to tolerate polar compounds.

Table 7 Esterification of hydroxycarboxylic acids in alcohols catalyzed by **17**

Entry	Temperature	Time (h)	Yield (%)	$\text{RCO}_2\text{H} \xrightarrow[\text{R}^2\text{OH (5 mL)}]{\text{17 (5 mol\%)} \text{ RCO}_2\text{R}^2} \text{Product}$		Entry	Temperature	Time (h)	Yield (%)	Product
				Yield (%)	Product					
1	rt	10 h	93			5 ^a	Reflux	15	95	
2	Reflux	15	92			6 ^a	Reflux	18	92	
3 ^a	Reflux	21	81			7 ^{b,c}	Reflux	20	84	
4	80°C	5	97			8	Reflux	22	89	

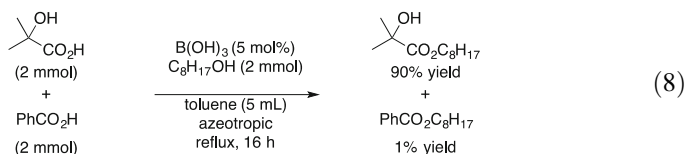
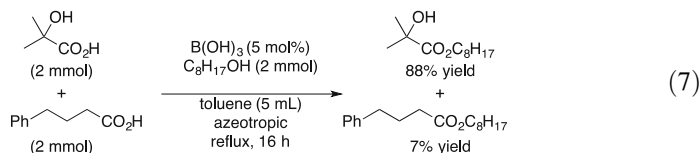
^aDicarboxylic acid is used as substrate^b10 mol% **17** is used^cDiisobutyl 4-hydroxyisophthalate and 2-hydroxy-5-(isobutoxycarbonyl)benzoic acid are produced in respective yields of 5 and 2%

Fig. 3 Correlation between catalytic activity of boron (III) compounds and molar ratio of mandelic acid and butanol



The generality and scope of the esterification of equimolar mixtures of α -hydroxycarboxylic acids and alcohols catalyzed by boric acid are shown in Table 8 (entries 1–6) [45, 47]. Not only are α -hydroxycarboxylic acids and primary alcohols applicable, but also β -hydroxycarboxylic acids and secondary alcohols are reactive.

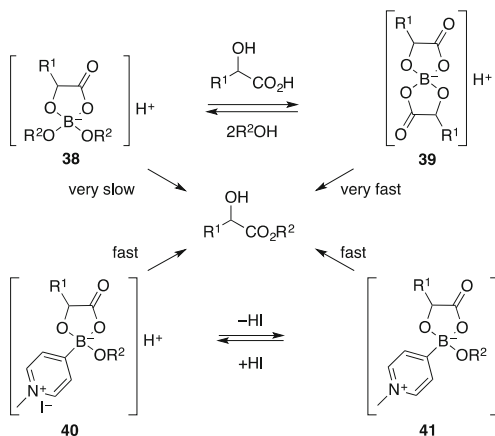
The boric acid-catalyzed chemoselective esterification of α -hydroxy- α -methylpropanoic acid proceeds in the presence of 4-phenylbutyric acid or benzoic acid (Eqs. 7 and 8).



Boric acid is known to react with 2 equiv. of α -hydroxycarboxylic acids to give dimeric borate complex **39**, which is more active than monomeric **38** (Scheme 15). However, an equilibrium is observed between **38** and **39**. The more active species **39** exists as a major intermediate in an esterification reaction solution with a higher molar ratio of α -hydroxycarboxylic acid, while the less active species **38** is a major intermediate in excess alcohol. Based on the experimental results shown in Fig. 3, the reactivity of the intermediates with alcohols increases in the order **38** < **40** and **41** < **39**.

Table 8 Esterification of equimolar mixture of hydroxycarboxylic acids and alcohols catalyzed by boric acid

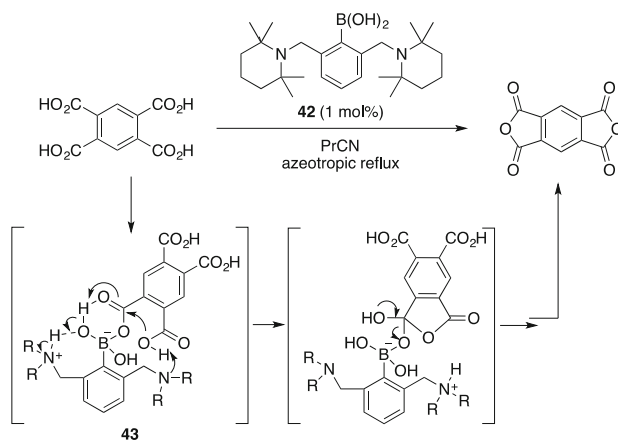
		RCO ₂ H + R ² OH		B(OH) ₃ (5 mol%)		RCO ₂ R ²	
		1 : 1		toluene, azeotropic reflux			
Entry	Time (h)	Product	Yield (%)	Entry	Time (h)	Product	Yield (%)
1	4		93	4 ^a	21		87
2	21		99	5 ^a	20		82
3	21		90	6 ^{a,b}	21		86

^aBoric acid (10 mol%) was used^b*o*-Xylene was used in place of toluene**Scheme 15** Proposed reaction mechanism

Compound **17** is effective for the esterification of L-phenylalanine and its *N*-protected derivatives in methanol (Table 9, entries 1–8). In particular, *N*-tosyl-L-phenylalanine (entry 1) and methoxyphenylacetic acid (entry 7) are much more reactive than L-phenylalanine and its *N*-carboxyl derivatives. In contrast, α -phenylpropionic acid is much less reactive (entry 8). The good results (entries 1 and 7) can be understood in terms of the weak coordination of α -tosylamino and α -methoxy groups to the boron(III) atom.

Table 9 Methyl esterification of α -functionalized carboxylic acids

		17 (5 mol%)			
		MeOH (5 mL), reflux, 20 h			
		Ph-CH ₂ -CO ₂ H $\xrightarrow{\hspace{1.5cm}}$ Ph-CH ₂ -CO ₂ Me			
Entry	X	Yield (%)	Entry	X	Yield (%)
1	TsNH	76	5	TfNH	24
2	CbzNH	61	6	NH ₂ ^a	N.R.
3	BzNH	45	7	OMe ^b	71
4	AcNH	28	8	Me ^c	28

^aL-Phenylalanine is not dissolved^b α -Methoxyphenylacetic acid is used as substrate^c α -Phenylpropanoic acid is used as substrate**Scheme 16** Intramolecular dehydrative condensation of 1,2-dicarboxylic acids

5 B(III)-Catalyzed Dehydrative Condensation to Carboxylic Anhydrides

Ishihara et al. developed 2,6-diaminomethylphenylboronic acid **42** to effectively catalyze the dehydrative intramolecular condensation of dicarboxylic acids to afford cyclic anhydrides under significantly milder temperatures compared to the thermal variant (Scheme 16) [48, 49]. The authors claimed that boronic acid **42** works as a bifunctional catalyst, with the amine substituent serving as a Brønsted base to deprotonate the carboxylic acid, thus increasing nucleophilicity of the carboxylate functionality in the proposed monoacyl boronate intermediate **43**. Moreover, the second protonated amine substituent can act as a Brønsted acid to further activate the carbonyl group through a relay of two hydrogen bonding interactions.

6 Other B(III)-Catalyzed Reactions

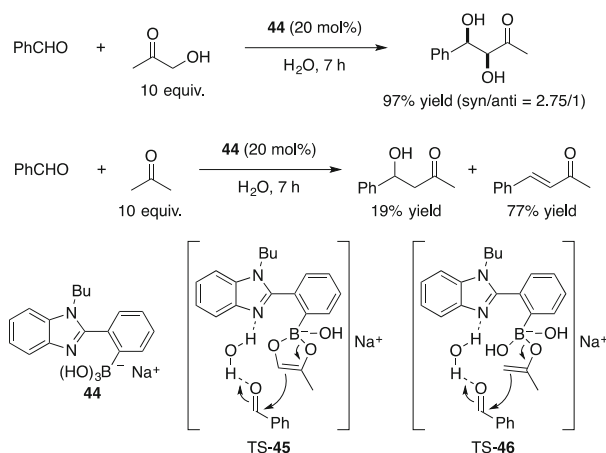
Boronic acid catalysis is emerging as a mild and effective strategy for the direct, covalent activation of not only carboxylic acids but also alcohols and enol derivatives. For example, imine hydrolysis [50], epoxide ring opening [51], the Biginelli reaction [52], and dipolar cycloaddition [53] have already been performed under boronic acid catalysis.

In 2008, Whiting et al. reported a catalytic aldol reaction and condensation through in situ boron ate complex enolate generation in water (Scheme 17) [54]. The sodium ate complex **44** of benzimidazolylphenylboronic acid shows high catalytic activity in water at 20 mol% for the aldol reaction of aldehydes with hydroxyacetone in high conversion and moderate to high *syn* selectivity. In contrast, the reaction of aldehydes with acetone mainly gives condensation products. Transition state structures **45** and **46** for the aldol reactions are proposed.

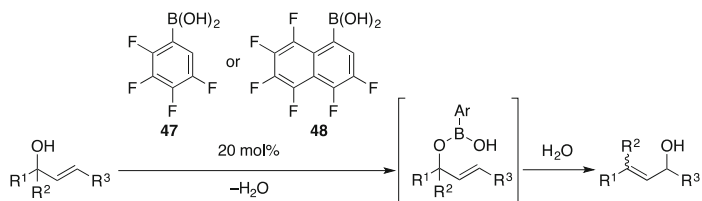
In 2010, Dixon et al. used 3-nitrophenylboronic acid **15** to promote the enolization of 1,3-dicarbonyl compounds [55]. In refluxing toluene, the generated enol subsequently undergoes a concerted ene carbocyclization with a pendant alkyne substituent to afford carbocyclic products in good yields.

In the same year, McCubbin et al. reported Friedel–Crafts-type alkylations by activation of allylic and benzylic alcohols with electron-poor boronic acids [56, 57]. Inspired by this approach, Hall et al. devised mild and effective reaction conditions for the stereoselective 1,3-transpositions of allylic and propargylic alcohols in the absence of an external nucleophile (Scheme 18) [58]. 2,3,4,5-Tetrafluorophenylboronic acid **47** and 3,4,5,6,7,8-hexafluoro-1-naphthylboronic acid **48** are more effective for the activation of hydroxyl groups.

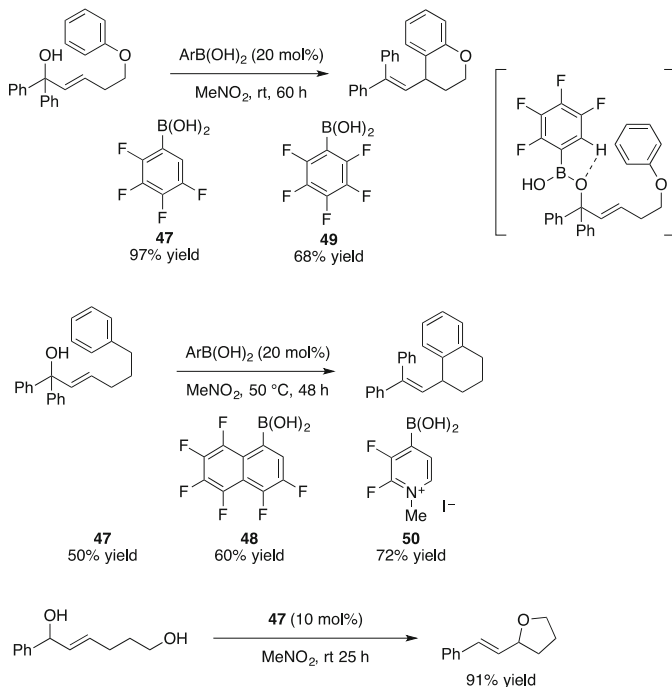
In 2012, Hall et al. reported direct carbo- and hetero-cyclizations of free allylic alcohols (Scheme 19) [59] with compounds **47** and **48** being effective as catalysts.



Scheme 17 Direct aldol reaction and condensation



Scheme 18 Stereoselective 1,3-transpositions of allylic alcohols

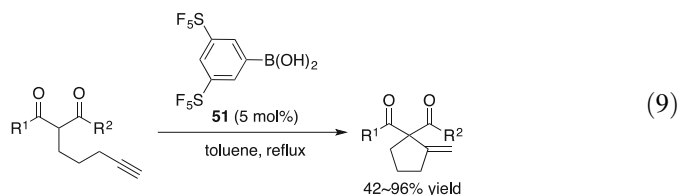


Scheme 19 Direct carbo- and hetero-cyclizations of free allylic alcohols

A comparison with pentafluorophenylboronic acid **49** confirmed that **47** was a superior catalyst. The inferior efficiency of **49** versus **47** was not thought to be due to a difference in stability because both catalysts could be recovered intact after the reaction. One explanation is the possibility for additional substrate activation from the relatively acidic *ortho* C–H bond of arylboronic acids. 2,3-Difluoro-4-methylpyridiniumboronic acid **50** is more effective for the intramolecular Friedel–Crafts cyclization of unactivated arene substrate.

In the same year, Shibata et al. introduced 3,5-bis(pentafluorosulfanyl)boronic acid **51** as an efficient organocatalyst for Conia-ene carbocyclization of 1,3-dicarbonyl compounds having terminal alkynes. A variety of 2-alkynic 1,3-dicarbonyl compounds were smoothly converted to ene-carbocyclization

products in moderate to excellent yields. Compared with the reported catalyst, 3-nitrophenylboronic acid **15**, catalyst **51** was slightly better in a nonpolar solvent such as toluene and 1,1,1,3,3-pentafluorobutane. These results indicate that the SF₅ function can be a lipophilic and sterically demanding alternative to the NO₂ group in catalyst design (Eq. 9) [60].



7 Conclusions

This review clearly demonstrates the recent progress in methods for the synthesis of carboxylic esters and carboxamides from classical methods with stoichiometric condensing agents to dehydrative condensation methods with reusable catalysts directed toward green and sustainable chemistry. Catalytic dehydrative condensation processes have recently matured with an impressive and steadily increasing number of reports regarding the synthesis of carboxylic esters. In contrast, there are only a few successful examples of catalytic methods for the synthesis of carboxamides. For the synthesis of carboxylic esters, several catalytic dehydrative condensation reactions have been realized without removal of the water produced. The application of organocatalysts has permitted the preparation of several valuable products, while excluding the use of hazardous metals and offering several economic and environmental advantages. These contributions from many academic groups have led to dramatic improvements in catalytic dehydrative condensation reactions. By improvements in practicality and environmental safety, these groups will undoubtedly continue to advance this field in a direction that benefits academic chemists, process chemists, material chemists, natural product chemists, and medicinal chemists alike. The use of boronic acids, for novel types of reactions not involving condensation, looks to be highly promising, and perhaps this is an area where major further developments might be expected.

References

1. Brown HC, Stocky TP (1977) *J Am Chem Soc* 99:8218
2. Brown HC, Stocky TP (1987) *J Am Chem Soc* 52:3925
3. Kato K, Furuta K, Yamamoto H (1992) *Synlett* 565
4. Hall DG (ed) (2011) *Boronic acids—preparation and applications in organic synthesis medicine and materials*, 2nd edn. Wiley-VCH, Weinheim
5. Lozada J, Liu Z, Perrin DM (2014) *J Org Chem* 79:5365

6. Ishihara K (2009) *Tetrahedron* 65:1085
7. Zheng H, Hall DG (2014) *Aldrichmica Acta* 47:41
8. Furuta K, Miwa Y, Iwanaga K, Yamamoto H (1988) *J Am Chem Soc* 110:6254
9. Ishihara K, Gao Q, Yamamoto H (1993) *J Am Chem Soc* 115:10412
10. Al-Zoubi RM, Marion O, Hall DG (2008) *Angew Chem Int Ed* 47:2876
11. Zheng H, Hall DG (2010) *Tetrahedron Lett* 51:3561
12. Gernigon N, Al-Zoubi RM, Hall DG (2012) *J Org Chem* 77:8386
13. Azuma T, Murata A, Kobayashi Y, Inokuma T, Takemoto Y (2014) *Org Lett* 16:4256
14. Mitchell JA, Reid EE (1931) *J Am Chem Soc* 53:1879
15. Jursie BS, Zdravkovski Z (1993) *Synth Commun* 23:2761
16. Charville H, Jackson DA, Hodges G, Whiting A, Wilson MR (2011) *Eur J Org Chem* 5981
17. Allen CL, Chhatwal AR, Williams MJ (2012) *Chem Commun* 48:666
18. Perreux L, Loupy A, Volatron F (2002) *Tetrahedron* 58:2155
19. Pelter A, Levitt TE, Nelson P (1970) *Tetrahedron* 26:1539
20. Trapani G, Reho A, Latrofa A (1983) *Synthesis* 1013
21. Tani J, Oine T, Inoue I (1975) *Synthesis* 714
22. Collum DB, Chen S, Ganem B (1978) *J Org Chem* 43:4393
23. Ishihara K, Ohara S, Yamamoto H (1996) *J Org Chem* 61:4196
24. Ishihara K, Ohara S, Yamamoto H (2000) *Macromolecules* 33:3511
25. Ishihara K, Ohara S, Yamamoto H (2002) *Org Synth* 79:176
26. Maki T, Ishihara K, Yamamoto H (2004) *Synlett* 1355
27. Ishihara K, Kondo S, Yamamoto H (2001) *Synlett* 1371
28. Wipf P, Wang X (2002) *J Comb Chem* 4:656
29. Liu S, Yang Y, Liu X, Ferdousi FK, Batsanov AS, Whiting A (2013) *Eur J Org Chem* 5692
30. Ohara S, Ishihara K, Yamamoto H (2000) The 78th spring meeting of chemical society of Japan, 3-B5-10
31. Ishihara K, Yamamoto H, Japan Kokai Tokkyo Koho JP 2001-270939 (2001-10-02), Application: JP 2000-87495 (2000-03-27)
32. Maki T, Ishihara K, Yamamoto H (2005) *Org Lett* 7:5043
33. Latta R, Springsteen G, Wang B (2001) *Synthesis* 1611
34. Gu L, Lim J, Cheong JL, Lee SS (2014) *Chem Commun* 50:7017
35. Yang W, Gao X, Springsteen G, Wang B (2002) *Tetrahedron Lett* 43:6339
36. Lanigan RM, Starkov P, Sheppard TD (2013) *J Org Chem* 78:4512
37. Maki T, Ishihara K, Yamamoto H (2006) *Org Lett* 8:1431
38. Tang P (2005) *Org Synth* 81:262
39. Mylavarapu RK, Kondaiah GCM, Kolla N, Veeramalla R, Koilkonda P, Bhattacharya A, Bandichhor R (2007) *Org Process Res Dev* 11:1065
40. Marcelli T (2010) *Angew Chem Int Ed* 49:6840
41. Wang C, Yu H-Z, Fu Y, Guo Q-X (2013) *Org Biomol Chem* 11:2140
42. Arnold K, Davies B, Giles RL, Grosjean C, Smith GE, Whiting A (2007) *Adv Synth Catal* 348:813
43. Arnold K, Davies B, Héroult D, Whiting A (2008) *Angew Chem Int Ed* 47:2673
44. Yamashita R, Sakakura A, Ishihara K (2013) *Org Lett* 15:3654
45. Maki T, Ishihara K, Yamamoto H (2005) *Org Lett* 7:5047
46. Houston TA, Wilkinson BL, Blanchfield JT (2004) *Org Lett* 6:679
47. Maki T, Ishihara K, Yamamoto H (2007) *Tetrahedron* 63:8645
48. Sakakura A, Ohkubo T, Yamashita R, Akakura M, Ishihara K (2011) *Org Lett* 13:892
49. Sakakura A, Yamashita R, Ohkubo T, Akakura M, Ishihara K (2011) *Aust J Chem* 64:1458
50. Rao G, Philipp M (1991) *J Org Chem* 13:892
51. Hu X-D, Fan C-A, Zhang F-M, Tu Y-Q (2004) *Angew Chem Int Ed* 43:1702
52. Debache A, Boumoud B, Amimour M, Belfaitah A, Rhousati S, Carboni B (2006) *Tetrahedron Lett* 47:5697
53. Zheng R, McDonald R, Hall DG (2010) *Chem Eur J* 16:5454

54. Aelvoet K, Batsanov AS, Blatch AJ, Grosjean C, Patrick LGF, Smethurst CA, Whiting A (2008) *Angew Chem Int Ed* 47:768
55. Li M, Yang T, Dixon DJ (2010) *Chem Commun* 46:2191
56. McCubbin JA, Hosseini H, Krokhin OV (2010) *J Org Chem* 75:959
57. McCubbin JA, Krokhin OV (2010) *Tetrahedron Lett* 51:2447
58. Zheng H, Lejkowski M, Hall DG (2011) *Chem Sci* 2:1305
59. Zheng H, Ghanbari S, Nakamura S, Hall DG (2012) *Angew Chem Int Ed* 51:6187
60. Yang Y-D, Lu X, Tokunaga E, Shibata N (2012) *J Fluorine Chem* 204

Reagent-Controlled Lithiation–Borylation

Daniele Leonori and Varinder K. Aggarwal

Contents

1	Introduction	272
2	Mechanism of Lithiation–Borylation Processes	272
3	α -Chloro-Stabilized Lithium Carbenoids	273
4	α -O-Stabilized Organolithiums	275
4.1	Primary Carbamates/Benzoates	276
4.2	Secondary Benzylic Carbamates	283
4.3	Secondary Allylic/Propargylic Carbamates	289
4.4	Secondary Benzoates	291
5	α -N-Stabilized Organolithiums	292
6	Conclusions and Outlook	293
	References	294

Abstract This chapter focuses on the stereo-controlled homologation of chiral boronic esters with chiral lithium carbenoid (lithiation–borylation) as a powerful method for the asymmetric synthesis of many complex molecules. It is highlighted that the potential methodology to create multiple contiguous stereogenic centers on “growing” carbon chains.

Keywords 1,2-Metallate rearrangement • Boronic esters • Stereospecific • Homologation • Lithiated carbamates • Total synthesis

D. Leonori • V.K. Aggarwal (✉)
School of Chemistry, University of Bristol, Cantock’s Close, Bristol, UK
e-mail: v.aggarwal@bristol.ac.uk

© Springer International Publishing Switzerland 2015
E. Fernández, A. Whiting (eds.), *Synthesis and Application of Organoboron Compounds*, Topics in Organometallic Chemistry 49,
DOI 10.1007/978-3-319-13054-5_9

271

1 Introduction

The stereo-controlled homologation of chiral boronic esters with chiral lithium carbenoid (lithiation–borylation) is a powerful method for the asymmetric synthesis of many complex molecules. Its importance is underscored by its capability to create multiple contiguous stereogenic centers on “growing” carbon chains often in a telescoped fashion [1, 2].

The fundamental work on the asymmetric homologation of organoborons was carried out by Matteson in the 1980s [3–5]. In his contributions, a chiral auxiliary was embedded in the diol unit of the boronic ester, and a two-step sequence, consisting of the (1) addition of chloromethyl lithium and (2) addition of an achiral Grignard, was employed. In this substrate-controlled approach, the stereochemical outcome was dictated by the chiral diol stereochemistry and was highly predictable. However, a limitation becomes evident when multiple stereocenters that are not set to benefit from the substrate bias need to be installed. In this case the chiral diol at boron needs to be exchanged in order to obtain the desired product [6].

The lithiation–borylation approach solves this issue due to its reagent-controlled nature. In this case the chirality is contained within the chiral lithium carbenoid, usually an α -lithiated carbamate. Having both enantiomers of the chiral lithium carbenoid enables access to any possible isomer at will.

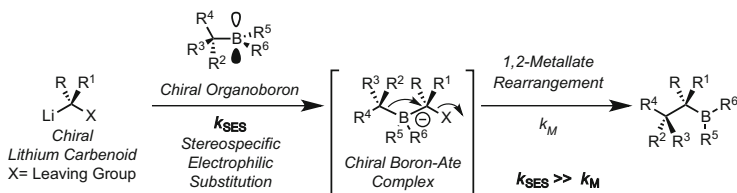
In this chapter we discuss the state of modern reagent-controlled homologation of chiral boronic esters and its application in organic synthesis with particular attention to papers published from 2005. We will first describe relevant mechanistic features of lithiation–borylation. After that, the discussion will be divided into the different types of lithium carbenoids that have been employed, and finally selected applications in the synthesis of complex molecules will be illustrated.

2 Mechanism of Lithiation–Borylation Processes

Organoboranes and boronic esters are good electrophiles and react with nucleophiles to give intermediate ate complexes. When the nucleophile also contains a good leaving group, 1,2 migration occurs creating a new C–C or C–X bond. This type of reaction is fundamental to many transformations of organoboron compounds. In the case of lithium carbenoid-based nucleophiles, the 1,2-metallate rearrangement creates a C–C bond leading to homologated products. The process is stereospecific since the migrating group aligns anti-periplanar to the leaving group.

For broad synthetic utility it is important that several factors are simultaneously satisfied (Scheme 1):

1. The chiral lithium carbenoid has to be chemically and configurationally stable under the reaction conditions. Should this not be the case, low yield and low selectivity will be observed.



Scheme 1 General mechanism for lithiation–borylation with chiral, non-racemic organolithiums and organoborons

2. The reaction of the lithium carbenoid with the boron electrophile needs to be fully stereospecific, either retentive ($S_{\text{E}}2_{\text{ret}}$) or invertive ($S_{\text{E}}2_{\text{inv}}$), so that only one chiral boronate complex is formed.
3. The boronate complex formation should be nonreversible. Should this not be the case, the re-formed organolithium might undergo decomposition or epimerization pathways.
4. The 1,2-metallate rearrangement has to proceed at temperature higher than the boronate complex formation (normally -78°C). This is required in order to avoid over-homologations.

α -Lithiated carbamates and benzoates are highly effective for these processes, and they represent the most commonly used source of chiral lithium carbenoids in modern lithiation–borylation methodologies. Regarding the organoboron reagents, there is a significant difference between boranes and boronic esters. Boranes display enhanced electrophilicity and undergo faster 1,2-metallate rearrangement compared to boronic esters [7]. However, boronic esters are easier to prepare and handle, and many are commercially available making them more practical to work with.

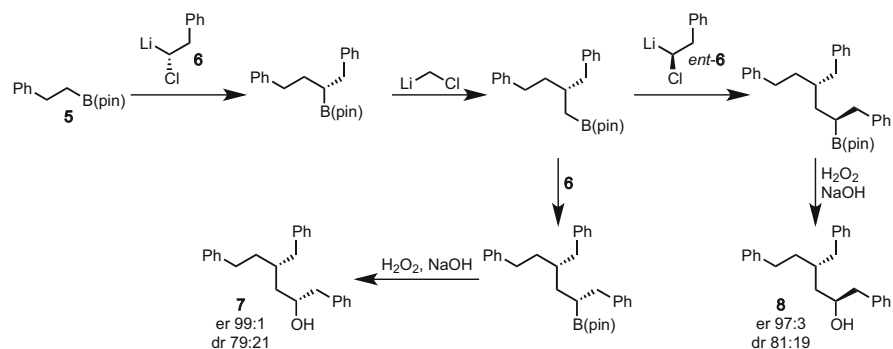
3 α -Chloro-Stabilized Lithium Carbenoids

Chiral α -chloro organolithiums have historically been the first class of chiral lithium carbenoids to be exploited in reagent-controlled homologation of boronic esters. This class of organometallic reagents was obtained by sulfoxide–lithium exchange from chiral α -chloro sulfoxides and *t*-BuLi as pioneered by Hoffmann [8]. However, due to the chemical and configurational lability of the organolithium, Barbier conditions are generally employed to trap the organolithium as soon as it is formed. Blakemore developed the reactions of chiral α -chloro organolithiums with neopentyl glycol and pinacol boronic esters (Table 1) [9]. This process involved the generation of the chiral α -chloro organolithiums from **1** (er 99:1) in the presence of the boronic esters at low temperature giving the chiral boronate complexes **2**. Upon warming to 0°C the desired 1,2-metallate rearrangement took place leading to the

Table 1 Homologation of boronic esters with enantioenriched α -chloro-alkyllithiums

$\text{B(OR)}_2 = \text{B(pin)} \quad \text{B(neo)}$

Entry	R	B(OR) ₂	R ¹	Yield (%)	es (%)
1	PhCH ₂	Neo	PhCH ₂ CH ₂	70	97
2	PhCH ₂	Pin	PhCH ₂ CH ₂	76	93
3	PhCH ₂	Pin	Cy	67	83
4	<i>i</i> -Bu	Pin	PhCH ₂ CH ₂	64	93
5	PhCH ₂ CH ₂	Neo	Cy	26	87
6	Et	Neo	PhCH ₂ CH ₂	29	99

**Scheme 2** Iterative homologations of pinacol boronic esters with enantioenriched α -chloro-alkyllithiums

homologated boronic esters **3** that after oxidation gave the desired chiral alcohols **4** in high yield and enantiospecificity (es).

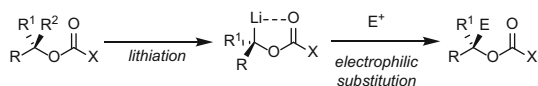
Blakemore has also successfully applied this chemistry to the synthesis of alkyl chains bearing 1,3-stereogenic centers (Scheme 2). In this example, starting from the primary boronic ester **5**, homologation with the chiral lithium carbenoid **6** was followed by a 1-C homologation using chloromethyl lithium and a second homologation with **6** or its enantiomer *ent*-**6**. Finally oxidation gave the desired products **7** and **8** in very high er and moderate dr. The reactions were under full reagent control without interference from substrate control [10].

4 α -O-Stabilized Organolithiums

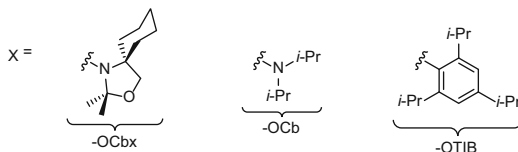
Lithiated carbamates and benzoates represent the most widely used class of chiral carbenoids in modern lithiation–borylation methodologies (Scheme 3). Three main factors account for their success:

1. They are easy to generate in excellent yield and selectivity by stereospecific deprotonation of chiral secondary carbamates, stereospecific Sn–Li exchange, or enantioselective deprotonation of primary carbamates/benzoates.
2. They display sufficient chemical and configurational stability under cryogenic conditions.
3. The addition of boron electrophiles is stereospecific.

The directing group choice (carbamate vs. benzoate) is frequently dictated by the substrate features and reflects their ability to serve as both directing groups and leaving groups. In general, carbamates (OCb and OCbx) give slightly higher levels of enantioselectivity by asymmetric deprotonation, but benzoates are better leaving groups and enable slow migrating groups on boron (e.g., Me, Ph, $(\text{CH}_2)_2\text{CN}$) to be employed. An especially difficult case is dialkyl α -O organolithiums which can only be generated with a benzoate as the directing group (*vide infra*).



$\text{R}^1 = \text{H}$	$\text{R}^2 = \text{H}$	\rightarrow	asymmetric deprotonation
$\text{R}^1 = \text{H/C}$	$\text{R}^2 = \text{Sn}$	\rightarrow	stereospecific Sn–Li exchange
$\text{R}^1 = \text{C}$	$\text{R}^2 = \text{H}$	\rightarrow	stereospecific deprotonation



Secondary Organolithiums



R = alkyl	\rightarrow	OCbx, OCb, OTIB
vinyl	\rightarrow	OCb
aryl	\rightarrow	OCbx, OCb

Tertiary Organolithiums



R = alkyl	$\text{R}^1 =$ alkyl	\rightarrow	OTIB
vinyl	alkyl	\rightarrow	OCbx, OCb
aryl	aryl	\rightarrow	OCbx, OCb
aryl	alkyl	\rightarrow	OCbx, OCb

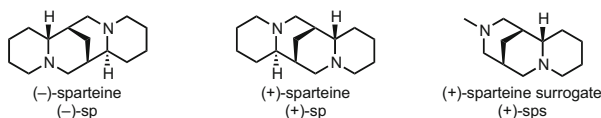
Scheme 3 Asymmetric deprotonation and electrophilic quench of carbamates and hindered benzoates

4.1 Primary Carbamates/Benzoates

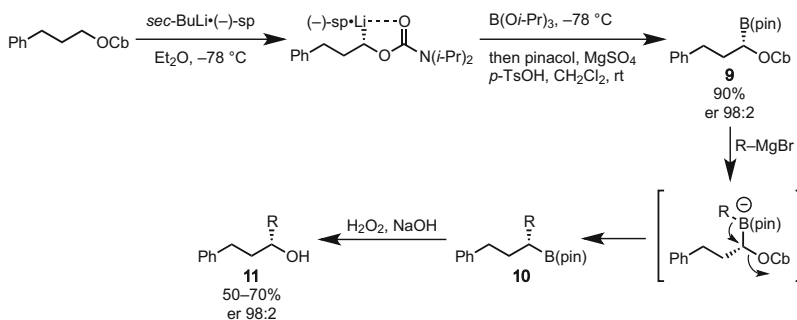
Primary alkyl carbamates can be lithiated with high selectivity and efficiently quenched with many electrophiles using *sec*-BuLi(-)-sparteine as demonstrated by Hoppe [11]. This chemistry has the advantage that by using (+)-sparteine, or the (+)-sparteine surrogate (Scheme 4 for their structures), the opposite enantiomer of the chiral organolithium can be accessed in similar yield and selectivity.

During his pioneering studies on asymmetric lithiation, Hoppe demonstrated that triisopropoxy borate [B(Oi-Pr)₃] was a competent electrophile for the asymmetric synthesis of α -O-boronic esters **9** upon *trans*-esterification with pinacol (Scheme 5). Following the addition of Grignard reagents and 1,2-metallate, rearrangement led to the homologated boronic esters **10** which were oxidized to give the corresponding chiral secondary alcohols **11** in high overall yield and selectivity [12, 13].

Kocienski [14] and Aggarwal [15] showed that the 3-step sequence could be streamlined to a single operation by directly adding a boronic ester to the intermediate chiral organolithium. As outlined in Table 2, a general lithiation–borylation process starts with the asymmetric deprotonation of primary carbamates to give the corresponding enantioenriched organolithiums **12**. The addition of a boron electrophile (a borane or a boronic ester) forms the intermediate boronate complexes **13** that upon 1,2-rearrangement affords the homologated organoborons **14**. Oxidative work-up gives the desired chiral alcohols **15** in excellent yield and enantioselectivity. Because the chiral organolithiums are normally generated with an er of 98:2, and because the electrophilic quench and the 1,2-migration occur with



Scheme 4 Chiral diamines used in asymmetric deprotonation



Scheme 5 1,2-Metallate rearrangement of boronate complexes generated by the addition of Grignard reagents to α -O-boronic esters

Table 2 Asymmetric deprotonation and lithiation–borylation with primary alkyl carbamates

Entry	R	R ¹ -B(R ₂) ₂	Conditions	Lewis acid	Yield (%)	er
1	PhCH ₂ CH ₂	B(Et) ₃	-40 °C → rt	–	91	98:2
2		B(Et) ₃	-40 °C → rt	–	67	95:5
3	PhCH ₂ CH ₂	<i>i</i> -Pr-BBN	-40 °C → rt	–	81	98:2
4	PhCH ₂ CH ₂	Ph-BBN	-40 °C → rt	–	85	88:12
5	PhCH ₂ CH ₂	Ph-BBN	-40 °C → rt	MgBr ₂	94	97:3
6		Ph-BBN	-40 °C → rt	MgBr ₂	73	98:2
7	PhCH ₂ CH ₂	Ph-B(pin)	reflux, 16 h	MgBr ₂	90	98:2
8	<i>i</i> -Pr	Ph-B(pin)	reflux, 16 h	MgBr ₂	70	98:2
9	PhCH ₂ CH ₂	Et-B(pin)	reflux, 16 h	–	75	97:3
10	PhCH ₂ CH ₂	Me-B(pin)	reflux, 16 h	MgBr ₂	50	95:5

complete stereospecificity, the homologated organoborons are formed in similarly high er. The key 1,2-metallate rearrangement is highly dependent on the nature of the organoboron employed and has been found to be affected by the following features [15]:

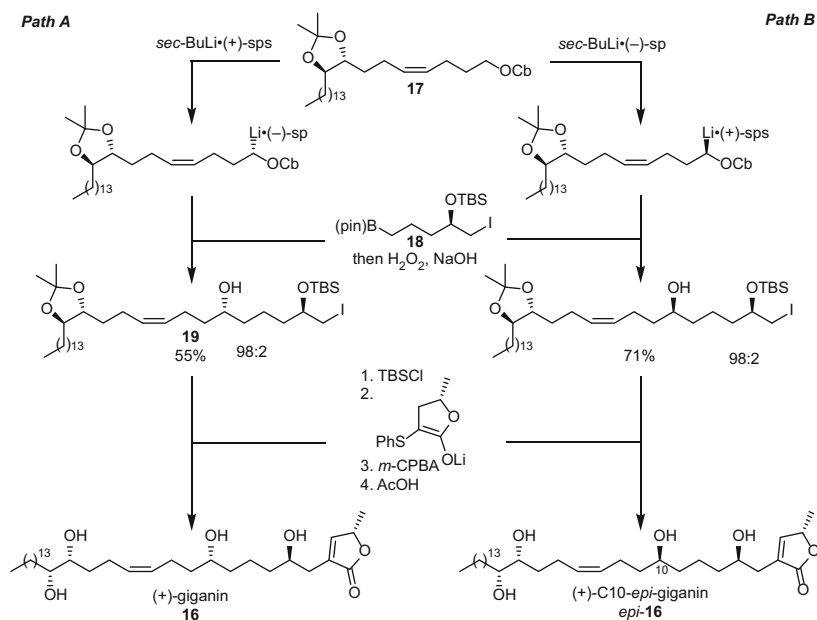
1. Boronate complexes of boranes rearrange quickly (upon warming) (entries 1–6).
2. Boronate complexes of boronic esters require refluxing Et₂O to effect 1,2-rearrangement (entry 9). Phenyl and Me are slow migrating groups, and a Lewis acid, e.g., MgBr₂, is required to promote the rearrangement (entries 7, 8, 10).

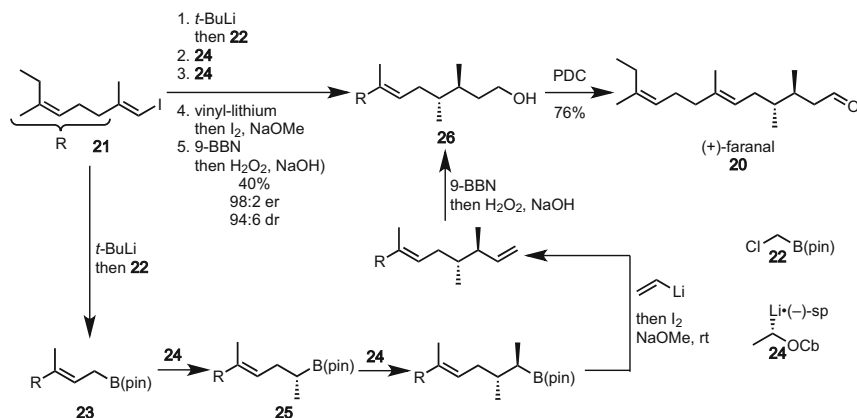
In the case of particularly slow 1,2-migrations [e.g., when Me–B(pin) is used], the employment of directing groups with improved leaving group abilities [tri-*i*-propyl benzoates (TIB)] was found to be beneficial (Table 3) [16]. In this case after asymmetric lithiation and electrophilic quench with a boronic ester, a more activated boronate complex was formed thus allowing faster 1,2-metallate rearrangements. However, slightly lower enantioselectivity was observed in the asymmetric deprotonation of benzoate esters (95:5 vs. 98:2 of carbamates).

Lithiation–borylation methodologies have found many applications in the total synthesis of complex natural products. In the synthesis of (+)-giganin **16**, the carbamate **17** (prepared in eight steps) was lithiated with *sec*-BuLi(–)-sp to give the intermediate chiral organolithium that upon quenching with the functionalized boronic ester **18** (prepared in four steps) gave an intermediate boronate complex. 1,2-Rearrangement and oxidation afforded the desired alcohol **19** in good yield and high dr. Following protection, alkylation, oxidation, and deprotection gave (+)-giganin **16** in very high selectivity and only 13 total steps (Scheme 6, Path A). The power of chemistry in creating stereogenic centers with high stereo-control was illustrated by employing (+)-sps in place of (–)-sp in the key lithiation–borylation

Table 3 Comparison of OCb carbamate and TIB ester in lithiation–borylation with slow migrating groups

Entry	DG	R	Conditions	Lewis acid	Yield (%)	er
1	Cb	Me	Reflux, 16 h	–	<10	–
2	Cb	Me	Reflux, 16 h	MgBr ₂	50	95:5
3	TIB	Me	Reflux, 2 h	–	76	96:4
4	Cb	(CH ₂) ₂ CO ₂ <i>t</i> -Bu	Reflux, 16 h	–	0	–
5	Cb	(CH ₂) ₂ CO ₂ <i>t</i> -Bu	Reflux, 16 h	MgBr ₂	35	93:7
6	TIB	(CH ₂) ₂ CO ₂ <i>t</i> -Bu	Reflux, 2 h	–	63	96:4
7	Cb	(CH ₂) ₂ CN	Reflux, 16 h	–	0	–
8	Cb	(CH ₂) ₂ CN	Reflux, 16 h	MgBr ₂	0	–
9	TIB	(CH ₂) ₂ CN	Reflux, 2 h	–	46	97:3

**Scheme 6** Total synthesis of (+)-giganin and its C10 epimer via lithiation–borylation

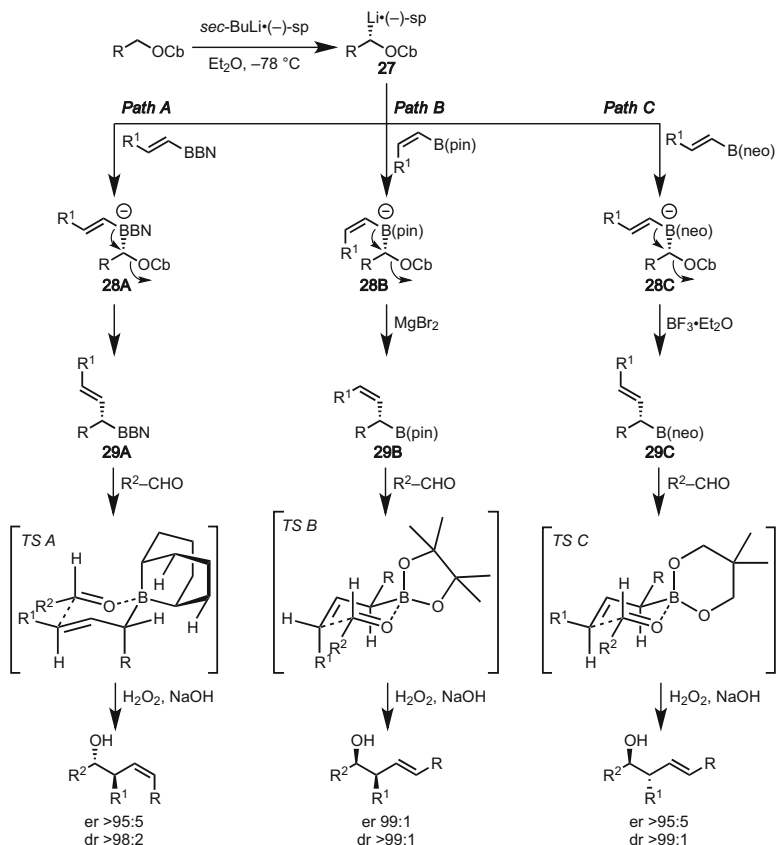


Scheme 7 Total synthesis of (+)-faranal via quadrupole homologation sequence

event (Scheme 6, Path B). This gave access to the C10-epimer of (+)-giganin *epi*-**16** in similar yield and selectivity without changing the synthetic sequence or any of the building blocks [17].

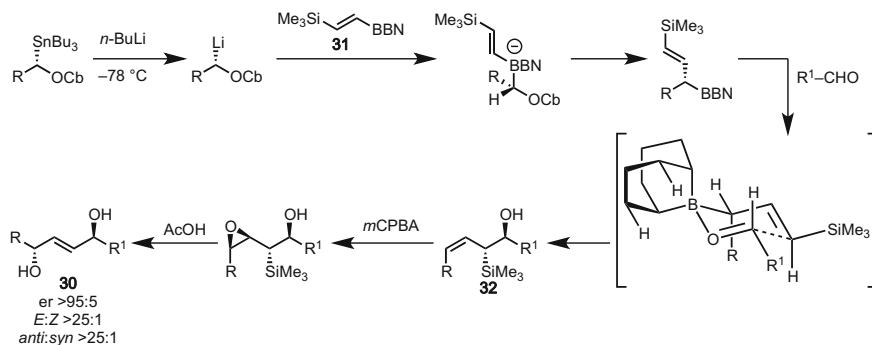
Another interesting application of lithiation–borylation in total synthesis was reported in the asymmetric synthesis of (+)-faranal **20** [18]. This insect pheromone was assembled in only six steps using a telescoped quadruple homologation sequence from the vinyl iodide **21** (Scheme 7). The key step in the synthesis started with I–Li exchange on **21** to give the corresponding organolithium which was reacted with the α -chloro boronic ester **22**. This process gave the intermediate homologated substrate **23** which was reacted with the lithiated carbamate **24** to set the first stereogenic center. Once the 1,2-metallate rearrangement occurred, the homologated product **25** was subjected to a second in situ lithiation–borylation reaction with **24**. Finally, Zweifel olefination [19] and hydroboration–oxidation gave the alcohol **26** in 40% yield and 94:6 dr in a single operation. Final oxidation with PDC gave (+)-faranal **20** with high stereo-control.

The homologation of boronic esters using lithiation–borylation is not restricted to the formation of new stereogenic centers but can also be used to create new chiral reactive intermediates. For example, using vinyl boranes/boronic esters in lithiation–borylation protocols enables the highly selective synthesis of α -substituted allyl boranes/boronic esters that can be exploited in allylboration processes. This has allowed the synthesis of challenging disubstituted homoallylic alcohols with excellent control over all the elements of stereochemistry (enantioselectivity, *E/Z*-stereochemistry and *syn/anti*-stereochemistry) [20]. Aggarwal has demonstrated that by choosing the appropriate set of reagents, almost all the combination of products (*syn*, *anti*, *E*, *Z*) can be accessed with similar levels of selectivity (Scheme 8). Hence, while *E*-vinyl BBN-boranes allowed the synthesis of the *anti-Z* isomers (Path A), *Z*-vinyl pinacol boronic esters (Path B) and the less hindered *E*-neopentyl glycol boronic esters (Path C) afford the *syn-E* and the *anti-E* isomers, respectively. As outlined in Scheme 8, all of these processes share very



Scheme 8 Synthesis of stereo-defined allylic boranes and boronic esters via lithiation–borylation and their use in allylboration of aldehydes

similar reaction conditions. The primary carbamate was lithiated using $sec-BuLi(-)-sp$ to give the enantioenriched organolithium **27** which upon treatment with different vinyl organoborons yielded the various boronate complexes **28A**, **B**, and **C**. Following 1,2-metallate rearrangement, the key allylic organoboron reagents **29A–C** were formed and immediately reacted with the aldehydes. The different stereochemical outcomes of the reaction can be rationalized by inspecting the 6-membered chair transition states for the various allylboration processes. Due to the severe steric hindrance imposed by the BBN moiety, the R group is forced into a pseudo axial position thus forming the Z -anti alcohol (Scheme 8, Path and TS A). When vinyl pinacol boronic ester is employed, the R group adopts a pseudo equatorial position in order to avoid severe $A^{1,3}$ strain with the *cis* R^1 group (Scheme 8, Path and TS B), and this forms the $syn-E$ alcohols. Finally, in order to access the $anti-E$ products, an E -vinyl organoboron with a small group at boron was required in order to allow the R group to adopt a pseudo equatorial position.



Scheme 9 Synthesis of stereo-defined 2-ene-*anti*-1,4-diols via lithiation–borylation–allylboration

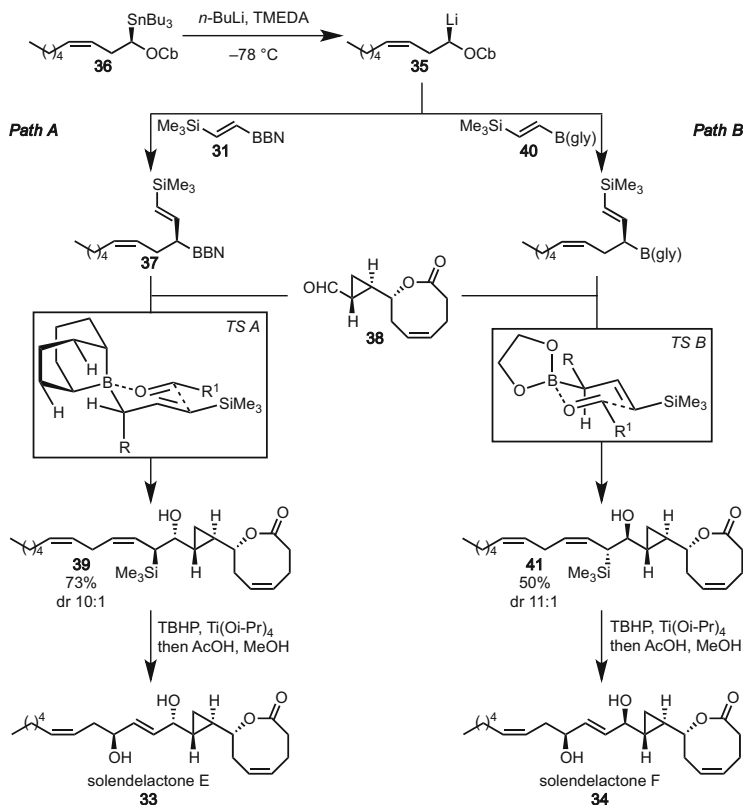
Neopentyl boronic esters have been found uniquely effective for this transformation, and they gave the desired products in excellent selectivities (Scheme 8, Path and TS C) [20].

A more sophisticated application of this chemistry was employed in the synthesis of valuable 2-ene-*anti*-1,4-diols **30** which required the use of β -silyl vinyl BBN-borane **31** (Scheme 9). In this case, after the diamine-free lithiation–borylation–allylboration sequence, the *anti-Z* allyl silane **32** was formed in very high dr. After stereoselective epoxidation of **32** and acid-promoted ring-opening/elimination, the 2-ene-*anti*-1,4-diols were formed with high stereocontrol (Scheme 9) [21].

This chemistry has been applied to the stereocontrolled synthesis of the complex natural products (–)-decastrictine D [21] and solandelactone E **33** [22] and F **34** [23]. The synthesis of the two solandelactones is instructive. These two marine oxylipins were assembled using an identical synthetic sequence but with different vinyl boron reagents. In the case of **33**, the chiral organolithium **35** was generated under diamine-free conditions from the enantioenriched stannane **36** by Sn–Li exchange. The addition of **31** gave the required boronate complex that rearranged to form the allylic boronic ester **37**. The addition of aldehyde **38** afforded the *Z-anti*-allyl silane **39** in high yield and selectivity (Scheme 10, Path A). Following diastereoselective epoxidation and ring-opening/elimination gave the natural product **33** [22].

Based on the factors responsible for stereo-control in the allylboration reaction (see Scheme 8), the isomeric solandelactone F **34** was prepared by the same sequence by simply changing the vinyl organoboron from the BBN-borane **31** to the sterically unhindered glycol boronic ester **40** (Scheme 10, Path B). This resulted in the formation of the isomeric *Z-anti*-allyl silane **41** en route to the title compound **34** [22].

While primary alkyl carbamates and benzoates can be lithiated in high yield and selectivity, primary benzylic carbamates cannot. This is due to their low configurational stability even at -78°C . However, Hoppe has reported that by using a chiral bisoxazoline ligand, a highly selective dynamic resolution under thermodynamic control (DTR) can occur thus allowing the use of these chiral



Scheme 10 Total synthesis of solandelactone E and F via lithiation–borylation–allylboration sequence

Table 4 Lithiation–borylation of primary benzylic carbamates

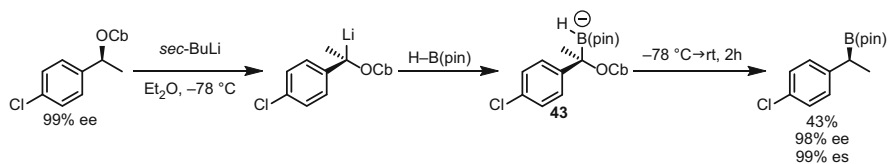
$$\text{Ar-CH}_2\text{-OCb} \xrightarrow[\text{then MgBr}_2, \text{reflux}]{\text{sec-BuLi, L}^*, \text{Et}_2\text{O, -78 }^\circ\text{C}; \text{ then Ar}^1\text{-B(neo), -78 }^\circ\text{C}}$$

$$\text{Ar-CH}(\text{Ar}^1)\text{-B(neo)} \quad \mathbf{42}$$

$$\text{L}^* = \begin{array}{c} \text{Et} \quad \text{Et} \\ | \quad | \\ \text{N} \quad \text{O} \\ / \quad \backslash \\ \text{O} \quad \text{N} \\ | \quad | \\ \text{i-Pr} \quad \text{i-Pr} \end{array}$$

Entry	Ar	Ar ¹	Yield (%)	er
1	Ph	<i>p</i> -Et-Ph	37	98:2
2	<i>m</i> -MeO-Ph	Ph	51	93:7
3	<i>m</i> -MeO-Ph	<i>p</i> -Et-Ph	55	90:10
4	<i>p</i> -MeO-Ph	<i>p</i> -F-Ph	43	80:20
5	2-Naphtyl	Ph	50	90:10

organometallics in asymmetric synthesis [24, 25]. Crudden has applied this chemistry to the synthesis of diaryl secondary benzylic boronic esters **42** (Table 4). The use of the less sterically hindered neopentyl boronic esters was necessary in order to obtain high levels of enantio-enrichment [26].



Scheme 11 Synthesis of a benzylic boronic ester via lithiation–borylation with H–B(pin)

Aggarwal has recently developed an alternative approach that gives access to similar substrates in high selectivity (Scheme 11) [27]. In this example, the configurationally stable tertiary benzylic α -*O* organolithium (vide infra) was reacted with H–B(pin). This formed a boronate complex **43** that after 1,2-shift of hydride gave the desired benzylic secondary boronic esters. This method is particularly useful in the synthesis of secondary benzylic boronic esters that cannot be accessed by transition-metal-catalyzed hydroboration in high ee.

4.2 Secondary Benzylic Carbamates

While lithiated primary benzylic carbamates are not configurationally stable, lithiated secondary benzylic carbamates are, and they have been successfully exploited in many lithiation–borylation processes. Interestingly, the addition of boronic esters occurs with retention of configuration at the Li-bearing C (S_E2ret , **44**), while the addition of boranes occurs with inversion (S_E2inv , **45**) (Table 5) [28]. Following 1,2-migration and oxidation, the desired chiral carbinols **46** are obtained in high yield and high selectivity in both cases. Because the stereoselectivity of the electrophilic quench (ret vs. inv) is dictated by nature of the B-substituents, either enantiomer of the tertiary alcohols can be prepared from the same lithiated carbamate. The rationale for this dichotomous behavior has been explained on the basis of the ability of the oxygen of boronic esters to coordinate to the lithium cation, delivering the boronic ester to the same face of the metal. Boranes cannot engage in this interaction, and therefore they react from the opposite face of the lithium where there is less steric hindrance but still significant electron density. This is however possible only for benzylic organolithiums due to the partially flattened nature of the carbanion. Alkyl carbamates do not benefit from the mesomeric stabilization offered by the aryl group and therefore always react with retention with both boranes and boronic esters. The process shows a broad scope, and alkyl, aryl, and heteroaryl groups can be transferred efficiently and in high stereospecificity [28, 29].

However when hindered boronic esters and/or carbamates with electron-withdrawing groups on the aromatic group were used, the intermediate boronate complexes reverted back to the lithiated carbamate thus leading to erosion of enantiopurity due to racemization. This dissociation–racemization pathway could be eliminated by (1) adding MgBr₂/MeOH as an additive if using pinacol boronic

Table 5 Stereodivergence in the lithiation–borylation of benzylic carbamates with pinacol boronic esters and boranes

Entry	Ar	Organoboron	Yield (%)	er
1	Ph	Et–B(pin)	95	99:1 (ret)
2	Ph	B(Et) ₃	91	99:1 (inv)
3	Ph	<i>i</i> -Pr–B(pin)	92	99:1 (ret) ^a
4	Ph	<i>i</i> -Pr–BBN	91	98:2 (inv)
5	Ph	<i>p</i> -MeO–Ph–B(pin)	92	98:2 (ret)
6	Ph	2-Furyl–B(pin)	94	98:2 (ret)
7	Ph		81	98:2 (ret)
8	Ph		52	99:1 (ret)
9	<i>o</i> -MeO–Ph	<i>i</i> -Pr–B(pin)	79	99:1 (ret) ^a
10	<i>p</i> -Cl–Ph	<i>i</i> -Pr–B(pin)	89	99:1 (ret) ^a
11		Et–B(pin)	69	99:1 (ret)
12		B(Et) ₃	90	95:5 (inv)

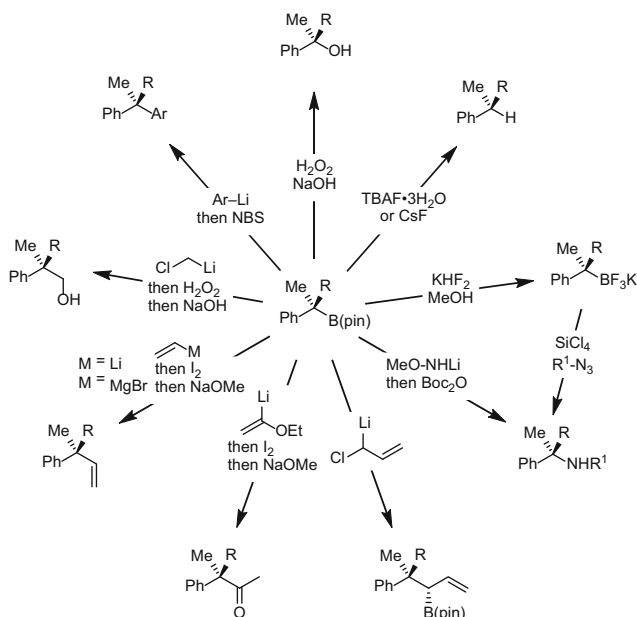
esters or (2) using less hindered neopentyl boronic esters in place of pinacol boronic esters (Table 6) [30].

The lithiation–borylation of this class of substrates has found considerable applications due to the further possible stereospecific transformations of the C–B into other functional groups (e.g., C–C, C–N, C–H) (Scheme 12) [31, 32].

A particularly useful transformation is represented by the conversion of C–B bonds into C–H bonds by means of stereoselective protodeboronation. Aggarwal has reported that by treating chiral tertiary benzylic boronic esters with fluoride sources (TABF·3H₂O or CsF) in the presence of H₂O, a highly stereoselective

Table 6 Comparison of pinacol and neopentyl boronic esters in the lithiation–borylation with hindered and electron-poor benzylic carbamates

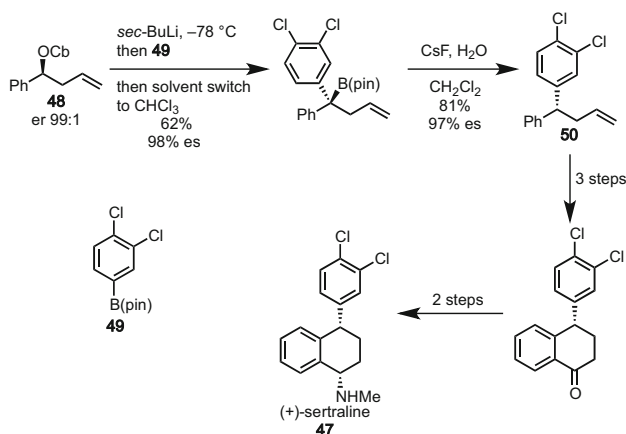
Entry	Ar	R	Conditions	Yield (%)	es (%)
<i>R-B(OR²)₂ = R-B(pin)</i>					
1	<i>p</i> -Cl-Ph	Et	–	63	40
2	<i>p</i> -Cl-Ph	Et	MgBr ₂ –MeOH	91	99
3	<i>p</i> -F-Ph	<i>i</i> -Pr	MgBr ₂ –MeOH	88	99
4	<i>o</i> -MeO-Ph	<i>i</i> -Pr	MgBr ₂ –MeOH	79	99
<i>R-B(OR²)₂ = R-B(neo)</i>					
5	<i>p</i> -Cl-Ph	<i>i</i> -Pr	–	95	99
6	<i>p</i> -F-Ph	<i>i</i> -Pr	–	79	99
7	<i>o</i> -MeO-Ph	<i>i</i> -Pr	–	92	96

**Scheme 12** Functionalizations of enantioenriched tertiary benzylic boronic esters

retentive protodeboration process was possible (Table 7) [33]. This method allowed the synthesis of challenging chiral aryl-alkane motifs in excellent stereo-control. The stereochemical outcome has been rationalized on the basis of the activation of the boronic ester by the fluoride followed by a front-side delivery of the proton due to the coordination of the H₂O molecules to the boronate complex.

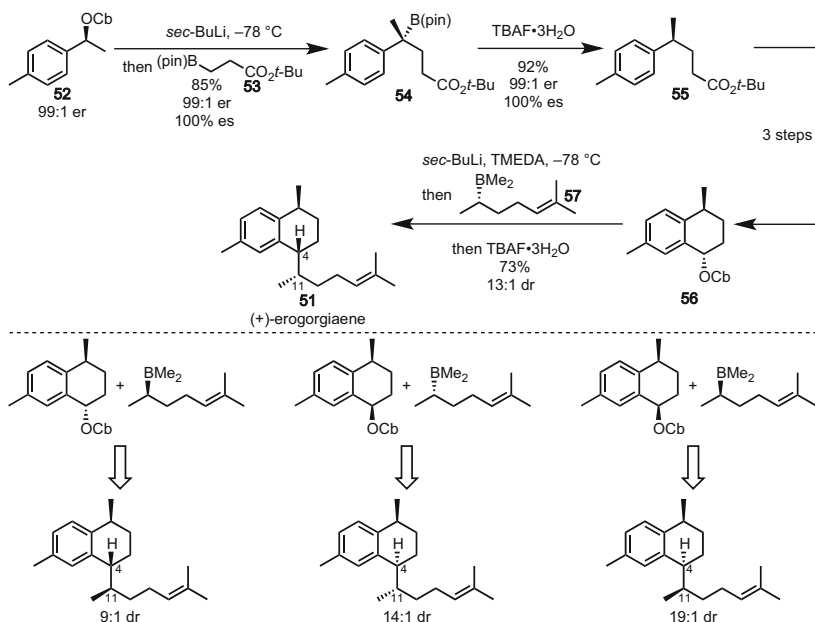
Table 7 Stereospecific protodeboronation of enantioenriched tertiary benzylic boronic esters

Entry	Ar	R	R ¹	Method	Yield (%)	es (%)
1	Ph	Me	<i>p</i> -Cl-Ph	A	82	98
2	<i>p</i> -MeO-Ph	Me	Ph	A	99	99
3	Ph	Me	Et	B	97	99
4	Ph	Me	Allyl	B	98	99
5	Ph	Et	Allyl	B	79	99

**Scheme 13** Synthesis of (+)-sertraline via lithiation–borylation–protodeboronation sequence

The use of lithiation–borylation–protodeboronation sequences has been applied to the synthesis of many complex molecules. As an example the top-selling drug (+)-sertraline **47** has been assembled from the enantioenriched carbamate **48** by lithiation–borylation with the aryl boronic ester **49** (Scheme 13) [34]. In this case the 1,2-metallate rearrangement proved difficult, but it was accelerated by switching the reaction media from Et₂O to the less polar CHCl₃. Following retentive protodeboronation, the 1,1-diaryllithium intermediate **50** was obtained in excellent stereospecificity. This intermediate was converted to (+)-sertraline in 5 steps.

The natural product (+)-erogorgiaene **51** and its diastereoisomers have all been synthesized using two lithiation–borylation–protodeboronation sequences as key steps [35]. As outlined in Scheme 14, lithiation–borylation of enantioenriched benzylic carbamate **52** with the ester-functionalized boronic ester **53** gave the tertiary organoboron **54** that was subjected to the protodeboronation protocol to give **55** in excellent yield and complete stereospecificity. This intermediate was elaborated into the cyclic *anti*-carbamate **56** in three steps. At this stage a second

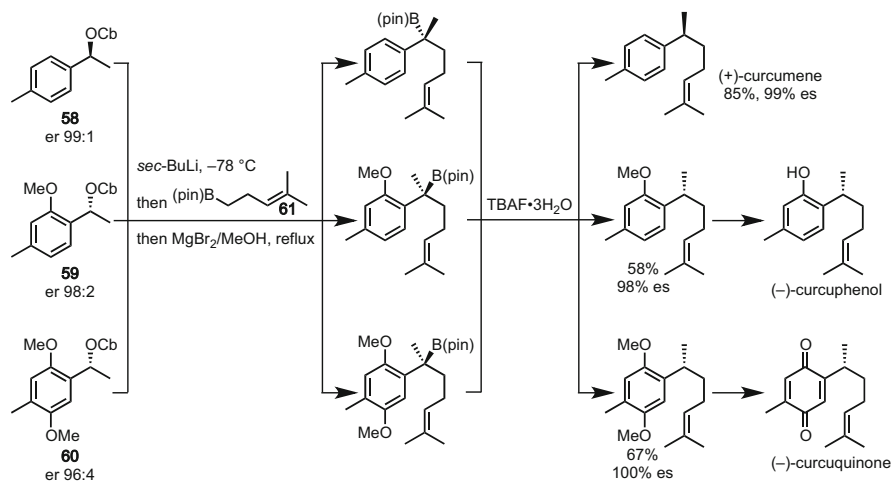


Scheme 14 Total synthesis of (+)-erogorgiaene and its epimers via lithiation–borylation–protodeboronation sequence

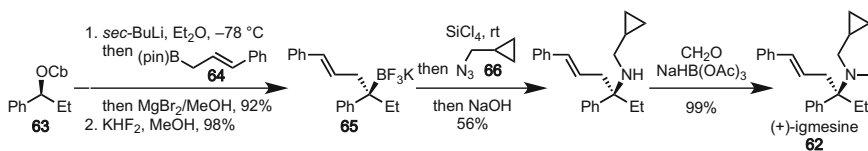
lithiation–borylation–protodeboronation sequence was used to complete the total synthesis. In contrast to acyclic- and indanol-derived carbamates, tetralol-derived carbamates give low ee in lithiation–borylation with boronic esters [28]. However, engaging the tetralol-derived lithiated carbamate in a lithiation–borylation process with the unhindered and more reactive dimethyl borane **57** gave the desired homologated borane that underwent in situ protodeboronation yielding (+)-erogorgiaene **51** in 13:1 dr and 44% overall yield. Furthermore by changing the chiral ligand used in the synthesis of carbamate **56**, or the chiral base used in the synthesis of borane **57**, the remaining diastereoisomers of (+)-erogorgiaene were accessed in similar yields and selectivities.

A lithiation–borylation–protodeboronation sequence has been used as a key step in the collective synthesis of three members of the bisabolane family of sesquiterpenes (Scheme 15) [36]. Starting from the readily available enantioenriched benzylic carbamates **58**, **59**, and **60**, lithiation–borylation with the boronic ester **61** gave the intermediate tertiary boronic esters that were protodeboronated by treatment with TBAF·3H₂O. Further elaboration gave the desired natural products.

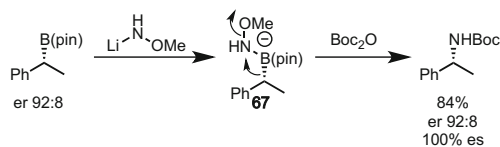
A very useful functionalization of boronic esters is the stereospecific conversion of the C–B bonds into C–N bonds. This allows the asymmetric synthesis of valuable chiral amines. Aggarwal reported the use of Matteson’s amination protocol [37, 38] in the asymmetric synthesis of C-tertiary amines in good yield and excellent stereospecificity [39]. This protocol required the initial conversion of the boronic



Scheme 15 Total synthesis of sesquiterpenes via lithiation–borylation–protodeboration



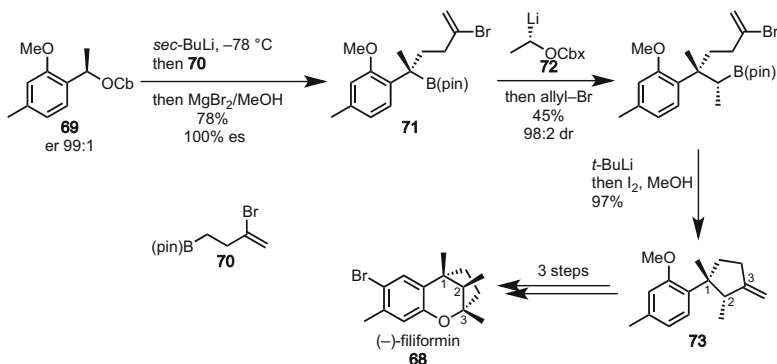
Scheme 16 Synthesis of (+)-igmesine via lithiation–borylation–Matteson amination sequence



Scheme 17 Morcken's amination protocol

esters into the corresponding trifluoroborates [40] and their rearrangement with SiCl_4 and an azide. This methodology has been successfully applied to the asymmetric synthesis of the pharmaceutical (+)-igmesine **62** (Scheme 16). The lithiation–borylation between the carbamate **63** and the boronic ester **64** proceeded in good yield and excellent enantiospecificity. The boronic ester was then converted into the corresponding tetrafluoroborate salt **65** which underwent the amination process with the cyclopropyl-functionalized azide **66** with complete stereospecificity. Finally, reductive amination gave (+)-igmesine **62**.

More recently Morcken has developed a mild amination protocol of pinacol boronic esters (Scheme 17) [41]. In this example the boronic ester was reacted with lithium methoxyamide to form an intermediate boronate complex **67** that



Scheme 18 Total synthesis of (–)-filiformin via lithiation–borylation and intramolecular Zweifel olefination

rearranged to give the desired primary amines. The addition of Boc_2O was required to aid the purification of the product. This reaction shows broad scope, but it could not be expanded to the more challenging tertiary boronic esters.

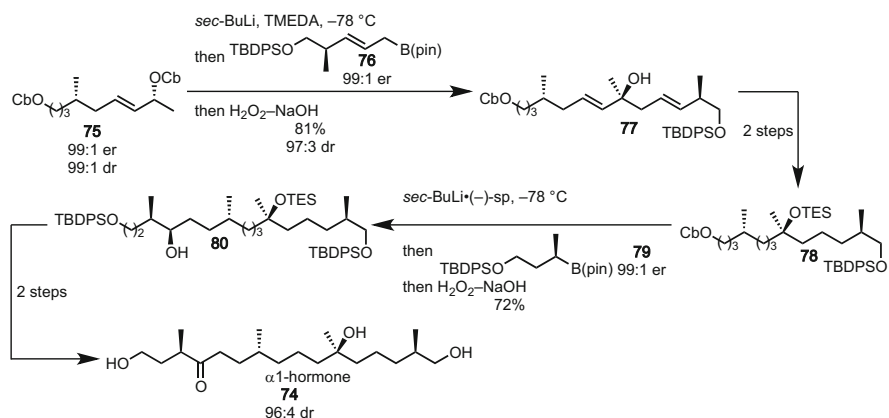
Chiral tertiary boronic esters can also be used for the construction of challenging all-carbon quaternary stereogenic centers via functionalization protocols such as the Matteson homologation or the Zweifel olefination (see Scheme 12) [31]. This was applied in a short total synthesis of the natural product (–)-filiformin **68** (Scheme 18) [42]. This sesquiterpene is characterized by the presence of a challenging quaternary–tertiary motif embedded in a bicyclic system. The synthesis started by lithiation of the enantioenriched carbamate **69** and borylation with the vinyl-bromide-functionalized boronic ester **70**. This reaction created the tertiary boronic ester **71** in high yield and complete stereospecificity. At this stage lithiation–borylation with lithiated carbamate **72** constructed the quaternary–tertiary motif in good yield and excellent dr. Then, an unprecedented intramolecular Zweifel olefination [19] assembled the cyclopentene-containing intermediate **73**. Following deprotection of the methoxy ether, acid-catalyzed cyclization and bromination gave (–)-filiformin **68** in just nine steps.

4.3 Secondary Allylic/Propargylic Carbamates

While lithiated primary allylic carbamates are not configurationally stable, secondary allylic carbamates are, and therefore they can be used in lithiation–borylation. The deprotonation–electrophilic quench of this class of substrates has been extensively studied by Hoppe who found that they usually give a mixture of α - and γ -addition products. However, Aggarwal has found that reaction with boronic esters occurs selectively at the α -position with complete retention of configuration (Table 8). In analogy with the borylation of benzylic carbamates (see Sect. 4.2),

Table 8 Lithiation–borylation with secondary allylic carbamates

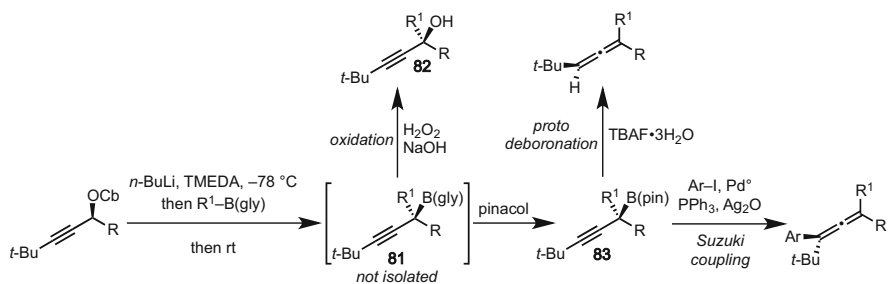
Entry	R	R ¹	R ²	R ³	Yield (%)	es (%)
1	Me	H	Me	<i>n</i> -Bu	75	99
2	<i>i</i> -Pr	H	Me	Vinyl	79	99
3	Me	H	Et	CH ₂ CH ₂ Ph	83	100
4	Me	Me	Me	CH ₂ CH ₂ Ph	81	98

**Scheme 19** Total synthesis of α -1-hormone via lithiation–borylation of an allylic carbamate

this selectivity has been rationalized on the basis of a pre-complexation of the oxygen of the boronic ester to the lithium cation [43–46].

Aggarwal used this methodology in the asymmetric synthesis of the *Phytophthora* universal mating hormone α -1 **74** (Scheme 19) [47]. The synthesis started from the enantioenriched bis-carbamate **75** (prepared in five steps from citronellal). Selective kinetic deprotonation of the more acidic allylic position gave the intermediate organolithium that reacted with complete α -selectivity with the chiral boronic ester **76** which itself was prepared in six steps from the Roche ester. 1,2-Metallate rearrangement followed by oxidation gave the tertiary alcohol **77** which was elaborated into the primary carbamate **78**. Following lithiation–borylation of the primary carbamate with the boronic ester **79** (prepared in four steps) assembled **80** that was converted in the natural product in just two steps.

An extension of this methodology is represented by the use of propargylic carbamates in lithiation–borylation (Scheme 20) [48]. However this is restricted to the use of *t*-Bu-substituted substrates due to the unique configurational stability of the lithiated species [49]. In this case the use of the less hindered glycol boronic esters was necessary in order to avoid issues associated to the reversibility of the boronate complex formation. After 1,2-metallate rearrangement, the in situ



Scheme 20 Synthesis of propargylic boronic esters via lithiation–borylation and their functionalizations

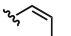
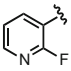
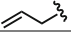
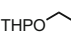
generated tertiary propargylic boronic esters **81** were oxidized to the alcohols **82** or *trans*-esterified with pinacol to enhance their stability and allow isolation. These tertiary propargylic boronic esters **83** were found to undergo stereospecific protodeboration and Suzuki–Miyaura cross-coupling to give chiral allenes with various substitution patterns.

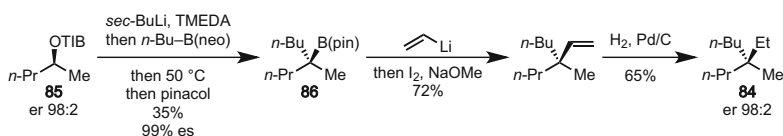
4.4 Secondary Benzoates

Secondary carbamates have been used extensively in lithiation–borylation. However, a major limitation that affects these class of substrates is imposed by the fact that one aromatic/allylic group is necessary to enable deprotonation. Without acidifying groups it had been reported such substrates could not be deprotonated [50, 51] and therefore could not be used in lithiation–borylation processes. This major limitation was recently addressed by Aggarwal who demonstrated that the combination of using TIB esters together with CPME as solvent enabled deprotonation of dialkyl benzoates [52]. Subsequent reaction with neopentyl boronic esters and 1,2-metallate rearrangement gave the homologated boronic esters which were oxidized to give the chiral carbinols in good yield and perfect stereospecificity (Table 9).

The newly generated boronic esters could also be *trans*-esterified in situ with pinacol to aid purification which enabled further stereospecific functionalization of the C–B bond. A trialkyl-substituted chiral boronic ester has been used in the shortest known synthesis of the simplest unbranched hydrocarbon bearing an all-C quaternary center (**84**) (Scheme 21). In this case the enantioenriched TIB ester **85** underwent lithiation–borylation with *n*-Bu–B(neo) to give the boronic ester **86** in moderate yield but excellent stereospecificity. Zweifel olefination [18] and hydrogenation installed the ethyl group and completed the synthesis of **84** in just four steps [52].

Table 9 Lithiation–borylation with secondary, dialkyl benzoates

Entry	Alkyl	Alkyl ¹	R	Yield (%)	es (%)
1	PhCH ₂ CH ₂	Me	Et	80	100
2	PhCH ₂ CH ₂	Me	CH ₂ CH ₂ CO ₂ <i>t</i> -Bu	69	99
3	PhCH ₂ CH ₂	Me		78	100
4	PhCH ₂ CH ₂	Me		73	100
5		Me	Et	72	100
6	THPO 	Me	Et	56	99
7	PhCH ₂ CH ₂	Et	Allyl	40	100

**Scheme 21** Synthesis of (*R*)-4-ethyl-4-methyloctane via lithiation–borylation

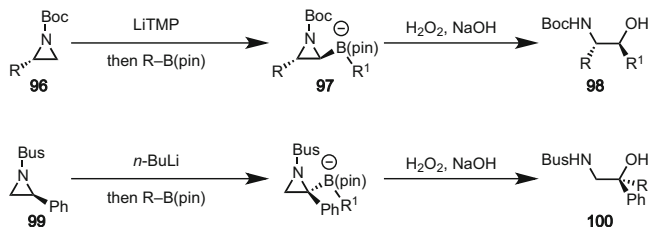
5 α -*N*-Stabilized Organolithiums

The lithiation–borylation is not restricted to the use of lithiated carbamates and benzoates. A few examples involving α -*N*-stabilized organolithiums have been described in the literature (Table 10). Beak's lithiated *N*-Boc-pyrrolidine **87** [53], indoline **88** [54], and benzyl amine **89** [55] reacted well with boranes to give various intermediate boronate complexes **90**, **91**, and **92**. In these cases the strong Lewis acid TMS–OTf was required in order to trigger the more challenging 1,2-migrations. Final oxidation resulted in the asymmetric synthesis of chiral (amino)-alcohols **93**, **94**, and **95** [56].

Another class of α -*N*-organolithiums that has been successfully applied to lithiation–borylation methodology is represented by lithiated aziridines (Scheme 22). Lithiation of *N*-Boc-protected aziridines **96** with LTMP followed by electrophilic quench with boronic esters gave the intermediate boronate complexes **97** that rearranged to give, after oxidation, various 1,2-aminoalcohols **98** in very high selectivity [57]. This methodology was then extended by using the enantioenriched *N*-Bus-phenyl aziridine **99**. In this case kinetic deprotonation of the more acidic benzylic position formed a chiral tertiary α -*N*-organolithium that reacted with boronic esters to give, after oxidation, tertiary β -amino alcohols **100** in excellent stereospecificity. The choice of the Bus as the *N*-protecting group was required as when *N*-Boc-phenyl aziridine was used a *N* \rightarrow *C* migration of the Boc group was observed [57].

Table 10 Lithiation–borylation using α -*N*-organolithiums and boranes

Entry	Substrate	R	Yield (%)	er
1	87	Et	58	95:5
2	88	Et	67	97:3
3	89	Et	83	95:5
4	87	<i>n</i> -Bu	59	92:8
5	88	<i>n</i> -Bu	64	96:4
6	89	<i>n</i> -Bu	82	95:5

**Scheme 22** Lithiation–borylation using lithiated aziridines and boronic esters

6 Conclusions and Outlook

The reagent-controlled asymmetric homologation of boronic esters is a powerful method for the stereo-controlled synthesis of substituted carbon chains. The reagents with the greatest scope are Hoppe's lithiated carbamates: a broad range of primary alkyl carbamates can react with a range of alkyl and aryl boranes and boronic esters. Since the chiral carbanions are derived from simple primary alcohols, access to these chiral reagents is especially facile. Furthermore, they can be used iteratively thus allowing carbon chains to be grown interspersed with substituents of specific stereochemistry. They therefore offer the greatest versatility and flexibility in the homologation of boranes and boronic esters in particular. The methodology has been extended to include primary benzylic carbamates where the enantioenriched lithiated carbamate is generated under thermodynamic control.

Secondary allylic, benzylic, and dialkyl carbamates/TIB esters can also be employed in lithiation–borylation reactions. The secondary alcohols are easily obtained in high enantiopurity and undergo stereospecific lithiation and stereoselective borylation leading to tertiary boronic esters (or boranes) with very high er.

This methodology has been applied effectively at various stages in the synthesis of a number of natural products. Its use at the start of a total synthesis requires large-scale applications, and its use at the end requires a certain degree of functional group compatibility. In terms of limitations, the carbamate cannot contain functional groups that could react with *s*-BuLi although the faster Sn–Li exchange enables a broader range of carbamates to be employed and the boronic ester component must not have functional groups that are more electrophilic than the pinacol boronic ester. Potential leaving groups β to the boronic ester should be avoided; otherwise, at the boronate complex stage, elimination competes with 1,2-migration. Providing these limitations are satisfied, this methodology can be applied with confidence. Indeed the methodology has been applied extensively in the synthesis of acyclic molecules with high stereo-control. It would be interesting to see if this methodology could also be applied to cyclic substrates since they too are very common in nature.

References

1. Thomas SP, French RM, Jheengut V, Aggarwal VK (2009) *Chem Rec* 9:24
2. Watson CG, Unsworth PJ, Leonori D, Aggarwal VK (2014) *Lithium–boron chemistry: a synergistic strategy in modern synthesis*. Wiley, Weinheim
3. Matteson DS (1989) *Chem Rev* 89:1535
4. Matteson DS (1995) *Reactivity and structure concepts in organic chemistry*, vol 32. Springer, Berlin
5. Matteson DS (2012) *J Org Chem* 78:10009
6. Matteson DS, Man H-W (1996) *J Org Chem* 61:6047
7. Aggarwal VK, Fang GY, Ginesta X, Howells DM, Zaja M (2006) *Pure Appl Chem* 78:215
8. Hoffmann RW, Nell PG, Leo R, Harms K (2000) *Chem Eur J* 6:3359
9. Blakemore PR, Marsden SP, Vater HW (2006) *Org Lett* 8:773
10. Blakemore PR, Burge MS (2007) *J Am Chem Soc* 129:3068
11. Hoppe D, Marr F, Bruggemann M (2003) *Organolithiums*. In: Hodgson DM (ed) *Enantioselective synthesis*, vol 2005. Springer, London, p 2073
12. Beckmann E, Desai V, Hoppe D (2004) *Synlett* 2275
13. Beckmann E, Hoppe D (2005) *Synthesis* 217
14. Besong G, Jarowicki K, Kocienski PJ, Sliwinskia E, Boyle FT (2006) *Org Biomol Chem* 4:2193
15. Stymiest JL, Dutheuil G, Mahmood A, Aggarwal VK (2007) *Angew Chem Int Ed* 46:7491
16. Larouche-Gauthier R, Fletcher CJ, Couto I, Aggarwal VK (2011) *Chem Commun* 47:12592
17. Fletcher CJ, Wheelhouse KMP, Aggarwal VK (2013) *Angew Chem Int Ed* 52:2503
18. Dutheuil G, Webster MP, Worthington PA, Aggarwal VK (2009) *Angew Chem Int Ed* 48:6317
19. Zweifel G, Arzoumanian H, Whitney CC (1967) *J Am Chem Soc* 89:3652
20. Althaus M, Mahmood A, Suárez JR, Thomas SP, Aggarwal VK (2010) *J Am Chem Soc* 132:4025

21. Binanzer M, Fang GY, Aggarwal VK (2010) *Angew Chem Int Ed* 49:4264
22. Robinson A, Aggarwal VK (2010) *Angew Chem Int Ed* 49:6673
23. Robinson A, Aggarwal VK (2012) *Org Biomol Chem* 10:1795
24. Lange H, Huenerbein R, Frohlich R, Grimme S, Hoppe D (2007) *Chem Asian J* 3:78
25. Lange H, Huenerbein R, Wibbeling B, Frohlich R, Grimme S, Hoppe D (2008) *Synthesis* 2095
26. Matthew SC, Glasspole BW, Eisenberger P, Crudden CM (2014) *J Am Chem Soc* 136:5828
27. Roesner S, Brown CA, Mohiti M, Pulis AP, Rasappan R, Blair DJ, Essafi S, Leonori D, Aggarwal VK (2014) *Chem Commun* 50:4053
28. Stymiest JL, Bagutski V, French RM, Aggarwal VK (2008) *Nature* 456:778
29. Watson CG, Aggarwal VK (2013) *Org Lett* 15:1346
30. Bagutski V, French RM, Aggarwal VK (2010) *Angew Chem Int Ed* 49:5142
31. Scott HK, Aggarwal VK (2011) *Chem Eur J* 17:13124
32. Sonawane RP, Jheengut V, Rabalakos C, Larouche-Gauthier R, Scott HK, Aggarwal VK (2011) *Angew Chem Int Ed* 50:3760
33. Nave S, Sonawane RP, Elford TG, Aggarwal VK (2010) *J Am Chem Soc* 132:17096
34. Roesner S, Casatejada JM, Elford TG, Sonawane RP, Aggarwal VK (2011) *Org Lett* 13:5740
35. Elford TG, Nave S, Sonawane RP, Aggarwal VK (2011) *J Am Chem Soc* 133:16798
36. Aggarwal VK, Ball LT, Carobene S, Connelly RL, Hesse MJ, Partridge BM, Roth P, Thomas SP, Webster MP (2012) *Chem Commun* 48:9230
37. Matteson DS, Kim GY (2002) *Org Lett* 4:2153
38. Kim GY, Matteson DS (2004) *Angew Chem Int Ed* 43:3056
39. Bagutski V, Elford TG, Aggarwal VK (2011) *Angew Chem Int Ed* 50:1080
40. Bagutski V, Ros A, Aggarwal VK (2009) *Tetrahedron* 65:9956
41. Mlynarski SN, Karns AS, Morken JP (2012) *J Am Chem Soc* 134:16449
42. Blair DJ, Fletcher CJ, Wheelhouse KMP, Aggarwal VK (2014) *Angew Chem Int Ed* 53:5552
43. Pulis AP, Aggarwal VK (2012) *J Am Chem Soc* 134:7570
44. Hoppe D (1984) *Angew Chem Int Ed* 23:932–948
45. Krämer T, Schwark J-R, Hoppe D (1989) *Tetrahedron Lett* 30:7037
46. Zschage O, Schwark J-R, Hoppe D (1990) *Angew Chem Int Ed* 29:296
47. Pulis AP, Fackler P, Aggarwal VK (2014) *Angew Chem Int Ed* 126:4471
48. Partridge BM, Chausset-Boissarie L, Burns M, Pulis AP, Aggarwal VK (2012) *Angew Chem Int Ed* 51:11795
49. Dreller S, Dyrbusch M, Hoppe D (1991) *Synlett* 397
50. Hoppe D, Hintze F, Tebben P (1990) *Angew Chem Int Ed* 29:1422
51. Beak P, Carter LG (1981) *J Org Chem* 46:2363
52. Pulis AP, Blair DJ, Torres E, Aggarwal VK (2013) *J Am Chem Soc* 135:16054
53. Beak P, Kerrick ST, Wu S, Chu J (1994) *J Am Chem Soc* 116:3231
54. Bertini Gross KM, Jun YM, Beak P (1997) *J Org Chem* 62:7679
55. Park YS, Boys ML, Beak P (1996) *J Am Chem Soc* 118:3757
56. Coldham I, Patel JJ, Raimbault S, Whittaker DTE, Adams H, Fang GY, Aggarwal VK (2008) *Org Lett* 10:141
57. Schmidt F, Keller F, Vedrenne E, Aggarwal VK (2009) *Angew Chem Int Ed* 48:1149

Recent Advances in the Synthesis and Applications of Organoborane Polymers

Frieder Jäkle

Contents

1	Introduction	299
2	Synthesis of Organoborane Polymers	299
2.1	Polymer Modification Reactions on Polyolefins	299
2.2	Direct Polymerization of Borane Monomers by Chain Growth Methods	302
2.3	Side-Chain Functionalization of Conjugated Polymers	303
2.4	Boron Incorporation into the Main Chain of Conjugated Polymers	306
3	Selected Examples of Polymers and Their Applications	307
3.1	Borane Polymers as Lewis Acids and Anion Sensors	307
3.2	Luminescent Polymers Based on Boron Chelate Complexes	311
3.3	Boronic and Borinic Acid-Functionalized Polymers for Biomedical Applications and as Smart Materials	315
3.4	Borate and Boronium-Functionalized Polymers as Polyelectrolytes and Polymeric Ligand	318
4	Conclusions	321
	References	321

Abstract Recent advances in the synthesis of organoborane polymers are reviewed in this chapter. The last decade has witnessed new approaches for the direct polymerization of functional borane monomers as well as the use of innovative polymer modification techniques. Powerful new methods that allow for positioning of functional borane moieties at well-defined positions in the polymer chain have also been developed. The resulting organoborane polymers have been investigated as luminescent and electro-active materials, electrolytes for batteries, supported Lewis acid catalysts, sensors for anions and biologically relevant molecules, building blocks of stimuli-responsive and dynamic (supramolecular) materials, and for biomedical applications.

F. Jäkle (✉)

Rutgers University-Newark, 73 Warren Street, Newark, NJ 07102, USA

e-mail: fjaekle@rutgers.edu

© Springer International Publishing Switzerland 2015

E. Fernández, A. Whiting (eds.), *Synthesis and Application of Organoboron*

Compounds, Topics in Organometallic Chemistry 49,

DOI 10.1007/978-3-319-13054-5_10

297

Keywords Boron • Lewis acids • Luminescence • Organoborane • Polyelectrolytes • Polymerization • Sensors

Abbreviations

9-BBN	9-Borabicyclononane
AIBN	Azobisisobutyronitrile
Alq ₃	Aluminum tris(8-hydroxyquinolate)
Ar	Aryl
ATRP	Atom transfer radical polymerization
COD	1,5-Cyclooctadiene
Cp	Cyclopentadienyl
Cp*	Pentamethylcyclopentadienyl
CTA	Chain transfer agent
DLS	Dynamic light scattering
dppb	Bis(diphenylphosphino)butane
dppp	Bis(diphenylphosphino)propane
dtbpy	4,4'-Di- <i>t</i> -butyl-2,2'-bipyridine
Fc	Ferrocenyl or ferrocenediyl
Hex	<i>n</i> -Hexyl
LCST	Lower critical solution temperature
LLDPE	Linear low-density polyethylene
Mes	Mesityl (2,4,6-trimethylphenyl)
NIR	Near infrared
NMP	Nitroxide-mediated polymerization
OLED	Organic light emitting device
PCL	Poly(ϵ -caprolactone)
PDMA	Poly(<i>N,N</i> -dimethylacrylamide)
PEG	Polyethylene glycol
PEO	Polyethylene oxide
pin	Pinacolato
PLA	Poly(lactic acid)
PMDETA	<i>N,N,N',N'',N'''</i> -Pentamethyldiethylenetriamine
PNIPAM	Poly(<i>N</i> -isopropylacrylamide)
PS	Polystyrene
PSBA	Polystyrene boronic acid
R	Organic substituent
RAFT	Reversible addition–fragmentation chain transfer
ROMP	Ring-opening metathesis polymerization
St	Styrene or styryl
TEM	Transmission electron microscopy
T_g	Glass transition temperature
Tip	Tripyl (2,4,6-tri- <i>iso</i> -propylphenyl)

TMS	Trimethylsilyl
UCST	Upper critical solution temperature
UV	Ultraviolet

1 Introduction

Boron-containing polymers represent an emerging class of inorganic and organo-metallic polymers [1, 2]. They have long been known for their unique properties, including flame retardance and high thermal stability, and their use as preceramic materials [3]. More recently, applications as electrolytes for lithium ion batteries and as photo- and electro-active polymers (including holographic, nonlinear optical, electroluminescent materials) have been explored [4–10]. Moreover, the attachment of Lewis acidic borane groups has been exploited for the development of supported reagents and immobilized catalysts, separation media, sensor systems, stimuli-responsive materials, and biomaterials [7, 11, 12].

Organoborane-functionalized polymers are accessed either by direct polymerization of organoborane monomers or by polymer modification reactions. Both methods have been applied successfully for the attachment of new functional borane substituents to the side chains of polyolefins and conjugated polymers [3]. In addition, a diverse range of new synthetic routes for the incorporation of boron into the polymer main chain have been reported [5, 7]. In another major accomplishment, reliable methods for the synthesis of well-defined organoborane-modified polymers of controlled molecular weight and chain-end functionality have been introduced [13]. These new synthetic tools allow for the formation of more sophisticated polymer architectures such as block and star polymers and provide an entry into nanostructured boron-containing materials.

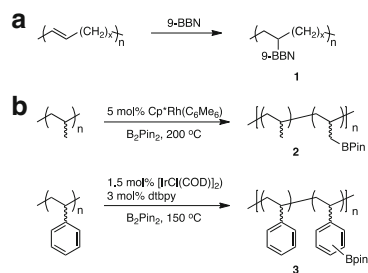
This review will highlight the recent advances in the field of boron-containing polymers with a specific focus on organoborane polymers. Polymeric materials based on carboranes are not included and those with B–N and B–P linkages [14] are discussed in a separate chapter in this book.

2 Synthesis of Organoborane Polymers

2.1 *Polymer Modification Reactions on Polyolefins*

One of the earliest and most commonly applied routes to borane-functionalized polymers involves the use of metalated polymers, especially polystyrene derivatives [3]. Suitable precursor polymers were lithiated, mercuriated, or converted to the Grignard reagent and then treated with an electrophilic borane species. However, these polymer analogous procedures often resulted in moderate chemo- and regioselectivity, and their utility was mostly limited to polymer resins [15]. In the

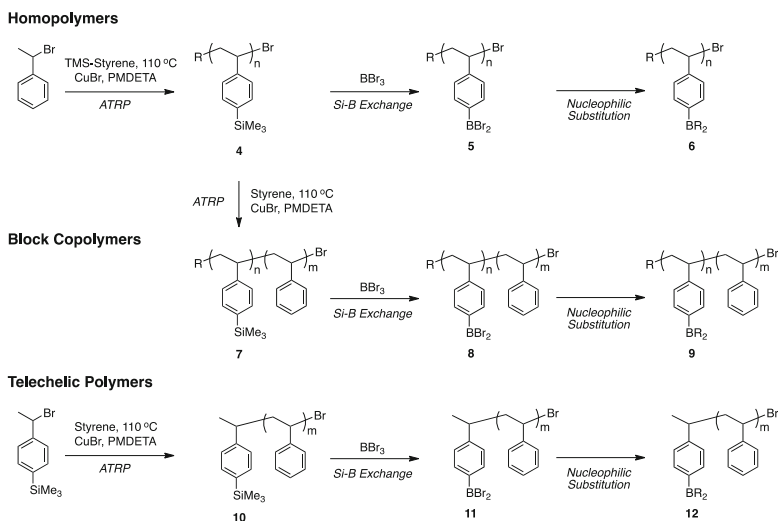
Scheme 1 Examples of polymer modification with borane groups by (a) hydroboration and (b) transition metal-catalyzed C–H activation methods



case of soluble polymers, side reactions that led to cross-linking were frequently observed [16]. Another approach entails the direct borylation of organic polymers. This method is well suited for vinyl-functionalized precursor polymers that readily undergo hydroboration (**1**, Scheme 1a) [17, 18]. However, for other less reactive polymers much harsher conditions are required; an example is the direct borylation of polystyrene with BH_2Cl , which proceeded only under forcing conditions and with low selectivity [19]. The last decade has witnessed two major advances: (a) transition metal-catalyzed direct functionalization of organic polymers using C–H activation protocols and (b) the use of highly selective Si–B exchange chemistries.

The direct borylation of polyolefins by C–H activation was first explored by Hartwig, Hillmyer, and coworkers [20–22]. They found that polypropylene can be selectively functionalized at the pendant methyl groups with B_2pin_2 (Pin = pinacolato) in the presence of $Cp^*Rh(C_6Me_6)_2$ as the catalyst (**2**, Scheme 1b) [21]. Similar methods were developed for the functionalization of LLDPE and for isotactic poly(1-butene) (up to 19% borylation) [22, 23]. Bae and coworkers investigated the borylation of atactic, isotactic, and syndiotactic polystyrene in the presence of an Ir catalyst (e.g., $[IrCl(COD)]_2/dtbpy$) and achieved high degrees of functionalization (**3**, up to 42% borylation) [24]. Since the regioselectivity of the borylation is determined by steric effects, a mixture of *meta*- and *para*-substitution patterns was observed. The boryl moieties in the products are typically converted to organic functional groups to enhance the hydrophilicity or to allow for the formation of brush-like polymer architectures.

We established a very efficient and versatile new route to organoborane-functionalized styrenic polymers. Our approach involved the “masking” of polystyrene with silyl groups, which were then quantitatively replaced with the desired borane functional groups (Scheme 2) [25, 26]. In the first step, the preparation of the TMS-functionalized polymer **4** was accomplished by ATRP [27], a controlled free radical polymerization technique that allows us to adjust the molecular weight by simply varying the ratio of initiator to monomer. The second step involved a highly selective polymer modification reaction, where **4** was treated with a slight excess of BBr_3 to form polymer **5**. This methodology represents an exceptionally simple and straightforward route to borane-functionalized polystyrene that avoids the use of toxic mercury or tin species, while at the same time providing outstanding selectivity without any apparent cross-linking of the polymer chains. The reactive



Scheme 2 Synthetic approach to borylated homo, block, and telechelic polymers via Si-B exchange (R=1-phenylethyl)

polymer **5** proved highly versatile in that the characteristics of the individual boron sites (e.g., Lewis acidity, photophysical and electronic properties) can be readily fine-tuned through high-yielding substitution reactions. A family of new organoborane polymers (**6**; R = H, alkyl, aryl, alkoxy, amino, etc.) was obtained, including different luminescent polymers and highly Lewis acidic triarylborane polymers that are otherwise difficult to prepare [28–32].

Another important benefit is that we were able to realize different polymer architectures. Thus, the same synthetic approach was successfully applied to the synthesis of *random copolymers*, *telechelic* (end-functionalized) polymers, and *block copolymers* containing organoborane moieties at well-defined positions of the polymer chain [33–35]. Random copolymers with both silyl and boryl groups were obtained by simply varying the ratio of BBr₃ to SiMe₃ functionalities in **4** [35]. Polymer **4** was also used as a macro-initiator for the polymerization of styrene [33]. The block copolymer **7** was then again treated with BBr₃, and the resulting polymer **8** served as a “universal” precursor to amphiphilic organoborane block copolymers such as the borate and boronium-functionalized materials discussed further in Sect. 3.4. Telechelic polymers were prepared using a silylated initiator, 1-bromo-1-(4-trimethylsilylphenyl)ethane, for the polymerization of styrene, followed by exchange of the TMS end group in **10** with BBr₃ [34]. Atom transfer radical coupling (ATRC) of **10** gave the respective di-telechelic α ,- ω -borane-functionalized polymers. The telechelic polymers **12** can be used, for example, in the construction of polymer assemblies as described in Sect. 3.1.

2.2 Direct Polymerization of Borane Monomers by Chain Growth Methods

The direct polymerization of borane monomers also has a long history. Early studies revolved around the free radical polymerization of styryl boronic acid derivatives for biomedical and related applications, and of vinyl-functionalized borazines and borane and carborane clusters for the preparation of preceramic polymers [3]. In recent years, significant advances have been made in that a much broader range of functional monomers can now be polymerized, including monomers with highly electron-deficient borane moieties [36–38]. In another major breakthrough, the controlled chain growth polymerization of boron-containing monomers has been popularized [13]. The latter has opened up avenues to polymers of well-defined architectures that can be used to develop new functional materials for nanotechnology and biomedical applications.

Relative to the polymer modification reactions described earlier, an advantage is that the borane monomers can be isolated and purified prior to polymerization. Moreover, the functional group tolerance is generally higher as the need for reactive borane species such as BBr_3 or transition metal catalysts can be circumvented. This allows for a greater variety of other functional comonomers to be incorporated, including acrylates, acrylamides, vinylpyridines, and ethylene oxide [39–44]. However, the polymerizability of each new monomer has to be investigated and the polymerization conditions carefully optimized.

For the preparation of block copolymers, at times it is advantageous to perform the polymerization of the boron monomer first, followed by the organic monomer. In other cases it is preferable to use the preformed organic polymer as a macro-initiator to generate the boron-containing block copolymers. Small molecule initiators that are functionalized with borane groups can be used to prepare telechelic polymers. This is schematically illustrated in Fig. 1, for the case of vinyl polymers, but similar considerations also apply to other chain growth polymerization processes such as ring-opening polymerizations.

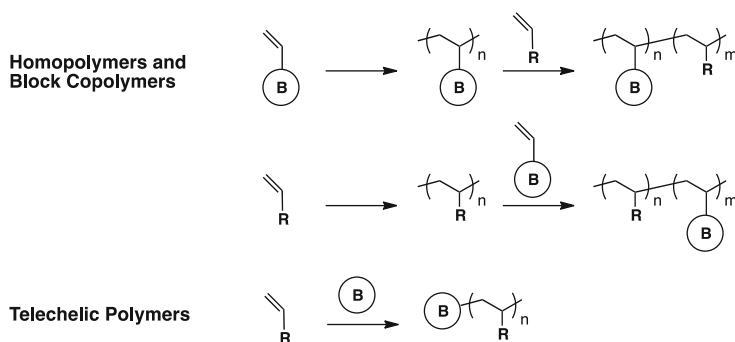


Fig. 1 Schematic illustration of the formation of homopolymers, block copolymers, and telechelic polymers from borane-functionalized vinyl monomers and initiators

Free radical polymerizations are most frequently employed, because of the unmatched tolerance to functional groups and the typically straightforward synthetic protocols. A range of different techniques including atom transfer radical polymerization (ATRP) [27], nitroxide-mediated polymerization (NMP) [45], and reversible addition–fragmentation chain transfer polymerization (RAFT) [46] are available. It is important to emphasize that these new methods not only offer control over the molecular weight, but also provide facile access to complex polymer architectures such as block and star-shaped polymers.

We used the ATRP technique to prepare the first organoborane-functionalized block copolymers. First, the borane homopolymer (PSBpin) was obtained by ATRP of the styryl boronic ester StBpin. Subsequent chain extension with styrene proceeded with excellent efficiency and control to give the block copolymer PSBpin-*b*-PS [33]. This approach was more recently applied to other block copolymers such as PEG-*b*-PSBA (PSBA=polystyrene boronic acid) [47]. Sumerlin and coworkers first explored RAFT methods for the preparation of boronic acid-functionalized acrylamide block copolymers (see Sect. 3.3) [48, 49]. RAFT polymerizations have since proven to be highly versatile and have been applied to a wide range of different functional monomers, including (8-hydroxyquinolato) borane derivatives [43, 44, 50, 51], BODIPY-functionalized monomers [52, 53], and even Lewis acidic dimesitylborane species [37] (see Sects. 3.1 and 3.2). The NMP method was utilized in the block copolymerization of tris(2-pyridyl)borate ligand-functionalized styrene (see Sect. 3.4) [54]. Alternative approaches include Ziegler-Natta [55, 56] and ring-opening metathesis polymerization (ROMP) of borane monomers [57].

The use of borane initiators in the ring-opening polymerization of cyclic esters such as lactide and ϵ -caprolactone gives telechelic polymers. Much work has been performed on the use of boron diketonate initiators that give rise to polymeric materials with intriguing luminescence properties (see Sect. 3.2) [58–60]. Shea and coworkers explored the homologation of ylides as a means to generate borane-terminated polymethylenes [61, 62]. In another novel approach Lalevée and Lacôte used borane–carbene adducts as initiators for the radical photopolymerization of vinyl monomers [63–66].

2.3 Side-Chain Functionalization of Conjugated Polymers

Polymer modification reactions have been widely utilized for the side-chain functionalization of conjugated polymers. Typically, the goal is to modify the electronic structure of the conjugated material and thereby enhance the properties. Si–B exchange reactions are a versatile tool for the preparation of borane-functionalized polythiophenes and thiophene copolymers (Scheme 3a) [67–69]. The direct attachment of borane moieties to the conjugated backbone in polymers **13** resulted in significantly lowered LUMO orbital energies and strong bathochromic shifts in the absorption spectra. The hydroboration of poly

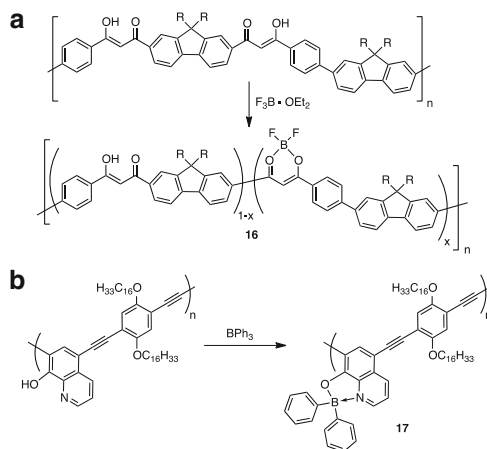
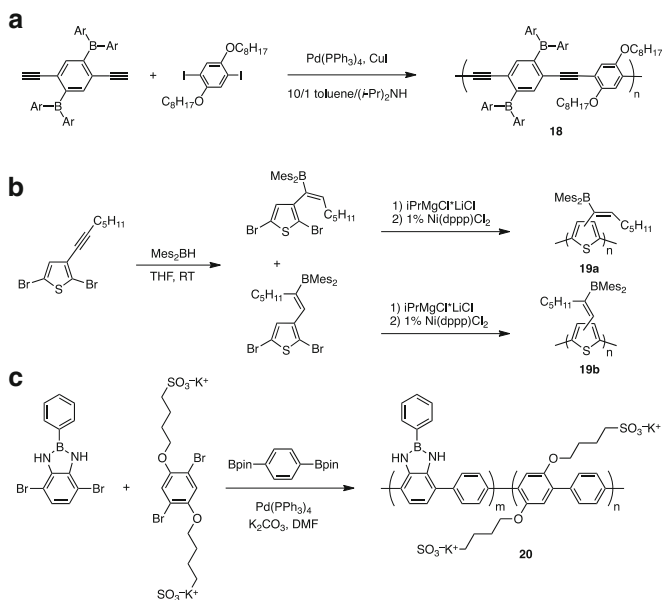


Fig. 2 (a) Functionalization of conjugated diketonate copolymers with varying amounts of $F_3B \cdot OEt_2$. (b) Functionalization of conjugated 8-hydroxyquinoline copolymer with BPh_3



Scheme 4 Examples of the synthesis of conjugated polymers with borane side groups from borane monomers via (a) Songashira–Hagihara, (b) Kumada, and (c) Suzuki–Miyaura-type polycondensation

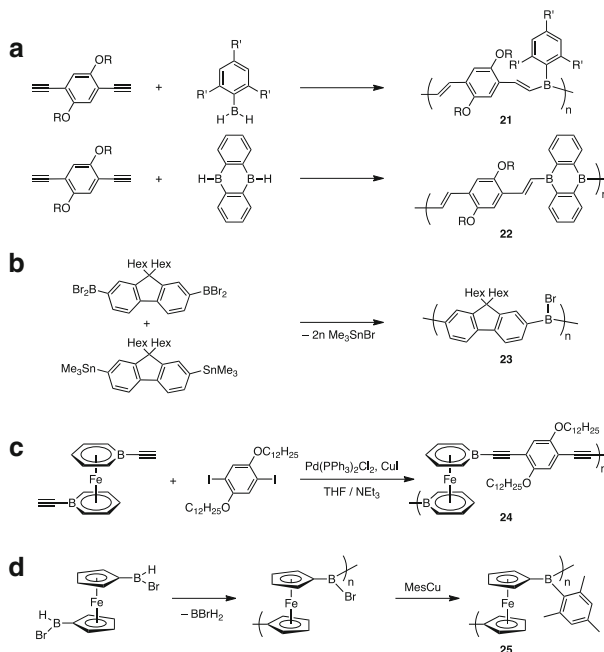
range of different diiodoarenes as comonomers [77]. We explored the Kumada coupling polymerization of thiophenes with vinylborane substituents (Scheme 4b) [78]. Hydroboration of the 3-(*n*-pentylethynyl)thiophene gave rise to two different regioisomers, which were separated by reverse phase column chromatography,

converted to the corresponding Grignard species, and then polymerized in the presence of $\text{Ni}(\text{dppp})\text{Cl}_2$. The optical properties of the polymeric products **19a** and **19b** differed significantly, highlighting the effects of the substitution pattern on the extent of cross-conjugation between polymer main chain and borane side groups. Diazaborole polymers were prepared by C–C coupling as well as electropolymerization methods [82]. For example, a water-soluble conjugated copolymer (**20**) was obtained by Suzuki–Miyaura coupling copolymerization of a dibrominated diazaborole (Scheme 4c) [83]. Finally, Chujo and coworkers incorporated BODIPY chromophores as pendant groups to polyfluorenes by Ni-catalyzed Yamamoto or Suzuki–Miyaura coupling methods [84]. The polymers exhibited interesting energy transfer from the BODIPY side chains to the polyfluorene main chain.

2.4 Boron Incorporation into the Main Chain of Conjugated Polymers

The first well-defined conjugated main chain-type polymers were prepared by Chujo and coworkers in 1998 via hydroboration polymerization (**21**, Scheme 5a) [85]. A wide range of different luminescent polymers have since been obtained by reaction of organic or organometallic dialkynes with MesBH_2 or TipBH_2 ($\text{Mes} = 2,4,6\text{-trimethylphenyl}$, $\text{Tip} = 2,4,6\text{-tri-iso-propylphenyl}$). The use of the bulkier Tip derivative results in enhanced stability of the products [86]. A diboraanthracene derivative with two spatially separated B–H functionalities was utilized by Wagner and coworkers to generate polymer **22** [87].

Organometallic polycondensation reactions present an attractive alternative, especially when hydroboration methods are not applicable as in poly(aryleneborane)s. Grignard and organolithium reagents were explored early on, but the molecular weights were relatively low [88]. We demonstrated more recently that reaction of distannyl species with arylboranes ArBX_2 or $\text{X}(\text{R})\text{B-Ar-B}(\text{R})\text{X}$ ($\text{X} = \text{Br}, \text{Cl}$) results in highly selective polymer formation under mild conditions via Sn–B exchange (**23**, Scheme 5b) [89–93]. Transition metal-catalyzed C–C coupling processes have also attracted increased attention. They have been widely used to incorporate luminescent BODIPY and boron 8-hydroxyquinolate heterocycles into conjugated polymers [94–101]. In addition, Sonogashira–Hagihara coupling was used to embed bis(borabenzene)iron complexes into conjugated polymers (**24**, Scheme 5c), while a recent report details the Stille-type polymerization of thiophene derivatives of diboraanthracene [102]. Other less frequently employed techniques include the spontaneous polymerization of in situ generated ferrocenylboranes, $\text{H}(\text{Br})\text{B-fc-B}(\text{Br})\text{H}$ ($\text{fc} = 1,1'\text{-ferrocenediyl}$) (**25**, Scheme 5d) [103], the spontaneous ring-opening polymerization of borafuorenes [104], and the use of preformed organoboranes in click reactions [105]. Electropolymerization



Scheme 5 Examples for the synthesis of main chain-type conjugated organoboron polymers via (a) hydroboration polymerization, (b) Sn–B exchange polymerization, (c) Sonogashira–Hagihara and Stille-type polycondensation, and (d) spontaneous polycondensation of arylboranes

presents yet another alternative; however, its use has been largely limited to monomers with boronic ester or carborane pendant groups.

3 Selected Examples of Polymers and Their Applications

In the following section we introduce selected classes of organoborane polymers and briefly discuss their application fields.

3.1 Borane Polymers as Lewis Acids and Anion Sensors

Among the earliest examples of polymer-supported borane Lewis acids are Merrifield resins that were functionalized with 9-BBN or Tip₂B moieties [106, 107]. These resins were used in hydroboration reactions and the reduction of ketones. More recently, we developed a new family of soluble polymers (26) using the Si–B exchange protocol discussed in Sect. 2.1 [108]. The Lewis acidity of the boranes in 26 was fine-tuned by modification of the substituent R (Fig. 3),



Fig. 3 Lewis acidity tuning of organoborane polymers

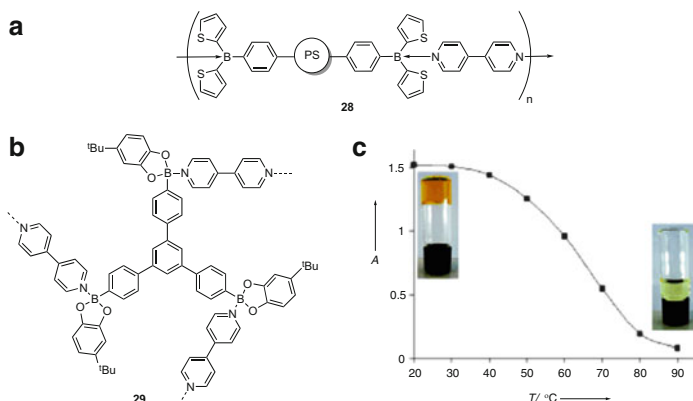
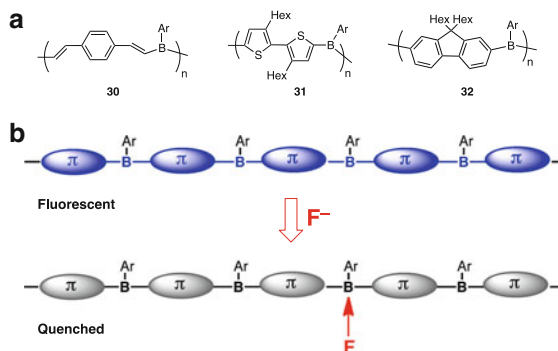


Fig. 4 (a) An example of a supramolecular 1D polymer formed via Lewis acid–base interactions (*PS* polystyrene). (b) Formation of a 3D network using a trifunctional boronate ester and 4,4′-bipyridine. (c) Illustration of the temperature-dependent properties of a related organogel in toluene. Adapted with permission from Sheepwash et al. [109]. Copyright 2011 Wiley-VCH Verlag GmbH & Co. KGaA

thereby offering control over the strength and reversibility of the donor–acceptor bonding to Lewis basic substrates. We found that the arylborane polymers **26** ($\text{R} = \text{C}_6\text{F}_5$, thienyl) and the related hydroborane polymer **27** strongly bind to Lewis bases as evidenced by the formation of soluble, isolable polymeric donor–acceptor complexes with pyridine ligands [28, 108]. With weaker donors, a temperature-dependent equilibrium between coordinated and uncoordinated sites was established [108]. On the other hand, more weakly Lewis acidic poly(styrene boronic esters) (**26**, $\text{R} = \text{alkoxy}$) were only partially coordinated even with very strong bases.

The self-assembly of polymeric Lewis acids and Lewis bases is expected to allow for reversible formation of complex polymer architectures such as *block* and *graft* copolymers and of reversibly cross-linked materials. An example of this concept is the assembly of borane-functionalized mono- and di-telechelic organoboron polymers into supramolecular structures by means of reversible noncovalent interactions with bifunctional donor molecules (**28**, Fig. 4a) [34]. Studies on the assembly of molecular polyfunctional organoboranes and polyfunctional amines to give 1D, 2D, and 3D-polymeric materials were also reported [109–113]. For example, Severin and coworkers discovered the formation of some very interesting temperature-responsive organogels in toluene (**29**, Fig. 4b, c) [109].

Fig. 5 (a) Examples of conjugated organoborane polymers that were studied for the recognition of anions and aromatic amines. (b) Schematic illustration of the amplified fluorescence quenching upon binding of fluoride to one of the borane sites in a conjugated organoborane polymer



At temperatures above 60°C, the organogel broke up due to rupture of the B–N bonded network and reformed again upon cooling to room temperature.

The Lewis acidity of tricoordinate organoborane polymers is also advantageous for the development of new luminescent materials for the recognition and sensing of anions. Figure 5a shows selected examples of conjugated organoborane polymers that are luminescent and at the same time act as Lewis acids [89, 90, 114]. An important feature is the overlap of the empty p-orbital of the electron-deficient boron atom with the π -conjugated organic bridges, which leads to bathochromic shifts in the absorption and frequently strong emission in the visible region. Steric shielding of the borane moiety is usually accomplished by the introduction of a bulky aryl groups (Ar = mesityl, triptyl) and results in high selectivity for small anions such as fluoride or cyanide. Coordination of these anions to boron then triggers a response in the photophysical characteristics (e.g., change in the absorption and emission color or quenching of the luminescence) [115–117], which is specific to the nature of the anion under investigation and can readily be verified via spectroscopic screening or even by naked eye observation.

An intriguing aspect of conjugated organoborane polymers is that energy transfer can occur from remote sites to the anion recognition site, which then acts as a quenching site [118]. This implies that coordination of the anion to only one of the borane moieties results in effective quenching of the fluorescence of the entire conjugated polymer chain as illustrated in Fig. 5b. This phenomenon was first qualitatively reported by Chujo and coworkers for polymer **30** [114], and a quantitative analysis of the binding of pyridine to a poly(bithiophene borane) system (**31**) was performed by our group [89]. The amplified quenching appears to be a quite general phenomenon as several other conjugated polymer systems have since been reported [90, 91, 119]. We also succeeded in the preparation of a conjugated organoborane macrocycle, which allowed for a more detailed investigation since polydispersity and end group effects do not come into play [120].

Related phenomena were also observed for nonconjugated polymers with borane chromophores as side chains [29–31, 55, 57]. As an example, polymers **33** (Fig. 6) are strongly emissive in the blue region with a maximum at $\lambda_{em} = 463$ nm when R = H, while the amino-functionalized derivative (R = NPh₂) emits in the green at

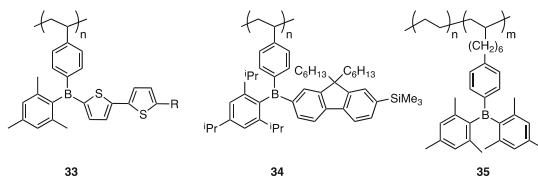


Fig. 6 Examples of polymers with fluorescent triarylborane side chains

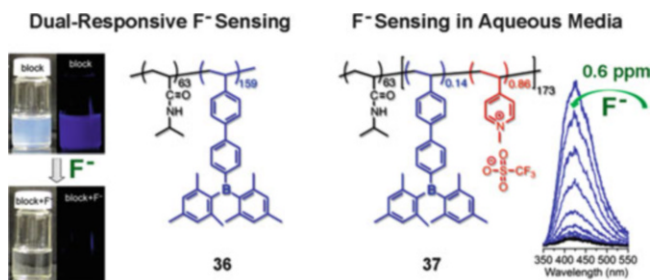


Fig. 7 Fluoride ion sensing with organoborane block copolymers. Adapted with permission from Cheng et al. [37]. Copyright 2013 American Chemical Society

$\lambda_{\text{em}} = 537 \text{ nm}$. These polymers selectively bind fluoride and cyanide over a range of other anions (e.g., Cl^- , Br^- , and NO_3^-) as reflected in a hypsochromic shift of the absorption maximum. Fluoride or cyanide binding to **33** ($\text{R} = \text{NPh}_2$) led to a change of the emission color from green to blue, but for **33** ($\text{R} = n\text{-hexyl}$) highly effective fluorescence quenching was observed. The amplified quenching effect was tentatively attributed to through-space exciton migration to lower energy fluoroborate quenching sites. Similar studies were reported by Do and Lee and coworkers for polymers **35**, which strongly emit in the violet/UV region with a maximum at 382 nm [55, 57].

We recently reported a new twist to this concept: i.e., the block copolymer **36** not only responds to fluoride anions with a color change but at the same time the solubility characteristics change dramatically (Fig. 7) [37]. In DMF solution, the borane-functionalized block forms the core of self-assembled aggregates, but upon addition of a small amount of fluoride anions the aggregates disassemble into individual polymer chains. The disassembly process can be monitored by a change in turbidity as well as the quenching of the fluorescence. We also prepared a novel block–random copolymer **37**, in which cationic pyridinium groups are inserted into the borane block. The pyridinium groups further enhance the anion binding strength due to favorable electrostatic interactions, allowing for the detection of very low levels of fluoride even in aqueous solution ($\text{DMF}/\text{H}_2\text{O} = 9:1$) [37].

3.2 Luminescent Polymers Based on Boron Chelate Complexes

Polymers that contain boron heterocycles, typically with boron in the tetracoordinate state, have been pursued vigorously due to their promise as new luminescent materials. Applications as emissive and electron-conduction materials for organic light emitting devices (OLEDs), lasing materials, in bioimaging, and as stimuli-responsive materials are most prominent. Architectural control tends to be an important aspect because it allows for the fabrication of controlled size nanoparticles, for example, by the assembly of block copolymers or star polymer.

The boron heterocycles come in many different flavors, but three classes have been studied most extensively: boron dipyrromethene (BODIPY), boron 8-hydroxyquinolate, and boron diketonate derivatives (Fig. 8). They stand out because of their high stability, typically strong emission, and facile tuning of the absorption and emission characteristics through simple substituent variations. There is a vast literature on the incorporation of these chromophores into the main chains or side chains of polymers. In the following sections, we offer a few selected examples and discuss pertinent applications where appropriate.

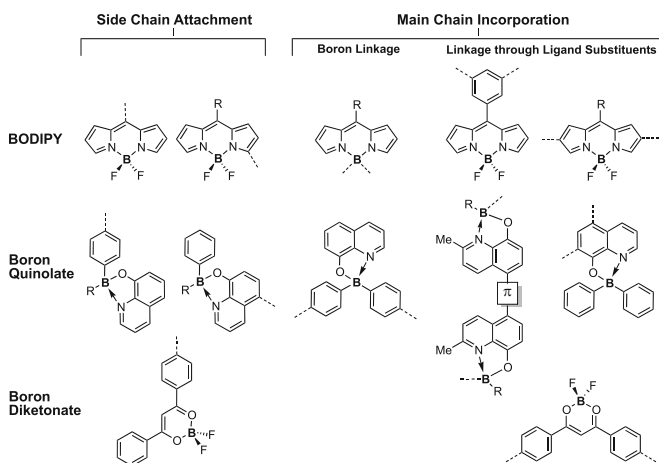
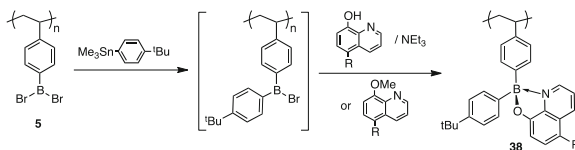


Fig. 8 Incorporation of fluorescent boron heterocycles into polymers. The linkages to the polymer chains are indicated with *dashed lines*; some of the substituents on the pyrrole and quinoline moieties are omitted for clarity reasons



Scheme 6 Synthesis of boron quinolate polymers **38**

3.2.1 Boron Quinolate-Functionalized Polymers

In 2004, we introduced the first class of polymers with boron quinolate chromophores attached to a polystyrene backbone using a facile one-pot polymer modification procedure (Scheme 6) [121–122] (see also ref. [123]). The polymeric products (**38**) proved to be highly soluble and luminescent thin films could be readily cast from solution. Importantly, we found that the emission characteristics could be tuned by simple variation of the substituent in the 5-position of the quinoline moiety ($\text{R} = \text{Bpin}$, C_6F_5 , Cl , $p\text{-C}_6\text{H}_4\text{OMe}$, $p\text{-C}_6\text{H}_4\text{NMe}_2$), covering almost the entire visible spectrum from blue to red emission [122, 124].

More recently, we explored the controlled radical polymerization of organoboron quinolate monomers in an effort at achieving architectural control. Well-defined block copolymers with polystyrene, poly(styrene-*alt*-maleic anhydride), polyethylene oxide, and poly(4-vinylpyridine) were prepared by RAFT polymerization using monomer **39** as the building block [43, 50]. A pyridine derivative of **39** ($\text{R} = 4\text{-pyridyl}$) was also prepared and incorporated into a block copolymer with PS [44]. The self-assembly of this amphiphilic block copolymer was investigated and the pyridine binding sites were exploited for the complexation to a Zn porphyrin derivative. Complexation to Zn resulted in interesting energy transfer phenomena from the boron quinolate chromophore to the porphyrin (Fig. 9a). We also prepared the first organoborane star polymers using an arm-first RAFT polymerization method, in which a distyrylboron quinolate cross-linker (**40**) was polymerized with AIBN in the presence of different macro-chain transfer agents (CTA, Fig. 9b) [51]. The successful formation of well-defined luminescent stars was confirmed by TEM and DLS analysis.

Chujo and coworkers studied the incorporation of boron quinolate chromophores into the main chain of conjugated polymers [73, 96, 125, 126]. A range of different methods were explored, including polymer modifications and the direct polymerization of preformed complexes via C–C coupling methods. For example, polymers **42** were prepared by treatment of **41** with BPh_3 or $(\text{C}_6\text{F}_5)_2\text{BF}\cdot\text{OEt}_2$ (Fig. 10) [127]. The application of **42** as an electron conducting material in OLEDs was explored. For the fluorinated polymer ($\text{Ar} = \text{C}_6\text{F}_5$), an electron mobility close to that of aluminum tris(8-hydroxyquinolate) (Alq_3) was recorded in an electron-only thin film device.

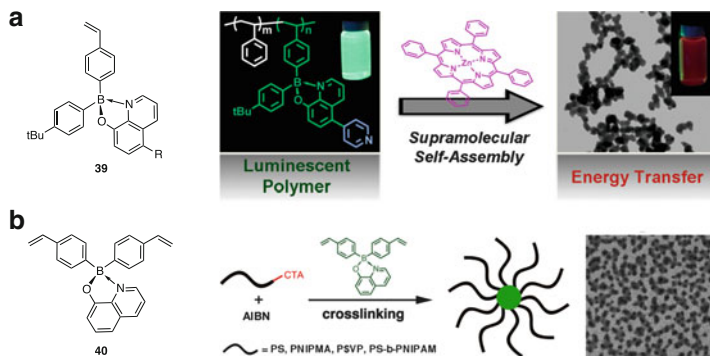


Fig. 9 (a) Structure of boron quinolate monomers (**39**) used to generate well-defined homo and block copolymers and illustration of the supramolecular assembly of a pyridyl derivative (R=4-pyridyl) with Zn tetraphenylporphyrin. Adapted with permission from Cheng et al. [44]. Copyright 2013 American Chemical Society. (b) Structure of a boron quinolate cross-linker (**40**) and its use in the formation of luminescent star polymers by arm-first RAFT polymerization. Adapted with permission from Cheng et al. [51]. Copyright 2012 The Royal Society of Chemistry

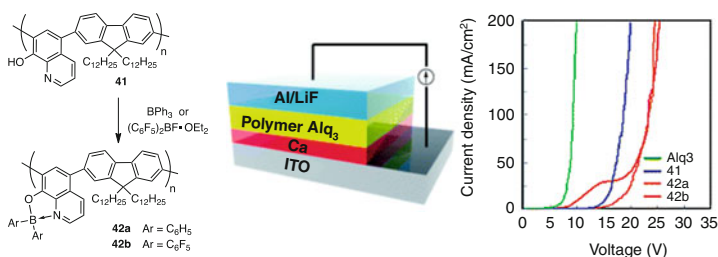


Fig. 10 Synthesis of boron quinolate polymers **42** via post-polymerization modification and current–voltage plots in comparison to an Alq₃ device. Adapted with permission from Nagai et al. [127]. Copyright 2010 American Chemical Society

3.2.2 BODIPY-Functionalized Polymers

Boron dipyrromethene dyes are among the most widely utilized fluorophores, because of their strong and sharp emission in the visible and in some cases even the NIR region. Numerous polymers have been developed with BODIPY as pendant groups or incorporated into the polymer main chain. Some examples of random and block copolymers that contain BODIPY side groups (**43–45**) are illustrated in Fig. 11 [52, 53, 128]. The first polymers with BODIPY in the main chain (**46**) were prepared by Li and Liu via Sonogashira–Hagihara coupling [94, 97]. Polymers **47** are linked through the boron atom itself; they were found to aggregate into nanosized particles and higher-order, fiber-like structures depending on the bridging aryl (Ar) moiety, possibly promoted by the presence of the long alkyl group on the dipyrromethene entity [129]. Polymers **48** are highly emissive as

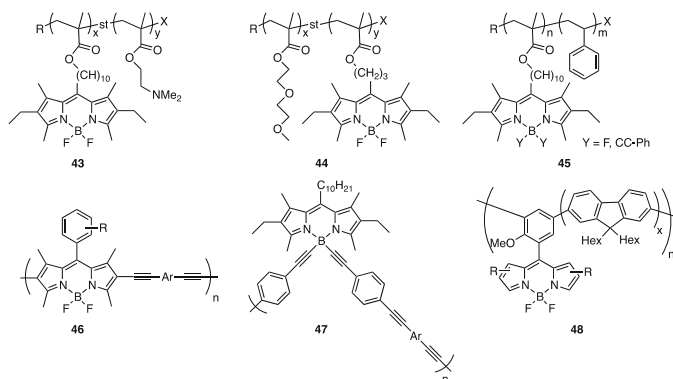


Fig. 11 Selected examples of BODIPY-functionalized polymers

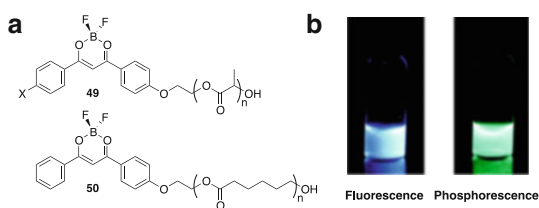


Fig. 12 (a) Boron diketonate-terminated PLA (**49**, X=H, I) and PCL (**50**). (b) Photographs of aqueous nanoparticle suspensions of **49** in the presence of air (fluorescence observed) and under N₂ atmosphere after turning off the excitation source (phosphorescence observed). Adapted with permission from Pfister et al. [131]. Copyright 2008 American Chemical Society

a result of efficient energy transfer from the oligofluorene bridging moieties to the BODIPY chromophores [130].

3.2.3 Boron Diketonate-Functionalized Polymers

The functionalization of polymers with boron diketonate chromophores was pioneered by Fraser and coworkers. They used boron diketonate derivatives with primary alcohol functionalities as initiators for the ring-opening polymerization of lactide and discovered that the resulting polymers (**49**, Fig. 12a) exhibited dual emission at room temperature, strong blue fluorescence, and simultaneous green phosphorescence [132]. In contrast, phosphorescence was only observed at temperatures below 0°C for polymers (**50**) derived from ϵ -caprolactone. The different behavior was attributed to the lower glass transition temperature (T_g) of poly(ϵ -caprolactone) (PCL) in comparison to that of poly(lactic acid) (PLA) [60]. The fluorescence emission color of the PLA material was found to be also molecular weight dependent (blue to green), indicating the importance of dye–dye interactions

[133]. Nanoparticles that can be dispersed in aqueous solution and exhibit both fluorescence and room temperature phosphorescence were fabricated via nanoprecipitation from DMF as a water-miscible organic solvent [131].

An intriguing aspect of these materials is that the phosphorescence but not the fluorescence is effectively quenched by oxygen. This is illustrated for an aqueous nanoparticle suspension of **49** in Fig. 12b. In the presence of air only the blue fluorescence is apparent, while under nitrogen atmosphere the longer-lived green phosphorescence can be observed after the excitation source is turned off. This property was exploited in tumor hypoxia imaging applications [134, 135]. For this purpose a polymer with an iodine substituent (**49**, X = I) was developed which showed enhanced phosphorescence, because the iodine heavy atom promotes intersystem crossing into the triplet manifold.

As already mentioned earlier, conjugated polymers were also modified with boron diketonate functional groups (see Fig. 2a) [75].

3.3 Boronic and Borinic Acid-Functionalized Polymers for Biomedical Applications and as Smart Materials

Boronic acid-functionalized polymers have garnered intense interest because of the ability of boronic acids to reversibly bind 1,2- or 1,3-diols as illustrated in Fig. 13.

This property allows for the detection and immobilization of sugars; especially the complexation of glucose is of great importance in diagnostics and treatment of diabetes. A range of other biomedical applications have been explored, and this topic is covered in a review by Sumerlin and coworkers [12]. We will focus here on recent advances in areas pertaining to (1) architectural control; (2) development of multiple responsive systems; (3) structural modification to allow for application at physiological pH; and (4) the discovery of new responsive materials.

To achieve architectural control where boronic acid sites are incorporated at well-defined positions of polymers and nanoparticles, controlled radical polymerization techniques are the method of choice. We prepared the first boronic acid block copolymer, PS-*b*-PSBA (**51**, Fig. 14), in 2005 using ATRP in combination with polymer modification procedures that involved the exchange of silyl for boryl groups [33]. The block copolymer was shown to self-assemble into micelles, vesicles, and bundles of rodlike structures, depending on the pH and the amount of THF used as an organic co-solvent [136]. Also, van Hest and Kim and coworkers

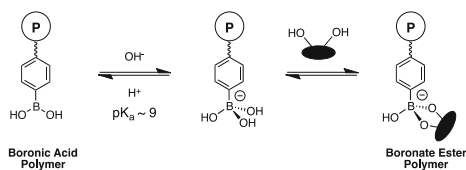


Fig. 13 Schematic illustration of the binding of sugars (1,2- or 1,3-diols) to boronic acid-functionalized polymers

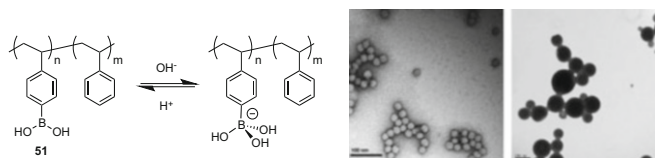


Fig. 14 Structure of PS-*b*-PSBA block copolymers (**51**) and TEM images of assemblies in 0.1 M NaOH (*left*) and in THF/H₂O mixture (*right*). Adapted with permission from Cui et al. [136]. Copyright 2010 Wiley-VCH Verlag GmbH & Co. KGaA

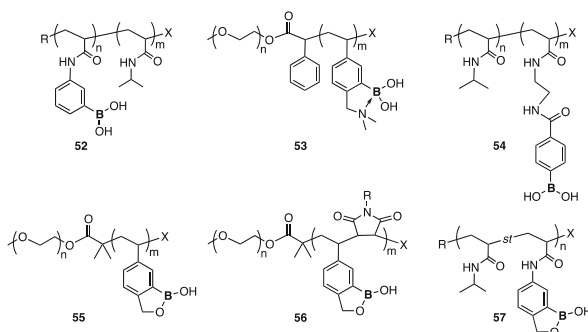


Fig. 15 Examples of boronic acid and boroxole-functionalized polymers that display dual responsive properties and/or are capable of binding sugars at physiological pH

utilized similar methods for the preparation of vesicles that consist of PEG-*b*-PSBA and PEG-*b*-PS and studied them as stimuli-responsive drug delivery vehicles [47].

Sumerlin and coworkers developed RAFT polymerization methods for the preparation of thermoresponsive acrylamide block copolymers [41, 48, 49, 137]. As an example, the acrylamide block copolymer **52** (Fig. 15) forms micellar aggregates in aqueous solution at low pH [137]. These aggregates break up when the pH is increased and sugar molecules are added to the solution. A secondary response is observed when the solution is heated above the lower critical solution temperature (LCST) of the PNIPAM block, which results in the formation of reverse micellar aggregates with PNIPAM in the core.

The sugar binding process is strongly pH dependent as the binding equilibrium relates to the $\text{p}K_{\text{a}}$ of the boronic acid moiety. For practical applications it is important to achieve sugar binding at physiological pH. Several approaches have been taken toward this goal: van Hest, Kim, and coworkers used an amino-functionalized Wulff-type phenylboronic acid derivative (**53**), which favors sugar binding due to an intramolecular B–N interaction [138]. Sumerlin and coworkers demonstrated that linkage of the phenylboronic acid moiety through the electron-withdrawing carboxyl rather than amino group of an amide (**54**) results in similarly enhanced sugar binding at neutral pH [41]. In a different approach, Kiser and coworkers incorporated more acidic boroxoles [139, 140] into polymer structures

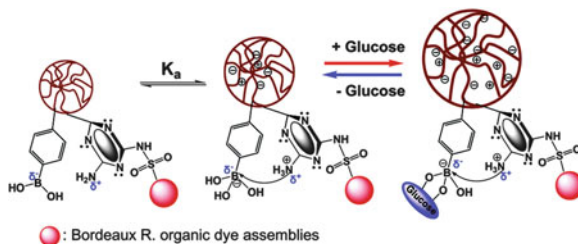


Fig. 16 Schematic illustration of glucose sensing with dye-functionalized boronic acid microgels. Reproduced with permission from Li and Zhou [146]. Copyright 2013 The Royal Society of Chemistry

[141–144]. Related block copolymers (**55**, **56**) were investigated by Kim and coworkers as building blocks of responsive vesicles for insulin release applications [36, 40]. Narain and coworkers found that the combination of boroxole-functionalized polyacrylamide copolymer **57** with glycopolymers resulted in temperature-, pH-, and glucose-responsive gels [39]. Finally, Zhou et al. developed microgels that allow for glucose sensing at physiological pH (due to the presence of quaternizable amino or pyridyl groups) and at the same time contain organic dyes as reporter molecules [145]. Glucose binding resulted in swelling of the gel, which affected the dye–dye separation and in turn triggered a change in the photoluminescence properties (Fig. 16) [146].

Boronic and borinic acid-functionalized polymers have also attracted interest as new responsive and smart materials. Sumerlin and coworkers reported that the cross-linking of a boronic acid-functionalized acrylamide block copolymer (**58**) with polyfunctional alcohols leads to formation of star-shaped polymer architectures as illustrated in Fig. 17a [147]. Addition of monofunctional diols triggered disassembly into the building blocks.

We recently introduced a new type of borinic acid polymer (**59**) that is capable of hydrogen bonding with Lewis bases [38]. In DMSO solution, the polymer shows an upper critical solution temperature (UCST) that strongly depends on the amount of water present (Fig. 17b). An essentially linear correlation of the UCST on the amount of water was found over an unusually wide temperature range. The solubility characteristics were also reversibly altered by the addition of a small amount of fluoride anions.

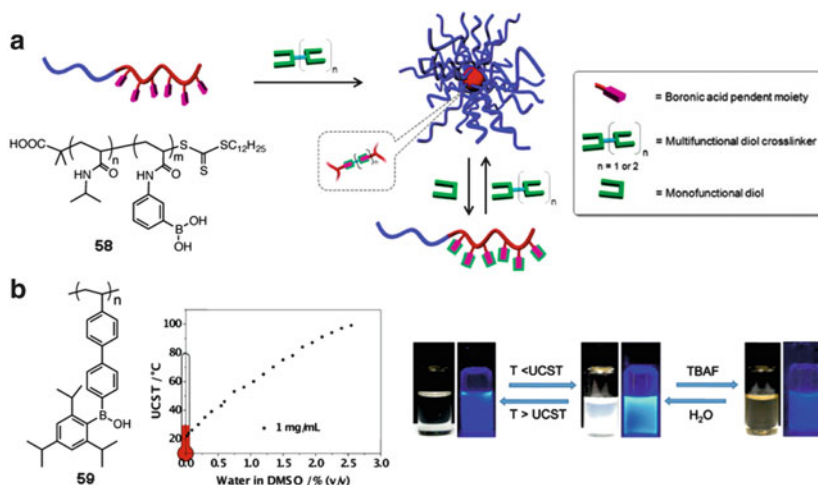


Fig. 17 (a) Schematic illustration of the reversible cross-linking of **58** with multifunctional diols to give starlike assemblies. Adapted with permission from Bapat et al. [147]. Copyright 2011 American Chemical Society. (b) Effect of water content on the UCST of **59** in DMSO solution and photographs (visible light/UV irradiation) illustrating changes with temperature and upon addition of fluoride anions. Adapted with permission from Wan et al. [38]. Copyright 2014 Wiley-VCH Verlag GmbH & Co. KGaA

3.4 Borate and Boronium-Functionalized Polymers as Polyelectrolytes and Polymeric Ligand

Organoborate polymers are attractive as catalyst supports and as new materials for lithium ion battery applications [10]. Typical structural motifs are shown in Fig. 18. For example, Ohno, Matsumi, and coworkers reacted lithium mesitylhydroborate with poly(ethylene oxide) (PEO) and then added different alcohols (ROH) to give polymers **60**. The organoborate moieties in the main chain act as weakly coordinating counterions to lithium ions [148].

The combination of imidazolium ions and borate functionalities in the zwitterionic polymer **61** was found to be beneficial as it resulted in high conductivity despite a relatively high glass transition temperature [149]. In polymer **62**, the amido group is stabilized by B–N π – π interactions, which leads to high ionic conductivity due to favorable ion dissociation. In recent years new composite materials, for example with cellulose, have also been developed [150].

Organoborate polymers are also advantageous as weakly coordinating counterions in catalysis. Many transition metal catalysts rely on the presence of coordinatively unsaturated cationic metal sites, which are stabilized by weakly coordinating counteranions [151, 152]. Especially fluorinated organoborate derivatives are highly effective [153]. Efforts at incorporating these weakly coordinating borate anions into polymeric materials resulted in a range of new ionic polymers [154–156]. Mecking, Vogt, and coworkers prepared borate-functionalized polymer

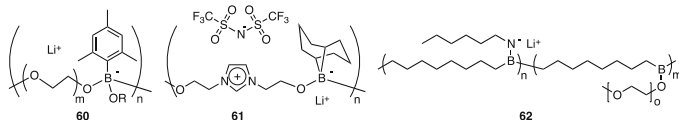


Fig. 18 Examples of boron-containing polymers as electrolytes for lithium ion batteries

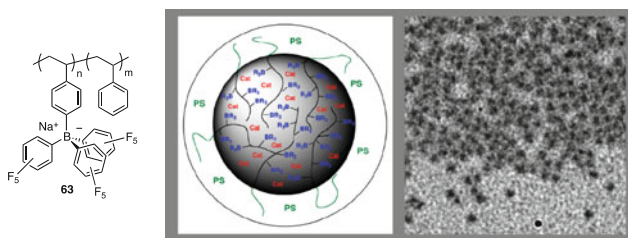


Fig. 19 Self-assembly of the amphiphilic block copolymer **63** in toluene solution. The TEM micrograph shows micelles that had been loaded with $[\text{Rh}(\text{COD})(\text{dppb})]^+$. Adapted with permission from Cui et al. [156]. Copyright 2010 American Chemical Society

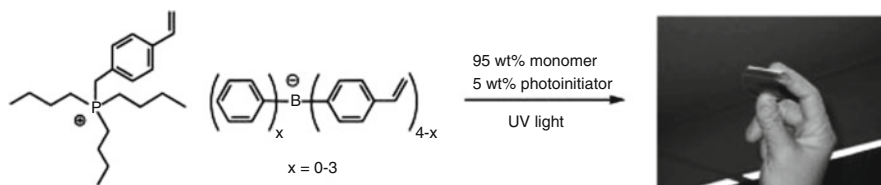


Fig. 20 Formation of highly cross-linked phosphonium borate films by photopolymerization of multifunctional monomers. Adapted with permission from Berven et al. [157]. Copyright 2013 Wiley-VCH Verlag GmbH & Co. KGaA

particles by emulsion copolymerization of styryltriphenylborate, styrene, and divinylbenzene and used the particles to immobilize $[\text{Rh}(\text{dppp})(\text{COD})]^+$. The immobilized catalyst was then applied in the hydrogenation of α -acetamidocinnamic acid [155]. We prepared polystyrene-based homo and block copolymers with perfluoroarylborate pendant groups using a polymer modification protocol [156]. In toluene, the block copolymer **63** assembled into micelles that contain the functional borate moieties in the core surrounded by an inert polystyrene shell (Fig. 19). These micelles were loaded with the $[\text{Rh}(\text{COD})(\text{dppb})]^+$ complex.

Ragogna and coworkers reported an innovative approach to cross-linked borate materials. Highly cross-linked films were generated by photoinitiated polymerization of styryl-functionalized phosphonium borate salts (Fig. 20) [157]. With an increasing number of styrene moieties in the phosphonium borates, the polymer films became harder and more scratch resistant, indicating the tunability of the material properties by simple structural modifications.

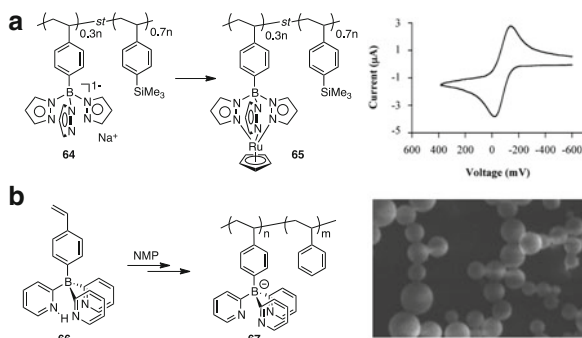


Fig. 21 (a) Metal complexation of a Tp-functionalized polymer **64** and cyclic voltammetry data of the product **65**. Adapted with permission from Qin et al. [35]. Copyright 2008 American Chemical Society. (b) Synthesis of Tpyb-functionalized block copolymer **67** and SEM picture of self-assembled particles after treatment with Cu²⁺ ions. Adapted with permission from Shipman et al. [54]. Copyright 2013 American Chemical Society

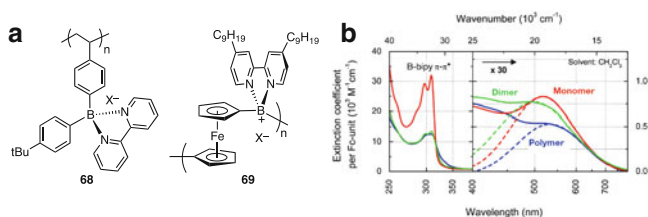


Fig. 22 (a) Structures of boronium-functionalized polymers. (b) UV-visible spectra of polymer **69** in comparison to the corresponding monomer and dimer. Adapted with permission from Cui et al. [161]. Copyright 2010 American Chemical Society

The organoborate polymers discussed thus far are weakly coordinating. Another approach is to attach strong binding sites to generate powerful polymeric ligands for applications in catalysis and supramolecular materials chemistry. We anchored tris(1-pyrazolyl)borate (Tp) [158] ligands to polystyrene by polymer modification processes and then complexed the polymer (**64**) with organoruthenium moieties [35]. Cyclic voltammetry data on **65** confirmed the metal attachment and revealed excellent reversibility for the metal oxidation process (Fig. 21a). We also investigated related Tp end-functionalized polymers as building blocks for supramolecular polymers [159]. More recently, we introduced a new class of tris(2-pyridyl)borate (Tpyb) ligands [160]. Tpyb ligands are more robust than the Tp ligands, allowing for direct polymerization of the styryl derivative **66** by NMP (Fig. 21b) [54]. The block copolymer **67** was generated by sequential polymerization and its nanostructures and metal complexation were studied.

In comparison to these anionic borate-functionalized polymers, cationic organoboron ionomers and polyelectrolytes remain quite rare. The boronium cation sites in polymers **68** (Fig. 22a) are isoelectronic to ammonium functionalities. They were introduced by simple “click”-like reaction of the corresponding bromoborane-

functionalized polymers with 2,2'-bipyridine. Essentially quantitative functionalization was achieved [161–163]. Corresponding amphiphilic block copolymers with polystyrene as a second block were also prepared and their micellar assembly was studied in MeOH. Potential utility as antibacterial materials similar to ammonium-functionalized polymers was suggested. Boronium cation-bridged polyferrocenes (**69**) were introduced as redox-active polyelectrolytes. The ferrocene moieties undergo reversible oxidation at moderate potentials, while the bipyridylboronium heterocycles can be reversibly reduced. These materials display an intense purple color in solution due to charge transfer between the electron-rich ferrocene and the electron-poor bipyridylboronium groups (Fig. 22b).

4 Conclusions

As this brief review indicates, the much greater sophistication of today's synthetic toolbox for borane incorporation into polymeric materials has enabled tremendous progress in terms of (1) the types of functionalities that can be incorporated; (2) the architectural precision that can be achieved; and (3) the new applications that are under pursuit as a consequence. The future of borane chemistry in polymer science is certain to be bright!

Acknowledgments The author thanks the National Science Foundation (NSF CHE-0956655, 1112195, 1308517, and 1362460) for the generous financial support. He is also indebted to all of his students and collaborators for their contributions to the work discussed in here.

References

1. Abd-El-Aziz AS, Carraher CE Jr, Pittman CU Jr, Zeldin M (eds) (2007) *Macromolecules containing metal and metal-like elements: boron-containing polymers*, vol 8. Wiley, Hoboken
2. He X, Baumgartner T (2013) *RSC Adv* 3:11334–11350
3. Jäkle F (2005) *J Inorg Organomet Polym Mater* 15:293–307
4. Entwistle CD, Marder TB (2004) *Chem Mater* 16:4574–4585
5. Matsumi N, Chujo Y (2008) *Polym J* 40:77–89
6. Elbing M, Bazan GC (2008) *Angew Chem Int Ed* 47:834–838
7. Jäkle F (2010) *Chem Rev* 110:3985–4022
8. Lorbach A, Hubner A, Wagner M (2012) *Dalton Trans* 41:6048–6063
9. Tanaka K, Chujo Y (2012) *Macromol Rapid Commun* 33:1235–1255
10. Matsumi N, Ohno H (2007) Organoboron polymer electrolytes for selective lithium cation transport. In: *Macromolecules containing metal and metal-like elements*, vol 8, pp 175–196
11. Jäkle F (2006) *Coord Chem Rev* 250:1107–1121
12. Cambre JN, Sumerlin BS (2011) *Polymer* 52:4631–4643
13. Cheng F, Jäkle F (2011) *Polym Chem* 2:2122–2132
14. Staubitz A, Robertson APM, Sloan ME, Manners I (2010) *Chem Rev* 110:4023–4078

15. Armitage P, Ebdon JR, Hunt BJ, Jones MS, Thorpe FG (1996) *Polym Degrad Stab* 54:387–393
16. Caze C, Moulaj NE, Hodge P, Lock CJ, Ma J (1995) *J Chem Soc Perkin Trans 1* 345–349
17. Ramakrishnan S (1991) *Macromolecules* 24:3753–3759
18. Chung TC, Lu HL, Li CL (1994) *Macromolecules* 27:7533–7537
19. Paetzold P, Hoffmann J (1980) *Chem Ber* 113:3724–3733
20. Kondo Y, Garcia-Cuadrado D, Hartwig JF, Boen NK, Wagner NL, Hillmyer MA (2002) *J Am Chem Soc* 124:1164–1165
21. Bae C, Hartwig JF, Harris NKB, Long RO, Anderson KS, Hillmyer MA (2005) *J Am Chem Soc* 127:767–776
22. Bae C, Hartwig JF, Chung H, Harris NK, Switek KA, Hillmyer MA (2005) *Angew Chem Int Ed* 44:6410–6413
23. Shin J, Chang AY, Brownell LV, Racoma IO, Ozawa CH, Chung H-Y, Peng S, Bae C (2008) *J Polym Sci A Polym Chem* 46:3533–3545
24. Shin J, Jensen SM, Ju J, Lee S, Xue Z, Noh SK, Bae C (2007) *Macromolecules* 40:8600–8608
25. Qin Y, Cheng G, Sundararaman A, Jäkle F (2002) *J Am Chem Soc* 124:12672–12673
26. Qin Y, Cheng G, Achara O, Parab K, Jäkle F (2004) *Macromolecules* 37:7123–7131
27. Matyjaszewski K, Xia J (2001) *Chem Rev* 101:2921–2990
28. Doshi A, Jäkle F (2006) *Main Group Chem* 5:309–318
29. Parab K, Venkatasubbaiah K, Jäkle F (2006) *J Am Chem Soc* 128:12879–12885
30. Parab K, Jäkle F (2009) *Macromolecules* 42:4002–4007
31. Parab K, Doshi A, Cheng F, Jäkle F (2011) *Macromolecules* 44:5961–5967
32. Kuhtz H, Cheng F, Schwedler S, Böhling L, Brockhinke A, Weber L, Parab K, Jäkle F (2012) *ACS Macro Lett* 1:555–559
33. Qin Y, Sukul V, Pagakos D, Cui C, Jäkle F (2005) *Macromolecules* 38:8987–8990
34. Qin Y, Cui C, Jäkle F (2007) *Macromolecules* 40:1413–1420
35. Qin Y, Cui C, Jäkle F (2008) *Macromolecules* 41:2972–2974
36. Kim H, Kang YJ, Kang S, Kim KT (2012) *J Am Chem Soc* 134:4030–4033
37. Cheng F, Bonder EM, Jäkle F (2013) *J Am Chem Soc* 135:17286–17289
38. Wan W, Cheng F, Jäkle F (2014) *Angew Chem Int Ed* 53:8934–8938
39. Kotsuchibashi Y, Agustin RVC, Lu J-Y, Hall DG, Narain R (2013) *ACS Macro Lett* 2:260–264
40. Kim H, Kang YJ, Jeong ES, Kang S, Kim KT (2012) *ACS Macro Lett* 1:1194–1198
41. Roy D, Sumerlin BS (2012) *ACS Macro Lett* 1:529–532
42. Roy D, Cambre JN, Sumerlin BS (2009) *Chem Commun* (16):2106–2108
43. Cheng F, Jäkle F (2010) *Chem Commun* 46:3717–3719
44. Cheng F, Bonder EM, Salem S, Jäkle F (2013) *Macromolecules* 46:2905–2915
45. Nicolas J, Guillauneuf Y, Lefay C, Bertin D, Gimes D, Charleux B (2013) *Prog Polym Sci* 38:63–235
46. Barner L, Barner-Kowollik C, Davis TP, Stenzel MH (2004) *Aust J Chem* 57:19–24
47. Kim KT, Cornelissen JJLM, Nolte RJM, van Hest JCM (2009) *Adv Mater* 21:2787–2791
48. Cambre JN, Roy D, Gondi SR, Sumerlin BS (2007) *J Am Chem Soc* 129:10348–10349
49. Roy D, Cambre JN, Sumerlin BS (2008) *Chem Commun* 2477–2479
50. Cheng F, Bonder EM, Jäkle F (2012) *Macromolecules* 45:3078–3085
51. Cheng F, Bonder EM, Doshi A, Jäkle F (2012) *Polym Chem* 3:596–600
52. Nagai A, Kokado K, Miyake J, Chujo Y (2009) *Macromolecules* 42:5446–5452
53. Nagai A, Kokado K, Miyake J, Chujo Y (2010) *J Polym Sci A Polym Chem* 48:627–634
54. Shipman PO, Cui C, Lupinska P, Lalancette RA, Sheridan JB, Jäkle F (2013) *ACS Macro Lett* 2:1056–1060
55. Park MH, Kim T, Huh JO, Do Y, Lee MH (2011) *Polymer* 52:1510–1514
56. Dong JY, Manias E, Chung TC (2002) *Macromolecules* 35:3439–3447
57. Sung WY, Park MH, Park JH, Eo M, Yu M-S, Do Y, Lee MH (2012) *Polymer* 53:1857–1863
58. Zhang G, Kooi SE, Demas JN, Fraser CL (2008) *Adv Mater* 20:2099–2104

59. Zhang G, Fiore GL, St. Clair TL, Fraser CL (2009) *Macromolecules* 42:3162–3169
60. Zhang G, St. Clair TL, Fraser CL (2009) *Macromolecules* 42:3092–3097
61. Wagner CE, Kim JS, Shea KJ (2003) *J Am Chem Soc* 125:12179–12195
62. Luo J, Shea KJ (2010) *Acc Chem Res* 43:1420–1433
63. Tehfe MA, Brahmī MM, Fouassier JP, Curran DP, Malacria M, Fensterbank L, Lacote E, Lalevee J (2010) *Macromolecules* 43:2261–2267
64. Tehfe MA, Monot J, Brahmī MM, Bonin-Dubarle H, Curran DP, Malacria M, Fensterbank L, Lacote E, Lalevee J, Fouassier JP (2011) *Polym Chem* 2:625–631
65. Tehfe MA, Monot J, Malacria M, Fensterbank L, Fouassier JP, Curran DP, Lacote E, Lalevee J (2012) *ACS Macro Lett* 1:92–95
66. Telitel S, Schweizer S, Morlet-Savary F, Graff B, Tschamber T, Blanchard N, Fouassier JP, Lelli M, Lacote E, Lalevee J (2013) *Macromolecules* 46:43–48
67. Li H, Sundararaman A, Venkatasubbaiah K, Jäkle F (2007) *J Am Chem Soc* 129:5792–5793
68. Li H, Jäkle F (2011) *Polym Chem* 2:897–905
69. Li H, Sundararaman A, Pakkirisamy T, Venkatasubbaiah K, Schödel F, Jäkle F (2011) *Macromolecules* 44:95–103
70. Pammer F, Lalancette RA, Guo F, Jäkle F (2012) *Macromolecules* 45:6333–6343
71. Hoven CV, Wang HP, Elbing M, Garner L, Winkelhaus D, Bazan GC (2010) *Nat Mater* 9:249–252
72. Yamaguchi I, Choi BJ, Koizumi TA, Kubota K, Yamamoto T (2007) *Macromolecules* 40:438–443
73. Nagata Y, Otaka H, Chujo Y (2008) *Macromolecules* 41:737–740
74. Nagai A, Kokado K, Nagata Y, Chujo Y (2008) *Macromolecules* 41:8295–8298
75. Tanaka K, Tamashima K, Nagai A, Okawa T, Chujo Y (2013) *Macromolecules* 46:2969–2975
76. Welch GC, Bazan GC (2011) *J Am Chem Soc* 133:4632–4644
77. Zhao C, Wakamiya A, Yamaguchi S (2007) *Macromolecules* 40:3898–3900
78. Pammer F, Jäkle F (2012) *Chem Sci* 3:2598–2606
79. Ma X, Jiao JM, Yang J, Huang XB, Cheng YX, Zhu CJ (2012) *Polymer* 53:3894–3899
80. Reitzenstein D, Lambert C (2009) *Macromolecules* 42:773–782
81. Guo F, Yin X, Pammer F, Cheng F, Fernandez D, Lalancette RA, Jäkle F (2014) *Macromolecules* 47:7831–7841
82. Hayashi S, Koizumi T (2012) *Polym Chem* 3:613–616
83. Son JH, Jang G, Lee TS (2013) *Polymer* 54:3542–3547
84. Yeo H, Tanaka K, Chujo Y (2013) *Macromolecules* 46:2599–2605
85. Matsumi N, Naka K, Chujo Y (1998) *J Am Chem Soc* 120:5112–5113
86. Nagai A, Murakami T, Nagata Y, Kokado K, Chujo Y (2009) *Macromolecules* 42:7217–7220
87. Lorbach A, Bolte M, Li H, Lerner H-W, Holthausen MC, Jäkle F, Wagner M (2009) *Angew Chem Int Ed* 48:4584–4588
88. Matsumi N, Naka K, Chujo Y (1998) *J Am Chem Soc* 120:10776–10777
89. Sundararaman A, Victor M, Varughese R, Jäkle F (2005) *J Am Chem Soc* 127:13748–13749
90. Li H, Jäkle F (2009) *Angew Chem Int Ed* 48:2313–2316
91. Li H, Jäkle F (2010) *Macromol Rapid Commun* 31:915–920
92. Chen P, Lalancette RA, Jäkle F (2011) *J Am Chem Soc* 133:8802–8805
93. Chai J, Wang C, Jia L, Pang Y, Graham M, Cheng SZD (2009) *Synth Met* 159:1443–1449
94. Zhu M, Jiang L, Yuan M, Liu X, Ouyang C, Zheng H, Yin X, Zuo Z, Liu H, Li Y (2008) *J Polym Sci A Polym Chem* 46:7401–7410
95. Tokoro Y, Nagai A, Kokado K, Chujo Y (2009) *Macromolecules* 42:2988–2993
96. Nagata Y, Chujo Y (2008) *Macromolecules* 41:2809–2813
97. Donuru VR, Vegesna GK, Velayudham S, Green S, Liu H (2009) *Chem Mater* 21:2130–2138
98. Meng G, Velayudham S, Smith A, Luck R, Liu H (2009) *Macromolecules* 42:1995–2001
99. Kim B, Ma B, Donuru VR, Liu H, Fréchet JMJ (2010) *Chem Commun* 46:4148–4150
100. Nagai A, Chujo Y (2010) *Macromolecules* 43:193–200

101. Yoshii R, Nagai A, Tanaka K, Chujo Y (2013) *J Polym Sci A Polym Chem* 51:1726–1733
102. Reus C, Guo F, John A, Winhold M, Lerner HW, Jäkle F, Wagner M (2014) *Macromolecules* 47:3727–3735
103. Heilmann JB, Scheibitz M, Qin Y, Sundararaman A, Jäkle F, Kretz T, Bolte M, Lerner H-W, Holthausen MC, Wagner M (2006) *Angew Chem Int Ed* 45:920–925
104. Hubner A, Qu ZW, Englert U, Bolte M, Lerner HW, Holthausen MC, Wagner M (2011) *J Am Chem Soc* 133:4596–4609
105. Pammer F, Lalancette RA, Jäkle F (2011) *Chem Eur J* 17:11280–11289
106. Smith K, El-Hiti GA, Hou DJ, DeBoos GA (1999) *J Chem Soc Perkin Trans 1* 2807–2812
107. Revell JD, Dörner B, White PD, Ganesan A (2005) *Org Lett* 7:831–833
108. Qin Y, Jäkle F (2007) *J Inorg Organomet Polym Mater* 17:149–157
109. Sheepwash E, Krampl V, Scopelliti R, Sereda O, Neels A, Severin K (2011) *Angew Chem Int Ed* 50:3034–3037
110. Grosche M, Herdtweck E, Peters F, Wagner M (1999) *Organometallics* 18:4669–4672
111. Ma K, Scheibitz M, Scholz S, Wagner M (2002) *J Organomet Chem* 652:11–19
112. Severin K (2009) *Dalton Trans* 5254–5264
113. Icli B, Solari E, Kilbas B, Scopelliti R, Severin K (2012) *Chem Eur J* 18:14867–14874
114. Miyata M, Chujo Y (2002) *Polym J* 34:967–969
115. Yamaguchi S, Akiyama S, Tamao K (2002) *J Organomet Chem* 652:3–9
116. Hudson ZM, Wang S (2009) *Acc Chem Res* 42:1584–1596
117. Wade CR, Broomsgrove AEJ, Aldridge S, Gabbai FP (2010) *Chem Rev* 110:3958–3984
118. Thomas SW III, Joly GD, Swager TM (2007) *Chem Rev* 107:1339–1386
119. Cai M, Daniel SL, Lavigne JJ (2013) *Chem Commun* 49:6504–6506
120. Chen P, Jäkle F (2011) *J Am Chem Soc* 133:20142–20145
121. Qin Y, Pagba C, Piotrowiak P, Jäkle F (2004) *J Am Chem Soc* 126:7015–7018
122. Qin Y, Kiburu I, Shah S, Jäkle F (2006) *Macromolecules* 39:9041–9048
123. Wang X-Y, Weck M (2005) *Macromolecules* 38:7219–7224
124. Qin Y, Kiburu I, Shah S, Jäkle F (2006) *Org Lett* 8:5227–5230
125. Nagata Y, Chujo Y (2008) *Macromolecules* 41:3488–3492
126. Nagata Y, Chujo Y (2007) *Macromolecules* 40:6–8
127. Nagai A, Kobayashi S, Nagata Y, Kokado K, Taka H, Kita H, Suzuri Y, Chujo Y (2010) *J Mater Chem* 20:5196–5201
128. Paris R, Quijada-Garrido I, Garcia O, Liras M (2011) *Macromolecules* 44:80–86
129. Nagai A, Miyake J, Kokado K, Nagata Y, Chujo Y (2008) *J Am Chem Soc* 130:15276–15278
130. Thivierge C, Loudet A, Burgess K (2011) *Macromolecules* 44:4012–4015
131. Pfister A, Zhang G, Zareno J, Horwitz AF, Fraser CL (2008) *ACS Nano* 2:1252–1258
132. Zhang G, Chen J, Payne SJ, Kooi SE, Demas JN, Fraser CL (2007) *J Am Chem Soc* 129:8942–8943
133. Fraser CL, Zhang GQ, Xu SP, Zestos AG, Evans RE, Lu JW (2010) *ACS Appl Mater Interfaces* 2:3069–3074
134. Zhang G, Palmer GM, Dewhirst MW, Fraser CL (2009) *Nat Mater* 8:747–751
135. Hamm-Alvarez SF, Contreras J, Xie JS, Chen YJ, Pei H, Zhang GQ, Fraser CL (2010) *ACS Nano* 4:2735–2747
136. Cui C, Bonder EM, Qin Y, Jäkle F (2010) *J Polym Sci A Polym Chem* 48:2438–2445
137. Roy D, Cambre JN, Sumerlin BS (2009) *Chem Commun* 16:2106–2108
138. Kim KT, Cornelissen JJLM, Nolte RJM, van Hest JCM (2009) *J Am Chem Soc* 131:13908–13909
139. Dowlut M, Hall DG (2006) *J Am Chem Soc* 128:4226–4227
140. Berube M, Dowlut M, Hall DG (2008) *J Org Chem* 73:6471–6479
141. Jay JI, Shukair S, Langheinrich K, Hanson MC, Cianci GC, Johnson TJ, Clark MR, Hope TJ, Kiser PF (2009) *Adv Funct Mater* 19:2969–2977
142. Jay JI, Lai BE, Myszka DG, Mahalingam A, Langheinrich K, Katz DF, Kiser PF (2010) *Mol Pharm* 7:116–129

143. Jay JI, Langheinrich K, Hanson MC, Mahalingam A, Kiser PF (2011) *Soft Matter* 7:5826–5835
144. Mahalingam A, Jay JI, Langheinrich K, Shukair S, McRaven MD, Rohan LC, Herold BC, Hope TJ, Kiser PF (2011) *Biomaterials* 32:8343–8355
145. Wu W, Zhou S (2013) *Macromol Biosci* 64:1464–1477
146. Li Y, Zhou S (2013) *Chem Commun* 49:5553–5555
147. Bapat AP, Roy D, Ray JG, Savin DA, Sumerlin BS (2011) *J Am Chem Soc* 133:19832–19838
148. Matsumi N, Sugai K, Sakamoto K, Mizumo T, Ohno H (2005) *Macromolecules* 38:4951–4954
149. Narita A, Shibayama W, Matsumi N, Ohno H (2006) *Polym Bull* 57:109–114
150. Matsumi N, Nakamura Y, Aoi K, Watanabe T, Mizumo T, Ohno H (2009) *Polym J* 41:437–441
151. Mager M, Becke S, Windisch H, Denninger U (2001) *Angew Chem Int Ed* 40:1898–1902
152. Moritz R, Zardalidis G, Butt HJ, Wagner M, Mullen K, Floudas G (2014) *Macromolecules* 47:191–196
153. Chen EY-X, Marks TJ (2000) *Chem Rev* 100:1391–1434
154. Kishi N, Ahn C-H, Jin J, Uozumi T, Sano T, Soga K (2000) *Polymer* 41:4005–4012
155. Sablong R, van der Vlugt JI, Thomann R, Mecking S, Vogt D (2005) *Adv Synth Catal* 347:633–636
156. Cui C, Bonder EM, Jäkle F (2010) *J Am Chem Soc* 132:1810–1812
157. Berven BM, Oviasuyi RO, Klassen RJ, Idacavage M, Gillies ER, Ragogna PJ (2013) *J Polym Sci A Polym Chem* 51:499–508
158. Trofimenko S (1999) *Scorpionates—the coordination chemistry of polypyrazolylborate ligands*. Imperial College Press, London
159. Qin Y, Shipman PO, Jäkle F (2012) *Macromol Rapid Commun* 33:562–567
160. Cui C, Lalancette RA, Jäkle F (2012) *Chem Commun* 48:6930–6932
161. Cui C, Heilmann-Brohl J, Perucha AS, Thomson MD, Roskos HG, Wagner M, Jäkle F (2010) *Macromolecules* 43:5256–5261
162. Cui C, Jäkle F (2009) *Chem Commun* (19):2744–2746
163. Cui C, Bonder EM, Jäkle F (2009) *J Polym Sci A Polym Chem* 47:6612–6618

Index

A

α -(Acylamino)benzylboronic esters, 231
Acyloxyalkyltrifluoroborates, 134
Acyloxybenzodioxaborolane, 253
Acyloxyboron, 243
Acyltrifluoroborates, 143
Alder-ene reaction, 104
Aldimines, boration, 21
Alkenylations, potassium
 alkenyltrifluoroborates, 133
Alkenyl(dialkyl)borane, 106
Alkenyl halides, 229
Alkoxyethylboron, 125
Alkoxyethyltrifluoroborates, 126
Alkoxyethyltrifluoroborates, 124, 136
Alkyl β -trifluoroboratoamides, 135
Alkynes, 14, 57, 93, 206, 266
Alkynylborates (ate-complexes), 105
Alkynylboronates, 93, 94
Alkynyl(dihalo)boranes, 96
Alkynyl(triaryl)borates, 105
Alkynyl(triorganyl)borates, 105
Alkynylzirconium, 1,1-hydroboration, 112
Allenamides, 84
Allenoates, 84
Allylhaloboranes, 106
Amidation, 243
 α -Amidoacrylates, Cu-catalyzed
 enantioselective β -borylation, 83
Amidoboranes, 192
Amine-boranes, dehydrocoupling, 153
Amino acid derivatives, 249
Aminoboranes, 155
Aminoboronic acid, 246, 259

Aminomethyltrifluoroborates, 122
Aminothiourea, 246
Ammonioalkynylborate, 108
Ammoniomethyltrifluoroborates, 123
Amphidinolide K, 104
Arylboroxines, 236
Aryl halides, 229
Arylsilanes, borodesilation, 53
Aryltrifluoroborates, 119
 amination, 145
 nitrosation, 144
Atom transfer radical polymerization
 (ATRP), 303
Atropisomers, enantioenriched, 224

B

Benzimidazolylphenylboronic acid, 266
Benzoates, secondary, 291
Benzo[*d*][1,3,2]dioxaborol-2-ol, 253
Benzotriazin-4(3*H*)-one, 101
Benzoylborane, 10
Benzoyltrifluoroborates, 142
Benzylic boronates, 229
Benzylic boronic esters, enantioenriched
 tertiary, 285
1-(Benzyloxy)alkyltrifluoroborates, 135
 α -Benzyloxytrifluoroborates, 233
Biaryls, axially chiral, 225
Bisboronic acid (BBA), 119
Bis(dimethylamino)borylphosphine, 32
Bis(dimethylamino)naphthalene, 54
Bis(oxazol-2-ylidene)borylene, 66
Bis(pentafluorosulfanyl)boronic acid, 267

- Bis(perfluorodecyl)phenylboronic acid, 247
Bis(pinacolato)diboron, 86, 119
Bis(trifluoromethyl)phenylboronic acid, 247, 260
Block copolymers, 302
Borane, 93, 297
Borane homopolymer, 303
Borazaronaphthalenes, 149
Borenium, 39
Boric acid, 243, 263
Borinium, 39, 48
Borocations, 39
 electrophilicity, 44
Borodestannylation, 51
Borole, 5
Boron diketonates, 303
Boron dipyrromethene (BODIPY), 64, 303, 311
 functionalized polymers, 313
Boron enolate, 2
Boron 8-hydroxyquinolate, 306, 311
Boronic acids, 243
Boronic esters, 271
Boronium, 39
4-Borono-*N*-methylpyridinium iodide, 260
Borono-Pschorr transformations, 137
Boronopyridinium chloride, 251
Boron quinolate-functionalized polymers, 312
Boroxacycles, 104
1-Boryl-1-alkenylzirconiums, 95
Borylaluminum, 29
Boryl anions, 1
Borylation, 39
 asymmetric, 73
Borylcadmium, 24
Borylcopper, 3
Borylcyanozincate, 17
Borylenes, 65
Borylgallium, 29
Boryllithiums, 1, 8
Borylmercury, 23
Boryl radicals, 65
1-Boryl-2-stannylalkene, 111
Boryl-substituted main group elements, 1
Boryl-transition metal complexes, 1, 22
Boryltrihydroborate, 29
4-Bromoacetophenone, nickel-catalyzed borylation, 120
Bromoborane, 3
Bromopentyltrifluoroborate, 122
Bromosulfoxides, 234
Brønsted acids, 243
Buchwald-Hartwig arylation, 132
- C**
Carbamates, 271
Carbinols, 283
Carboxamides, 247, 253, 268
Carboxylic acid esters, 260
Carboxylic acids, 243
Catalysis, 73, 93, 153, 221
 borocations, 61
Catecholborane, 247, 253
C-C bond formation, 221
 enantioselective, 133
 α -Chloro-alkyllithiums, 274
Chloroborole, 5
Chloroborylene dimanganese, 6
Chlorophosphanes, 106
Chlorophosphine, 33
C-N bond formation, 142
Cross-coupling, 2, 117, 221
 stereoselective, 221
 Suzuki-Miyaura, 2
Cu-catalyzed β -borylation, 74
Cu-QuinoxP, 81
C-X bond formation, 145
 α -Cyanohydrin triflates, 235
Cyclic borinate ester, 106
Cyclobutyltrifluoroborate, 129
Cyclohexadienylboronic esters, 101
Cyclohexadienylborane, 95
Cyclopentadienones, 97
Cyclopentenones, 102
Cyclopropanes, borylation, 121
Cyclopropylboronate esters, 121
Cyclopropylboronic acid, 128, 227
Cyclopropyltrifluoroborate, 129
- D**
Decarestrictine, 281
Dehydrative condensation, 243
Dehydroboration, 39, 49
Dehydrocoupling, 153
 amine-boranes, 155
Dialkoxy-4-oxo-dioxaborolan-2-uide, 260
Di(alkynylboryl)methanes, 102
Di(alkynyl)hafnocene, 113
Dialkynylzirconocene, 113
Diaminomethylphenylboronic acid, 265
1,8-Diazabicyclo[5.4.0]undec-7-ene (DBU), 86
Dibenzo-18-crown-6, 6
Diborane(4), 18, 66
Diborazanes, 157
Diboronyl carboxyesters, 232, 233

Diborylacetylene, 99
Diboryllead, 31
Diboryl-2-silylalkenes, 95
Diborylstannylene, 31
Diborylzinc, 24
Dichloroborenium cations, 55
Dicyanoborane, 6
1,4-Dienes, 104
Dienoates, Cu-catalyzed enantioselective δ -borylation, 84
Dienones, Cu-catalyzed enantioselective δ -borylation, 84
1,4-Dienylboronates, 104
Difluoro-4-methylpyridiniumboronic acid, 267
3,5-Dihalo-2*H*-1,4-oxazin-2-ones, 97
2-(*N,N*-Diisopropylaminomethyl)phenylboronic acid, 246
Di(isopropylprenyl)borane, 125
Dioxaborolan-2-ol, 255
Dipeptides, 248
Directing group, 93
Dötz reaction, 103

E

Electrophiles, 39
Elemento-boration, 58
Enantioselectivity, 73
Enones, enantioselective β -borylation, 79
Enyne metathesis, 104
Erogorgiaene, 286
Erythroccamide B, 246
Esterification, 243
Ethynylboronic acid catechol ester, hydroboration, 96
Ethynylboronic acid MIDA ester, hydroboration, 96

F

Faranal, 279
Filiformin, 289
Fischer carbene, 103
Fluorescent boron heterocycles, 311
Fluoride, abstraction, 45
N-Fluorotrimethylpyridinium triflate (NFTPT), 147

G

Giganin, 277
Glucose sensing, 317

H

Hafnocene, 113
Haloboration, 39
Halomethyltrifluoroborates, 122
2-Halophenylboronic acids, 245, 256
Heteroaryltrifluoroborates, 147
Heteroatom conversion, 117
N-Heterocyclic carbene (NHC), 2, 19, 58, 77
Hexaborylbenzene, 99
Hexafluoro-1-naphthylboronic acid, 266
Homoallylboronates, 83, 88
Homologation, 271
Hydroboration, 2, 39, 58, 94, 111, 156, 185, 229, 300
Hydroborole, 5
1-(Hydroxy)alkyltrifluoroborates, 134
Hydrozirconation, 95, 102

I

Ibuprofen, 257
Igmesine, 288
Imines, α,β -unsaturated, 81
Iminium ions, 81
2-Iodoalkenylboranes, 106
Iodoborane, 5
2-Iodophenylboronic acid, 256
Isoxazoleboronates, 98

J

Josiphos, 19, 76, 77, 86

K

KenPhos, 225

L

Lepidine, 137
Lewis acids, 243, 297
borane polymers, 307
boron-mediated reactions, 2
catalysis, 39
Lithiated carbamates, 271
Lithiation-borylation, 271
Lithium borylcyanozincate, 17
Lithium carbenoids, α -chloro-stabilized, 273
Luminescence, 297, 303
Luminescent polymers, 306, 311

M

Mandyphos, 76
Mating hormone α -1, 290

1,2-Metallate rearrangement, 271
Methyl cinnamate, NHC–Cu-catalyzed
enantioselective β -borylation, 79
N-Methylindol-2-yltrifluoroborate, 145
Monoacyloxyboronates, 258
Monoborylacetylenes, 99

N

Naproxen, 131
Neopentyl boronic esters, 284
Nickel, 221
 β -borylation, 85
3-Nitrophenylboronic acid, 266
Nitrosation, 144
Nitrosoarenes, 145
Nitrosonium tetrafluoroborate, 144
Nitroxide-mediated polymerization
(NMP), 303
Norbornadieneboronate, 95

O

Oligo(arylenevinylene)s, 108
Organic light emitting devices (OLEDs), 311
Organic synthesis, 93
Organoboranes, 297
Organoboron reagents, 221
Organotrifluoroborates, 117
C–H functionalization, 131
radical reactions, 136
trifluoromethylation, 130
Oxazaborolidines, 61
3-Oxoalkynyltrifluoroborates, 99

P

Palladium, 221
Pd-catalyzed β -borylation, 85
Pentafluorophenylboronic acid, 267
Phenylacetyltrifluoroborate, 143
Phosphine–boranes, catalytic
dehydrocoupling, 153
Pinacol boronic esters, 284
N-Pivaloyl morpholine, borylation, 121
Polyaminoboranes, 155
Polyborazylene, 155
Polyelectrolytes, 297, 318
Poly(ethylene oxide) (PEO), 318
Polymerization, 64, 297
Polyolefins, 299
Polystyrene–poly(ethylene glycol) copolymer
(PS–PEG), 226

Potassium alkoxyethyltrifluoroborates, 126
Potassium β -aminoethyltrifluoroborate, 125
Potassium bromomethyltrifluoroborate, 122
Potassium diaryltrifluoroboratomethanes, 134
Potassium dioxolanylethyltrifluoroborate, 126
Potassium iodomethyltrifluoroborate, 122
Potassium methyl 3-trifluoroboratobenzoate,
144
Potassium phenyltrifluoroborate, 141
Potassium styryltrifluoroborate, 128
Potassium sulfonamidomethyltrifluoroborate,
124
Potassium trifluoro(*N*-methylheteroaryl)
borates, 123
Potassium trifluoro(*N*-methylpyrazolo)borate,
123
Potassium(2-(trimethylsilyl)ethoxy)
methyltrifluoroborate, 125
Potassium vinyltrifluoroborate, 127
PQXPhos, 226
Propargylic boronates, 230
Propylene oxide, 64
Protodeboration, 51, 243
Pseudohalides, 234
Pyrazoles, 98
Pyridine–*N*-oxide–borane, 108
Pyrones, 97

Q

Quinolineboronic acid, 236

R

Regioselectivity, 93
Reversible addition–fragmentation chain
transfer polymerization (RAFT), 303
Rhodium–bisoxazolinyphenyl acetate, 85
Rhodium-catalyzed β -borylation, 84
Ring-opening metathesis polymerization
(ROMP), 303

S

Sensors, 297
Sertraline, 286
Sesquiterpenes, 288
Side-chain functionalization, 303
Silacyclopentadiene, 112
Silylboranes, 95
Sodium 2'-dicyclohexylphosphino-
2,6-dimethoxy-1,1'-biphenyl-3-
sulfonate hydrate (^tSPhos), 123

Solandelactones, 281
Sonogashira–Hagihara coupling, 304, 306, 313
Sparteine, 276
Stannacyclopentadienes, 111
Stereoselectivity, 60, 95, 102, 140, 221, 237,
266, 271
Stereospecificity, 230, 271
Styryltrifluoroborate, 133
Subporphyrin borenium cation, 64
Sugar binding, 316
Suzuki–Miyaura cross-coupling, 2, 94, 101,
108, 223, 306
Sydnones, 98

T

Taniaphos, 85
Tetrachloroaluminate, 54
Tetrachlorobenzo[*d*]dioxaborol-2-ol, 255
Tetrafluorophenylboronic acid, 266
Tolylboronic acids, 248
Transition metals, 93, 108
Transmetallation, 15, 18, 86, 111, 223, 229,
236, 239
Triarylmethanes, enantiomerically enriched,
230

Triboranes(5), 29
 β -Trifluoroboratoamides, 136, 232
4-Trifluoroboratotetrahydroisoquinolones, 131
Trifluorodiazaoethane, 131
Trifluoromethyl radicals, 130
Trifluoro(*N*-methylheteroaryl)borates, 123
Trifluorophenylboronic acid, 247
Triisopropyl borate, 94
Tris(pentafluorophenyl)borane, 105

U

α,β -Unsaturated compounds, 73

V

Vancomycin, 224
Vinylcarbene chromium, 103
Vinyltrifluoroborate, 127
C–H insertion, 132

Z

Zircocenes, 102, 113, 168
Zirconacycles, 102